

Green Chemistry and Sustainable Technology

Mahendra Rai

Silvio Silvério da Silva *Editors*

---

# Nanotechnology for Bioenergy and Biofuel Production

 Springer

# Green Chemistry and Sustainable Technology

## Series editors

Prof. Liang-Nian He

State Key Laboratory of Elemento-Organic Chemistry, Nankai University, Tianjin, China

Prof. Robin D. Rogers

Department of Chemistry, McGill University, Montreal, Canada

Prof. Dangsheng Su

Shenyang National Laboratory for Materials Science, Institute of Metal Research, Chinese Academy of Sciences, Shenyang, China

and

Department of Inorganic Chemistry, Fritz Haber Institute of the Max Planck Society, Berlin, Germany

Prof. Pietro Tundo

Department of Environmental Sciences, Informatics and Statistics, Ca' Foscari University of Venice, Venice, Italy

Prof. Z. Conrad Zhang

Dalian Institute of Chemical Physics, Chinese Academy of Sciences, Dalian, China

## **Aims and Scope**

The series *Green Chemistry and Sustainable Technology* aims to present cutting-edge research and important advances in green chemistry, green chemical engineering and sustainable industrial technology. The scope of coverage includes (but is not limited to):

- Environmentally benign chemical synthesis and processes (green catalysis, green solvents and reagents, atom-economy synthetic methods etc.)
- Green chemicals and energy produced from renewable resources (biomass, carbon dioxide etc.)
- Novel materials and technologies for energy production and storage (bio-fuels and bioenergies, hydrogen, fuel cells, solar cells, lithium-ion batteries etc.)
- Green chemical engineering processes (process integration, materials diversity, energy saving, waste minimization, efficient separation processes etc.)
- Green technologies for environmental sustainability (carbon dioxide capture, waste and harmful chemicals treatment, pollution prevention, environmental redemption etc.)

The series *Green Chemistry and Sustainable Technology* is intended to provide an accessible reference resource for postgraduate students, academic researchers and industrial professionals who are interested in green chemistry and technologies for sustainable development.

More information about this series at <http://www.springer.com/series/11661>

Mahendra Rai • Silvio Silvério da Silva  
Editors

# Nanotechnology for Bioenergy and Biofuel Production

 Springer

*Editors*

Mahendra Rai  
Department of Biotechnology  
Sant Gadge Baba Amravati University  
Amravati, India

Silvio Silvério da Silva  
Department of Biotechnology  
University of São Paulo  
Lorena/SP  
São Paulo, Brazil

ISSN 2196-6982                      ISSN 2196-6990 (electronic)  
Green Chemistry and Sustainable Technology  
ISBN 978-3-319-45458-0              ISBN 978-3-319-45459-7 (eBook)  
DOI 10.1007/978-3-319-45459-7

Library of Congress Control Number: 2016959554

© Springer International Publishing AG 2017

This work is subject to copyright. All rights are reserved by the Publisher, whether the whole or part of the material is concerned, specifically the rights of translation, reprinting, reuse of illustrations, recitation, broadcasting, reproduction on microfilms or in any other physical way, and transmission or information storage and retrieval, electronic adaptation, computer software, or by similar or dissimilar methodology now known or hereafter developed.

The use of general descriptive names, registered names, trademarks, service marks, etc. in this publication does not imply, even in the absence of a specific statement, that such names are exempt from the relevant protective laws and regulations and therefore free for general use.

The publisher, the authors and the editors are safe to assume that the advice and information in this book are believed to be true and accurate at the date of publication. Neither the publisher nor the authors or the editors give a warranty, express or implied, with respect to the material contained herein or for any errors or omissions that may have been made.

Printed on acid-free paper

This Springer imprint is published by Springer Nature  
The registered company is Springer International Publishing AG  
The registered company address is: Gewerbestrasse 11, 6330 Cham, Switzerland

# Preface

There is a greater need to search for alternative sources of energy due to the limited availability of fossil fuels. The use of biofuels is the common alternative in front of the whole world, and its use is significantly increased in many countries. Generally, biodiesel is used as a fuel for diesel engines due to its technical, environmental, and strategic advantages. Apart from these, biodiesel is technically competitive with conventional, petroleum-derived diesel fuel and requires virtually no changes in the fuel distribution infrastructure. Other advantages of biodiesel as compared to petrodiesel include reduction of most exhaust emissions, biodegradability, higher flash point, inherence, and the fact that it is of domestic origin. However, ethanol is mostly used for Otto cycle engines as an alternative to gasoline.

Nanotechnology is one of the most important research areas in the twenty-first century. The potential applications of nanobiotechnology in the production of sustainable bioenergy and biosensors have encouraged researchers in recent years to investigate new novel nanoscaffolds to build robust nanobiocatalytic systems. Different kinds of nanomaterials have been developed as per the need for application purpose.

Various metal nanomaterials are found to have direct or indirect application in the production of biofuels. Among these, nanoparticle-mediated enzyme hydrolysis of lignocellulosic residues for the production of ethanol is in practice. Magnetic and metal oxide nanoparticles such as  $\text{TiO}_2$ ,  $\text{ZnO}$ ,  $\text{SnO}_2$ , etc. are commonly used matrices for enzyme immobilization. Magnetic nanoparticles are found to have potential uses in the field of biofuel and bioenergy, i.e., in the production of bioethanol from lignocellulosic materials by immobilization of enzymes like cellulases and hemicellulases by physical adsorption, covalent binding, cross-linking, or specific ligand spacers. Such nanomaterials are generally called as nanocatalysts, which are fabricated by immobilizing enzymes with functional nanomaterials as enzyme carriers.

The book would be immensely useful for a diverse group of readers including physicists, chemists, microbiologists, biotechnologists, food technologists, agriculture engineers, nanotechnologists, and those who are interested in clean technologies. The students should find this book useful.

Amravati, Maharashtra, India  
Lorena, SP, Brazil

Mahendra Rai  
Silvio Silvério da Silva

# Contents

## Part I Nanotechnological Applications in Bioenergy and Biofuel

- 1 Bioenergy and Biofuels: Nanotechnological Solutions for Sustainable Production . . . . . 3**  
Felipe Antonio Fernandes Antunes, Swapnil Gaikwad, Avinash P. Ingle, Raksha Pandit, Júlio César dos Santos, Mahendra Rai, and Silvio Silvério da Silva
- 2 Nanotechnology Applications on Lignocellulosic Biomass Pretreatment . . . . . 19**  
Johnatt Allan Rocha de Oliveira, Luiza Helena da Silva Martins, Andrea Komesu, and João Moreira Neto
- 3 Applications of Carbon-Based Nanomaterials in Biofuel Cell . . . . . 39**  
Ming-Guo Ma, Bo Liu, and Ling-Yan Meng
- 4 Multifunctional Nanoparticle Applications to Microalgal Biorefinery . . . . . 59**  
Jung Yoon Seo, Minjeong G. Kim, Kyubock Lee, Young-Chul Lee, Jeong-Geol Na, Sang Goo Jeon, Seung Bin Park, and You-Kwan Oh

## Part II Nanotechnology in Biomass Conversion

- 5 Potential Applications of Nanotechnology in Thermochemical Conversion of Microalgal Biomass . . . . . 91**  
Abdul Raheem, Liaquat Ali Memon, Sikandar Ali Abbasi, Y.H. Taufiq Yap, Michael K. Danquah, and Razif Harun
- 6 Hierarchy Nano- and Ultrastructure of Lignocellulose and Its Impact on the Bioconversion of Cellulose . . . . . 117**  
Xuebing Zhao, Feng Qi, and Dehua Liu



<b>7</b>	<b>Role of Nanoparticles in Enzymatic Hydrolysis of Lignocellulose in Ethanol</b> . . . . .	153
	Mahendra Rai, Avinash P. Ingle, Swapnil Gaikwad, Kelly J. Dussán, and Silvio Silvério da Silva	
<b>8</b>	<b>Physicochemical Characterizations of Nanoparticles Used for Bioenergy and Biofuel Production</b> . . . . .	173
	Rafaella O. do Nascimento, Luciana M. Rebelo, and Edward Sacher	
<b>Part III Nano-characterization and Role of Catalysts</b>		
<b>9</b>	<b>From Biomass to Fuels: Nano-catalytic Processes</b> . . . . .	195
	Mohammad Barati	
<b>10</b>	<b>Catalytic Conversion on Lignocellulose to Biodiesel Product</b> . . . . .	207
	Samira Bagheri, Nurhidayatullaili Muhd Julkapli, and Rabi'atul Adawiyah Zolkepli	
<b>11</b>	<b>Heterogeneous Catalysts for Advanced Biofuel Production</b> . . . . .	231
	Vorranutch Itthibenchapong, Atthapon Srifa, and Kajornsak Faungnawakij	
<b>12</b>	<b>An Overview of the Recent Advances in the Application of Metal Oxide Nanocatalysts for Biofuel Production</b> . . . . .	255
	Mandana Akia, Esmail Khalife, and Meisam Tabatabaei	
<b>13</b>	<b>Nanocatalysis for the Conversion of Nonedible Biomass to Biogasoline via Deoxygenation Reaction</b> . . . . .	301
	Hwei Voon Lee and Joon Ching Juan	
<b>14</b>	<b>Impact of Nanoadditive Blended Biodiesel Fuels in Diesel Engines</b> . . . . .	325
	J. Sadhik Basha	
<b>Part IV Risk Management</b>		
<b>15</b>	<b>Nanotechnologies and the Risk Management of Biofuel Production</b> . . . . .	343
	Maria de Lourdes Oshiro, Edgar Oshiro, Tânia Elias Magno da Silva, William Waissmann, and Wilson Engelmann	
	<b>Index</b> . . . . .	365

# Contributors

**Abdul Raheem** Department of Chemical and Environmental Engineering, Universiti Putra Malaysia, Serdang, Malaysia

**Andrea Komesu** Faculdade de Engenharia Química, UNICAMP, Campinas, Brazil

**Atthapon Srifa** National Nanotechnology Center (NANOTEC), National Science and Technology Development Agency (NSTDA), Khlong Luang, Pathumthani, Thailand

**Avinash P. Ingle** Nanobiotechnology Laboratory, Department of Biotechnology, Sant Gadge Baba Amravati University, Amravati, Maharashtra, India

**Bo Liu** Engineering Research Center of Forestry Biomass Materials and Bioenergy, Beijing Key Laboratory of Lignocellulosic Chemistry, College of Materials Science and Technology, Beijing Forestry University, Beijing, PR China

**Dehua Liu** Department of Chemical Engineering, Institute of Applied Chemistry, Tsinghua University, Beijing, China

**Edgar Oshiro** Dr. Jorge David Nasser Public Health School, Mato Grosso do Sul State Health Secretariat, Campo Grande, Mato Grosso do Sul, Brazil

**Edward Sacher** Département de Génie Physique, Montréal, QC, Canada

**Esmail Khalife** Biofuel Research Team (BRTeam), Karaj, Iran

Department of Agricultural Machinery, College of Agricultural Technology and Natural Resources, University of Mohaghegh Ardabili, Ardabil, Iran

**Feng Qi** College of Life Sciences/Engineering Research Center of Industrial Microbiology, Fujian Normal University, Fuzhou, China

**Hwei Voon Lee** Nanotechnology & Catalysis Research Centre (NANOCAT), Institute of Postgraduate Studies, University of Malaya, Kuala Lumpur, Malaysia

**Jeong-Geol Na** Biomass and Waste Energy Laboratory, Korea Institute of Energy Research (KIER), Daejeon, Republic of Korea

**João Moreira Neto** Faculdade de Engenharia Química, UNICAMP, Campinas, Brazil

**Johnatt Allan Rocha de Oliveira** Faculdade de Nutrição, UFPA, Universidade Federal do Pará, Instituto de Ciências da Saúde, Belém, Brazil

**Joon Ching Juan** Nanotechnology & Catalysis Research Centre (NANOCAT), Institute of Postgraduate Studies, University of Malaya, Kuala Lumpur, Malaysia  
School of Science, Monash University, Bandar Sunway, Malaysia

**J. Sadhik Basha** Mechanical Engineering, International Maritime College Oman, Sohar, Al Liwa, Sultanate of Oman

**Jung Yoon Seo** Department of Chemical and Biomolecular Engineering, Korea Advanced Institute of Science and Technology (KAIST), Daejeon, Republic of Korea

**Kajornsak Faungnawakij** National Nanotechnology Center (NANOTEC), National Science and Technology Development Agency (NSTDA), Khlong Luang, Pathumthani, Thailand

**Kelly Johana Dussán** Biotechnology Department, Engineering School of Lorena, University of Sao Paulo, Lorena, Brazil

**Kyubock Lee** Biomass and Waste Energy Laboratory, Korea Institute of Energy Research (KIER), Daejeon, Republic of Korea

**Liaquat Ali Memon** Mechanical Department, Quaid-e-Awam University of Engineering, Science and Technology, Nawabshah, Pakistan

**Ling-Yan Meng** Engineering Research Center of Forestry Biomass Materials and Bioenergy, Beijing Key Laboratory of Lignocellulosic Chemistry, College of Materials Science and Technology, Beijing Forestry University, Beijing, PR China

**Luiza Helena da Silva Martins** Faculdade de Engenharia Química, UNICAMP, Campinas, Brazil

**Luciana M. Rebelo** Faculdade Católica Rainha do Sertão (FCRS), Quixadá, Ceará, Brazil

**Mahendra Rai** Nanobiotechnology Laboratory, Department of Biotechnology, Sant Gadge Baba Amravati University, Amravati, Maharashtra, India

**Mandana Akia** Department of Mechanical Engineering, University of Texas Rio Grande Valley, Edinburg, TX, USA

Biofuel Research Team (BRTeam), Karaj, Iran

**Maria de Lourdes Oshiro** Dr. Jorge David Nasser Public Health School, Mato Grosso do Sul State Health Secretariat, University Católica Dom Bosco, Campo Grande, Mato Grosso do Sul, Brazil

**Meisam Tabatabaei** Biofuel Research Team (BRTeam), Karaj, Iran

Microbial Biotechnology Department, Agricultural Biotechnology Research Institute of Iran (ABRII), AREEO, Karaj, Iran

**Michael K. Danquah** Department of Chemical Engineering, Curtin University, Sarawak, Malaysia

**Ming-Guo Ma** Engineering Research Center of Forestry Biomass Materials and Bioenergy, Beijing Key Laboratory of Lignocellulosic Chemistry, College of Materials Science and Technology, Beijing Forestry University, Beijing, PR China

**Minjeong G. Kim** Department of Chemical and Biomolecular Engineering, Korea Advanced Institute of Science and Technology (KAIST), Daejeon, Republic of Korea

**Mohammad Barati** Department of Applied Chemistry, Faculty of Chemistry, University of Kashan, Kashan, Iran

**Nurhidayatullaili Muhd Julkapli** Nanotechnology & Catalysis Research Centre (NANOCAT), University of Malaya, Kuala Lumpur, Malaysia

**Rabi'atul Adawiyah Zolkepli** Nanotechnology & Catalysis Research Centre (NANOCAT), University of Malaya, Kuala Lumpur, Malaysia

**Rafaella O. do Nascimento** Chemistry Department, Université de Montréal (UdeM), Montreal, QC, Canada

**Razif Harun** Department of Chemical and Environmental Engineering, Universiti Putra Malaysia, Serdang, Malaysia

**Samira Bagheri** Nanotechnology & Catalysis Research Centre (NANOCAT), University of Malaya, Kuala Lumpur, Malaysia

**Sang Goo Jeon** Biomass and Waste Energy Laboratory, Korea Institute of Energy Research (KIER), Daejeon, Republic of Korea

**Seung Bin Park** Department of Chemical and Biomolecular Engineering, Korea Advanced Institute of Science and Technology (KAIST), Daejeon, Republic of Korea

**Silvio Silvério da Silva** Biotechnology Department, Engineering School of Lorena, University of Sao Paulo, Lorena, Brazil

**Swapnil Gaikwad** Biotechnology Department, Engineering School of Lorena, University of Sao Paulo, Lorena, Brazil

**Tânia Elias Magno da Silva** Social Sciences Graduation and Research Group, Itinerary, Intellectuals, Image and Society, Sergipe Federal University, São Cristóvão, Sergipe, Brazil

**Y.H. Taufiq Yap** Catalysis Science and Technology Research Centre, Faculty of Science, Universiti Putra Malaysia, Serdang, Malaysia

**Vorranutch Itthibenchapong** National Nanotechnology Center (NANOTEC), National Science and Technology Development Agency (NSTDA), Khlong Luang, Pathumthani, Thailand

**W.A.K.G. Wan Azlina** Department of Chemical and Environmental Engineering, Universiti Putra Malaysia, Serdang, Malaysia

**William Waissmann** Research Group, Labour's Health and Human Ecology Studies Center, Sérgio Arouca National Public Health School, Rio de Janeiro, Brazil

**Wilson Engelmann** Vale do Rio Sinos University – UNISINOS, São Leopoldo, RS, Brazil

**Xuebing Zhao** Department of Chemical Engineering, Institute of Applied Chemistry, Tsinghua University, Beijing, China

**You-Kwan Oh** Biomass and Waste Energy Laboratory, Korea Institute of Energy Research (KIER), Daejeon, Republic of Korea

**Young-Chul Lee** Department of BioNano Technology, Gachon University, Seongnam-Si, Gyeonggi-Do, Republic of Korea

**Part I**  
**Nanotechnological Applications**  
**in Bioenergy and Biofuel**

# Chapter 1

## Bioenergy and Biofuels: Nanotechnological Solutions for Sustainable Production

Felipe Antonio Fernandes Antunes, Swapnil Gaikwad, Avinash P. Ingle, Raksha Pandit, Júlio César dos Santos, Mahendra Rai, and Silvio Silvério da Silva

**Abstract** Rather than using fossil fuels, the world is focusing on finding or developing alternative modes of energy production. This is due to the fact that fossil fuels are exhausting and the emission products of these fuels have been causing several damages to the environment. In this context, nanotechnology can play an important role for sustainable bioenergy and biofuel production. Different nanomaterials, such as metal nanoparticles, nanofiber, nanotubes, nanosheets, and others, have been reported to have a number of direct or indirect applications (as nanocatalyst) in the production of biofuels such as bioethanol and biodiesel. Actually, these biofuels are eco-friendly and renewable energy resources and hence have been receiving attention as an alternative energy source. Also, nanotechnology offers interesting approaches such as the use of magnetic nanoparticles. These particles can be used as carrier to immobilize enzymes that can be applied in bioethanol or biodiesel production. Moreover, magnetic nanoparticles can also be used for biogas production due to strong paramagnetic property and high coercivity during the process of methanogenesis. In this chapter, after introducing a global view about bioenergy and biofuel, different and interesting approaches regarding the application and solutions that nanotechnology can offer to bioenergy and biofuel production will be discussed followed by a section about safety issue concerning this technology.

**Keywords** Nanotechnology • Bioenergy • Biofuels • Ethanol • Biodiesel • Nanocatalysts

---

F.A.F. Antunes • S. Gaikwad • J.C. dos Santos  
Engineering School of Lorena, University of São Paulo, Estrada Municipal do Campinho, s/n°, 12.602-810 Lorena, São Paulo, Brazil

A.P. Ingle • R. Pandit • M. Rai  
Biotechnology Department, SGB Amravati University, Amravati 444 602, Maharashtra, India

S.S. da Silva (✉)  
Biotechnology Department, Engineering School of Lorena, University of Sao Paulo, Lorena, Brazil  
e-mail: [silviosilverio@gmail.com](mailto:silviosilverio@gmail.com)

## 1.1 Introduction

Worldwide, the concerns about environmental problems have driven a number of researchers to seek for innovative solutions. Particularly, the requirement for replacing resources as petroleum and coal by renewable energy and biofuel sources has motivated a large number of professionals to search for novel technological approaches. In fact, this requirement has gained pivotal importance regarding current problems as depletion of more readily available oil reserves, forcing to seek it in places more difficult to access, resulting in higher production costs. As a consequence, there is intense demand for energy in developing countries. The environmental problems such as greenhouse gas emission, especially due to the CO<sub>2</sub> generated during the burning of fossil fuels, has resulted into climate change that has become more clear for the scientific community (Huber et al. 2006; Cherubini 2010; Boudet 2011). For example, the importance of replacing fossil fuels in motors for energy derived from renewable sources can be easily verified considering that the transport sector can be responsible by 60 % of the estimated oil demand for 2030, in around 116 million barrels per day (IEA 2007).

Renewable energy includes a number of options such as solar, wind, geothermal, and biomass. The interest in the latter has been increased considering the abundant quantity of vegetable waste that can be used to generate electricity or liquid and gaseous fuels. This use can be in direct from burning biomass to generate vapor and electricity or after some transformation that allows a more efficient use of this energy source. However, the technologies for biomass processing remain limited by technological and economical constraints. Thus, new and creative approaches are necessary to achieve feasible processes as well as larger and faster change of global energy matrix.

Among the new developments, nanotechnology has been a fertile field of research, which includes promising possibilities in different application areas of social and industrial interest. This technology can be used in different fields such as electronics, material development, pharmaceutical, and life sciences, among others, and has along other converging technologies (biotechnology, information technology, and cognitive sciences) great potential to enhance human life (Wolf and Medikonda 2012; Demetzos 2016).

In biofuels and bioenergy field, nanotechnology has different applications such as modification in feedstocks, development of more efficient catalysts, and others. For example, enzymes have been largely used to hydrolyze biomass to produce biofuels such as ethanol and biogas or to catalyze biodiesel production from oils and fats (Michalska et al. 2015; Verma and Barrow 2015; Terán-Hilares et al. 2016). In this context, nanostructures can be used to replace the enzymes or to immobilize them, resulting into more efficient catalysis or favoring the recovery of biocatalysts from medium. Moreover, this technology includes alternatives in which magnetic properties are added to immobilized systems (Verma and Barrow 2015; Rai et al. 2016).



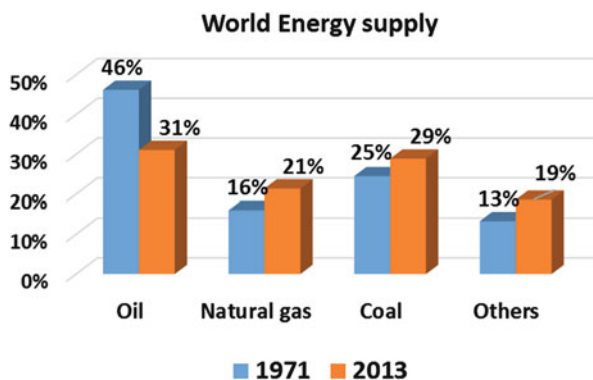
This chapter presents an overview of the possibilities of the use of nanotechnology as an interesting tool to solve some technological problems in bioenergy and biofuels production. It also includes a global view of the world energetic matrix, mainly considering renewable resources. Moreover, it is complemented with a section regarding safety issues.

## 1.2 Global View of Bioenergy and Biofuel

Currently, world energy supply is provided predominantly by coal, oil, natural gas, nuclear, hydro, and renewable sources (Brazilian Energy Balance 2015). From the last decades, total global energy primary production has been increased, and the mainly current producers are (Mtoe) China (2555), United States (1989), Russia (1334), Saudi Arabia (630), India (571), Indonesia (457), Canada (452), Australia (357), Iran (308), and Brazil (26) (Yearbook Enerdata 2015a). Considering different sources, the world energy supply has been provided mainly from oil, followed by natural gas and coal. Figure 1.1 presents world energy supply profile in 1971 and in 2013.

As can be clearly observed, the world remains strongly dependent on fossil fuels. Renewable energy, on the other hand, accounts for only about 10 % of total in world scenario from around 40 years (Brazilian Energy Balance 2015). In spite of this, several countries have been using the green energy. For example, from renewable energy, electricity production is the first source of power generation (%) in Norway (98.0), New Zealand (79.0), Brazil (73.4), Colombia (70.0), Venezuela (62.8), Portugal (62.6), Canada (62.5), Sweden (58.5), Chile (42.8), and Italy (42.1) (Yearbook Enerdata 2015b). In addition to this, share of wind and solar in electricity production is strongly diffused in Portugal (24.5), Spain (23.9), New Zealand (21.7), Italy (16.7), Germany (15.2), United Kingdom (10.3), Belgium (10.0), Romania (9.6), Sweden (7.6), and the Netherlands (6.6) (Yearbook Enerdata 2015c).

**Fig. 1.1** World energy supply profile in 1971 and in 2013 (Source: Based on IEA data from the Key World Energy Statistics © OECD/IEA 2015, [www.iea.org/statistics](http://www.iea.org/statistics). Licence: [www.iea.org/t&c](http://www.iea.org/t&c); as modified by present authors)



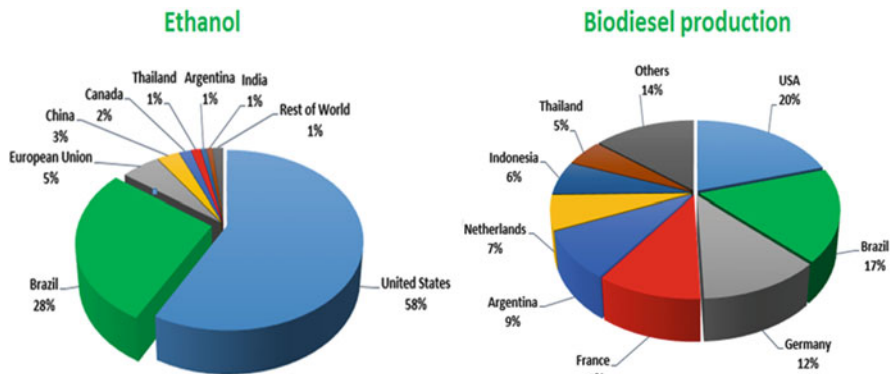


**Fig. 1.2** Main world renewable fuel producers in 2015 (Source: Statista 2016b; Renewable Fuels Association 2015)

Currently, biofuels have also gained special highlight and have been manufactured in different countries, with an increasing production. Among them, for example, bioethanol has world production of around 25 millions of gallons per year. The larger producers of bioethanol include the United States, with around 14,000 millions of gallons per year by using corn as a raw material, followed by Brazil, with around 7000 millions of gallons per year, by using sugarcane juice as carbon source (Renewable Fuels Association 2015). According to Goldemberg (2006), if just ethanol produced from sugarcane juice could replace 10% of total consumed gasoline in the world, carbon emissions could be reduced up to 66 million tons per year. Biodiesel, another important biofuel, is usually produced by a chemically catalyzed transesterification reaction between low chain length alcohols (mainly methanol) and oils and fats from animals or plants. The manufacturing of this compound has also been increased. For example, European Union currently produces around 3.35 billions litre of biodiesel, which can be increased up to around 4.14 billion gallons in 2025 (Statista 2016a). In 2014, the world's biggest biodiesel producers were (billion liters) the United States (4.7) followed by Brazil (3.4), Germany (3.4), Indonesia (3.1), and Argentina (2.9) (Statista 2016b). Figure 1.2 shows an overview of the main world renewable fuel producers in 2015.

One of the most important potential materials for biofuel production is the vegetal biomass, mainly taking into account lignocellulosic compounds that are the most abundant renewable carbon source in the world. These materials have an estimated generation from 10 to 50 billion tons per year, with about billion tons of primary biomass potentially available for reuse (Zhao et al. 2012). In many industrial processes, biomass is burning in boilers for self-sustainable energy production. Also, vegetal biomass is composed of two thirds polymeric carbohydrates such as cellulose and hemicellulose (Antunes et al. 2014) and hence can be used in bioprocesses for producing biofuels or other value-added compounds.

In this scenario, green technology along with nanotechnology has great potential to supply different industrial sectors with high demand of production within the required conception of sustainable development process.

### 1.3 Nanotechnological Solutions

Nanotechnology is the developing branch of science, which is applied for assessment of new technological replacements. It is the most significant study in modern science, which allows chemists, engineers, biotechnologists, and physicians to work at molecular and cellular levels.

Current researches have indicated that nanotechnology applied in nanomaterials can exhibit advanced properties that are exceptional in science (Engelmann et al. 2013). Nanotechnology can deal promising solutions for bioenergy production by changing the features of feed materials. Different nanomaterials, such as carbon nanotubes, magnetic and metal oxide nanoparticles, and others, are advantageous to become an essential part of sustainable bioenergy production (Rai et al. 2016).

#### 1.3.1 *Nanotechnology in Bioenergy Production*

Nanotechnology has the potential to enhance the bioenergy production by using different forms of the nanoparticles. Nanoparticles have potential physical, chemical, and electrical properties, which differ from the bulk material. They have ability to increase the energy production and can serve as solution, which can tackle the problem of energy production. Water, solar, and biogas energies are different kinds of renewable sources and its production can be enhanced by applying nanotechnology (Hussein 2015).

##### 1.3.1.1 **Nanotechnology in Biogas Production**

Biogas is produced from anaerobic digestion of organic wastes such as plant, agriculture, and animal and human wastes. Organic waste is rich in carbon and nitrogen sources, and the release of energy from anaerobic process depends on the C:N ratio (Feng et al. 2014). There are evidences that addition of certain metal ions in trace amounts increase the activity of methanogenic bacteria, and thus, acts as a catalyst which increases the production of energy. Since methanogenic bacteria require small amount of iron, cobalt, and nickel for the anaerobic digestion, researchers demonstrated that instead of using atomic or bulky materials, nanomaterials are beneficial (Feng et al. 2010). Magnetic nanoparticles have a strong paramagnetic property and high coercivity, and hence, can be used in the process of methanogenesis (Yang et al. 2015). Abdelsalam et al. (2015) found that

cobalt and nickel nanoparticles enhanced the methane gas production. They have also compared the activity of iron nanoparticles with iron oxide nanoparticles and reported that the latter presented more activity as compared to iron nanoparticles. In a more recent study, Abdelsalam et al. (2016) reported that the effect of different nanoparticles such as Fe, Fe<sub>3</sub>O<sub>4</sub>, nickel (Ni), and cobalt (Co) yields the highest biogas and methane production from anaerobic digestion of cattle dung. Also, Casals et al. (2014) reported that when Fe<sub>3</sub>O<sub>4</sub> nanoparticles were applied to the organic waste in the anaerobic digester, enhancement of the activity of disintegration as well as increasing yield of methane and biogas production was observed.

### ***1.3.2 Nanotechnology in Biofuel Production***

The first-generation biofuel is produced from different food feedstocks such as starch from corn, sucrose from sugarcane, animal fats, and plant oils (Naik et al. 2010). The regular use of these feedstocks present some concerns, and hence, new notion of second-generation biofuel has been gaining ground in the world scenario for production of biofuel by using non-food feedstock, e.g., lignocellulosic materials such as, wood wastes, agricultural residues, and others. (Patumsawad 2011; Eggert and Greker 2014). Although, second-generation biofuels have certain benefits as waste materials used in this case, they have some drawbacks such as high cost of production and infrastructure as well as technological problems. Therefore, keeping these truths in mind, researchers need to develop proficient technologies to solve these concerns in mass processing and increase productivity in biofuels. Aiming to these perspectives, application of nanotechnology can overcome the aforementioned difficulties by proposing the chance to modify the characteristics of feedstock materials for biofuel production.

Nanoparticles have strategic uses in biofuel production because of its exceptional physiochemical properties. Many nanomaterials such as TiO<sub>2</sub>, Fe<sub>3</sub>O<sub>4</sub>, SnO<sub>2</sub>, ZnO, carbon, graphene, and fullerene, presenting unique properties, have been applied for biofuel production. Moreover, magnetic nanoparticles have wide applications in biofuel production because of its high surface to the volume ratio, quantum properties, and immobilizing property due to their small size. Besides, the most significant property of these nanoparticles is that they can be easily recovered from reaction mixture by applying suitable magnetic field (Ahmed and Douek 2013).

#### **1.3.2.1 Nanocatalysts in Biodiesel Production**

Biodiesel is a mix of esters, which are commonly produced by transesterification of vegetable oils or animal fats with short-chain alcohols (methanol or ethanol) that meets specific standards to be used as fuel in diesel engines. Compared to

**Table 1.1** Different nanocatalyst and feedstock used for biodiesel production

Sr. No.	Nanocatalyst	Feedstock	Yield (%)	Reference
1	MgO	Sunflower oil and rape-seed oil	98.0	Verziu et al. (2008)
2	K <sub>2</sub> O/ $\gamma$ -Al <sub>2</sub> O <sub>3</sub>	Rapeseed oil	94.0	Heyou and Yanping (2009)
3	KF/CaO	Chinese tal-low seed oil	96.8	Wen et al. (2010)
4	Lithium-impregnated calcium oxide (Li-Cao)	Karanja oil and <i>Jatropha</i> oil	99.0	Kaur and Ali (2011)
5	ZrO <sub>2</sub> loaded with C <sub>4</sub> H <sub>4</sub> O <sub>6</sub> HK	Soybean oil	98.03	Qiu et al. (2011)
6	Hydrotalcite-derived particles with Mg/Al oxides	<i>Jatropha</i> oil	95.2	Deng et al. (2011)
7	ZnO nanorods	Olive oil	94.8	Molina (2013)
8	MgO nanoparticles on TiO <sub>2</sub> support	Soybean oil	95.0	Mguni et al. (2012)
9	Cs/Al/Fe <sub>3</sub> O <sub>4</sub>	Sunflower oil	94.8	Feyzi et al. (2013)
10	TiO <sub>2</sub> -ZnO	Palm oil	92.2	Madhuvilakku and Piraman (2013)
11	Iron/cadmium and iron/tin oxide nanoparticles	Soybean oil	84.0	Alves et al. (2014)
12	KF/ $\gamma$ -Al <sub>2</sub> O <sub>3</sub> /honeycomb ceramic (HC) monolithic catalyst	Palm oil	96.0	Gao et al. (2015)
13	Sulfamic and sulfonic acid-functionalized silica-coated crystalline Fe/Fe <sub>3</sub> O <sub>4</sub> core/shell magnetic nanoparticles	Glyceryl trioleate	95.0	Wang et al. (2015)
14	Ca/Fe <sub>3</sub> O <sub>4</sub> @SiO <sub>2</sub>	Sunflower oil	97.0	Feyzi and Norouzi (2016)
15	CaO	<i>Jatropha</i> oil	98.54	Reddy et al. (2016)

fossil fuels, biodiesel presents many advantages, such as biodegradable and superior lubricant properties, without generation of harmful emissions, as well as the possibility to be produced by renewable resources (Feyzi and Norouzi 2016).

About application of nanotechnology, Table 1.1 summarizes different nanocatalysts and feedstock used for the production of biodiesel, as well as the yield related to each process.

As shown, there are a number of different possibilities of application of nanocatalysts in this field. Several functionalized nanomaterials have been successfully used in the production of biodiesel. For example, Wang et al. (2015) synthesized acid-functionalized magnetic nanoparticles and demonstrated their use as heterogeneous nanocatalysts for biodiesel production. In this study, acid-functionalized, i.e., sulfamic and sulfonic silica-coated crystalline Fe/Fe<sub>3</sub>O<sub>4</sub> core/shell, magnetic nanoparticles were synthesized and used for the production of biodiesel from transesterification of glyceryl trioleate. Authors reported that both acid-functionalized nanocatalysts showed the significant catalytic activities. However, the sulfamic acid-functionalized nanocatalysts showed comparatively more activity than the sulfonic acid-functionalized nanocatalysts. In another investigation, Tahvildari et al. (2015) investigated the production of biodiesel from cooking oils, using CaO and MgO nanoparticles synthesized by sol-gel and sol-gel self-combustion methods, respectively. CaO nanoparticles showed significant increase in the biodiesel yield compared to MgO nanoparticles.

Other interesting approach is the use of magnetic nanocatalysts that can be easily recovered and reused, favoring the economic viability of the process. In this context, Alves et al. (2014) proposed a rapid and easy nanotechnological approach for the production of biodiesel from soybean oil. In this study, authors used a mixture of iron/cadmium and iron/tin oxide nanoparticles with magnetic properties, prepared by coprecipitation method as nanocatalysts for the biodiesel production. Between the two used nanocatalysts, iron/tin oxide nanoparticles showed maximum efficacy by producing about 84 % biodiesel. These nanocatalysts presented significant potential toward hydrolysis, transesterification, and esterification of soybean oil and their fatty acids. Similarly, Qiu et al. (2011) demonstrated the synthesis by ZrO<sub>2</sub> nanocatalyst loaded with C<sub>4</sub>H<sub>4</sub>O<sub>6</sub>HK (potassium bitartrate), in size range of 10–40 nm. Further, authors investigated the production of biodiesel by using the synthesized nanocatalysts for the transesterification of soybean oil and methanol in different molar ratios and other parameters like reaction temperature, nanocatalyst concentration, and reaction time. The obtained results showed that reaction mixture containing methanol and oil in the ratio 16:1 having 6.0 % nanocatalyst at 60 °C for 2.0 h resulted in maximum biodiesel yield of about 98.03 %.

Several other studies have been reported using nanocatalysts for biodiesel production. For example, Wen et al. (2010) synthesized KF/CaO nanocatalyst by impregnation method having size in the range of 30–100 nm and further used it for the production of biodiesel from Chinese tallow seed oil. This study reported about 96.8 % of biodiesel yield showing potential of such nanocatalyst for biodiesel industry. In another study, Deng et al. (2011) obtained about 95.2 % yield of biodiesel from pretreated *Jatropha* oil using nanocatalysts, hydrotalcite-derived particles with Mg/Al oxides synthesized by a coprecipitation method using urea as precipitating agent. In a novel proposal, Feyzi et al. (2013) reported a new nanocatalyst, Cs/Al/Fe<sub>3</sub>O<sub>4</sub>, that was synthesized and evaluated regarding its catalytic efficacy for biodiesel production. This investigation demonstrated the effect of different Cs/Al and Cs/Fe molar ratio and calcination conditions on the catalytic

performance. These nanocatalysts, in the molar ratio of 2.5:1 and 4:1, respectively, showed potential for production of biodiesel, resulting in 94.8 % of process yield at 58 °C with constant stirring for 120 min.

In other approach, Verziu et al. (2008) demonstrated the synthesis of MgO nanocatalyst in nanosheet form by aerogel method and proposed its use for the production of biodiesel from rapeseed and sunflower oil, verifying process yield up to 98 %. Recently, Feyzi and Norouzi (2016) synthesized a nanocatalyst  $\text{Ca/Fe}_3\text{O}_4@\text{SiO}_2$  with strong magnetic properties using combination of two different approaches, i.e., sol-gel and incipient wetness impregnation method for the production of biodiesel. Synthesized nanocatalysts were shown to be very effective at optimum conditions and resulted in maximum yield of about 97 %. The magnetic nature of nanocatalyst supported its reuse for several times without significant loss in its catalytic activity. In another current report, Reddy et al. (2016) demonstrated the synthesis of novel calcium oxide (CaO) nanocatalyst, using seashell, *Polymesoda erosa*, through different steps such as calcination, hydration, and dehydration techniques. Authors also investigated the efficacy of the synthesized nanocatalyst toward biodiesel production from the non-edible crude oils like *Jatropha* oil. Maximum of 98.54 % biodiesel yield was reported at conditions of methanol to oil ratio in 5.15:1 molar ratio, 133.1 min reaction time at 0.02:1 (w/w) nanocatalyst ratio.

### 1.3.2.2 Nanocatalysts in Bioethanol Production

Bioethanol (ethyl alcohol) is generally produced by carbon sources of sugarcane juice, grains, and others. However, production of this alcohol by using fermentable sugars, released from vegetal biomass, such as lignocellulosic materials, is also possible. These materials are mainly composed by cellulose and hemicellulose, polymeric structures of carbohydrates, and lignin, a complex organic polymer composed mainly by phenolic compounds (Antunes et al. 2014). For the use of sugars present in cellulose and hemicellulose fractions, some pretreatments are required to break down the recalcitrance of biomass, disrupting polymeric fraction in fermentable monomers. Usually, after an initial pretreatment, cellulosic fraction of these materials is enzymatically hydrolyzed (Rai et al. 2016). By this method, monomeric glucose can be produced in milder conditions of process (lower temperature, without requirement of pressure), compared to chemical process, as well as the non-formation of undesirable fermentation inhibitor compounds.

For example, the use of cellulases for the hydrolysis of lignocellulosic biomass is responsible for about 18 % of total costs involved in the process of the bioethanol production. Therefore, the development of advanced strategies, which could provide the recovery and recycling of enzymes, can reduce production cost. Considering this fact, nanotechnology offers immobilization of various enzymes such as cellulases and hemicellulases, involved in the bioethanol production on different nanomaterials. For example, immobilization of enzyme on magnetic nanomaterials is a promising method that provides easy recovery of enzyme by applying magnetic

field that allows enzyme recovery and reuse for several cycles (Alftren 2013; Rai et al. 2016).

Studies that were carried out by using magnetic nanoparticles were reported for immobilization of enzymes involved in the bioethanol production. Generally, enzyme immobilization on nanoparticles is achieved by covalent binding or physical adsorption. However, covalent binding method is more suitable because it reduces protein desorption due to formation of covalent bonds between enzyme and nanoparticles (Abraham et al. 2014). For stable immobilization of enzyme on nanomaterials, these compounds need to be modified or coated with chemically active polymer to provide the functional group for linkage of enzyme.

Lee et al. (2010) demonstrated the immobilization of  $\beta$ -glucosidase enzyme on polymer magnetic nanofibers by entrapment method for cellulosic ethanol production.  $\beta$ -Glucosidase is the enzyme responsible for the conversion of cellobiose into glucose, which can be metabolized by microorganisms to produce bioethanol. In fact, the entrapment of  $\beta$ -glucosidase on magnetic nanofibers provide stability to the enzyme and also the possibility of repeated use, separating them by applying magnetic field. Similarly, Verma et al. (2013b) evaluated  $\beta$ -glucosidase (isolated from fungus) immobilization on magnetic nanoparticles, used as nanobiocatalyst for bioethanol production. Authors verified that 93 % of enzyme-binding efficiency was recorded, showing about 50 % of its initial activity at 16th cycle. Jordan et al. (2011) also tested recycling of enzyme in the hydrolysis of microcrystalline cellulose by using carbodiimide as linking polymer for enzyme immobilization on  $\text{Fe}_3\text{O}_4$  nanoparticles. Due to magnetic nature of nanoparticles, the enzyme could be recovered easily and recycled for six times.

In another study, Goh et al. (2012) demonstrated that enzyme involved in the bioethanol production was immobilized in single-walled carbon nanotubes, which was already incorporated by magnetic iron oxide nanoparticles to give magnetic properties. In this study, the performance of immobilized enzyme could be controlled by altering the concentration of iron oxide nanoparticles in nanotubes. Thus, immobilized enzyme can be stored in acetate buffer at 4 °C for its longer storage.

Different nanomaterials have been studied for immobilization of enzymes. For example, Xie and Wang (2012) demonstrated the immobilization of lipase on magnetic chitosan microspheres synthesized by chemical coprecipitation method. In this work, glutaraldehyde was used as linking molecules for the covalent binding between lipase enzyme and magnetic chitosan microspheres. Moreover, enzyme immobilized on  $\text{TiO}_2$  nanoparticles by adsorption methods was also successfully used for the hydrolysis of lignocellulosic materials, aiming for the use of bioethanol production (Ahmad and Sardar 2014). In another study, Cherian et al. (2015) reported the immobilization of cellulase recovered from *Aspergillus fumigatus* on manganese dioxide nanoparticles by covalent binding. Authors verified that immobilized enzyme showed potential to enhance in its thermostability property compared to free enzymes, presenting stability up to 70 °C. Immobilized cellulase-mediated hydrolysis followed by the use of yeast leads to the production of bioethanol (21.96 g/L) from agricultural waste. After repeated use for about five cycles, immobilized enzyme showed 60 % of its activity.



Apart from magnetic nanoparticles, other nanomaterials can be used in nanotechnology process, such as silica and TiO<sub>2</sub>, polymeric nanoparticles, and carbon materials such as fullerene, graphene, carbon nanotubes, and others. These materials have been successfully reported for immobilization of different enzymes regarding the processes of bioethanol production (Huang et al. 2011; Cho et al. 2012; Pavlidis et al. 2012; Verma et al. 2013a). For instance, Pan et al. (2007) demonstrated the use of carbon nanotubes entrapped with Rh particles to enhanced catalytic activity for production of ethanol. Actually, free cores available on the carbon nanotubes are reported as a way to facilitate the incorporation of materials of different interests. In another investigation, Lupoi and Smith (2011) studied the immobilization of cellulase on silica nanoparticles, demonstrating the efficacy of immobilized and free enzymes in hydrolysis of cellulose into glucose. Authors observed that immobilized cellulase enzyme showed increased yield of glucose when compared to free enzyme, verifying that immobilized enzymes can be used in simultaneous saccharification and fermentation.

Microbial cells can also be immobilized on the nanoparticles and applied to fermentation step of ethanol production. For example, Ivanova et al. (2011) developed an approach for immobilization of *Saccharomyces cerevisiae* cells on magnetic nanoparticles. Further, authors demonstrated continuous fermentation process for the production of bioethanol; immobilized *S. cerevisiae* cells showed high ethanol production capability. Hence, the studies performed either on the immobilization of enzyme or whole microbial cells on the different nanomaterials provide evidence that such approaches will be convenient for the safe and economical production of bioethanol from cheapest lignocellulosic materials.

## 1.4 Safety Issues

Unfortunately, a few studies have been made on the safety assessment of nanoparticles used for biofuel and bioenergy production. During the course of their synthesis and application, nanoparticles can be released in the environment posing threat to human and environment (Gupta et al. 2015). However, as far as human exposure is concerned, nanoparticles have ability to enter inside the human body and may affect its most sensitive areas (Pourmand and Abdollahi 2012). The easy entry is possible via the process of ingestion, inhalation, and the penetration through intact and/or fractured dermis layers (Tang et al. 2009; Gupta et al. 2012). This is because nanoparticles have smaller size, and therefore, they can easily penetrate into the human and animal cells. They can cause trouble to the normal functioning of the cell (Vishwakarma et al. 2010). For instance, metal nanocatalyst (Asharani et al. 2011), catalyst support such as carbon nanotube and carbon fiber (Simon-Deckers et al. 2008; Erdely et al. 2013), and zirconia-based nanoparticles have been reported to induce the toxicity.

As far as the use of nanoparticles in biofuel is concerned, their emission from the vehicles and industry can cause harmful effects. They can be deposited into the lung

tissues through respiration. Such deposition may lead to the development of abnormality in the lung tissues, which can lead to various respiratory ailments including asthma, bronchitis, etc. (Upadhyay et al. 2015). Moreover, the worker manufacturing, along the processing of nanoparticles, has the chances of getting exposed through their dermal contact or through breathing. Platinum nanoparticles have also been investigated for their exposure effects on early stage of development. Literature reported that, depending on their concentration, they lower the heart rate, delay the hatching process, and also affect the touch response, axis curvature (Asharani et al. 2011).

Even though in-depth mechanism of toxicity is hitherto not understood, the toxicity is dependent on size (Mostafalou et al. 2013), shape, dose (Foldbjerg et al. 2011), composition, surface capping, and structure (Gupta et al. 2012). At cellular level, nanoparticles interact with the lipid bilayer envelope of the cell. This interaction disturbs the normal functioning of the cell membrane, thereby causing the pits in it, subsequently forming the cell content leakage. The nanoparticles, if exposed to the biological systems, can interact, followed by entering inside the cell, through mitochondrial membrane thereby disturbing its potential (Chen et al. 2008). The damage to mitochondria affects the energy balance of the cell consequently disturbing normal cell metabolism. Nanoparticles also induce the reactive oxygen species such as oxygen ions. The accumulated reactive radicals interact with proteins, especially with the enzymatic machinery. DNA damage by nanoparticles has also been reported to be induced by nanoparticle interaction (Kim et al. 2009; Guan et al. 2012).

On the basis of increased use of nanoparticles for biofuel applications, their exposure effect on human and environment is obvious. Therefore, for safe use of nanoparticles in such studies, safety assessment is of utmost importance. In the present scenario, various approaches are being made for assessing the toxicity of nanoparticles. Most of the studies involve in vitro evaluation of nanotoxicity. However, extensive studies are needed to focus on in vivo interaction of nanoparticles particularly used for biofuel and bioenergy production.

## 1.5 Conclusions

The global environmental problems, such as greenhouse effect generated by different chemicals including the use of petroleum and coal, have necessitated to search for alternative renewable energy and biofuel sources. The demand of alternative sources is also due to the rapid depletion of existing oil reserves. Among the new alternatives, nanotechnology is gaining importance to tackle the problem of bioenergy and biofuels by different applications including use of operative catalysts and amendments in feedstocks.

Encouragingly, various nanomaterials, such as carbon nanotubes and magnetic and metal oxide nanoparticles, having unique properties, are used for biofuel production. Among all the nanoparticles tested for biofuel production, magnetic

nanoparticles are frequently used because they can be easily recovered due to their magnetic property. The nanoparticles also can enhance the activity of enzymes after their immobilization. Although the use of nanotechnology for the production of biofuel and bioenergy has been beneficial and can be recommended for large-scale processing, there are safety issues concerning the environment and human being that need to be addressed meticulously after extensive long-term studies.

## References

- Abdelsalam E, Samer M, Abdel-Hadi MA, Hassan HE, Badr Y (2015) Effects of  $\text{CoCl}_2$ ,  $\text{NiCl}_2$  and  $\text{FeCl}_3$  additives on biogas and methane production. *Misr J Agric Eng* 32(2):843–862
- Abdelsalam E, Samer M, Attia YA, Abdel-Hadi MA, Hassan HE, Badr Y (2016) Comparison of nanoparticles effects on biogas and methane production from anaerobic digestion of cattle dung slurry. *Renew Energy* 87:592–598
- Abraham RE, Verma ML, Barrow CJ, Puri M (2014) Suitability of magnetic nanoparticle immobilised cellulases in enhancing enzymatic saccharification of pre-treated hemp biomass. *Biotechnol Biofuels* 7:90
- Ahmad R, Sardar M (2014) Immobilization of cellulase on  $\text{TiO}_2$  nanoparticles by physical and covalent methods: a comparative study. *Indian J Biochem Biophys* 51:314–320
- Ahmed M, Douek M (2013) The role of magnetic nanoparticles in the localization and treatment of breast cancer. *BioMed Res* 2013:1–11
- Alftren J (2013) Immobilization of cellulases on magnetic particles to enable enzyme recycling during hydrolysis of lignocellulose. PhD thesis submitted to Institute for Food, Technical University of Denmark, Lyngby, Denmark
- Alves MB, Medeiros FCM, Sousa MH, Rubim JC, Suarez PAZ (2014) Cadmium and tin magnetic nanocatalysts useful for biodiesel production. *J Braz Chem Soc* 25(12):2304–2313
- Antunes FAF, Chandel AK, Mmillessi TSS, Santos JC, Rosa CA, Da Silva SS (2014) Bioethanol production from sugarcane bagasse by a novel Brazilian pentose fermenting yeast *Scheffersomyces shehatae* UFMG-HM 52:2: evaluation of fermentation medium. *Int J Chem Eng* 2014:1–8
- Asharani PV, Lianwu Y, Gong Z, Valiyaveetil S (2011) Comparison of the toxicity of silver, gold and platinum nanoparticles in developing zebrafish embryos. *Nanotoxicology* 5(1):43–54
- Boudet AM (2011) Editorial: A new era for lignocellulosics utilization through biotechnology. *Comptes Rendus Biol* 334:777–780
- Brazilian Energy Balance (2015) Final Report 2015. [https://ben.epe.gov.br/downloads/Relatorio\\_Final\\_BEN\\_2015.pdf](https://ben.epe.gov.br/downloads/Relatorio_Final_BEN_2015.pdf). Accessed June 2016
- Casals E, Barrena R, García A, González E, Delgado L, Busquets-Fité M, Font X, Arbiol J, Glatzel P, Kvashnina K, Sánchez A, Puentes V (2014) Programmed iron oxide nanoparticles disintegration in anaerobic digesters boosts biogas production. *Small* 10(14):2801–2808
- Chen L, Yokel RA, Hennig B, Toborek M (2008) Manufactured aluminum oxide nanoparticles decrease expression of tight junction proteins in brain vasculature. *J Neuroimmune Pharmacol* 3(4):286–295
- Cherian E, Dharmendrakumar M, Baskar G (2015) Immobilization of cellulase onto  $\text{MnO}_2$  nanoparticles for bioethanol production by enhanced hydrolysis of agricultural waste. *Chinese J Catal* 36(8):1223–1229
- Cherubini F (2010) The biorefinery concept: using biomass instead of oil for producing energy and chemicals. *Energy Convers Manage* 51:1412–1421

- Cho EJ, Jung S, Kim HJ, Lee YG, Nam KC, Lee HJ, Bae HJ (2012) Co-immobilization of three cellulases on Au-doped magnetic silica nanoparticles for the degradation of cellulose. *Chem Commun* 48:886–888
- Demetzos C (2016) Introduction to nanotechnology. In: Demetzos C (ed) *Pharmaceutical nanotechnology, fundamentals and practical applications*. Adis, pp 3–16. ISBN 978-981-10-0790-3
- Deng X, Fang Z, Liu YH, Yu CL (2011) Production of biodiesel from *Jatropha* oil catalyzed by nanosized solid basic catalyst. *Energy* 36(2):777–784
- Eggert H, Greker M (2014) Promoting second generation biofuels: does the first generation pave the road? *Energies* 7:4430–4445
- Engelmann W, Aldrovandi A, Guilherme A, Filho B (2013) Prospects for the regulation of nanotechnology applied to food and biofuels. *Vigilancia Sanitaria em Debate* 1(4):110–121
- Erdelyi A, Dahm M, Chen BT, Zeidler-Erdelyi PC, Fernback JE, Birch ME, Evans DE, Kashon ML, Deddens JA, Hulderman T, Bilgesu SA, Battelli L, Schwegler-Berry D, Leonard HD, McKinney W, Frazer DG, Antonini JM, Porter DW, Castranova V, Schubauer-Berigan MK (2013) Carbon nanotube dosimetry: from workplace exposure assessment to inhalation toxicology. *Part Fibre Toxicol* 10(1):53
- Feng XM, Karlsson A, Svensson BH, Bertilsson S (2010) Impact of trace element addition on biogas production from food industrial waste-linking process to microflora. *FEMS Microbiol Ecol* 74:226
- Feng Y, Zhang Y, Quan X, Chen S (2014) Enhanced anaerobic digestion of waste activated sludge digestion by the addition of zero valent iron. *Water Resour* 52:242–250
- Feyzi M, Norouzi L (2016) Preparation and kinetic study of magnetic Ca/Fe<sub>3</sub>O<sub>4</sub>@SiO<sub>2</sub> nanocatalysts for biodiesel production. *Renew Energy* 94:579–586
- Feyzi M, Hassankhani A, Rafiee HR (2013) Preparation and characterization of Cs/Al/Fe<sub>3</sub>O<sub>4</sub> nanocatalysts for biodiesel production. *Energy Convers Manage* 71:62–68
- Foldbjerg R, Dang DA, Autrup H (2011) Cytotoxicity and genotoxicity of silver nanoparticles in the human lung cancer cell line, A549. *Arch Toxicol* 85(7):743–750
- Gao L, Wang S, Xu W, Xiao G (2015) Biodiesel production from palm oil over monolithic KF/γ-Al<sub>2</sub>O<sub>3</sub>/honeycomb ceramic catalyst. *Appl Energy* 146:196–201
- Goh WJ, Makam VS, Hu J, Kang L, Zheng M, Yoong SL, Udalgama CN, Pastorin G (2012) Iron oxide filled magnetic carbon nanotube-enzyme conjugates for recycling of amyloglucosidase: toward useful applications in biofuel production process. *Langmuir* 28(49):16864–16873
- Goldemberg J (2006) The ethanol program in Brazil. *Environ Res Lett* 1 (5 pages)
- Guan R, Kang T, Lu F, Zhang Z, Shen H, Liu M (2012) Cytotoxicity, oxidative stress, and genotoxicity in human hepatocyte and embryonic kidney cells exposed to ZnO nanoparticles. *Nanoscale Res Lett* 7(1):602
- Gupta I, Duran N, Rai M (2012) Nano-silver toxicity: emerging concerns and consequences in human health. In: Cioffi N, Rai M (eds) *Nano-antimicrobials: progress and prospects*. Springer, Berlin, pp 525–548
- Gupta IR, Anderson AJ, Rai M (2015) Toxicity of fungal-generated silver nanoparticles to soil-inhabiting *Pseudomonas putida* KT2440, a rhizospheric bacterium responsible for plant protection and bioremediation. *J Hazard Mater* 286:48–54
- Heyou H, Yanping G (2009) Synthesis of biodiesel from rapeseed oil using K<sub>2</sub>O/γ-Al<sub>2</sub>O<sub>3</sub> as nano-solid-base catalyst. *Wuhan University J Natural Sci* 14(1):75–79
- Huang XJ, Chen PC, Huang F, Ou Y, Chen MR, Xu ZK (2011) Immobilization of *Candida rugosa* lipase on electrospun cellulose nanofiber membrane. *J Mol Catal B Enzym* 70:95–100
- Huber GW, Iborra SS, Corma A (2006) Synthesis of transportation fuels from biomass: chemistry, catalysts, and engineering. *Chem Rev* 106:4044–4098
- Hussein AK (2015) Applications of nanotechnology in renewable energies — A comprehensive overview and understanding. *Renew Sust Energy Rev* 42:460–476
- IEA – International energy agency (2007) *World energy outlook world energy outlook*. International Energy Agency, Paris

- Ivanova V, Petrova P, Hristov J (2011) Application in the ethanol fermentation of immobilized yeast cells in matrix of alginate/magnetic nanoparticles, on chitosan-magnetite microparticles and cellulose-coated magnetic nanoparticles. *Int Rev Chem Eng* 3(2):289–299
- Jordan J, Kumar CSS, Theegala C (2011) Preparation and characterization of cellulase-bound magnetite nanoparticles. *J Mol Catal B Enzym* 68:139–146
- Kaur M, Ali A (2011) Lithium ion impregnated calcium oxide as nano catalyst for the biodiesel production from karanja and jatropha oils. *Renew Energy* 36:2866–2871
- Kim YJ, Choi HS, Song MK, Youk DY, Kim JH, Ryu JC (2009) Genotoxicity of aluminum oxide ( $Al_2O_3$ ) nanoparticle in mammalian cell lines. *Mol Cell Toxicol* 150:55–59
- Lee S, Jin LH, Kim JH, Han SO, Na HB, Hyeon T, Koo YM, Kim J, Lee JH (2010)  $\beta$ -Glucosidase coating on polymer nanofibers for improved cellulosic ethanol production. *Bioprocess Biosyst Eng* 33:141–147
- Lupoi JS, Smith EA (2011) Evaluation of nanoparticle-immobilized cellulase for improved yield in simultaneous saccharification and fermentation reactions. *Biotechnol Bioeng* 108: 2835–2843
- Madhuvilakku R, Piraman K (2013) Biodiesel synthesis by  $TiO_2$ - $ZnO$  mixed oxide nanocatalyst catalyzed palm oil transesterification process. *Bioresour Technol* 150:55–59
- Mguni LL, Meijboom R, Jalama K (2012) Biodiesel production over nano- $MgO$  supported on titania. *Int J Chem Mol Nucl Mater Metallurg Eng* 6(4):380–384
- Michalska K, Bizukojć M, Ledakowicz S (2015) Pretreatment of energy crops with sodium hydroxide and cellulolytic enzymes to increase biogas production. *Biomass Bioenergy* 80: 213–221
- Molina CMM (2013)  $ZnO$  nanorods as catalyst for biodiesel production from olive oil. M.Sc. Thesis, University of Louisville
- Mostafalou S, Mohammadi H, Ramazani A, Abdollahi M (2013) Different biokinetics of nano-medicines linking to their toxicity; an overview. *DARU* 21(1):14
- Naik SN, Goud VV, Rout PK, Dalai AK (2010) Production of first and second generation biofuels: a comprehensive review. *Renew Sustainable Energy Rev* 14(2):578–597
- OECD/IEA - International Energy Agency (2015) Key world energy statistics, based on IEA data from the Key World Energy Statistics © OECD/IEA 2015. [www.iea.org/statistics](http://www.iea.org/statistics). Licence: [www.iea.org/t&c](http://www.iea.org/t&c). [https://www.iea.org/publications/freepublications/publication/KeyWorld\\_Statistics\\_2015.pdf](https://www.iea.org/publications/freepublications/publication/KeyWorld_Statistics_2015.pdf). Accessed July 2016
- Pan X, Fan Z, Chen W, Ding Y, Luo L, Bao X (2007) Enhanced ethanol production inside carbon-nanotube reactors containing catalytic particles. *Nat Mater* 6:507–511
- Patumsawad S (2011) 2nd Generation biofuels: technical challenge and R and D opportunity in Thailand. *J Sustain Energy Environ (Special Issue)*:47–50
- Pavlidis IV, Vorhaben T, Gournis D, Papadopoulos GK, Bornscheuer UT, Stamatis H (2012) Regulation of catalytic behaviour of hydrolases through interactions with functionalised carbon-based nanomaterials. *J Nanopart Res* 14:842
- Pourmand A, Abdollahi M (2012) Current opinion on nanotoxicology. *DARU* 20(1):95
- Qiu F, Li Y, Yang D, Li X, Sun P (2011) Heterogeneous solid base nanocatalyst: preparation, characterization and application in biodiesel production. *Bioresour Technol* 102:4150–4156
- Rai M, dos Santos JC, Soler MF, Marcelino PRF, Brumano LP, Ingle AP, Gaikwad S, Gade A, da Silva SS (2016) Strategic role of nanotechnology for production of bioethanol and biodiesel. *Nanotechnol Rev* 5(2):231–250
- Reddy ANR, Saleh AA, Islam MS, Hamdan S, Maleque MA (2016) Biodiesel production from crude Jatropha oil using a highly active heterogeneous nanocatalyst by optimizing transesterification reaction parameters. *Energy Fuels* 30:334–343
- Renewable Fuels Association (2015) World Fuel Ethanol in 2015. <http://www.ethanolrfa.org/resources/industry/statistics/#1454098996479-8715d404-e546>. Accessed June 2016
- Simon-Deckers A, Gouget B, Mayne-L'hermite M, Herlin-Boime N, Reynaud C, Carrière M (2008) In vitro investigation of oxide nanoparticle and carbon nanotube toxicity and intracellular accumulation in A549 human pneumocytes. *Toxicology* 253(1–3):137–146

- Statista, The statistic portal (2016a) Biodiesel production in the European Union from 2010 to 2025 (in million gallons). <http://www.statista.com/statistics/202236/eu-biodiesel-production-from-2010/>. Accessed June 2016
- Statista, The statistic portal (2016b) The world's biggest biodiesel producers in 2014, by country (in billion liters). <http://www.statista.com/statistics/271472/biodiesel-production-in-selected-countries/>. Accessed June 2016
- Tahvildari K, Anaraki YN, Fazaeli R, Mirpanji S, Delrish E (2015) The study of CaO and MgO heterogenic nano-catalyst coupling on transesterification reaction efficacy in the production of biodiesel from recycled cooking oil. *J Environ Health Sci Eng* 2015:13
- Tang J, Xiong L, Wang S, Wang J, Liu L, Li J, Yuan F, Xi T (2009) Distribution, translocation and accumulation of silver nanoparticles in rats. *J Nanosci Nanotechnol* 9(8):4924–4932
- Terán-Hilares R, Reséndiz AL, Martínez RT, Silva SS, Santos JC (2016) Successive pretreatment and enzymatic saccharification of sugarcane bagasse in a packed bed flow-through column reactor aiming to support biorefineries. *Bioresour Technol* 203:42–49
- Upadhyay S, Ganguly K, Palmberg L (2015) Wonders of nanotechnology in the treatment for chronic lung diseases. *J Nanomed Nanotechnol* 6:337
- Verma ML, Barrow CJJ (2015) Recent advances in feedstocks and enzyme-immobilised technology for effective transesterification of lipids into biodiesel. In: Kalia VC (ed) *Microbial factories. Biofuels, waste treatment*, 1st edn, vol 1. Springer India, pp 87–103
- Verma ML, Barrow CJ, Puri M (2013a) Nanobiotechnology as a novel paradigm for enzyme immobilization and stabilization with potential applications in biodiesel production. *Appl Microbiol Biotechnol* 97:23–39
- Verma ML, Chaudhary R, Tsuzuki T, Barrow CJ, Puri M (2013b) Immobilization of  $\beta$ -glucosidase on a magnetic nanoparticle improves thermostability: application in cellobiose hydrolysis. *Bioresour Technol* 135:2–6
- Verziu M, Cojocar B, Hu J, Richards R, Ciuculescu C, Filip P, Parvulescu VI (2008) Sunflower and rapeseed oil transesterification to biodiesel over different nanocrystalline MgO catalysts. *Green Chem* 10:373–378
- Vishwakarma V, Samal SS, Manoharan N (2010) Safety and risk associated with nanoparticles—a review. *JMMCE* 9(5):455
- Wang H, Covarrubias J, Prock H, Wu X, Wang D, Bossmann SH (2015) Acid-functionalized magnetic nanoparticle as heterogeneous catalysts for biodiesel synthesis. *J Phys Chem C* 119: 26020–26028
- Wen L, Wang Y, Lu D, Hu S, Han H (2010) Preparation of KF/CaO nanocatalyst and its application in biodiesel production from Chinese tallow seed oil. *Fuel* 89:2267–2271
- Wolf EL, Medikonda M (2012) *Understanding the nanotechnology revolution*. Wiley-VCH, Weinheim, p 214
- Xie W, Wang J (2012) Immobilized lipase on magnetic chitosan microspheres for transesterification of soybean oil. *Biomass Bioenergy* 36:373–380
- Yang Z, Shi X, Wang C, Wang C, Wang L, Guo R (2015) Magnetite nanoparticles facilitate methane production from ethanol via acting as electron acceptors. *Sci Rep* 5:16118
- Yearbook Enerdata (2015a) *Global Energy Statistical Yearbook 2015*. <https://yearbook.enerdata.net/renewable-in-electricity-production-share-by-region.html#energy-primary-production.html>
- Yearbook Enerdata (2015b) *Global Energy Statistical Yearbook 2015*. <https://yearbook.enerdata.net/renewable-in-electricity-production-share-by-region.html#renewable-in-electricity-production-share-by-region.html>. Accessed June 2016
- Yearbook Enerdata (2015c) *Global Energy Statistical Yearbook 2015*. <https://yearbook.enerdata.net/renewable-in-electricity-production-share-by-region.html#wind-solar-share-electricity-production.html>. Accessed June 2016
- Zhao X, Zhang L, Liu D (2012) Biomass recalcitrance. Part I: the chemical compositions and physical structures affecting the enzymatic hydrolysis of lignocellulose. *Biofuel Bioprod Biorefin* 6:465–482

## Chapter 2

# Nanotechnology Applications on Lignocellulosic Biomass Pretreatment

Johnatt Allan Rocha de Oliveira, Luiza Helena da Silva Martins,  
Andrea Komesu, and João Moreira Neto

**Abstract** Global population growth raises questions concerning the environment and energy production. Fossil fuels are well known and utilized energy source. These are not renewable and contribute to the greenhouse gas effect. The search for alternative energy sources and solution for environmental problems has a growing concern in recent years. The lignocellulosic biomass has emerged as a solution to our energy and environmental concerns since it is rich within feedstock and can be converted to biofuels and/or biomaterials. This approach is interesting because these biomasses can become renewable sources of energy and pollute less than fossil fuels when transformed into biofuels, which is a green fuel. However, some steps are necessary to transform these lignocellulosic biomasses into biofuels or biomaterials. Nanotechnology is a multidisciplinary area of study with several applications that can be used to improve the lignocellulose bioconversion process, used both in production of liquid fuels through conversion by fermentation, gasification, or catalysis and development of new nanoscale catalyzers/materials. Nanoscale or sub-nanoscale instrumentation facilitates understanding of the lignocellulosic biomass cell wall ultrastructure and enzymatic mechanisms. This aspect contributes in the development of sophisticated instrumentation techniques for lignocellulosic fiber analysis such as scanning electronic microscopy (SEM), transmission electronic microscopy (TEM), and atomic force microscopy (AFM).

**Keywords** Lignocellulosic biomass • Pretreatment • Nanotechnology • Biomaterials

---

J.A.R. de Oliveira (✉)

Health Sciences Institute, School of Nutrition, Federal University of Pará, Belém, Brazil  
e-mail: [johnatt@ufpa.br](mailto:johnatt@ufpa.br)

L.H. da Silva Martins • A. Komesu • J.M. Neto

School of Chemical Engineering, University of Campinas, Campinas, Brazil

© Springer International Publishing AG 2017

M. Rai, S.S. da Silva (eds.), *Nanotechnology for Bioenergy and Biofuel Production*,  
Green Chemistry and Sustainable Technology, DOI 10.1007/978-3-319-45459-7\_2

## 2.1 Introduction

Nanotechnology and lignocellulosic biomass may seem unrelated or at best tenuously connected, but it is important to acknowledge that lignocellulosic biomass-forming units are in nanometric size, so nanotechnology can be used to enhance properties of the lignocellulosic material (Wegner and Jones 2009).

Currently, fossil fuel and nuclear and hydroelectric power are the main sources of energy. These sources are harmful to the environment, causing global warming as well as destruction of biosphere and geosphere. Energy production is considered harmful in terms of both pollution generation and environmental impact. Since industrial revolution in eighteenth century, around 80% of world production of CO<sub>2</sub> is a result of energy production (Serrano et al. 2009). The unavoidable exhaustion of fossil fuels, the concerns on energy safety, and the growing environmental problems reinforced interest in finding alternative sources of energy. With this in mind, lignocellulosic materials have become an appealing feedstock to biofuel energy alternative (Huang et al. 2015).

Lignocellulosic biomasses are plant or agricultural residues that are primarily cellulose (38–50%), hemicellulose (23–32%), and lignin (15–25%), including other minor components, such as proteins, pectin, and extractives (Fengel and Wegener 1989). The cellulose corresponds to the glucose homopolymer linked by the glycolic bond  $\beta$ -1,4. The hydrogen bonds form to link the cellulose inside (intramolecular) and outside the chains (intermolecular). The hemicelluloses are pentose (xylose, arabinose) and hexose (glycose, mannose, galactose) heteropolysaccharides. It also contains uronic acids and acetates. Lastly, the lignin is a complex biomolecule composed of three phenolic compounds: *p*-cumaryl, coniferyl, and alcohol sinapil (Wang 2012).

One of the greatest challenges in the twenty-first century is to develop technologies for renewable energy production, due to the serious problems on energy production and use. In this context, nanotechnology is a promising research area with fast growing interest and considered the most suitable choice to solve the energy issue (Hussein 2015).

Nanotechnology offer tools to develop new industries, granting great results in both cost-effectiveness and efficiency, which contributes to sustainable economic growth. It is a well-known term typically used to describe materials and phenomena at nanometric scale, in other words, in the tens of billionth meter scale (Serrano et al. 2009). It is a promising multidisciplinary research field with a wide range of opportunities in several areas as medicine, pharmaceutical, electronic, energy, and agriculture (Prasad et al. 2014).

Among the most recent technological innovations, nanotechnology stands a prominent position in food and agricultural production. The development of nanodevices and nanomaterials could supply new applications in plant biotechnology and agriculture (Scrini and Lyons 2007; Prasad et al. 2014).

There is growing interest in sustainable production of chemical products and/or biomass materials traditionally obtained from petroleum. Biodegradable plastics



and biocompatibles generated from renewable feedstock, such as biomass, are promising materials, which can replace petroleum-based polymers by reducing global dependence on fossil fuels (Brinchi et al. 2013).

Cellulose is an inexhaustible source of feedstock, which could meet a demand of environment-friendly products and biocompatibles. In the current millennia, cellulose has been used from wood and plant fibers as energy source, construction material, paper, textiles, and clothing (Brinchi et al. 2013).

Bioethanol produced from lignocellulosic biomass is obtained in a multiple step process. Three primary steps are proposed and developed: the pretreatment, ethanol production by lignocellulosic biomass enzymatic hydrolysis, and fermentation (Huber et al. 2006; Wang 2012; Zhuang et al. 2016).

One of the nanotechnology aspects involved in biofuel production is development and processing of new materials/catalysis at nanoscale, which is one of the most recent subjects that has garnered great interest from the scientific community (Zhang and Zhao 2009). A significant aspect in biofuel production is the nanoscale or sub-nanoscale instrumentation, which contributed to the understanding of the cell wall ultrastructure and the enzymatic hydrolysis mechanisms. In the long-term, this aspect of nanotechnology contributes to biofuel production, advances in instrumentation, and sample preparation techniques (Himmel et al. 2007).

In this chapter, we have discussed about the use of nanotechnology to transform lignocellulosic biomass into biofuels and production of biomaterials.

## 2.2 Using Nanotechnology to Transform Lignocellulosic Agricultural Residues

Every year, transformation of animal and plant feedstock, and its intermediate and final products, produces 140 billion tons of industrial and agricultural residues. Only 3 % of the 13 billion tons/year of plant biomass residues produced is utilized in manufacturing goods (Morganti 2013).

All phases in the production or consumption process generate a specific kind of residue, which demands a specific management solution. It is important to know the feedstock and the energy necessary in residue production, transportation, distribution, and utilization. Although it is fundamental to have a comprehensive view of the residue generation, it is also necessary to be able to evaluate its life cycle and understand the development, use, and regulation of its biological systems, which leads to properly remediate contaminated systems and organize environment-friendly processes (green technologies and sustainable development) (Morganti 2013).

Sustainable development and sustainability concepts provide a convenient environment to examine the importance of nanotechnology and biomass correlation. Sustainability is recurrently seen as a desirable objective in environmental development and management. Its meaning is strongly dependent on the context in which

it is applied and if its utilization is based on a social, economic, or ecological perspectives (Wegner and Jones 2009).

Fusing nanotechnology and lignocellulosic biomass utilization in a sustainable way is vital to satisfy the needs of the people for food, clothing, shelter, commerce, and goods, which is necessary to achieve quality of life by balancing both individual comfort and ecological needs (Mäki-Arvela et al. 2011).

Reuse of agro-industrial residue is essential to the biotechnology field, due to the constant search for decreasing human environmental impacts over nature. In addition, any agro-industry-rejected materials should be evaluated to assemble potential value in reusing it. Plant materials are primary sources of potential feedstock in manufacture of biotechnological products (Mäki-Arvela et al. 2011; Albuquerque et al. 2014).

Nanotechnology can also be one of the solutions for environmental issues, such as lignocellulosic residue accumulation, which could be used in biofuels and biomaterial production. Proper use of residue could highly reduce its accumulation, and the transformed products could generate income.

### 2.3 Nanotechnology Significance in Biofuel Production

Nanotechnology has played a significant role in the scientific and technological advances in biofuel production. As described by Wang (2012), at least two aspects are highlighted:

1. Nanoscale or sub-nanoscale instrumentation facilitates understanding of the cell wall ultrastructure, deconstruction microscopic analysis, and enzymatic mechanisms. These aspects offer long-term contribution to the biofuel production field and continue to contribute in the development of sophisticated instrumentation, as well as advances in sample preparation techniques. For example, the cellulose fibril can be measured by AFM (atomic force microscopy), and it is about 3–5 nm (Himmel et al. 2007; Wang 2012).
2. The other aspect concerns the pretreatment development and new nanoscale catalyzers/materials. This emerged in recent years and received the attention of the scientific community by its diversified studies (Wang 2012). Some topics on the latter aspect will be addressed in the following paragraphs.

Nanotechnology plays an important role in the production of liquid biofuels obtained from lignocellulosic biomass. Because the cell wall structures are in the nanometric scale and are to be easily modified by the deconstruction of constitutive materials, which is used in producing liquid fuels through conversion by fermentation, gasification, or catalysis.

It is also interesting to use a nanocatalyst to break the recalcitrant cellulose, once it exists in the 15–25 % order in lignocellulosic material carbohydrates, hindering sugar conversion in alcohol production during fermentation. Thus, transport of

nanocatalyzers to the reaction places, over the solid and recalcitrant cellulose substrate, will produce water and soluble polyols (Wegner and Jones 2009).

In the majority of catalytic systems, the reagents are washed away by the catalyst. In this case, it is necessary to place the catalyst on the solid substrate reaction bonds. The products of reaction, soluble in water, enable the recovery of the catalysts (Wegner and Jones 2009).

Other possible approaches of nanotechnology in biofuel production lie in enzymes or enzyme systems (including glycol hydrolases and lignin-degrading enzymes) developing to improve efficiency in nanoscale conversion. It could also be done by changing tree biology and designing plants to create and stock enzyme and enzymatic systems in the living tree until the harvest. Then it is activated to be used by engineering in order to decompose the lignocellulosic biomass. At last, this creates new biological systems to work symbiotically with nanotechnology to produce ethanol and other biofuels (Wegner and Jones 2009).

## **2.4 Application of Nanotechnology in Pretreatment of Lignocellulosic Biomass**

The objective in lignocellulosic biomass pretreatment is to change biomass structure, which allows availability of cellulose to cellulolytic enzymes. They will convert polysaccharides in fermentable sugars to later production of cellulosic bioethanol (Agbor et al. 2011; Timilsena et al. 2013; Zhuang et al. 2016). This step aims high yield in cellulosic fermentable sugar production. During this step, little or no sugar degradation should occur because toxic products generated (furfural and 5-hydroxymethylfurfural) can hinder cellulose enzymatic hydrolysis as well as fermentation (Timilsena et al. 2013).

The next topic will address pretreatment methods using nanotechnology techniques to lignocellulosic biomass deconstruction in second-generation ethanol production.

### ***2.4.1 Use of Nanoscale Instrumentation for Analysis of Lignocellulosic Fibers***

Instrumentation techniques used in lignocellulosic biomass structure studies are very useful to understand feedstock transformations after the pretreatment stage because of the nanometric size of the fibers. Electron microscopy is mostly utilized in nanoscale instrumentation to evaluate these types of materials. It is also extensively used by researchers of several areas, because it covers techniques that are used for characterization of morphology, chemical composition, and atomic

structure of various materials such as metal, ceramic, polymers, and biological specimens (Bonevich and Haller 2010).

Scanning electron microscopy (SEM) is vastly used in observation and analysis of microstructure of solid objects due to its high versatility. The reason for so much interest is due to its high resolution, reaching 2–5 nm in commercial instruments and 1 nm in advanced research instruments. Another important feature is the tridimensional aspect of sample images, which results in a wide depth of field, highly useful once electronic imaging complements optical imaging information (Dedavid et al. 2007). It is broadly used in lignocellulosic material structure micrography visualization before and after the pretreatment step. It is also used in enzymatic hydrolysis after biomass solubilization of the lignin, and hemicellulose (Zhao et al. 2009) has a structural change, which is visualized in electron microscopy. It provides a great advantage due to its simple preparation aspect.

Despite its higher resolution, in comparison to other electronic microscopes, it does not meet the necessary requirements of study. The drawback to SEM use lies in the required high-energy electron beam, which can shatter polymeric samples limiting practical equipment operation in less than 50,000 times zooming, utilized in most of polymers (Bonevich and Haller 2010).

Transmission electron microscopy (TEM) is used to reach high resolution, which usually requires thin films of ultramicrotomy in solid samples. TEM has proven to be a great tool for characterization of nanoparticle size. Projected particle size is the main determinant to measure particle diameter. Therefore, carefully following guidelines is important for good results. Otherwise, this method could cause a series of undesirable risks to the material analyses (Bonevich and Haller 2010). TEM is effective in determining biomass pretreatment effect inside plant cell walls (Chundawat et al. 2011; Corrales et al. 2012).

Atomic force microscopy (AFM) is important due to its higher resolution and lower cost in comparison to SEM and TEM (Herrmann et al. 1997); as part of this methodology, mode-synthesizing atomic force microscopy (MSAFM) has emerged, which is an advanced technique in AFM and applied to study of plant cell structure (Tetard et al. 2010).

The main advantages in AFM in comparison to SEM, in terms of morphological and material structure analysis, include the higher-resolution, tridimensional image, no need of conductive coating, no specific sample preparation methods, direct quantification of sample roughness, measuring of ultrathin films over subtracts, fractal analysis, analyses of different viscoelasticity phases, mechanical properties of sampled material in nanometric scale, liquid immersed sample analysis, and lower cost in comparison to conventional electron microscopes (Herrmann et al. 1997).

Corrales et al. (2012) pretreated sugarcane bagasse in vapor with CO<sub>2</sub> and SO<sub>2</sub>. TEM image of non-treated sugarcane bagasse clearly showed well-preserved primary cell wall (PCW), secondary cell wall (SCW), and medium lamellae (ML), as observed in Fig. 2.1a, b. These structures are strongly bounded creating a highly compact structure, typical of cell walls. As sugarcane bagasse is thicker and stiffer, SCW has cellulose microfibrils arranged parallel to each other, which are

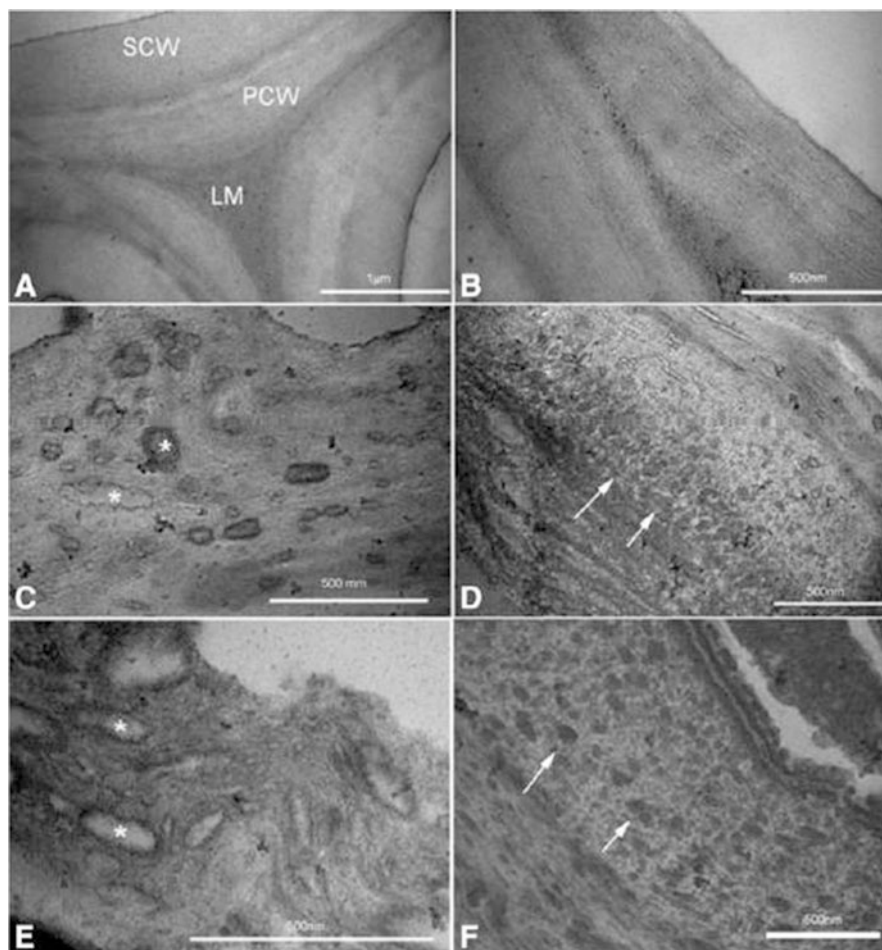
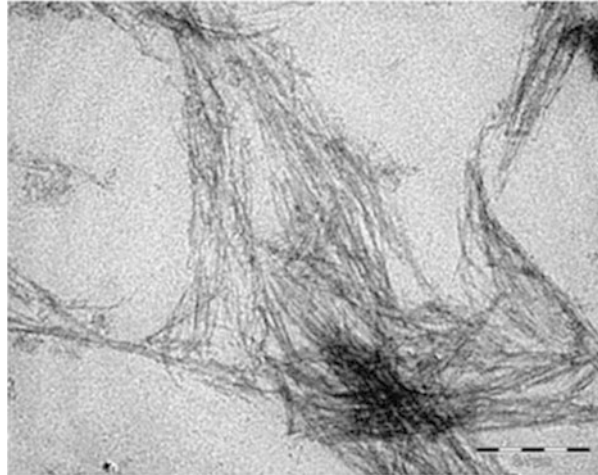


**Fig. 2.1** (a) Untreated bagasse TEM images exhibiting: (PCW) primary cell wall, (SCW) secondary cell wall, and (ML) middle lamella. (b) SCW zoom displaying microfibrils orientation. (c) (*asterisks*): Large pores with well-defined size and shape. (d) (*arrows*): Cell wall matrix compact ion origin structures with round and elongate forms. (c, d): CO<sub>2</sub> (205 °C/15 min)-pretreated cell wall. (e, f): SO<sub>2</sub> (190 °C/5 min)-pretreated cell wall. Spread at the exterior of the second cell wall (SCW) after the treatment can be seen pores (e, *asterisks*) and cell wall matrix compact ion structures (f, *arrows*). With Permission from Biotechnology and Biofuels

responsible for the cell wall integrity (Fig. 2.1b). Figure 2.1c, d represents samples treated with CO<sub>2</sub> (205 °C/15 min) and shows different sizes and forms pores in the cell wall. They concluded that most of the pores are formed in the exterior cell wall. When we utilized SO<sub>2</sub> (190 °C/5 min), the secondary cell wall, especially the exterior region, was strongly disturbed leading to the appearance of big pores with an irregular surface, as observed in Fig. 2.2e, f, as the result of partial solubilization of the cell wall structural components.

**Fig. 2.2** TEM picture of cotton linter nanowhiskers (Source: Morais et al. 2013) with permission from Carbohydrate Polymers



Morais et al. (2013) used TEM to evaluate dimensions of nanocellulose obtained from cotton linter and treated with sulfuric acid at 60 % (m/m), as observed in Fig. 2.2. This analysis showed nanocellulose dimensions of 177 nm of length and 12 nm of width.

Tetard et al. (2010) assessed cell structure of several wood types through AFM and MSAFM, as observed in Fig. 2.3. They concluded the need to develop robust analysis techniques, higher resolution, and detection of imaging in order to better understand plant cell wall structure (which is complex) as well as its chemical structure and specific features. MSAFM utilization is revealed to be potentially important to lignocellulosic biological materials.

As discussed by Tetard et al. (2010), MSAFM provides better results to plant tissue characterization. Results show variations in the mechanical properties of different layers of the cell walls as well as differences in composition inside the tissue sample. Both complimentary techniques can be used to determine lignocellulosic material structural and mechanical properties. The arrows on Fig. 2.3 indicate clear areas of cell wall, presenting different mechanical properties and corresponding to the middle lamellae (ML).

#### **2.4.2 Lignocellulose Pretreatment Using Nano-shear Hybrid Alkaline Technique**

Nano-shear Hybrid Alkaline (NSHA) pretreatment consists of high-speed shear and chemical reagent synergy and milder thermal effect application. These reactions occur in specific reactors (nanomixing in general), as observed in Fig. 2.1, in which the high shearing work axis is transferred to the biomass nanostructure,

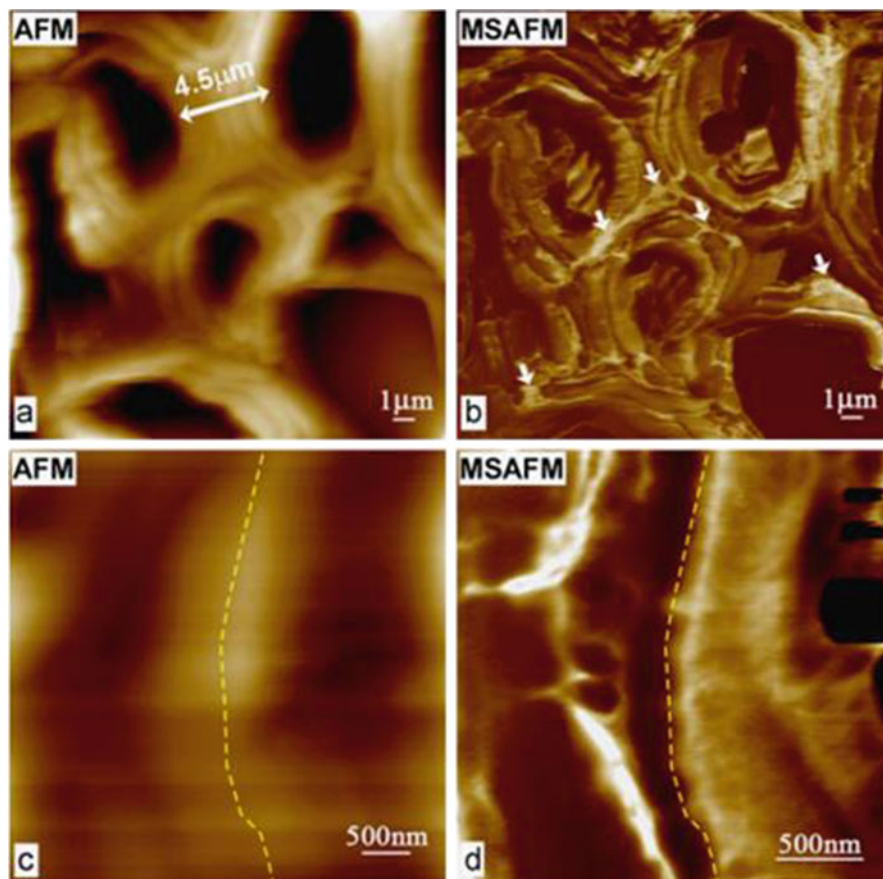


**Fig. 2.3** AFM (left) and MFM (right) images of a cross section of *Populus* timber (Source: Tetard et al. 2010) with permission from Ultra microscopy

which allows efficient lignin elimination with cellulose and hemicellulose exposition in a short period of time (Wang et al. 2013). Patent (n° 2009147512 A2 2011) created the nano-shear hybrid method pretreatment of lignocelluloses, and patent (n° 20120036765 A1 2014) made it in one step using other kinds of chemical reagents as pretreatment agent (Fig. 2.4).

Wang et al. (2013) used corn straw as feedstock to test NSHA pretreatment in biofuel production. They used 1:1 NaOH and biomass proportions, room temperature, and shear rate of  $12,500 \text{ s}^{-1}$  during 2 min; they obtained cellulose conversion rate over 70%. This mechanism points to positive aspects in incorporating high shearing to existing pretreatment methodologies and many other chemical products, due to the high shear rate synergic effects.

Ji and Lee (2013) studied wheat straw pretreatment through NSHA. They used 0.4–4% (w/v) NaOH and adding a cationic polyelectrolyte, 0.081 and 0.485 in

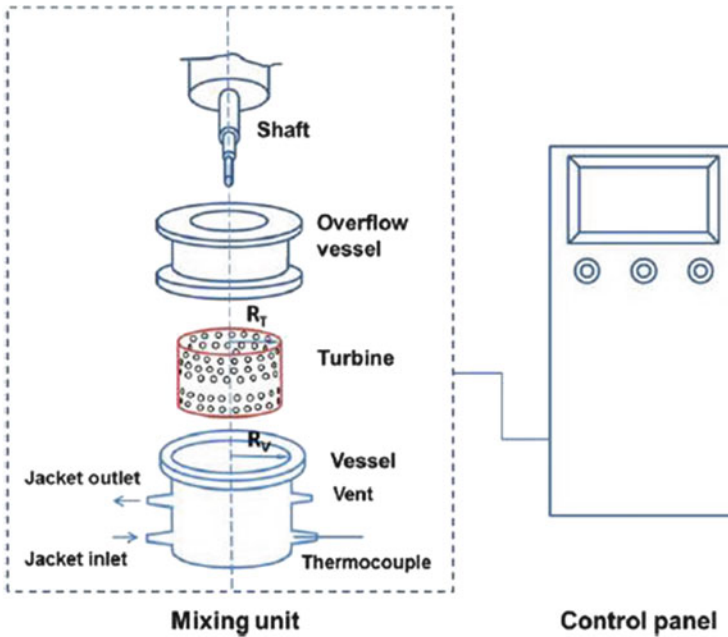


**Fig. 2.4** Schematic illustration of the Taylor-Couette modified reactor (nanomixer) (Source: Wang et al. 2013) with permission from Biomass and Bioenergy

mass weight, as an additive. It showed that lignin was distributed over the interior and exterior cell wall surfaces in the form of aggregate droplets instead of being leached out, as well as microfibrils on the residues. Enzymatic hydrolysis yield raised above 70% to corn straw pretreated with cationic polyelectrolyte. It is believed that lignin transformed effectively, once it opened the cell wall structure during pretreatment process in a short period of time. This prevented nonproductive bonds between lignin and enzyme in the enzymatic hydrolysis; therefore, cationic polyelectrolyte showed its potential as a pretreatment additive, because it eased lignin redistribution and raised cellulose and hemicellulose conversion in enzymatic hydrolysis.

Lignin forms globular complexes with the cationic polyelectrolyte and was placed on the pretreated corn straw surface or microfibril matrix. Cell wall layers showed significant changes in morphology after this pretreatment. The lignin and fibrillated cellulose droplets were retained, which contributed to a weaker inhibitory lignin effect and a bigger enzyme accessibility to the substrates. The addition of polyelectrolyte could be an effective way to reduce the use of pretreatment chemical products; also the change in cellulose surface is easily reached.

Other nonvolatile chemical compounds, besides NaOH, such as potassium hydroxide, sulfuric acid, hydrogen, and ionic liquids can be incorporated in synergy to the high shear rate allowing a faster and efficient pretreatment (as pointed out



previously). However, a pretreatment using volatile chemical compound (organic solvents, ammoniac, ozone, etc.) requires sealed reactors in order to avoid vaporization and depletion. Therefore, higher shearing causes rise in temperature and pressure leading to longer reactor runs. Security issues are minimized in shorter retention times (minutes or seconds) (Patent n° 20120036765 A1 2014).

Without temperature control, calcium hydroxide is not a suitable chemical compound, once it presents decreasing solubility with increasing temperature (Kaar and Holtzaple 2000; Kim and Holtzaple 2006). The high shear temperature increase will result in an even more heterogeneous solid phase weakening the reaction synergic effects (Patent n° 20120036765 A1 2014).

NSHA pretreatment has proven to remove lignin and hemicelluloses significantly and promotes cellulose nanostructure disruption. These capabilities aided a better corn straw digestibility, in terms of enzyme load reduction and saccharification time. Besides that, Wang et al. (2013) reported that during enzymatic hydrolysis, no enzyme mixture optimization was made; therefore, additional improvements in saccharification rate and enzyme load reduction could be studied. Yet this pretreatment has shown to be efficient in production of biofuels.

It should be noted that this pretreatment does not seem as effective without NaOH synergistic effect. Wang et al. (2013) observed no significant removal of lignin and hemicellulose using shearing only, as well as in low NaOH concentrations, such as 4 g L<sup>-1</sup>.

### ***2.4.3 Immobilization of Enzymes on Nanoparticles for Lignocellulosic Biomass Conversion***

Among several methods to improve efficiency in enzymatic degradation of lignocellulosic materials, the most effective was found to be the ball mill, because it reduces cellulose particle size and crystallinity (Hendriks and Zeeman 2009; Liao et al. 2010; Cherian et al. 2015).

Cellulose saccharification is improved by combining pretreatment in the ball mill and enzymatic hydrolysis; however, the milling process has drawbacks, such as enzymatic activity reduction (Liao et al. 2010; Zhou et al. 2010). Many researchers report that immobilization of nanoparticles can maintain enzymatic activity efficiently and obtain desirable performance, such as low cost and high stability (Wu et al. 2005; Dinçer and Telefoncu 2007; Ho et al. 2008; Liao et al. 2008, 2010; Cherian et al. 2015; Liu et al. 2015). These studies show that nanotechnology can aid the improvement in efficiency of lignocellulosic biomass conversion to biofuels.

## 2.5 Lignocellulosic Biomass Use in Nanocellulose Production

Interest in renewable polymers is driven by the same factors as renewable energy: awareness that petroleum and other fossil resources have a finite supply, access, and control of these resources lies on a small number of countries, many with unstable governments, and lastly, burning of fossil fuels significantly impact the environment, contributing to release of greenhouse gases (Vermerris 2008; Ten and Vermerris 2013; Han et al. 2016). According to the EUA Energy Information Administration (EIA), around 5 % of EUA petroleum is used in plastic production and 1.5 % in energy generation to industries (Ten and Vermerris 2013; Hamid et al. 2016).

Biological-based products do not compete with petroleum by being renewable sources of energy. Production of biological-based chemicals from effluents of biofuel installations (biorefineries) has the potential to generate extra income, reducing cost of biofuel production and making it more competitive with fossil fuels. Consequently, investments for biological-based products have the potential to lead the way to a future in which fossil fuels play a less important role (Ten and Vermerris 2013).

According to Ten and Vermerris (2013) renewable polymers are referred as polymers produced from biological materials, which are different from polymer production from fossil fuels, especially petroleum, which cannot be replaced once it has been used. In the last years there has been increasing interest in nanocomposite production, due to its extraordinary properties.

Another nanocellulose application is related to the paper and cellulose sectors, which is recent but provides interesting results that caught companies' attention (Hassan et al. 2011; Luu et al. 2011; González et al. 2012; Viana 2013). Cellulose nanofibrils are hydrophilic and present great capacity to form interfibrillar hydrogen bonds. They produce high resistant material, which is used in coating nanocellulose films or as reinforcement in several paper industry products (Biao et al. 2011; Viana 2013; Rambabu et al. 2015). They are also applied in pharmaceutical products, such as hydrogels. Development of nanocellulose is interesting due to its functionality, both as active surface area and low cost (Huber et al. 2006; Li et al. 2012a, b; Rambabu et al. 2015).

Cellulose microfibrils contain crystalline structure and have amorphous regions distributed randomly along its length. The first is strongly bounded, while the second is in disorder, which breaks up easily in severe pretreatment (Lee et al. 2014a, b).

Nanocellulose is classified into two categories: nanocrystalline cellulose (NCC) and nanofibrillated cellulose (NFC). Both types are chemically similar; however, its physical properties are different (different colloidal forms). Nanocellulose has rigid structure in a rod shape, varying 1–100 nm in diameter and 10–100 nm in length. Relative crystallinity degree and geometric aspect relation (length and diameter, L/d)

are very important parameters, which controls nanocellulose properties (Siró and Plackett 2010; Lavoine et al. 2012; Lee et al. 2014a, b).

Microfibril proportions of amorphous and crystalline regions vary strongly among plant species. Characteristics of nanocellulose materials, particularly dimensions, greatly depend on feedstock. Even if all cellulose nanocrystals are made of the same polymer, different feedstocks can be used to obtain the specific needs of adapted nanocellulose (Beck-Candanedo et al. 2005; Eichhorn et al. 2010; Pandey et al. 2010; Rosa et al. 2010; Morais et al. 2013).

Recently, preparation of nanoscale cellulose in mild conditions is attracting researchers' attention. Cellulosic fiber disruption is realized using mechanical reaction (grinding and high-pressure homogenization), biological reaction (enzymatic treatment), and chemical reaction (oxidation and acid hydrolysis). However, a major obstacle needs to be overcome to achieve successful nanocellulose commercialization, which is the high-energy consumption in fiber mechanical disruption to produce nanofibers; this involves many steps through disintegration. Considering this fact, researchers combine mechanical pretreatment with chemical techniques to raise efficiency in size reduction, before homogenization, which reduces energy consumption (Lee et al. 2014a, b).

Among cellulose depolymerization treatments, oxidation pretreatment is the mostly used technique to degrade cellulose in nanocellulose through 2,2,6,6-tetramethylpiperidine-1-oxyl (TEMPO). TEMPO is the oxidation method used to generate repulsion forces between fibrils and interfibrils through native cellulose surface modification. This leads to cellulose primary hydroxyl conversion into carboxylate groups, which later becomes negatively charged resulting into nanofiber repulsion, contributing to a fast and easy fibrillation (Saito et al. 2007).

Nanocellulose production is also an alternative to industrial lignocellulosic residue utilization, as shown by Morais et al. (2013) who conducted a study in nanocellulose production from cotton residue (lint); these authors used concentrated sulfuric acid treatment method (60 %, w/w) in 1:20 proportion (w/v) at 45 °C, during 60 min. Successful cellulose nanocrystals were obtained with aspect ratio of 19, crystallinity of 91 %, and high hydrophilicity; besides there was no need for pulping cotton lint to nanocellulose extraction. Li et al. (2012a, b) extracted nanocellulose from sugarcane bagasse using high-pressure homogenization coupled with an ionic liquid pretreatment, which resulted in 10–20 nm diameter nanocellulose. They found low thermal solubility and crystallinity due to hydrogen bond disruption in cellulose in response to the pretreatment. So, there is acute need for further study to explore the applications of nanocellulose.

Mariño et al. (2015) produced nanocellulose fiber from citric residue. They observed morphological alterations of fibers after a three-phase treatment, namely, physical, chemical, and enzymatic using NaOH (4 % w/v) at 120 °C for 20 min and NaClO<sub>2</sub> (1.7 % w/v) for 30 min at 12 °C and pH 4.5 and enzymatic action for 48 h at 45 °C and pH 5.0. Low NaOH concentration preserves cellulose-activated structure and aids the amorphous component hydrolysis by the use of *Xanthomonas axonopodis* pv. citri (Xac) enzymes. Later, sonication allowed obtaining high proportion nanocellulose fibers, adding value to a previously considered

agricultural residue. Cellulose nanofibers showed approximately 55 % of crystallinity and 10 nm average diameter. Mariño et al. (2015) reported that citric biomass residues have great potential as renewable substance to important nanobiomaterial fabrication, such as nanocellulose.

## 2.6 Utilization of Residues of Bioethanol Process in Nanocellulose Production

The costs of production of second-generation ethanol have been reduced by coproduction of chemicals and natural materials (Cardona and Sánchez 2007; Oksman et al. 2011). An interesting by-product is crystal cellulose, which is the hardest part of cellulose to dissolve in hydrolysis process during ethanol production.

As previously discussed, lignocellulosic biomass is composed of polysaccharides (cellulose and hemicellulose), lignin, and, to a less extent, extractives. Cellulose and hemicellulose can be utilized for sugar and ethanol production, while lignin cannot be utilized for this purpose (Oksman et al. 2011).

Nanocellulose is needlelike structure of cellulose single crystal. These crystals are bounded by cellulosic microfibril and amorphous cellulose, which reinforces the cell wall structure. It has been attracting great interest in the last few years (Saïd et al. 2004; Angles and Dufresne 2000; Kvien et al. 2005; Bondeson et al. 2006; Lu et al. 2006; Oksman et al. 2011).

Nanocellulose is only produced in laboratory scale from different feedstocks, such as tunicate, cotton, bacterial cellulose, beet, saccharin, wood, ramie, and wheat straw. Nanocellulose size depends on the source (Oksman et al. 2011).

Exploitation of industrial bioresidues as feedstock source to nanocellulose production could be achieved from a bioethanol pilot plant. The first step involves purification process using chemical extraction and whitening. Then the bioresidue is separated in mechanical treatment, such as ultrasound homogenization, high pressure, and acid hydrolysis of lignocellulosic feedstock (Oksman et al. 2011).

Oksman et al. (2011) studied the viability of nanocellulose production from bioethanol production process residues, which is a simple and low-cost source of feedstock, adding up value to the bioethanol process. The results showed that the bioethanol process residues are a great source for large-scale nanocellulose production. Lignin residue exhibited extremely high cellulose content, mainly crystalline cellulose, which can be isolated to nanocellulose production through mechanical treatment, such as ultrasound and homogenization. Total yield calculated to this process was 48 % of cellulose.

Li et al. (2012a, b) studied nanocellulose production from Norway spruce (*Picea abies*) and proposed a nanocellulose isolation model through a purely physical method, using ultrasonic intensity in microcrystalline cellulose, producing nanocellulose diameter of 10–20 nm and 50–250 nm length. These authors

observed decreasing length of nanocellulose and crystallinity with increasing ultrasonication.

Bondeson et al. (2006) discovered a high yield and fast process to obtain nanocellulose stable colloidal aqueous suspension. Large amounts of feedstock are necessary to obtain this material, once it is used as polymers in the extraction process in production of nanobiocomposites. Microcrystalline cellulose (MCC), derived from Norway spruce (*Picea abies*), was a feedstock to this nanocellulose production. These authors used sulfuric acid at 63.5 % (m/m), obtaining nanocellulose with 200–400 nm length and less than 10 nm width in around 2 h, yielding 30 % (initial weight).

## 2.7 Liquor Extraction as By-product of NCC (Nanocrystalline Cellulose)

As mentioned in Sect. 2.5, cellulose is one of the richest renewable sources in the world, among its applications; NCC production arises as promising. NCC is a low-cost product and can be used in production of several materials.

As mentioned before, NCC can be extracted from cellulose crystalline chain phases (Brinchi et al. 2013), and the liquor by-product can also be a feedstock to second-generation ethanol production (Pirani and Hashaikeh 2013).

In Pirani and Hashaikeh (2013), a modified process is utilized to produce NCC, and, at the same time, the liquor by-product is recovered as a new form of cellulose. This recovered cellulose presented reasonably opened structure, becoming more susceptible to enzymatic hydrolysis and producing high rates of fermentable sugar conversion, which makes a great candidate for a potential feedstock to biofuel. In addition, because it is a secondary product of acid hydrolysis to produce NCC, it could be eliminated in the residue treatment process, avoiding the cost of this process. Therefore, NCC can be used as a composite material component due to its great mechanical properties. In this case, the production of a high-value product, such as NCC, pays for the low-value product, like the biofuels. The low-value product is therefore promising and environmental friendly (Pirani and Hashaikeh 2013).

It is known that both cellulose biofuels and nanocellulose production are economically viable; its production in the biorefinery could generate many new employment opportunities and increase venture profits (Duran et al. 2012). There are several reports for integrated production of nanocellulose and biofuels from liquor by-product (Zhu et al. 2011; Oksman et al. 2011).

Optimization of residual liquor transformation obtained in NCC production as well as its valorization could decrease the cost to process and could face environmental issues related to strong acids and concentrated solutions utilized in this process. It is important to remember that this liquor contains monomeric and

oligomeric forms of sugar, besides residual sulfuric acid (Patent n° 8,709,203, 2014).

The use of nanofiltering membrane to separate acid and sugars in residual liquor and the utilization of second filtering membrane to separate monomeric and oligomeric sugar have been studied by Jemaa et al. (2014).

## 2.8 Conclusion

With decreasing amount of fossil fuel resources for energy production, there is an urgent need for the use of alternative sources such as lignocellulosic biomass, which is both an available and accessible option. This bioenergy is environmental friendly; however, its bioconversion is still an onerous process, whereas the pretreatment step, being reasonably recent, still has some issues to be solved. Nanotechnology arises as an interesting option to lignocellulosic biomass transformation. Its use in biofuel production is still a developing science with rapid pace. It will be interesting once it has become one of the solutions to minimize the concerns around energy and environmental issues. In relation to biomaterials, nanotechnology can be used for lignocellulosic biomass transformation, which will be used in nanocomposite production, mainly cellulose nanocrystals.

## References

- Agbor V, Cicek NS, Berlin A, Levin D (2011) Biomass pretreatment: fundamentals toward application. *Biotechnol Adv* 29(6):675–685
- Albuquerque T, Gomes S, Marques J Jr, da Silva I Jr, Rocha M (2014) Xylitol production from cashew apple bagasse by *Kluyveromyces marxianus* CCA510. *Catal Today* 225:33–40
- Angles M, Dufresne A (2000) Plasticized starch/tunicin whiskers nanocomposites. 1. Structural analysis. *Macromolecules* 33(22):8344–8353
- Beck-Candanedo S, Roman M, Gray DG (2005) Effect of reaction conditions on the properties and behavior of wood cellulose nanocrystal suspensions. *Biomacromolecules* 6(2):1048–1054
- Biao H, Xue-rong C, Dai Da-song TL, Wen O, Li-rong T (2011) Preparation of nanocellulose with cation-exchange resin catalysed hydrolysis. INTECH Open Access Publisher. <http://cdn.intechweb.org/pdfs/19706.pdf>
- Bondeson D, Mathew A, Oksman K (2006) Optimization of the isolation of nanocrystals from microcrystalline cellulose by acid hydrolysis. *Cellulose* 13(2):171–180
- Bonevich JE, Haller WK (2010) Measuring the size of nanoparticles using transmission electron microscopy (TEM). NIST-NCL Joint Assay Protocol, PCC-7 Version, 1
- Brinchi L, Cotana F, Fortunati E, Kenny JM (2013) Production of nanocrystalline cellulose from lignocellulosic biomass: technology and applications. *Carbohydr Polym* 94(1):154–169
- Cardona CA, Sánchez ÓJ (2007) Fuel ethanol production: process design trends and integration opportunities. *Bioresour Technol* 98(12):2415–2457
- Cherian E, Dharmendirakumar M, Baskar G (2015) Immobilization of cellulase onto MnO<sub>2</sub> nanoparticles for bioethanol production by enhanced hydrolysis of agricultural waste. *Chin J Catal* 36(8):1223–1229

- Chundawat SP, Donohoe BS, da Costa Sousa L, Elder T, Agarwal UP, Lu F, Dale BE (2011) Multi-scale visualization and characterization of lignocellulosic plant cell wall deconstruction during thermochemical pretreatment. *Energy Environ Sci* 4(3):973–984
- Corrales RC, Mendes FM, Perrone CC, Sant’Anna C, de Souza W, Abud Y, Bon EP, Ferreira-Leitão V (2012) Structural evaluation of sugar cane bagasse steam pretreated in the presence of CO<sub>2</sub> and SO<sub>2</sub>. *Biotechnol Biofuels* 5(1):1–8
- Dedavid BA, Gomes CI, Machado G (2007) Microscopia eletrônica de varredura: aplicações e preparação de amostras: materiais poliméricos, metálicos e semicondutores. Rio Grande do Sul, Brazil: EdiPUCRS, 9–26
- Diñer A, Telefoncu A (2007) Improving the stability of cellulase by immobilization on modified polyvinyl alcohol coated chitosan beads. *J Mol Catal B: Enzym* 45(1):10–14
- Duran N, Paula Lemes A, Seabra BA (2012) Review of cellulose nanocrystals patents: preparation, composites and general applications. *Recent Pat Nanotechnol* 6(1):16–28
- Eichhorn SJ, Marcovich NE, Capadona JR, Rowan SJ, Peijs T (2010) Review: current international research into cellulose nanofibres and nanocomposites. *J Mater Sci* 45(1):1–33
- Fengel D, Wegener G (1989) Wood: chemistry, ultrastructure, reactions. Walter de Gruyter, Berlin, 613p
- González I, Boufi S, Pèlach MA, Alcalà M, Vilaseca F, Mutjé P (2012) Nanofibrillated cellulose as paper additive in eucalyptus pulps. *Bioresources* 7(4):5167–5180
- Hamid SBA, Zain SK, Das R, Centi G (2016) Synergic effect of tungstophosphoric acid and sonication for rapid synthesis of crystalline nanocellulose. *Carbohydr Polym* 138:349–355
- Han Y, Yuan L, Li G, Huang L, Qin T, Chu F, Tang C (2016) Renewable polymers from lignin via copper-free thermal click chemistry. *Polymer* 83:92–100
- Hassan EA, Hassan ML, Oksman K (2011) Improving bagasse pulp paper sheet properties with microfibrillated cellulose isolated from xylanase-treated bagasse. *Wood Fiber Sci* 43(1):76–82
- Hendriks AT, Zeeman G (2009) Pretreatments to enhance the digestibility of lignocellulosic biomass. *Bioresour Technol* 100(1):10–18
- Herrmann PS, da Silva MA, Bernardes R, Job AE, Colnago LA, Frommer JE, Mattoso LH (1997) Microscopia de varredura por força: uma ferramenta poderosa no estudo de polímeros. *Polímeros: ciência e tecnologia* 7:51–61
- Himmel ME, Ding SY, Johnson DK, Adney WS, Nimlos MR, Brady JW, Foust TD (2007) Biomass recalcitrance: engineering plants and enzymes for biofuels production. *Science* 315 (5813):804–807
- Ho KM, Mao X, Gu L, Li P (2008) Facile route to enzyme immobilization: core–shell nanoenzyme particles consisting of well-defined poly (methyl methacrylate) cores and cellulase shells. *Langmuir* 24(19):11036–11042
- Huang Y, Qin X, Luo XM, Nong Q, Yang Q, Zhang Z, Gao Y, Lv F, Chen Y, Yu Z, Liu J, Feng J (2015) Efficient enzymatic hydrolysis and simultaneous saccharification and fermentation of sugarcane bagasse pulp for ethanol production by cellulase from *Penicillium oxalicum* EU2106 and thermotolerant *Saccharomyces cerevisiae* ZM1-5. *Biomass Bioenergy* 77:53–63
- Huber GW, Iborra S, Corma A (2006) Synthesis of transportation fuels from biomass: chemistry, catalysts, and engineering. *Chem Rev* 106(9):4044–4098
- Hussein AK (2015) Applications of nanotechnology in renewable energies—A comprehensive overview and understanding. *Renew Sustain Energy Rev* 42:460–476
- Jemaa N, Paleologou M, Zhang X (2014) U.S. Patent and Trademark Office, Washington, DC. Patente N° 8,709,203
- Ji S, Lee I (2013) Impact of cationic polyelectrolyte on the nanoshear hybrid alkaline pretreatment of corn stover: morphology and saccharification study. *Bioresour Technol* 133:45–50
- Kaar WE, Holtzapple MT (2000) Using lime pretreatment to facilitate the enzymic hydrolysis of corn stover. *Biomass Bioenergy* 18(3):189–199
- Kim S, Holtzapple MT (2006) Lime pretreatment and enzymatic hydrolysis of corn stover. *Bioresour Technol* 96(18):1994–2006

- Kvien I, Tanem BS, Oksman K (2005) Characterization of cellulose whiskers and their nanocomposites by atomic force and electron microscopy. *Biomacromolecules* 6(6):3160–3165
- Lavoine N, Desloges I, Dufresne A, Bras J (2012) Microfibrillated cellulose—its barrier properties and applications in cellulosic materials: a review. *Carbohydr Polym* 90(2):735–764
- Lee HV, Hamid SB, Zain SK (2014a) Conversion of lignocellulosic biomass to nanocellulose: structure and chemical process. *Scientific World J* 2014: Article ID 631013. doi:[10.1155/2014/631013](https://doi.org/10.1155/2014/631013)
- Lee I, Wang W, Ji S (2014b) US Patente N° US20120036765 A1
- Li J, Wei X, Wang Q, Chen J, Chang G, Kong L, Liu Y (2012a) Homogeneous isolation of nanocellulose from sugarcane bagasse by high pressure homogenization. *Carbohydr Polym* 90(4):1609–1613
- Li W, Yue J, Liu S (2012b) Preparation of nanocrystalline cellulose via ultrasound and its reinforcement capability for poly (vinyl alcohol) composites. *Ultrason Sonochem* 19(3):479–485
- Liao HD, Yuan L, Tong CY, Zhu YH, Li D, Liu XM (2008) Immobilization of cellulase based on polyvinyl alcohol/Fe<sub>2</sub>O<sub>3</sub> nanoparticles. *Chem J Chin Univ* 8:1564–1568
- Liao H, Chen D, Yuan L, Zheng M, Zhu Y, Liu X (2010) Immobilized cellulase by polyvinyl alcohol/Fe<sub>2</sub>O<sub>3</sub> magnetic nanoparticle to degrade microcrystalline cellulose. *Carbohydr Polym* 82(3):600–604
- Liu MQ, Huo WK, Xu X, Jin DF (2015) An immobilized bifunctional xylanase on carbon-coated chitosan nanoparticles with a potential application in xylan-rich biomass bioconversion. *J Mol Catal B: Enzym* 120:119–126
- Lu Y, Weng L, Cao X (2006) Morphological, thermal and mechanical properties of ramie crystallites—reinforced plasticized starch biocomposites. *Carbohydr Polym* 63(2):198–204
- Luu W, Bousfield DW, Kettle J (2011) Application of nano-fibrillated cellulose as a paper surface treatment for inkjet printing. TAPPI PaperCon Conference, Atlanta, USA
- Mäki-Arvela P, Salmi T, Holmbom B, Willför S, Murzin DY (2011) Synthesis of sugars by hydrolysis of hemicelluloses—a review. *Chem Rev* 111(9):5638–5666
- Mariño M, Lopes da Silva L, Durán N, Tasic L (2015) Enhanced materials from nature: nanocellulose from citrus waste. *Molecules* 20(4):5908–5923
- Morais JP, de Freitas Rosa M, Nascimento LD, do Nascimento DM, Cassales AR (2013) Extraction and characterization of nanocellulose structures from raw cotton linter. *Carbohydr Polym* 91(1):229–235
- Morganti P (2013) Saving the environment by nanotechnology and waste raw materials: use of chitin nanofibrils by EU research projects. *J Appl Cosmetol* 31:89–96
- Oksman K, Etang JA, Mathew AP, Jonoobi M (2011) Cellulose nanowhiskers separated from a bio-residue from wood bioethanol production. *Biomass Bioenergy* 35(1):146–152
- Pandey JK, Ahn SH, Lee CS, Mohanty AK, Misra M (2010) Recent advances in the application of natural fiber based composites. *Macromol Mater Eng* 295(11):975–989
- Pirani S, Hashaikeh R (2013) Nanocrystalline cellulose extraction process and utilization of the byproduct for biofuels production. *Carbohydr Polym* 93(1):357–363
- Prasad R, Kumar V, Prasad KS (2014) Nanotechnology in sustainable agriculture: present concerns and future aspects. *Afr J Biotechnol* 13(6):705–713
- Rambabu N, Panthapulakkal S, Sain M, Dalai AK (2015) Production of nanocellulose fibers from pinecone biomass: evaluation and optimization of chemical and mechanical treatment conditions on mechanical properties of nanocellulose films. *Indus Crops Products*. doi:[10.1016/j.indcrop.2015.11.083](https://doi.org/10.1016/j.indcrop.2015.11.083)
- Rosa MF, Medeiros ES, Malmonge JA, Gregorski KS, Wood DF, Mattoso LH et al (2010) Cellulose nanowhiskers from coconut husk fibers: effect of preparation conditions on their thermal and morphological behavior. *Carbohydr Polym* 81(1):83–92
- Saïd Azizi Samir MA, Alloin F, Paillet M, Dufresne A (2004) Tangling effect in fibrillated cellulose reinforced nanocomposites. *Macromolecules* 37(11):4313–4316



- Saito T, Kimura S, Nishiyama Y, Isogai A (2007) Cellulose nanofibers prepared by TEMPO-mediated oxidation of native cellulose. *Biomacromolecules* 8(8):2485–2491
- Scrinis G, Lyons K (2007) The emerging nano-corporate paradigm: nanotechnology and the transformation of nature, food and agri-food systems. *Int J Sociol Food Agric* 15(2):22–44
- Serrano E, Rus G, Garcia-Martinez J (2009) Nanotechnology for sustainable energy. *Renew Sustain Energy Rev* 13(9):2373–2384
- Siró I, Plackett D (2010) Microfibrillated cellulose and new nanocomposite materials: a review. *Cellulose* 17(3):459–494
- Ten E, Vermerris W (2013) Functionalized polymers from lignocellulosic biomass. State of the art. *Polymers* 5(2):600–642
- Tetard LP, Farahi RH, Kalluri UC, Davison BH, Thundat T (2010) Spectroscopy and atomic force microscopy of biomass. *Ultramicroscopy* 110(6):701–707
- Timilsena YP, Audu IG, Rakshit SK, Brosse N (2013) Impact of the lignin structure of three lignocellulosic feedstocks on their organosolv delignification. Effect of carbonium ion scavengers. *Biomass Bioenergy* 52:151–158
- Vermerris W (2008) Why bioenergy makes sense. Springer, New York, NY
- Viana LC (2013) Desenvolvimento de filmes celulósicos nanoestruturados a partir da polpa kraft de Pinus sp. Doctoral thesis, UFV, Viçosa, MG, Brazil
- Wang W (2012) Nanotechnology applications for biomass pretreatment, functional material fabrication and surface modification. Ph.D. Dissertation, Chemical Engineering, Michigan State University, East Lansing, MI
- Wang W, Ji S, Lee I (2013) Fast and efficient nanoshear hybrid alkaline pretreatment of corn stover for biofuel and materials production. *Biomass Bioenergy* 51:35–42
- Wegner TH, Jones EP (2009) A fundamental review of the relationships between nanotechnology and lignocellulosic biomass. *Nanosci Technol Renew Biomater* 1:1–41
- Wu L, Yuan X, Sheng J (2005) Immobilization of cellulase in nanofibrous PVA membranes by electrospinning. *J Membr Sci* 250(1):167–173
- Zhang Z, Zhao ZK (2009) Solid acid and microwave-assisted hydrolysis of cellulose in ionic liquid. *Carbohydr Res* 344(15):2069–2072
- Zhao X, Peng F, Cheng K, Liu D (2009) Enhancement of the enzymatic digestibility of sugarcane bagasse by alkali-peracetic acid pretreatment. *Enzyme Microbial Technol* 44(1):17–23
- Zhou J, Chen DZ, Liao HY, Chen Z, Liu X (2010) Simultaneous wet ball milling and mild acid hydrolysis of rice hull. *J Chem Technol Biotechnol* 85(1):85–90
- Zhu JY, Sabo R, Luo X (2011) Integrated production of nano-fibrillated cellulose and cellulosic biofuel (ethanol) by enzymatic fractionation of wood fibers. *Green Chem* 13(5):1339–1344
- Zhuang X, Wang W, Yu Q, Qi W, Wang Q, Tan X, Zhou G, Yuan Z (2016) Liquid hot water pretreatment of lignocellulosic biomass for bioethanol production accompanying with high valuable products. *Bioresour Technol* 199:68–75

# Chapter 3

## Applications of Carbon-Based Nanomaterials in Biofuel Cell

Ming-Guo Ma, Bo Liu, and Ling-Yan Meng

**Abstract** Bioenergy and biofuels are promising candidates as alternative fossil fuel. Nanotechnology has been accepted as important tool for the synthesis and modification of bioenergy and biofuel production. In this chapter, we have focused on the recent development of carbon-based nanomaterials in the applications of biofuel cell. Obviously, carbon-based nanomaterials could be obtained from biomass, which possess the properties of nanomaterials, implying the complete combination of biofuel and nanotechnology. We have described the preparation of carbon-based nanomaterials with various structures and shapes by all kinds of synthesis methods. It is well known that carbon-based nanomaterials have wide applications in photocatalysis, biomedical, sensor, etc. Special attention has been paid on the potential applications of carbon-based nanomaterials in the biofuel cell. We also suggested the problems and future developments of carbon-based nanomaterials in these special fields. In this chapter, our purpose was to review the development and problems on the carbon-based nanomaterials in biofuel cell application.

**Keywords** Carbon-based nanomaterials • Biofuel cell • Nanotechnology • Applications

### 3.1 Introduction

Nanomaterials display one size in nano-dimension with special properties. The nanotechnology is the science and technology on the manufacturing materials via single atom and molecular, which is on the synthesis, properties, and applications of material in the range of 1–100 nm. There are many methods for the preparation of nanomaterials, including physical, chemical, and biological methods. In general, we can obtain nanomaterials from “top-down” and “bottom-up” routes (Lu and

---

M.-G. Ma (✉) • B. Liu • L.-Y. Meng

Engineering Research Center of Forestry Biomass Materials and Bioenergy, Beijing Key Laboratory of Lignocellulosic Chemistry, College of Materials Science and Technology, Beijing Forestry University, Beijing 100083, PR China  
e-mail: [mg\\_ma@bjfu.edu.cn](mailto:mg_ma@bjfu.edu.cn)

Lieber 2007). Among the various synthetic methods, most attention was paid on the sol-gel method (Avnir et al. 2006), hydrothermal method (Cundy and Cox 2003), and so on. Some methods such as microwave-assisted method (Zhu and Chen 2014), ultrasound method (Bang and Suslick 2010), and UV-assisted method (Lu et al. 2007) were also applied for the fabrication of nanomaterials.

Nanomaterials have demonstrated many applications in bioenergy and biofuel fields. There are various reports on the synthesis of nanomaterials for the applications in these fields. Based on our knowledge, nanocellulose and carbon are major nanomaterials in biomass fields (Moran et al. 2008; Navarro et al. 2007). Nanocellulose includes cellulose nanocrystals (CNC), cellulose nanofibrils (CNF), and bacterial cellulose (BC), which belongs to typical organic nanomaterials. Carbon is mainly obtained from biomass via thermal cracking or calcination without  $O_2$ . There are many reports on the synthesis and applications of nanocellulose (Yan et al. 2014). Therefore, in this chapter, we will discuss carbon and carbon-based nanomaterials such as the carbon nanotubes and graphene which displayed different properties and have wide applications as photocatalysts, electrode materials, and sensors and in biomedical fields (Fang et al. 2001). Moreover, attention was paid on the synthesis, property, and potential applications of carbon-based nanomaterials in the biofuel cell applications through typical examples.

## 3.2 Synthesis of Carbon-Based Nanomaterials

Du et al. (2013) prepared activated carbon hollow fibers with high surface area from renewable ramie fibers by the activation method under low temperature. For the activated carbon hollow fiber electrode, they obtained the maximum capacity of  $287 \text{ F g}^{-1}$  at  $50 \text{ mA g}^{-1}$  and reported the ramie fibers with a smooth surface without voids (Fig. 3.1a) and activated carbon hollow fibers with a heterogeneous surface (Fig. 3.1b–d).

Apparently the cyclic voltammetry curve of RZ400-2 was deformed due to the poor conductivity (Fig. 3.2a). The authors further observed that the cyclic voltammetry curves of both RZ650-2 and RZ750-2 preserve the excellent capacitive behavior due to the high specific area. At both low and high current density, RZ650-2 possessed the highest specific capacitance of  $287 \text{ F g}^{-1}$  at  $50 \text{ mA g}^{-1}$  (Fig. 3.2c). With activation temperature or activation time, carbon conductivity had a positive effect on electrochemical double-layer capacitance. Figure 3.2d provides the values of specific capacitance. It was also observed that only RZ400-2 showed obvious capacity fluctuation and lowest capacity retention, due to the low conductivity. Ramie-based activated carbon hollow fibers with high electrochemical performances may be desirable to large-scale commercial applications.

The effect of  $ZnCl_2$  impregnation concentration on the microstructure and electrochemical performances of supercapacitor showed that the development of morphology and pore structure depended to a great extent on  $ZnCl_2$  concentration, which displayed the maximum capacity of  $287 \text{ F g}^{-1}$ .

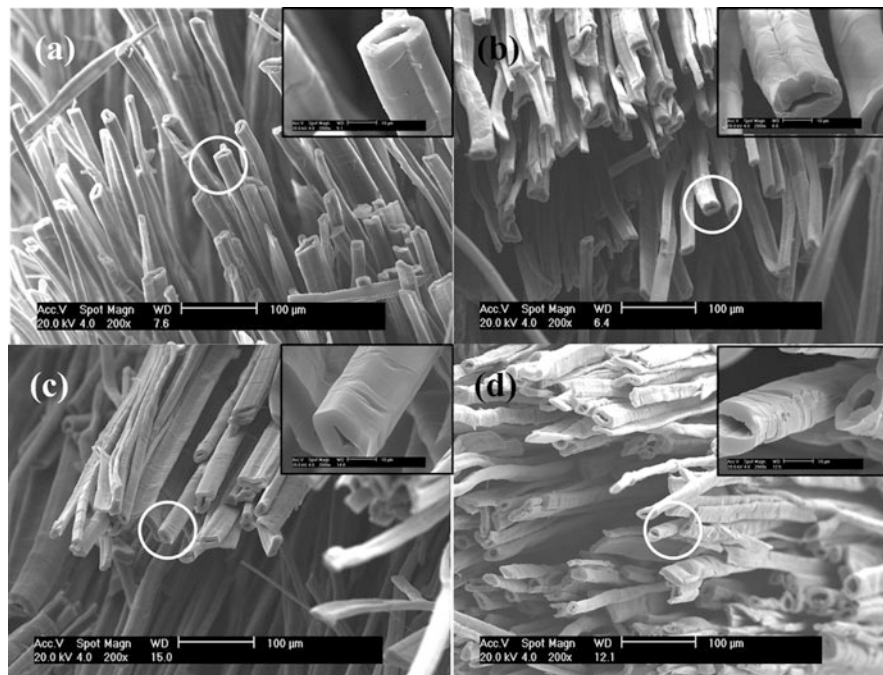


**Fig. 3.1** SEM images of (a) raw RFs, (b) RZ400-2, (c) RZ500-2, and (d) RZ650-2. From Du et al. (2013). Reprinted with permission from Elsevier

Figure 3.3 displayed the schematic diagram of the formation of porous activated carbon hollow fibers under  $\text{ZnCl}_2$  activation.  $\text{ZnCl}_2$  concentration had an effect on the development of pore structure, and the electrical energy storage of activated carbon-based supercapacitor mainly relies on the adsorption capacity of electrical charges on the inner pores.

Our group also explored a green synthesis strategy for the fabrication of cellulose-based hybrids and its thermal transformation to carbon/metal hybrids. The hybrids from cellulose and  $\text{Cu}(\text{OH})_2/\text{CuO}$  were fabricated by the sonochemistry method (Fu et al. 2014). The Cu/C hybrids were obtained by thermal transformation of the hybrids at  $800^\circ\text{C}$  for 3 h in the Ar atmosphere. During the thermal transformation process in the Ar atmosphere, carbon materials were obtained by the thermal decomposition of cellulose. However, only CuO crystals were observed in the air atmosphere.

Hybrids from cellulose and  $\text{Cu}(\text{OH})_2/\text{CuO}$  were heated to  $800^\circ\text{C}$  in the Ar atmosphere and kept at  $800^\circ\text{C}$  for 3 h. It was found that all the samples were indexed to well-crystallized Cu with a cubic structure (JCPDS 04-0836). The peak intensities increased with increasing of calcination temperature, indicating the better crystallinity. When hybrids are calcined in the Ar atmosphere, carbon materials are obtained from the thermal decomposition of cellulose, and Cu crystals are obtained from  $\text{Cu}(\text{OH})_2/\text{CuO}$  using carbon materials as reducing reagents.

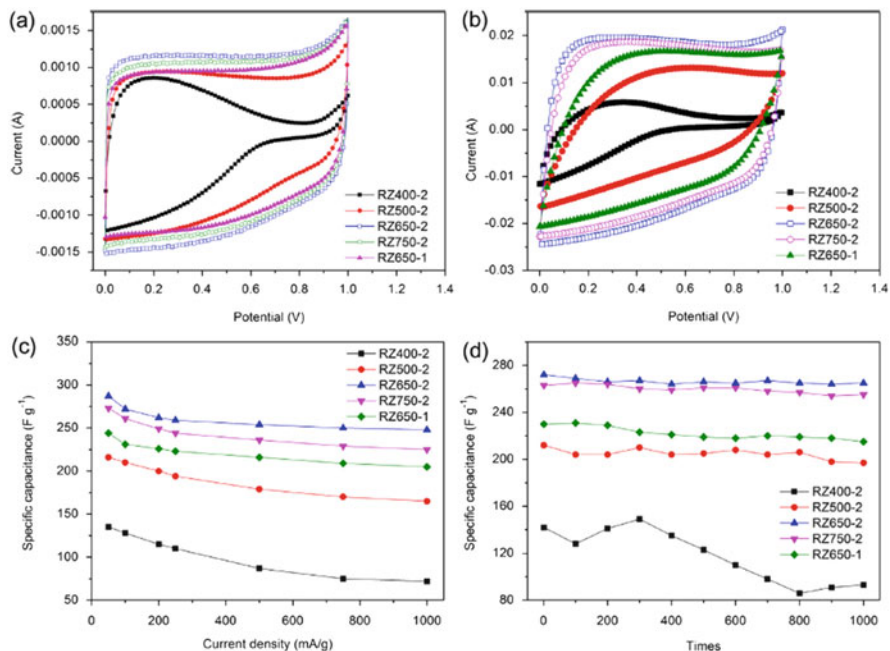


**Fig. 3.2** Cyclic voltammetry curves of activated carbon hollow fibers at different scan rate of (a) 1 mV s<sup>-1</sup> and (b) 20 mV s<sup>-1</sup>; (c) specific capacitance at various current densities for activated carbon hollow fibers samples; (d) cycling performance of activated carbon hollow fibers at current density of 100 mA g<sup>-1</sup>. From Du et al. (2013). Reprinted with permission from Elsevier

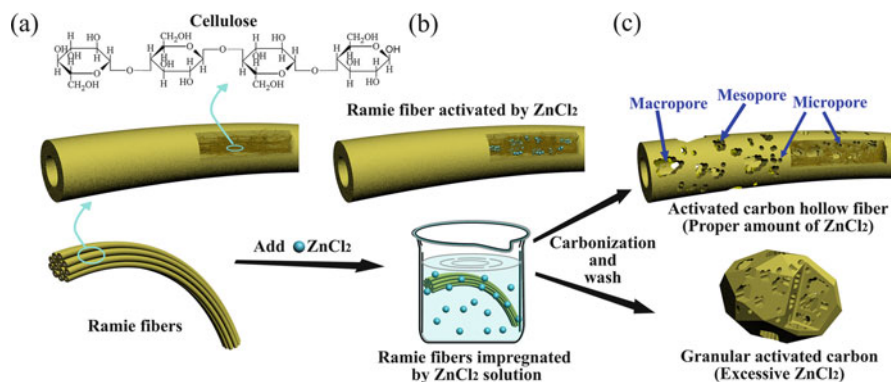
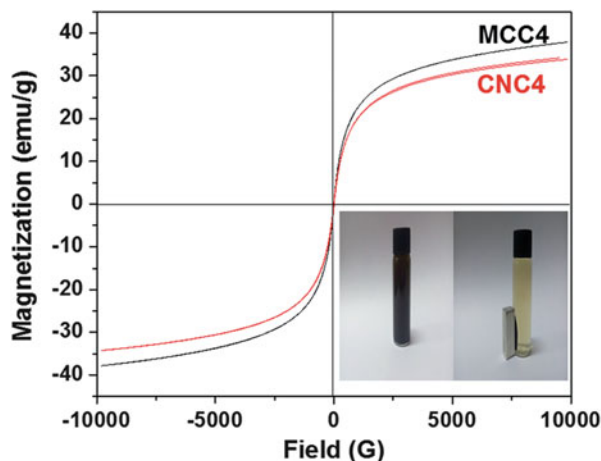


**Fig. 3.3** Scheme for the preparation of activated carbon hollow fibers-based activated carbons. From Du et al. (2013). Reprinted with permission from Elsevier

The residue carbon materials and Cu crystals form C/Cu hybrids. It is observed that Cu crystals display uniform particle-like shape and small size using hybrids from cellulose and Cu(OH)<sub>2</sub> synthesized for 10 min as precursor. Cu particles are

**Fig. 3.4** The magnetic hysteresis loop of the MCC4 and CNC4. The *down inset* is the picture of the separation of  $\text{Fe}_3\text{O}_4/\text{C}$  nanocomposites with external magnetic field. From Liu et al. (2015). Reprinted with permission from RSC



abounded on the surface of carbon materials with increasing synthetic time to 20 min. Increased synthetic time to 40 min, Cu particles are abounded on the surface of carbon materials with fibers and irregular sheets.

Our group also studied  $\text{Fe}_3\text{O}_4/\text{C}$  nanocomposites by different cellulose types (microcrystalline cellulose and cellulose nanocrystal) through the sonochemistry method (Liu et al. 2015). Cellulose nanocrystals were prepared by acid-hydrolyzed commercial microcrystalline cellulose. Experimental results demonstrated that the different cellulose types play a considerable role in the phases, crystallinities, and morphologies of as-obtained  $\text{Fe}_3\text{O}_4/\text{C}$  nanocomposites.

$\text{Fe}_3\text{O}_4/\text{C}$  nanocomposites show both superparamagnetic and ferromagnetic behaviors. The saturation magnetizations of samples MCC4 and CNC4 are 37.85 and 34.24  $\text{emu}\cdot\text{g}^{-1}$  (Fig. 3.4). What's important is that the black  $\text{Fe}_3\text{O}_4/\text{C}$  nanocomposite powder was easily separated from dispersion by using an external magnetic field (the right down inset of Fig. 3.4). This visual experiment proved that the  $\text{Fe}_3\text{O}_4/\text{C}$  nanocomposites possessed ferromagnetism and could be favorably employed as a magnetic adsorbent for dye removal and wastewater treatment fields.

The MCC4 is observed to display an excellent adsorption rate of methylene blue up to 95.0% (Fig. 3.5a). The blue color for the original methylene blue solution was observed (the left of Fig. 3.5b), which disappeared by the addition of  $\text{Fe}_3\text{O}_4/\text{C}$  nanocomposites. More importantly, the dye-loaded  $\text{Fe}_3\text{O}_4/\text{C}$  nanocomposites could be easily separated with external magnetic field.

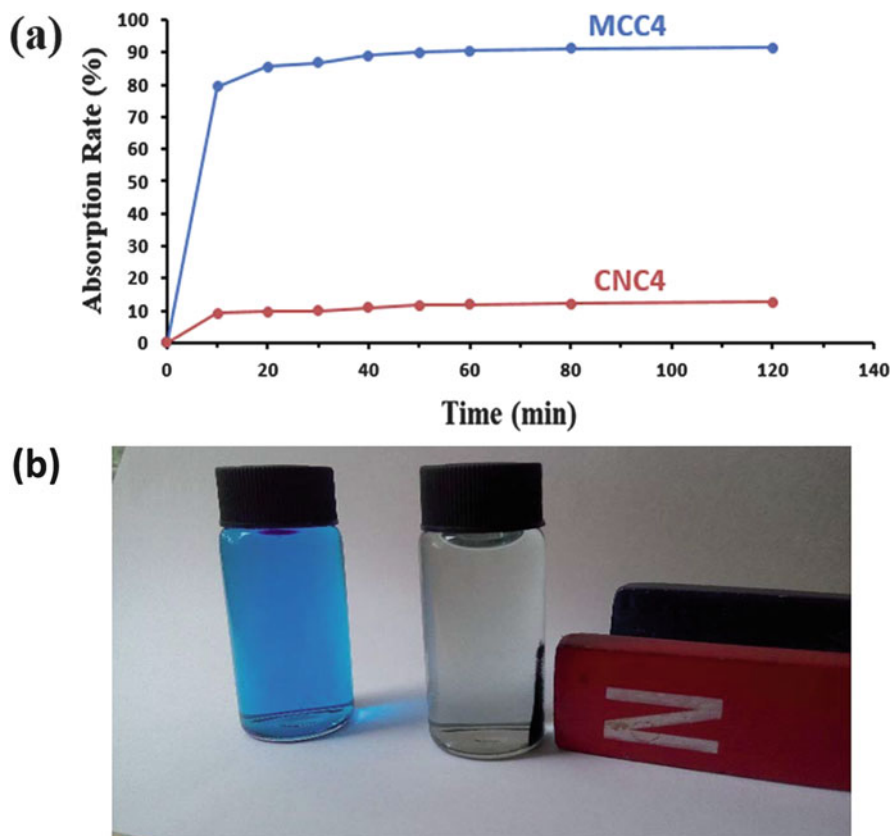


**Fig. 3.5** (a) The adsorption rates of methylene blue using the samples of MCC4 and CNC4, (b) the picture of the original methylene blue solution and the separation of the dye-loaded  $\text{Fe}_3\text{O}_4/\text{C}$  nanocomposites with external magnetic field. From Liu et al. (2015). Reprinted with permission from RSC

### 3.3 Applications of Carbon-Based Nanomaterials in Biofuel Cell

Enzymes are known to have advantages of high specificity and reaction rates. Enzyme electrodes are reported to show great potential applications as biosensors, anodes, and cathodes in biocatalytic fuel cells for power generation. There are a few reports on the applications of carbon-based nanomaterials in biofuel cell fields.

**Single-Walled Carbon Nanotubes** Considerable effort has been devoted to the synthesis of single-walled carbon nanotubes (SWCNTs) due to its interesting properties and wide applications in many fields. More importantly, single-walled carbon nanotubes also display important application in biofuel cell. Wen et al. (2011) demonstrated a miniature biofuel cell with single-walled carbon

nanohorn-modified carbon fiber microelectrodes as the substrate by using glucose dehydrogenase as the biocatalyst on single-walled carbon nanohorn-modified carbon fiber microelectrodes, which display a high efficient and stably confined electrocatalyst for the oxidation of the nicotinamide adenine dinucleotide (NADH) cofactor of glucose dehydrogenase. Electrically contacted bilirubin oxidase–single-walled carbon nanohorn/carbon fiber microelectrodes were reported as the bio-cathode, which shows direct bioelectrocatalytic functions for the reduction of  $O_2$  to  $H_2O$ . It obtained the maximum power output of the cell  $140 \mu W cm^{-2}$  at 0.51 V. The authors indicated that the present glucose/air biofuel cell can directly harvest energy from different kinds of soft drinks, which could promise potential applications of the biofuel cell as portable power sources.

Krzysztof et al. (2012) used SWCNTs covalently phenylated, naphthylated, or terphenylated for construction of cathodes in a bio-battery and biofuel cell. SWCNTs are covalently modified with glucose oxidase/catalase on the biofuel cell anode. The maximum power density of ca.  $1 mW cm^{-2}$  for the hybrid biofuel cell with zinc wire anode and graphitized carbon cloth cathode covered with phenylation–carbon nanotubes (CNTs) and laccase in Nafion film is achieved using the bio-battery with phenylated nanotubes at the cathode, and the open-circuit potential is 1.5 V. The fully enzymatic fuel cell has power density of  $40 \mu W cm^{-2}$  at  $20 k\Omega$  loading, and the open-circuit potential for the biofuel cell is 0.4 V. The cell voltage is shown to be stable for more than 2 weeks of continuous work of the cell. The authors suggested that bio-batteries employing functionalized CNTs are demonstrated to be important alternative devices as well as a convenient choice for testing new types of bio-cathodes due to its much high open-circuit potentials and power outputs.

Krzysztof et al. (2014) also used single-walled carbon nanotubes covalently biphenylated with glucose oxidase and catalase for the construction of cathodes and zinc covered with a hopeite layer as the anode in a flow bio-battery and biofuel cell. It obtains the power density of the bio-battery with biphenylated nanotubes at the cathode of ca.  $0.6 mW cm^{-2}$  and the open-circuit potential of ca. 1.6 V. It carries out the open-circuit potential of ca. 4.8 V and power density  $2.1 mW cm^{-2}$  at 3.9 V under  $100 k\Omega$  load using three connected bio-batteries in a series. The biofuel cell is reported to show power densities of ca.  $60 \mu W cm^{-2}$  at  $20 k\Omega$  external resistance and the open-circuit potential for biofuel cell of only 0.5 V. The authors indicated that the bio-battery showing significantly large power densities and open-circuit voltages is especially useful for testing novel cathodes and applications such as powering units for clocks and sensing devices.

Kenath et al. (2014) reported enzymatic biofuel cells with high stability (open-circuit voltage of  $\sim 1.2$  V) and the high-power density of  $2.27 \pm 0.11 mW cm^{-2}$  equipped with enzyme-functionalized graphene–SWCNT hybrid electrodes using the naturally abundant glucose as the fuel and oxygen as the oxidizer. It observes graphene with a monolithic macroporous structure (Fig. 3.6a). It is found that graphene is covered inside-out by a dense thin-film network of single-walled carbon nanotubes with a mesh size comparable to a macromolecule (Fig. 3.6b). The hybrid exhibits characteristic D band from carboxylated single-walled carbon nanotubes



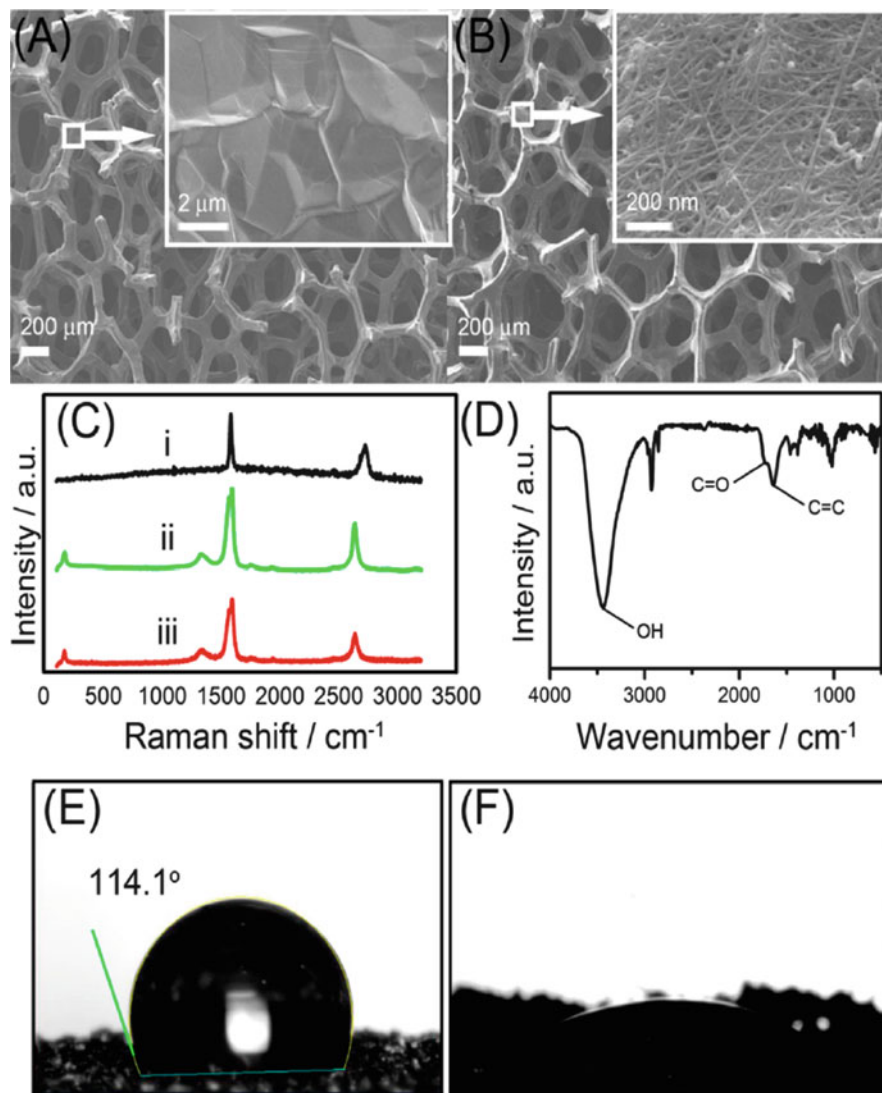


**Fig. 3.6** FESEM images of (a) bare graphene and (b) graphene single-walled carbon nanotubes hybrid. Each *inset* shows the surface of the skeleton at a large magnification. (c) Raman spectra of (i) graphene, (ii) single-walled carbon nanotubes, and (iii) graphene single-walled carbon nanotubes hybrid. (d) FTIR of single-walled carbon nanotubes. Contact angle of (e) graphene and (f) graphene single-walled carbon nanotubes hybrid. From Kenath et al. (2014). Reprinted with permission from ACS

(Fig. 3.6d). The contact angle measurement indicated the hydrophilic hybrid structure to ensure electrolyte penetration (Fig. 3.6e and f). It obtains the  $E_{\text{cell}}^{\text{ocv}}$  of the enzymatic biofuel cells  $\sim 1.20$  V (Fig. 3.7), which is close to the theoretical potential

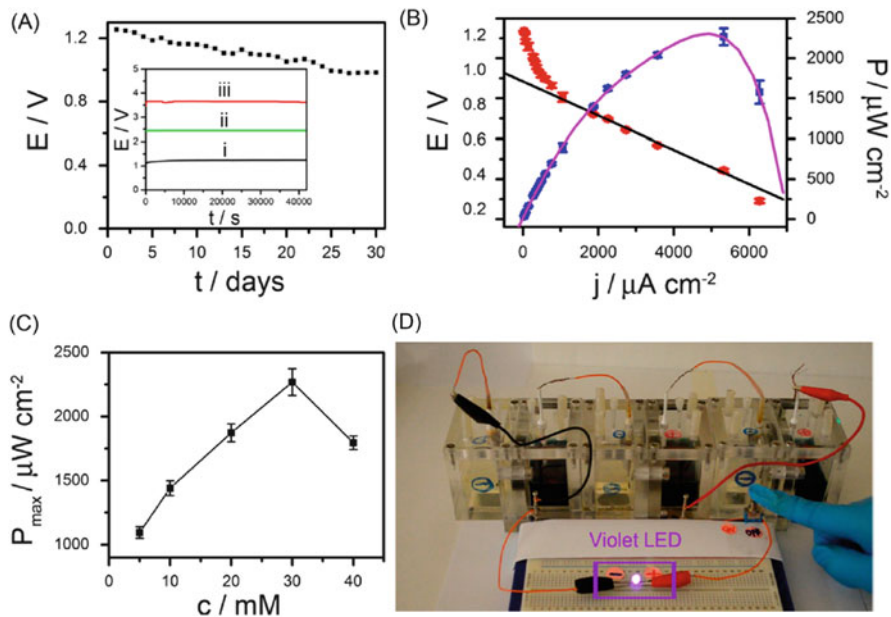


**Fig. 3.7** (a) The open circuit voltage from one cell over 30 days. *Inset*: the open circuit voltages from (i) single EBFC, (ii) double EBFCs, and (iii) triple EBFCs in series. (b) Polarization curve and power output curve of the EBFC. (c) The maximum power output of the EBFC with different glucose concentrations. (d) A violet LED powered by three EBFCs in series. From Kenath et al. (2014). Reprinted with permission from ACS

difference between the  $O_2/H_2O$  couple and the gluconolactone/glucose couple at thermodynamic equilibrium. It observes only a 20% drop of  $E_{cell}^{ocv}$  after 30 days, indicating the high stability of enzymatic biofuel cells (EBFCs). It is calculated the internal resistance of  $245 \Omega$  based on the fitting of the linear region of the polarization curve and the maximal power output density of  $2.27 \pm 0.11 \text{ mW cm}^{-2}$  ( $n = 3$ ) using 30 mM the glucose concentration in the anolyte (Fig. 3.7b). It is found that three enzymatic biofuel cells in the series are able to lighten up a violet LED with  $\sim 3 \text{ V}$  turn-on voltage and the optimal concentration of  $\sim 30 \text{ mM}$  (Fig. 3.7c).

Campbell et al. (2015) reported the membrane/mediator-free enzymatic biofuel cells with ultrahigh surface area ( $\sim 800 \text{ m}^2 \text{ g}^{-1}$ ), high enzyme loading, large porosity for unhindered glucose transport, and moderate electrical conductivity ( $\sim 0.2 \text{ S cm}^{-1}$ ) utilizing novel electrodes of graphene oxide (GO) and SWCNTs co-gel, which were fabricated by mixing suspensions of GO and individually dispersed SWCNTs (Fig. 3.8). The co-gel displays the density of  $7.1 \text{ mg mL}^{-1}$  and is made up of pores having a radius greater than 10 nm. It observes micron-scale graphene sheets with scroll-like structures within the single-walled carbon nanotube matrix (Fig. 3.8b). It is reported that glucose oxidase and bilirubin oxidase are physically adsorbed onto these electrodes to form anodes and cathodes. Enzymatic biofuel cells are obtained to produce power densities up to  $0.19 \text{ mW cm}^{-2}$

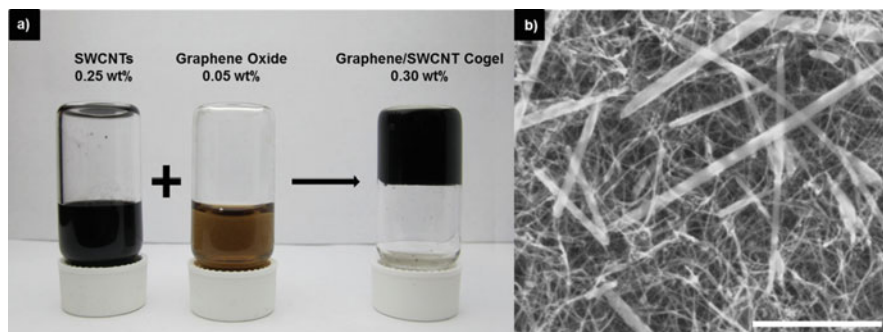


**Fig. 3.8** Graphene/single-walled carbon nanotube co-gel. (a) Graphene/single-walled carbon nanotube co-gel was formed by mixing individually dispersed single-walled carbon nanotube with graphene oxide in a 5:1 ratio by weight. (b) Scanning electron microscopy (SEM) micrograph of graphene/single-walled carbon nanotube aerogel with scale bar representing 5  $\mu\text{m}$ . From Campbell et al. (2015). Reprinted with permission from ACS

that correlated to  $0.65 \text{ mW mL}^{-1}$  or  $140 \text{ mW g}^{-1}$  of glucose oxidase with an open-circuit voltage of 0.61 V. They suggested that these electrodes will be useful for biosensing applications.

**Multi-walled Carbon Nanotubes (MWCNTs)** There are various applications of MWCNTs including catalyst support, field effect emission materials, polymer reinforcing agent, and nano-electronic components. An extensive effort has been made to study the role of MWCNTs in biofuel cell. For example, Junichi et al. (2011) focused on the synthesis of Au nanoparticle-decorated functionalized MWCNTs for monosaccharide (biofuel) oxidation reactions and practical application in air biofuel cells. The samples demonstrated better catalytic activities and stability with a maximum power density of  $220 \mu\text{W cm}^{-2}$ . Further, it was found that two small air–glucose fuel cells using Au nanoparticle-decorated functionalized MWCNTs can run a LED lamp which can also be applied to other equivalent power handy devices. However, the monosaccharide oxidation reaction mechanism still needs to be unraveled in the near future.

Neto et al. (2015) reported the synthesis of Au nanoparticles by using different protocols and supported on the surface of MWCNTs containing different functional groups. The authors further focused on the electrochemical performance toward NADH oxidation, ethanol bioelectrocatalysis, and ethanol/ $\text{O}_2$  biofuel cell, which generated high-power output for the hybrid bioelectrodes containing small and better distributed Au nanoparticles on the surface of carbon nanotubes using ethanol/ $\text{O}_2$  biofuel cell tests.

Zhang et al. (2012) developed a hybrid system of carbon nanotubes coated with poly(amidoamine) dendrimer-encapsulated platinum nanoparticles and glucose oxidase through the layer-by-layer self-assembly approach, which were used as anode in enzyme-based biofuel cells. Interestingly, the enzyme-based biofuel cells operate in a solution containing glucose generated an open-circuit voltage of

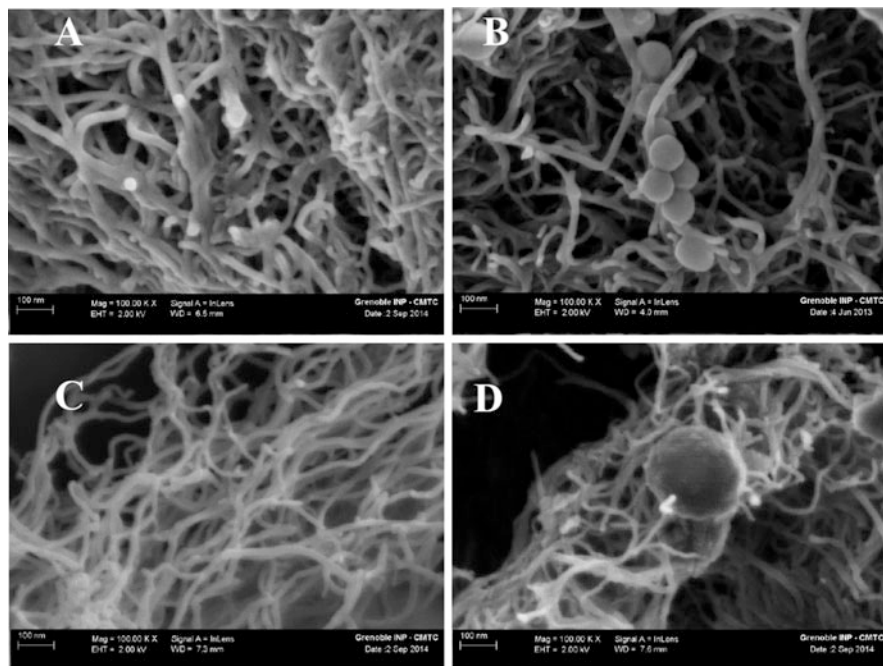


**Fig. 3.9** SEM image of a cross section of different bio-cathodes based on (a) Chitosan-MWCNTs, (b) Chitosan-MWCNTs-laccase, (c) MWCNTs, (d) MWCNTs-laccase. The agglomerates of laccase are the spherical attachments to the chitosan matrix. MWCNTs are not visible in chitosan nanofibers presented in (a) and (b). It can be assumed that they are dispersed within the fibers and act as fillers. From Sarra et al. (2014). Reprinted with permission from RSC

approximately 640.0 mV and a maximum current density of about  $90.0 \mu\text{A cm}^{-2}$  by employing the products modified electrodes as anode.

The biofuel cell with high performances such as stability, easy-handling electrodes, and biofluid-flow controllable system are the important issues for future human body implant by using the effective platform regarding the high surface area from MWCNTs-conducting polymer with poly(3,4-ethylenedioxythiophene), and size/shape dependent flexible yarn electrodes for the implantation of biofuel cell (Cheong et al. 2015). Experimental results showed that a high surface area yarn-based biofuel cell retained over 70% of its initial power output after an extended 20-day period of continuous operation in human blood serum while delivering a power density of  $\sim 1.0 \text{ mW cm}^{-2}$ .

A combined chitosan-CNT-enzyme bio-cathode with a greatly enhanced and stable long-term current density of  $-0.19 \text{ mA mL}^{-1}$  was demonstrated by Sarra et al. (2014). The authors reported that the chitosan matrix is composed of nanofibers with diameters varying from 25 to 35 nm (Fig. 3.9a). CNTs showed more likely tens of nanometers and didn't exceed 20 nm (Fig. 3.9c). They further

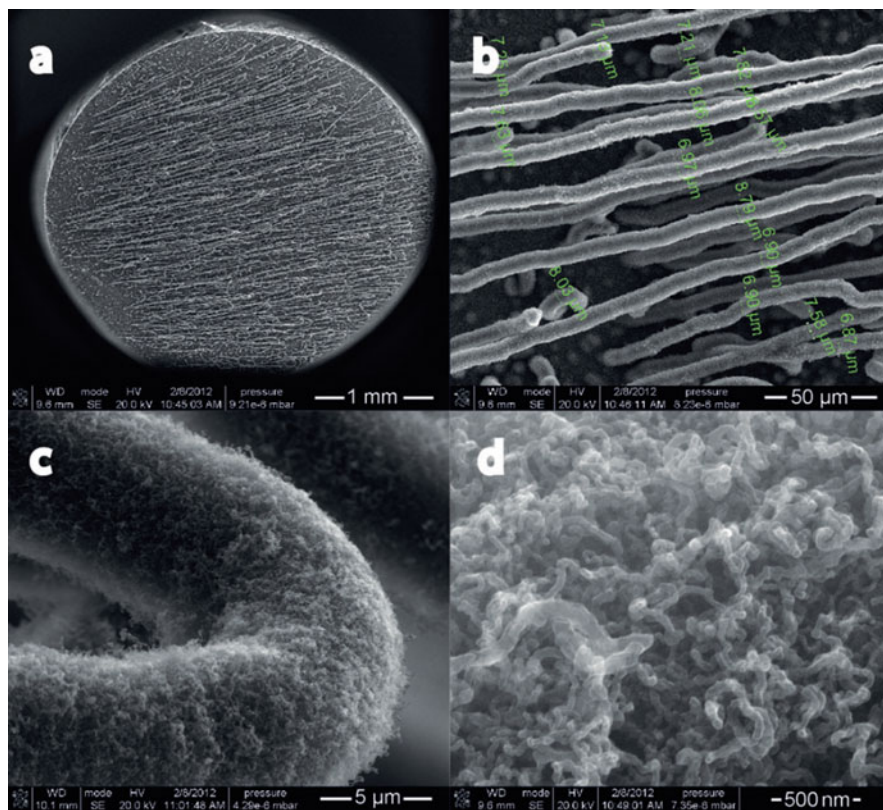


**Fig. 3.10** SEM images of 3D hierarchically structured CNT/carbon microfiber modified/graphite electrodes. (a) Graphite rod with hierarchically structured carbon surfaces, (b) carbon microfiber modified with CNTs, (c) magnification of one carbon microfiber modified with CNT, and (d) close up of the CNT. From Jeevanthi et al. (2014). Reprinted with permission from Wiley

recorded spherical agglomerates in the matrix in proximity of the chitosan nanofibers (Fig. 3.9b) and carbon nanotubes (Fig. 3.9d) in presence of the enzyme.

Jeevanthi et al. (2014) studied different modification methods to stabilize and control the orientation of *Myrothecium verrucaria* bilirubin oxidase on 3D CNT/carbon microfiber-modified graphite electrode surfaces for the improvement of biofuel cell cathodes. The authors reported the maximal current response at a pH value of 6.5 with temperatures between 20 and 35 °C. It carried the high current density ( $1600 \mu\text{A cm}^{-2}$ ) for the bio-cathode based on *Myrothecium verrucaria* bilirubin oxidase immobilized through an imino bond to the electrode and demonstrated a maximal power of  $54 \mu\text{W cm}^{-2}$  at 350 mV with an open-circuit voltage of about 600 mV using a cellobiose dehydrogenase-based bio-anode and glucose as the fuel.

A hierarchical composition of dense CNTs on long and mostly straight modified carbon microfiber anchored to a graphite surface was observed (Fig. 3.10). It was

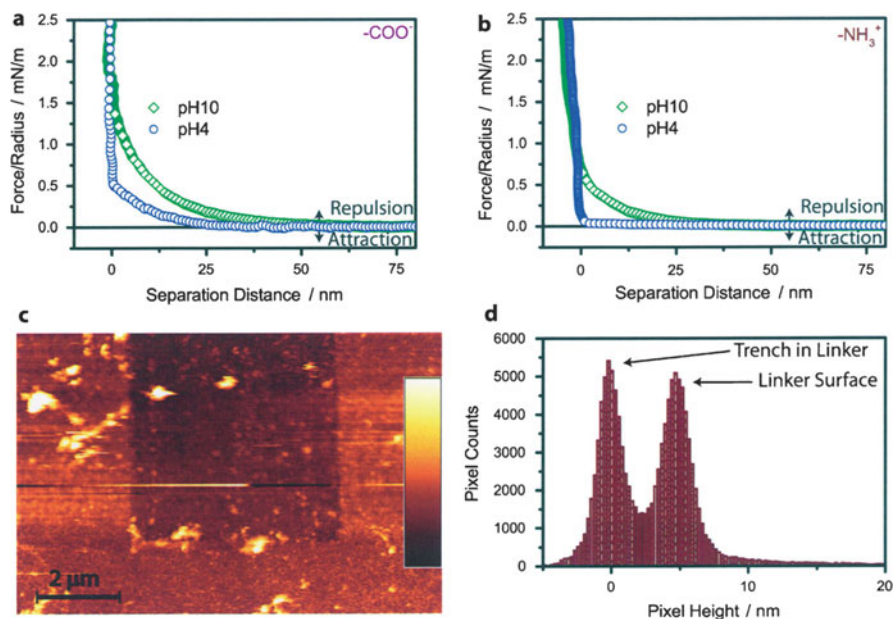


**Fig. 3.11** Representative interaction force profiles between a silica colloidal probe (negatively charged) and a glassy carbon (a) after the diazotization step (methods B–D) and (b) after the amine-linker coupling step in aqueous solutions with 1 mM KCl as the supporting electrolyte. The profiles were obtained upon approach to the surfaces. (c) AFM image of a trench in a grafted linker prepared on a flat glassy carbon surface by method C. The AFM-based lithographic removal of the linker layer and the AFM imaging in tapping mode were performed in liquid. Height color scale is 30 nm. (d) Pixel height distribution taken from the AFM image in (c). Two well-defined peaks represent the topographical surface levels of the trench and linker layer. Pixel statistics instead of an exemplary cross section were used, owing to the strong adhesion of debris to the sample, which created an apparently high surface roughness on the bottom of the trench. Visible debris was excluded from the statistical analysis. From Jeevanthi et al. (2014). Reprinted with permission from Wiley

also found that all carbon microfiber modified/CNTs with the diameter of 6–9  $\mu\text{m}$  lie at the top of the electrode surface and are oriented in one direction (Fig. 3.10b). Further, a homogeneous and densely packed distribution of the CNTs on top of the as-modified carbon microfiber was observed (Fig. 3.10c). The short, curled, and very dense CNTs show the diameters range between 20 and 50 nm (Fig. 3.10d).

The force versus separation distance curves between the silica colloidal probe and a glassy carbon plate after the diazotization step under acidic (pH 4.0) and basic (pH 10) conditions with 1 mM KCl as the supporting electrolyte were recorded (Fig. 3.11a). The area adjacent after scratching a quadratic region of  $5 \times 5 \mu\text{m}$  with a sharp AFM tip at a loading force of 60–80 nN in tapping mode was observed (Fig. 3.11c). Finally, two well-defined peaks with the pixel height distribution were recorded as shown in Fig. 3.11d.

**Porous Carbon** Porous carbon materials exhibit the advantages of light weight, high toughness, high modulus, and stability. Especially, porous carbon materials show clear electrocatalytic oxidation performance for glucose with short response time and large response current due to its high surface area. Gao et al. (2011) reported micro-structured carbon hollow spheres with excellent electrocatalytic activity to the oxidation of dihydronicotinamide adenine dinucleotide. The carbon hollow sphere-coated glassy carbon electrode allows high-sensitive and direct amperometric detection of dihydronicotinamide adenine dinucleotide at low potential, ranging from 0.20 to 100  $\mu\text{M}$  with a high sensitivity of  $7.3 \pm 0.2 \text{ nA } \mu\text{M}^{-1}$ , low detection limit of  $0.08 \pm 0.03 \mu\text{M}$ , and minimization of surface fouling. A lactate biosensor displays rapid and high-sensitive amperometric response to lactate ranging from 0.5 to 12 mM with a detection limit of  $3.7 \pm 0.2 \mu\text{M}$ , a sensitivity of  $4.1 \pm 0.2 \text{ nA } \mu\text{M}^{-1}$ , good reproducibility, and excellent stability with lactate dehydrogenase as a model. It also contains a high open-circuit potential of 0.60 V for a membrane-less lactate/oxygen biofuel cell. The authors reported that these materials show potential applications for dehydrogenase-based amperometric biosensors and biofuel cells.

Alexander et al. (2013) implemented the porous high surface area and conducting properties of mesoporous carbon nanoparticles with <500 nm diameter and pore dimensions  $\sim 6.3 \text{ nm}$  to design electrically contacted enzyme electrodes for biosensing and biofuel cell applications. The as-synthesized relay/enzyme-functionalized mesoporous carbon nanoparticles are immobilized on glassy carbon electrodes, and the relays encapsulated in the pores are sufficiently free to electrically contact the different enzymes with the bulk electrode supports. These materials provide an effective electrically contacted material for the bioelectrocatalyzed reduction of  $\text{O}_2$ , which is reported to yield a biofuel cell revealing a power output of  $\sim 95 \mu\text{W cm}^{-2}$ .

Shitanda et al. (2013) demonstrated a paper-based biofuel cell using porous carbon inks for high-power output. It obtained the power density of the as-fabricated biofuel cell of  $0.12 \text{ mW cm}^{-2}$  (at 0.4 V). It reached  $4.6 \text{ mA cm}^{-2}$  with the catalytic current at 0.5 V, which is 12 times higher than that for previously reported paper-based biofuel cells. It displayed  $0.1 \text{ mA cm}^{-2}$  for the same enzyme and mediator loadings without the porous carbon layer. Obviously, the present flexible paper-based biofuel cell is highly applicable to the development of low-cost, flexible, ubiquitous energy devices.

Anne de et al. (2014) reported herringbone carbon nanofiber mesoporous films as platforms for enhanced bio-oxidation of hydrogen, which is found to allow mediator-less hydrogen oxidation by the membrane-bound hydrogenase from the hyperthermophilic bacterium *Aquifex aeolicus*. The authors discovered the limit catalytic current by mass transport inside the mesoporous carbon nanofiber film and obtained very high efficiency of the bio-electrode by the combination of the hierarchical porosity of the carbon nanofiber film with the hydrophobicity of the treated carbon material. It reached current densities of  $4.5 \text{ mA cm}^{-2}$  with a turnover frequency of  $48 \text{ s}^{-1}$ . Authors suggested that carbon nanofibers can be efficiently used in future sustainable  $\text{H}_2/\text{O}_2$  biofuel cells.

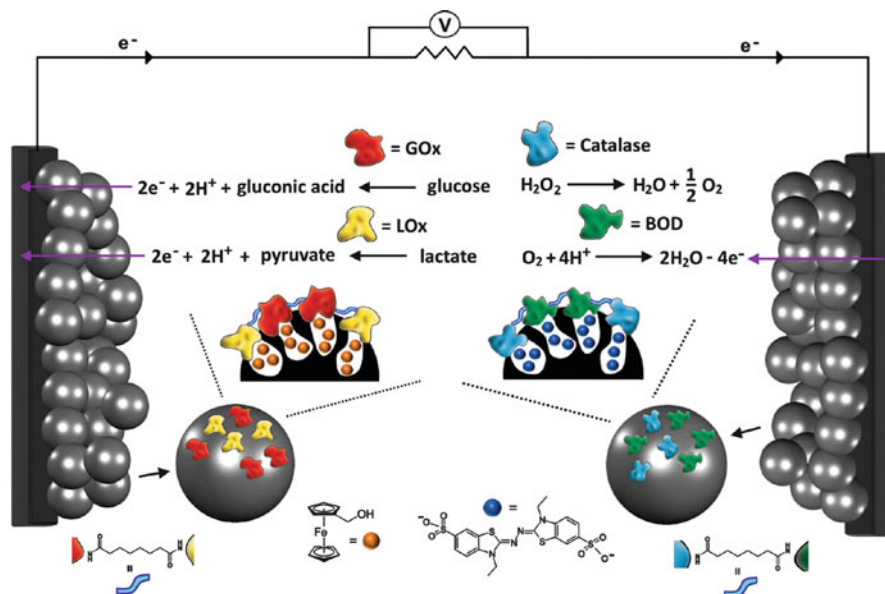
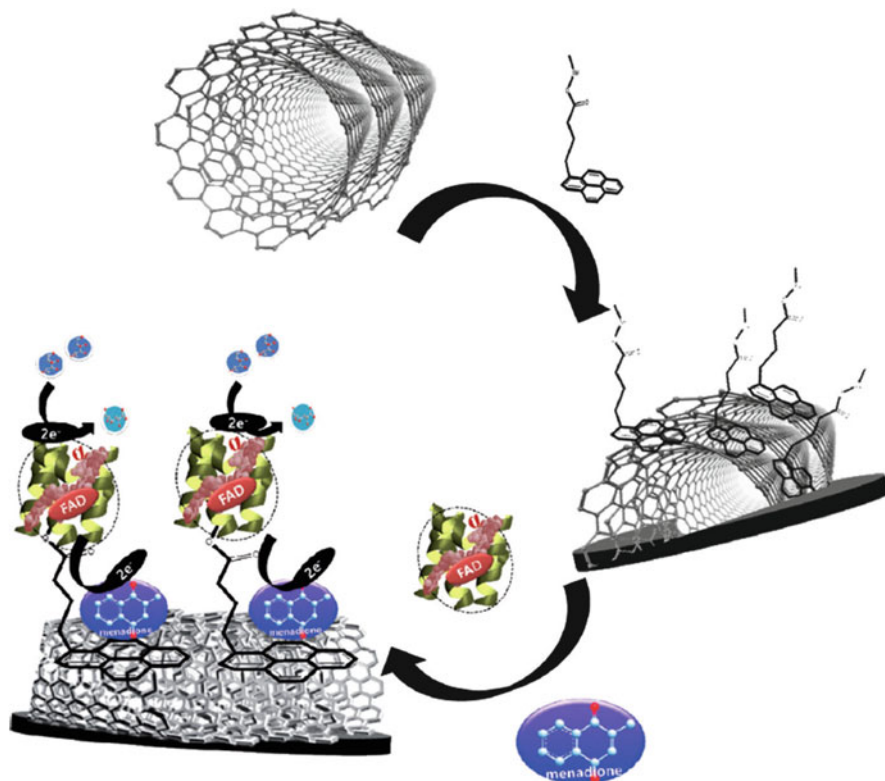


**Fig. 3.12** Schematic configuration of a biofuel cell composed of the (1)-loaded, glucose oxidase/lactate oxidase-capped mesoporous carbon nanoparticles-modified anode, oxidizing both the glucose and lactate fuels and the (3)-loaded, bilirubin oxidase and catalase-capped mesoporous carbon nanoparticles-modified cathode that utilizes  $O_2$  and  $H_2O_2$  as oxidizers. From Alexander et al. (2015). Reprinted with permission from Wiley

Alexander et al. (2015) reported the capping of electron relay units in mesoporous carbon nanoparticles by cross-linking of different enzymes on mesoporous carbon nanoparticle matrices to integrate electrically contacted bienzyme electrodes acting as dual biosensors or as functional bienzyme anodes and cathodes for biofuel cells. They used the capping of ferrocenemethanol and methylene blue in mesoporous carbon nanoparticles by the cross-linking of glucose oxidase and horseradish peroxidase to yield a functional sensing electrode for both glucose and  $H_2O_2$ . The schematic configuration of a biofuel cell based on the integrated bienzyme anode and the bienzyme cathode is shown in Fig. 3.12. They also reported that the glucose oxidase/lactate oxidase electrode mediates the simultaneous oxidation of glucose and lactate, and the bilirubin oxidase and catalase cathode implement the oxidizers  $O_2$  and  $H_2O_2$  (as an oxygen source). This biofuel cell display a power efficiency of  $\sim 90 \mu W cm^{-2}$  in the presence of the two fuels. They demonstrated that multi-enzyme mesoporous carbon nanoparticle electrodes may improve the performance of biofuel cells by oxidizing mixtures of fuels in biomass.

**Enzymatic Biofuel Cell** Biofuel cell used organic materials as fuel and enzyme as catalyst. Enzymatic biofuel cell is a real green battery due to its high-energy conversion efficiency, good biocompatibility, and raw material sources.





**Scheme 3.1** Immobilization of the flavin adenine dinucleotide-dependent glucose dehydrogenase a subunit–menadione system onto the surface of graphitized carbon nanofiber paper through a bifunctional molecule. From Deby et al. (2014). Reprinted with permission from Wiley

Deby et al. (2014) fabricated free-standing graphitized carbon nanofiber paper as immobilizer enzymes and an electrode for enzymatic biofuel cell applications using a dispersion–filtration method, modified by non-covalent functionalization with 1-pyrenebutyric acid *N*-hydroxysuccinimide ester—a bifunctional linker reagent through  $\pi$ – $\pi$  stacking. Scheme 3.1 depicts the non-covalent immobilization of the flavin adenine dinucleotide-dependent glucose dehydrogenase–menadione system on graphitized carbon nanofiber paper. The maximum power density was obtained at a glucose concentration of 100 mM, yielding  $834.9 \pm 200$ ,  $262.9 \pm 15.6$ , and  $147.2 \pm 4.70 \mu\text{W cm}^{-2}$  for flavin adenine dinucleotide-dependent glucose dehydrogenase–menadione, glucose oxidase–menadione, and glucose oxidase-only systems (as the anode), respectively, with laccase as the cathode.

Dai et al. (2012) reported the biofuel cells similarly to those conventional fuel cells as one of potential substitutes for fossil fuel, which exhibited the advantages on reduction of greenhouse gas emissions as well as increasing energy security. Glucose oxidase and laccase are immobilized onto carbon paper as bio-anode and

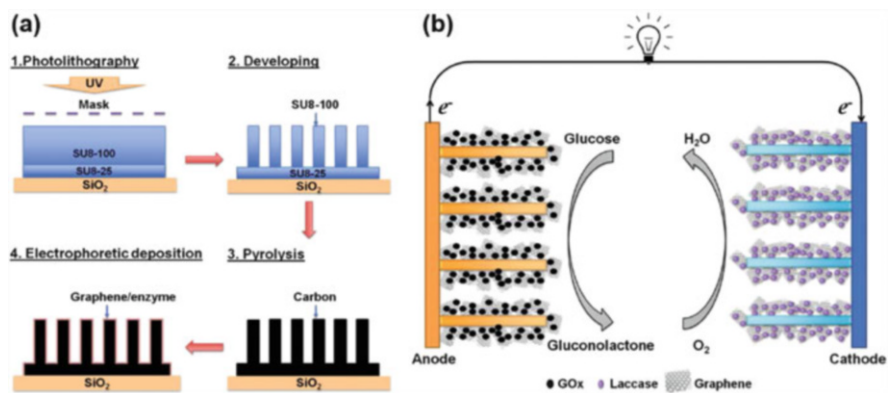


**Fig. 3.13** (a) Schematic showing the fabrication of enzymatic biofuel cells based on carbon microelectromechanical systems micropillar arrays. (b) Illustration of the enzymatic biofuel cells with graphene/enzyme encrusted three-dimensional carbon micropillar arrays (not to scale). From Song et al. (2015). Reprinted with permission from RSC

bio-cathode, respectively, in enzyme-based biofuel cells system, which convert chemical energy into electrical energy via specific enzymes as biocatalysts. It achieved the power voltage up to 0.114 V with the carbon nanoball surface using plasma surface modification with oxygen bubbling in cathode directly in the cell and the power density of  $65.5 \mu\text{W cm}^{-2}$ . The hydrophilicity on the electrode is found to play a crucial role in enhancing power density.

Song et al. (2015) integrated graphene/enzyme onto three-dimensional micropillar arrays with excellent electrochemical activity for use in high-performance enzymatic biofuel cells. The authors showed an illustration of the typical carbon microelectromechanical system fabrication procedure (Fig. 3.13). As per authors' report, a maximum power density of  $136.3 \mu\text{W cm}^{-2}$  at 0.59 V was generated.

Rosalba et al. (2011) reported the development of a fully enzymatic biofuel cell under a continuous flow-through regime. It operated the enzymatic malate dehydrogenase–laccase biofuel cell with an open-circuit voltage of 0.584 V and sustained the alcohol dehydrogenase–laccase biofuel cell with an open-circuit voltage of 0.618 V, and the maximum volumetric power densities approaching  $20 \mu\text{W cm}^{-3}$  were reported.

Peter et al. (2012) reported the development of mass-producible, completely enzymatic printed glucose/oxygen biofuel cells based on filter paper coated with conducting carbon inks containing mediators and laccase, for reduction of oxygen, or aldose dehydrogenase, for oxidation of glucose. The highest power output of  $3.5 \mu\text{W cm}^{-2}$  at 0.34 V for ThL/ABTS cathodes was observed. It obtained highest stability for a printed fuel cell using osmium complexes as mediators of glucose oxidation by aldose dehydrogenase and oxygen reduction by *Trametes hirsuta laccase*, maintaining cell voltage above 200 mV for 137 h at pH 5.

Selloum et al. (2014) presented the construction of an ethanol microfluidic biofuel cell based on a bio-cathode and bio-anode in a Y-shaped microfluidic channel, which was obtained using ethanol oxidized by alcohol dehydrogenase as anode and the oxygen reduced by laccase as cathode. It generated the maximum power density of  $90 \mu\text{W cm}^{-2}$  for the miniaturized device at 0.6 V for a flow rate  $16 \mu\text{L min}^{-1}$ . They will develop a compact fuel cell stack comprising multiple microfluidic biofuel cells and get more durable and stable bioelectrodes to produce adequate power for practical applications.

### 3.4 Conclusion

In summary, the synthesis of carbon-based nanomaterials by using various methods and its applications in biofuel cell have been described in the chapter. Obviously, the topic has been receiving more and more attention due to its practical industrial applications. For the preparation of carbon-based nanomaterials, environmentally friendly methods should be developed at low cost and high efficiency. More importantly, we should pay more attention to the synthesis of the carbon-based nanomaterials with various shapes, sizes, self-assembly, and microstructures. For example, the hierarchically nanostructured carbon-based nanomaterials display high specific surface area, which provide better choices in biofuel cell. There are some reports on the carbon-based nanomaterials such as carbon–ferric oxide, carbon–titanium oxide, carbon–g- $\text{C}_3\text{N}_4$ , etc. Moreover, more and more carbon-based nanomaterials should be developed via theoretical and computer simulations. The following problems should be focused on in the near future, such as the detailed mechanism between carbon and nanomaterials, comparative studies between carbon and carbon-based nanomaterials, and the relationship of composition–structure–property of carbon-based nanomaterials. Undoubtedly, for the industry applications of carbon-based nanomaterials in biofuel cell, there is still a long way to go. The major challenge for biofuel cells is that the carbon–carbon bond is not easy to decompose by traditional catalysts such as noble metals. Although microorganisms or enzymes are capable of decomposing biomass, there are still many drawbacks including the limited power output, selectively decompose certain types of biomass by microorganisms or enzymes, and microbial system failure. Moreover, the power output and long-term stability should be required to optimize so as to meet requirements for practical applications. Therefore, more and more efforts should be devoted to the research of carbon-based nanomaterials in biofuel cell.

**Acknowledgments** Financial support from the Fundamental Research Funds for the Central Universities (No. 2015ZCQ-CL-03, JC2013-3) and Beijing Higher Education Young Elite Teacher Project (No. YETP0763) is gratefully acknowledged.

## References

- Alexander T, Katharina H, Ran TV, Omer Y, Michael W, Itamar W (2013) Enzyme-capped relay-functionalized mesoporous carbon nanoparticles: effective bioelectrocatalytic matrices for sensing and biofuel cell applications. *ACS Nano* 7:11358–11368
- Alexander T, Ran TV, Michael F, Itamar W (2015) Electrically contacted bienzyme-functionalized mesoporous carbon nanoparticle electrodes: applications for the development of dual amperometric biosensors and multifuel-driven biofuel cells. *Adv Energy Mater* 5:1401853
- Avnir D, Coradin T, Lev O, Livage J (2006) Recent bio-applications of sol-gel materials. *J Mater Chem* 16:1013–1030
- Bang JH, Suslick KS (2010) Applications of ultrasound to the synthesis of nanostructured materials. *Adv Mater* 22:1039–1059
- Campbell AS, Yeon JJ, Geier SM, Koepsel RR, Russell AJ, Islam MF (2015) Membrane/mediator-free rechargeable enzymatic biofuel cell utilizing graphene/single-wall carbon nanotube co-gel electrodes. *ACS Appl Mater Interfaces* 7:4056–4065
- Cheong HK, Jae AL, Choi YB, Kim HH, Spinks GM, Lima MD, Baughman RH, Kim SJ (2015) Stability of carbon nanotube yarn biofuel cell in human body fluid. *J Power Sources* 286:103–108
- Cundy CS, Cox PA (2003) The hydrothermal synthesis of zeolites: History and development from the earliest days to the present time. *Chem Rev* 103:663–701
- Dai DJ, Chan DS, Wu HS (2012) Modified carbon nanoball on electrode surface using plasma in enzyme-based biofuel cells. *Energy Procedia* 14:1804–1810
- de Anne P, Helena MK, Veronique W, Marie TGO, Roger G, Elisabeth L (2014) Carbon nanofiber mesoporous films: efficient platforms for bio-hydrogen oxidation in biofuel cells. *Phys Chem Chem Phys* 16:1366–1378
- Deby F, Yooseok L, Chyi YL, Ahn JH, Kim SW, Chang IS (2014) Immobilisation of flavin-adenine-dinucleotide-dependent glucose dehydrogenase a subunit in free-standing graphitised carbon nanofiber paper using a bifunctional cross-linker for an enzymatic biofuel cell. *ChemElectroChem* 1:1844–1848
- Du X, Zhao W, Wang Y, Wang CY, Chen MM, Qi T, Hua C, Ma MG (2013) Preparation of activated carbon hollow fibers from ramie at low temperature for electric double-layer capacitor applications. *Bioresour Technol* 149:31–37
- Fang J, Chen A, Peng C, Zhao S, Ci L (2001) Changes in forest biomass carbon storage in China between 1949 and 1998. *Science* 292:2320–2322
- Fu LH, Yao K, Shi CM, Ma MG, Zhao JJ (2014) Ultrasonic-assisted synthesis of cellulose/Cu(OH)<sub>2</sub>/CuO hybrids and its thermal transformation to CuO and Cu/C. *Sci Adv Mater* 6:1117–1125
- Gao F, Guo XY, Yin J, Zhao D, Li MG, Wang L (2011) Electrocatalytic activity of carbon spheres towards NADH oxidation at low overpotential and its applications in biosensors and biofuel cells. *RSC Adv* 1:1301–1309
- Jeevanthi V, Rosalba AR, Volodymyr K, Sascha P, Wolfgang S (2014) Biofuel-cell cathodes based on bilirubin oxidase immobilized through organic linkers on 3D hierarchically structured carbon electrodes. *ChemElectroChem* 1:1901–1908
- Junichi N, Le QH, Yasuhito S, Tomohiko I, Hiroyuki Y, Masato S, Eiichi T (2011) Development of biofuel cells based on gold nanoparticle decorated multi-walled carbon nanotubes. *Bio-sensors Bioelectron* 30:204–210
- Kenath PP, Chen Y, Chen P (2014) Three-dimensional graphene-carbon nanotube hybrid for high-performance enzymatic biofuel cells. *ACS Appl Mater Interfaces* 6:3387–3393
- Krzysztof S, Dominika Ł, Kamila Z, Jan FB, Jerzy R, Renata B (2012) Arylated carbon nanotubes for biobatteries and biofuel cells. *Electrochim Acta* 79:74–81
- Krzysztof S, Michal K, Dominika M, Kamila Z, Jan FB, Jerzy R, Renata B (2014) Biobatteries and biofuel cells with biphenylated carbon nanotubes. *J Power Sources* 249:263–269

- Liu S, Liu YJ, Deng F, Ma MG, Bian J (2015) Comparison of the effects of microcrystalline cellulose and cellulose nanocrystals on the  $\text{Fe}_3\text{O}_4/\text{C}$  nanocomposites. *RSC Adv* 5:74198–74205
- Lu W, Lieber CM (2007) Nanoelectronics from the bottom up. *Nat Mater* 11:841–850
- Lu Y, Mei Y, Schrunner M (2007) In situ formation of Ag nanoparticles in spherical polyacrylic acid brushes by UV irradiation. *J Phys Chem C* 111:7676–7681
- Moran JJ, Alvarez VA, Cyras VP, Vazquez A (2008) Extraction of cellulose and preparation of nanocellulose from sisal fibers. *Cellulose* 15:149–159
- Navarro RM, Pena MA, Fierro JLG (2007) Hydrogen production reactions from carbon feedstocks: fossils fuels and biomass. *Chem Rev* 10:3952–3991
- Neto SA, Almeida TS, Belnap DM, Minter SD, De Andrade AR (2015) Enhanced reduced nicotinamide adenine dinucleotide electrocatalysis onto multi-walled carbon nanotubes-decorated gold nanoparticles and their use in hybrid biofuel cell. *J Power Sources* 273:1065–1072
- Peter J, Saara T, Anu V, Matti V, Maria S, Dónal L (2012) A mediated glucose/oxygen enzymatic fuel cell based on printed carbon inks containing aldose dehydrogenase and laccase as anode and cathode. *Enzyme Microb Technol* 50:181–187
- Rosalba AR, Carolin L, Heather RL, Kristen EG, Emily A, Glenn RJ, Plamen A (2011) Enzymatic fuel cells: integrating flow-through anode and air-breathing cathode into a membrane-less biofuel cell design. *Biosensors Bioelectron* 27:132–136
- Sarra EI, Abdelkader Z, Awatef L, Reverdy-Bruasc N, Didier C, Mohamed NB, Philippe C, Martin DK (2014) Chitosan improves stability of carbon nanotube biocathodes for glucose biofuel cells. *Chem Commun* 50:14535–14538
- Selloum D, Tingry S, Techer V, Renaud L, Innocent C, Zouaoui A (2014) Optimized electrode arrangement and activation of bioelectrodes activity by carbon nanoparticles for efficient ethanol microfluidic biofuel cells. *J Power Sources* 269:834–840
- Shitanda I, Kato S, Hoshi Y, Itagaki M, Tsujimura S (2013) Flexible and high-performance paper-based biofuel cells using printed porous carbon electrodes. *Chem Commun* 49:11110–11112
- Song Y, Chen CH, Wang CL (2015) Graphene/enzyme-encrusted three-dimensional carbon micropillar arrays for mediatorless micro-biofuel cells. *Nanoscale* 7:7084–7090
- Wen D, Xu XL, Dong SJ (2011) A single-walled carbon nanohorn-based miniature glucose/air biofuel cell for harvesting energy from soft drinks. *Energy Environ Sci* 4:1358–1363
- Yan CY, Wang JX, Kang WB, Cui MQ, Wang X, Foo CY, Chee KJ, Lee PS (2014) Highly stretchable piezoresistive graphene-nanocellulose nanopaper for strain sensors. *Adv Mater* 26:2022–2027
- Zhang JM, Zhu YH, Chen C, Yang XL, Li CZ (2012) Carbon nanotubes coated with platinum nanoparticles as anode of biofuel cell. *Particuology* 10:450–455
- Zhu YJ, Chen F (2014) Microwave-assisted preparation of inorganic nanostructures in liquid phase. *Chem Rev* 114:6462–6555

# Chapter 4

## Multifunctional Nanoparticle Applications to Microalgal Biorefinery

Jung Yoon Seo, Minjeong G. Kim, Kyubock Lee, Young-Chul Lee, Jeong-Geol Na, Sang Goo Jeon, Seung Bin Park, and You-Kwan Oh

**Abstract** Microalgal feedstocks are leading candidates for application to large-scale production of sustainable biochemicals and biofuels, due to the inherent potentials of microalgae including high biomass and lipid productivities, carbon neutrality, a wide range of end products, and cultivation in nonarable lands. However, the overall process, starting from microalgae cultivation and ending in conversion to biofuels, entails complicated processes and, moreover, faces technological and economic challenges for commercialization. Recently, the application of multifunctional nanoparticles has been suggested as a potential tool to open commercialization of microalgae-based biofuels. In this context, this chapter will discuss the extensive research that has been conducted to improve process efficiency in microalgal biorefinery. Attention will be focused mainly on nanoparticle-aided microalgae harvesting, extraction, and conversion. With respect to microalgae harvesting, a diverse range of functionalized magnetic nanoparticles are utilized to enhance harvesting efficiency in a short time. Further, nanoparticles with multiple functions or recyclability are developed to reduce process costs. Aminoclay-conjugated nanoparticles are applied to increase lipid extraction yields through destabilization of cell walls or generation of hydroxyl radicals for cell disruption. Also, the various nanocatalysts for conversion yield enhancement and biodiesel upgrading are covered. It is hoped that this chapter of the current state of nanoparticle-based technology will prove a useful guide to future improvements in microalgal biorefinery.

---

J.Y. Seo • M.G. Kim • S.B. Park

Department of Chemical and Biomolecular Engineering, Korea Advanced Institute of Science and Technology (KAIST), Daejeon 34141, Republic of Korea

K. Lee

Graduate School of Energy Science and Technology, Chungnam National University, Daejeon 34134, Republic of Korea

Y.-C. Lee

Department of BioNano Technology, Gachon University, Seongnam-Si, Gyeonggi-Do 13120, Republic of Korea

J.-G. Na • S.G. Jeon • Y.-K. Oh (✉)

Biomass and Waste Energy Laboratory, Korea Institute of Energy Research (KIER), Daejeon 34129, Republic of Korea

e-mail: [ykoh@kier.re.kr](mailto:ykoh@kier.re.kr)

**Keywords** Nanoparticle • Microalgal biorefinery • Harvesting • Lipid extraction • Conversion

## 4.1 Introduction

The demand for alternative sources of energy continues to rise due to global concerns over rapidly depleting fossil fuels, increasing energy consumption, and serious environmental problems (Brentner et al. 2011). Microalgae are considered to be very promising feedstocks for future energy resources, due to their numerous benefits such as fast growth rates and high lipid contents (Williams and Laurens 2010; Cho et al. 2011; Sharma et al. 2011). According to the recent assessment of the lipid productivity potentials of microalgal biomass, many countries could obtain 30% of their transportation fuel from microalgal biomass cultivated using nonarable lands (Moody et al. 2014). In addition to their high lipid productivity compared with terrestrial feedstocks, microalgae are composed of polysaccharides, proteins, lipids, nucleic acids, and pigments, which enable them to serve as feedstocks for a variety of end products ranging from nutrients, pharmaceuticals, bioplastics, and biofuels (Williams and Laurens 2010; Sharma et al. 2011; Moody et al. 2014; Kim et al. 2016). Microalgae are also attractive in that they sequester and more efficiently capture CO<sub>2</sub> during photosynthetic growth (Praveenkumar et al. 2014a). Unlike terrestrial oilseeds, moreover, microalgae can be grown in saline or contaminated environments as well as freshwater, without the need of large amounts of nitrogen fertilizers (Mata et al. 2010; Christenson and Sims 2011; Lam and Lee 2012).

These advantages of microalgae as feedstocks have boosted the extensive research efforts ongoing to commercialize microalgal biofuels; however, unfortunately microalgal biorefineries still faced with a number of technological and economic challenges (Lee et al. 2015b). Microalgal biorefinery is divided into four major downstream processes including cultivation, harvesting, lipid extraction, and conversion. Firstly, the mass cultivation of selected algal species while maximizing lipid contents is thought to be important (Mata et al. 2010; Christenson and Sims 2011). Growth rates and lipid yields are affected by various factors including cultivation methods, temperature, light, CO<sub>2</sub>, salinity, and nutrients (Williams and Laurens 2010; Praveenkumar et al. 2014b). After cell growth attains the stationary phase for lipid accumulation, the second step is to harvest microalgae from the low-concentration medium (open pond, 0.5–1 g/L; photobioreactor, 1–10 g/L) (Pienkos and Darzins 2009; Praveenkumar et al. 2014a). Due to the inherent small size and stable dispersion of microalgae, the harvesting step is much more difficult than is the case with terrestrial oilseed crops (Christenson and Sims 2011; Milledge and Heaven 2013). Indeed, according to recent reports, the harvesting step incurs the highest energy consumption as well as the greatest cost uncertainty in microalgal biorefinery (Sander and Murthy 2010; Williams and Laurens 2010; Lee et al. 2015b). The difficulty of lipid extraction reflects the robust cell walls that inhibit recovery of intracellular lipids. Most conventional extraction methods are fraught with environmental issues (through their use of toxic organic solvents) and

incur significant costs (through the requirements for high pressure and temperature, supercritical conditions, microwave treatment, etc.) (Lam and Lee 2012; Kim et al. 2016). Moreover, downstream processes such as lipid extraction and conversion are highly dependent on feedstock conditions (e.g., species, water content, composition of feedstock oil) (Williams and Laurens 2010; Park et al. 2015). The extracted lipid is converted to biodiesel in the presence of a catalyst. Most heterogeneous catalysts and conversion conditions for microalgal biodiesel are adapted from those for vegetable-oil-based biodiesel (Mata et al. 2010). As such, the development of more suitable catalysts for microalgal oil is necessary, in that the conversion yield and selectivity are affected by the composition of the feedstock oil.

In the face of the various technological limitations on the commercialization of microalgal biofuel production, nanoparticle engineering has been proposed as the key to the solution of the above-noted problems related to each of the downstream processes (Lee et al. 2015b; Wang et al. 2015). As shown in Fig. 4.1, multifunctional nanoparticles have been applied to microalgal biorefinery to improve biomass productivity, lipid extraction yield, and biodiesel productivity and to enhance the overall economics of microalgae-based biodiesel production. Figure 4.2 provides images of nanoparticles and nanostructured particles that are actually utilized in microalgal downstream processing. In this chapter, we provide a review of the recent research into the various specialized nanoparticles that have been applied in microalgal biorefinery. The chapter is organized based on the



**Fig. 4.1** Utilization of multifunctional nanoparticles in microalgal biorefinery



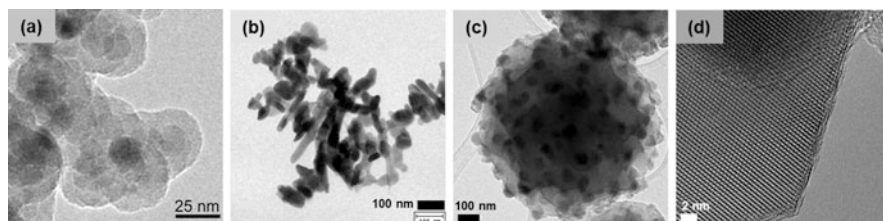


**Fig. 4.2** Transmission electron microscopy (TEM) images of (a) dual-functionalized (OTES and APTES)  $\text{SiO}_2\text{-Fe}_3\text{O}_4$  nanoparticles. Reprinted with permission from Lee et al. (2015a). Copyright (2015) American Chemical Society. (b) APTES-coated  $\text{BaFe}_{12}\text{O}_{19}$  nanoparticles, (c)  $\text{Fe}_3\text{O}_4$ -nanoparticle-embedded carbon microparticles, and (d) high-resolution image of (c). Images of (b–d) are unpublished data of references (Seo et al. 2014, 2015)

various nanoparticle-aided approaches to microalgal biorefinery. Accordingly, Sect. 4.2 discusses nanoparticle-aided microalgae harvesting through functionalized magnetic nanoparticles and aminoclay nanoparticles. Additionally, multifunctional nanoparticles for integrated use as well as recyclable nanoparticles are explored. In Sect. 4.3, aminoclay-based lipid extraction and potential pathways for efficient extraction are introduced. Section 4.4 explores heterogeneous nanocatalysts for lipid-to-diesel conversion or biodiesel upgrading.

## 4.2 Nanoparticle-Aided Microalgae Harvesting

Microalgae harvesting is regarded as one of the critical bottlenecks in microalgae-based biorefinery, due to several biological and physicochemical characteristics of microalgae, including the low upper end of culture concentration, the very small cell size, and the cells' high dispersity (Pienkos and Darzins 2009; Wang et al. 2015). To date, various harvesting technologies ranging from centrifugation to flocculation, filtration, sedimentation, flotation, electrophoresis, immobilization, and magnetophoretic separation have been reported (Lee et al. 2015b; Wang et al. 2015). Nanoparticle-aided microalgae harvesting has become the latest trend to enhance harvesting effectiveness in view of energy consumption, final microalgal concentration, reliability, environmental toxicity, and process cost (Lee et al. 2015b). In this section, the research progress and directions of nanoparticle-aided microalgae harvesting are introduced.

### 4.2.1 Functionalized Magnetic Nanoparticles

Nanoparticles used for microalgae harvesting are mainly magnetic nanoparticles, because magnetic separation enables fast, automatable, and scalable processing

with high harvesting efficiency and low contamination (Borlido et al. 2013). Most microalgae present in negatively charged form in a culture broth due to cell-wall functional groups such as  $-\text{COOH}$ ,  $-\text{OH}$ , and  $-\text{SH}$ , the properties of which could be taken advantage for nanoparticle-based microalgae harvesting. In general, naked magnetic particles such as  $\text{Fe}_3\text{O}_4$  allow harvesting through nanoparticle adsorption or pH control. However, they show lower harvesting efficiency or capacity, since they have a negative zeta potential under a common cultivation condition (around pH 7). According to Hu et al. (2014), harvesting capacity of naked  $\text{Fe}_3\text{O}_4$  nanoparticles was 3.07 g DCW/g nanocomposites, whereas that of  $\text{Fe}_3\text{O}_4$ -PEI nanocomposites was 32.61 g DCW/g nanocomposites. In this context, functionalized magnetic nanoparticles, especially as positively charged, have drawn the attention of many researchers in the field.

Lim et al. (2012) reported that positively charged poly (diallyldimethylammonium chloride) (PDDA)-coated  $\text{Fe}_3\text{O}_4$  rodlike nanoparticles allowed harvesting of *Chlorella* sp. with 99 % efficiency under a low magnetic field gradient through their enhanced dispersibility and full attachment to cells. They also compared the “immobilized-on” and “attached-to” strategies, the former entailing the introduction of PDDA-coated magnetic nanoparticles into microalgal culture and the latter the introduction of magnetic nanoparticles into a culture containing PDDA-adsorbed microalgae, and reported that the “immobilized-on” strategy is more effective. Also, the harvesting efficiency of  $\text{Fe}_3\text{O}_4$  rodlike nanoparticles is superior to that of sphere-like nanoparticles, due to the stable magnetic moment (Lim et al. 2012). As extended research, Lim’s group (Toh et al. 2012) discussed the feasibility of magnetophoretic removal of naturally grown mixed microalgae from a fishpond using PDDA- $\text{Fe}_3\text{O}_4$  rodlike nanoparticles. One  $\text{m}^3$  of pond water containing six species of algae (*Scenedesmus* sp., *Spirulina* sp., *Chlorella* sp., *Tetraedron* sp., *Haematococcus* sp., and *Dictyosphaerium* sp.) was treated by a combination of a low magnetic field gradient and these magnetic nanoparticles at an estimated cost of US\$0.13. Furthermore, they demonstrated the fundamental principle behind magnetophoretic flocculation of microalgae, which is based on the extended Derjaguin-Landau-Verwey-Overbeek (XDLVO) theory (Toh et al. 2014a, b, c). According to their XDLVO predictions and experimental results, electrostatic interaction had the largest influence on the total interaction energy in the case of the freshwater *Chlorella* sp., while the total interaction energies of the marine *Nannochloropsis* sp. and PDDA- $\text{Fe}_3\text{O}_4$  nanoparticles were governed dominantly by van der Waals attraction and Lewis acid-base interaction. The XDLVO profile of the interaction between PDDA- $\text{Fe}_3\text{O}_4$  and microalgae showed the secondary minimum ( $-3.12$  kT), differently from the case of bare- $\text{Fe}_3\text{O}_4$ , proving that functionalization with a cationic polymer binder is preferable for magnetic nanoparticle attachment (Toh et al. 2014b).

In recent years, various kinds of cationic functionalized magnetic nanoparticles have been used for microalgae harvesting according to the “immobilized-on” strategy. Polyethylenimine (PEI) is one of the representative coating agents due to its high amine-group contents. Prochazkova et al. (2013) reported that PEI-coated magnetic beads (500 nm) achieve harvesting of *Chlorella vulgaris* cells

with efficiencies better than 90 % under controlled conditions (10 mM KCl, pH 2–10) and, moreover, that the particle dosage (about 0.1 g particles/g cell) is most effective at pH 4. Compared with diethylaminoethyl (DEAE)-coated magnetic beads, which show a weaker ion-exchange character, PEI-coated magnetic beads harvest cells more efficiently in the overall pH 4–10, whereas with the latter, detachment from cells is significantly less effective. This result indicates that the interaction of microalgae and magnetic beads follows physicochemical interactions such as ion exchange, electrostatic interaction, and covalent bonding. Hu et al. (2014) reported the use of PEI for magnetophoretic harvesting of *Chlorella ellipsoidea*. They obtained a harvesting efficiency of 97 % with a particle dosage of 20 mg/L within 2 min, based on the mechanism of electrostatic attraction and the nanoscale effect for adsorption. They also examined harvesting capacity as a function of cultivation period and revealed that harvesting capacity increased to 32.61 g cell/g particle over 14 days due to particle/cell collision and decreased thereafter due to organic matter formed by cell autolysis. Also, increasing of harvesting temperature brings about a more favorable harvesting efficiency (Hu et al. 2014). Ge et al. (2015a) functionalized Fe<sub>3</sub>O<sub>4</sub> nanoparticles with PEI as well and applied them to the separation of *Scenedesmus dimorphus*. They confirmed that the PEI coating could reduce the required dosage for achieving efficiency above 80 % and demonstrated, according to the prediction of the XDLVO theory, increased attraction between particles and cells. Moreover, they reported that harvesting efficiency increased as a function of both ultraviolet (UV) irradiation and its intensity (Ge et al. 2015a).

Wang et al. (2014a) reported that cationic polyacrylamide (CPAM)-modified Fe<sub>3</sub>O<sub>4</sub> nanocomposites enable better than 95 % microalgae harvesting within 10 min with different dosages, specifically 25 mg/L for *Botryococcus braunii* and 120 mg/L for *Chlorella ellipsoidea*. They insisted that the harvesting mechanism of microalgae by CPAM-Fe<sub>3</sub>O<sub>4</sub> nanocomposites is mainly based on bridging as aided by charge neutralization, which was confirmed by optical microscopy observation. This nanocomposite shows a tendency to heterogeneous multilayer adsorption in that the adsorption isotherm data are fitted well to the Freundlich model compared with the Langmuir model (Wang et al. 2014a). This differs from the adsorption isotherm data of PEI-Fe<sub>3</sub>O<sub>4</sub> nanocomposites that were closely fitted to the Langmuir model in their other study (Hu et al. 2014). As extended research, Wang et al. (2014b) introduced a scaled-up experiment that integrated 200 L outdoor cultivation with a continuous magnetic separator. This system enabled continuous separation of *B. braunii* with 90 % efficiency at a flow rate 100 mL/min, requiring a total estimated production cost of US\$25.14 to produce the 1 kg of *B. braunii* dry biomass (Wang et al. 2014b).

Seo et al. (2014) reported that BaFe<sub>12</sub>O<sub>19</sub> nanoparticles of different sizes (108 nm ~1.2 μm) could be used for harvesting of *Chlorella* sp. through functionalization with (3-aminopropyl)triethoxysilane (APTES). APTES, having an amine group (-NH<sub>2</sub>), increases the isoelectric point of APTES-functionalized BaFe<sub>12</sub>O<sub>19</sub> nanoparticles, which completes microalgae harvesting within 2–3 min with 98.6–99.5 % efficiency. Unlike common Fe<sub>3</sub>O<sub>4</sub>, BaFe<sub>12</sub>O<sub>19</sub> offers the

advantages of high saturation magnetization, coercivity, and chemical stability. Recently, Seo et al. (2015) used polyvinylpyrrolidone (PVP) as a functionalizing agent to endow a cationic property to embedded  $\text{Fe}_3\text{O}_4$  nanoparticles. A quaternary nitrogen species is formed in carbonaceous composites, embedding  $\text{Fe}_3\text{O}_4$  through short-time pyrolysis of the optimal content of PVP, which results in the positive zeta potential (24.9 mV) of PVP/ $\text{Fe}_3\text{O}_4$  composites (PVP/Fe nit = 0.8) required for microalgae separation (*Chlorella* sp.). The harvesting efficiency of this composite is as high as 99 % with a dosage of 10 mg/mL, while that of PVP/ $\text{Fe}_3\text{O}_4$  composite (PVP/Fe nit = 0.33) particles showing negative zeta potential (−6.05 mV) is only 31.4 % with a dosage of 25 mg/mL. As a means of reducing the required dosage, which is to say, the relative weight of particles,  $\text{Fe}_3\text{O}_4$  nanoparticles have been incorporated into light carbonaceous materials.

Lee et al. (2013a) developed the biocompatible magnetic flocculants composed of chitosan and  $\text{Fe}_3\text{O}_4$  nanoparticles. With them, the harvesting efficiency of *Chlorella* sp. was improved to better than 99 % as the dosage of flocculants and the ratio of chitosan to  $\text{Fe}_3\text{O}_4$  were increased. The biocompatibility of the chitosan/ $\text{Fe}_3\text{O}_4$  composites was proved by a re-cultivation experiment using recycled culture medium, the results of which indicating that chitosan/ $\text{Fe}_3\text{O}_4$  flocculants could be economically exploited in the harvesting step of microalgae-based biorefinery (Lee et al. 2013a). Toh et al. (2014c) reported that chitosan-functionalized  $\text{Fe}_3\text{O}_4$  nanoparticles had no side effect on the extractable lipids or their quality, even though internal intrusion of chitosan/ $\text{Fe}_3\text{O}_4$  nanoparticles into *Chlorella* sp. was confirmed by cross-section TEM/EDX investigation.

Overall, microalgae harvesting by magnetic nanoparticles relies predominantly on electrostatic attraction as well as other interactions such as bridging, nanoscale adsorption, ion-exchange mechanism, and sweeping, which assist flocculation between microalgae and functionalized magnetic nanoparticles (Toh et al. 2014b; Wang et al. 2014a, b, 2015; Ge et al. 2015a). As shown in Table 4.1, the harvesting-condition variables for every group, such as cell species, its concentration, particle dosage, culture medium pH, mixing speed, and so on, are impractically diverse. Thus, it is not easy to determine the superiority or inferiority of functionalized magnetic particles that have been tried. On the whole, harvesting efficiency is increased when  $\text{Fe}_3\text{O}_4$  nanoparticles are functionalized with various positively charged materials such as PDDA, PEI, chitosan, APTES, etc. In addition, the use of smaller nanoparticles can reduce the particle dosage necessary for sufficient harvesting efficiency.

### 4.2.2 Aminoclay Nanoparticles

Aminoclays are amine-group-rich organophyllosilicates composed of amino-functionalized phyllosilicate sheets and metal cations (Farooq et al. 2013; Lee et al. 2013d, 2014c, d). Generally, aminoclay denotes 3-aminopropyl-functionalized magnesium phyllosilicate, which is synthesized by sol-gel reaction

**Table 4.1** Comparison of microalgae harvesting performances according to various functionalized magnetic particles

Magnetic nanoparticles			Microalgae				Harvesting performances				Ref.
Type	Size (nm)	Dosage (mg/L)	Species	Cell conc. (g/L or cells/mL)	Efficiency (%)	Capacity (mg cell/mg particles)	Time (min)	Working medium	Ref.		
Bare Fe <sub>3</sub> O <sub>4</sub>	8.8	1200	<i>Scenedesmus dimorphus</i>	1 g/L	80.3	5	2-3	Culture	Ge et al. (2015a)		
PDDA-Fe <sub>3</sub> O <sub>4</sub> (rod like)	40 (D) 380 (L)	200	<i>Chlorella</i> sp.	5 × 10 <sup>6</sup> cells/mL	~99	-	<3	Culture	Lim et al. (2012)		
PDDA-Fe <sub>3</sub> O <sub>4</sub> (spherical)	20-30	-	<i>Nannochloropsis</i> sp.	3 × 10 <sup>7</sup> cells/mL	97.9	2.38	6	Seawater	Toh et al. (2014b)		
PEI-Fe <sub>3</sub> O <sub>4</sub>	12	20	<i>Chlorella ellipsoidea</i>	0.75 g/L	97	32.61	2	Culture	Hu et al. (2014)		
PEI-Fe <sub>3</sub> O <sub>4</sub>	8.8	600	<i>Scenedesmus dimorphus</i>	1 g/L	82.7	10	2-3	Culture	Ge et al. (2015a)		
Chitosan-Fe <sub>3</sub> O <sub>4</sub>	10-30	1400	<i>Chlorella</i> sp. KR-1	1 g/L	99	-	2-5	Culture	Lee et al. (2013a)		
APTES-BaFe <sub>12</sub> O <sub>19</sub>	246	-	<i>Chlorella</i> sp. KR-1	1.8 g/L	99	0.43	2-3	Culture	Seo et al. (2014)		
OTES/ATPES-Fe <sub>3</sub> O <sub>4</sub> @SiO <sub>2</sub>	~20	-	<i>Chlorella</i> sp. KR-1	1.6 g/L	98.5	0.625	2.5	Culture	Lee et al. (2015a)		
Fe <sub>3</sub> O <sub>4</sub> NP-embedded carbon microparticle	~2000	10,000	<i>Chlorella</i> sp. KR-1	~2 g/L	99	-	1	Culture	Seo et al. (2015)		
Aminoclay-nZVI composite	~100	19,130	<i>Chlorella</i> sp. KR-1	1.5 g/L	~100	-	3	Culture	Lee et al. (2014c)		
CPAM-Fe <sub>3</sub> O <sub>4</sub>		25	<i>Botryococcus braunii</i>	1.8 g/L	>95	114.8	<10	Culture (pH 7)	Wang et al. (2014a)		

CPAM-Fe <sub>3</sub> O <sub>4</sub>	120	<i>Chlorella ellipsoidea</i>	1.8 g/L	96	21.4	<10	Culture (pH 7)	Wang et al. (2014a)
DEAE-Fe <sub>3</sub> O <sub>4</sub>	–	<i>Chlorella vulgaris</i>	0.2 g/L	90	5	–	Culture (pH 4)	Prochazkova et al. (2013)
Stearic acid-Fe <sub>3</sub> O <sub>4</sub> -ZnO composite	–	<i>Scenedesmus dimorphus</i>	0.8 g/L	–	3.33	5	Culture	Ge et al. (2015c)
Triazabicyclodecene-Fe <sub>3</sub> O <sub>4</sub> @SiO <sub>2</sub>	–	<i>Chlorella vulgaris</i>	–	–	–	1	Culture	Chiang et al. (2015)

Extended from the table in the reference (Lee et al. 2015b)

of aminosilane [3-[2-(2-aminoethylamino)ethylamino]propyltrimethoxysilane (hereafter, N3) or 3-aminopropyl]triethoxysilane (APTES)] with magnesium salts under ambient conditions. In recent years, the range of metal cations has been extended to others such as  $\text{Fe}^{3+}$ ,  $\text{Al}^{3+}$ ,  $\text{Ca}^{2+}$ ,  $\text{Mn}^{2+}$ , and  $\text{Sn}^{4+}$  (Lee et al. 2014c, 2015b). Owing to the abundance of amine groups, aminoclay has been intensively researched in the field of microalgae harvesting (Farooq et al. 2013; Lee et al. 2013d, 2014c, d).

Farooq et al. (2013) reported the harvesting route of the freshwater species *Chlorella vulgaris* and the marine species *Nannochloropsis oculata* using aminoclay with  $\text{Mg}^{2+}$  and  $\text{Fe}^{3+}$  (polydisperse distribution of aminoclay sheets; 50–100 nm to submicron range). Many protonated amine groups in aqueous solution result in efficient microalgae harvesting within about 5 min for *C. vulgaris* and 120 min for *N. oculata*, which is dependent on the mechanism of sweep flocculation, irrespective of species or culture medium. It should be noted that microalgae harvesting by aminoclays is independent of culture pH, while most of the other flocculation methods are sensitive to pH. Furthermore, Fe-aminoclay nanoparticles coated on cotton membrane resulted in 95 % harvesting efficiency, which represents a cost-efficient and up-scalable utilization of aminoclay-based harvesting. Al-aminoclay, Mg-aminoclay, and Ca-aminoclay have been synthesized via sol-gel reaction with APTES and N3 for microalgae harvesting (*Chlorella* sp.) and Al-aminoclay and Mg-aminoclay attaining almost 100 % efficiency at dosages above 0.6 g/L without change of pH (Lee et al. 2013d).

Humic acid is one of the organic constituents that are easily found in soil, streams, lakes, oceans, and wastewater. Lee et al. (2014d) reported utilization of humic acid in microalgae harvesting as a way of cost reduction. When aminoclay and humic acid were used together, the same loading of Mg-aminoclay resulted in fast and effective microalgae harvesting (*Chlorella* sp.) with almost 100 % efficiency. The microalgae harvesting by humic acid/Mg-aminoclay accelerated by formation of network-like precipitants (Lee et al. 2014d).

Lee et al. (2014c) developed Mg-aminoclay/nanoscale zerovalent iron (nZVI) composites for efficient separation of *Chlorella* sp. The composites (Mg-aminoclay-coated nZVI nanoparticles) were synthesized through reduction of ferric ( $\text{Fe}^{3+}$ ) ions by sodium borohydride ( $\text{NaBH}_4$ ) in an aqueous solution containing solubilized aminoclay. The optimum ratio of aminoclay to nZVI was 1.0 among the tested ones (0–7.5); that is, at that ratio, the obtained composites showed both the smallest aggregate size (130 nm) and the highest zeta potential (~40 mV). Microalgae harvesting, furthermore, was completed within 3 min with ~100 % efficiency at a dosage of over 20 g/L. They also demonstrated the availability of aminoclay-nZVI composites for large-scale (24 L) treatment of microalgae culture.

### 4.2.3 Multifunctional Nanoparticles for Integrated Use

In the microalgae harvesting process, the use of nanoparticles incurs extra expense. Alternatively, integrated use of nanoparticles, applicable to several of the downstream stages, is a key strategy for process cost reduction. A number of groups have reported new harvesting routes that innovatively utilize nanoparticles not only in the harvesting stage but also in other downstream stages including cell disruption, lipid extraction, and oil conversion.

Lee et al. (2014b) reported aminoclay-conjugated  $\text{TiO}_2$  composites that serve both flocculation and cell-disruption roles.  $\text{TiO}_2$  nanoparticles are the most popular photocatalysts under UV-light irradiation by virtue of several benefits, namely, high photocatalytic activity, low price, superior stability, and environmental benignity. Here, hydroxyl radicals ( $\text{OH}\cdot$ ), generated from the surface of  $\text{TiO}_2$  nanoparticles in aminoclay/ $\text{TiO}_2$  composites, could attack the surfaces of microalgae and induce cell disruption. The addition of aminoclay-conjugated  $\text{TiO}_2$  composites (dosage, 3 g/L) then brought about 85 % efficient harvesting of *Chlorella* sp., 95 % of which were disrupted by simple UV irradiation at 365 nm for 3 h (Lee et al. 2014b).

Cationic, magnetic, and lipophilic microparticles (PVP/ $\text{Fe}_3\text{O}_4$  composites), noted in Sect. 4.2.1, have been synthesized through incorporation of  $\text{Fe}_3\text{O}_4$  nanoparticles into carbonaceous microparticles (Seo et al. 2015). The trifunctionality of these microparticles enables effective recovery of intracellular microalgal lipids in a simplified way, as shown in Fig. 4.3. The quaternary nitrogen species in the carbonaceous shell endows the cationic property that is capable of flocculating microalgae with 99 % efficiency. The synergetic effect of carbon functional groups (e.g., polyene, amide, carbonyl) and the surface roughness results in the lipophilic property by which extracted microalgal lipids can be adsorbed. They proved that the one-pot recovery method of microalgal lipids does not cause adverse effects on lipid quality in biodiesel production. Due to the incorporated  $\text{Fe}_3\text{O}_4$  nanoparticles, the desired components (here, microalgae and extracted lipids) could be separated quickly using an external magnetic field.

Triazabicyclodecene (TBD)-functionalized  $\text{Fe}_3\text{O}_4$ @silica core-shell nanoparticles (TBD- $\text{Fe}_3\text{O}_4$ @Silica NPs) have been prepared for harvesting of microalga (*Chlorella vulgaris*) and catalyzed transesterification reaction of algal oil (Chiang et al. 2015). For the catalytic function of the magnetic harvester

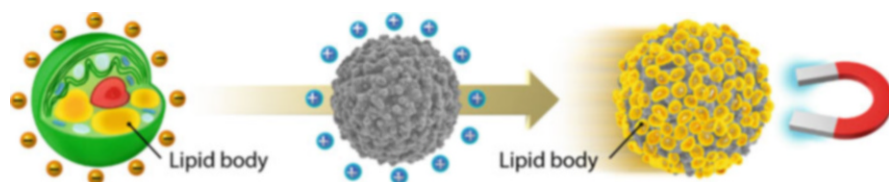


**Fig. 4.3** Schematic illustration of integrated use of trifunctional  $\text{Fe}_3\text{O}_4$ -embedded carbon microparticles. Reprinted from Seo et al. (2015). Trifunctionality of  $\text{Fe}_3\text{O}_4$ -embedded carbon microparticles in microalgal harvesting, 280:206–214, Copyright (2015), with permission from Elsevier



( $\text{Fe}_3\text{O}_4$ @silica), the TBD, as a strong base, was introduced onto the surface of  $\text{Fe}_3\text{O}_4$ @silica through the grafting of epoxysilane (trimethoxysilylpropoxymethyloxirane) onto mesoporous silica and the covalent bonding with the silanol group. Interestingly, although the zeta potential of TBD- $\text{Fe}_3\text{O}_4$ @Silica NPs showed a negative charge of  $-38$  mV, TBD- $\text{Fe}_3\text{O}_4$ @Silica NPs could harvest negatively charged microalgae. The authors explained that the approximately 1000 times difference in size (microalgae, several tens of micrometers; TBD- $\text{Fe}_3\text{O}_4$ @Silica NPs, several tens of nanometers) make microalgae harvesting possible by nanoparticle adsorption. More details on catalytic transesterification by TBD- $\text{Fe}_3\text{O}_4$ @Silica NPs will be provided in Sect. 4.4.2.

#### 4.2.4 Recyclable Nanoparticles

In the field of nanoparticle-based microalgae harvesting, recycling of nanoparticles recently has been considered as an important issue. Although a few approaches have been reported, the level of recycling technology remains at a fledgling stage. In order to recycle nanoparticles for microalgae harvesting, the necessary preliminary phase is their detachment from microalgal-particle flocs. In general, most studies have been based on pH control of the medium, which changes the surface charge potential of positively functionalized nanoparticles to negative, thereby separating them from negatively charged microalgae by electrostatic repulsion forces (Lee et al. 2014a; Seo et al. 2014). Lee et al. (2014a) demonstrated the 10 times repeated use of bare micro-sized  $\text{Fe}_3\text{O}_4$  particles by controlling to pH 2 for harvesting and to pH 12 for particle recovery. The harvesting and detaching (recovery) efficiencies were 99% and 97%, respectively. In large-scale applications, the cost of adjusting pH would be very expensive and cause environmental problems. Such concerns might be resolved to a certain extent by using exhaust  $\text{CO}_2$  flue gas to decrease pH. It has been confirmed that the re-cultured cell concentration in the used medium was similar to the case in which supernatant medium was used after centrifugation (Lee et al. 2014a).

The effect of particle size on detachment efficiency from algae-particle flocs has been investigated using size-controlled APTES-functionalized  $\text{BaFe}_{12}\text{O}_{19}$  nanoparticles (APTES; (3-aminopropyl)triethoxysilane) (Seo et al. 2014). The mechanism of harvesting and detaching could be explained by electrostatic interaction, as shown in Fig. 4.4. APTES- $\text{BaFe}_{12}\text{O}_{19}$  nanoparticles had a positive charge of 35 mV at pH 7 and a negative charge of  $-24.7$  mV at pH 12 (isoelectric point (IEP): 9.85), whereas the microalgae, *Chlorella* sp., had a negative charge throughout the pH range. Therefore, the pH of the culture medium (6.5–7) induced attachments between *Chlorella* sp. and APTES- $\text{BaFe}_{12}\text{O}_{19}$ , and the control of the pH to 12 enabled detachment of the nanoparticles from the conglomerates or particle recycling. According to this report, the detachment efficiency was increased from 12.5% at about 100 nm to 85% at about 1.2  $\mu\text{m}$ , even though the required weight of the magnetic particles was increased. As smaller  $\text{BaFe}_{12}\text{O}_{19}$

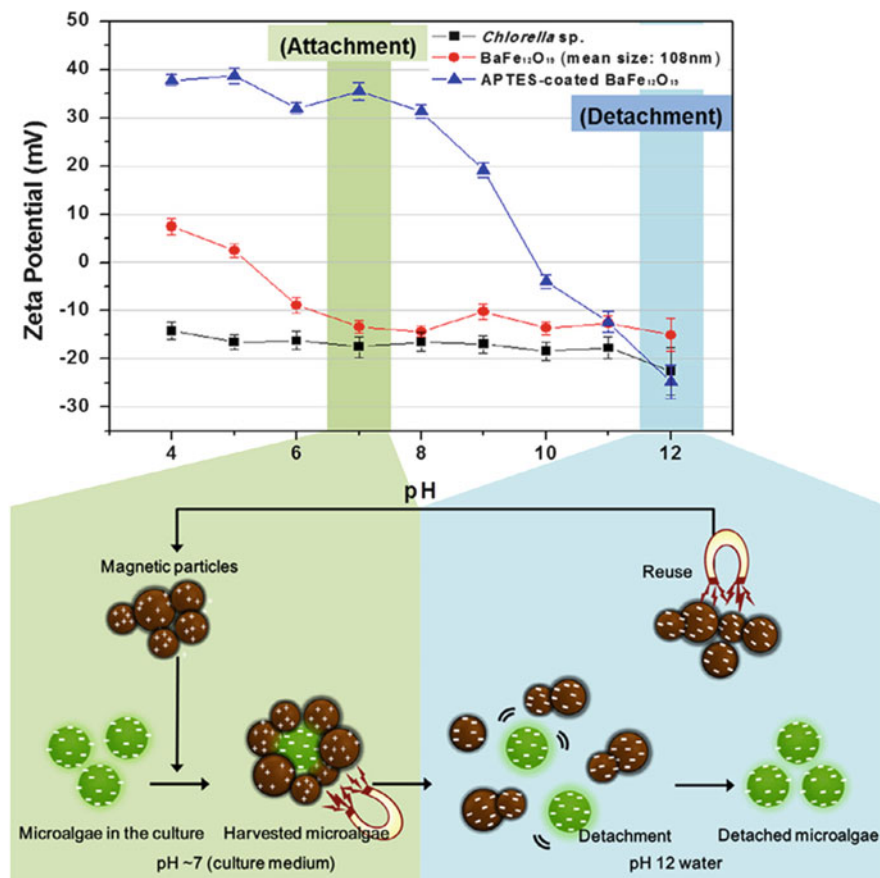


**Fig. 4.4** Schematic illustration of microalgae harvesting and sequential detachment of magnetic particles based on electrostatic interaction. Reprinted from Seo et al. (2014). Effect of barium ferrite particle size on detachment efficiency in magnetophoretic harvesting of oleaginous *Chlorella* sp., 152:562–566, Copyright (2014), with permission from Elsevier

nanoparticles form a strong binding due to the existence of more contact sites, detachment from conglomerates is more difficult with smaller  $BaFe_{12}O_{19}$  particles.

The extended Derjaguin-Landau-Verwey-Overbeek (EDLVO or XDLVO) theory has been used to interpret or predict the colloidal interaction between particles and cells (Prochazkova et al. 2013; Toh et al. 2014b; Ge et al. 2015b, c). In the first approach using the XDLVO theory, Prochazkova et al. (2013) compared their experimental results on harvesting and detachment of *C. vulgaris* with results predicted by the XDLVO theory. In addition to van der Waals attraction and electrostatic interaction, covered in the DLVO theory, the XDLVO theory explains the total interaction energy of colloidal particles in a liquid medium versus separation distance, including Lewis acid-base interaction originating from functionalized layers on nanoparticles. In the case of diethylaminoethyl (DEAE)-

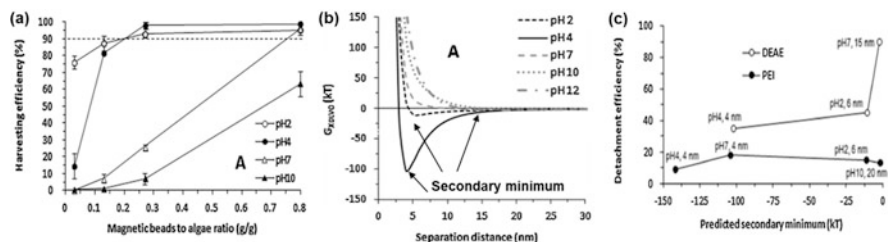


**Fig. 4.5** (a) Harvesting efficiencies of *C. vulgaris* cells at different ratios of DEAE-magnetic beads to microalgae mass in 10 mM KCl of different pH. (b) Total interaction energy ( $G_{XDLVO}$ ) as function of separation distance between *C. vulgaris* cells and DEAE-magnetic beads. (c) Detachment efficiencies versus secondary minima as predicted by XDLVO theory for interactions during harvesting. The data symbols represent the pH of the harvesting and the separation distance (nm) of the secondary minimum. The detachment experiments were carried out in 10 mM KCl at pH 12. Reprinted from Prochazkova et al. (2013), Physicochemical approach to freshwater microalgae harvesting with magnetic particles, 112:213–218. Copyright (2013), with permission from Elsevier

coated magnetic beads (0.5  $\mu\text{m}$ ), the detachment efficiency depended on harvesting conditions such as pH, as represented in Fig. 4.5. It increased rapidly to about 90 % when *C. vulgaris* was harvested by DEAE-magnetic beads at pH 7, where the secondary minimum, predicted by the XDLVO theory, had the lowest value of  $-2.3$  kT at a distance of 15 nm. Here, secondary minimum (represented by arrow) means the minimal value of total interaction energy before the high-energy barrier where the adhesion of particles and cells can be reversible. On the other hand, as the secondary minimum was deeper, *C. vulgaris* was harvested efficiently by DEAE-magnetic beads at a lower dose (Prochazkova et al. 2013).

Ge et al. (2015a) reported a chemical-free and sonication-aided method for detachment of magnetic nanoparticles (MNPs) from microalgal flocs, unlike previously reported methods using acid or base. The microalgae species *Scenedesmus dimorphus* (length,  $7.6 \pm 1.7$   $\mu\text{m}$ ; width,  $3.7 \pm 0.9$   $\mu\text{m}$ ; zeta potential,  $-29.0 \pm 1.3$  mV) was selected for harvesting and detachment experiments. The harvesting and detachment efficiencies showed particle-size-dependent behavior; the harvesting efficiency was increased gradually from 60 % at 9 nm to 85 % at 53 nm and decreased to approximately 70 % with 247 nm PEI-coated MNPs under the same dosage condition (0.075 g MNP/g cell), whereas the detachment efficiency was 72 % for 9 nm and increased to 92.6 % for 247 nm (Ge et al. 2015b), which is consistent with the previous results for differently sized APTES-BaFe<sub>12</sub>O<sub>19</sub> MNPs by Seo et al. (2014). It should be noted, however, that the harvesting efficiency of the 247 nm PEI-MNPs was about 15 % lower than that of the 53 nm versions. Furthermore, comparable levels of microalgae harvesting were accomplished by using detached PEI-MNPs, even though detached PEI-MNPs require refunctionalization with PEI. In fact, it seems that PEI coating is delaminated during harvesting and detachment (Ge et al. 2015b).

Ge et al. (2015c) also presented an intriguing method, still in the prototype stage, of recovering MNPs from algae-MNP flocs. The principle of detachment was to

control the surface wetting property from hydrophobicity to hydrophilicity. To control the surface wettability, MNPs were functionalized with hydrophobic stearic acid (SA) and composited with photocatalytic ZnO nanoparticles. Here, the ZnO nanoparticles (diameter: 50 nm) played an important role in degrading the hydrophobic SA to hydrophilic fragments such as carboxylate through the generation of reactive OH radicals under UV-light irradiation (wavelength: 365 nm). The SA-coated Fe<sub>3</sub>O<sub>4</sub>-ZnO nanocomposites achieved a detachment efficiency of around 55 % when the algae-MNP flocs were shaken rotationally and irradiated with UV light for 210 min. The XDLVO calculation supported these results indicating that the surface wettability change to hydrophilic resulted in a shift of the total interaction energy between the MNPs and algae toward the positive side, showing that the attraction between the MNPs and algae was diminished, thus enabling the MNPs' detachment (Ge et al. 2015c).

Lee et al. (2015a) have attempted to detach MNPs from algae-MNP flocs in entirely new ways. Specifically, a water-nonpolar organic solvent (NOS) interface was used as the selective sieve, which confined the hydrophilic microalgae to the water phase, and the external magnetic field applied from the side of the NOS phase caused the lipophilicity-controlled MNPs to migrate to the NOS phase. To obtain desirable positive charge and lipophilicity of MNPs, (3-aminopropyl) triethoxysilane (APTES) and octyltriethoxysilane (OTES) were used, respectively, the ratio of APTES having been set to 35 % of the total silane (APTES/(APTES + OTES) = 0.35). The dually functionalized magnetic nanoparticles (dMNPs) achieved a harvesting efficiency of 98.5 % at a dosage of 1.6 g dMNP/g cell. After harvesting of *Chlorella* sp. with the above-noted dosage, microalgae (or dMNPs) were recovered at 68 %, 79 %, and 83 % efficiency by using dichloromethane (DCM), hexane, and dodecane, in order. The microalgae culture concentration was increased from ~1.5 g/L to ~60 g/L through the harvesting and detachment process using the dMNPs and the water-NOS interface (Lee et al. 2015a).

### 4.3 Nanoparticle-Aided Lipid Extraction

Lipid extraction from microalgae is considered to be particularly difficult due to the rigid cell walls, unlike typical lipid extraction from terrestrial oil crops. The degradation of rigid structures, unfortunately, requires either an energy-intensive pretreatment process or the use of highly toxic organic solvents, which are viewed to be obstructive factors to the commercial viability of microalgal biofuel (Johnson and Wen 2009; Lee et al. 2015b; Kim et al. 2016). Traditionally, most microalgal lipid extraction methods rely on solvent extraction methods, which are modified and improved methods starting from the Folch method and the Bligh and Dyer method in the 1950s (Ranjith Kumar et al. 2015). Some mechanical approaches using expeller press, bead beating, ultra-sonication, and microwave have been suggested to assist lipid extraction, but these methods are accompanied by

significant energy consumption and capital cost or concerns about deterioration of target components (Lee et al. 2010; Mercer and Armenta 2011; Ranjith Kumar et al. 2015). Up to now, it is hard to find a single lipid extraction method satisfying all following features: efficiency and quality of extracted lipid, process cost, energy consumption, environmental effect, and scalability. Lately, a few attempts utilizing nanoparticles have been made, which have marginally improved the lipid extraction process. In fact, considering the existing lipid extraction technology, the lipid extraction process leaves much room for improvement by application of nanoparticles. For example, dielectric, hard, spinose, magnetic, and enzymatic nanomaterials have been applied to aid lipid extraction from microalgae.

### 4.3.1 Aminoclay-Based Lipid Extraction

A few types of aminoclay nanoparticles, such as Mg-APTES clay, Al-APTES clay, Ca-APTES clay, and Mg-N3 clay, introduced as flocculants for microalgae harvesting in Sect. 4.2.2, have had positive impacts on lipid extraction yield, FAME (fatty acid methyl ester) content, and FAME productivity (Lee et al. 2013b). The postulated mechanism proceeds as follows: solubilized aminoclays, especially amino groups, cause destabilization of cell walls (not denoted as cell disruption) and, subsequently thereby, enhance lipid extraction yields from wet microalgal biomass. Docosahexaenoic acid (DHA)-rich *Chlorella* sp. and oleaginous *Chlorella* sp. KR-1, with 87.6 and 330.2 mg FAME/g cell, respectively, have been selected as species models for microalgal lipid extraction. The lipid extraction yield and FAME productivity were examined as a function of Mg-APTES clay dosage, showing the requirement of 10–20 % Mg-APTES clay over dry cell weight for both microalgae. Significantly, the achieved efficiency of the conversion of extracted lipid oils to FAME, in the case of *Chlorella* sp. KR-1, was almost 100 %. Among the four types of aminoclays, Al-APTES clay showed the superior FAME productivity from *Chlorella* sp. KR-1 (105 mg FAME/g cell), followed by Mg-APTES clay (90 mg FAME/g cell). Lee et al. (2013c) suggested a Fenton-like reaction of Fe-APTES clay, Mn-APTES clay, and Cu-APTES clay to assist lipid extraction. In this process, cationic ions such as  $\text{Fe}^{3+}$ ,  $\text{Mn}^{2+}$ , and  $\text{Cu}^{2+}$  allowed the activation of hydrogen peroxide ( $\text{H}_2\text{O}_2$ ) to hydroxyl radical ( $\text{OH}\cdot$ ), similarly to the Fenton reaction, and the generated hydroxyl radicals ( $\text{OH}\cdot$ ) gave rise to cell-wall damage and consequent effective release of internal lipids from wet microalgae, as shown in Fig. 4.6. Fe-APTES clays with 5 %  $\text{H}_2\text{O}_2$  attained the lipid extraction efficiency of 30.74 %, a level similar to the lipid content in oleaginous *Chlorella* sp. KR-1 and also higher than the case of only 5 %  $\text{H}_2\text{O}_2$  addition without clays (25.63 %) (Lee et al. 2013c). Further, composites of aminoclay and  $\text{TiO}_2$  have been utilized as cell-disruption agents through photocatalytic reaction of UV-irradiated  $\text{TiO}_2$ , as discussed in Sect. 4.2.3 (Lee et al. 2014b).

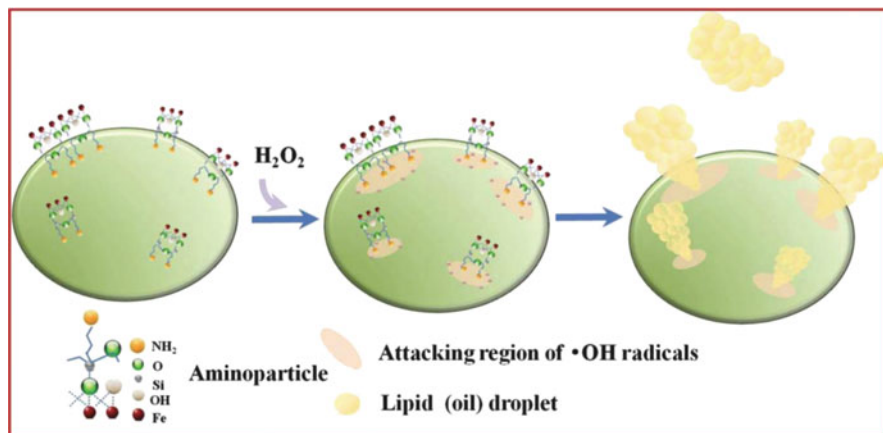


**Fig. 4.6** Schematic illustration of microalgal cell-wall damage by OH radical attacks in the presence of  $H_2O_2$ , with surrounding aminoparticles. Reproduced from Lee et al. (2013c) with permission from The Royal Society of Chemistry, Copyright (2013)

### 4.3.2 Potential Engineered Nanoparticles

With advanced nanotechnology, nanoparticles could be engineered with various functionalizing materials to disrupt rigid cell walls or to enhance lipid extraction efficiency. For example, surfactant-functionalized or enzyme-functionalized nanoparticles have a potential to be utilized in lipid extraction processes including pretreatment. Surfactants are known to be antimicrobial and biotoxic and, as such, have been applied for inhibition of the growth of microorganisms such as microalgae and bacteria (Coward et al. 2014; Mohareb et al. 2015). Among surfactants, a cationic surfactant, especially quaternary ammonium compound, not only is endowed with superior biocidal activity but also is relatively harmless to the environment and less irritative to the skin (Mohareb et al. 2015). According to Coward et al. (2014), CTAB-aided foam floatation (CTAB; cetyltrimethylammonium bromide) enhanced the amount of extractable lipid from *Chlorella* sp. through adsorption onto the cell surface during harvesting. This successful outcome was owed to the fact that CTAB causes solubilization of the phospholipid bilayer. Moreover, CTAB-aided foam floatation resulted in higher percentages of monounsaturated fatty acids and saturated fatty acids, which are beneficial to the quality standards of biodiesel (e.g., FAME content, diesel's energy yield, cetane #, and oxidative stability). The effect of CTAB on cell deterioration has also been confirmed by another group (Huang and Kim 2013). In their study, CTAB simultaneously enabled harvesting and cell-wall disruption of microalgae. The extracted FAME from the microalgal biomass (~50 mg) harvested and disrupted by CTAB was about 6.34 mg. In this context, our group is working on developing CTAB-decorated MNPs for effective cell-wall disruption.

There have been reports that enzyme pretreatment enables an increase in lipid extraction yield and FAME productivity from wet microalgal biomass. Enzymes such as cellulases (Celluclast 1.5 L) and  $\beta$ -glucosidases (Novozyme 188) could hydrolyze glucan to glucose and then increase the lipid extraction yield from wet *Chlorella vulgaris* by 29.2–73.1% and the FAME productivity by 10.1–68.9% (Cho et al. 2013). The enzymatic hydrolysis yield showed a maximum under the pH 4.8, temp. 50 °C, and incubation time 72 h conditions. Enzyme effectiveness on lipid extraction from *Scenedesmus* sp. also was confirmed by Taher et al. (2014), wherein lysozyme from chicken egg white and cellulase from *Trichoderma longibrachiatum* were used to reduce the rigidity of cell walls. Lysozyme treatment for 30 min at 37 °C helped to achieve a lipid extraction yield of 16.6%, while the total lipid content obtained from the lyophilized *Scenedesmus* sp. cells by the soxhlet extraction method was 21.1% (Taher et al. 2014). The above results suggest that cell-wall disruption using enzymes diminishes the need of a costly drying process. Indeed, in this regard, enzyme-functionalized nanoparticles are expected to improve the efficiency of the lipid extraction process. In two recent studies, lipase from the bacterium *Burkholderia* sp. was immobilized on alkyl-grafted  $\text{Fe}_3\text{O}_4@\text{SiO}_2$  nanoparticles using dimethyloctadecyl[3-(trimethoxysilyl)propyl] ammonium chloride as a linker (Tran et al. 2012, 2013). Those nanoparticles were used as biocatalysts for conversion of microalgal oil to biodiesel, not as accelerators for cell-wall disruption and lipid extraction. This immobilized lipase accomplished the direct transesterification from ultrasonicated wet microalgal biomass (*C. vulgaris* ESP-31), even with a high water content (>71.4%), while attaining a FAME productivity of 97.3 wt% oil or 58.3 wt% cell. This means that downstream stages such as biomass dry and oil extraction can be skipped by applying immobilized biocatalysts for biodiesel production (Tran et al. 2012).

#### 4.4 Nanoparticle-Aided Conversion of Oil to Biodiesel

The conversion to biodiesel (fatty acid methyl ester [FAME] or diesel-range alkanes) from extracted microalgal oil is the final downstream process in microalgae-based biorefinery (Pienkos and Darzins 2009). Many kinds of nanostructured catalysts for conversion of lipid to biodiesel have been developed during the last few years (Hara 2010; Sani et al. 2013). Extensive research on the catalytic conversion of microalgal oil has begun from the basic idea of terrestrial oil's conversion. Conventionally, homogeneous catalysts such as acids (e.g.,  $\text{H}_2\text{SO}_4$ , HCl) and bases (e.g., NaOH, KOH) are used for esterification and transesterification, respectively, but there are accompanying environmental and economic issues such as wastewater neutralization, catalyst recycling problems, and expensive corrosion-resistant equipment (Lam and Lee 2012; Chiang et al. 2015). To resolve these issues, research on heterogeneous solid catalysts as alternatives is being carried out vigorously, since they can be easily recovered for recycling and, thus, are considered to offer enhanced cost and environmental

acceptability (Carrero et al. 2011; Lam and Lee 2012). Furthermore, an added advantage is that the conversion yield and selectivity can be manipulated with tailored catalyst designs. Variables including catalyst formulation and content, alcohol-to-oil ratio, temperatures, pressures, and reaction time determine the possible reaction pathways for conversion of microalgal oil (Vyas et al. 2010; Zhao et al. 2013). Recently, hydrotreatment with sulfided catalysts or decarboxylation and decarbonylation with supported noble metal catalysts has been suggested for upgrading to high-grade fuels (e.g., C<sub>15</sub>–C<sub>18</sub> alkanes) (Peng et al. 2012a; Kandel et al. 2013; Zhao et al. 2013).

#### 4.4.1 Acid Nanocatalyst

Compared with microporous crystalline zeolites, hierarchical nanocrystalline zeolite endows a high external surface area with a bimodal porosity, which allows large molecules such as microalgal oil an increased accessibility to acid sites. The hierarchical nanocrystalline ZSM-5 and beta (hereafter denoted HZSM-5 and HBeta, respectively) have been explored for application to the conversion of *Nannochloropsis* oil (Carrero et al. 2011). As shown in Table 4.2, the FAME yield was much higher in HBeta (ca. 25 wt%) than in HZSM-5 (ca. 2 wt%), though the HBeta yield was significantly lower than that of homogeneous H<sub>2</sub>SO<sub>4</sub> (90 wt%). The lower yield in HZSM-5 was attributed to the narrow pores of HZSM-5 restricting the access of reactant oil. Moreover, it is worthy of note that the reaction temperature and pressure for catalytic conversion were mild considering the typical reaction conditions for solid acid catalysts (Carrero et al. 2011). The crude oil of *Nannochloropsis* sp. obtained through hydrothermal liquefaction was treated hydrothermally over HZSM-5, resulting in a great drop in the content of heteroatom (N, O, and S) (Li and Savage 2013). The reaction temperature was one of the major factors affecting the composition and yield of the treated oil. Catalytic treatment at 400 °C generated a paraffinic oil of 75 wt% suitable for liquid transportation fuels, while treatment at 500 °C generated an aromatic hydrocarbon oil of 44 wt% and a hydrocarbon gas stream of 19 wt%.

Sulfonated carbon-based catalyst is one of the promising solid acid catalysts, as it contains highly acidic functional groups such as –SO<sub>3</sub>H, –COOH, and phenolic –OH (Hara 2010; Fu et al. 2013; Sani et al. 2013). The catalytic performance of amorphous carbon-based catalysts is about 60 % of the performance obtained by homogeneous H<sub>2</sub>SO<sub>4</sub> and is superior to conventional solid acid catalysts (e.g., Amberlyst-15, Nafion NR50, and niobic acid) (Sani et al. 2013). Fu et al. (2013) introduced a microalgae-residue-based carbon catalyst (denoted MBC catalyst) synthesized through in situ partial carbonization and sulfonation under the hydrothermal conditions. They applied this MBC catalyst to the esterification of oleic acid and the transesterification of triolein in the presence of methanol. It showed an approximately 1.15 times higher conversion of esterification and a 3 times higher transesterification yield than the ion-exchange resin Amberlyst-15. The high



**Table 4.2** Catalytic conditions and performances of various acid and base nanocatalysts

Catalyst	Loading	Feedstock oil	Temp. (°C)	Time (h)	Pressure	Alcohol-to-oil molar ratio	Conversion yield (wt%)	Ref.
HBeta HZSM-5	2 wt% of oil +methanol feed	<i>Nannochloropsis gaditana</i> oil	115	4	Autogenous pressure in the autoclave	100	ca. 25 % (FAME) ca. 2 % (FAME)	Carrero et al. (2011)
		Oleic acid Triolein	80	12	–	10 30	98 % (esterification) 24 % (transesterification)	
CBMM's HY-340 (Nb <sub>2</sub> O <sub>5</sub> )	10 %	<i>Monoraphidium contortum</i> oil	200	1	Autoclave	30	94.27 % (FAME)	Hara (2010)
		<i>Nannochloropsis oculata</i>	60	19	Atmospheric	600	~17 %	Velasquez-Orta et al. (2013)
SA-SBA-15-p	2–3 wt% of reaction mixture	Lauric acid/ palmitic acid	50 & 60	35	Atmospheric	ca. 5	~100 %	Chen et al. (2011)
		<i>Nannochloropsis oculata</i> oil	50	4	–	30	97.5 % (biodiesel)	Umdu et al. (2009)
80 wt% CaO/Al <sub>2</sub> O <sub>3</sub>	2 wt% of oil	<i>Nannochloropsis oculata</i> oil	50	4	–	6	16 % (biodiesel)	Umdu et al. (2009)
		<i>Nannochloropsis oculata</i> oil	60	3	–	60	85.3 % (FAME)	Teo et al. (2014)
CaMgO	20 wt% of oil						75.5 % (FAME)	

Mg-Zr catalyst	10 wt% of dried biomass	<i>Nannochloropsis</i> sp.	65	4	–	–	28 % (FAME)	Li et al. (2011)
TBD-Fe <sub>3</sub> O <sub>4</sub> @SiO <sub>2</sub>	32.5 mg	Dried algae ( <i>C. vulgaris</i> )	65	2	–	1 mL MeOH/ 2.5 mg dried algae	6.7 % (FAME)	Chiang et al. (2015)

catalytic activity of the MBC catalyst could be explained by synergistic reasons such as the high density of acidic  $-\text{SO}_3\text{H}$ , the good accessibility to active sites, the strong affinity between reactants and catalysts, and the desirable dispersion in methanol.

In the hydroesterification process, a serial reaction of hydrolysis and esterification, niobium oxide (CBMM's HY-340) was used as the catalyst under the conditions described in Table 4.2. The wet microalgal biomass (*Monoraphidium contortum*) was subjected to in situ hydrolysis reaction, resulting in the obtainment of fatty acids without incurring of high cost or an energy-intensive process such as lyophilization and oil extraction. The FAME yield of niobium-oxide-catalyzed esterification was as high as 94.27 %. In addition to the above-described catalysts, some catalysts such as molecular-sieve zeolites and sulfonic acid-functionalized platelet SBA-15(SA-SBA-15-p) have been used in biodiesel production; their catalytic performances are summarized in Table 4.2 (Chen et al. 2011; Velasquez-Orta et al. 2013).

#### 4.4.2 Base Nanocatalyst

Base catalysts allow significantly faster transesterification of microalgal oil than do acid catalysts (Carrero et al. 2011). However, feedstock oils for base catalysts are limited to refined oils with low contents of free fatty acid (FFA, below 0.5 wt%), because the presence of FFA causes an undesirable soap formation from FFA (Sharma et al. 2008; Vyas et al. 2010; Kandel et al. 2013). In case of feedstock oil with a low amount of FFA, basic catalysts are most effective for the transesterification reaction (Umdu et al. 2009; Park et al. 2015). The solid base catalysts first applied to the transesterification of microalgal oil (*Nannochloropsis oculata* oil) were  $\text{Al}_2\text{O}_3$ -supported CaO and  $\text{Al}_2\text{O}_3$ -supported MgO. While pure CaO or pure MgO could not convert microalgal oil to biodiesel, 80 % CaO-loaded  $\text{Al}_2\text{O}_3$  and 80 % MgO-loaded  $\text{Al}_2\text{O}_3$  achieved enhanced conversion yields of 23 % and 16 %, respectively (Umdu et al. 2009). Very interestingly, the change in the methanol-to-oil ratio from 6:1 to 30:1 led to a very steep biodiesel yield increase, from 23 to 97.5 %. The conversion yield was affected not only by basicity but also by the basic strength of the catalyst. Teo et al. (2014) investigated the effect of reaction parameters on transesterification of *N. oculata* oil by CaMgO or CaMgO/ $\text{Al}_2\text{O}_3$  catalysts; the parameters included the methanol-to-oil molar ratio, the reaction time and temperature, the catalyst loading, and the presence of an  $\text{Al}_2\text{O}_3$ -support matrix. The  $\text{Al}_2\text{O}_3$ -supported CaMgO catalysts showed the highest FAME yield of 85.3 % when loaded up to 10 % (based on the weight of oil), and the transesterification reaction was conducted at 60 °C for 3 h (Teo et al. 2014). Unlike the basic CaMgO catalysts, the  $\text{Al}_2\text{O}_3$ -supported CaMgO catalysts were less sensitive to moisture in microalgal oil and showed a higher density of basic sites. Heterogeneous base Mg-Zr catalysts have been used to directly convert microalgal biomass *Nannochloropsis* sp. to biodiesel (Li et al. 2011). This direct

transesterification method using 10 wt% Mg-Zr catalysts (based on dried biomass) attained a FAME yield of 28 % while extracting microalgal lipid with an organic solvent mixture (methanol/methylene dichloride:3/1, v/v).

As addressed in Sect. 4.2.3, Chiang et al. (2015) developed a new type of solid base catalyst through attachment of triazabicyclodecene (as a strong base) to the surfaces of  $\text{Fe}_3\text{O}_4/\text{SiO}_2$  core-shell nanoparticles (hereafter denoted TBD- $\text{Fe}_3\text{O}_4@/\text{SiO}_2$  NPs). Owing to the magnetism of the core  $\text{Fe}_3\text{O}_4$  and the catalytic function of the shell TBD, TBD- $\text{Fe}_3\text{O}_4@/\text{SiO}_2$  NPs could be applied to two steps, harvesting and transesterification. For microalgae oil (*C. vulgaris*) without FFA, a significantly high FAME yield (97.1 %) was attained by using these TBD- $\text{Fe}_3\text{O}_4@/\text{SiO}_2$  NPs, which yield is superior to those of commercially available catalysts such as  $\text{H}_2\text{SO}_4$ ,  $\text{AlCl}_3$ , Amberlyst-15, and  $\text{CuCl}_2$ .

### 4.4.3 Nanocatalysts for Greener Biodiesel

The need and desire for greener biodiesel has grown in importance with tightening international standards. The first-generation biodiesel, FAME, is produced via transesterification reaction of triglycerides with alcohol with the aid of catalysts (Park et al. 2015). However, the FAMEs are relatively poor in terms of their cold-flow property storage stability and engine compatibility, due to the high oxygen contents and unsaturation. For that reason, recent and various biodiesel upgrades have been attempted (Shim et al. 2014, 2015). The sulfided Co-Mo-, Ni-Mo-, and Ni-W-based catalysts have been used for hydrotreatment of vegetable oils (Kumar et al. 2010; Peng et al. 2012a); however, issues such as product contamination and catalyst deactivation via sulfur leaching remain. Alternatively, FFA deoxygenation has been performed using supported noble metal catalysts (e.g., Pt, Pd), though at increased cost (Immer et al. 2010).

Peng et al. (2012a) developed, for the first time, Ni-supported zeolites for conversion of microalgal oil to diesel-range alkanes. Herein, Ni facilitated some reactions including hydrogenolysis of TAG (triacylglycerol), decarbonylation of aldehyde intermediates, and hydrogenation of carboxylic acids, aldehydes, and alkenes. Meanwhile, the acidic zeolites promoted the formation of alkenes or isomers and lighter alkanes through dehydration or isomerization and cracking, respectively. When 5 wt% Ni was loaded onto the zeolite (HBeta), the Si/Al molar ratio was 75, and the yield of diesel-range alkanes, composed of 82 %  $\text{C}_{18}$  and 18 %  $\text{C}_{17}$ , was 96 %. This result means that the cracking of intermediates by Ni/HBeta was almost minimized. On the other hand, Ni/ZSM-5 led to much more cracking, which was attributed to the longer residence time inside the narrower pores of HZSM-5. Additionally, the isomerized alkanes content decreased with the increased Si/Al molar ratio.

In further research, the same group reported on ZrO<sub>2</sub>-promoted Ni catalysts for conversion of microalgal oil to diesel-range hydrocarbons (Peng et al. 2012b). In a search for a suitable support material, various metal oxides including SiO<sub>2</sub>, TiO<sub>2</sub>,

CeO<sub>2</sub>, Al<sub>2</sub>O<sub>3</sub>, and ZrO<sub>2</sub> were tested with stearic acid. Among the explored support materials, ZrO<sub>2</sub> showed the highest conversion (~100 %) and selectivity for n-C<sub>17</sub> alkanes (96 %). At 270 °C and 40 bar H<sub>2</sub>, Ni/ZrO<sub>2</sub> catalysts transformed microalgal oil to liquid alkanes with 76 % conversion efficiency and 68 % selectivity for n-heptadecane(C<sub>17</sub>).

The introduction of an adsorbent group, aminopropyl, to Ni-impregnated mesoporous silica nanoparticles (Ni-MSN) changed the catalytic selectivity for favored reaction from hydrocracking to hydrotreating. Aminopropyl-functionalized Ni-MSN (AP-Ni-MSN) catalysts allowed about a fourfold increase in octadecane yield (~13 %) compared with Ni-MSN catalysts (~3 %) (Kandel et al. 2013). Furthermore, aminopropyl groups enabled the selective adsorption of FFAs, thereby increasing the yield of octadecane to 43 % via sequential batch reaction (preloading of oleate prior to hydrodeoxygenation). Also, AP-Ni-MSN was demonstrated to selectively adsorb FFAs in crude oil, meaning that the available range of feedstock oil could be broadened to FFA-rich feedstocks. The successful catalytic performance of Ni has arisen considerable research interest in the development of inexpensive and multifunctional nanocatalysts. As an attractive candidate, supported iron nanoparticles (Fe-MSN) have shown very superior selectivity for hydrodeoxygenation over decarbonylation. Fe-MSN catalyst enables conversion of oleic acid to n-octadecane (C<sub>18</sub>) and n-heptadecane (C<sub>17</sub>) with selectivities of 83 % and 12 %, respectively (Kandel et al. 2014). It is noteworthy that Fe-MSN catalyst has been demonstrated to achieve almost perfect upgrading of fatty acids to diesel-range alkanes, while the abovementioned Ni-MSN catalysts led to the formation of 25 % n-heptadecane (C<sub>17</sub>) and 3 % n-octadecane (C<sub>18</sub>). Detailed information on heterogeneous catalysts for high-quality biodiesel is summarized in Table 4.3.

## 4.5 Conclusion

Throughout this chapter, we have reviewed the various nanoparticle-aided approaches to the enhancement of process efficiency, and ultimately thereby, increased microalgal biodiesel productivity. The merging of microalgal biorefinery with nanoparticle technology has led to breakthroughs from the viewpoint of microalgae harvesting efficiency, lipid extraction yield, conversion yield, and selectivity for green diesel. Furthermore, bifunctional or trifunctional nanoparticles could be utilized to integrate the complicated and fragmented downstream processes for obtainment of the end product, biodiesel, thereby resulting in cost savings in microalgal biorefinery. In its present state, microalgae-based biodiesel is inferior to fossil- or terrestrial-biomass-based biodiesels in price competitiveness. Resolution of the remaining economic and technological issues and problems surrounding microalgal biorefinery will require further active exploration of novel nanoparticles.

**Table 4.3** Production of high-quality biodiesels using different heterogeneous nanocatalysts

Catalyst	Loading	Feedstock oil	Temp. (°C)	Time (h)	Pressure	Selectivity	Ref.
HZSM-5	50 wt%	Crude oil of <i>Nannochloropsis</i> sp. (hydrothermal liquefaction)	400	4	4.35 MPa=43.5 bar	Oil ~ 75 % Solid ~ 16.2 % Gas ~ 8.8 %	Li and Savage (2013)
Ni/ HZSM-5	20 wt%	Stearic acid	260	8	40 bar H <sub>2</sub>	n-C <sub>18</sub> 41.1 % iso-C <sub>18</sub> 6.3 % n-C <sub>17</sub> 9.2 % iso-C <sub>17</sub> 0.4 % Cracking 42.7 %	Peng et al. (2012a)
		Stearic acid				n-C <sub>18</sub> 82.8 % iso-C <sub>18</sub> 6.0 % n-C <sub>17</sub> 10.2 % iso-C <sub>17</sub> 0.2 % Cracking 0.4 %	
Ni/ZrO <sub>2</sub>	50 wt%	Microalgal oil (or stearic acid)	270	8	40 bar H <sub>2</sub>	n-C <sub>17</sub> 68 % (liquid alkane 76 %)	Peng et al. (2012b)
AP-Ni-MSN	10 mg/1 mM OA in hexane (10 mL)	Oleic acid (OA)	290	6	30 bar H <sub>2</sub>	C <sub>18</sub> (hydrodeoxygenation) 43 % C <sub>17</sub> (decarbonylation) 49 % Cracking 8 %	Kandel et al. (2013)
		Oleic acid (OA)	290	6	30 bar H <sub>2</sub>	C <sub>18</sub> (hydrodeoxygenation) 83 % C <sub>17</sub> (decarbonylation) 12 % Cracking 5 %	

**Acknowledgment** This study was conducted within the framework of the Research and Development Program of the Korea Institute of Energy Research (KIER) (B6-2444). Further support was received from the Advanced Biomass R&D Center (ABC) of the Global Frontier Project funded by the Ministry of Science, ICT and Future Planning (ABC-2012M3A6A205388), the Korea Institute of Energy Technology Evaluation and Planning (KETEP), and the Ministry of Knowledge Economy (MKE) of Korea as part of the “Process demonstration for bioconversion of CO<sub>2</sub> to high-valued biomaterials using microalgae” (20152010201900) project of the “Energy Efficiency and Resources R&D project.” Some part of this chapter is presented Ph.D. dissertation of the first author.

## References

- Borlido L, Azevedo A, Roque A, Aires-Barros M (2013) Magnetic separations in biotechnology. *Biotechnol Adv* 31(8):1374–1385
- Brentner LB, Eckelman MJ, Zimmerman JB (2011) Combinatorial life cycle assessment to inform process design of industrial production of algal biodiesel. *Environ Sci Technol* 45(16):7060–7067
- Carrero A, Vicente G, Rodríguez R, Linares M, Del Peso G (2011) Hierarchical zeolites as catalysts for biodiesel production from *Nannochloropsis* microalga oil. *Catal Today* 167(1):148–153
- Chen S-Y, Yokoi T, Tang C-Y, Jang L-Y, Tatsumi T, Chan JC, Cheng S (2011) Sulfonic acid-functionalized platelet SBA-15 materials as efficient catalysts for biodiesel synthesis. *Green Chem* 13(10):2920–2930
- Chiang YD, Dutta S, Chen CT, Huang YT, Lin KS, Wu J, Suzuki N, Yamauchi Y, Wu KCW (2015) Functionalized Fe<sub>3</sub>O<sub>4</sub>@ silica core-shell nanoparticles as microalgae harvester and catalyst for biodiesel production. *ChemSusChem* 8(5):789–794
- Cho S, Lee D, Luong TT, Park S, Oh Y-K, Lee T (2011) Effects of carbon and nitrogen sources on fatty acid contents and composition in the green microalga, *Chlorella* sp. 227. *J Microbiol Biotechnol* 21(10):1073–1080
- Cho H-S, Oh Y-K, Park S-C, Lee J-W, Park J-Y (2013) Effects of enzymatic hydrolysis on lipid extraction from *Chlorella vulgaris*. *Renew Energy* 54:156–160
- Christensen L, Sims R (2011) Production and harvesting of microalgae for wastewater treatment, biofuels, and bioproducts. *Biotechnol Adv* 29(6):686–702
- Coward T, Lee JG, Caldwell GS (2014) Harvesting microalgae by CTAB-aided foam flotation increases lipid recovery and improves fatty acid methyl ester characteristics. *Biomass Bioenergy* 67:354–362
- Farooq W, Lee Y-C, Han J-I, Darpito CH, Choi M, Yang J-W (2013) Efficient microalgae harvesting by organo-building blocks of nanoclays. *Green Chem* 15(3):749–755
- Fu X, Li D, Chen J, Zhang Y, Huang W, Zhu Y, Yang J, Zhang C (2013) A microalgae residue based carbon solid acid catalyst for biodiesel production. *Bioresour Technol* 146:767–770
- Ge S, Agbakpe M, Wu Z, Kuang L, Zhang W, Wang X (2015a) Influences of surface coating, UV irradiation and magnetic field on the algae removal using magnetite nanoparticles. *Environ Sci Technol* 49(2):1190–1196
- Ge S, Agbakpe M, Zhang W, Kuang L (2015b) Heteroaggregation between PEI-coated magnetic nanoparticles and algae: effect of particle size on algal harvesting efficiency. *ACS Appl Mater Interfaces* 7(11):6102–6108
- Ge S, Agbakpe M, Zhang W, Kuang L, Wu Z, Wang X (2015c) Recovering magnetic Fe<sub>3</sub>O<sub>4</sub>-ZnO nanocomposites from algal biomass based on hydrophobicity shift under UV irradiation. *ACS Appl Mater Interfaces* 7(21):11677–11682
- Hara M (2010) Biomass conversion by a solid acid catalyst. *Energy Environ Sci* 3(5):601–607

- Hu Y-R, Guo C, Wang F, Wang S-K, Pan F, Liu C-Z (2014) Improvement of microalgae harvesting by magnetic nanocomposites coated with polyethylenimine. *Chem Eng J* 242:341–347
- Huang W-C, Kim J-D (2013) Cationic surfactant-based method for simultaneous harvesting and cell disruption of a microalgal biomass. *Bioresour Technol* 149:579–581
- Immer JG, Kelly MJ, Lamb HH (2010) Catalytic reaction pathways in liquid-phase deoxygenation of C18 free fatty acids. *Appl Catal A* 375(1):134–139
- Johnson MB, Wen Z (2009) Production of biodiesel fuel from the microalga *Schizochytrium limacinum* by direct transesterification of algal biomass. *Energy Fuels* 23(10):5179–5183
- Kandel K, Frederickson C, Smith EA, Lee Y-J, Slowing II (2013) Bifunctional adsorbent-catalytic nanoparticles for the refining of renewable feedstocks. *ACS Catal* 3(12):2750–2758
- Kandel K, Anderegg JW, Nelson NC, Chaudhary U, Slowing II (2014) Supported iron nanoparticles for the hydrodeoxygenation of microalgal oil to green diesel. *J Catal* 314:142–148
- Kim D-Y, Vijayan D, Praveenkumar R, Han J-I, Lee K, Park J-Y, Chang W-S, Lee J-S, Oh Y-K (2016) Cell-wall disruption and lipid/astaxanthin extraction from microalgae: *Chlorella* and *Haematococcus*. *Bioresour Technol* 199:300–310
- Kumar R, Rana BS, Tiwari R, Verma D, Kumar R, Joshi RK, Garg MO, Sinha AK (2010) Hydroprocessing of jatropha oil and its mixtures with gas oil. *Green Chem* 12(12):2232–2239
- Lam MK, Lee KT (2012) Microalgae biofuels: a critical review of issues, problems and the way forward. *Biotechnol Adv* 30(3):673–690
- Lee J-Y, Yoo C, Jun S-Y, Ahn C-Y, Oh H-M (2010) Comparison of several methods for effective lipid extraction from microalgae. *Bioresour Technol* 101(1):S75–S77
- Lee K, Lee SY, Na J-G, Jeon SG, Praveenkumar R, Kim D-M, Chang W-S, Oh Y-K (2013a) Magnetophoretic harvesting of oleaginous *Chlorella* sp. by using biocompatible chitosan/magnetic nanoparticle composites. *Bioresour Technol* 149:575–578
- Lee Y-C, Huh YS, Farooq W, Chung J, Han J-I, Shin H-J, Jeong SH, Lee J-S, Oh Y-K, Park J-Y (2013b) Lipid extractions from docosahexaenoic acid (DHA)-rich and oleaginous *Chlorella* sp. biomasses by organic-nanoclays. *Bioresour Technol* 137:74–81
- Lee Y-C, Huh YS, Farooq W, Han J-I, Oh Y-K, Park J-Y (2013c) Oil extraction by aminoparticle-based H<sub>2</sub>O<sub>2</sub> activation via wet microalgae harvesting. *RSC Adv* 3(31):12802–12809
- Lee Y-C, Kim B, Farooq W, Chung J, Han J-I, Shin H-J, Jeong SH, Park J-Y, Lee J-S, Oh Y-K (2013d) Harvesting of oleaginous *Chlorella* sp. by organoclays. *Bioresour Technol* 132:440–445
- Lee K, Lee SY, Praveenkumar R, Kim B, Seo JY, Jeon SG, Na J-G, Park J-Y, Kim D-M, Oh Y-K (2014a) Repeated use of stable magnetic flocculant for efficient harvest of oleaginous *Chlorella* sp. *Bioresour Technol* 167:284–290
- Lee Y-C, Lee HU, Lee K, Kim B, Lee SY, Choi M-H, Farooq W, Choi JS, Park J-Y, Lee J (2014b) Aminoclay-conjugated TiO<sub>2</sub> synthesis for simultaneous harvesting and wet-disruption of oleaginous *Chlorella* sp. *Chem Eng J* 245:143–149
- Lee Y-C, Lee K, Hwang Y, Andersen HR, Kim B, Lee SY, Choi M-H, Park J-Y, Han Y-K, Oh Y-K (2014c) Aminoclay-templated nanoscale zero-valent iron (nZVI) synthesis for efficient harvesting of oleaginous microalga, *Chlorella* sp. KR-1. *RSC Adv* 4(8):4122–4127
- Lee Y-C, Oh SY, Lee HU, Kim B, Lee SY, Choi M-H, Lee G-W, Park J-Y, Oh Y-K, Ryu T (2014d) Aminoclay-induced humic acid flocculation for efficient harvesting of oleaginous *Chlorella* sp. *Bioresour Technol* 153:365–369
- Lee K, Na J-G, Seo JY, Shim TS, Kim B, Praveenkumar R, Park J-Y, Oh Y-K, Jeon SG (2015a) Magnetic-nanoflocculant-assisted water–nonpolar solvent interface sieve for microalgae harvesting. *ACS Appl Mater Interfaces* 7(33):18336–18343
- Lee Y-C, Lee K, Oh Y-K (2015b) Recent nanoparticle engineering advances in microalgal cultivation and harvesting processes of biodiesel production: a review. *Bioresour Technol* 184:63–72



- Li Z, Savage PE (2013) Feedstocks for fuels and chemicals from algae: treatment of crude bio-oil over HZSM-5. *Algal Res* 2(2):154–163
- Li Y, Lian S, Tong D, Song R, Yang W, Fan Y, Qing R, Hu C (2011) One-step production of biodiesel from *Nannochloropsis* sp. on solid base Mg–Zr catalyst. *Appl Energy* 88 (10):3313–3317
- Lim JK, Chieh DCJ, Jalak SA, Toh PY, Yasin NHM, Ng BW, Ahmad AL (2012) Rapid magnetophoretic separation of microalgae. *Small* 8(11):1683–1692
- Mata TM, Martins AA, Caetano NS (2010) Microalgae for biodiesel production and other applications: a review. *Renew Sustain Energy Rev* 14(1):217–232
- Mercer P, Armenta RE (2011) Developments in oil extraction from microalgae. *Eur J Lipid Sci Technol* 113(5):539–547
- Milledge JJ, Heaven S (2013) A review of the harvesting of micro-algae for biofuel production. *Rev Environ Sci Bio/Technol* 12(2):165–178
- Mohareb RM, Badawi AM, El-Din MRN, Fatthallah NA, Mahrous MR (2015) Synthesis and characterization of cationic surfactants based on N-hexamethylenetetramine as active microfouling agents. *J Surfactants Deterg* 18(3):529–535
- Moody JW, McGinty CM, Quinn JC (2014) Global evaluation of biofuel potential from microalgae. *Proc Natl Acad Sci U S A* 111(23):8691–8696
- Park J-Y, Park MS, Lee Y-C, Yang J-W (2015) Advances in direct transesterification of algal oils from wet biomass. *Bioresour Technol* 184:267–275
- Peng B, Yao Y, Zhao C, Lercher JA (2012a) Towards quantitative conversion of microalgae oil to diesel-range alkanes with bifunctional catalysts. *Angew Chem* 124(9):2114–2117
- Peng B, Yuan X, Zhao C, Lercher JA (2012b) Stabilizing catalytic pathways via redundancy: selective reduction of microalgae oil to alkanes. *J Am Chem Soc* 134(22):9400–9405
- Pienkos PT, Darzins A (2009) The promise and challenges of microalgal-derived biofuels. *Biofuels Bioprod Biorefin* 3(4):431–440
- Praveenkumar R, Kim B, Choi E, Lee K, Cho S, Hyun J-S, Park J-Y, Lee Y-C, Lee HU, Lee J-S (2014a) Mixotrophic cultivation of oleaginous *Chlorella* sp. KR-1 mediated by actual coal-fired flue gas for biodiesel production. *Bioprocess Biosyst Eng* 37(10):2083–2094
- Praveenkumar R, Kim B, Choi E, Lee K, Park J-Y, Lee J-S, Lee Y-C, Oh Y-K (2014b) Improved biomass and lipid production in a mixotrophic culture of *Chlorella* sp. KR-1 with addition of coal-fired flue-gas. *Bioresour Technol* 171:500–505
- Prochazkova G, Podolova N, Safarik I, Zachleder V, Branyik T (2013) Physicochemical approach to freshwater microalgae harvesting with magnetic particles. *Colloids Surf B* 112:213–218
- Ranjith Kumar R, Hanumantha Rao P, Arumugam M (2015) Lipid extraction methods from microalgae: a comprehensive review. *Front Energy Res* 2:61
- Sander K, Murthy GS (2010) Life cycle analysis of algae biodiesel. *Int J Life Cycle Assess* 15 (7):704–714
- Sani YM, Daud WMAW, Aziz AA (2013) Solid acid-catalyzed biodiesel production from microalgal oil—the dual advantage. *J Environ Chem Eng* 1(3):113–121
- Seo JY, Lee K, Lee SY, Jeon SG, Na J-G, Oh Y-K, Park SB (2014) Effect of barium ferrite particle size on detachment efficiency in magnetophoretic harvesting of oleaginous *Chlorella* sp. *Bioresour Technol* 152:562–566
- Seo JY, Lee K, Praveenkumar R, Kim B, Lee SY, Oh Y-K, Park SB (2015) Tri-functionality of Fe<sub>3</sub>O<sub>4</sub>-embedded carbon microparticles in microalgae harvesting. *Chem Eng J* 280:206–214
- Sharma YC, Singh B, Upadhyay S (2008) Advancements in development and characterization of biodiesel: a review. *Fuel* 87(12):2355–2373
- Sharma YC, Singh B, Korstad J (2011) A critical review on recent methods used for economically viable and eco-friendly development of microalgae as a potential feedstock for synthesis of biodiesel. *Green Chem* 13(11):2993–3006
- Shim J-O, Jeong D-W, Jang W-J, Jeon K-W, Jeon B-H, Cho SY, Roh H-S, Na J-G, Ko CH, Oh Y-K (2014) Deoxygenation of oleic acid over Ce<sub>(1-x)</sub>Zr<sub>(x)</sub>O<sub>2</sub> catalysts in hydrogen environment. *Renew Energy* 65:36–40

- Shim J-O, Jeong D-W, Jang W-J, Jeon K-W, Kim S-H, Jeon B-H, Roh H-S, Na J-G, Oh Y-K, Han SS (2015) Optimization of unsupported CoMo catalysts for decarboxylation of oleic acid. *Catal Commun* 67:16–20
- Taher H, Al-Zuhair S, Al-Marzouqi AH, Haik Y, Farid M (2014) Effective extraction of microalgae lipids from wet biomass for biodiesel production. *Biomass Bioenergy* 66:159–167
- Teo SH, Taufiq-Yap Y, Ng F (2014) Alumina supported/unsupported mixed oxides of Ca and Mg as heterogeneous catalysts for transesterification of *Nannochloropsis* sp. microalga's oil. *Energy Convers Manage* 88:1193–1199
- Toh PY, Yeap SP, Kong LP, Ng BW, Chan DJC, Ahmad AL, Lim JK (2012) Magnetophoretic removal of microalgae from fishpond water: feasibility of high gradient and low gradient magnetic separation. *Chem Eng J* 211:22–30
- Toh PY, Ng BW, Ahmad AL, Chieh DCJ, Lim J (2014a) Magnetophoretic separation of *Chlorella* sp.: role of cationic polymer binder. *Process Saf Environ Prot* 92(6):515–521
- Toh PY, Ng BW, Ahmad AL, Chieh DCJ, Lim J (2014b) The role of particle-to-cell interactions in dictating nanoparticle aided magnetophoretic separation of microalgal cells. *Nanoscale* 6 (21):12838–12848
- Toh PY, Ng BW, Chong CH, Ahmad AL, Yang J-W, Lim J (2014c) Magnetophoretic separation of microalgae: the role of nanoparticles and polymer binder in harvesting biofuel. *RSC Adv* 4 (8):4114–4121
- Tran D-T, Yeh K-L, Chen C-L, Chang J-S (2012) Enzymatic transesterification of microalgal oil from *Chlorella vulgaris* ESP-31 for biodiesel synthesis using immobilized *Burkholderia* lipase. *Bioresour Technol* 108:119–127
- Tran D-T, Le B-H, Lee D-J, Chen C-L, Wang H-Y, Chang J-S (2013) Microalgae harvesting and subsequent biodiesel conversion. *Bioresour Technol* 140:179–186
- Umdu ES, Tuncer M, Seker E (2009) Transesterification of *Nannochloropsis oculata* microalga's lipid to biodiesel on Al<sub>2</sub>O<sub>3</sub> supported CaO and MgO catalysts. *Bioresour Technol* 100 (11):2828–2831
- Velasquez-Orta S, Lee J, Harvey A (2013) Evaluation of FAME production from wet marine and freshwater microalgae by in situ transesterification. *Biochem Eng J* 76:83–89
- Vyas AP, Verma JL, Subrahmanyam N (2010) A review on FAME production processes. *Fuel* 89 (1):1–9
- Wang S-K, Wang F, Hu Y-R, Stiles AR, Guo C, Liu C-Z (2014a) Magnetic flocculant for high efficiency harvesting of microalgal cells. *ACS Appl Mater Interfaces* 6(1):109–115
- Wang S-K, Wang F, Stiles AR, Guo C, Liu C-Z (2014b) *Botryococcus braunii* cells: ultrasound-intensified outdoor cultivation integrated with in situ magnetic separation. *Bioresour Technol* 167:376–382
- Wang S-K, Stiles AR, Guo C, Liu C-Z (2015) Harvesting microalgae by magnetic separation: a review. *Algal Res* 9:178–185
- Williams PJB, Laurens LM (2010) Microalgae as biodiesel & biomass feedstocks: review & analysis of the biochemistry, energetics & economics. *Energy Environ Sci* 3(5):554–590
- Zhao C, Brück T, Lercher JA (2013) Catalytic deoxygenation of microalgal oil to green hydrocarbons. *Green Chem* 15(7):1720–1739

**Part II**  
**Nanotechnology in Biomass Conversion**

# Chapter 5

## Potential Applications of Nanotechnology in Thermochemical Conversion of Microalgal Biomass

**Abdul Raheem, Liaquat Ali Memon, Sikandar Ali Abbasi, Y.H. Taufiq Yap, Michael K. Danquah, and Razif Harun**

**Abstract** The rapid decrease in fossil reserves has significantly increased the demand of renewable and sustainable energy fuel resources. Fluctuating fuel prices and significant greenhouse gas (GHG) emission levels have been key impediments associated with the production and utilization of nonrenewable fossil fuels. This has resulted in escalating interests to develop new and improve inexpensive carbon neutral energy technologies to meet future demands. Various process options to produce a variety of biofuels including biodiesel, bioethanol, biohydrogen, bio-oil, and biogas have been explored as an alternative to fossil fuels. The renewable, biodegradable, and nontoxic nature of biofuels make them appealing as alternative fuels. Biofuels can be produced from various renewable resources. Among these

---

A. Raheem

Department of Chemical and Environmental Engineering, Universiti Putra Malaysia, 43400 Serdang, Malaysia

Energy and Environment Department, Dawood University of Engineering and Technology, Karachi 74800, Pakistan

L.A. Memon

Mechanical Department, Quaid-e-Awam University of Engineering Science and Technology, 67450 Nawabshah, Pakistan

S.A. Abbasi

Energy and Environment Department, Dawood University of Engineering and Technology, Karachi 74800, Pakistan

Y.H. Taufiq Yap

Catalysis Science and Technology Research Centre, Faculty of Science, Universiti Putra Malaysia, Serdang, Malaysia

M.K. Danquah

Department of Chemical Engineering, Curtin University, Sarawak, Malaysia

R. Harun (✉)

Department of Chemical and Environmental Engineering, Universiti Putra Malaysia, 43400 Serdang, Malaysia

e-mail: [mh\\_razif@upm.edu.my](mailto:mh_razif@upm.edu.my)

renewable resources, algae appear to be promising in delivering sustainable energy options.

Algae have a high carbon dioxide (CO<sub>2</sub>) capturing efficiency, rapid growth rate, high biomass productivity, and the ability to grow in non-potable water. For algal biomass, the two main conversion pathways used to produce biofuel include biochemical and thermochemical conversions. Algal biofuel production is, however, challenged with process scalability for high conversion rates and high energy demands for biomass harvesting. This affects the viable achievement of industrial-scale bioprocess conversion under optimum economy. Although algal biofuels have the potential to provide a sustainable fuel for future, active research aimed at improving upstream and downstream technologies is critical. New technologies and improved systems focused on photobioreactor design, cultivation optimization, culture dewatering, and biofuel production are required to minimize the drawbacks associated with existing methods.

Nanotechnology has the potential to address some of the upstream and downstream challenges associated with the development of algal biofuels. It can be applied to improve system design, cultivation, dewatering, biomass characterization, and biofuel conversion. This chapter discusses thermochemical conversion of microalgal biomass with recent advances in the application of nanotechnology to enhance the development of biofuels from algae. Nanotechnology has proven to improve the performance of existing technologies used in thermochemical treatment and conversion of biomass. The different bioprocess aspects, such as reactor design and operation, analytical techniques, and experimental validation of kinetic studies, to provide insights into the application of nanotechnology for enhanced algal biofuel production are addressed.

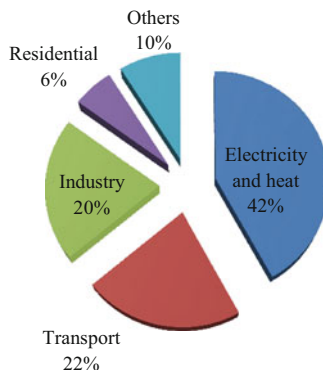
**Keywords** Microalgae • Gasification • Nanotechnology • Thermogravimetric analysis • Thermochemical conversion

## 5.1 Introduction

The combustion of fossil fuels is known to be the primary cause of global warming, and this has become a global environmental challenge (Demirbas 2010). The concentration of greenhouse gases has presently reached higher levels (CO<sub>2</sub> concentration >455 ppm) and is continuously increasing due to high dependency on fossil fuels for various applications such as heat, electricity, and transportation. CO<sub>2</sub> emission data for 2012, as shown in Fig. 5.1, indicates that electricity and heat generation account for the highest CO<sub>2</sub> emission of 42 % followed by transportation (22 %) and then industrial emissions (20 %).

Subhadra and Edwards (2010) discussed strategies to reduce CO<sub>2</sub> emissions: (1) direct capture of CO<sub>2</sub> at source before it is vented out to the atmosphere, (2) removal of atmospheric CO<sub>2</sub> by microorganisms such as algae, and (3) reduction

**Fig. 5.1** Global CO<sub>2</sub> emissions by sectors in 2012 (Maria 2014)



in the consumption of fossil fuel by developing nonconventional and GHG emission-free sources such as hydro, solar, wind, and biomass.

Biomass is considered as the leading energy source by contributing to more than 10% of global energy supply and ranks as the fourth major primary source of energy (Saidur et al. 2011; Wu et al. 2012). This makes biomass a potential alternative feedstock to replace fossil fuels in terms of availability. Biomass development relies on CO<sub>2</sub> uptake from the atmosphere, and this constitutes a potential measure to control atmospheric CO<sub>2</sub>. It has been projected that biomass will provide nearly 38% of global fuel supply by 2050 (Demirbas 2000).

Currently, first-generation biofuel sources such as sucrose, starch, and oil-based materials are extensively used to produce bioethanol, biodiesel, and syngas (Naik et al. 2010). However, considerations for large-scale biofuel production result in a series of problems relating to the requirement of a vast arable land area and the associated effects on the food versus fuel debate (Sims et al. 2011). Therefore, biofuels from oil/food crops are not socioeconomically advantageous to meet current and future energy demands. Second-generation biofuel feedstock materials, referred to as lignocellulosic biomass (nonfood materials), have progressed to solve some of the problems associated with first-generation biofuel sources (Chen and Kuo 2010). However, they still face challenges relating technological performance and consistency, cost-effectiveness, and biomass collection networks (Nigam and Singh 2011).

Algae have been widely researched as a suitable feedstock with the capacity to solve major challenges of first- and second-generation biofuel feedstock. They constitute third-generation biofuel feedstock, represent a huge diversity of photosynthetic species (Mata et al. 2010; Nigam and Singh 2011), and are either heterotrophic or autotrophic in nature (John et al. 2011). Algae are characterized by their ability to grow in varied environments with high carbon dioxide (CO<sub>2</sub>) absorption and uptake rate. Algae have the potential to produce approximately 40–50% of oxygen available in the atmosphere to support life on the planet (Schenk et al. 2008; Brennan and Owemde 2010; Verma et al. 2010; Jorquera et al. 2010). Furthermore, algae have high growth rates, a high potential to convert

energy from the sun into biomass, about 3–8 % compared to 0.5 % for other land-based plants. The high contents of proteins, carbohydrates, and lipids make algal biomass an excellent choice for biofuel production (Singh et al. 2011a, b). Extensive research into process development has enabled the effective use of algal biomass to produce liquid and gaseous fuels such as bioethanol, biodiesel, and BioSyngas via biochemical and thermochemical conversions (Yu et al. 2011; Vinu and Broadbelt 2012; Zhang et al. 2013; Brandenberger et al. 2013). Algal biofuels, however, face some process challenges relating to:

- The development of a robust industrial-scale production process
- The economics of biomass production and harvesting
- Efficient technologies to convert biomass to biofuels

Table 5.1 illustrates the chemical and elemental composition of various microalgae species. Some of the species contain high lipid contents, hence appropriate for biodiesel production via transesterification. Bioethanol is produced from the fermentation of simple sugars, while biogas is produced via anaerobic digestion (Spolaore et al. 2006). Gasification (Brennan and Owemde 2010), pyrolysis (Grierson et al. 2009), and liquefaction (Barreiro et al. 2013) are examples of thermochemical conversion methods. Figure 5.2 shows the operating parameters and key products of liquefaction, pyrolysis, and gasification.

Thermochemical conversion appears to be a promising technology to rapidly produce various biofuels, while biochemical processing of biomass typically requires a longer time to produce biofuels (Nahak et al. 2011). In addition, thermochemical technology can be applied to various types of biomass without the use of toxic chemicals. Hence, there exists the potential to use thermochemical conversion to produce renewable fuels including chemicals (condensable organics) (Levine et al. 2010; Brown et al. 2010; Duan and Savage 2011), solid (char), and gaseous (noncondensable organics) (Haiduc et al. 2009; Brown et al. 2010) from algal biomass. The relative fractions of various solids, liquids, and gaseous products are highly dependent on the gasification reactor type, as shown in Table 5.2, and other operating conditions include temperature, pressure, heating rate, and residence time.

## 5.2 Gasification Principles

Gasification is a versatile and clean approach to produce environmental sustainable fuels. In gasification, the biomass or virtually any carbon-based material is partially oxidized in the presence of air, oxygen, or steam to produce a mixture of inflammable gases at high temperatures (700–1000 °C). Under such conditions, chemical and structural bonds within the biomass break, initiating chemical reactions that typically produce a mixture of gases known as synthesis gas (syngas), mainly composed of H<sub>2</sub>, CO, CO<sub>2</sub>, and CH<sub>4</sub> (Brennan and Owemde 2010; Khoo et al. 2013). Gasification adds value to low- or negative-value feedstocks by

**Table 5.1** Summary of chemical and elemental compositions of various microalgae species

Method	Microalgae species	Chemical composition			Elemental composition							HHV (MJ kg <sup>-1</sup> )	Reference	
		Carbohydrates	Protein	Lipids	C	H	N	O	S					
Liquefaction	<i>Chlorella vulgaris</i>	9.00	55.00	25.00	52.6	7.1	08.20	32.2	0.5			36.50	Biller et al. (2012)	
	<i>Chlorogloopsis fritschii</i>	44.00	50.00	7.00	54.4	6.9	07.30	31.4				32.00	Biller et al. (2012)	
	<i>Dunaliella tertiolecta</i>	21.69	61.32	3.00	39.0	5.37	02.00	53.03				20.08	Shuping et al. (2010a)	
	<i>Nannochloropsis oculata</i>	22.70	20.00	25.00	50.0	7.46	07.54	34.47	0.47			21.46	Cheng et al. (2014)	
	<i>Spirulina platensis</i>	30.21	48.36	13.30	46.16	7.14	10.56	35.44	0.74			20.52	Jena and Das (2011)	
	<i>Scenedesmus</i>	25.00	56.00	13.00	52.1	7.4	08.80	31.1	0.5			22.60	Vardon et al. (2012)	
	<i>Spirulina</i>	20.00	64.00	5.00	45.2	6.4	10.00	40	0.8			17.70	Vardon et al. (2012)	
	<i>Scenedesmus dimorphus</i>	16.00	43.00	18.00	53.4	7.8	07.90	31.0				33.60	Biller et al. (2012)	
	<i>Spirulina platensis</i>	20.00	65.00	5.00	55.7	6.8	11.20	26.4	0.8			36.00	Biller et al. (2012)	
	<i>Chlorella</i>	15.50	34.00	07.00	50.20	07.25	09.30	33.20				21.20	Babich et al. (2011)	
Pyrolysis	<i>Chlorella vulgaris</i>	21.00	42.50		42.50	06.70	06.60	28.00				17.00	Wang and Brown (2013)	
	<i>Chlorella vulgaris</i>		55.00	15.50	44.00	6.20	06.70	43.30				18.00	Keblmann et al. (2013)	
	<i>Chlorella pyrenoidosa</i>	22.50	71.50	00.20	51.20	6.8	11.30	30.70					Gai et al. (2013)	
	<i>Chlorella</i> spp.	16.50	29.60	13.00	46.10	6.1	6.7	19.10				20.40	Rizzo et al. (2013)	
	<i>Chlorella vulgaris</i>	12.40	58.10	13.50	44.80	07.00	07.00	40.40	1.0				Lopez-Gonzalez et al. (2014)	
	<i>Dunaliella tertiolecta</i>	21.69	61.32	02.87	39.00	5.37	2.00	53.02	0.6			20.00	Shuping et al. (2010b)	
	<i>Dunaliella tertiolecta</i>	40.50	27.20	22.00	38.23	6.2	11.00	44.46				11.66	Kim et al. (2015)	
	<i>Nannochloropsis gaditana</i>	25.10	40.50	26.30	49.40	07.70	7.00	34.70	1.1					Lopez-Gonzalez et al. (2014)

(continued)



Table 5.1 (continued)

Method	Microalgae species	Chemical composition			Elemental composition							HHV (MJ kg <sup>-1</sup> )	Reference
		Carbohydrates	Protein	Lipids	C	H	N	O	S				
Gasification	<i>Scenedesmus</i> sp.	29.30	36.40	19.50	50.0	7.11	07.25	30.70	0.5	21.10	Kim et al. (2014)		
	<i>Scenedesmus</i> sp.	07.80	27.80	11.50	32.10	04.80	05.30	22.10	0.5	19.00	Harman-Ware et al. (2013)		
	<i>Scenedesmus almeriensis</i>	25.20	44.20	24.60	42.00	06.70	6.00	44.70	0.8		Lopez-Gonzalez et al. (2014)		
	<i>Tetraselmis suecica</i>	19.81	63.04	<1	25.00	04.00	4.12	67.54	0.6		Kassim et al. (2014)		
	<i>Spirulina platensis</i>	19.30	65.00	04.80	50.00	6.2	10.80	33.40			Gai et al. (2013)		
	<i>Nannochloropsis gaditana</i>	14.00	24.05	18.67	47.26	7.03	6.72	38.5	0.5		Sanchez-Silva et al. (2013)		
	<i>Chlorella vulgaris</i>	20.45	30.00	50.75	44.00	6.1	7.4	29.3			Kirtania et al. (2014)		
	<i>Chlamydomonas reinhardtii</i>		47.65	19.00	52.7	7.2	9	20.4			Hognon et al. (2014)		
	<i>Nannochloropsis oculata</i>	17	40	20	23.00	4.2	2.5	55.4	1.0		Duman et al. (2014)		

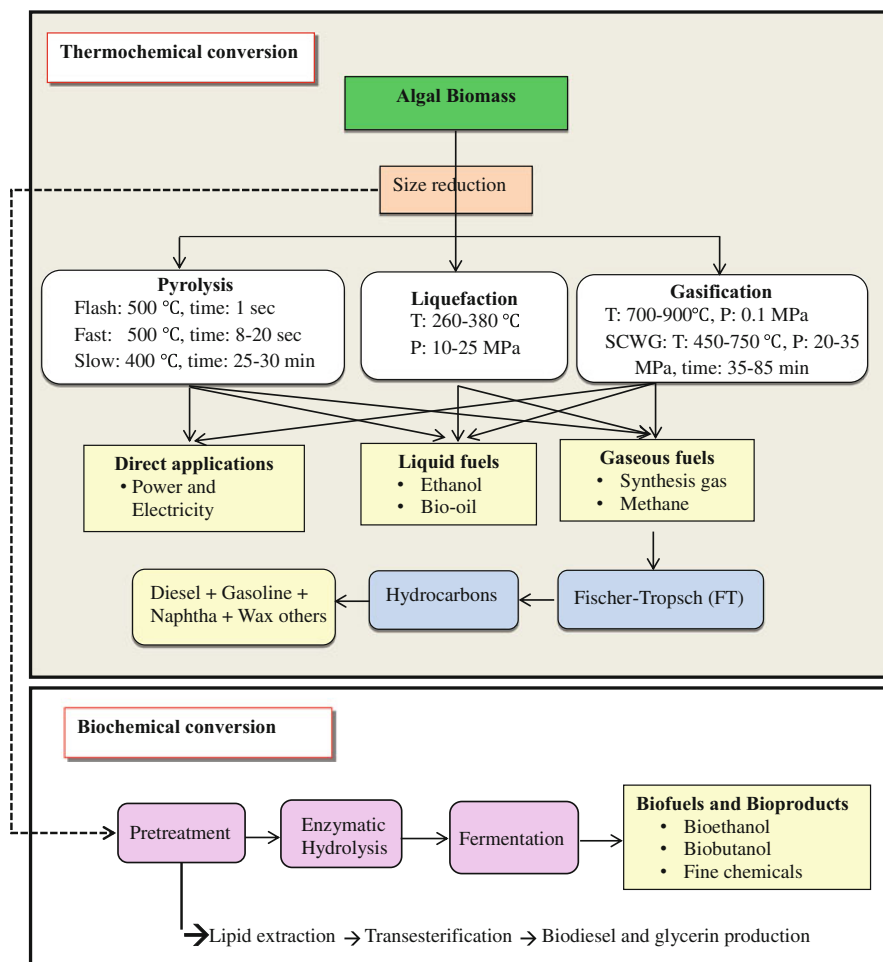


Fig. 5.2 Algal biomass conversion processes

converting them into marketable fuels and products. Syngas can be converted into liquid fuels by means of Fischer-Tropsch (FT) processes or combusted directly for power generation (Lange 2007).

The entire reaction mechanism of biomass gasification involves various reactions due to thermal effects within the gasifier. These can be broadly characterized into four phases: (1) dehydration or moisture removal, (2) devolatilization or pyrolysis, (3) secondary reactions of volatile matter or combustion, and (4) char gasification or reduction. Homogeneous reactions (water-gas shift and methanation reactions) and heterogeneous (water-gas and Boudouard reactions) reactions are involved in the process. Figure 5.3 shows the simplified reaction sequence for microalgal biomass gasification to produce char, liquid, gaseous products, and ash. Dehydration or moisture removal (1) phase takes place around 150–200 °C.

**Table 5.2** Types of gasification reactors and effects on fuel composition

Reactor type	Max: temp (°C)	Cold gas eff: (%)	Char conversion (%)	Tar (g/Nm <sup>3</sup> )	References
Fluidized bed (FBR)	750–950	60–70	65–70	15–25	Gomez-Barea et al. (2013)
Fixed bed (down-draft) reactor	850–1100	25–62	60–80	0.02–0.49	Sheth and Babu (2009)
Fixed bed (updraft) reactor	900–1150	25–55	38–84	30–145	Brandin et al. (2010), Plis and Wilk (2011)
Fluidized circulating bed reactor (FCB)	800–900	45–68	65–90	4–15	Alauddin et al. (2010) and Meng et al. (2011)
Microscale fluidized bed reactor	700–900	60–75	70–85	5–10	Raheem et al. (2015a)
Horizontal axis quartz tube furnace	500–900	65–75	60–80	10–20	Raheem et al. (2015b)

The steam produced from this phase is mixed with gas flow and may trigger a subsequent chemical reaction, typically the water-gas shift reaction. The devolatilization or pyrolysis (2) phase occurs between 250 and 500 °C leading to the formation of pyrolysis products such as hydrocarbons and liquid. 70 % of weight loss occurs in this phase due to volatiles and tar production. The third (3) phase refers to the formation of volatiles and solid carbon formed in the second phase of the pyrolysis reaction. The combustion of volatiles and solid carbon takes place around 500–900 °C, and primary volatiles undergo gasification by reacting with a gasifying agent (O<sub>2</sub>/air or steam) to form permanent gases (H<sub>2</sub>, CO, CO<sub>2</sub>, CH<sub>4</sub>) and small quantities of tar and ash as final products. Table 5.3 shows a typical gasification reaction mechanism.

Table 5.4 summarizes different methods used to gasify microalgal biomass, and these include conventional and supercritical water/hydrothermal gasification. Khoo et al. (2013) gasified *Nannochloropsis* sp. in a fixed bed reactor at ~850 °C. It was found that the product consisted of 14, 28, and 58.2 weight percent (wt%) of bio-oil, synthesis gas, and char, respectively. Sanchez-Silva et al. (2013) carried out a thermogravimetric study of *Nannochloropsis gaditana* to observe the syngas pattern under steam as the gasifying agent. The main gaseous products were H<sub>2</sub>, CO, and CO<sub>2</sub>. Increase in the moisture content of the feed gas resulted in an increase in H<sub>2</sub> yield and a decrease in CH<sub>4</sub> yield, indicating the occurrence of water-gas shift reaction. A study conducted by Alghurabie et al. (2013) investigated the gasification of *Tetraselmis* sp. in a fluidized bed reactor with low-rank coal as a co-gasification agent at temperature ranging 830–880 °C. 10 wt% of *Tetraselmis* sp. was mixed with 90 wt% of coal. Gasification of the biomass was ineffective as a result of ash accumulation and defluidization phenomenon inside the reactor. H<sub>2</sub> and CO<sub>2</sub> contents decreased with increasing reactor temperature; however, CO showed an increasing pattern. It was concluded that microalgae have the potential

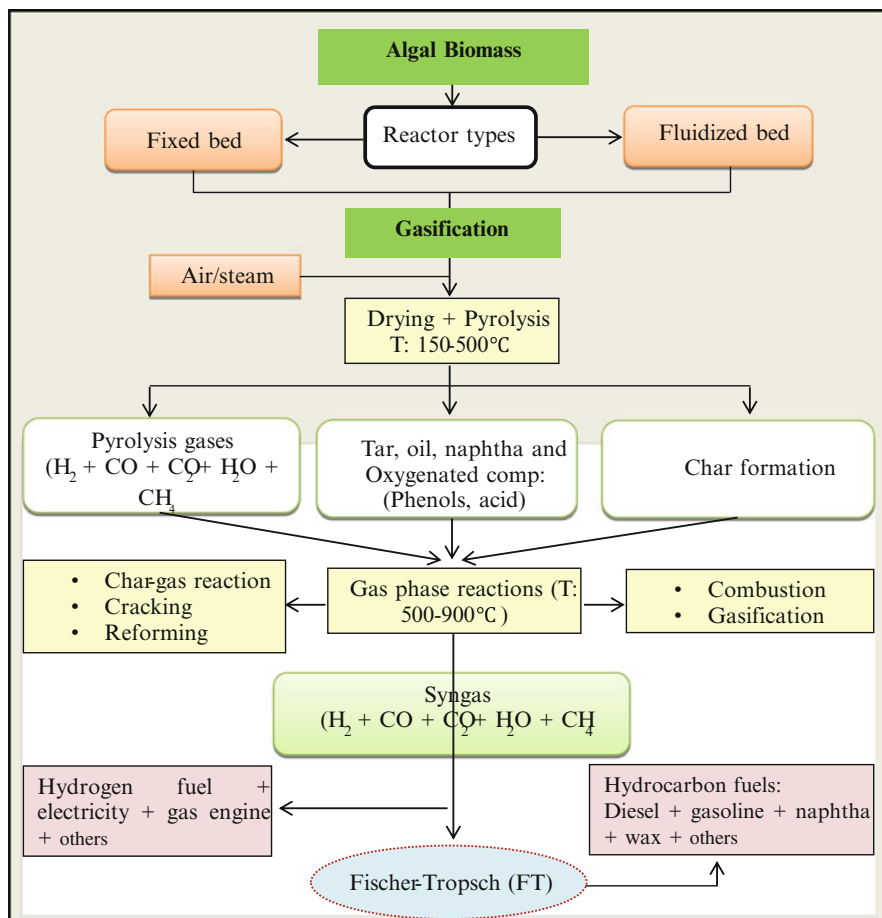


**Fig. 5.3** Stagewise development of biofuels and chemical products from algal gasification

**Table 5.3** A typical biomass gasification reaction mechanism (Raheem et al. 2015a)

Type of reaction	Name
$2C + O_2 \leftrightarrow CO_2$	Partial oxidation reaction
$C + O_2 \leftrightarrow CO_2$	Complete oxidation reaction
$C + H_2O \leftrightarrow H_2 + CO$	Water-gas reaction
$CO + H_2O \leftrightarrow CO_2 + H_2$	Water-gas shift reaction
$C + CO_2 \leftrightarrow 2CO$	Boudouard reaction
$C + 2H_2 \leftrightarrow CH_4$	Hydrogasification reaction
$CH_4 + CO_2 \leftrightarrow 2H_2 + CO$	Dry reforming reaction
$CH_4 + H_2O \leftrightarrow CO + 3H_2$	Methane reforming reaction

**Table 5.4** Effect of operating parameters on gas composition in microalgae in conventional and supercritical microalgal biomass gasification

Mode	Aquatic biomass	Operating parameters			Syngas composition (vol %)						Reference
		Temperature (°C)	Agent (mL min <sup>-1</sup> )/catalyst	Technology	H <sub>2</sub>	CO	CO <sub>2</sub>	CH <sub>4</sub>			
Conventional gasification	<i>Spirulina</i>	1000	O <sub>2</sub> , 0.39	FB <sup>a</sup>	34–48	10–18	31–37	09–11	Hirano et al. (1997)		
	<i>Spirulina platensis</i> <sup>i</sup>	800	Air/steam	FB <sup>a</sup>	19.00	40.00	25.00	08.00	Yang et al. (2013)		
	<i>Spirulina platensis</i>	800	Air/steam	FB <sup>a</sup>	21	36	40	3	Yang et al. (2013)		
	<i>Nannochloropsis</i> sp.	850	N <sub>2</sub>	FB <sup>b</sup>	Total produced gas (85%)						Khoo et al. (2013)
	<i>Nannochloropsis</i>	850	Steam	FB <sup>b</sup>	40–53	<7	30–40	10.00	Duman et al. (2014)		
	<i>Nannochloropsis gaditana</i>	850	Steam/Air: 200	TGA	45	33	12	4	Sanchez-Silva et al. (2013)		
Supercritical water/hydrothermal gasification	<i>Tetraselmis</i> sp. <sup>j</sup>	885	Air, 35,000	FB <sup>a</sup>	09.00	12.00	13.00	02.00	Alghurabie et al. (2013)		
	<i>Chlorella vulgaris</i>	350	Air/nickel	EF <sup>c</sup>	10–35		44–49	16–38	Minowa and Sawayama (1999)		
	<i>Chlorella vulgaris</i>	700	Ru/TiO <sub>2</sub>	R-QC <sup>d</sup>	07.00	22.00	26.00	25.00	Chakimala et al. (2010)		
	<i>Chlorella vulgaris</i>	450	NaOH, Ni	BR <sup>c</sup>	18–57	0.45–5.2	34.6–45	17.28	Onwudili et al. (2013)		
	Gulfweed	900	He/O <sub>2</sub> = 79/21	D-FB <sup>f</sup>	22.00	29.00	10.50	02.10	Hanaoka et al. (2013)		

<i>Phaeodactylum tricornutum</i>	400	Argon/Ru/C	BR <sup>g</sup>	06–08	34–46	40–84	Haiduc et al. (2009)
<i>Spirulina platensis</i>	>400	Ru/ZrO <sub>2</sub> ; Ru/C		06–29	38–77	02–52	Stucki et al. (2009)
<i>Spirulina platensis</i>	450	NaOH, Ni	BR <sup>e</sup>	21–60	36–38	21.2–26.5	Onwuodili et al. (2013)
<i>Saccharina latissima</i>	450	NaOH, Ni	BR <sup>e</sup>	25–69	50–51	12–29	Onwuodili et al. (2013)
<i>Nannochloropsis</i> sp.	450	Ru/C	M-BR <sup>h</sup>	48.00	36.00	15.00	Guan et al. (2013)

<sup>a</sup>Fluidized bed reactor, <sup>b</sup>Fixed bed reactor, <sup>c</sup>Electric furnace, <sup>d</sup>Quartz capillary reactor, <sup>e</sup>Batch reactor (Inconel), <sup>f</sup>Downdraft bed reactor, <sup>g</sup>Batch reactor, <sup>h</sup>Mini-batch reactor, <sup>i</sup>Co-gasification of coal, <sup>j</sup>Co-gasification of wood

to be utilized as a co-gasification agent with coal. However, microalgae with high ash content are not recommended, in order to avoid ash accumulation. Also, Yang et al. (2013) co-gasified *Spirulina platensis* (pellet) and woody biomass (pellet) using a bubbling fluidized bed reactor. CO<sub>2</sub> and CO contents increased with increasing equivalence ratio (ER), while H<sub>2</sub> and CH<sub>4</sub> decreased with increasing feeding ratio of microalgae pellets. The ash content in the microalgae pellets was found to be higher compared to the woody biomass pellets. However, the presence of ash catalyzes the reaction under certain conditions to enhance the gasification process. High ash content can cause sintering in gasification, affecting gasification products (Asadullah 2014). Lopez-Gonzalez et al. (2014) investigated the steam gasification behavior of three microalgae species (*Scenedesmus almeriensis*, *Nannochloropsis gaditana*, and *C. vulgaris*).

The main products from the gasification process were CO<sub>2</sub>, H<sub>2</sub>, and CO, with trace concentrations of light hydrocarbons (CH<sub>4</sub>, C<sub>2</sub>H<sub>2</sub>, and C<sub>2</sub>H<sub>5</sub>). *Scenedesmus almeriensis* produced the highest amount of gaseous products (H<sub>2</sub>, CO<sub>2</sub>, CO, and CH<sub>4</sub>), and this can be explained by the presence of higher concentrations of catalytic elements such as K and Mg. The highest production of H<sub>2</sub> from *Scenedesmus almeriensis* was favored by water-gas shift ( $\text{CO} + \text{H}_2\text{O} \leftrightarrow \text{CO}_2 + \text{H}_2$ ) and steam reforming ( $\text{CH}_4 + \text{H}_2\text{O} \leftrightarrow \text{CO} + 3\text{H}_2$ ) reactions. Chakinala et al. (2010) studied hydrothermal gasification of *Chlorella vulgaris* under temperature conditions 400–700 °C. The gasification efficiency increased with temperature, and *C. vulgaris* was completely gasified at 700 °C in the presence of excess Ru/TiO<sub>2</sub> catalysts. The catalyst increased H<sub>2</sub> yield as well as gasification efficiency up to 85%. Gasification product composition is also influenced by type of catalyst and gasifying agent. Dolomite, nickel, and potassium carbonate are commonly used catalysts (Sutton et al. 2001). Gasifying agents react with solid carbon and heavier hydrocarbons to convert them into low molecular weight gases such as CO and H<sub>2</sub>. The most commonly used gasifying agents are oxygen, steam, and compressed air. Although air is generally considered as the best gasifying agent, it results in increased tar formation (Kumar et al. 2009). Increasing the flow rate of air during gasification can reduce tar formation (Kumar et al. 2009).

## 5.3 Analytical Approach

### 5.3.1 Thermogravimetric Analysis

Thermogravimetric analysis (TGA) is an analytical method used to study changes in the physical and chemical properties of different types of biomass in response to increase in temperature with time. Various properties such as thermal stability, moisture content, and volatile matter content can be measured. However, the most important significant information generated from TGA is weight loss, rate of weight loss (differential thermogravimetry, DTG), and temperature. The original weight of

the sample starts to degrade from dehydration and continues until devolatilization of its organic matter content. A DTG is considered as the first derivative of the sample mass with respect to temperature and time. DTG thermogram could offer scientific insights on the quantitative and qualitative aspects of the sample composition. Table 5.5 shows the decomposition behavior and proximate analysis of various microalgal biomass materials. Most of the studies are in pyrolytic atmosphere except those used oxygen/air (Babich et al. 2011; Chen et al. 2011) to evaluate the gasification behavior. TGA of microalgae is typically characterized into three stages; first stage (I) appears between room temperature and initial devolatilization temperature ( $T_1$ ) 200 °C, where some internal molecular rearrangements, such as cellular and external water elimination, bond breakup, and free radical generation, take place; second stage (II) of TGA represents the main pyrolysis process where the biomass undergoes solid devolatilization ( $T_2 = 200\text{--}500$  °C). It proceeds at a high rate, leading to the formation of pyrolysis products. In the final stage (III), the decomposition of char and carbonaceous (carbon-rich solid form) materials take place at a very slow rate (Demirbas and Arin 2002). Pane et al. (2001) investigated the influence of temperature on *Tetraselmis suecica* (planktonic marine algae). The three weight loss stages were reported within 40–179 °C, corresponding to the external and loosely bound water molecules in the cellular structure. In this region, the cellular structure is progressively destroyed, and reorganizations in the lipid and protein structures affecting their thermal properties may occur (Pane et al. 2001).

During the second stage, decomposition of carbohydrates and proteins takes place within the temperature range 179–400 °C. More weight loss occurs in this devolatilization stage. The final of complete oxidation of organic matter occurs at around 400–760 °C.

Peng et al. (2001) studied the pyrolytic characterization of *Chlorella protothecoides* and *Spirulina platensis* at 800 °C under varying heating rates of 15, 40, 60, and 80 °C min<sup>-1</sup>. The three stages (moisture removal, devolatilization, and organic solid decomposition) were observed during the pyrolysis process, where *Chlorella protothecoides* and *S. platensis* were devolatilized within the temperature ranges of 149–539 °C and at 190–558 °C, respectively. Similarly, Marcilla et al. (2009) explained the three major stages of *Nannochloropsis* sp. decomposition at temperature 25–180 °C (stage 1) corresponding to moisture removal, 180–540 °C (stage 2) corresponding to devolatilization, and 540–800 °C (stage 3) corresponding to low-rate solid material decomposition. The major stages such as devolatilization and decomposition were observed to give a slightly complex chemistry by showing three overlapped trends at temperatures 292, 338, and 458 °C evidenced by FTIR analysis. It was discussed that the chemical composition of the microalgae seems to be decomposed in the order of carbohydrates (polysaccharides), proteins, and lipids.



**Table 5.5** Summary of some reported TGA studies on microalgal biomass devolatilization

	Experimental setup			Devolatilization			Proximate analysis (wt %)				Reference	
	SM (mg)	Temp. (°C)	Carrier gas (mL min <sup>-1</sup> )	$\beta$ (°C min <sup>-1</sup> )	T <sub>1</sub> (1st peak, °C)	T <sub>2</sub> (2nd peak, °C)	T <sub>3</sub> (3rd peak, °C)	M	V.M	F.C		A
Microalgae												
<i>Chlorella</i> sp.	10	R-750	Nitrogen, 100	10-30	R-130 R-160	130-390 160-435	400-525 440-650	7.0	72.0	15.0	6.0	Phukan et al. (2011)
<i>Chlorella</i>	20	R-1000	Air, 30	10-00	R-140	150-400	500-650	6.5	65.5	18.5	9.5	Babich et al. (2011)
<i>Chlorella vulgaris</i>	10	R-800	Nitrogen + Oxygen, 100	10-40	R-170	170-657	657-800		55.4	34.4	10.3	Chen et al. (2011)
<i>Chlorella vulgaris</i>	10	R-800	Nitrogen, 30	10-40	R-200	200-600	600-800					Thangalazhy-G et al. (2012)
<i>Chlorella pyrenoidosa</i>	14	25-800	Nitrogen, 60	10-80	25-150	227-477	477-800	6.1	94.3		6.0	Gai et al. (2013)
<i>Chlorella vulgaris</i>	20	105-1000	Argon, 200	40-00	R-178	150-346	1000-00	4.4	67.2	12.4	16.0	Lopez-Gonzalez et al. (2014)
<i>Chlorella pyrenoidosa</i>	2.5-5	R-800	Nitrogen, 100	20-00	R-145	145-640	640-800	5.8	66.5	16.0	6.0	Hu et al. (2015)
<i>Chlorella</i> sp.	10	R-600	Nitrogen, 100	05-15	R-187	188-511	512-600	7.0	57.0	19.0	21.0	Kassim et al. (2014)
<i>Dunaliella tertiolecta</i>	10	R-900	Nitrogen, 50	05-40	R-165	165-342	342-900	5.0	55.0	27.0	14.0	Shuping et al. (2010a, b)
<i>Enteromorpha prolifera</i>	10	R-1000	Nitrogen, 100	05-40	R-162	162-319	319-1000	2.7	50.0	25.0	23.0	Wu et al. (2015)
<i>Saccharina japonica</i>	25	R-800	Nitrogen, 25	10-20	R-190	200-270	270-350	6.9	68.8	04.1	20.2	Kim et al. (2012)

<i>Sargassum</i> sp.	25	R-800	Nitrogen, 25	05-20	R-180	200-270	270-350	9.3	44.5	09.3	37.0	Kim et al. (2013)
<i>Scenedesmus almeriensis</i>	20	105-1000	Argon, 200	40-00	R-142	142-336	1000-00	3.0	68.0	08.0	19.4	Lopez-Gonzalez et al. (2014)
<i>Scenedesmus</i> sp. <sup>a</sup>	03	R-800	N <sub>2</sub> , 25	30-00	80-160	170-410	410-500	4.6	75.4	12.7	7.3	Kim et al. (2014)
<i>Nannochloropsis gaditana</i>	10	R-900	Helium, 200	15-00	R-130	140-540	540-880		83.1	10.1	6.8	Sanchez-Silva et al. (2013)
<i>Nannochloropsis gaditana</i>	20	105-1000	Argon, 200	40-00	R-160	160-344	1000-00	3.5	80.0	10.2	6.4	Lopez-Gonzalez et al. (2014)
<i>Tetraselmis suecica</i>	10	R-600	Nitrogen, 100	05-15	R-155	156-475	476-600	7.0	55.0	20.5	20.5	Kassim et al. (2014)

SM sample mass, R room temperature, T<sub>1</sub> initial devolatilization temperature, T<sub>2</sub> peak devolatilization temperature, T<sub>3</sub> final decomposition temperature, M moisture, VM volatile matter, F, C fixed carbon, A ash

<sup>a</sup>Lipids extracted

## 5.4 Kinetic Modeling of Microalgal Biomass Gasification

Describing the kinetics and other governing principles of algal biomass gasification by providing models is important to design equipment and reactor chambers for thermochemical conversion (Koufopoulos et al. 1991). TGA is an analytical technique broadly used to investigate the thermal decomposition and kinetic parameters corresponding to the decomposition of various biomass materials such as cotton stalk, cornstalk, and wheat straw (Cai and Liu 2008), wood (Saddawi et al. 2010), wheat straw and corn straw (Min et al. 2007), and cellulose and hemicellulose (Stenseng et al. 2001; Fisher et al. 2002). However, very limited information is available on the kinetics of algal biomass pyrolysis or gasification. There is no acceptable model that could be used to predict pyrolysis rate and stipulate prior information relating to the final conversion over a larger variety of culture conditions for microalgae (García-Quesada et al. 2001).

As the decomposition of microalgal biomass typically occurs via complex mechanisms, including varied reactions with distinctive degree of overlapping, it is more challenging to elucidate the occurrence of single or multiple processes. These complexities result in the determination of pseudo kinetic parameters (Marcilla et al. 2013). Rigorous experimental data based on parametric evidence of kinetic triplet [conversion degree, pre-exponential factor, and activation energy ( $f(\alpha)$ ,  $k_o$ , and  $E_a$ )] will significantly demonstrate dependence on the conversion degree (Conesa et al. 2001; Maciejewski 2000). During experimental analysis, it is usually problematic to clearly resolve the reactions involved. Thus, consideration of the kinetic constants ( $K_o$  and  $E_a$ ) should be of interest. There are general practices in analyzing kinetic data which reveal that kinetic energy is dependent on the conversion degree ( $\alpha$ ). Therefore, necessary steps are required to improve the proposed kinetic analysis model instead of using assumptions to avoid the present contradiction between kinetic constants and the degree of conversion. Existing kinetic analysis methods are outdated, and despite the great evolution of powerful computational tools, the use of models based on rough assumptions is common. Although these assumptions are acceptable and helpful when computational methods were not so effective, they are considered absurd in the current state. In present literature on pyrolysis and gasification of microalgal biomass, the kinetic study reveals some weak points that cause several uncertainties (Marcilla et al. 2013). These can be expressed as follows: (a) the complexities associated with the reaction mechanism are not consistent with the applied kinetic model. Isoconversional approaches (Friedman 1964; Ozawa 1965; Flynn and Wall 1966; Akahira and Sunose 1971) are suitable in terms of single-stage reactions, and they have been extensively used for microalgae thermal decomposition to estimate kinetic characteristics.

However, according to Marcilla et al. (2013), these assumptions for thermal decomposition of microalgae are not valid. Consequently, the obtained activation energy reveals obvious dependency on conversion degree, representing that the procedure must be explained within multiple stage kinetics to obtain kinetic triplets. Hence, these methods would be properly used if the deconvolution of the peaks

were verified through DTG thermogram. The use of kinetic differential equations is another option to perform the kinetic study. It includes multiple steps to find the mass of sample or its derivative and the reduction of the sum of the squares of variations between the experimental and calculated mass and their derivatives (García-Quesada et al. 2001; Vyazovkin et al. 2011). Table 5.6 shows the results of activation energy ( $E_a$ ) of various microalgae species obtained from Kissinger (KAS) and Flynn-Wall-Ozawa (FWO) methods according to their conversion degree in different environments. The data shows that there can be variations in activation energy for the same conversion degrees.

Li et al. (2011) studied three different species of microalgae *Corallina pilulifera*, *Porphyra yezoensis*, and *Plocamium telfairiae* Harv to determine their activation energies. However, all three species showed different activation energies at the same conversion degree of 0.1 for both methods: Kissinger (290, 118, and 153 kJ mol<sup>-1</sup>) and FWO (283, 221, and 153 kJ mol<sup>-1</sup>). Chen et al. studied *C. vulgaris* by varying O<sub>2</sub> concentration, and the obtained activation energy was within the range of 134–243 kJ mol<sup>-1</sup>. Tahmasebi et al. (2013) reported activation energies ranging from 70 to 71 kJ mol<sup>-1</sup> for *Tetraselmis suecica*. Shuping et al. (2010a, b) studied *Dunaliella tertiolecta* and reported activation energies of 139.6 kJ mol<sup>-1</sup> and 141.3 kJ mol<sup>-1</sup> at a conversion degree of 0.2 using Kissinger and FWO methods. The difference in activation energy values for microalgae species is due to factors including difference in the type and nature of species, compositions, cultivation conditions and pyrolysis or gasification parameters such as heating rate, and the biomass feeding rate.

## 5.5 Nanotechnology for Algal Biofuel Production

Although the development of algal biofuels is a promising engineering research endeavor, large-scale production and commercialization of algal biofuels still seem challenging due to various factors such as (a) selection of high-yield lipids, carbohydrates, and protein algal strains for biofuel production (inherent adaption could be the option to increase production efficiency) and (b) advanced technologies for algal cultivation (different reactor designs have been used for algae growth). However, there still exist some limitations regarding effective gas transfer, stirring, lighting, and biomass production. Therefore, advanced technologies with improved reactor design is critical to address these limitations.

The introduction of nanotechnology to the upstream and downstream operations of microalgal bioprocess engineering is another option that potentially addresses the challenges confronting full-scale production and commercialization of algal biofuels. Nanotechnology can be applied to improve system design and biomass characterization and enhanced production of biochemical such as lipid, carbohydrates, and proteins. Various types of nanomaterials such as electrospun nanomaterials, nanophotocatalysts, metal oxides, and mesoporous materials have been incorporated in technologies to improve algal biofuel production

**Table 5.6** Activation energy of different algae species obtained using Kissinger and FWO methods

Species	Conversion degree ( $\alpha$ )		Kissinger $E$ (kJ mol <sup>-1</sup> )		FWO $E$ (kJ mol <sup>-1</sup> )		$R^2$		References
	Min	Max	Min	Max	Min	Max	Kissinger	FWO	
<i>Corallina pilulifera</i>	0.1	0.4	290	291.2	283.4	285.1	0.99-0.98	0.99-0.98	Li et al. (2011)
<i>Chlorella vulgaris</i>	0.10	0.60	45.8	143.5	44.2	146.5	0.90-0.98	0.96-0.98	Thangalazhy-G et al. (2012)
<i>Chlorella vulgaris</i> (20%O <sub>2</sub> -80%N <sub>2</sub> )	0.2	0.3	175.5	174	166.9	153.9	0.96-0.96	0.96-0.97	Chen et al. (2011)
<i>Dunaliella tertiolecta</i>	0.2	0.4	139.6	152.7	141.3	152.9	0.99-0.99	0.99-0.99	Shuping et al. (2010a, b)
<i>Porphyra yezoensis</i>	0.1	0.8	118.7	176	121.1	173.2	0.99-0.95	0.99-0.95	Li et al. (2011)
<i>Plocamium telfairiae</i> Harv	0.1	0.9	153.0	320.8	153.4	314.9	0.98-0.99	0.98-0.99	Li et al. (2011)
<i>Tetraselmis suecica</i>	0.2	0.6	23.22	146.59	29.78	178.47	0.99-0.98	0.99-0.98	Kassim et al. (2014)
<i>Tetraselmis suecica</i>	0.2	0.4	47.21	99.1	51.32	79.2	0.96-0.99	0.99-0.99	Tahmasebi et al. (2013)

(Laudenslager et al. 2010; Crossley et al. 2010; Metzler et al. 2011). These materials have proven to deliver cost-effective energy efficient protocols for algal biofuel synthesis. Various articles have discussed the application of nanotechnology to optimize cultivation, reactor design, and product yields to enable enhanced biofuel production (Laudenslager et al. 2010; Pugh et al. 2010). However, the appropriate catalytic technologies are not well developed and require optimization to obtain economic and commercial viability.

Nanomaterials play an important role in improving conventional biochemical and thermochemical biomass conversion technologies. These relate to the application of advanced materials for enzyme control, materials with improved enzyme loading capacity, nanocatalysts, materials to store bioenergy products, materials to separate and purify liquid biofuels, and nanomaterials to improve bioreactor performance. Conventional thermo-/biochemical methods for producing algal biofuels include gasification to produce syngas, pyrolysis to liquid fuels, lipid transesterification to biodiesel, and anaerobic digestion to methane. Recently, different types of nanomaterials or catalysts have been developed and used to produce biofuels. These include electrospun nanomaterials (Verdugo et al. 2014), mesoporous material (Bautista et al. 2015), and nanocatalysts (Li et al. 2015). These nanomaterials have been considered as effective tools for enhanced microalgal conversion processes.

### ***5.5.1 Nanomaterials for Biomass Gasification***

During gasification, unwanted production of char and tar constitutes a critical issue that needs to be addressed. Tar is one of the complex structures of condensable hydrocarbons and causes major problems such as corrosion, failure of engines, and blockage of piping as well as filters. Char contains carbonaceous materials including aromatic structural units (Li et al. 2008; Nordgreen 2011). Tar formations can be controlled via reactor conditions. The most crucial parameters for this approach are the reactor temperature, gasifying agent, reaction time, equivalence ratio, and catalysts, and these can have considerable effects on tar reduction (Balat et al. 2009; Luo and Zhou 2012). The use of various nanocatalysts is important for product distributions. The catalyst does not only decrease tar formation but also increase the quality of producer gas and biomass conversion efficiency. Nickel (Ni), potassium (K), calcium (Ca), and sodium (Na) have been discovered as the most efficient catalysts to promote char gasification (Nzihou et al. 2013). The main reactions during tar cracking include thermal cracking, steam reforming, hydrocracking, and water-gas shift reactions (Anis and Zainal 2011). The conversion of tar products using dolomite, alkali metals, and nickel-based catalysts at high temperatures (800–1000 °C) is efficient in tar cracking (Han and Kim 2008; Nzihou et al. 2013; Asadullah 2014). In gasification, nickel-based catalysts are most preferable as the catalytic hot gas cleanup and tar removal can be achieved at high rate. In addition, Ni-based catalysts have been utilized to produce hydrogen-

rich gas (Balat et al. 2009; Sinag 2012). Anis and Zainal (2011) stated that among all catalysts for tar conversion into producer gas, nickel catalysts are the most capable.

Recently, nanomaterials, particularly nano-sized NiO (nano-NiO), have received an extensive attention for their distinctive properties for biomass gasification. Functional hybrid catalyst can be prepared by integrating nanoparticles of NiO on the surface of metal carriers, such as alumina, for a more economical operation (Li et al. 2008). Li et al. (2008) studied biomass pyrolysis using nano-NiO and micro-NiO particles as a catalyst. They reported the formation of char from both catalysts, and the obtained results were comparable with pyrolysis conducted in the absence of catalyst. The devolatilization of cellulose using micro-NiO was 10 °C lower than pure cellulose, while the decomposition of cellulose using nano-NiO began at 295 °C, which was 20 °C less than pure cellulose. The absolute char production was 5.65 wt%, which was less than that of micro-NiO. The nano-NiO displayed a lower pyrolysis temperature to achieve high efficiency. It was concluded that the presence of nano-NiO catalyst during gasification significantly improves the quality of gaseous products and considerably reduces tar formation.

Aradi et al. (2010) investigated the effect of organometallic nanocatalysts and Ni<sub>3</sub>Cu (SiO<sub>2</sub>)<sub>6</sub> nanoalloy catalyst on biomass gasification. The results exhibited a considerable increment in hydrogen yield. They showed that the presence of the nanoalloy catalyst amplified biomass conversion efficiency at moderately low gasification temperature. Many other types of nanocatalysts have been used for gasification. These include nano-ZnO and nano-SnO<sub>2</sub>. Sinag et al. (2011) studied nano-ZnO and showed its effectiveness for lower temperature (300 °C) water-gas shift reaction. The gaseous products produced at 300 °C were mainly CO<sub>2</sub> and H<sub>2</sub>. Also, nano-SnO<sub>2</sub> was found to be an effective catalyst for higher temperature (400–500 °C) water-gas shift reaction. It was observed that the larger surface area of nano-ZnO improved the rate of the water-gas shift reaction.

## 5.6 Conclusion

In response to the growing energy demand and the tremendous increase in environmental issues such as global warming, more renewable and sustainable biofuel options are required. It seems impractical to produce biofuels from terrestrial crops due to climatic constraints and the use of vast availability of arable land for crop production. The production of biofuels using algae has the potential to offer renewable energy development with the prospect of contributing significantly to future sustainable energy mix.

Thermochemical conversion technology offers simplicity in terms of biomass conversion and maximizing output yield over biochemical conversion technology. However, certain key challenges associated with the technology coupled with low biomass production offer new research endeavors for enhancing biomass yield, product quality, and other related drawbacks. In this chapter, microalgal

thermochemical conversion technology was discussed extensively. The potential of nanomaterial for enhanced thermochemical conversion of algal biomass to biofuels was also highlighted. Nanotechnology provides physicochemical and catalytic advantages to improve current processes used in the production of algal biofuels. It can be used to improve the system design, characterization, treatment, and conversion of biomass. Algae biofuel production can be greatly improved by integrating nanomaterials to the process system. Further research is however required to investigate, evaluate, and establish the effectiveness of nanotechnology on algal thermochemical conversion, as the number of current published reports is limited.

## References

- Akahira T, Sunose T (1971) Method of determining activation deterioration constant of electrical insulating materials. *Res Rep Chiba Inst Technol (Sci Technol)* 16:22–31
- Alauddin ZA, Lahijani P, Mohammadi M, Mohamed AR (2010) Gasification of lignocellulosic biomass in fluidized beds for renewable energy development: a review. *Renew Sust Energy Rev* 14:2852–2862
- Alghurabie IK, Hasan BO, Jackson B, Kosminski A, Ashman PJ (2013) Fluidized bed gasification of Kingston coal and marine microalgae in a spouted bed reactor. *Chem Eng Res Des* 91:1614–1624
- Anis S, Zainal ZA (2011) Tar reduction in biomass producer gas via mechanical, catalytic and thermal methods: a review. *Renew Sust Energy Rev* 15:2355–2377
- Aradi A, Roos J, Jao TC (2010) Nanoparticle catalyst compounds and/or volatile organometallic compounds and method of using the same for biomass gasification. US 20100299990A1
- Asadullah M (2014) Barriers of commercial power generation using biomass gasification gas: a review. *Renew Sust Energy Rev* 29:201–215
- Babich IV, Hulst MVD, Lefferts L, Moulijn JA, O'Connor P, Seshan K (2011) Catalytic pyrolysis of microalgae to high-quality liquid bio-fuels. *Biomass Bioenergy* 35:3199–3207
- Balat M, Balat M, Kirtay E, Balat H (2009) Main routes for the thermo-conversion of biomass into fuels and chemicals. Part 2: Gasification systems. *Energy Convers Manage* 50:3158–3168
- Barreiro DL, Prins W, Ronsse F, Brilman W (2013) Hydrothermal liquefaction (HTL) of microalgae for biofuel production: state of the art review and future prospects. *Biomass Bioenergy* 53:113–127
- Bautista LF, Vicente G, Mendoza Á, González S, Morales V (2015) Enzymatic production of biodiesel from *Nannochloropsis gaditana* microalgae using immobilized lipases in mesoporous materials. *Energy Fuels* 29:4981–4989
- Biller P, Ross AB, Skill SC, Lea-Langton A, Balasundaram B, Hall C, Riley R, Llewellyn CA (2012) Nutrient recycling of aqueous phase for microalgae cultivation from the hydrothermal liquefaction process. *Algal Res* 1:70–76
- Brandenberger M, Matzenberger J, Vogel F, Ludwig C (2013) Production synthetic natural gas from microalgae via supercritical water gasification: a techno-economic sensitivity analysis. *Biomass Bioenergy* 51:26–34
- Brandin J, Tuner M, Odenbrand I (2010) Small scale gasification: gas engine CHP for biofuels. Swedish Energy Agency Report, pp 27–29
- Brennan L, Owemde P (2010) Biofuel from microalgae – a review of technologies for production, processing and extraction of biofuel and co-products. *Renew Sust Energy Rev* 14:557–577
- Brown TM, Duan PG, Savage PE (2010) Hydrothermal liquefaction and gasification of *Nannochloropsis* sp. *Energy Fuels* 24:3639–3646



- Cai J, Liu R (2008) Application of Weibull 2-mixture model to describe biomass pyrolysis kinetics. *Energy Fuels* 22:675–678
- Chakinala AG, Brilman DWF, Swaaij WPMV, Kersten SRA (2010) Catalytic and non-catalytic supercritical water gasification of microalgae and glycerol. *Ind Eng Chem Res* 49:1113–1122
- Chen WH, Kuo PC (2010) A study on torrefaction of various biomass materials and its impact on lignocellulosic structure simulated by a thermogravimetry. *Energy* 35:2580–2586
- Chen C, Ma X, Liu K (2011) Thermogravimetric analysis of microalgae combustion under different oxygen supply concentrations. *Appl Energy* 88:3189–3196
- Cheng J, Huang R, Yu T, Li T, Zhou J, Cen K (2014) Biodiesel production from lipids in wet microalgae with microwave irradiation and bio-crude production from algal residue through hydrothermal liquefaction. *Bioresour Technol* 151:415–418
- Conesa JA, Marcilla A, Caballero JA, Font R (2001) Comments on the validity and utility of the different methods for kinetics analysis of thermogravimetric data. *J Analyt Appl Pyrolysis* 58–59:617–633
- Crossley S, Faria J, Shen M, Resasco DE (2010) Solid nanoparticles that catalyze biofuel upgrade reactions at the water/oil interface. *Science* 327:68–72
- Demirbas A (2000) Biomass resources for energy and chemical industry. *Energy Edu Sci Technol* 5:21–45
- Demirbas A (2010) Use of algae as biofuel sources. *Energy Convers Manage* 51:2738–2749
- Demirbas A, Arin G (2002) An over view of biomass pyrolysis. *Energy Sources* 24:471–482
- Duan PG, Savage PE (2011) Hydrothermal liquefaction of a microalga with heterogeneous catalysts. *Ind Eng Chem Res* 50:52–61
- Duman G, AzharUddin M, Yanik J (2014) Hydrogen production from algal biomass via steam gasification. *Bioresour Technol* 166:24–30
- Fisher T, Hajjaligol M, Waymack B, Kellogg D (2002) Pyrolysis behavior and kinetics of biomass derived materials. *J Analyt Appl Pyrolysis* 62:331–349
- Flynn JH, Wall LA (1966) A quick, direct method for the determination of activation energy from thermogravimetric data. *J Polym Sci* 4:323–328
- Friedman HL (1964) Kinetics of thermal degradation of char-forming plastics from thermogravimetry: application to a phenolic plastic. *J Polym Sci* 6:183–195
- Gai C, Zhang Y, Chen WT, Zhang P, Dong Y (2013) Thermogravimetric and kinetic analysis of thermal decomposition characteristic of low-lipid microalgae. *Bioresour Technol* 150:139–148
- García-Quesada JC, Marcilla A, Gilbert M (2001) Study of the pyrolysis behaviour of peroxide cross linked unplasticized PVC. *J Analyt Appl Pyrolysis* 58–59:651–666
- Gomez-Barea A, Leckner B, Villanueva-Perales A, Nilsson S, Fuentes-Cano D (2013) Improving the performance of fluidized bed biomass/waste gasifiers for distributed electricity: a new three-stage gasification system. *Appl Therm Eng* 50:1453–1462
- Grierson S, Strezov V, Ellem G, McGregor R, Herbertson J (2009) Thermal characterization of microalgae under slow pyrolysis conditions. *J Appl Energy* 85:118–123
- Guan Q, Wei C, Ning P, Tian S, Gu J (2013) Catalytic gasification of algae *Nannochloropsis* sp. in sub/supercritical water. *Procedia Environ Sci* 18:844–848
- Haiduc AG, Brandenberger M, Suquet S, Vogel F, Bernier-Latmani R, Ludwig C (2009) An integrated process for the hydrothermal production of methane from microalgae and CO<sub>2</sub> mitigation. *J Appl Phycol* 21:529–541
- Han J, Kim H (2008) The reduction and control technology of tar during biomass gasification/pyrolysis: an overview. *Renew Sust Energy Rev* 12:397–416
- Hanaoka T, Hiasa S, Edashige Y (2013) Syngas production by CO<sub>2</sub>/O<sub>2</sub> gasification of aquatic biomass. *Fuel Process Technol* 116:9–15
- Harman-Ware AE, Morgan T, Wilson M, Crocker M, Zhang J, Liu K, Stork J, Debolt S (2013) Microalgae as a renewable fuel source: fast pyrolysis of *Scenedesmus* sp. *Renew Energy* 60:625–632
- Hirano A, Ueda R, Hirayama S, Ogushi Y (1997) CO<sub>2</sub> fixation and ethanol production with microalgal photosynthesis and intracellular anaerobic fermentation. *Energy* 22:137–142

- Hognon C, Dupont C, Grateau M, Delrue F (2014) Comparison of steam gasification reactivity of algal and lignocellulosic biomass: influence of inorganic elements. *Bioresour Technol* 164:347–353
- Hu M, Chen Z, Guo D, Liu C, Xiao B, Hu Z, Liu S (2015) Thermogravimetric study on pyrolysis kinetics of *Chlorella pyrenoidosa* and bloom-forming cyanobacteria. *Bioresour Technol* 177:41–50
- Jena U, Das KC, Kastner JR (2011) Effect of operating conditions of thermochemical liquefaction on biocrude production from *Spirulina platensis*. *Bioresour Technol* 102:6221–6229
- John RP, Anisha GS, Nampoothiri KM, Pandey A (2011) Micro and macroalgal biomass: a renewable source for bioethanol. *Bioresour Technol* 102:186–193
- Jorquera O, Kiperstok A, Sales EA, Embirucu M, Ghirardi ML (2010) Comparative energy life-cycle analyses of microalgal biomass production in open ponds and photobioreactors. *Bioresour Technol* 101:1406–1413
- Kassim MA, Kirtania K, De C, Cura N, Srivatsa SC, Bhattacharya S (2014) Thermogravimetric analysis and kinetic characterization of lipid-extracted *Tetraselmis suecica* and *Chlorella* sp. *Algal Res* 6:39–45
- Kebelmann K, Hornung A, Karsten U, Griffiths G (2013) Intermediate pyrolysis and product identification by TGA and Py-GC/MS of green microalgae and their extracted protein and lipid components. *Biomass Bioenergy* 49:38–48
- Khoo HH, Koh CY, Shaik MS, Sharratt PN (2013) Bioenergy co-products derived from microalgae biomass via thermochemical conversion – life cycle energy balances and CO<sub>2</sub> emissions. *Bioresour Technol* 143:298–307
- Kim SS, Ly HV, Choi GH, Kim J, Woo HC (2012) Pyrolysis characteristics and kinetics of the alga *Saccharina japonica*. *Bioresour Technol* 123:445–451
- Kim SS, Ly HV, Kim J, Choi JH, Woo HC (2013) Thermogravimetric characteristics and pyrolysis kinetics of Alga *Sagarssum* sp. biomass. *Bioresour Technol* 139:242–248
- Kim SW, Koo BS, Lee DH (2014) A comparative study of bio-oils from pyrolysis of microalgae and oil seed waste in a fluidized bed. *Bioresour Technol* 162:96–102
- Kim SS, Ly HV, Kim J, Lee EY, Wo HC (2015) Pyrolysis of microalgae residual biomass derived from *Dunaliella tertiolecta* after lipid extraction and carbohydrate saccharification. *Chem Eng J* 263:94–199
- Kirtania K, Joshua J, Kassim MA, Bhattacharya S (2014) Comparison of CO<sub>2</sub> and steam gasification reactivity of algal and woody biomass chars. *Fuel Process Technol* 117:44–52
- Koufopoulos CA, Papayannakos N, Maschio G, Lucchesi A (1991) Modelling of the pyrolysis of biomass particles. Studies on kinetics, thermal and heat transfer effects. *Can J Chem Eng* 69:907–915
- Kumar A, Jones DD, Hanna MA (2009) Thermochemical biomass gasification: a review of the current status of the technology. *Energies* 2:556–581
- Lange J-P (2007) Lignocellulosic conversion: an introduction to chemistry, process and economics. *Biofuels Bioprod Biorefin* 1:39–48
- Laudenslager M, Scheffer RH, Sigmund W (2010) Electrospun materials for energy harvesting, conversion and storage: a review. *Pure Appl Chem* 82:2137–2156
- Levine RB, Pinnarat T, Savage PE (2010) Biodiesel production from wet algal biomass through in situ lipid hydrolysis and supercritical transesterification. *Energy Fuels* 24:5235–5243
- Li J, Yan R, Xiao B, Liang DT, Du L (2008) Development of nano-NiO/Al<sub>2</sub>O<sub>3</sub> catalyst to be used for tar removal in biomass gasification. *Environ Sci Technol* 42:6224–6229
- Li D, Chen L, Zhang X, Ye N, Xing F (2011) Pyrolytic characteristics and kinetic studies of three kinds of red algae. *Biomass Bioenergy* 35:1765–1772
- Li F, Liang Z, Zheng X, Zhao W, Wu M, Wang Z (2015) Toxicity of nano-TiO<sub>2</sub> on algae and the site of reactive oxygen species production. *Aquat Toxicol* 158:1–13
- Lopez-Gonzalez D, Fernandez-Lopez M, Valverde JL, Sanchez-Silva L (2014) Pyrolysis of three different types of microalgae: kinetic and evolved gas analysis. *Energy* 73:33–43

- Luo Z, Zhou J (2012) Thermal conversion of biomass. In: Chen WY, Seiner J, Suzuki T, Lackner M (eds) Handbook of climate change mitigation. Springer Science Business Media, LLC, New York, NY, pp 1002–1037
- Maciejewski M (2000) Computational aspects of kinetic analysis. Part B: The ICTAC Kinetics Project Ð the decomposition kinetics of calcium carbonate revisited, or some tips on survival in the kinetic minefield. *Thermochim Acta* 355:145–154
- Marcilla A, Gómez-Siurana A, Gomis C, Chápuli E, Catalá MC, Valdés FJ (2009) Characterization of microalgal species through TGA/FTIR analysis: application to *nannochloropsis* sp. *Thermochim Acta* 484:41–47
- Marcilla A, Catalá L, García-Quesada JC, Valdés FJ, Hernández MR (2013) A review of thermochemical conversion of microalgae. *Renew Sust Energy Rev* 27:11–19
- Maria VH (2014) CO<sub>2</sub> emissions from fuel combustion highlights. <https://www.iea.org/publications/freepublications/publication/CO2EmissionsFromFuelCombustionHighlights2014.pdf>
- Mata TM, Martins AA, Caetano NS (2010) Microalgae for biodiesel production and other applications: a review. *Renew Sust Energy Rev* 14:217–232
- Meng X, de Jong W, Fu N, Verkooijen AHM (2011) Biomass gasification in a 100 kWth steam-oxygen blown circulating fluidized bed gasifier: effects of operational conditions on product gas distribution and tar formation. *Biomass Bioenergy* 35:2910–2924
- Metzler DM, Li M, Erdem A, Huang CP (2011) Responses of algae to photocatalytic nano-TiO<sub>2</sub> particles with an emphasis on the effect of particle size. *Chem Eng J* 170:538–546
- Min FF, Zhang MX, Chen QR (2007) Non-isothermal kinetics of pyrolysis of three kinds of fresh biomass. *J China Univ Min Technol* 17:105–111
- Minowa T, Sawayama S (1999) A novel microalgal system for energy production with nitrogen cycling. *Fuel* 78:1213–1215
- Nahak S, Nahak G, Pradhan I, Sahu RK (2011) Bioethanol from marine algae: a solution to global warming problem. *J Appl Environ Biol Sci* 1:74–80
- Naik SN, Goud VV, Rout PK, Dalai AK (2010) Production of first and second generation biofuels: a comprehensive review. *Renew Sust Energy Rev* 14:578–597
- Nigam P, Singh A (2011) Production of liquid biofuels from renewable resources. *Prog Energy Combust Sci* 37:52–68
- Nordgreen T (2011) Iron-based materials as tar cracking catalyst in waste gasification. Ph.D. Thesis, Department of Chemical Engineering and Technology Chemical Technology, KTH-Royal Institute of Technology, SE-100 44 Stockholm, Sweden
- Nzihou A, Stanmore B, Sharrock P (2013) A review of catalysts for the gasification of biomass char, with some reference to coal. *Energy* 58:305–317
- Onwudili JA, Lea-Langton AR, Ross AB, Williams PT (2013) Catalytic hydrothermal gasification of algae for hydrogen production: composition of reaction products and potential for nutrient recycling. *Bioresour Technol* 127:72–80
- Ozawa T (1965) A new method of analyzing thermogravimetric data. *Bull Chem Soc Jpn* 38:1881–1886
- Pane L, Franceschi E, Denuccio L, Carli A (2001) Applications of thermal analysis on the marine phytoplankton, *Tetraselmis Suecica*. *J Therm Anal Calorim* 66:145–154
- Peng W, Wu Q, Tu P, Zhao N (2001) Pyrolytic characteristics of microalgae as renewable energy source determined by thermogravimetric analysis. *Bioresour Technol* 80:1–7
- Phukan MM, Chutia RS, Konwar BK, Kataki R (2011) Microalgae *Chlorella* as a potential bio-energy feedstock. *Appl Energy* 88:3307–3312
- Plis P, Wilk RK (2011) Theoretical and experimental investigation of biomass gasification process in a fixed bed gasifier. *Energy* 36:3838–3845
- Pugh S, McKenna R, Moolick R, Neilson DR (2010) Advances and opportunities at the interface between microbial bioenergy and nanotechnology. *Can J Chem Eng* 89:1–12
- Raheem A, Sivasangar S, Azlina WAK, Yap YT, Danquah MK, Harun R (2015a) Thermogravimetric study of *Chlorella vulgaris* for syngas production. *Algal Res* 12:52–59

- Raheem A, Azlina WAK, Yap YT, Danquah MK, Harun R (2015b) Optimization of the microalgae *Chlorella vulgaris* for syngas production using central composite design. RSC Adv 5:71805–71815
- Rizzo AM, Prussi M, Bettucci L, Libelli IM, Chiaramonti D (2013) Characterization of microalgae *Chlorella* as a fuel and its thermogravimetric behavior. Appl Energy 102:24–31
- Saddawi A, Jones JM, Williams A, Wojtowicz MA (2010) Kinetics of the thermal decomposition of biomass. Energy Fuels 24:1274–1282
- Saidur R, Abdelaziz EA, Demirbas A, Hossain MS, Mekhilef S (2011) A review on biomass as a fuel for boilers. Renew Sust Energy Rev 15:2262–2289
- Sanchez-Silva L, López-González D, Garcia-Minguillan AM, Valverde JL (2013) Pyrolysis, combustion and gasification characteristics of *Nannochloropsis gaditana* microalgae. Bioresour Technol 130:321–331
- Schenk PM, Thomas-Hall SR, Stephens E, Marx UC, Mussgnug JH, Posten C, Kruse O, Hankamer B (2008) Second generation biofuels: high-efficiency microalgae for biodiesel production. Bioenergy Res 1:20–43
- Sheth PN, Babu BV (2009) Experimental studies on producer gas generation from wood waste in a downdraft gasifier. Bioresour Technol 100:3127–3133
- Shuping Z, Yulong W, Mingde Y, Kaleem I, Chun L, Tong J (2010a) Production and characterization of bio-oil from hydrothermal liquefaction of microalgae *Dunaliella tertiolecta* cake. Energy 35:5406–5411
- Shuping Z, Yulong W, Mingde Y, Chun L, Junmao T (2010b) Pyrolysis characteristics and kinetics of the marine microalgae *Dunaliella tertiolecta* using thermogravimetric analyzer. Bioresour Technol 101:359–365
- Sims REH, Mabee W, Saddler JN, Taylor M (2011) An overview of second generation biofuel technologies. Bioresour Technol 101:1570–1580
- Sinag A (2012) Catalysts in thermochemical biomass conversion. In: Baskar S, Baskar C, Dhillon RS (eds) Biomass conversion. Springer, Berlin, pp 187–197
- Sinag A, Yumak T, Balci V, Kruse A (2011) Catalytic hydrothermal conversion of cellulose over SnO<sub>2</sub> and ZnO nanoparticle catalysts. J Supercrit Fluid 56:179–185
- Singh A, Nigam PS, Murphy JD (2011a) Renewable fuels from algae: an answer to debatable land based fuels. Bioresour Technol 102:10–16
- Singh A, Nigam PS, Murphy JD (2011b) Mechanism and challenges in commercialization of algal biofuels. Bioresour Technol 102:26–34
- Spolaore P, Joannis-Cassan C, Duran E, Isambert A (2006) Commercial applications of microalgae. J Biosci Bioeng 101:87–96
- Stenseng M, Jensen A, Dam-Johansen K (2001) Investigation of biomass pyrolysis by thermogravimetric analysis and differential scanning calorimetry. J Analyt Appl Pyrolysis 58–59:765–780
- Stucki S, Vogel F, Ludwig C, Haiduc AG, Brandenberger M (2009) Catalytic gasification of algae in supercritical water for biofuel production and carbon capture. Energy Environ Sci 2:535–541
- Subhadra B, Edwards M (2010) An integrated renewable energy park approach for algal biofuel production in United States. Energy Policy 38:4897–4902
- Sutton D, Kelleher B, Ross JRH (2001) Review of literature on catalyst for biomass gasification. Fuel Process Technol 73:155–173
- Tahmasebi A, Kassim MA, Yu J, Bhattacharya S (2013) Thermogravimetric study of the combustion of *Tetraselmis suecica* microalgae and its blend with a Victorian brown coal in O<sub>2</sub>/N<sub>2</sub> and O<sub>2</sub>/CO<sub>2</sub> atmospheres. Bioresour Technol 150:15–27
- Thangalazhy-Gopakumara S, Adhikaria S, Chattanathana SA, Gupta RB (2012) Catalytic pyrolysis of green algae for hydrocarbon production using H-ZSM-5 catalyst. Bioresour Technol 118:150–157

- Vardon DR, Sharma BK, Blazina GV, Rajagopalan K, Strathmann TJ (2012) Thermochemical conversion of raw and defatted algal biomass via hydrothermal liquefaction and slow pyrolysis. *Bioresour Technol* 109:178–187
- Verdugo M, Lim LT, Rubilar M (2014) Electrospun protein concentrate fibers from microalgae residual biomass. *J Polym Environ* 22:373–383
- Verma NM, Mehrotra S, Shukla A, Mishra BN (2010) Prospective of biodiesel production utilizing microalgae as the cell factories: a comprehensive discussion. *Afr J Biotechnol* 9:1402–1411
- Vinu R, Broadbelt LJ (2012) A mechanistic model of fast pyrolysis of glucose-based carbohydrates to predict bio-oil composition. *Energy Environ Sci* 5:9808–9826
- Vyazovkin S, Burnham AK, Criado JM, Pérez-Maqueda LA, Popescu C, Sbirraz-zuoli N (2011) ICTAC kinetics committee recommendations for performing kinetic computations on thermal analysis data. *Thermochim Acta* 520:1–19
- Wang K, Brown RC (2013) Catalytic pyrolysis of microalgae for production of aromatics and ammonia. *Green Chem* 15:675–681
- Wu KT, Tsai CJ, Chen CS, Chen HW (2012) The characteristics of torrefied microalgae. *Appl Energy* 100:52–57
- Wu S, Li Y, Zhao X, Du Q, Wang Z, Xia Y, Xia L (2015) Biosorption behavior of ciprofloxacin onto *Enteromorpha prolifera*: isotherm and kinetic studies. *Int J Phytoremed* 17:957–961
- Yang K-C, Wu K-T, Hsieh M-H, Hsu H-T, Chen C-S, Chen H-W (2013) Co-gasification of woody biomass and microalgae in a fluidized bed. *J Taiwan InstChemEng* 44:1027–1033
- Yu G, Zhang Y, Schideman L, Funk T, Wang Z (2011) Distributions of carbon and nitrogen in the products from hydrothermal liquefaction of low-lipid microalgae. *Energy Environ Sci* 4:4587–4595
- Zhang JX, Chen WT, Zhang P, Luo ZY, Zhang YH (2013) Hydrothermal liquefaction of *Chlorella pyrenoidosa* in sub and supercritical ethanol with heterogeneous catalysts. *Bioresour Technol* 133:389–397

# Chapter 6

## Hierarchy Nano- and Ultrastructure of Lignocellulose and Its Impact on the Bioconversion of Cellulose

Xuebing Zhao, Feng Qi, and Dehua Liu

**Abstract** Lignocellulose has been considered as one of the most promising biomass feedstock for producing biofuels and biochemicals. However, lignocellulose is indeed a complicated natural biomaterial at nano- and microscales. This is because the chemical compositions of lignocellulose cell wall construct a bulwark with a spatially hierarchy nano- and ultrastructure to protect the structural carbohydrates from degradation, which is known as the biomass recalcitrance. In this chapter, we have reviewed the structural features of lignocellulosic biomass, particularly on the hierarchy nano- and ultrastructure of plant cell wall and its impact on the bioconversion of the biomass. The effects of various pretreatments on the structure changes of the biomass substrates have been discussed. The tools and methodologies to characterize the nano- and ultrastructure of lignocellulosic biomass also have been reviewed.

**Keywords** Lignocellulosic biomass • Hierarchy structure • Cell wall ultrastructure • Biomass recalcitrance • Bioconversion • Pretreatment

### 6.1 Introduction

Lignocellulose, mostly existing in the form of plant materials, is one of the most abundant organic materials in natural world. It has been estimated that there is an annual worldwide production of 10–50 billion tons of dry lignocellulose, accounting for about half of the global biomass yield (Zhao et al. 2012a). However, much of the lignocellulosic biomass is just thrown away (Sanderson 2011). Typical lignocellulose refers to grass, woody, and agricultural residues. Straw biomass such as corn stover,

---

X. Zhao (✉) • D. Liu

Department of Chemical Engineering, Institute of Applied Chemistry, Tsinghua University, Beijing 100084, China

e-mail: [zhaoxb@mail.tsinghua.edu.cn](mailto:zhaoxb@mail.tsinghua.edu.cn)

F. Qi

College of Life Sciences/Engineering Research Center of Industrial Microbiology, Fujian Normal University, Fuzhou 350108, China

wheat straw, rice straw, and bagasse is the most abundant agricultural lignocellulose distributed worldwide. In some countries, such as Canada and the USA, woody biomass is also an important lignocellulosic biomass for biorefinery (Zhu and Pan 2010). Some energy crops for producing lignocellulosic biomass have been developed and cultured in a relatively large scale, such as switchgrass in North America (David and Ragauskas 2010) and *Miscanthus* in Europe (Brosse et al. 2012).

In recent years, as the depletion of fossil resources, continuously serious environmental pollutions, and the increasing demand of fuels, lignocellulose has been considered as one of the most promising feedstock to produce fuels and chemicals as a substitute of fossil resource. Lignocellulosic biomass can offer the possibility of a renewable, geographically distributed, and relatively greenhouse-gas-favorable source of sugars that can be further converted to liquid fuels and chemicals via chemical or biological ways, which is known as the conception of “biomass biorefinery” (Demirbas 2009). According to the National Renewable Energy Laboratory of the USA, biorefinery is defined as “a facility that integrates biomass conversion processes and equipment to produce fuels, power, and chemicals from biomass,” which is analogous to today’s petroleum refineries (<http://www.nrel.gov/biomass/biorefinery.html>). It has been considered that lignocellulose biorefinery will most probably be pushed through with highest success among the potential industrial biorefineries, because the raw material situation is optimal and the conversion products have a good position in the traditional petrochemical as well as in the future bio-based product market (Kamm and Kamm 2007). Many products can be produced from lignocellulosic sugars by either chemical or biological conversions or combination of both in the biorefinery. However, lignocellulose is indeed a complex heterogeneous composite at multiple scales, and recalcitrant to deconstruction and saccharification due to its fundamental molecular architecture and multicomponent laminate composition. At the molecular scale, the chemical compositions of cell wall vary widely among and within plant species. At the nanoscale, domains within a single cell wall contain specific sets of polymers and molecular interaction characteristic of the developmental stage. At the mesoscale, emergent biophysical properties are imparted by differing proportions of cell types, sizes, shapes, and sites of cell-cell adhesion (McCann and Carpita 2015). In this chapter, we focus on the structural features of lignocellulosic biomass, particularly on the hierarchy nano- and ultrastructures of plant cell wall and their impacts on the bioconversion of the biomass.

## 6.2 Chemical Compositions of Lignocellulose

Lignocellulose actually mainly refers to the agricultural and forest residuals, the part of cell wall tissues. It is mainly composed of cellulose, hemicellulose, and lignin. Cellulose and hemicellulose are also known as holocellulose, the total carbohydrates of lignocellulosic biomass. Generally, woody lignocellulose contains 40–55 % cellulose, 8–30 % hemicellulose, and 18–35 % lignin, while grass

lignocellulose contains 25–50 % cellulose, 20–50 % hemicellulose, and 10–30 % lignin (Zhao et al. 2012a). Carbohydrates usually account for more than 60 % of lignocellulosic biomass, and whereby they are the main feedstock in biomass biorefinery system. Cellulose is the most important carbohydrate for lignocellulose biorefinery, which is a polysaccharide consisting of  $\beta$ -(1 $\rightarrow$ 4)-linked D-glucose units. Hemicelluloses are a diverse group of short-chain branched and substituted polymer of sugars with much lower degree of polymerization (~70 to 200) (Scheller and Ulvskov 2010). It has a backbone composed of 1, 4-linked  $\beta$ -D-hexosyl residues and may contain pentose (xylose, arabinose), hexoses (glucose, galactose, mannose), and/or uronic acids (hexuronic acids) (Girio et al. 2010). Hemicelluloses are also important carbohydrate feedstocks for lignocellulose biorefinery. Lignin is a large group of aromatic polymers resulting from the oxidative combinatorial coupling of 4-hydroxyphenylpropanoids (Vanholme et al. 2010) with three basic monomeric units (monolignols): p-hydroxyphenyls (H), guaiacyls (G), and syringyls (S) (Chundawat et al. 2011a). During lignocellulose biorefining system, lignin is usually used as a feedstock for aromatic compounds production or as a fuel for heat recovery. Generally, woody biomass contains more glucan and lignin, while non-woody biomass contains more ash, extractives, and hemicellulose. The contents of the major compositions are varied significantly as lignocellulose types, and even different parts of a plant have different contents of the major compositions. However, although lignocellulose is of variety in its contents of compositions, much has been known on its chemistry and structural characteristics, particularly on the chemical features of cellulose, hemicellulose, and lignin.

## 6.2.1 Cellulose Chemistry and Structure

Since cellulose was discovered in 1838 by the French chemist Anselme Payen, it has been widely used in many areas for about 150 years (Klemm et al. 2005). Significant process also has been made to understand cellulose chemistry and structure; however, there are still lots of aspects that should be further understood, particularly on the complex hydrogen-bonding networks and supermolecular structure of cellulose.

### 6.2.1.1 Chemical Features of Cellulose

It has been known that cellulose is a homopolymer of glucose with “cellobiose” as a repeat unit (Fig. 6.1a). Generally, the chemical features of cellulose can be summarized as following aspects:

1. Cellulose consists of elements C, H, and O, and corresponding contents are 44.44 %, 6.17 %, and 49.39 %, respectively. The basic monomer of cellulose is D-glucose, more accurately D-anhydroglucopyranose units (AGU). Therefore,



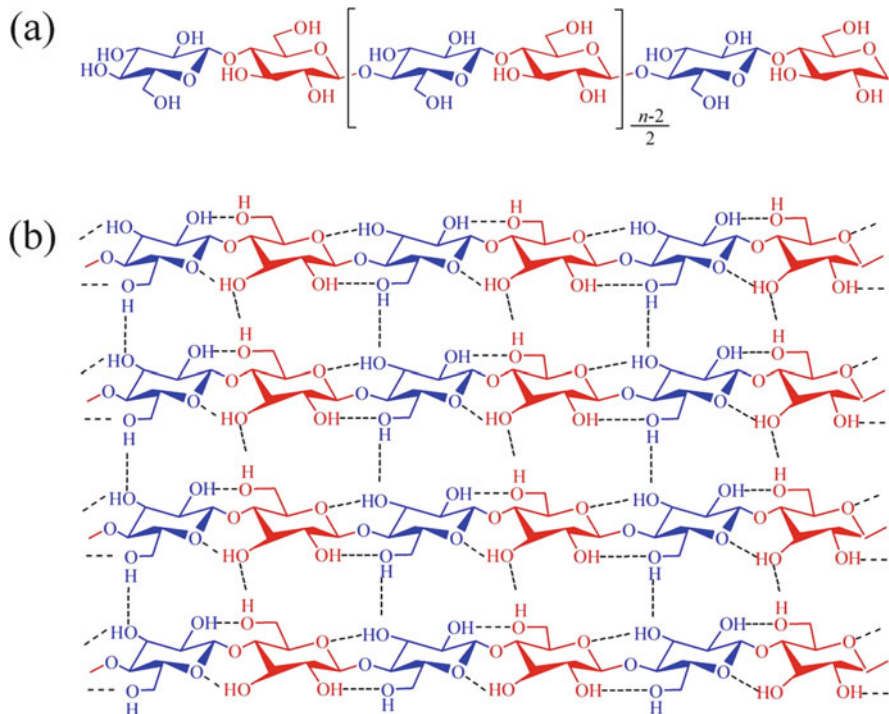


**Fig. 6.1** Molecular structure of cellulose (a) and its hydrogen bond network (b)

the chemical formula of cellulose can be expressed as  $(\text{C}_6\text{H}_{10}\text{O}_5)_n$ , where  $n$  is the number of D-glucose unit (degree of polymerization, DP). The value of  $n$  can be varied in the range of 500 and 14,000 depending on the cellulose source (Mohnen et al. 2008). Naturally occurring vascular plant cellulose has an average DP higher than 10,000 (Krässig 1996). However, cellulose DP decreases to some extent after processing depending on the treatment process. For example, wood dissolving pulp has a cellulose DP of 600–1200, and man-made cellulose filaments and fiber have a DP of 250–500, while the DP of cellulose powder decreases to 100–200 (Klemm et al. 1998). By acid treatment and cellulase-catalyzed hydrolysis, cellulose can be quantitatively decomposed to D-glucose.

2. Cellulose is a linear polymer of glucose by  $\beta$  (1 $\rightarrow$ 4) glycosidic bonds formed between C-1 and C-4 of adjacent glucose moieties (Fig. 6.1a) (Klemm et al. 1998). Each successive glucose unit is rotated 180 degrees around the axis of the polymer backbone chain, relative to the last repeat unit. This kind of glycosidic bond is relatively stable, so that cellulose is not easy to hydrolyze unless using concentrated acid or at high temperature. Another evidence for the high stability of  $\beta$ -1,4 glycosidic linkage refers that cellulose is much difficult to hydrolyze than starch. Starch is a glucose polymer linked together by  $\alpha$ -1,4 and

$\alpha$ -1,6 glycosidic bonds, and all the glucose repeat units are oriented in the same direction. Generally, the acid hydrolysis of starch is three times quicker than that of cellulose.

3. Three hydroxyl groups are equatorially positioned in the AGU at C2, C3, and C6 sites, corresponding to one primary (C6-OH) and two secondary groups (C2, C3-OH). These hydroxyl groups determine the chemical characteristics and reactivity of cellulose (Granström 2009). Cellulose can be modified by esterification, etherification, oxidation, and graft copolymerization due to the presence of these hydroxyl groups. The acidity of these three hydroxyl groups follows the order of C2>C3>C6. The reactivities of the hydroxyl groups are also different. Generally, the esterification rate of C6-OH is ten times faster than those of C2, C3-OH, while the etherification rate of C2-OH is two times faster than that of C3-OH (Zhan 2005). Hydroxyl group also play an important role in the solubility of cellulose. Native cellulose is insoluble in common organic solvents and in water, due to the fact that extensive hydrogen-bonding network is formed by hydroxyl groups via intra- and intermolecular hydrogen bonding. In order to dissolve cellulose, the prevailing hydrogen-bonding network must be broken (Granström 2009).
4. Cellulose molecule has a reducing end and nonreducing end. The reducing end has a free hemiacetal (or aldehyde) group at C-1, and the nonreducing end has a free hydroxyl at C-4 (Festucci-Buselli et al. 2007). The presence of reducing end endows cellulose several properties and reactivity for modification. For example, the thermal stability of cellulose is relevant to the amount of reducing end (Matsuoka et al. 2011), and the dissolution of cellulose in ionic liquid (IL) might be caused by the reaction between the reducing end of cellulose and IL (Ebner et al. 2008). Moreover, the presence of reducing and nonreducing ends makes cellulose have a molecular polarity and polymorphs directionality.

### 6.2.1.2 Crystalline Structures of Cellulose

Cellulose contains amorphous and crystalline structures. In amorphous region, the cellulose is present in a less order form because the hydrogen bond network is not well established. Therefore, amorphous cellulose is much less recalcitrant to chemical reagent and enzymes. In crystalline region, cellulose chains are present in high order due to the hydrogen bond network (Fig. 6.1b), so that crystalline cellulose is much more stable and even water molecule is hard to permeate into it. Ordered hydrogen bond systems are formed by the OH groups at C2, C3, and C6 sites and the oxygen atoms of both the pyranose ring and the glycosidic bond (Fig. 6.1b), which form various types of supramolecular semicrystalline structures (Klemm et al. 2002). Both intra- and intermolecular hydrogen bonding are found in cellulose. However, although the crystal structure of cellulose has been investigated for almost a century (Nishiyama et al. 2003), the detailed structure of the hydrogen bond system is still a subject of discussion. The presence of intramolecular hydrogen bonds is of high relevance with regard to the single-chain conformation and

stiffness, while the intermolecular hydrogen bonding is responsible for the sheetlike nature of the native polymer (Klemm et al. 2002).

Pure cellulose can exist in several crystalline polymorphs with different packing arrangements (Zugenmaier 2007). One polymorph can be reversibly or irreversibly transformed to another. Natural cellulose exists as cellulose I. It is now recognized that cellulose I simultaneously crystallizes in a one-chain triclinic structure  $I_{\alpha}$  and a two-chain modification  $I_{\beta}$  (Zugenmaier 2007). In cellulose  $I_{\alpha}$ , all chains are crystallographically identical, but alternating glucose units in each chain and adjacent chains are linked by a zigzag, repeating  $O-H\cdots O-H\cdots$  motif. In cellulose  $I_{\beta}$  chains of two distinct kinds are arranged in alternating sheets (Jarvis 2003). Cellulose  $I_{\alpha}$  and  $I_{\beta}$  are of various ratios in a fiber depending on the origin. The cell wall of some algae and bacterial cellulose are rich in  $I_{\alpha}$ , while cotton, wood, and ramie fibers are rich in  $I_{\beta}$  (Nishiyama et al. 2003). However, cellulose  $I_{\alpha}$  can be transformed to  $I_{\beta}$  by a hydrothermal treatment in an alkaline solution (Yamamoto and Horii 1993) or a heat treatment at 280 °C in an inert gas (helium) (Wada et al. 2003). The crystal structure and hydrogen-bonding system of cellulose  $I_{\alpha}$  and  $I_{\beta}$  have been intensively studied by Nishiyama et al. (2002, 2003) with synchrotron X-ray and neutron fiber diffraction, and more data can be found in their works.

### 6.2.1.3 Effect of Crystalline and Nanostructure on Cellulose Susceptibility

Due to the presence of highly ordered hydrogen-bonding network, crystalline structure is much more stable than amorphous structure. Mazeau and Heux (2003) demonstrated by molecular simulation that the total number of hydrogen bonds per repeat unit is 8 in the crystalline form of cellulose  $I_{\alpha}$  but is only 5.3 in the amorphous form, and the crystalline form of cellulose has much larger cohesive energy density than noncrystalline forms. Therefore, amorphous regions are much more easily penetrated by chemical species and enzymes for hydrolysis. It has been found that amorphous celluloses are typically 3–30 times faster to hydrolyze than high crystalline cellulose (Zhang and Lynd 2004). Zhao et al. (2006) found that acid hydrolysis rate of cellulose increased more than doubled when crystallinity index of cellulose decreased from 0.773 to 0.523. This increased hydrolysis rate was attributed to disruption of hydrogen bonding and a concomitant increase in the number of  $\beta$ -1,4-glycosidic bonds accessible to the acid involved in hydrolysis. By comparing the hydrolysis behavior of amorphous and crystalline cellulose in hot-compressed water system, Yu and Wu (2010) found the minimal temperature for breaking the glycosidic bonds in those short-chain segments to form glucose monomer from amorphous portion of microcrystalline cellulose was 150 °C; however, the minimal temperature is around 180 °C for the crystalline portion. During enzymatic hydrolysis of cellulose, amorphous cellulose was hydrolyzed first followed by the hydrolysis of the more recalcitrant crystalline composition (Szijarto et al. 2008; Hall et al. 2010). This is mainly because that amorphous cellulose is much easier to allow the penetration of cellulase enzymes to perform the catalytic actions.

Since the cellulose susceptibility is strongly affected by its hydrogen-bonding system, the different cellulose polymorphs show different stability, reactivity, and accessibility. For heating cellulose  $I_{\alpha}$ , the intermolecular hydrogen bonds cannot be broken unless the temperature is higher than 200 °C. Above this temperature, cellulose molecular chains may become more flexible with a thermal expansion of the crystal lattice and form a transformation intermediate structure, but after cooling new types of hydrogen bonds may reform (Wada et al. 2003). Cellulose  $I_{\alpha}$  is metastable and mostly converts to  $I_{\beta}$  by a heat treatment. It indicates that  $I_{\beta}$  is thermodynamically more stable than  $I_{\alpha}$ . Moreover, when comparing the acetylation reaction of Valonia cellulose  $I_{\alpha}$  and  $I_{\beta}$  by partial homogeneous acetylation, Sassi et al. (2000) found that cellulose  $I_{\alpha}$  indeed was more reactive than cellulose  $I_{\beta}$ . Beckham et al. (2011) conducted molecular simulation to calculate the free energy for decrystallization of several cell polymorphs. They found that the order of decrystallization work for edge chain follows an order of  $I_{\beta} > I_{\alpha} > III_1 > II$ , indicating  $I_{\beta}$  is the most stable of these cellulose polymorphs. However, Ciolacu et al. (2012) assessed the accessibility of different allomorphic forms of cellulose through a water vapor sorption method and found that the accessibility for crystal surfaces and amorphous regions was in the order of Cellulose II > Cellulose I > Cellulose III. It indicates that the determined reactivities of cellulose polymorphs are also dependent on the reagents.

Enzymatic hydrolysis rate of cellulose can be improved by reconstructing the crystalline hydrogen bond network. As found by Chundawat et al. (2011b), the transformation of allomorph  $I_{\beta}$  to  $III_1$  by ammonia led to the decrease in the number of cellulose intrasheet hydrogen bonds and an increase in the number of intersheet hydrogen bonds, resulting in enhancement of the cellulose hydrolysis rates by up to fivefold (closest to that of amorphous cellulose). Generally, the relative rates of digestibility of cellulose are in the order of amorphous >  $III_1 > IV_1 > III_{II} > I > II$  (Balan et al. 2011). However, the accessibility of cellulose in lignocellulose cell wall is not only influenced by cellulose structure of itself but also, maybe more significantly, by the other compositions and spatial structure of cell wall.

## 6.2.2 Hemicelluloses Chemistry and Structures

Hemicelluloses are the second abundant natural carbohydrates. As an important component of plant cell wall, hemicelluloses are also paid great attention for application to produce biofuels and chemicals. Various processes have been developed to industrially isolate hemicelluloses from lignocellulosic biomass, but the hemicelluloses may degrade to some extent with different properties (Puls and Saake 2004) Being different from cellulose, hemicelluloses are not homopolymers, but heteropolymers of several monosaccharide groups and uronic acid groups (Fig. 6.2), including D-xylose, L-arabinose, D-glucose, D-galactose, D-mannose, D-glucuronic acid, 4-O-methyl-D-glucuronic acid, D-galacturonic acid, and, to a lesser extent, L-rhamnose, L-fucose, and various O-methylated neutral sugars (Xu 2010).

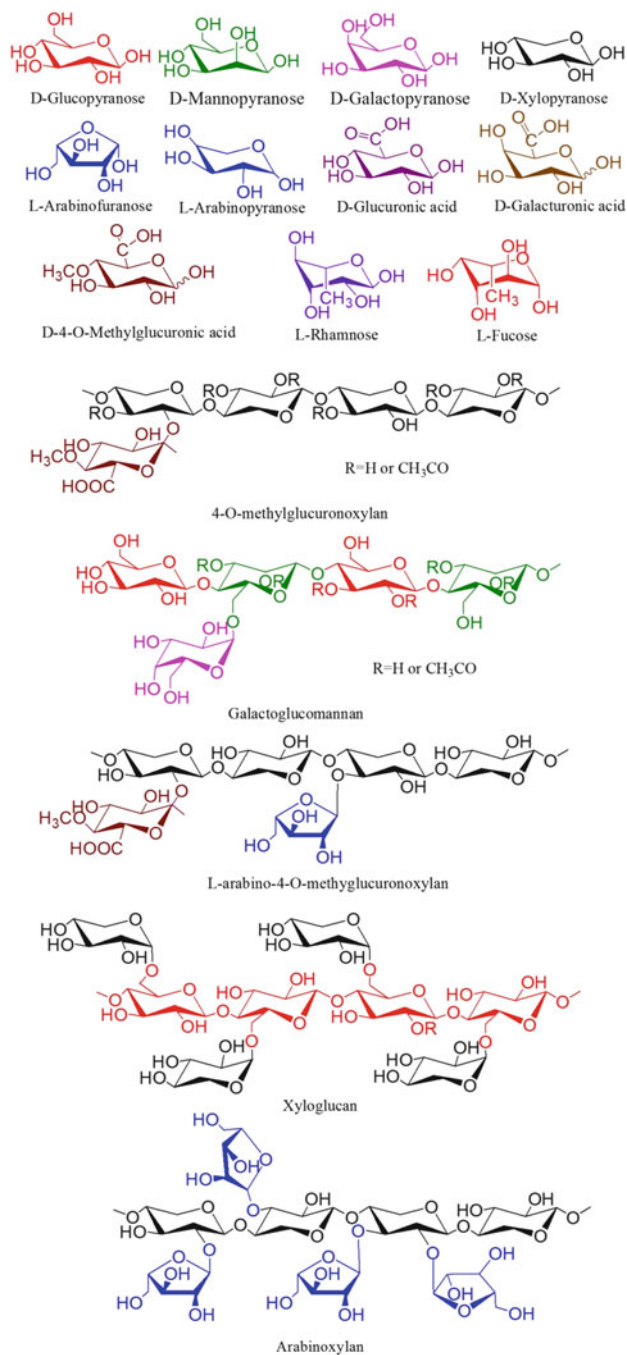


**Fig. 6.2** Main monosaccharide monomers and structure of hemicelluloses in plant cell wall (Ren and Sun 2010) (Adapted and redrawn with permission from the authors)

They are groups of polysaccharides having  $\beta$ -(1 $\rightarrow$ 4)-linked backbones with an equatorial configuration (Maki-Arvela et al. 2011). Uronic acid groups and acetyl group are also found to link with the polysaccharide backbone as side chains. The chemical structure, characterization, and hydrolysis of hemicelluloses have been comprehensively reviewed (Sun et al. 2004; Ebringerova et al. 2005; Girio et al. 2010; Ren and Sun 2010; Scheller and Ulvskov 2010; Maki-Arvela et al. 2011). Generally, hemicelluloses account for about one-fourth to one-third of most lignocellulosic materials, and this content varies according to the particular plant species. Hemicelluloses have much lower molecular weight than cellulose with degree of polymerization (DP) of 80–200 (Xu 2010). No crystalline structure is formed in hemicelluloses, so that they are much more susceptible to chemicals. Therefore, hemicelluloses are usually characterized as the heterogeneous polysaccharides being soluble in strong alkali (Ragauskas et al. 2006).

The structure of hemicelluloses varies with the plant species. In hardwoods the principal hemicellulose structure is O-acetyl-4-O-methylglucuronoxylan (GX) with amount between 15 % and 30 % depending on the species (Peng et al. 2012). GX consists of a linear backbone of  $\beta$ -D-xylopyranosyl units via  $\beta$ -(1,4) glycosidic bonds linkage with some xylose units acetylated at C2 and C3. Uronic acid group (4-O-methylglucuronic acid) is found to link on the xylan chain by  $\alpha$ -(1,2) linkages (Fig. 6.2) (Pereira and Graça 2003). In softwood (Gymnospermae), galactoglucomannans (O-acetyl-galactoglucomannans) are the main hemicelluloses with content of 10–25 % of dry mass. It consists of a backbone of randomly distributed (1 $\rightarrow$ 4)-linked mannose and glucose units with (1 $\rightarrow$ 6)-linked galactose units attached to mannose units. The hydroxyl groups in locations C2 and C3 in mannose are partially substituted by acetyl groups (Willfor et al. 2008). Hemicelluloses from non-woody materials such as agricultural crops mainly consist of arabinoglucuronoxylans (arabino-4-O-methylglucuronoxylans), which contain a linear  $\beta$ -(1 $\rightarrow$ 4)-D-xylopranose backbone with 4-O-methyl-D-glucuronic acid and  $\alpha$ -L-arabinofuranosyl units attached at C2 and C3, respectively (Fig. 6.2) (Peng et al. 2012). Xyloglucan is the quantitatively predominant hemicellulosic polysaccharide in the primary walls of dicots and non-graminaceous monocots and may account for up to 20 % of the dry weight of the primary wall (Hayashi 1989). It binds to the surface of cellulose microfibrils by forming hydrogen bonds thus increasing the structural integrity of the cellulose network (de Vries and Visser 2001). Arabinoxylans are the major hemicellulose structures of the cereal grain cell walls, which are similar to hardwoods xylan but with higher amount of L-arabinose (Girio et al. 2010). It consists of  $\alpha$ -L-arabinofuranose residues attached as branch points to  $\beta$ -(1,4)-linked D-xylopyranose polymeric backbone chains, which may be 2- or 3-substituted or 2- and 3-di-substituted (Izydorczyk and Biliaderis 1995).

### 6.2.3 Lignin Chemistry and Structures

Lignin is an aromatic polymer composed of phenylpropane units and is found in all vascular plants. It binds the cells, fibers, and vessels like a “glue” to reinforce cell walls and keep them from collapsing. Lignin has been studied for more than one century, but its biosynthesis and structure still has not been clearly elucidated yet. However, it has been widely accepted that the biosynthesis of lignin stems from the polymerization of three types of phenylpropane units (monolignols), namely, *p*-coumaryl, coniferyl, and sinapyl alcohols as shown in Fig. 6.3 (Lisperguer et al. 2009), and corresponding aromatic residues constituting lignin polymer are termed as *p*-hydroxyphenyl (H), guaicyl (G), and syringyl (S) units (Calvo-Flores and Dobado 2010). The ratio of H/G/S units in the lignin is highly dependent on plant taxonomy. Generally, there are three main groups of lignins: the lignins from softwoods (gymnosperms), hardwoods (angiosperms), and grasses (non-woody or herbaceous crops) (Buranov and Mazza 2008). Hardwood lignins are predominantly composed of G and S units with trace amounts of H units. Softwood lignins are composed of mostly G units, whereas grass lignins contain all three units in significant amounts with different ratios (Buranov and Mazza 2008; Chundawat et al. 2011a). The linkages between the phenylpropane units and their abundance are dominant structural features of lignin. Although the structure of native lignin still remains unclear, approximately 85 % of the lignin interunit linkages have been identified (Capanema et al. 2005). The phenylpropane units are linked by various ether and C–C bonds (Fig. 6.3), and  $\beta$ -O-4 is the dominant linkage.

Generally,  $\beta$ -O-4 linkage accounts for more than 50 % of the total linkages (Table 6.1). However, the percentages of the linkage types between phenylpropane units vary with plant species and the isolation process. On the other hand, the frequency of these linkages is found to have significant consequences on the lignin’s overall reactivity. For example, during organosolv delignification process, cleavage of ether linkages is primarily responsible for lignin breakdown. Under acidic conditions  $\alpha$ -ether bonds are most readily broken, but  $\beta$ -ether cleavage also plays a role, while in alkaline systems, the cleavage of  $\beta$ -ethers is more important (McDonough 1993). Lignin macromolecule also contains a variety of functional groups that have an important impact on its reactivity. The main chemical functional groups are the hydroxyl (including aliphatic and phenolic), methoxyl, carbonyl, and carboxylic groups (El Mansouri and Salvado 2007). Only a small proportion of the phenolic hydroxyl groups are free since most of them are occupied in linkages to neighboring phenylpropane units. The proportion of these functional groups greatly depends on the genetic origin and isolation processes.

Lignin is covalently bound to the side chains of branched hemicelluloses to form lignin-carbohydrate complex (LCC). The proposed linkages between lignin and carbohydrates are classified into six types as reviewed by Azuma (1989): (1) glycosidic linkages between sugars and hydroxyl groups at the side chain of lignin, (2) phenolic glycosidic linkages, (3) ester linkages between the carboxyl groups of uronic acid and the hydroxyl group at  $\beta$ - or  $\gamma$ -position of lignin, (4) benzyl ether

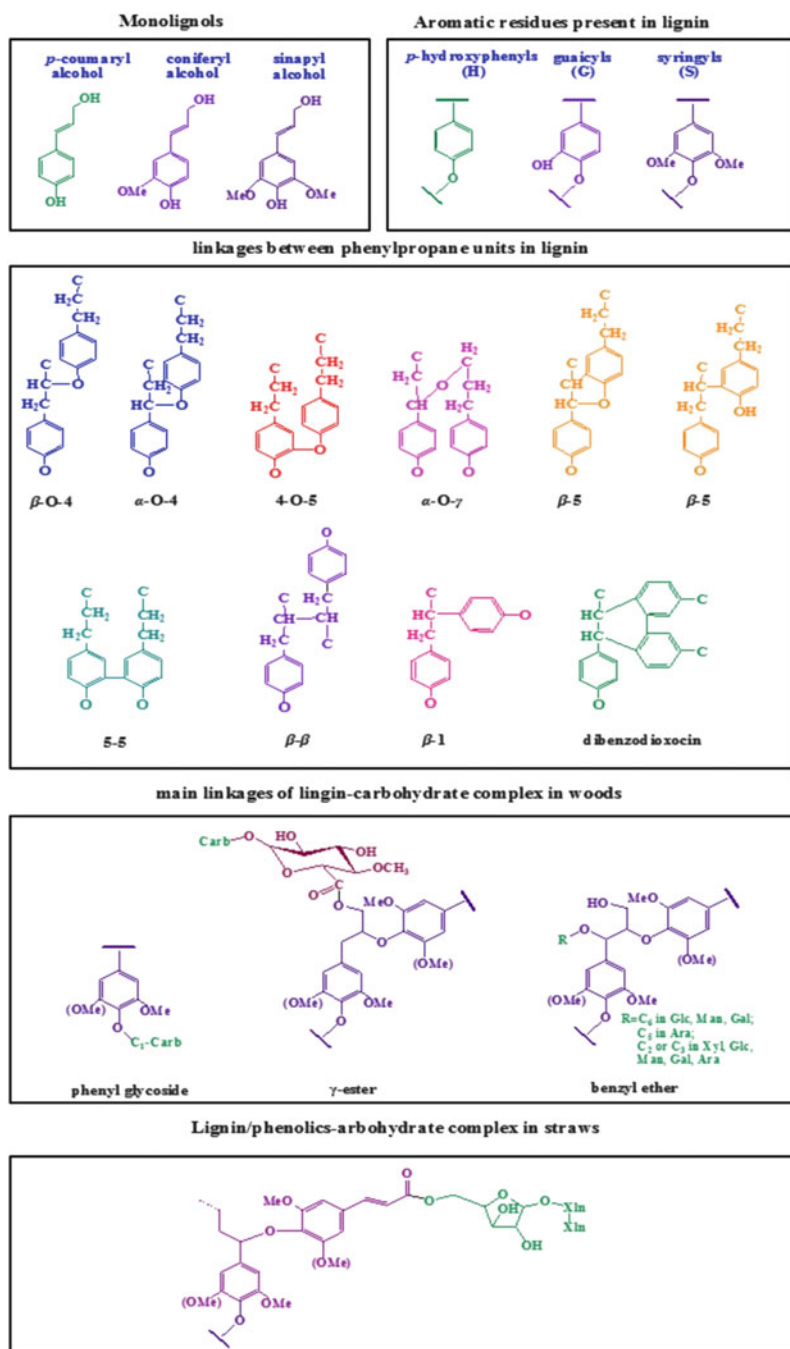


**Fig. 6.3** Monolignols and aromatic units of lignin and linkages between phenylpropane units in lignin and lignin-carbohydrate complex (Adapted with permission from Buranov and Mazza (2008), *Ind Crop Prod* 28: 237–259. Copyright (2008), Elsevier B.V.; Adapted with permission



**Table 6.1** Main linkages between phenylpropane units and their abundance in lignin

Linkage type	Dimmer structure	Percentage of total linkage		
		Softwood <sup>a</sup>	Hardwood <sup>a</sup>	Wheat straw <sup>b</sup>
$\beta$ -O-4	Arylglycerol- $\beta$ -aryl ether	50	60	67
$\alpha$ -O-4	Noncyclic benzyl aryl ether	2–8	7	13
$\beta$ -5	Phenylcoumaran	9–12	6	9
5-5	Biphenyl	10–11	5	2
4-O-5	Diaryl ether	4	7	-
$\beta$ -1	1,2-Diaryl propane	7	7	2
$\beta$ - $\beta$	Pinoresinol/lignan type	2	3	3
$\alpha$ -O- $\gamma$	Resinol type	-	-	3

<sup>a</sup>Data from Adler (1977)

<sup>b</sup>Data calculated according to the results of del Rio et al. (2012)

linkages, (5) benzyl ester linkages, and (6) hemiacetal or acetal linkage between carbonyl groups and  $\beta$ -position of lignin and hydroxyl groups of sugar. Among these linkages, it is believed that in wood LCCs the main types are phenyl glycoside bonds, esters, and benzyl ethers as shown in Fig. 6.3 (Koshijima and Watanabe 2003), and in monocots the majority of LCC linkages are ester bond between hemicellulose and phenolic acids such as ferulate and diferulate (Chundawat et al. 2011a). According to Laine et al. (2004), the LCCs isolated enzymatically from spruce and pine pulps contained 4.9–9.4 % carbohydrates, and the main carbohydrate units were 4-substituted xylose, 4,3- and 3,6-substituted galactose, 4-substituted glucose, and 4- and 4,6-substituted mannose, which were assigned to carbohydrate residues of xylan, 1,4- and 1,3/1,6-linked galactan, cellulose, and glucomannan. According to Yuan et al. (2011), acetylated 4-O-methylgluconoxylan was the main carbohydrate associated with lignins of poplar wood, and isolation process showed important influence on the determined amounts of phenyl glycoside, benzyl ether, and  $\gamma$ -ester linkages of LCCs. In herbaceous plants, the LCC structure is different from those in woods. Ferulic bridges are found between lignin and carbohydrates (arabinoxylans) via ester-linked ferulic acids (Fig. 6.3). These linkages are alkali-labile, so that half of the total phenolics in herbaceous plants can be removed with NaOH at ambient temperature (Buranov and Mazza 2008). LCC is believed as an important factor to biomass recalcitrance, since they are thought to exclude water and prevent cell walls from chemical or enzymatic deconstruction (Shevchenko and Bailey 1996). Cleavage of LCCs can facilitate the extraction and removal of cell wall polymers (e.g., hemicellulose and lignin) which in turn increases the accessibility to the intact carbohydrates (Chundawat et al. 2011a).

**Fig. 6.3** (continued) from Yuan et al. (2011), J Agr Food Chem 59: 10604–10614. Copyright (2011), American Chemical Society)

## 6.3 Hierarchy Structure of Cell Wall and Its Impact on Bioconversion

### 6.3.1 Multilayered Architecture of Cell Wall

Lignocellulosic biomass used for bioconversion in a biorefinery usually is the dead plant tissue composed of chambers enclosed by cell walls referred to as lumen (Fig. 6.4). The plant cell wall is largely honeycomb-like and composed of distinct layers, with the oldest layer being furthest from the plasma membrane and the youngest layer being closest (Gibson 2012). This multilayered structure was firstly observed in wood cells. Typically, normal wood cell wall is made up of several layers termed as middle lamella (ML), primary wall (P), and secondary wall (S), and there is a common area among three or four cells called cell corner (CC) (Xu 2010) (Fig. 6.4). Primary wall (P) is a thin layer, with about 100–200 nm of thickness, consisting of cellulose, hemicelluloses, pectin, and protein, all completely embedded in lignin. According to the cross-link types, primary wall can be classified to two types, namely, type I and type II. Type I is found in dicotyledonous plants and consists of equal amounts of glucan and xyloglucan, while type II is present in cereals and other grasses having glucuronoarabinoxylans as their cross-linking glucans. The ML which glues the cells together usually shows no clear transition to the adjacent wall layers. Therefore, ML and both adjacent primary walls are termed compound middle lamella (CML), with approximate 50–300 nm width and with higher concentration of hemicelluloses and lignin (Fromm et al. 2003). The second wall usually consists of three sublayers, namely, S<sub>1</sub> (outer), S<sub>2</sub> (middle), and S<sub>3</sub> (inner) lamellae, respectively (Chundawat et al. 2011a). The outer layer (S<sub>1</sub>) is thinner and forms only 10–20 % of the total cell wall. The middle layer (S<sub>2</sub>) forms the main portion of the cell wall taking up 70–90 % of the total cell wall. The inner layer (S<sub>3</sub>) is the thinnest layer, 2–8 % of the total cell wall. The change in thickness of S<sub>2</sub> is determined by the growing seasons, age, and morphological position. Therefore, the cell wall thickness mainly depends on that of S<sub>2</sub> lamellae (Xu 2010).

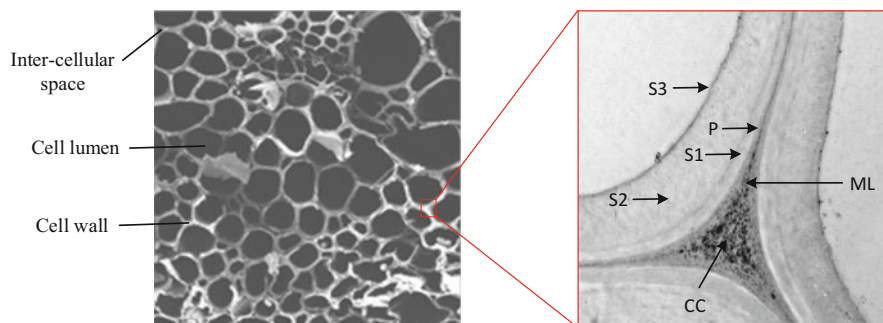


**Fig. 6.4** Multilayered structure of wheat straw cell wall

Cellulose, hemicelluloses and lignin have different distributions in these wall layers. Generally, cellulose concentration in cell wall layers follows an order of  $S > P > M$ , and  $S_2$  and  $S_3$  lamellae have the highest cellulose concentration (Agarwal 2006; Yang 2001). Most of cellulose distributes in S layer, particularly in  $S_2$  lamellae since  $S_2$  is the thickest among the wall layers (Yang 2001; Zhang et al. 2012). The distribution of hemicelluloses shows similar tendency as that of cellulose, with most of hemicelluloses distributing in the second wall.  $S_2$  lamella has the highest hemicellulose concentration among the cell wall layers (Yang 2001). Various imaging technologies have revealed that lignin concentration is the highest on average in CC and ML than in other cell wall layers (Fromm et al. 2003; Agarwal 2006; Gierlinger and Schwanninger 2006). However, since S layer is much thicker than CC and CML, most of lignin still distributes in the second wall (McMillan 1994).

### **6.3.2 Ultrastructure, Nanoporosity, and Recalcitrance of Cell Wall**

The compositions of lignocellulose cell wall construct a complicated network via chemical and physical interactions. The biomass recalcitrance is actually mainly ascribed to such compact and complex structure. The structure of plant cell wall covers a wide range of size from nanometer scale (cellulose fibril size) to micrometer scale (cell size) (Fig. 6.5). In cell wall, cellulose molecules align to form microfibrils with diameter of about 3–4 nm. These microfibrils themselves are aligned and bound together into fibril aggregates (or macrofibrils) with roughly 10–25 nm in diameter by a matrix of hemicellulose and lignin. Cell wall is further assembled by gluing together these macrofibrils under the “gluing” action of lignin (Gibson 2012). According to Donaldson (2007), the size of macrofibrils varies among cell wall types within the range of 14–23 nm, and the fibrillar structure of the secondary wall varies from microfibril-sized structures of 3–4 nm up to large aggregates of 60 nm in diameter. The macromolecular structure within a cellulose microfibril is not uniform since it contains both crystalline and amorphous regions (Ponni et al. 2012). However, the structure of cellulose microfibrils is not known in detail yet, even though a variety of techniques, such as atomic force microscopy, electron tomography, wide-angle X-ray scattering (WAXS), X-ray diffraction, and solid-state  $^{13}\text{C}$  NMR, have been employed to study the microfibril structure (Donaldson 2007; Fernandes et al. 2011). Previous studies suggested that microfibril has a diameter ranged from 2.2 nm to 3.6 nm, corresponding to about 12 and 32 chains (Jakob et al. 1995; Newman 1999); however, a 36-chain model is frequently suggested since cellulose is naturally synthesized by large multi-meric protein complexes visualized as hexameric rosette-like structures in plasma membrane freeze etches (Endler and Persson 2011). According to Fernandes et al. (2011), the structure of spruce microfibrils is of 3.0 nm in diameter with

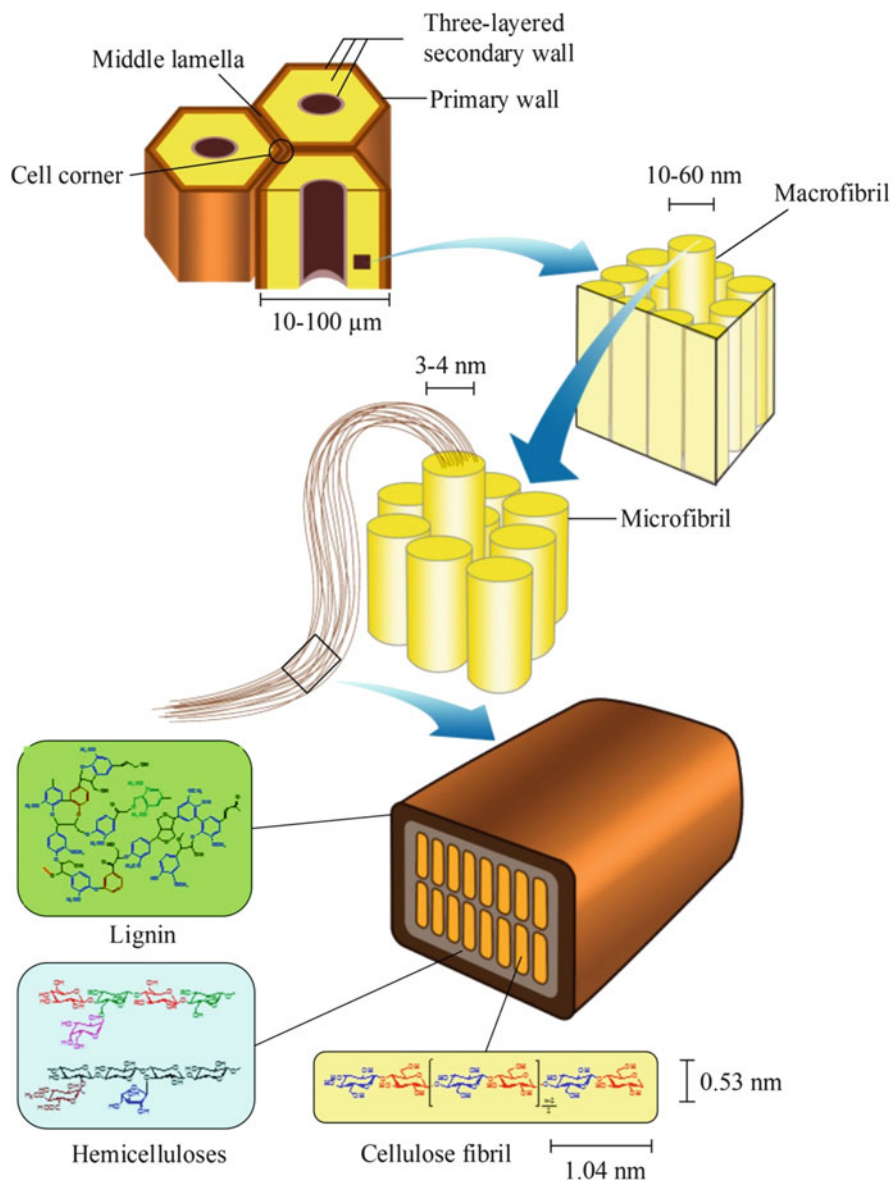


**Fig. 6.5** Hierarchical structure of plant cell wall

only about 24 cellulose chains, and the microfibrils are aggregated into bundles about 15–20 nm across. It seems that the reported sizes of microfibrils and their aggregation are different. This is mainly because that the cellular structure of plant varies with species and cell types.

Naturally, pores or pits in the cell wall are observed with size of about 20–100 nm in diameter. They are the regions where no secondary cell wall was deposited and an open pore is maintained between adjacent cell lumen. Therefore, these pits provide good initial access for cellulase enzyme to the two surfaces of the cell wall. However, these small openings can close up due to cell wall drying and can become occluded by relocalized lignin globules during pretreatment for enzymatic conversion. Generally, the architecture of the plant cell wall is a complex biomatrix with porosity on the scale of 5–10 nm. Pectins may have been the controlling factor in primary cell wall porosity, while lignin becomes the porosity limitation in cells with lignified secondary cell walls. The pore structures are also dependent on the cell wall organs and can be classified into tissue level, cell level, and cell wall level as summarized in Table 6.2 for corn stover (Zhao and Chen 2013). The pores in tissue level mainly consist of different cell lumen and intercellular spaces with size of 1–130  $\mu\text{m}$ . The pores in cell level mainly refer to the pit in cell wall, especially vessel cell wall with size of 30 nm–50  $\mu\text{m}$ . The pores in cell wall level consist of space among polymers, including lignin, hemicellulose, cellulose, as well as microfiber, with size in the range of 1–100 nm. The main exoglucanase in a *Trichoderma reesei* enzyme mixture has a size of  $4 \times 5 \times 13$  nm, but its hydration shell increases its effective size, thus requiring a much larger pore space for effective penetration. It is suggested by mass transfer consideration that the pore size should be in the range of 50–100 nm to allow sufficient penetration of enzymes into cell walls (Davison et al. 2013). Therefore, pretreatment is usually prerequisite to increase the porosity and pore size to enhance enzyme accessibility to a reactive surface, especially for cell wall.

Besides the restricted nanoporosity of the cell wall, other structural features of substrates also contribute to the biomass recalcitrance, including the epidermal tissue and chemicals, chemical compositions, cellulose structure, and pretreatment-induced causes (Zhao et al. 2012a). Actually, the enzymatic digestibility of cell wall cellulose is influenced by many factors, which can be divided into direct and indirect factors. The former refers to the accessible surface area, and the latter includes biomass structure-relevant factors (pore size, volume and distribution, particle size, and specific surface area), chemical compositions (lignin,

**Table 6.2** Pore distribution in corn stover (Zhao and Chen 2013)

Level	Origin	Width ( $\mu\text{m}$ )	Level	Origin	Width ( $\mu\text{m}$ )	
Tissue	Rectangular cell	20–35	Cell	Pit	0.5–50.0	
	Stomata	2–10		Plasmodesma	0.03–0.06	
	Vessel cell	30–130	Cell wall	Space among macrofibrils	0.001–0.100	
	Sieve tube	5–50		Space among microfibrils	0.001–0.030	
	Sieve cell	5–50		Lamellar gaps among polyphenols		0.001–0.030
	Fiber cell	13				
Intercellular space	<1					

hemicelluloses, and acetyl group), and cellulose structure-relevant factors (cellulose crystallinity and degree of polymerization). Strong interaction effects usually observed between these factors. Pretreatment is actually the process to alter indirect factors and improve direct factors, thus enhancing the accessibility of cellulose (Zhao et al. 2012a).

## 6.4 Pretreatment and Its Influence on the Ultrastructure of Cell Wall

Various pretreatment techniques have been developed during last decades in order to improve cellulose digestibility. Generally, these pretreatments can be divided into physical, physicochemical, chemical, and biological pretreatments or their combinations (Zhao et al. 2012b). However, the objective of these pretreatments is the same, namely, to disrupt cell wall structure and substantially expose cellulose to cellulolytic enzymes.

### 6.4.1 Mechanical and Chemi-mechanical Pretreatment

Mechanical pretreatment, usually referred as physical pretreatment, refers to pretreating biomass using mechanical comminution by a combination of chipping, grinding, and milling, which actually is a prerequisite step for further chemical or biochemical processing. The size of the feedstock is usually 10–30 mm after chipping and 0.2–2 mm after milling or grinding (McMillan 1994). However, to increase efficiently cellulose digestibility for enzymatic hydrolysis, the size of the substrates has to be decreased to a certain extent in order to substantially disrupt the ultrastructure of cell wall. Therefore, ball milling is usually the most effective because not only the particle size is greatly reduced but also the cellulose crystallinity decreases. However, physical pretreatment is usually energy-intensive. Combination of various thermal or chemical pre-pretreatment could greatly reduce the energy consumption (Zhu 2011). Actually, various mechanic pulping processes, such as thermomechanical pulping (TMP), chemi-thermomechanical pulping (CTMP), and refiner mechanical pulping (RMP), can be modified into pretreatment technologies, because pulping and pretreatment usually involve similar mechanisms. These pulping processes use mechanical energy to weaken and separate fibers from lignocellulose cell wall via a grinding action, especially for woody biomass. Typical energy consumption in first pass refining of wood chips for RMP and TMP is about 800 and 500 kWh/ton oven-dry (od) wood, while energy consumption of CTMP is often lower than that of TMP (Zhu 2011). Zakaria et al. (2015) found that combined pretreatment with hot-compressed water and wet disk milling resulted in nanofibrillation of fiber and loosening of the tight

biomass structure, thus increasing the subsequent enzymatic hydrolysis of cellulose to glucose. The SPORL pretreatment, which consists of sulfite treatment of wood chips under acidic conditions followed by mechanical size reduction using disk refining, is a successful demonstration on modifying biomass pulping to pretreatment (Zhu et al. 2009). This process caused a significant removal of hemicelluloses, delignification, and modification of lignin structure, resulting in a loosened fiber cell wall with significant delamination, which increased cellulose accessible surface area from 0.39 m<sup>2</sup>/g of untreated biomass to 6.15 m<sup>2</sup>/g of pretreated solid (Li et al. 2012). Generally, mechanical or chemi-mechanical pretreatment causes fibrillation of biomass and increase of specific surface area, thus enhancing the accessibility of cellulose toward cellulolytic enzymes. Disruption of cellulose crystalline structure by milling is also responsible to the improvement of cellulose digestibility (Xu et al. 2013; Kumagai et al. 2015). However, how mechanical pretreatment breaks the nanostructure of cell wall and improve the nanoporosity of the substrates has not been clearly elucidated.

#### **6.4.2 Physicochemical Pretreatment**

Steam explosion is one of the most promising physicochemical pretreatments to break the structure of lignocellulosic materials. This process combines the chemical modification of the biomass compositions and physical fracture of the cell wall structure. In this process, the material is subjected to high pressures and temperatures for a short duration of time after which the system is depressurized sharply, disrupting the structure of the fibrils (Brodeur et al. 2011). The increase of cellulose accessibility by steam explosion is attributed to removal of a great part of hemicelluloses, partial degradation of lignin macromolecule, and redistribution of the lignin in the cell wall. Steam explosion has been described as a thermo-mechanochemical process, because the massive disruption of lignocellulosic structure is aided by heat of steam (thermo), shear forces due to the expansion of moisture (mechano), and hydrolysis of glycosidic bonds (chemical), which leads to cleavages of some accessible glycosidic links,  $\beta$ -ether linkages of lignin, and lignin-carbohydrate complex (LCC) bonds (Zhao et al. 2012b). Evidences on the melting of lignin and reprecipitation as agglomerates on fiber surface have been frequently reported for steam explosion of various biomass feedstock (Biermann et al. 1987; Donaldson et al. 1988; Kallavus and Gravitis 1995; Angles et al. 2001). The migration and redistribution of lignin in the cell wall are important to the increase of cellulose accessibility for subsequent bioconversion. Kallavus and Gravitis (1995) observed using transmission electron micrographs (TEM) that lignin redistribution occurred not only on both the inner and outer surfaces of the cell wall but also inside the cell wall itself. Lamellar deposition of lignin within the secondary cell wall and free fibrils in the extract were also observed. Cellulose regions become more porous due to the formation of numerous pores greater than 2 nm, as found by Donaldson et al. (1988). Because of these disruptions of cell wall ultrastructure, the

bioconversion of cellulose to sugars or ethanol from various lignocellulosic biomass is greatly improved from less than 20 % of untreated substrate to higher than 80 % of pretreated substrates (Chen and Liu 2015; Jacquet et al. 2015).

Ammonia fiber expansion (AFEX) is another promising physicochemical pretreatment for bioconversion of lignocellulosic biomass. In this process, biomass is soaked with liquid ammonia under moderate pressure (0.68–4.8 Mpa) and temperature (70–200 °C) depending on feedstock followed by a rapid releasing of the pressure (Yang and Wyman 2008; Kumar et al. 2009; Bals et al. 2010). Cellulose accessibility is thus enhanced by decrystallization of cellulose, prehydrolysis of hemicelluloses, and alteration of lignin structure in the process (Yang and Wyman 2008; Kumar et al. 2009). Chundawat (2010) investigated the ultrastructural and physicochemical modifications of corn stover cell wall by AFEX pretreatment and their influence on enzymatic digestibility. He found that ammonolysis of lignin-carbohydrate complex (LCC) ester linkages resulted in the extraction and redeposition of decomposition products on outer cell wall surfaces and the formation of a nanoporous network. The shape, size (e.g., ranged from 100 to 1000 nm), and spatial distribution of the porous network were dependent on cell wall composition (e.g., middle lamella vs. secondary walls) and ammonia pretreatment conditions. The exposed pore surface area per unit of AFEX pretreated cell wall volume ranged between 0.005 and 0.05 nm<sup>2</sup> per nm<sup>3</sup>. This highly porous structure greatly enhances enzyme accessibility to embedded cellulosic microfibrils, with enzymatic hydrolysis yield enhanced by four- to fivefolds over that of untreated cell walls (Chundawat 2010; Chundawat et al. 2011c). It is also found by molecular dynamics (MD) simulations that ammonia treatment could transform the naturally occurring crystalline allomorph I<sub>β</sub> to III<sub>I</sub>, which led to a decrease in the number of cellulose intrasheet hydrogen bonds and an increase in the number of intersheet hydrogen bonds. This rearrangement of the hydrogen bond network increased the number of solvent-exposed glucan chain hydrogen bonds with water by ~50 %, accompanied by enhanced saccharification rates by up to fivefold (closest to amorphous cellulose) and 60–70 % lower maximum surface-bound cellulase capacity (Chundawat et al. 2011b).

Hydrothermal pretreatment is considered as a promising and green pretreatment because no or only a small amount of external chemicals are consumed in the process. The principle of this pretreatment is that high temperature causes autoionization of water and hydrolysis of acetyl group in hemicelluloses to generate hydrogen ions that can play as a catalyst for hemicellulose hydrolysis and cleavage of some intramolecular bonds in lignin (Cybulska et al. 2013). However, hydrothermal pretreatment initially removes the lignin-free hemicellulose from the middle layer of secondary wall, followed by the lignin-bound hemicelluloses, but the cellulose-bound hemicelluloses are seldom removed by this pretreatment (Ma et al. 2015). Ma et al. (2014) found that the hydrothermal pretreatment (HTP) caused in a time-depend manner the alterations of surface morphological and chemical features in different cell wall sublayers. The loss of lignin concentration in the S2 layer was more than that in the compound middle lamella (CML) after 30 min of pretreatment, whereas the drop of hemicellulose concentration



exhibited an opposite trend. Using transmission electron microscopy (TEM) in combination with immunogold labeling technologies, Ma et al. (2015) found HTP caused greater decline in the density of xylan labeling in the S2 layer of fiber wall than in the S1 layer. It indicates that the removal of lignin and hemicelluloses from the S2 layer and CML is important to the increasing enzymatic hydrolysis of cell wall cellulose.

### **6.4.3 Chemical Pretreatment**

Chemical pretreatments, which employ various chemicals or solvent to pretreat lignocellulosic biomass, are the most efficient pretreatment methods to deconstruct cell wall structure and expose cellulose. The leading chemical pretreatments mainly include dilute acid, alkaline, oxidative, and organosolv pretreatments.

#### **6.4.3.1 Dilute Acid Pretreatment**

Dilute acid pretreatment has received considerable attention over the years. Typically, effective dilute acid pretreatment is performed at a temperature higher than 130 °C with sulfuric acid concentration of 0.1–5 wt%. Dilute acid pretreatment not only causes significant removal of hemicelluloses but also, maybe more importantly, results in melting and redistribution of lignin in cell wall layers and the fiber surfaces. Pingali et al. (2010) found that dilute acid pretreatment increased the cross-sectional radius of the crystalline cellulose fibril accompanied by removal of hemicellulose and the formation of ~13.5 nm lignin aggregates. These lignin droplets showed negative effects on cellulose hydrolysis, not only by nonproductive adsorption of cellulase but also by blocking the cellulose surface for enzymatic recognition (Li et al. 2014). Dilute acid pretreatment also resulted in loss in the matrix between neighboring cell walls, selective removal of hemicelluloses, redistribution of phenolic polymers, and increased exposure of cellulose, which causes damage to cell wall, increase of porosity, and loss of mechanical resistance, thus enhancing enzyme access to cellulose and sugar yield (Ji et al. 2015). Modification of cell wall surface morphology is also important to the increase of cellulose digestibility by dilute acid pretreatment. Using time-of-flight secondary ion mass spectrometry (ToF-SIMS) technology, Jung et al. (2010) found that the relative content of xylan after dilute acid pretreatment increased by 30 %, and the relative content of cellulose and G-lignin units doubled on the surface of the poplar stem sections. Zhang et al. (2013) found, using atomic force microscopy (AFM) single molecular recognition imaging technology, that the cell wall surface crystalline cellulose coverage increased from 17–20 % to 18–40 % after dilute acid pretreatment at 135 °C under different acid concentrations and reached to 40–70 % after delignification. Such changes in the cell wall surface structure may substantially increase cellulose accessibility.

### 6.4.3.2 Alkaline Pretreatment

Alkaline pretreatment refers to the processes of biomass pretreatment with various alkalis or bases such as NaOH, KOH, lime, ammonia, etc. The intermolecular ester bonds cross-linking xylan hemicellulose and lignin are saponified in alkaline pretreatment, thus resulting in delignification of biomass (Zhao et al. 2012b). Temperature and alkali concentration are important factors affecting the deconstruction of cell wall architecture, especially the migration and redistribution of lignin in cell wall. Lignin droplets with size of several hundreds of nanometers were observed on the surface of pretreated solid, and more droplets were observed at lower alkali concentration. This is because higher NaOH concentration (e.g., 4 %) is sufficient to keep most of the coalesced lignin dispersed in the pretreatment liquor and lower concentrations used (less than 1 %) is not adequate to peel off the cellulose microfibrils and to expose the crystalline surfaces (Lima et al. 2013). During alkaline pretreatment, the active alkalis gradually permeate into the cell wall structures, etching away the lignin-containing matrix at the lumen surface. For example, a lime pretreatment caused partially unsheathed layers of microfibrils, while aqueous ammonia pretreatment results in an irregularly eroded surface. Such etching typically does not have an impact on the cell wall beyond 10–20 nm into the surface, but can still provide a substantial increase in the initial enzyme binding (Davison et al. 2013). Increasing the pretreatment severity, for example, alkali concentration and pretreatment temperature may achieve a high degree of delignification, causing substantial deconstruction of cell wall and liberation of cellulose fibers, which is known as the pulping process.

### 6.4.3.3 Organosolv Pretreatment

Organosolv pretreatment refers to the process to pretreat lignocellulosic feedstocks using organic solvents or their aqueous solutions with or without added catalysts in temperature range of 100–250 °C (Zhao et al. 2009). This process is similar to organosolv pulping, by which significant parts of lignin and hemicelluloses are removed while cellulose is recovered as solid (pulp). Due to the delignification and hydrolysis of hemicelluloses, biomass structure becomes loosen, and cellulose fibers are liberated with resulted increase of accessibility. When studying the two-stage delignification of spruce wood using methanol, Fengel et al. (1989) found that during the methanol-water pulping stage, the lignin content of the secondary cell walls decreases slowly, but in the compound middle lamella, only the reactivity of lignin increases. However, during the methanol-sodium hydroxide stage, the delignification proceeds fast in both layers, but the residual lignin content in the compound middle lamella remains higher than in the secondary walls. The delignification order of cell wall layers is influenced by the lignin nature of the secondary walls and the ultrastructure of cell walls. As found by Fujii et al. (1994), in acetosolv pulping of cryptomeria and beech wood, compound middle lamellae (CML) were delignified

preferably compared with the secondary walls of tracheids in the case of cryptomeria sapwoods and heartwoods; however, secondary walls of fiber tracheids and vessels were delignified more rapidly than the CML for beech wood. In our group, we studied the change of structural features of sugarcane bagasse before and after Formiline pretreatment (formic acid delignification followed by an alkaline deformylation). Formic acid played as a “hammer” to destroy the “concrete structure” (cell wall), removing “mesh,” “sand,” and “cement” (hemicelluloses and lignin), thus liberating the “rebars” (cellulose fibers) (Fig. 6.6). The rigid and compact structure of the raw bagasse thus was destroyed, and the specific surface area of the pretreated substrates increased by more than two times (Wu et al. 2016).

#### 6.4.3.4 Oxidative Pretreatment

Oxidative pretreatment refers to the process using various oxidants such as oxygen,  $H_2O_2$ , peroxy acids, sodium chlorite, ozone, etc. to pretreat biomass. In this pretreatment, lignin is oxidized and depolymerized to form small molecules with much higher hydrophilicity. Zhao et al. (2008) pretreated sugarcane bagasse with peracetic acid (PAA) and find that the enhancement of enzymatic digestibility of cellulose was achieved mainly by delignification and an increase in the surface area and exposure of cellulose fibers. Li et al. (2015) analyzed the chemical and structural changes associated with Cu-catalyzed alkaline-oxidative delignification of hybrid poplar. They found that lignin modification and/or removal resulted in disruption of cell wall by dislocations between individual cell walls as well as delaminations within cell walls. Fractures and disruptions were also observed in other lignin-rich regions including cell corners and compound middle lamellae. Ding et al. (2012) found that acid chlorite treatment effectively removes lignins in the second wall (SW) and the warty layer in sclerenchyma-type SW, thereby exposing microfibrils to enzyme access, resulting in near-complete digestion of all cell walls.

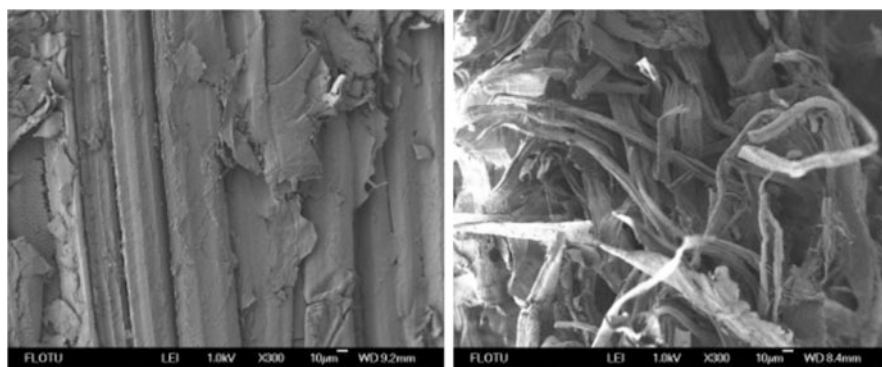


**Fig. 6.6** SEM images of sugarcane bagasse (*left*,  $\times 300$ ) and formiline-pretreated solid (*right*,  $\times 300$ )

### 6.4.3.5 Ionic Liquid Pretreatment

Ionic liquid (IL) pretreatment is the process using various ILs to deconstruct biomass and increase cellulose accessibility. IL pretreatment can achieve a considerable removal of lignin and depolymerization of hemicelluloses (Brandt et al. 2013); however, what is most important is that IL pretreatment significantly alters the macro- and microstructure of cellulose, especially the degree of crystallinity. The regenerated cellulose becomes nearly completely amorphous and much easier to hydrolyze. Singh et al. found that pretreatment of ground switchgrass with ionic liquid 1-*n*-ethyl-3-methylimidazolium acetate resulted in the disruption and solubilization of the plant cell wall at mild temperatures, due to the disruption of inter- and intramolecular hydrogen bonding between cellulose fibrils and lignin (Singh et al. 2009). Using confocal fluorescence imaging technology, they found that the lignin-rich sclerenchyma and middle lamella in plant tissues disintegrate immediately and simultaneously as primary and secondary cell walls start separating from the middle lamella. Complete breakdown of organized plant cell wall structure was observed after 2 h pretreatment. Similarly, Sun et al. found that cell wall swelling occurs primarily in the secondary cell walls and the IL had little effect on compound middle lamella in terms of swelling. Lignin dissolution was faster in the secondary cell walls, while there was no preferential cellulose dissolution. A synergistic interaction of lignocellulose dissolution regarding cellulose and lignin dissolution and cell wall swelling occurs during IL pretreatment (Sun et al. 2013).

## 6.5 Techniques to Characterize the Ultrastructure and Porosity of Cell Wall and Accessibility of Cellulose

Cellulose accessibility (accessible surface area) is the direct factor limiting the enzymatic hydrolysis of lignocellulosic cellulose, which directly determines the rate and degree of enzymatic hydrolysis of the substrates. However, cellulose accessibility is closely affected by several indirect factors, including biomass structure-relevant factors (pore size and volume, particle size, and specific surface area), chemical compositions (lignin, hemicelluloses, and acetyl group), and cellulose structure-relevant factors (cellulose crystallinity and degree of polymerization) (Zhao et al. 2012a). These factors usually show significant interactions. Therefore, characterizing the ultrastructure and porosity of cell wall and accessibility of cellulose is important to investigating the fundamentals of pretreatment and further optimizing the process. Many techniques can be used to analyze ultrastructure and porosity of cell wall and accessibility of cellulose as summarized in Table 6.3. However, some limitations still exist due to the specificity of biomass substrate and the enzymatic hydrolysis systems.

Convictional porosimetries to study the porous structure of powder or catalyst, such as Brunauer-Emmett-Teller (BET) and mercury intrusion porosimetry, have

**Table 6.3** Techniques commonly used to analyze ultrastructure and porosity of cell wall and accessibility of cellulose

Techniques	Principles or procedures	Merits and limitations	References
Electron microscopy (EM) such as SEM, TEM, FE-SEM, and combination with other techniques	These methods use a high-energy beam of electrons to produce images by interaction of electrons with the atoms of the samples. Very thin samples have to be prepared for TEM, while for SEM a thin layer of gold is usually sputter coated on the substrate surface to make the fibers conductive, avoiding degradation and buildup of charge on the specimen	These methods can obtain a visualized overview of cell wall structures and the lignin distribution across the different layers of the cell wall. However, (1) complicated procedure is needed to prepare specimens, and (2) drying is usually required	Fromm et al. (2003), Khalil et al. (2010)
Laser scanning confocal microscopy (LSCM)	LSCM uses the principle of fluorescence excitation to investigate the structural properties of cell wall	CLSM is an excellent method to investigate the internal structures of biomass in 3D. However, drying is usually required	Claxton et al. (2015)
Atomic force microscope (AFM)	AFM operates by measuring force between a probe and the sample. AFM cannot only image in three-dimensional topography but also provides various types of surface measurements	AFM is versatile and powerful for studying samples at nanoscale. It can generate images at atomic resolution with angstrom-scale resolution height information, with minimum sample preparation. However, drying is usually required	Sant'Anna and de Souza (2012)
Brunauer-Emmett-Teller (BET)	Determination of specific surface area of biomass substrates by BET method is based on nitrogen multilayer adsorption as a function of relative pressure. When the substrate is surrounded by and in equilibrium with nitrogen at certain temperature, $T$ , and relative vapor pressure, $p/p_0$ , it adsorbs physically a certain amount of gas. The amount of adsorbed	BET method has been well established and widely used for measuring the SSA of solid. However, (1) nitrogen is much smaller than cellulase enzymes, which can result in overestimating the cellulose accessibility to cellulase, and (2) drying is required	Afzal et al. (1973), Zhao et al. (2012b)

(continued)

**Table 6.3** (continued)

Techniques	Principles or procedures	Merits and limitations	References
	gas is dependent on its relative vapor pressure and is proportional to the total external and internal surface		
Solute exclusion	This technique is based on the accessibility of solute molecules (probe molecules) to the substrate pores of different sizes. The pore is considered accessible when the pore is connected to the bulk water and large enough to hold the probe molecule. The probe molecule solution is diluted by water contained in the initial substrate when the solute solution is added into the wet substrate. The water presented in the pores that are not accessible to the probe molecules will not contribute to the dilution. The substrate pore size and volume distribution can be determined using the concentration of a set of different solute solutions with various molecule sizes	Solute exclusion technique can be used for wet samples; thus drying can be avoided. However, this method (1) cannot measure the accessibility of external surfaces and (2) is laborious and unspecific to cellulose and (3) is not acceptable for determination of absolute pore size and volume distribution and (4) is easily effected by pore shape and osmotic pressure; thus the repeatability is not good	Beecher et al. (2009), Meng and Ragauskas (2014)
Simons' stain	This technique uses two direct dyes (Direct Blue 1 and Direct Orange 15) as molecular probes based on the different molecular sizes and affinity for cellulose. Direct Blue 1 has a smaller molecular size and weaker affinity for cellulose compared to Direct Orange 15, which has a larger molecular size and stronger affinity. The adsorption of direct dye probes on	Simons' stain method can be used for determining the porosity of substrate at wet state. It is relatively fast, simple, and sensitive and can measure both interior and exterior surface area. However, this method (1) may overestimate the surface area due to the smaller size of dye molecules than cellulase enzymes and (2) cannot be used for fully quantitative	Chandra et al. (2008)

(continued)

**Table 6.3** (continued)

Techniques	Principles or procedures	Merits and limitations	References
	cellulose follows the Langmuir isotherm. The ratio of adsorbed orange and blue dye and combined adsorption of both dyes can be then calculated and used to estimate the relative porosity and overall accessible surface area	analysis, and (3) the interference of lignin is not clear	
Fusion protein adsorption	This technique uses a fusion protein containing a cellulose-binding module (CBM) and a green fluorescent protein (GFP) (CBM-GFP) as probe molecules. Quantitative determination of cellulose accessibility to cellulase thus can be calculated based on the Langmuir adsorption of the fusion protein	This technique can correctly determine the cellulose accessibility because the protein contains CBM and the measurement can be performed in aqueous phase. However, this method (1) can be interfered by presence of non-cellulose components such as lignin and hemicellulose and (2) can be affected by the stability of the fusion protein	Hong et al. (2007)
Mercury intrusion porosimetry	This technique uses mercury as the probe molecules to measure the porosity and surface area. Mercury can gradually permeate into the pores under external pressure. The pore diameter and applied pressure can be correlated by the Washburn equation. The volume of mercury entering the pore is measured as the pressure increased, indicating the cumulative volume of all available pores of radius equal to or greater than a corresponding pore diameter	This method is time-saving and can provide a wide range of information, e.g., the pore size distribution, the total pore volume or porosity, the skeletal and apparent density, and the specific surface area of a sample. However, this method (1) measures the largest entrance toward a pore but not the actual inner size of a pore and (2) may overestimate the accessible surface of substrates and (3) needs drying the substrates	Giesche (2006), Meng and Ragauskas (2014)

(continued)

**Table 6.3** (continued)

Techniques	Principles or procedures	Merits and limitations	References
Differential scanning calorimetry (DSC)	This technique for pore size distribution measurements is based on the principle that water contained inside pores has a lower freezing point than that of bulk water. The relations between the specific melting enthalpy and pore size are described by the Gibbs-Thompson equation	This method can be used for a substrate at wet state. However, this method (1) shows some hysteresis when the freezing and melting cycle is repeated several times, and (2) osmotic pressure can also cause melting point depression and that the pore size distribution may change with freezing or with raising temperature	Beecher et al. (2009)
Nuclear magnetic resonance (NMR)	NMR method is based on the fact that water inside the cell wall has a much slower diffusion rate than free water. In NMR measurements, this diffusion rate influences the T2 relaxation time, and thus T2 relaxation time can be used for quantifying the amount of water in different environments such as the cell wall and cell lumen	This method is a nondestructive measurement with no influence by pore inlet size or shape and can be used for a substrate at wet state. However, this method is time-consuming and requires complicated experiment setup	Beecher et al. (2009), Meng and Ragauskas (2014)

been widely applied for determining the specific surface area of biomass substrate. These methods use small probe molecules (nitrogen for BET and liquid mercury for mercury porosimetry) to measure the pore volume, specific surface area, size distribution, etc. Using these methods, many researchers have gained consistent conclusions that pretreatment greatly increase the specific surface area of the substrates regarding to different feedstocks and pretreatment processes (Zhao et al. 2008; Yu et al. 2009; Xiao et al. 2013; Zhao and Chen 2013; Muzamal et al. 2015; Yuan et al. 2015). However, BET method and mercury porosimetry cannot well reflect the accessible surface area of cellulose due to the difference in size between the nitrogen molecule and cellulase enzymes. Moreover, drying of the substrate is required, but conventional drying or dewatering usually causes hornification of the fibers and collapse of porous structures (Luo and Zhu 2011). Therefore, determining the accessible surface area of substrates at wet state is important. Several techniques can achieve this goal, including solute exclusion, Simons' stain, and fusion protein adsorption. However, the solute exclusion method is usually laborious, unspecific to cellulose, and not acceptable for determination of



absolute pore size and volume distribution and cannot measure the accessibility of external surfaces. The Simon's stain method may overestimate the surface area due to the smaller size of dye molecules than cellulase enzymes. Moreover, the interactions of non-cellulose components such as hemicellulose and lignin with the dye probe molecules are not clear yet. The fusion protein adsorption method also has such limitation, because lignin usually can adsorb protein, even though CBM is contained in the fusion protein.

Some modern techniques have provided powerful tools to characterize the ultrastructure of biomass. Electron microscopy (EM), such as SEM and TEM, has been widely used to investigate the surface morphology and cell wall structures. More detailed structural information can be provided by using laser scanning confocal microscope (LSCM) and atomic force microscope (AFM). However, there are still many puzzles on the biomass ultrastructure, especially at nano-level, and how these nanostructures impact the cellulose accessibility.

## 6.6 Conclusion

Lignocellulosic biomass is one of the most promising biomass feedstock for biorefinery to produce biofuels, chemicals, and materials. However, lignocellulosic biomass is indeed a complicated natural biomaterial at nano- and microscales. This is because the polymeric compositions of lignocellulose cell wall, cellulose, hemicellulose, and lignin have complicated chemical structures, but more importantly, these compositions construct a compact and recalcitrant spatial structure in three dimension via chemical bonding. Such structure is analogue to a world of reinforced concrete, where cellulose fibers act as the rebars or steel rods to provide strength over long distances; hemicellulose represents the wire mesh or cable that wraps around the celluloses rods, providing extra strength and linkages; and lignin acts as the concrete that fills the remaining gaps and sets, holding everything in place and excludes water from the polysaccharide environment (Davison et al. 2013). Therefore, to enhance the bio-convertibility of lignocellulosic biomass, the substrates usually have to be pretreated through physical, chemical, or biological pretreatments or their combinations to increase cellulose accessibility by cellulase enzymes. These pretreatments expose cellulose by removing lignin and/or hemicelluloses, modifying lignin structure, or redistribute lignin in the cell wall layers, with associated deconstruction of cell wall hierarchy ultrastructure. Various techniques have been employed to characterize the cell wall structure, porosity, and cellulose accessibility, while each method has its own merits and limitations. However, there are still many puzzles on the cell wall structure and its relation with bioconversion of lignocellulosic biomass. Future works should be focused but not limited on the following aspects:

1. Deeply investigating the cell wall structure at multi-scales. The enzymatic hydrolysis of lignocellulosic cellulose is greatly affected by the microscale and

- nanoscale features of the plant cell wall. Investigating the structural features, especially the pore structure, distribution, and accessibility to cellulase enzymes, can be helpful to understand the micro-mechanisms of biomass recalcitrance.
2. Insights into the biomass recalcitrance at molecular and atomic levels. This needs to investigate the chemical bonding between carbohydrate and lignin, lignin moieties, and the hydrogen bond networks and their contributions to biomass recalcitrance. The effects of lignin structure and distribution in cell wall on its inhibitive action to cellulases have to be deeply investigated.
  3. Developing novel technique to characterize biomass ultrastructure. To accurately measure the accessible surface area of lignocellulosic cellulose, the probe molecules should have similar size with that of cellulase enzymes and can recognize cellulose as the CBM of cellobiohydrolases. However, such a compound or protein is still difficult to completely mimic the recognition of cellobiohydrolases toward cellulose.

**Acknowledgment** Authors are grateful for the supports of this work by National Natural Science Foundation of China (No. 21406130), National Energy Administration Project (No. NY20130402) and Dongguan Social and Technical Development Project (No. 2015108101004).

## References

- Adler E (1977) Lignin chemistry—past, present and future. *Wood Sci Technol* 11:169–218
- Afzal M, Butt PK, Ahmad N (1973) Determination of specific surface area of solids by the BET method. *Pakistan J Sci* 25:171–174
- Agarwal UP (2006) Raman imaging to investigate ultrastructure and composition of plant cell walls: distribution of lignin and cellulose in black spruce wood (*Picea mariana*). *Planta* 224:1141–1153
- Angles MN, Ferrando F, Farriol X, Salvado J (2001) Suitability of steam exploded residual softwood for the production of binderless panels. Effect of the pre-treatment severity and lignin addition. *Biomass Bioenergy* 21:211–224
- Azuma J (1989) Analysis of lignin-carbohydrate complexes of plant cell walls. In: Linskens H, Jackson J (eds) *Modern methods of plant analysis*. Springer, New York, NY, pp 100–126
- Balan V, Bals B, da Costa Sousa B, Garlock R, Dale B (2011) A short review on ammonia-based lignocellulosic biomass pretreatment. In: Blake A (ed) *Chemical and biochemical catalysis for next generation biofuels*. Royal Society of Chemistry, London, pp 89–114
- Bals B, Rogers C, Jin MJ, Balan V, Dale B (2010) Evaluation of ammonia fibre expansion (AFEX) pretreatment for enzymatic hydrolysis of switchgrass harvested in different seasons and locations. *Biotechnol Biofuels* 3:1. doi:10.1186/1754-6834-3-1
- Beckham G, Matthews J, Peters B, Bomble Y, Himmel M, Crowley M (2011) Molecular-level origins of biomass recalcitrance: decrystallization free energies for four common cellulose polymorphs. *J Phys Chem B* 115:4118–4127
- Beecher J, Hunt C, Zhu J (2009) Tools for the characterization of biomass at the nanometer scale. In: Lucia L, Rojas O (eds) *The nanoscience and technology of renewable biomaterials*. Blackwell, Oxford, pp 61–90
- Biermann CJ, McGinnis GD, Schultz TP (1987) Scanning electron microscopy of mixed hardwoods subjected to various pretreatment processes. *J Agr Food Chem* 35:713–716
- Brandt A, Grasvik J, Hallett J, Welton T (2013) Deconstruction of lignocellulosic biomass with ionic liquids. *Green Chem* 15:550–583

- Brodeur G, Yau E, Badal K, Collier J, Ramachandran K, Ramakrishnan S (2011) Chemical and physicochemical pretreatment of lignocellulosic biomass: a review. *Enzyme Res* 2011:787532
- Brosse N, Dufour A, Meng X, Sun Q, Ragauskas A (2012) Miscanthus: a fast-growing crop for biofuels and chemicals production. *Biofuel Bioprod Bior* 6:580–598
- Buranov A, Mazza G (2008) Lignin in straw of herbaceous crops. *Ind Crop Prod* 28:237–259
- Calvo-Flores F, Dobado J (2010) Lignin as renewable raw material. *Chemsuschem* 3:1227–1235
- Capanema EA, Balakshin MY, Kadla JF (2005) Quantitative characterization of a hardwood milled wood lignin by nuclear magnetic resonance spectroscopy. *J Agr Food Chem* 53:9639–9649
- Chandra R, Ewanick S, Hsieh C, Saddler JN (2008) The characterization of pretreated lignocellulosic substrates prior to enzymatic hydrolysis, Part 1: A modified Simons' staining technique. *Biotechnol Progr* 24:1178–1185
- Chen HZ, Liu ZH (2015) Steam explosion and its combinatorial pretreatment refining technology of plant biomass to bio-based products. *Biotech J* 10:866–885
- Chundawat S (2010) Ultrastructural and physicochemical modifications within ammonia treated lignocellulosic cell walls and their influence on enzymatic digestibility. PhD thesis, Michigan State University
- Chundawat S, Beckham G, Himmel M, Dale B, Prausnitz J (2011a) Deconstruction of lignocellulosic biomass to fuels and chemicals. *Annu Rev Chem Biomol* 2:121–145
- Chundawat S, Bellesia G, Uppugundla N, Sousa L, Gao D, Cheh A, Agarwal U, Bianchetti C, Phillips G, Langan P, Balan V, Gnanakaran S, Dale B (2011b) Restructuring the crystalline cellulose hydrogen bond network enhances its depolymerization rate. *J Am Chem Soc* 133:11163–11174
- Chundawat SPS, Donohoe BS, Sousa LD, Elder T, Agarwal UP, Lu FC, Ralph J, Himmel ME, Balan V, Dale BE (2011c) Multi-scale visualization and characterization of lignocellulosic plant cell wall deconstruction during thermochemical pretreatment. *Energy Environ Sci* 4:973–984
- Ciolacu D, Pitol-Filho L, Ciolacu F (2012) Studies concerning the accessibility of different allomorphic forms of cellulose. *Cellulose* 19:55–68
- Claxton N, Fellers T, Davidson M (2015) Laser scanning confocal microscopy. <http://www.olympusconfocal.com/theory/LSCMIntro.pdf>
- Cybulska I, Brudecki G, Lei H (2013) Hydrothermal pretreatment of lignocellulosic biomass. In: Gu T (ed) *Green biomass pretreatment for biofuels production*. Springer, Dordrecht, pp 87–106
- David K, Ragauskas A (2010) Switchgrass as an energy crop for biofuel production: a review of its ligno-cellulosic chemical properties. *Energy Environ Sci* 3:1182–1190
- Davison B, Parks J, Davis M, Donohoe B (2013) Plant cell walls: basics of structure, chemistry, accessibility and the influence on conversion. In: Wyman C (ed) *Aqueous pretreatment of plant biomass for biological and chemical conversion to fuels and chemicals*, 1st edn. Wiley, Chichester, pp 23–38
- de Vries RP, Visser J (2001) Aspergillus enzymes involved in degradation of plant cell wall polysaccharides. *Microbiol Mol Biol R* 65:497–522
- del Rio JC, Rencoret J, Prinsen P, Martinez AT, Ralph J, Gutierrez A (2012) Structural characterization of wheat straw lignin as revealed by analytical pyrolysis, 2D-NMR, and reductive cleavage methods. *J Agr Food Chem* 60:5922–5935
- Demirbas A (2009) Biorefineries: current activities and future developments. *Energy Convers Manage* 50:2782–2801
- Ding S-Y, Liu Y-S, Zeng Y, Himmel ME, Baker JO, Bayer EA (2012) How does plant cell wall nanoscale architecture correlate with enzymatic digestibility? *Science* 338:1055–1060
- Donaldson L (2007) Cellulose microfibril aggregates and their size variation with cell wall type. *Wood Sci Technol* 41:443–460
- Donaldson LA, Wong KKY, Mackie KL (1988) Ultrastructure of steam-exploded wood. *Wood Sci Technol* 22:103–114

- Ebner G, Schiehser S, Potthast A, Rosenau T (2008) Side reaction of cellulose with common 1-alkyl-3-methylimidazolium-based ionic liquids. *Tetrahedron Lett* 49:7322–7324
- Ebringerova A, Hromadkova Z, Heinze T (2005) Hemicellulose. *Polysaccharides 1: Structure, characterization and use*. *Adv Polym Sci* 186:1–67
- El Mansouri N-E, Salvado J (2007) Analytical methods for determining functional groups in various technical lignins. *Ind Crop Prod* 26:116–124
- Endler A, Persson S (2011) Cellulose synthases and synthesis in Arabidopsis. *Mol Plant* 4:199–211
- Fengel D, Wegener G, Greune A (1989) Studies on the delignification of spruce wood by organosolv pulping using SEM-EDXA and TEM. *Wood Sci Technol* 23:123–130
- Fernandes AN, Thomas LH, Altaner CM, Callow P, Forsyth VT, Apperley DC, Kennedy CJ, Jarvis MC (2011) Nanostructure of cellulose microfibrils in spruce wood. *Proc Natl Acad Sci U S A* 108:E1195–E1203
- Festucci-Buselli RA, Otoni WC, Joshi CP (2007) Structure, organization, and functions of cellulose synthase complexes in higher plants. *Braz J Plant Physiol* 19:1–13
- Fromm J, Rockel B, Lautner S, Windeisen E, Wanner G (2003) Lignin distribution in wood cell walls determined by TEM and backscattered SEM techniques. *J Struct Biol* 143:77–84
- Fujii T, Shimada K, Shimizu K (1994) Ultrastructural changes of cryptomeria and beechwood during acetosolv pulping. *Mokuzai Gakkaishi* 40:527–533
- Gibson L (2012) The hierarchical structure and mechanics of plant materials. *J R Soc Interface* 9:2749–2766
- Gierlinger N, Schwanninger M (2006) Chemical imaging of poplar wood cell walls by confocal Raman microscopy. *Plant Physiol* 140:1246–1254
- Giesche H (2006) Mercury porosimetry: a general (practical) overview. *Part & Part Syst Char* 23 (1):9–19
- Girio F, Fonseca C, Carvalheiro F, Duarte L, Marques S, Bogel-Lukasik R (2010) Hemicelluloses for fuel ethanol: a review. *Bioresour Technol* 101:4775–4800
- Granström M (2009) Cellulose derivatives: synthesis, properties and applications. Academic dissertation, Department of Chemistry, University of Helsinki, Finland
- Hall M, Bansal P, Lee JH, Realff MJ, Bommarius AS (2010) Cellulose crystallinity – a key predictor of the enzymatic hydrolysis rate. *FEBS J* 277:1571–1582
- Hayashi T (1989) Xyloglucans in the primary cell wall. *Annu Rev Plant Physiol Plant Mol Biol* 40:139–168
- Hong J, Ye X, Zhang YHP (2007) Quantitative determination of cellulose accessibility to cellulase based on adsorption of a nonhydrolytic fusion protein containing CBM and GFP with its applications. *Langmuir* 23:12535–12540
- Izydorczyk MS, Biliaderis CG (1995) Cereal arabinoxylans: advances in structure and physico-chemical properties. *Carbohydr Polym* 28:33–48
- Jacquet N, Maniet G, Vanderghem C, Delvigne F, Richel A (2015) Application of steam explosion as pretreatment on lignocellulosic material: a review. *Ind Eng Chem Res* 54:2593–2598
- Jakob HF, Fengel D, Tschegg SE, Fratzl P (1995) The elementary cellulose fibril in *Picea abies*: comparison of transmission electron microscopy, small-angle X-ray scattering, and wide-angle X-ray scattering results. *Macromolecules* 28:8782–8787
- Jarvis M (2003) Chemistry – cellulose stacks up. *Nature* 426:611–612
- Ji Z, Zhang X, Ling Z, Zhou X, Ramaswamy S, Xu F (2015) Visualization of *Miscanthus x giganteus* cell wall deconstruction subjected to dilute acid pretreatment for enhanced enzymatic digestibility. *Biotechnol Biofuels* 8:103. doi:10.1186/s13068-015-0282-3
- Jung S, Foston M, Sullards MC, Ragauskas AJ (2010) Surface characterization of dilute acid pretreated populus deltoides by ToF-SIMS. *Energy Fuel* 24:1347–1357
- Kallavus U, Gravitis J (1995) A comparative investigation of the ultrastructure of steam exploded wood with light, scanning and transmission electron microscopy. *Holzforschung* 49:182–188
- Kamm B, Kamm M (2007) Biorefineries—multi product processes. *Adv Biochem Eng/Biotechnol* 105:175–205

- Khalil HPSA, Yusra AFI, Bhat AH, Jawaid M (2010) Cell wall ultrastructure, anatomy, lignin distribution, and chemical composition of Malaysian cultivated kenaf fiber. *Ind Crop Prod* 31:113–121
- Klemm D, Philipp B, Heinze T, Heinze U, Wagenknecht W (1998) *Comprehensive cellulose chemistry: fundamentals and analytical methods*, vol 1. Wiley-VCH, Weinheim
- Klemm D, Schmauder H, Heinze T (2002) Cellulose. In: De Baets S, Vandamme E, Steinbüchel A (eds) *Polysaccharides II: Polysaccharides from eukaryotes*. Wiley-Blackwell, pp 275–320
- Klemm D, Heublein B, Fink H, Bohn A (2005) Cellulose: fascinating biopolymer and sustainable raw material. *Angew Chem Int Edit* 44:3358–3393
- Koshijima T, Watanabe T (2003) Association between lignin and carbohydrates in wood and other plant tissues. Springer, Berlin
- Krässig H (1996) Cellulose. Gordon and Breach Science, Amsterdam
- Kumagai A, Wu L, Iwamoto S, Lee S-H, Endo T, Rodriguez M Jr, Mielenz JR (2015) Improvement of enzymatic saccharification of Populus and switchgrass by combined pretreatment with steam and wet disk milling. *Renew Energy* 76:782–789
- Kumar R, Mago G, Balan V, Wyman CE (2009) Physical and chemical characterizations of corn stover and poplar solids resulting from leading pretreatment technologies. *Bioresour Technol* 100:3948–3962
- Laine C, Tamminen T, Hortling B (2004) Carbohydrate structures in residual lignin-carbohydrate complexes of spruce and pine pulp. *Holzforschung* 58:611–621
- Li X, Luo X, Li K, Zhu JY, Fougere JD, Clarke K (2012) Effects of SPORL and dilute acid pretreatment on substrate morphology, cell physical and chemical wall structures, and subsequent enzymatic hydrolysis of lodgepole pine. *Appl Biochem Biotechnol* 168:1556–1567
- Li H, Pu Y, Kumar R, Ragauskas AJ, Wyman CE (2014) Investigation of lignin deposition on cellulose during hydrothermal pretreatment, its effect on cellulose hydrolysis, and underlying mechanisms. *Biotechnol Bioeng* 111:485–492
- Li Z, Bansal N, Azarpira A, Bhalla A, Chen CH, Ralph J, Hegg EL, Hodge DB (2015) Chemical and structural changes associated with Cu-catalyzed alkaline-oxidative delignification of hybrid poplar. *Biotechnol Biofuels* 8:123. doi:10.1186/s13068-015-0300-5
- Lima M, Lavorente G, da Silva H, Bragatto J, Rezende C, Bernardinelli O, deAzevedo E, Gomez L, McQueen-Mason S, Labate C, Polikarpov I (2013) Effects of pretreatment on morphology, chemical composition and enzymatic digestibility of eucalyptus bark: a potentially valuable source of fermentable sugars for biofuel production – part 1. *Biotechnol Biofuels* 6:75. doi:10.1186/1754-6834-6-75
- Lisperguer J, Perez P, Urizar S (2009) Structure and thermal properties of lignins: characterization by infrared spectroscopy and differential scanning calorimetry. *J Chil Chem Soc* 54:460–463
- Luo X, Zhu JY (2011) Effects of drying-induced fiber hornification on enzymatic saccharification of lignocelluloses. *Enzyme MicrobTech* 48:92–99
- Ma J, Zhang X, Zhou X, Xu F (2014) Revealing the changes in topochemical characteristics of poplar cell wall during hydrothermal pretreatment. *Bioenergy Res* 7:1358–1368
- Ma J, Ji Z, Chen JC, Zhou X, Kim YS, Xu F (2015) The mechanism of xylans removal during hydrothermal pretreatment of poplar fibers investigated by immunogold labeling. *Planta* 242:327–337
- Maki-Arvela P, Salmi T, Holmbom B, Willfor S, Murzin D (2011) Synthesis of sugars by hydrolysis of hemicelluloses—a review. *Chem Rev* 111:5638–5666
- Matsuoka S, Kawamoto H, Saka S (2011) Reducing end-group of cellulose as a reactive site for thermal discoloration. *Polym Degrad Stabil* 96:1242–1247
- Mazeau K, Heux L (2003) Molecular dynamics simulations of bulk native crystalline and amorphous structures of cellulose. *J Phys Chem B* 107:2394–2403
- McCann M, Carpita N (2015) Biomass recalcitrance: a multi-scale, multi-factor, and conversion-specific property. *J Exp Bot* 66:4109–4118
- McDonough TJ (1993) The chemistry of organosolv delignification. *Tappi J* 76:186–193

- McMillan JD (1994) Pretreatment of lignocellulosic biomass. In: Himmel ME, Baker JO, Overend RP (eds) *Enzymatic conversion of biomass for fuels production*. American Chemical Society, Washington, pp 292–324
- Meng X, Ragauskas A (2014) Recent advances in understanding the role of cellulose accessibility in enzymatic hydrolysis of lignocellulosic substrates. *Curr Opin Biotechnol* 27:150–158
- Mohnen D, Bar-Peled M, Somerville C (2008) Cell wall polysaccharide synthesis. In: Himmel M (ed) *Biomass recalcitrance: deconstructing the plant cell wall for bioenergy*. Wiley-Blackwell, Singapore, pp 94–159
- Muzamal M, Jedvert K, Theliander H, Rasmuson A (2015) Structural changes in spruce wood during different steps of steam explosion pretreatment. *Holzforschung* 69:61–66
- Newman RH (1999) Estimation of the lateral dimensions of cellulose crystallites using C-13 NMR signal strengths. *Solid State Nucl Mag* 15:21–29
- Nishiyama Y, Langan P, Chanzy H (2002) Crystal structure and hydrogen-bonding system in cellulose I beta from synchrotron X-ray and neutron fiber diffraction. *J Am Chem Soc* 124:9074–9082
- Nishiyama Y, Sugiyama J, Chanzy H, Langan P (2003) Crystal structure and hydrogen bonding system in cellulose I(alpha), from synchrotron X-ray and neutron fiber diffraction. *J Am Chem Soc* 125:14300–14306
- Peng F, Peng P, Xu F, Sun RC (2012) Fractional purification and bioconversion of hemicelluloses. *Biotechnol Adv* 30:879–903
- Pereira H, Graça J (2003) Wood chemistry in relation to quality. In: Barnett J, Jeronimidis G (eds) *Wood quality and its biological basis*. Blackwell, Oxford, pp 53–86
- Pingali SV, Urban VS, Heller WT, McGaughey J, O'Neill H, Foston M, Myles DA, Ragauskas A, Evans BR (2010) Breakdown of cell wall nanostructure in dilute acid pretreated biomass. *Biomacromolecules* 11:2329–2335
- Ponni R, Vuorinen T, Kontturi E (2012) Proposed nano-scale coalescence of cellulose in chemical pulp fibers during technical treatments. *Bioresources* 7:6077–6108
- Puls J, Saake B (2004) Industrially isolated hemicelluloses. In: Gatenholm P, Tenhanen M (eds) *Hemicelluloses: science and technology*, vol 864, ACS Symposium Series. American Chemical Society, Washington, DC, pp 24–37
- Ragauskas AJ, Williams CK, Davison BH, Britovsek G, Cairney J, Eckert CA, Frederick WJ, Hallett JP, Leak DJ, Liotta CL, Mielenz JR, Murphy R, Templer R, Tschaplinski T (2006) The path forward for biofuels and biomaterials. *Science* 311:484–489
- Ren J, Sun R (2010) Hemicelluloses. In: Sun R (ed) *Cereal straw as a resource for sustainable biomaterials and biofuels*. Elsevier, Amsterdam, pp 73–130
- Sanderson K (2011) A chewy problem. *Nature* 474:S12–S14
- Sant'Anna C, de Souza W (2012) Microscopy as a tool to follow deconstruction of lignocellulosic biomass. Formatex Research Center, Espanha. <http://www.formatex.info/microscopy5/book/639-645.pdf>
- Sassi JF, Tekely P, Chanzy H (2000) Relative susceptibility of the I-alpha and I-beta phases of cellulose towards acetylation. *Cellulose* 7:119–132
- Scheller HV, Ulvskov P (2010) Hemicelluloses. *Annu Rev Plant Biol* 61:263–289
- Shevchenko SM, Bailey GW (1996) The mystery of the lignin-carbohydrate complex: a computational approach. *J Mol Struct-Theochem* 364:197–208
- Singh S, Simmons B, Vogel K (2009) Visualization of biomass solubilization and cellulose regeneration during ionic liquid pretreatment of switchgrass. *Biotechnol Bioeng* 104:68–75
- Sun RC, Sun XF, Tomkinson I (2004) Hemicelluloses and their derivatives. In: Gatenholm P, Tenhanen M (eds) *Hemicelluloses: science and technology*, vol 864, ACS Symposium Series. American Chemical Society, Washington, DC, pp 2–22
- Sun L, Li C, Xue Z, Simmons B, Singh S (2013) Unveiling high-resolution, tissue specific dynamic changes in corn stover during ionic liquid pretreatment. *RSC Adv* 3:2017–2027

- Szijarto N, Siika-aho M, Tenkanen M, Alapuranen M, Vehmaanpera J, Reczey K, Viikari L (2008) Hydrolysis of amorphous and crystalline cellulose by heterologously produced cellulases of *Melanocarpus albomyces*. *J Biotechnol* 136:140–147
- Vanholme R, Demedts B, Morreel K, Ralph J, Boerjan W (2010) Lignin biosynthesis and structure. *Plant Physiol* 153:895–905
- Wada M, Kondo T, Okano T (2003) Thermally induced crystal transformation from cellulose I-alpha to I-beta. *Polym J* 35:155–159
- Willfor S, Sundberg K, Tenkanen M, Holmbom B (2008) Spruce-derived mannans – a potential raw material for hydrocolloids and novel advanced natural materials. *Carbohydr Polym* 72:197–210
- Wu RC, Zhao XB, Liu DH (2016) Structural features of formalin pretreated sugar cane bagasse and their impact on the enzymatic hydrolysis of cellulose. *ACS Sustain Chem Eng* 4:1255–1261
- Xiao L-P, Shi Z-J, Xu F, Sun R-C (2013) Hydrothermal treatment and enzymatic hydrolysis of *Tamarix ramosissima*: evaluation of the process as a conversion method in a biorefinery concept. *Bioresour Technol* 135:73–81
- Xu F (2010) Structure, ultrastructure, and chemical composition. In: Sun R (ed) *Cereal straw as a resource for sustainable biomaterials and biofuels*. Elsevier, Amsterdam, pp 9–49
- Xu M, Xu M, Dai H, Wang S, Wu W (2013) The effects of ball milling and PFI pretreatment on the cellulose structure and fiber morphology. *J Cellulose Sci Tech* 21:46–52
- Yamamoto H, Horii F (1993) Carbon-13 NMR analysis of the crystal transformation induced for Valonia cellulose by annealing at high temperatures. *Macromolecules* 26:1313–1317
- Yang S (2001) *Plant fiber chemistry*, 3rd edn. China Light Industry Press, Beijing
- Yang B, Wyman C (2008) Pretreatment: the key to unlocking low-cost cellulosic ethanol. *Biofuel Bioprod Bior* 2:26–40
- Yu Y, Wu H (2010) Significant differences in the hydrolysis behavior of amorphous and crystalline portions within microcrystalline cellulose in hot-compressed water. *Ind Eng Chem Res* 49:3902–3909
- Yu CT, Chen WH, Men LC, Hwang WS (2009) Microscopic structure features changes of rice straw treated by boiled acid solution. *Ind Crop Prod* 29:308–315
- Yuan T-Q, Sun S-N, Xu F, Sun R-C (2011) Characterization of lignin structures and lignin-carbohydrate complex (LCC) linkages by quantitative C-13 and 2D HSQC NMR spectroscopy. *J Agr Food Chem* 59:10604–10614
- Yuan Z, Long J, Wang T, Shu R, Zhang Q, Ma L (2015) Process intensification effect of ball milling on the hydrothermal pretreatment for corn straw enzymolysis. *Energy Convers Manage* 101:481–488
- Zakaria MR, Hirata S, Fujimoto S, Hassan MA (2015) Combined pretreatment with hot compressed water and wet disk milling opened up oil palm biomass structure resulting in enhanced enzymatic digestibility. *Bioresour Technol* 193:128–134
- Zhan H (2005) *Fiber chemistry and physics*. Science Press, Beijing
- Zhang YHP, Lynd LR (2004) Toward an aggregated understanding of enzymatic hydrolysis of cellulose: noncomplexed cellulase systems. *Biotechnol Bioeng* 88:797–824
- Zhang ZH, Ma JF, Xu F (2012) Confocal Raman microspectroscopy study on the distribution of cellulose and lignin in *Daphne odora* Thunb. *Spectrosc Spect Anal* 32:1002–1006
- Zhang MM, Chen GJ, Kumar R, Xu BQ (2013) Mapping out the structural changes of natural and pretreated plant cell wall surfaces by atomic force microscopy single molecular recognition imaging. *Biotechnol Biofuels* 6:147. doi:10.1186/1754-6834-6-147
- Zhao J, Chen H (2013) Correlation of porous structure, mass transfer and enzymatic hydrolysis of steam exploded corn stover. *Chem Eng Sci* 104:1036–1044
- Zhao H, Kwak J, Wang Y, Franz J, White J, Holladay J (2006) Effects of crystallinity on dilute acid hydrolysis of cellulose by cellulose ball-milling study. *Energy Fuel* 20:807–811
- Zhao X, Wang L, Liu D (2008) Peracetic acid pretreatment of sugarcane bagasse for enzymatic hydrolysis: a continued work. *J Chem Technol Biot* 83:950–956

- Zhao X, Cheng K, Liu D (2009) Organosolv pretreatment of lignocellulosic biomass for enzymatic hydrolysis. *Appl Microbiol Biotechnol* 82:815–827
- Zhao X, Zhang L, Liu D (2012a) Biomass recalcitrance. Part I: The chemical compositions and physical structures affecting the enzymatic hydrolysis of lignocellulose. *Biofuel Bioprod Bior* 6:465–482
- Zhao X, Zhang L, Liu D (2012b) Biomass recalcitrance. Part II: Fundamentals of different pre-treatments to increase the enzymatic digestibility of lignocellulose. *Biofuel Bioprod Bior* 6:561–579
- Zhu JY (2011) Physical pretreatment – woody biomass size reduction – for forest biorefinery. Sustainable production of fuels, chemicals, and fibers from forest biomass, American Chemical Society, Washington, DC, pp 89–107
- Zhu J, Pan X (2010) Woody biomass pretreatment for cellulosic ethanol production: technology and energy consumption evaluation. *Bioresour Technol* 101:4992–5002
- Zhu JY, Pan XJ, Wang GS, Gleisner R (2009) Sulfite pretreatment (SPORL) for robust enzymatic saccharification of spruce and red pine. *Bioresour Technol* 100:2411–2418
- Zugenmaier P (2007) Crystalline cellulose and derivatives-characterization and structures. Springer, Berlin, pp 101–174



# Chapter 7

## Role of Nanoparticles in Enzymatic Hydrolysis of Lignocellulose in Ethanol

Mahendra Rai, Avinash P. Ingle, Swapnil Gaikwad, Kelly J. Dussán,  
and Silvio Silvério da Silva

**Abstract** The depletion in the limited sources of fossil fuels has generated the problem of energy crisis all over the world. This hunt forces scientific community towards the search for cost-effective, environment-friendly, renewable alternative sources which can replace fossil fuels and fulfill the increasing demands of energy. In this context, the use of lignocellulosic material (plant residues) composed of cellulose, hemicellulose, and lignin becomes the first choice. In the process of ethanol production, first lignocellulosic material is broken down and hydrolyzed into simple sugars like cellulose, and then these sugars are fermented into biofuels such as ethanol in the presence of enzymes like cellulases. The use of cellulases makes the process expensive, and therefore, immobilization of these enzymes on solid supports like nanoparticles can help to recover the enzyme, which ultimately decreases the cost of process. Therefore, the use of nanotechnology and nanomaterials could be one possible avenue to improve biofuel production efficiency and reduction in the processing cost.

This chapter discusses important existing pretreatment approaches involved in the pretreatment of plant biomass use for biofuel production. The emphasis is given on the role of nanotechnological solutions for the development of novel, efficient, and inexpensive strategies for the production of biofuels.

**Keywords** Biofuel • Ethanol • Fossil fuels • Nanotechnology • Pretreatments

---

M. Rai (✉) • A.P. Ingle  
Nanobiotechnology Laboratory, Department of Biotechnology, Sant Gadge Baba Amravati University, Amravati 444 602, Maharashtra, India  
e-mail: [mahendrarai@sgbau.ac.in](mailto:mahendrarai@sgbau.ac.in)

S. Gaikwad • S.S. da Silva  
Biotechnology Department, Engineering School of Lorena, University of Sao Paulo, Lorena, Brazil

K.J. Dussán  
Department of Biochemistry and Technological Chemistry, Institute of Chemistry, State University of São Paulo - UNESP, R. Professor Francisco Degni no 55, 14801-060, Araraquara, São Paulo, Brazil

## 7.1 Introduction

It is widely known that presently all nations have been facing the huge problem of energy crisis due to depletion of fossil fuel reserves. Moreover, the continuous consumption of this energy source is not accepted as sustainable energy source due to depletion of resources and emissions of greenhouse gases in the environment. Excessive dependence and limited sources of petroleum have forced researchers around the globe to search for alternative renewable energy source like biofuels (bioethanol and biodiesel) (Farrell et al. 2006). Only biofuels can mitigate the grave threat of global warming and also reduce dependency on petroleum (Kumar and Sharma 2014; Lee et al. 2014). Therefore, development of novel, eco-friendly, and economically viable renewable energy sources has become a very intense research area in the last few decades.

Initially, biofuel (bioethanol) was produced from feedstock such as vegetable oils, animal fats, and the sucrose from sugarcane or starch from corn which are called as the first-generation biofuels (Naik et al. 2010). The common use of these feedstocks creates certain limitations; therefore, new concept of the second-generation biofuels was put forward for the production of bioethanol using nonfood feedstock like lignocellulosic materials (viz., wood wastes, agricultural residues, etc.) (Patumsawad 2011; Eggert and Greaker 2014). Although the second-generation biofuels have some advantages like the use of waste materials, the production technologies for these generation biofuels are facing certain challenges with respect to production cost (which is relatively higher), requiring sufficient infrastructure facility, and these technologies also have many technological barriers. Therefore, considering these facts, more efforts are needed for the development of efficient technologies and to solve the problems associated with pretreatment of lignocellulosic materials and also to increase the efficacy of fermentation processes involved in the production of bioethanol (Patumsawad 2011). In this context, nanotechnology could offer a significant solution to overcome all the above mentioned problems by offering the opportunity to change the characteristics of feed materials for fuels.

Nanotechnology is emerging as a new frontier branch of science. It represents one of the most fascinating technoscientific revolutions ever undertaken. It has huge applications in variety of sectors including production and commercial sectors. These things become possible for nanotechnology because the nanomaterials involved in it exhibit innovative properties and characteristics that are unprecedented in science (Engelmann et al. 2013). The vast list of applications of nanotechnology also impacts all areas of energy generation, storage, and distribution. The potential applications of nanotechnology in bioenergy and biosensors have encouraged and attracted researchers in recent years to investigate novel nanotechnological solutions for the production of biofuel through the development of robust nanobiocatalytic systems (Verma et al. 2013a). Nanotechnology will also help to increase the efficiency of preexisting methods used in bioethanol production.

The main aim of this chapter is to examine the possibilities of nanotechnology in the production of bioethanol and discuss the role of nanomaterials in different pretreatment methods of lignocellulosic materials and optimization of other methods involved in the production of bioethanol from lignocellulosic materials.

## 7.2 Lignocellulosic Materials

Different types of lignocellulosic biomass, such as agricultural crop residues, hardwood, softwood, grasses, waste paper from chemical pulp, aquatic plants, switch grass, sugarcane bagasse, agricultural and municipal solid waste, and manures, contain different amounts of polymers, cellulose, hemicellulose, lignin, and extractives (Table 7.1). In general, lignocellulose is composed of three main components: cellulose (30–50 %), hemicellulose (15–35 %), and lignin (10–20 %). Cellulose and hemicelluloses make up approximately 70 % of the entire biomass and are tightly linked to the lignin component through covalent and hydrogenic bonds that make the structure highly robust and resistant to any treatment (Limayema and Ricke 2012).

Development of sustainable energy using cheaper renewable sources like biomass feedstocks is now a global attention. The use of lignocellulosic material is a better choice. As mentioned above, lignocellulosic biomass mainly consists of polymers of cellulose, hemicellulose, and lignin which are present in a complex structure. The biofuels such as bioethanol can be produced from such biomass through the fermentation of sugars derived from the cellulose and hemicellulose within lignocellulosic materials. But to liberate the sugars such as hexoses (glucose, galactose, mannose, etc.), pentoses (xylose, arabinose), different acids (acetic acid, formic acid, levulinic acid, etc.), and many others (Taherzadeh and Karimi 2007) from lignocellulosic materials, pretreatment processes of the biomass are necessary. In addition, productions of valuable byproducts along with biofuels create the need for selectivity during pretreatment (Agbor et al. 2011). Various pretreatment methods, which are in practice, have been discussed in brief.

**Table 7.1** Potential lignocellulosic biomass sources and their composition (% dry weight)

Raw materials	Cellulose	Hemicellulose	Lignin	Other (i.e., ash)	References
Agricultural residues	37–50	25–50	5–15	12–16	Limayema and Ricke (2012)
Hardwood	45–47	25–40	20–25	0.80	
Softwood	40–45	25–29	30–60	0.50	
Grasses	25–40	35–50	–	–	
Waste paper from chemical pulp	50–70	12–20	6–10	–	
Newspapers	40–55	25–40	18–30	–	
Switch grass	40–45	30–35	12	–	
Sugarcane grass	38.8	26	32.4	–	da Silva et al. (2010)

## 7.3 Pretreatment Methods for Lignocellulosic Materials

The ideal pretreatment methods should meet the following requirements: (1) improve the formation of sugars or the ability to subsequently form sugars by hydrolysis, (2) avoid the degradation or loss of sugars, (3) avoid the formation of byproducts that are inhibitory to the subsequent hydrolysis and fermentation processes, and (4) be cost-effective (Kumar et al. 2009). Generally, the methods involved in pretreatment of lignocellulosic material are grouped into physical, chemical, biological, and multiple or combinatorial pretreatment methods. Multiple or combinatorial pretreatment methods involves the use of more than one method mentioned above. The use of physical and chemical methods together is known as physicochemical method. Similarly, the combined use of biological and chemical methods is termed as biochemical method, whereas the involvement of physical and biological methods is called as biophysical methods. According to Sun and Cheng (2002), ammonia fiber explosion (AFEX) is a good example of a physicochemical method. However, bio-organosolv is a good example of a biochemical method for biomass pretreatment (Itoh et al. 2003). It was reported that multiple or combinatorial pretreatment strategies are generally more effective in enhancing digestibility of the lignocellulosic biomass and often used in designing suitable pretreatment technologies. The various physical, chemical, biological, and multiple or combinatorial pretreatment methods are briefly discussed here.

### 7.3.1 Physical Pretreatment Methods

Physical pretreatment methods mainly include milling and grinding of the biomass, which are carried out as mechanical comminution and extrusion. Mechanical comminution incorporates chipping, shredding, grinding, milling, etc., which help to reduce the size of bulk lignocellulosic materials and, ultimately, enhance the digestibility of lignocellulosic biomass (Palmowski and Muller 1999). It was demonstrated that by using these methods, lignocellulosic biomass is reduced from 10–50 mm to 10–30 mm by chipping and further reduced up to 0.2–2 mm by grinding and milling. Kumar et al. (2009) reviewed that vibratory ball milling was more effective than ordinary ball milling in reducing cellulose crystallinity. Whereas, disk milling is reported to be efficient in enhancing cellulose hydrolysis than hammer milling because disk milling produces fibers and hammer milling produces finer bundles (Zhua et al. 2009). The small size of biomass helps in early hydrolysis of available sugars.

Similarly, extrusion can also be used for the pretreatment of lignocellulosic biomass. In this method the cellulose present in lignocellulosic biomass rapidly

decomposes to gaseous products and residual char on the treatment of biomass at the temperatures greater than 300 °C (Zheng and Rehmann 2014). Other physical approach involves the use of gamma radiations (Takacs et al. 2000) that cleave the  $\beta$ -1,4 glycosidic bonds, thus generating larger surface area and lower crystallinity. Imai et al. (2004) demonstrated that when a suspension of cellulose is treated with irradiation, the reaction rate of the subsequent enzymatic hydrolysis may increase by approximately 200 %. But the use of such radiations makes the method very expensive and also has huge environmental and safety concerns.

### 7.3.2 Chemical Pretreatment Methods

Various chemicals/chemical compounds like acids, alkali, organic solvents, ionic liquids, etc., have been reported to have the ability to affect the complex structure of lignocellulosic biomass (Agbor et al. 2011). It was reported that pretreatment of lignocellulosic biomass with alkali such as sodium, potassium, and calcium hydroxide, anhydrous ammonia, and hydrazines is responsible for the swelling of biomass and thus increases the internal surface area of the biomass and decreases the degree of polymerization as well as cellulose crystallinity. Swatloski et al. (2002) demonstrated the mode of action of alkali in pretreatment. According to them, alkali disrupts the complex structure of lignin and also breaks the linkage between lignin and other carbohydrates present in lignocellulosic biomass and finally leads to liberation of sugars, thus making it more accessible. However, the use of dilute acids like sulfuric acid, hydrochloric acid, and phosphoric acid is mostly preferred for hydrolysis of biomass over the concentrated acids due to their corrosive action and economic viability (Sivers and Zacchi 1995; Nguyen 2000).

### 7.3.3 Biological Pretreatment Methods

The abovementioned conventional physical and chemical methods used for pretreatment of lignocellulosic biomass require high-energy inputs and also cause pollution. Therefore, biological pretreatment methods of lignocellulosic biomass are most preferably used as an efficient, eco-friendly, and cost-effective alternative (Wan and Li 2012). Biological methods used for pretreatment of lignocellulosic biomass are mostly associated with the involvement of fungi which are capable of producing enzymes and can degrade lignin, hemicellulose, and polyphenols. It was demonstrated that white and soft-rot fungi like *Phanerochaete chrysosporium*, *Phlebiaradiata*, *Dichomitus squalens*, *Rigidoporus lignosus*, and *Jungua separabilima* have the ability to secrete enzymes which can degrade lignocellulose material; further it was also observed that white-rot-causing fungi were effective at biological pretreatment of biomass (Hatakka 1994; Sun and Cheng 2002). Similarly, many other white-rot fungi such as *Phanerochaete chrysosporium*,

*Bjerkanderaadusta*, *Ganoderma resinaceum*, *Irpex lacteus*, *Trametes versicolor*, *Fomes fomentarius*, etc., have been successfully used for the treatment of wheat straw by solid state and submerged fermentations (Pinto et al. 2012). According to Saritha et al. (2012), *Streptomyces griseus* plays an important role in the treatment of hardwood and softwood.

The mechanisms involved in the degradation of lignocellulose by fungal enzymes are fully understood and categorized into two main types, i.e., oxidative and hydrolytic. In oxidative mechanism, lignin present in lignocellulosic biomass was degraded via generation of reactive oxygen species (ROS) mainly hydroxyl radicals by the fungi (Hammel et al. 2002), whereas, in hydrolytic mechanism, hydrolytic enzymes secreted by fungi degrade glycosidic linkages in cellulose and hemicellulose liberating monomeric sugars (Feijoo et al. 2008). Generally, the degradation of cellulose is achieved by three classes of hydrolytic enzymes: cellobiohydrolase (exocellulase), endo-(1,4)- $\beta$ -glucanase (endocellulase), and  $\beta$ -glucosidase (bG) (Baldrian and Valaskova 2008). Moreover, hemicellulose degradation is achieved by the action of hydrolytic enzymes such as endo-xylanases, endo- $\alpha$ -L-arabinase, endo-mannanase,  $\beta$ -galactosidase, and  $\beta$ -glucosidases (Shallom and Shoham 2003). Although the rate of biological pretreatment is comparatively slow for a large scale and required more time, these are very specific and efficient.

## 7.4 Multiple or Combinatorial Pretreatment Methods

This category includes various combinatorial pretreatments like physicochemical strategies such as wet oxidation pretreatment, liquid hot water pretreatment, ammonia recycle percolation, ammonia fiber/freeze explosion (AFEX), steam pretreatment, aqueous ammonia pretreatment, and organosolv pretreatment. These forms of pretreatment exploit the use of conditions and compounds that affect the physical and chemical properties of biomass (Zhu et al. 2009; Agbor et al. 2011) and biochemical approaches such as bio-organosolv (Itoh et al. 2003). Out of these AFEX and bio-organosolv are briefly discussed.

**AFEX** In this approach, lignocellulosic biomass is treated with liquid ammonia at high temperature and under suitable pressure (Teymouri et al. 2005). After few seconds, the pressure is suddenly reduced. A typical AFEX process can be carried out with 1–2 kg ammonia/kg dry biomass at 90 °C during 30 min. It reduces the lignin content and liberates some hemicellulose while decrystallizing cellulose.

**Bio-organosolv** This biochemical approach of pretreatment was generally used for the production of bioethanol by simultaneous saccharification and fermentation of beech wood chips. In this approach beech wood chips are subjected to pretreatment with the white-rot fungi for 2–8 weeks without the addition of any nutrients. The wood chips were then subjected to ethanolysis to separate them into pulp and soluble fractions. Further, the pulp fraction was used for the production of

bioethanol by simultaneous saccharification and fermentation using *Saccharomyces cerevisiae* AM12. It was reported that the yield thus obtained is 1.6 times higher than that of obtained without the fungal treatments. This approach of pretreatments saved 15 % of the electricity needed for the ethanolysis (Itoh et al. 2003).

De Maria et al. (2015) suggested that optimization of all the above mentioned existing pretreatment processes is necessary to reduce cost of ethanol production by increasing catalyst efficiency, effluents recirculation, or lignin valorization which can be achieved by altering the normal pretreatment processes.

## 7.5 Role of Nanotechnology in Biofuel Production

Nanomaterials are the building blocks of nanotechnology, which possess unique properties than that of their bulk metals. Verma et al. (2013a) reviewed that different nanomaterials like nanoparticles, nanofibers, nanotubes, nanosheets, etc., have a number of direct or indirect applications in the production of biofuels. Recently, the use of nanoparticles in enzyme-mediated hydrolysis of lignocellulosic biomass is in practice. Ahmad and Sardar (2014) and Goh et al. (2012) demonstrated the involvement of magnetic and metal oxide nanoparticles as matrices for enzyme immobilization. Immobilization of enzymes like cellulases and hemicellulases on magnetic nanoparticles by physical adsorption, covalent binding, cross-linking, or specific ligand spacers helped in the nanoparticle-mediated enzyme hydrolysis of sugars in ethanol. Such nanomaterials are generally called as nanocatalysts. These are fabricated by immobilizing enzymes with functional nanomaterials as enzyme carriers (Misson et al. 2015). Immobilized enzymes on magnetic nanoparticles could be magnetically recovered easily after use and can be reused for a new cycle of enzymatic hydrolysis of cellulose (Alftren and Hogley 2013; Rai et al. 2016).

### 7.5.1 Potential Nanoparticles for Bioethanol Production

Increase in price of fossil fuels has generated much interest in renewable energies like bioethanol and biodiesel production. An extensive research work has been carried out to use ethanol as a substitute for gasoline. Enzymatic hydrolysis of cellulose and fermentation is one of the leading procedures to produce bioethanol. The largest producers of bioethanol in the world are the United States, Brazil, and China by using corn feedstock and sugarcane. But, the main difficulty in producing the cellulosic ethanol is the higher cost of cellulase. The economical enzymatic hydrolysis of biomass could be enhanced by increasing efficiency, thermal stability, and reusability of enzymes. These entire enhancements could be possible by immobilizing enzymes on support.

Cost of production could be reduced by applying different nanoparticles in production of cellulosic ethanol or bioethanol. Various nanoparticles have extensive applications in biomedical, material science, biotechnology, engineering, and environmental areas, and therefore more devotion has been paid to the production of various kinds of nanoparticles. Due to unique size and physicochemical properties, nanoparticles have advantageous applications in bioethanol production. In current nanotechnology, development of trustworthy protocols for the synthesis of different nanomaterials with small size and high monodispersity are interesting issues (Mandal et al. 2005). Many nanoparticles like  $\text{Fe}_3\text{O}_4$ ,  $\text{TiO}_2$ ,  $\text{ZnO}$ ,  $\text{SnO}_2$ , carbon, fullerene, and graphene have been used in sugar and alcohol production.

### 7.5.2 Magnetic Nanoparticles

Similar to other metal nanoparticles, magnetic nanoparticles also have extensive uses in biotechnology, biomedical, material science, engineering, and environmental areas, therefore, much attention has been paid to the synthesis of different kinds of magnetic nanoparticles (Abraham et al. 2014). Magnetic nanoparticles retain exceptional properties including their high surface to volume ratio, quantum properties, and ability to carry other molecules due to their small size. Most important advantage of magnetic nanoparticles over other metal nanoparticles is that these can be easily removed or recovered by applying appropriate magnetic field, which reduces the probabilities of nanotoxicity (Ahmed and Douek 2013). Magnetic nanoparticles have potential uses in the field of biofuel and bioenergy, i.e., in the production of sugars and bioethanol from lignocellulosic materials by immobilizing enzymes like cellulases and hemicellulases on magnetic nanoparticles. These immobilized enzymes could be magnetically recovered and recycled for a new cellulosic hydrolysis process (Abraham et al. 2014) (Fig. 7.1). For immobilization of enzyme nowadays, many metal oxides are being used (Mei et al. 2009). Two techniques are generally used for immobilization of enzymes on nanoparticles, and these are covalent binding and physical adsorption. The most consistent method to reduce protein desorption is covalent binding which is attained by forming covalent bonds between enzyme and nanoparticles (Abraham et al. 2014).

In cellulosic ethanol production,  $\beta$ -glucosidase (bG) is a cellobiose inhibitor which converts it into glucose. For potential reuse of it, Lee et al. (2010) immobilized bG on polymer nanofibers. For this application they synthesized polymer nanofibers entrapped with magnetic nanoparticles. The bG was fixed and stabilized on these magnetic nanofibers, which could be easily recovered by applying magnetic field and reused for multiple cycles. Synthesis of new carrier material for immobilization and its use in continuous fermentation is a developing area.

Researchers also worked on direct immobilization of organisms with nanoparticles for continuous ethanol production. Ivanova et al. (2011) performed a study for continuous ethanol production by immobilizing *Saccharomyces*



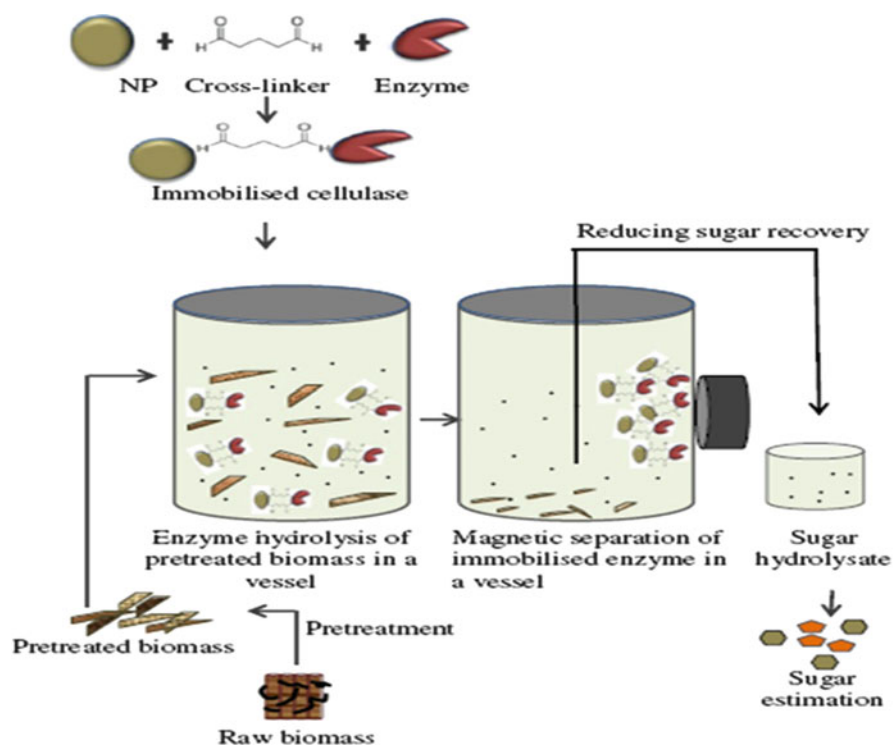


**Fig. 7.1** The use of magnetic nanoparticles (MNPs) immobilized cellulase enzyme in hydrolysis of lignocellulosic biomass for biofuel production [Source: Abraham et al. (2014), Reproduced by permission of Biomed Central]

*cerevisiae* on magnetic nanoparticles. Throughout the continuous fermentation, *S. cerevisiae*-immobilized cells showed high-yield ethanol production capability. Also, this enzyme-nanoparticle system can be used for the production of bioethanol by simultaneous saccharification and fermentation (SSF) process, which is more prominent in the present epoch. Experiments performed by Cherian et al. (2015) explained immobilization of cellulase produced by *Aspergillus fumigatus*, on manganese dioxide nanoparticles which were carried out by covalent binding. Particle size of nanoparticles was increased from 76 nm to 101 nm after immobilization of enzyme. Immobilized enzyme showed increased thermostability as compared to free enzyme and found to be stable at 70 °C. Immobilized cellulase in combination with yeast produced bioethanol of concentration 21.96 g/L by simultaneous saccharification and fermentation process from agricultural waste. Even after five cycles, immobilized enzyme retained 60% of its activity.

Goh et al. (2012) produced magnetic single-walled carbon nanotubes by incorporating iron oxide nanoparticles into carbon nanotubes. They immobilized the enzyme on magnetic carbon nanotubes for application in biofuel production. The activity of enzyme is reduced after immobilization, but it is reimbursed by the

ability to recycle the enzyme which could reduce the cost of biofuel production. They also concluded that immobilized enzyme retained their activity at least 1 month when stored in acetate buffer at 4 °C. In future study increasing the concentration of iron oxide nanoparticles in nanotubes will result in improved performance of immobilized nanoparticles for efficient biofuel production. Verma et al. (2013b) functionalized the magnetic nanoparticles and immobilized them with  $\beta$ -glucosidase isolated from fungus for biofuel production. Enzyme showed 93 % of binding efficiency and retained 50 % of its activity at 16th cycle. They concluded that this nanobiocatalyst system has more potential for biofuel production with great immobilization competence, greater thermostability and reusability, and more economical.

Many researchers are using magnetic nanoparticles in production of biodiesel. Hu et al. (2011) proved that the biodiesel production can be increased up to 95 % by using nano-magnetic solid base catalyst when reaction is carried out at 65 °C for 3 h. Also, this nano-magnetic catalyst can be reused 14 times with catalyst recovery more than 90 %. Their research concluded that application of nano-magnetic catalyst in biodiesel production provided good vision of its growth and use. Ren et al. (2011) developed a method for immobilization of lipase on polydopamine-coated magnetic nanoparticles (PD-MNPs) (Fig. 7.2). They found 73.9 % of binding efficiency of lipase enzyme with enhanced pH and thermal stability as

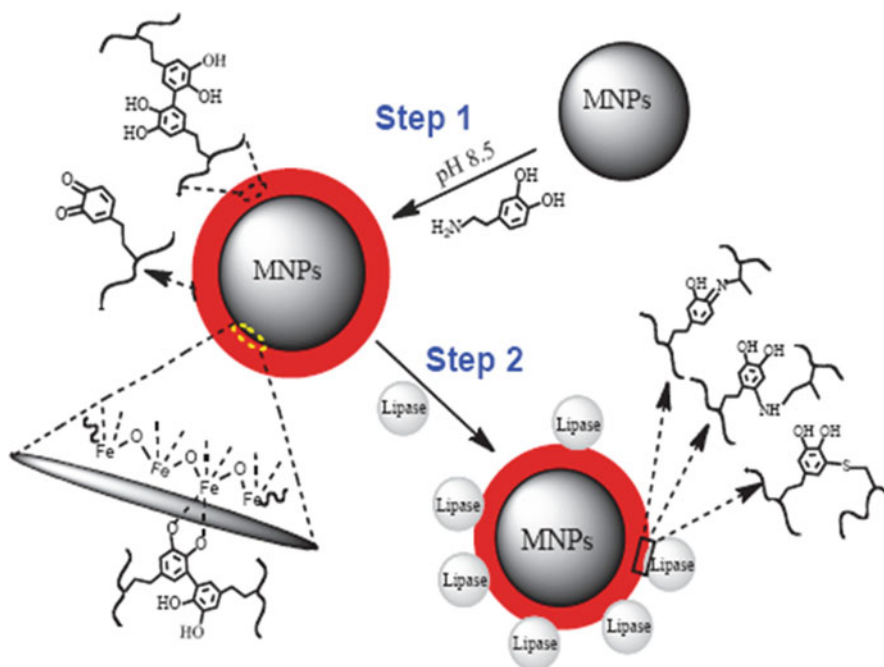


**Fig. 7.2** Fabrication of lipase immobilized polydopamine-coated magnetic nanoparticles (PD-MNPS) [Source: Ren et al. (2011), Reproduced by permission of Biomed Central]

compared to free enzyme. Moreover, lipase immobilized on PD-MNPs can be easily separated from reaction mixture with more than 70 % activity even after 21 repeated cycles.

### 7.5.3 Carbon, Silica, Gold, and Other Nanoparticles

Like magnetic nanoparticles other nanoparticles such as carbon, silica, cellulose, gold, TiO<sub>2</sub>, and polymeric, fullerene, and graphene nanomaterials have also been used for immobilization and biofuel production (Huang et al. 2011; Cho et al. 2012; Pavlidis et al. 2012a, b; Verma et al. 2013a). Carbon nanotubes have distinct free cores and have mechanical and thermal stability which promotes scientists to introduce other materials into it. Pan et al. (2007) used carbon nanotubes to entrap Rh particles to enhance catalytic activity. They reported outstanding improvement in catalytic activity of Rh particles for production of ethanol (30.0 mol/molRh/h) from CO and H<sub>2</sub>O. This study has inspired other researchers to use carbon nanotubes for immobilization.

Mahmood and Hussain (2010) used spent tea to convert it into biofuels by using nanobiotechnology. In their three-step reaction, first spent tea was gasified using co-nanocatalyst which produced liquid extract, fuel gases (ethane, methanol, and ethane), and charcoal. In the second step, transesterification of liquid extract from spent tea produced ethyl ester (biodiesel). And in the final step, growth of *Aspergillus niger* on spent tea gave bioethanol. Wen et al. (2010) prepared KF/CaO nanocatalyst for biodiesel production from tallow seed oil. They studied the effect of different conditions on yield of biodiesel and concluded that production of biodiesel increased up to 96.8 % by using KF/CaO nanocatalyst and also it is one of the efficient options to produce biodiesel with higher concentration of acid. Qiu et al. (2011) prepared heterogeneous solid base nanocatalyst for biodiesel production from soybean oil and methanol. In their work, they achieved yield of biodiesel about 98.03 % at 16:1 molar ratio of methanol to oil at 60 °C and 6 % nanocatalyst.

Recently, by using physical adsorption method, cellulase was immobilized on silica nanoparticles (Lupoi and Smith 2011). Immobilized cellulase showed increased ethanol production in the simultaneous saccharification and fermentation process. In their work they confirmed that cellulase immobilized on silica nanoparticles gave more yield of glucose compared to free cellulase since nanoparticles stabilized enzyme and stimulated activity under extreme conditions. Sakai et al. (2008) used PCL immobilized on PAN nanofiber for biodiesel production in batch and continuous fermenter. Enzyme immobilized on nanoparticles by physical adsorption achieved 94 % production of biodiesel in 48 h. Also, the starting reaction rates were 65 times higher as compared to commercial immobilized lipase (Novozym 435). Improved catalytic activity of attached lipase on nanofibers is due to admirable changes in lipase that assists free contact of substrate to active points of enzyme. Tran et al. (2012) applied lipase immobilized on ferric silica nanocomposites for biodiesel production. Lipase produced from

*Burkholderia* sp. showed adsorption capacity (29.45 mg/g particles). Biodiesel produced by using immobilized lipase was higher than 90%; also immobilized enzyme showed high methanol tolerance and reusability. Gold nanoparticles were also used for functional immobilization of cystine-tagged protein cellulases. Cho et al. (2012) demonstrated the feasible results for ethanol production using this enzyme-cascade immobilization. The organic-inorganic nanoparticles were synthesized and *Rhizomucor miehei* lipase (RML) immobilized on it by encapsulation technique (Macario et al. 2013). Lipase was encapsulated in liposome nanosphere coated with porous inorganic silica which stabilized and protected the lipase. Transesterification process of triolein with methanol, by using immobilized lipases, produced biodiesel. Immobilized lipases showed faster conversion of triolein as compared to lipase encapsulated into mesoporous/surfactant matrix. This work concluded that immobilized lipase preserves its free and stable structure because the liposome membrane has biocompatible microenvironment. Also, productivity is higher than the same amount of free enzyme.

## 7.6 Immobilization of Enzymes on Nanoparticles for Bioethanol Production

The immobilization of enzymes and cells is a process in which these biocatalysts are confined or localized in a defined region of space, to give rise to insoluble forms, which retain their catalytic activity and can be reused repeatedly in bioprocess (Tischer and Wedekind 1999).

In biofuel production, enzyme immobilization in nanomaterials has major potential to improve the economic viability of all processes. Some advantages of the use of immobilized nanobiocatalysts are the increase of their stability, the possibility of reuse of derivatives lowering costs of the process, and the designing specific reactors of easy handling and control. In addition to the possibility of recycling the biocatalyst, dispensing purification steps of products and preventing microbial growth during bioprocess are also the major advantages (Tischer and Wedekind 1999; Bornscheuer 2003; Datta et al. 2013). In general, immobilization methods are usually classified into two categories: physical retention and chemical bonding. The methods of immobilization of physical retention are divided into attachment including membranes, and immobilization methods by chemical bonding are divided into binding supports and cross-linking (Tischer and Wedekind 1999; Ahmad and Sardar 2015). Binding on support (nanoparticles) type is also divided into four subtypes, i.e., adsorption on support, ionic binding, covalent binding with support, and entrapment into support (Fig. 7.3).

In industrial point of view, covalent linking of an enzyme to a support is the most interesting method of immobilization. The method of covalent linking is based on activation of chemical groups of the support to react with protein nucleophiles (Ahmad and Sardar 2015; Mateo et al. 2000). The choice of substrate and the type

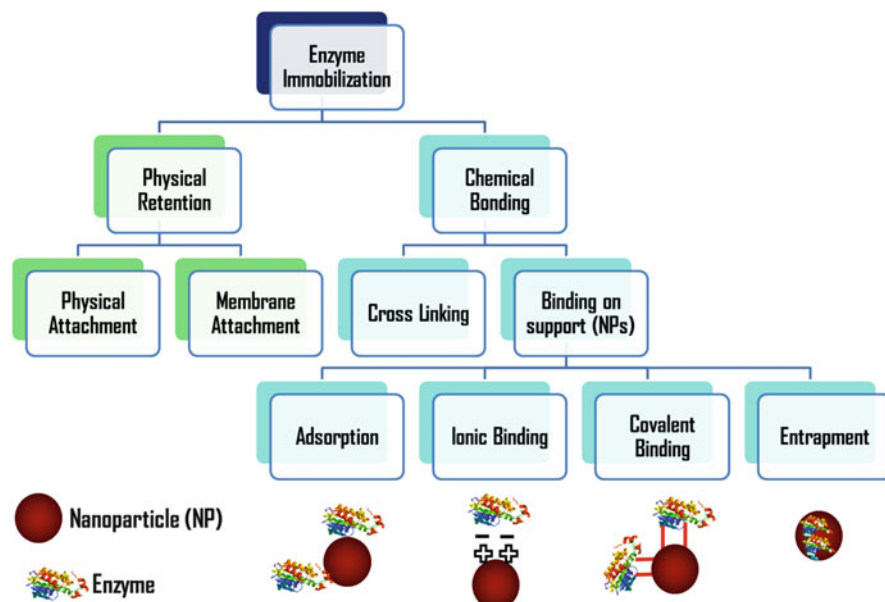


Fig. 7.3 Methods of immobilization of enzymes

of link are critical in the subsequent behavior of the immobilized biocatalyst. The immobilization process should increase the substrate affinity, decrease inhibition, expand the range of optimal pH in the case of enzymes, and reduce possible microbial contamination. Furthermore, the support must have adequate mechanical strength for the operating conditions of the reactor and be easily separable from the liquid medium so that it can be reused (Tischer and Wedekind 1999; Datta et al. 2013).

There are varieties of materials as supports have been used for immobilization of many enzymes. These materials differ in size, density, porosity, and shape, although generally found in a cylinder, sheets, and fibers and more usually in the form of spheres, and can be classified into two groups, inorganic and organic substrates. The inorganic supports can be natural (e.g., clays, pumice, silica, zeolite) or manufactured materials (e.g., glass and metal oxides with controlled pore size, nonporous glass, alumina, ceramics, silica gel, magnetic materials), and the organic carriers can be classified as natural polymers (e.g., cellulose, starch, dextrans, agar-agar, alginate, chitosan) (Ansari and Husain 2012; Datta et al. 2013; Ahmad and Sardar 2015).

The use of nanomaterial support with activated surface area offers unbreakable covalent bonds (cross-linking). Cross-linking is a technique that has been widely used in the stabilization of many enzymes, including cell immobilization, which uses bifunctional reagents such as dialdehydes, diiminoesters, diisocyanates, bisdiazonio salts, and even carbodiimide-activated diamines to cause intermolecular bonds between molecules of the biocatalyst (Han et al. 1984; Pundir

2015). Cross-linking results in biocatalysts with irreversible intermolecular bonds that can withstand pH and temperature extremes. Co-cross-linking eliminates the losses of enzyme activity due to diffusion effects, by cross-linking enzymes with a protein without enzymatic activity and rich in lysine residues (e.g., bovine albumin). A mixed process of immobilization is very common to immobilize the catalyst by adsorption onto an ion exchange resin or a polymeric support (which is achieved with a high enzyme load) and then adding the bifunctional reagent.

For bioethanol production,  $\beta$ -glucosidase and cellobiase enzymes immobilized on different nanomaterials have been used for the hydrolysis of pretreated lignocellulosic materials exhibiting improved biochemical properties and stability when compared with free enzymes. Several reviews on enzyme immobilization on different nanomaterials (metal, oxide, magnetic, porous, and polymeric nanomaterials) have been reported earlier (Ansari and Husain 2012; Datta et al. 2013; Puri et al. 2013; Verma et al. 2013a).  $\beta$ -Glucosidase immobilized on nanomaterials carrier for bioethanol production has been studied by several authors (Verma et al. 2013b; Zheng et al. 2013; Borges et al. 2014; Tsai and Meyer 2014; Honda et al. 2015). Verma et al. (2013b), e.g., developed a thermostable enzyme ( $\beta$ -glucosidase from *Aspergillus niger*) immobilized on functionalized magnetic nanoparticles by covalent binding. This biocatalyst showed 93 % immobilization efficiency and reached more than 50 % enzyme retained when used up to 16 cycles. In another work, Zheng et al. (2013) observed the same behavior when using  $\beta$ -glucosidase immobilized on magnetic chitosan microspheres and demonstrated the potential of this biocatalyst in recycling process. Finally, the biocatalyst immobilized was applied in hydrolysis of corn straw, producing 60 g/L reducing sugars with 78 % conversion rate, and this conversion was maintained after recycling the enzyme for up to eight cycles. On the other hand, cellulase (from *Trichoderma reesei*) immobilized on porous solid silica was used in the hydrolysis of oxalic acid-pretreated biomass, which reached efficiency up to 81 % when compared to free enzyme. Similar to other studies, the biocatalyst was easily recycled and reused in multiple batches, its enzymatic activity being retained (Das et al. 2011). Abraham et al. (2014) also studied cellulase (from *Trichoderma reesei*) immobilization onto activated magnetic nanoparticles using glutaraldehyde as a cross-linker for the hydrolysis of hemp hurd biomass for the production of sugars. The immobilization efficiency was 94 % and demonstrated the thermal stability of the enzyme immobilized (increased 10 °C when compared with free enzyme). Therefore, this magnetic biocatalyst was recycled, thus lowering the biocatalyst cost, and was used for seven cycles. Enzyme saccharification using free and immobilized cellulase resulted in 89 % and 95 % hydrolysis, respectively. Recently, Cherian et al. (2015) immobilized cellulase (from *Aspergillus fumigatus*) onto MnO<sub>2</sub> nanoparticles for bioethanol production and reached 75 % binding efficiency. Furthermore, immobilized cellulase (relative activity 89 %) was more stable than the free enzyme (relative activity 55 %), which could be used over a broad range of temperature (40–80 °C) and pH (4.00–8.00) and reused for the fifth cycle. Finally, bioethanol production by SSF from sugarcane leaves using free and immobilized cellulase showed about 18 and 22 g/L of bioethanol, respectively.

Considering the aforementioned facts, it can be concluded that the immobilized enzyme increases the bioethanol production and improves the optimum pH and temperature when compared with free enzyme.

## 7.7 Conclusion

The fast depletion of fossil fuels has generated the demand for alternative, new, and eco-friendly energy sources. Due to certain limitations in using valuable feedstock for the production of first-generation biofuels, there has been a greater need to use lignocellulosic materials (viz., wood wastes, agricultural residues, etc.) in second-generation biofuels. Unfortunately, the production technologies for this generation of biofuels are facing certain challenges with respect to higher production cost. Therefore, considering these facts, concerted efforts are needed for the development of efficient technologies to solve the problems of second-generation biofuels. Encouragingly, nanotechnology has been emerging as a powerful tool, which can offer solutions for sustainable production of bioethanol. The application of nanocatalysts such as  $\text{Fe}_3\text{O}_4$ ,  $\text{TiO}_2$ ,  $\text{ZnO}$ ,  $\text{SnO}_2$ , carbon, fullerene, and graphene is an eco-friendly, reusable, and cost-effective technology. Moreover, the immobilization of enzymes on nanomaterials (nanobiocatalysts) has played a crucial role to enhance the economic viability of production process. The additional advantages of these immobilized nanobiocatalysts are their increased stability, the possibility of reuse of derivatives, and the designing of specific reactors that are easy to handle and control. In the future, the use of nanotechnology may open up new avenues for the sustainable production of bioethanol.

**Acknowledgments** The authors wish to acknowledge CNPq for their financial assistance (Process No. 401308/2014-6) and Biomed Central Limited for permitting to reproduce the figures from their publications. SCG would like to thank CNPq for providing postdoctoral research fellowship (Process No. 150745/2015-0).

## References

- Abraham RE, Verma ML, Barrow CJ, Puri M (2014) Suitability of magnetic nanoparticle immobilised cellulases in enhancing enzymatic saccharification of pretreated hemp biomass. *Biotechnol Biofuels* 7:90
- Agbor VB, Cicek N, Sparling R, Berlin A, Levin DB (2011) Biomass pretreatment: fundamentals toward application. *Biotechnol Adv* 29:675–685
- Ahmad R, Sardar M (2014) Immobilization of  $\text{TiO}_2$  nanoparticles on cellulose by physical and covalent method: a comparative study. *Indian J Biochem Biophys* 51:314–320
- Ahmad R, Sardar M (2015) Enzyme immobilization: an overview on nanoparticles as immobilization matrix. *Biochem Anal Biochem* 4(2):178
- Ahmed M, Douek M (2013) The role of magnetic nanoparticles in the localization and treatment of breast cancer. *BioMed Res*, 11 pages. doi:[10.1155/2013/281230](https://doi.org/10.1155/2013/281230)

- Alftren J, Hobley TJ (2013) Covalent immobilization of  $\beta$ -glucosidase on magnetic particles for lignocellulose hydrolysis. *Appl Biochem Biotechnol* 169:2076–2087
- Ansari SA, Husain Q (2012) Potential applications of enzymes immobilized on/in nano materials: a review. *Biotechnol Adv* 30(3):512–523
- Baldrian P, Valaskova V (2008) Degradation of cellulose by basidiomycetous fungi. *FEMS Microbiol Rev* 32(3):501–521
- Borges DG, Baraldo A, Farinas CS Jr, Giordano Rde L, Tardioli PW (2014) Enhanced saccharification of sugarcane bagasse using soluble cellulase supplemented with immobilized beta-glucosidase. *Bioresour Technol* 167:206–213
- Bornscheuer UT (2003) Immobilizing enzymes: how to create more suitable biocatalysts. *Angew Chem Int Ed Engl* 42(29):3336–3337
- Cherian E, Dharmendirakumar M, Baskar G (2015) Immobilization of cellulase onto MnO<sub>2</sub> nanoparticles for bioethanol production by enhanced hydrolysis of agricultural waste. *Chin J Catal* 36(8):1223–1229
- Cho EJ, Jung S, Kim HJ, Lee YG, Nam KC, Lee HJ, Bae HJ (2012) Co-immobilization of three cellulases on Au-doped magnetic silica nanoparticles for the degradation of cellulose. *Chem Commun* 48:886–888
- da Silva AS, Inoue H, Endo T, Yano S, Bon EPS (2010) Milling pretreatment of sugarcane bagasse and straw for enzymatic hydrolysis and ethanol fermentation. *Bioresour Technol* 101:7402–7409
- Das S, Berke-Schlessel D, Ji HF, McDonough J, Wei Y (2011) Enzymatic hydrolysis of biomass with recyclable use of cellobiase enzyme immobilized in sol-gel routed mesoporous silica. *J Mol Catal B: Enzym* 70(1–2):49–54
- Datta S, Christena LR, Rajaram YRS (2013) Enzyme immobilization: an overview on techniques and support materials. *Biotech* 3(1):1–9
- de Maria PD, Grande PM, Leitner W (2015) Current trends in pretreatment and fractionation of lignocellulose as reflected in industrial patent activities. *Chem Ing Tech* 87(12):1686–1695
- Eggert H, Greaker M (2014) Promoting second generation biofuels: does the first generation pave the road? *Energies* 7:4430–4445
- Engelmann W, Aldrovandi A, Guilherme A, Filho B (2013) Prospects for the regulation of nanotechnology applied to food and biofuels. *Vigilancia Sanitaria em Debate* 1(4):110–121
- Farrell AE, Plevin RJ, Turner BT, Jones AD, O'Hare Kammen MD (2006) Ethanol can contribute to energy and environmental goals. *Science* 311(5760):506–508
- Feijoo G, Moreira MT, Alvarez P, Lu-Chau TA, Lema JM (2008) Evaluation of the enzyme manganese peroxidase in an industrial sequence for the lignin oxidation and bleaching of eucalyptus kraft pulp. *J Appl Polym Sci* 109(2):1319–1327
- Goh WJ, Makam VS, Hu J, Kang L, Zheng M, Yoong SL, Udalgama CN, Pastorin G (2012) Iron oxide filled magnetic carbon nanotube-enzyme conjugates for recycling of amyloglucosidase: toward useful applications in biofuel production process. *Langmuir* 28(49):16864–16873
- Hammel KE, Kapich AN, Jensen KA Jr, Ryan ZC (2002) Reactive oxygen species as agents of wood decay by fungi. *Enzyme Microb Technol* 30(4):445–453
- Han KK, Richard C, Delacourte A (1984) Chemical cross-links of proteins by using bifunctional reagents. *Int J Biochem* 16(2):129–145
- Hatakka A (1994) Lignin-modifying enzymes from selected white-rot fungi: production and role from in lignin degradation. *FEMS Microbiol Rev* 13:125–135
- Honda T, Tanaka T, Yoshino T (2015) Stoichiometrically controlled immobilization of multiple enzymes on magnetic nanoparticles by the magnetosome display system for efficient cellulose hydrolysis. *Biomacromolecules* 16(12):3863–3868
- Hu S, Guan Y, Wang Y, Han H (2011) Nano-magnetic catalyst KF/CaO-Fe<sub>3</sub>O<sub>4</sub> for biodiesel production. *Appl Energy* 88:2685–2690
- Huang XJ, Chen PC, Huang F, Ou Y, Chen MR, Xu ZK (2011) Immobilization of *Candida rugosa* lipase on electrospun cellulose nanofiber membrane. *J Mol Catal B: Enzym* 70:95–100



- Imai M, Ikari K, Suzuki I (2004) High-performance hydrolysis of cellulose using mixed cellulase species and ultrasonication pretreatment. *Biochem Eng J* 17(2):79–83
- Itoh H, Wada M, Honda Y, Kuwahara M (2003) Bioorganosolve pretreatments for simultaneous saccharification and fermentation of beech wood by ethanolysis and white-rot fungi. *J Biotechnol* 103:273–280
- Ivanova V, Petrova P, Hristov J (2011) Application in the ethanol fermentation of immobilized yeast cells in matrix of alginate/magnetic nanoparticles, on chitosan-magnetite microparticles and cellulose-coated magnetic nanoparticles. *Int Rev Chem Eng* 3(2):289–299
- Kumar M, Sharma MP (2014) Potential assessment of microalgal oils for biodiesel production: a review. *J Mater Environ Sci* 5(3):757–766
- Kumar P, Barrett DM, Delwiche MJ, Stroeve P (2009) Methods for pretreatment of lignocellulosic biomass for efficient hydrolysis and biofuel production. *Ind Eng Chem Res* 48:3713–3729
- Lee S, Jin LH, Kim JH, Han SO, Na HB, Hyeon T, Koo YM, Kim J, Lee JH (2010) *b*-Glucosidase coating on polymer nanofibers for improved cellulosic ethanol production. *Bioprocess Biosyst Eng* 33:141–147. doi:10.1007/s00449-009-0386-x
- Lee AF, Bennett JA, Manayil JC, Wilson K (2014) Heterogeneous catalysis for sustainable biodiesel production via esterification and transesterification. *Chem Soc Rev* 43:7887–7916
- Limayema A, Ricke SC (2012) Lignocellulosic biomass for bioethanol production: current perspectives, potential issues and future prospects. *Prog Energy Combust Sci* 38:449–467
- Lupoi JS, Smith EA (2011) Evaluation of nanoparticle-immobilized cellulase for improved yield in simultaneous saccharification and fermentation reactions. *Biotechnol Bioeng* 108:2835–2843
- Macario A, Verri F, Diaz U, Cormab A, Giordano G (2013) Pure silica nanoparticles for liposome/lipase system encapsulation: application in biodiesel production. *Catal Today* 204:148–155
- Mahmood T, Hussain S (2010) Nanobiotechnology for the production of biofuels from spent tea. *Afr J Biotechnol* 9:858–868
- Mandal D, Bolander ME, Mukhopadhyay D, Sarkar G, Mukherjee P (2005) The use of microorganism for the formation of metal nanoparticles and their application. *Appl Microbiol Biotechnol* 69:485–492
- Mateo C, Abian O, Fernandez-Lafuente R, Guisan JM (2000) Increase in conformational stability of enzymes immobilized on epoxy-activated supports by favoring additional multipoint covalent attachment. *Enzyme Microb Technol* 26(7):509–515
- Mei XY, Liu RH, Shen F, Wu HJ (2009) Optimization of fermentation conditions for the production of ethanol from stalk juice of sweet sorghum by immobilized yeast using response surface methodology. *Energy Fuels* 23:487
- Misson M, Zhang H, Jin B (2015) Nanobiocatalyst advancements and bioprocessing applications. *J R Soc Interface* 12(102):20140891
- Naik SN, Goud VV, Rout PK, Dalai AK (2010) Production of first and second generation biofuels: a comprehensive review. *Renew Sustain Energy Rev* 14(2):578–597
- Nguyen LM (2000) Organic matter composition, microbial biomass and microbial activity in gravel-bed constructed wetlands treating farm dairy wastewaters. *Ecol Eng* 16:199–221
- Palmowski L, Muller J (1999) Influence of the size reduction of organic waste on their anaerobic digestion. In: II International Symposium on anaerobic digestion of solid waste, Barcelona, 15–17 June, pp 137–144
- Pan X, Fan Z, Chen W, Ding Y, Luo L, Bao X (2007) Enhanced ethanol production inside carbon-nanotube reactors containing catalytic particles. *Nat Mater* 6:507–511
- Patumsawad S (2011). 2nd Generation biofuels: technical challenge and R and D opportunity in Thailand. *J Sustain Energy Environ Special Issue*:47–50
- Pavlidis IV, Vorhaben T, Gournis D, Papadopoulos GK, Bornscheuer UT, Stamatis H (2012a) Regulation of catalytic behaviour of hydrolases through interactions with functionalised carbon-based nanomaterials. *J Nanopart Res* 14:842

- Pavlidis IV, Vorhaben T, Tsoufis T, Rudolphe P, Bornscheuer UT, Gournisd D, Stamatis H (2012b) Development of effective nanobiocatalytic systems through the immobilization of hydrolases on functionalized carbon-based nanomaterials. *Bioresour Technol* 115:164–171
- Pinto PA, Dias AA, Fraga I, Marques G, Rodrigues MAM, Colaco J, Sampaio A, Bezerra RMF (2012) Influence of ligninolytic enzymes on straw saccharification during fungal pretreatment. *Bioresour Technol* 111:261–267
- Pundir CS (2015) Immobilization of enzyme nanoparticles. In: Pundir CS (ed) *Enzyme nanoparticles*. William Andrew Publishing, Boston, CA, pp 23–32
- Puri M, Barrow CJ, Verma ML (2013) Enzyme immobilization on nanomaterials for biofuel production. *Trends Biotechnol* 31(4):215–216
- Qiu F, Li Y, Yang D, Li X, Sun P (2011) Heterogeneous solid base nanocatalyst: preparation, characterization and application in biodiesel production. *Bioresour Technol* 102:4150–4156
- Rai MK, dos Santos JS, Soler MF, Marcelino PRF, Brumano LP, Ingle AP, Gaikwad SC, Gade AK, da Silva SS (2016) Strategic role of nanotechnology for production of bioethanol and biodiesel. *Nanotechnol Rev* 5(2):231–250
- Ren YH, Rivera JG, He L, Kulkarni H, Lee DK, Messersmith PB (2011) Facile, high efficiency immobilization of lipase enzyme on magnetic iron oxide nanoparticles via a biomimetic coating. *BMC Biotechnol* 11:63
- Sakai S, Antoku K, Yamaguchi T, Kawakami K (2008) Transesterification by lipase entrapped in electrospun poly(vinyl alcohol) fibers and its application to a flow-through reactor. *J Biosci Bioeng* 105:687–689
- Saritha M, Arora A, Lata (2012) Biological pretreatment of lignocellulosic substrates for enhanced delignification and enzymatic digestibility. *Indian J Microbiol* 52(2):122–130
- Shallom D, Shoham Y (2003) Microbial hemicellulases. *Curr Opin Microbiol* 6(3):219–228
- Sivers MV, Zacchi G (1995) A techno-economical comparison of three processes for the production of ethanol from pine. *Bioresour Technol* 51:43–52
- Sun Y, Cheng J (2002) Hydrolysis of lignocellulosic materials for ethanol production: a review. *Bioresour Technol* 83:1–11
- Swatloski RP, Spear SK, Holbrey JD, Rogers RD (2002) Ionic liquids: new solvents for non-derivitized cellulose dissolution. *Abstr Pap Am Chem Soc* 224:U622
- Taherzadeh MJ, Karimi K (2007) Acid hydrolysis processes for ethanol from lignocellulosic materials. *Bioresour* 2:472–499
- Takacs E, Wojnarovits L, Foldavary C, Hargagittai P, Borsa J, Sajo I (2000) Effect of combined gamma irradiation and alkali treatments on cotton cellulose. *Radiat Phys Chem* 57:339–402
- Teymouri F, Laureano-Perez L, Alizadeh H, Dale BE (2005) Optimization of the ammonia fibre explosion (AFEX) treatment parameters for enzymatic hydrolysis of corn stover. *Bioresour Technol* 96:2014–2018
- Tischer W, Wedekind F (1999) Immobilized enzymes: methods and applications. In: Fessner W-D, Archelas A, Demirjian DC, Furstoss R, Griengl H, Jaeger KE, Moris-Varas E, Öhrlein R, Reetz MT, Reymond JL, Schmidt M, Servi S, Shah PC, Tischer W, Wedekind F (eds) *Biocatalysis – from discovery to application*, vol 200. Springer, Berlin, pp 95–126
- Tran DT, Chen CL, Chang JS (2012) Immobilization of *Burkholderia* sp. lipase on a ferric silica nanocomposite for biodiesel production. *J Biotechnol* 158:112–119
- Tsai CT, Meyer AS (2014) Enzymatic cellulose hydrolysis: enzyme reusability and visualization of beta-glucosidase immobilized in calcium alginate. *Molecules* 19(12):19390–19406
- Verma ML, Barrow CJ, Puri M (2013a) Nanobiotechnology as a novel paradigm for enzyme immobilization and stabilization with potential applications in biodiesel production. *Appl Microbiol Biotechnol* 97:23–39
- Verma ML, Chaudhary R, Tsuzuki T, Barrow CJ, Puri M (2013b) Immobilization of  $\beta$ -glucosidase on a magnetic nanoparticle improves thermostability: application in cellobiose hydrolysis. *Bioresour Technol* 135:2–6
- Wan C, Li Y (2012) Fungal pretreatment of lignocellulosic biomass. *Biotechnol Adv* 30(6):1447–1457

- Wen L, Wang Y, Lu D, Hu S, Han H (2010) Preparation of KF/CaO nanocatalyst and its application in biodiesel production from Chinese tallow seed oil. *Fuel* 89:2267–2271
- Zheng J, Rehmann L (2014) Extrusion pretreatment of lignocellulosic biomass: a review. *Int J Mol Sci* 15:18967–18984
- Zheng P, Wang J, Lu C, Xu Y, Sun Z (2013) Immobilized  $\beta$ -glucosidase on magnetic chitosan microspheres for hydrolysis of straw cellulose. *Process Biochem* 48(4):683–687
- Zhu ZG, Sathitsuksanoh N, Vinzant T, Shell DJ, McMillan JD, Zhang Y-HP (2009) Comparative study of corn stover pretreated by dilute acid and cellulose solvent-based lignocellulose fractionation: enzymatic hydrolysis, supramolecular structure, and substrate accessibility. *Biotechnol Bioeng* 103:715–724
- Zhua JY, Wang GS, Pan XJ, Gleisner R (2009) Specific surface to evaluate the efficiencies of milling and pretreatment of wood for enzymatic saccharification. *Chem Eng Sci* 64:474–485

# Chapter 8

## Physicochemical Characterizations of Nanoparticles Used for Bioenergy and Biofuel Production

Rafaella O. do Nascimento, Luciana M. Rebelo, and Edward Sacher

**Abstract** Understanding the physicochemical properties of nanomaterials and how functionalizations modify their surface, altering their properties, is fundamental to defining better strategies of use. In fact, it is known that the surface characteristics of nanomaterials present batch-to-batch differences. Therefore, a good understanding of nanoparticle surface requires the use of several physicochemical and morphological techniques to adequately determine their shape, size and charge, as well as the presence of coatings and their functional groups. Furthermore, those parameters are crucial to determine acceptable differences of the surface chemistry that do not alter their properties and applications. Thus, in this chapter, we will discuss several physicochemical techniques that focus on nanoparticles for bioenergy and biofuel production.

**Keywords** Nanoparticles • Physicochemical characterization • Biofuels • Bioenergy • Surface • Size • Shape • Coatings

### 8.1 Introduction

Nanoparticles (NPs) and nanomaterials (NMs) have unique properties, which often differ from bulk materials. In fact, NPs have been successfully used in several areas, such as drug delivery (Masood 2015; Xie et al. 2015; Agiotis et al. 2016), sensors (Choi et al. 2015; Segura et al. 2015; Webster et al. 2015; Zhang et al. 2016;

---

R.O. do Nascimento (✉)

Chemistry Department, Université de Montréal (UdeM), 2900 Boulevard Edouard, Montpetit, Pavillon Jean - Armand Bombardier (PJAB), Montreal, QC, Canada H3T 1K4  
e-mail: [raffa.nascimento1@gmail.com](mailto:raffa.nascimento1@gmail.com)

L.M. Rebelo

Faculdade Católica Rainha do Sertão (FCRS), Putiú, Quixadá, Ceará 63900-000, Brazil

E. Sacher

Département de Génie Physique, École Polytechnique de Montréal, Montreal, QC, Canada H3C 3A7

Gong et al. 2016), environmental remediation (Feng et al. 2015; Ravi and Vadukumpully 2015; Bounab et al. 2016), antimicrobial products (Samiei et al. 2016; Nayak et al. 2016), biomedical devices (Arsiwala et al. 2014; Covarrubias et al. 2015; Kuthati et al. 2015), coatings, biofuels, bioenergy (Saravanakumar et al. 2016), etc. Concerning biofuels and bioenergy, NPs and other NMs can be obtained either directly from biological sources or synthesized by chemical or physical methods.

Biological techniques seem to be eco-friendlier, compared with physicochemical methods. However, the NPs and NMs obtained from biological sources can present more complex surfaces, due to intrinsic protein coatings or variations in their coronas. Therefore, the simultaneous application of several surface characterization techniques is fundamental to understand the physicochemical properties of NPs and NMs, in order to assure their efficiency and to ensure consistent yields of biofuel and the bioenergy production process. In this regard, it is necessary to understand the inconsistencies observed in the batch-to-batch production of NPs. For example, França et al. (2013) described the variations of silane-coated magnetite NPs, in terms of functional groups, using NPs prepared by the same protocols and chemicals made by the same experienced chemist. The variations were evaluated through scanning electron microscopy (SEM), transmission electron microscopy (TEM), X-ray photoelectron spectroscopy (XPS), Fourier transform infrared spectroscopy (FTIR), etc. They also noted that the inconsistencies observed can lead to variations in the cytotoxicity of the NPs. Such variations can also affect the efficiency of bioenergy or biofuel production. Thus, in this chapter, we will describe several physicochemical characterization techniques which are useful to understand possible inconsistencies in NP and NM syntheses, as well as some selected criteria for these techniques. Finally, we will give examples of the most common variations described in the biofuel and bioenergy production literature.

This chapter is divided as follows: “Technique Selection Criteria for the Physicochemical Characterizations of NPs and NMs” (Sect. 8.2), “Physicochemical Techniques Commonly Used to Characterize NPs and NMs” (Sect. 8.3), “General Remarks” (Sect. 8.4) and “References”.

## 8.2 Technique Selection Criteria for the Physicochemical Characterizations of NPs and NMs

NPs and NMs can be used as catalysts for the production of biofuels and bioenergy. Due to their huge surface areas, a small amount of NPs can be used for the low-cost direct production of biofuels, bioenergy or syngas. Therefore, it is necessary to have a complete study of their physicochemical properties, in order to assure the reproducibility of the protocols for biofuel and bioenergy production, as well as to optimize their translation from the research laboratory to industry. Thus, in this

chapter, we present some techniques that are commonly used to characterize NPs and NMs.

The selection of techniques to use to evaluate NPs and NMs is directly conditioned to the parameters that will be evaluated, such as size distribution, shape, surface charge, crystallinity, coating homogeneity, functionalization, magnetic properties, etc.

In order to evaluate the size distribution and shape of NPs and NMs, various microscopies are powerful tools, among them are direct measurements, such as transmission electron microscopy (TEM), scanning electron microscopy (SEM), atomic force microscopy (AFM) and scanning tunnelling microscopy (STM). Another technique, which can be used to measure size indirectly, is dynamic light scattering (DLS). The surface charge of NPs and NMs can be evaluated by zeta potential, which also provides information on stability in the dispersion medium used.

Crystallinity can be studied by X-ray diffraction (XRD). In fact, the synthesis of several NPs and NMs can be followed by this technique, showing changes as the material crystallizes.

Functionalization can be evaluated by several techniques, including Fourier transform infrared spectroscopy (FTIR), Raman spectroscopy, nuclear magnetic resonance (NMR) and X-ray photoelectron spectroscopy (XPS), which provide information about chemical bonding; each probes a different depth.

Regarding metal NPs or NMs, plasmon bands can be observed by ultraviolet-visible (UV-Vis) spectroscopy.

### 8.3 Physicochemical Techniques Commonly Used to Characterize NPs and NMs

As mentioned earlier, many techniques can be used to evaluate the NPs and NMs. Thus, some techniques will be described below.

Electromagnetic spectroscopies are the techniques which describe the interaction between electromagnetic waves and atoms, molecules, NPs, NMs, etc. Those interactions can be observed by emission or absorption of electromagnetic radiation. Such interactions are mediated by adsorption or emission of photons which are particle-like resulting from mutually perpendicular propagating electric and magnetic waves. These interactions are also strongly dependent on the nature of the sample, as well as the environment to which the sample is submitted.

Furthermore, several processes occur after the sample (material) absorbs energy. According to Kalantar-zadeh and Fry (2008), these processes can be explained by changes in the *vibrational and rotational relaxations*, *electronic energy*, *intersystem crossings* as well as *internal conversions*, as presented in Fig. 8.1.

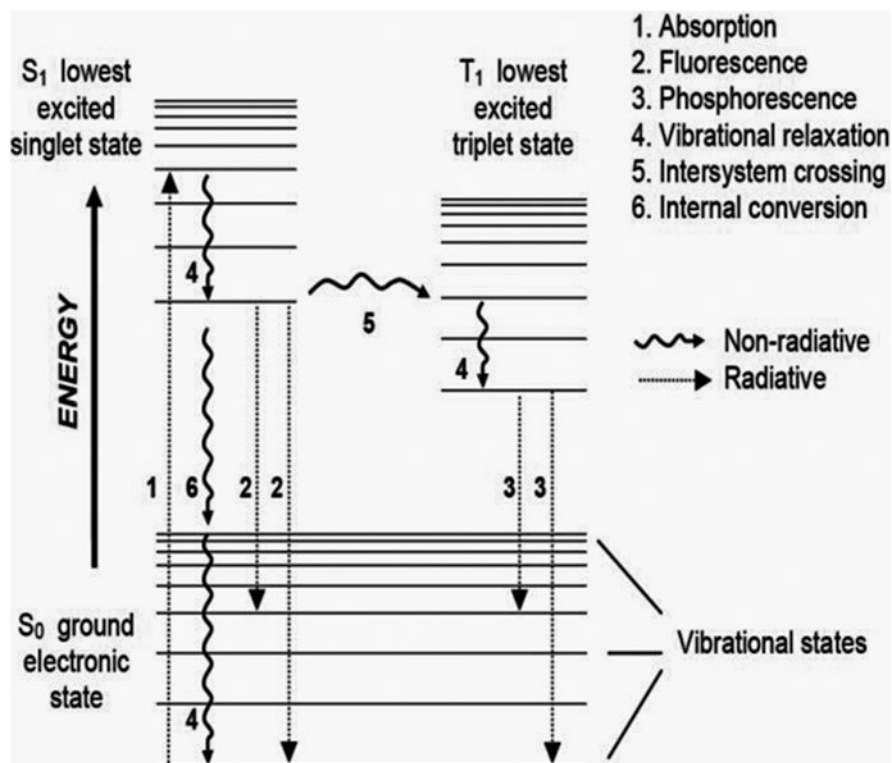


Fig. 8.1 Scheme of possible process following the absorption of photon. Reproduced with permission of Springer (Kalantar-zadeh and Fry 2008)

Electronic transitions occur when the molecule absorbs visible or ultraviolet electromagnetic radiations through electron transitions. These electrons are localized at specific bonds or delocalized over structures such as aromatic rings.

Vibrational spectroscopies are included in electromagnetic spectroscopies and can provide valuable information about coatings on NPs and NMs.

### 8.3.1 Infrared Spectroscopy

Infrared (IR) radiation refers to the part of the electromagnetic spectrum between  $14,290$  and  $200\text{ cm}^{-1}$ , which corresponds to the near-IR ( $14,290\text{--}4000\text{ cm}^{-1}$ ), the IR ( $4000\text{--}400\text{ cm}^{-1}$ ) and far-IR ( $700\text{--}200\text{ cm}^{-1}$ ) regions. IR spectroscopy is related to the light absorbed by the molecules in those regions (Rodrigues and Galzerani 2012). Groups of atoms absorb the light in the IR region, producing absorption bands over a given range of frequencies, regardless of the molecules to which they belong (Silverstein et al. 2005). This is commonly called the infrared signature. The

vibration frequencies are related to many factors, the most important being bond strength and atomic mass. The atomic bonds can exhibit several kinds of motion, such as stretching (symmetrical and asymmetrical), wagging, bending, scissoring, twisting, rocking, etc. (Table 8.1).

The broad application of IR spectroscopy is related to its being a non-destructive technique and well known in many fields. Furthermore, basically all organic compounds absorb IR radiation, which permits a rapid characterization of coatings on NPs and NMs, inasmuch as many of them are made of polymers or at least contain a reasonable quantity of functional groups with strong signal in the IR region.

Sample preparation for IR spectroscopy varies according to the type of material or IR technique that will be used. Thus, for powder samples, it is possible to add a small amount of the sample to dried potassium bromide (KBr). The mixture should be ground to a fine powder and then compressed to form a thin and *quasi*-transparent disc. In order to investigate thin films with IR spectroscopy, other tools can be applied, such as attenuated total reflectance (ATR), reflection-absorption infrared spectroscopy (RAIRS), etc. Regarding NP and NM dispersions, a few drops of the dispersion can be added to an ATR crystal and dried, to obtain a thin film.

Regarding biogenic NPs and NMs, IR spectroscopy can be used to evaluate the molecules that act as stabilizers of these NPs. Commonly, biogenic NPs are stabilized by polysaccharides, aliphatic amines and phenolic acids, among other groups, that also contribute to the reduction of cations (e.g.  $\text{Ag}^+$ ), which will generate the core of those NPs (Kuppusamy et al. 2015).

### 8.3.2 Plasmon Band Identification Using UV-Vis Spectroscopy

The UV-Vis spectroscopy is also classified as electromagnetic spectroscopy and is used to characterize organic molecules and NPs. Briefly, a sample is irradiated with ultraviolet and visible ranges of electromagnetic waves and the light absorbed is detected. The absorbance ( $A$ ) is directly proportional to the concentration ( $c$ ) of the sample in mol/l. The relation between the concentration and absorbance is expressed by the *Beer-Lambert law*:

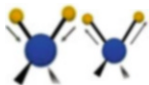
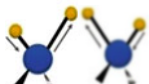
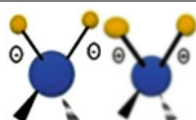
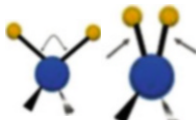
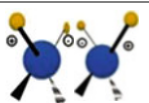

$$A = \epsilon bc \quad (8.1)$$

Where  $\epsilon$  is the *molar absorptivity* or *molar extinction coefficient* (l/mol cm) and  $b$  (cm) is the path length. The *molar absorptivity* is an inherent characteristic of the substances and indicates the amount of light absorbed at a particular wavelength.

UV-Vis spectroscopy can be used to investigate the presence of plasmon band generated due to the collective oscillations of free electrons at optical frequencies (Pines and Bohm 1952). Concerning this, Saravanakumar et al. (2016) used UV-Vis



**Table 8.1** Scheme of atomic bond motions

Type of vibration	Schematic representation
Symmetrical stretching	
Asymmetrical stretching	
Wagging	
Scissoring	
Twisting	
Rocking	

spectroscopy to evaluate the generation of biogenic metallic NPs (AuNPs and AgNPs) by the signal from their plasmon bands, in order to select the *Trichoderma* strain that produces more NPs in a shorter time under controlled incubation conditions.

Kim et al. (2014) used UV-Vis spectroscopy to measure the optical densities of their samples, in order to determine the dry cell weight of *Clostridium ljungdahlii* necessary to be added into syngas fermentation media for bioethanol production. In the same study, silica NPs were added to the fermentation media to increase the liquid-gas transfer and enhance the bioethanol production.

### 8.3.3 X-Ray-Based Characterizations

#### 8.3.3.1 X-Ray Diffraction

XRD involves the study of X-rays after their interaction with a sample. It is a technique which provides information about the crystalline phases present in powders and other solid materials. Crystalline structure and grain size, as well as NP size, can be determined by XRD. The crystalline structure can be determined by comparing the data obtained with those available in international databases

(e.g. *International Centre of Diffraction Data, ICDD*). XRD is widely used to study inorganic materials and is useful to solve the crystalline structure of inorganic and metallic NPs and NMs.

Samples that can be well characterized by XRD should have a space lattice with an ordered three-dimensional distribution of atoms, which form parallel distributed planes separated by a distance that varies according to the nature of the material. Because the crystalline planes are separated by a distance  $d$  from the material, when an X-ray beam is irradiated with a wavelength  $\lambda$  at an angle  $\theta$ , it will diffract when the distance travelled by the rays reflected by the successive planes differs by an integer number  $n$  of wavelengths to produce a constructive interference, as described by Bragg (Eq. 8.2).

$$n\lambda = 2d \sin \theta \quad (8.2)$$

The limitations of XRD include the study of materials with many phases with low or poor symmetry. Furthermore, this technique cannot be used to study amorphous materials or those with very low crystallinities.

Singh and Verma (2015) used XRD to characterize nickel NPs (NiNPs) dispersed at carbon micro-nanofibre (ACFs/CNFs) electrodes that were used in a microbial fuel cell (MFC) for bioenergy production, using *Escherichia coli* as a microbial catalyst. The XRD measurements were carried out to determine the structure of the crystalline phase of the carbon micro-nanofibres, as well as that of the NiNPs themselves. The results showed that NiNPs deposited on ACF presented peaks that correspond to at least five to the crystallographic index of crystalline Ni.

Briefly, MFCs are classified as electrochemical devices that convert microbial metabolic power into electricity (Mansoorian et al. 2013). Potentially, MFCs can be used to produce electricity from wastewater treatment plants (Liu et al. 2008), as well as to recover metals and nutrients from industrial effluents (C. Choi and Cui 2012).

### 8.3.3.2 X-Ray Photoelectron Spectroscopy

XPS is a sensitive, quantitative technique that measures the elemental composition in the parts per thousand range. XPS data are obtained by irradiating a material with X-rays and measuring the kinetic energy and number of electrons that emerge from the top 0 to 10 nm of the material surface:

$$E_{\text{binding}} = E_{\text{photon}} - (E_{\text{kinetic}} + \varnothing) \quad (8.3)$$

where  $E_{\text{binding}}$  is the binding energy of the electron,  $E_{\text{photon}}$  is the energy of the X-ray photons being used,  $E_{\text{kinetic}}$  is the kinetic energy of the electron measured by the instrument and is the work function, whose value depends on both the spectrometer and the chemical composition of the sample.

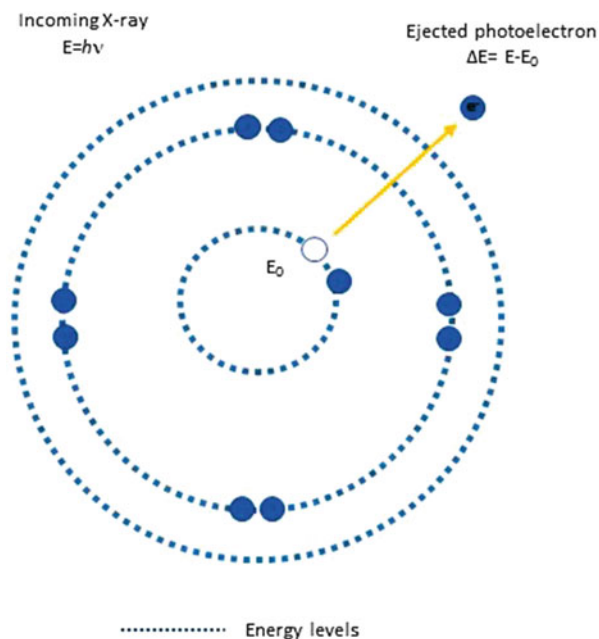
In XPS, the X-rays cause the ejection of photoelectrons from a surface; in other words, XPS is based on the photoelectric effect (Bagus et al. 2013). Each element produces characteristic XPS spectra having binding energies (Eq. 8.3) that identify the material at the surface (Fig. 8.2).

XPS is a technique that can be used to determine the surface chemistries of materials, as well as to understand chemical surface changes; thus, XPS can help to elucidate the mechanisms of coating bare NPs or shell formation. XPS can offer information about the surface chemistry of NPs and is a powerful tool to understand NP oxidation, degradation (or ageing) and interaction with other materials.

As mentioned earlier, França et al. (2013) used XPS to describe batch-to-batch inconsistencies in the synthesis of NPs and how they affect the application of NPs.

According to Baer et al. (2010), many parameters should be considered during the analysis of NPs by XPS. Note that while most XPS analyses are conducted by assuming that the sample covers a homogeneous and flat layer on the specimen holder, the shape and structure of NPs can play an important role in the accurate interpretation of the results. Additionally, other factors should be considered during the XPS analysis, in order to properly understand the results; these include (a) a low surface density of NPs to avoid NP overlapping, providing more realistic information on peak ratios and binding energies (Piyakis et al. 2003; Tougaard 2005), (b) an increased signal/noise (S/N) ratio by using spectral co-additions (i.e. adding several scans) and (c) size and curvature effects, as the electron path lengths and the surface curvature of the NPs can directly affect the signal strength of a coating or functional groups and can vary with particle size.

**Fig. 8.2** Scheme of electronic orbits showing the ejection of photoelectrons after absorption of a photon



Tang et al. (2015) used XPS to characterize capacitive layers of 3D electrodes. Such layers are composed of titanium dioxide ( $\text{TiO}_2$ ) and egg white protein (EWP)-derived carbon, assembled into core-shell NPs; these were then integrated into loofah sponge carbon (LSC). XPS revealed that Ti, O, C and N are the main elements of the electrode (LSC- $\text{TiO}_2$ @C). Regarding N 1s, for example, high-resolution XPS spectra showed the presence of N-containing components such as pyridinic N, pyrrolic or pyridonic N, quaternary N and oxidized N, which were compatible with those described at the literature (Zhou et al. 2011).

### ***8.3.4 Time of Flight of Secondary Ion Mass Spectrometry***

Time of flight of secondary ion mass spectrometry (TOF-SIMS) is a surface-sensitive analytical method that investigates the time of flight of charged fragments from the outermost layers of samples. The fragments are accelerated into a “flight tube” until reaching the detector. The masses of those fragments are determined by measuring their times of flight from the sample surface to the detector. During the SIMS measurements, ions of beams of  $\text{C}_{60}^+$ ,  $\text{O}_2^+$ ,  $\text{Ar}^+$ ,  $\text{Au}^+$ , etc., strike the sample surface and cause the ejection of these secondary ionic fragments (Baer et al. 2010).

TOF-SIMS, as other ion spectroscopies, is useful to obtain information about the chemical structures of coatings, as well as contaminations on their surfaces; however, the influence of the ion beams and the non-linear signal dependence should also be considered during the quantitative analysis. This technique has been successfully used to identify peptide conjugates on the surface of AuNPs. Note that TOF-SIMS is a powerful technique to sputter NPs and NMs in general; however, the results for thin films or bulk materials may be more complex to interpret.

TOF-SIMS has been combined with TEM to determine the composition and plasmon resonance of NPs. Furthermore, TOF-SIMS results are commonly correlated with XPS results in order to offer a concerted information about functional groups or coatings on the NP surface.

### ***8.3.5 Elucidation of the Size and Surface Charge of Nanoparticles***

The study of the charge of NPs can help to understand their aggregation in different media and also eventual changes in particle size. Light scattering techniques evaluate the scattered light from the NPs. The light scattering can be divided into elastic, where the wavelength of the scattered light is the same as the incident light, and inelastic, where the wavelength of the scattered light is different from the incident light. Rayleigh scattering is an example of elastic scattering which occurs when the particles are much smaller than the wavelength of the impinging light.

Such techniques can also provide information about particle size, structure as well as the chemical composition of NPs. Thus, light scattering techniques can also be used to monitor functionalization, coating and other changes in NPs. Raman spectroscopy and dynamic light scattering (DLS) are examples of light scattering characterization techniques extensively used for nanotechnology.

Colloidal systems are commonly studied by DLS because it is a rapid and uncomplicated technique, in which the light beam is directly focused onto a sample that scatters the light elastically. DLS is well suited to examine the monodispersity of NPs and, also, eventual changes in their sizes as the result of coatings, functionalization or degradation, which might affect the hydrodynamic radius.

Briefly, DLS use a monochromatic light source that passes through a solution containing particles, and light scatter occurs. The size of the particles, as well as the wavelength of the incident light, plays an important role in DLS, inasmuch as the intensity of scattered light is uniform in all directions as is the amount of Rayleigh scattering.

In solutions, particles undergo Brownian motion, which is the movement of the particles in small random patterns. Larger particles move more slowly than smaller ones, at a constant temperature.

The spherical radius ( $r$ ) of a particle can be calculated by the Stokes-Einstein relation:

$$r = \kappa T / 6\pi\eta D \quad (8.4)$$

where  $\kappa$  is Boltzmann's constant,  $T$  is the absolute temperature and  $\eta$  is the viscosity of a known dispersion of NPs.

DLS also has some limitations. It is limited to analysing NPs with Rayleigh scattering. Furthermore, DLS requires the dispersion to be highly diluted and well dispersed, inasmuch as DLS cannot differentiate particle aggregates from particles.

### ***8.3.6 Investigation of Nanoparticle Morphology by Atomic Force Microscopy***

Nanoparticles have electronic, optical, magnetic, mechanical and chemical reactivity properties that are highly correlated with their size. NPs constitute one of the most widely studied materials in various research fields, such as biological applications (Salata 2004), catalysis (Johnson 2003), devices (Willner and Willner 2002) and others. The proper characterization of NPs still presents a major challenge and is of utmost importance in all research fields.

The atomic force microscopy has shown to be a very promising technique in their investigation (Vesenka et al. 1993; Ebenstein et al. 2002; Klapetek et al. 2011), due to its high-resolution, three-dimensional images, without the need for an elaborate analysis preparation. Other microscopic techniques, such as

TEM, can provide high-resolution images of nanostructured systems, but many of them can cause damage to the sample, due to their high-energy electron beams (EB), apart from the difficulty due to the low atomic number of many such samples.

AFM topographic images provide quantitative and qualitative information about nanoparticle features, such as 3D visualization, size, morphology, surface roughness, particle counting, size distribution, surface area distribution and volume, and can be carried out in different environments (liquid, air, gas and others).

In addition, AFM permits the acquisition of phase images and electric and magnetic contrast images, providing information beyond topographic images and offering a correlation of these data with topography, permitting qualitative and quantitative analyses of the NPs. AFM has been extensively used for the topographic analysis of nanoparticles (Ramesh et al. 1998), such as NP interaction forces with AFM tips (Ong and Sokolov 2007), NP manipulation (Junno et al. 1995), observation of NP encapsulation (Fiel et al. 2011), NP agglomeration behaviour (Viguié et al. 2007) and others.

The technique basically consists of a sensor probe (tip + cantilever) that scans the surface of the sample with the aid of a piezoelectric scanner that precisely positions the probe relative to the sample, essential when working with nanoscale systems. The AFM tip is situated at the free end of the probe cantilever, where a laser beam is positioned, following the cantilever deflection due to topography and the interaction forces between the tip and the sample surface.

The AFM technique can be carried out in three modes of operation: non-contact (only for long-range interactions), contact and tapping. In the contact mode, the tip scans the surface of the sample continuously touching the surface. In the study of nanoparticles, this mode of operation is often inadequate, since the particles that are not well attached to the substrate can be dragged away, because of the continuous contact maintained with the tip and the lateral forces applied by the tip onto the sample. In intermittent contact or tapping mode, the tip scans the sample surface with small regular beats with a frequency close to the cantilever resonance frequency, thereby reducing the lateral forces (since it reduces the duration of tip-sample contact) and enabling the imaging of highly sensitive materials. Moreover, with this scanning mode, we can access the phase difference image (Magonov et al. 1997) of the material studied.

The phase image obtained with AFM measurements is of utmost importance to determine many characteristics of NPs. Tapping on the heterogeneous surface of the sample will result in a phase lag between the input signal and that acquired after the interaction with the sample.

In nanoparticle agglomeration studies, for example, by analysing only the height image, one might conclude that there has been a single particle; however, observing the corresponding phase image of the particle topography image, it is actually observed having a cluster of nanoparticles with diameters even lower than previously observed, thus being able to set up the pH and other characteristics of the solution that contains the nanoparticles, with the aim to disperse these particles (Fig. 8.3). This is possible because in the phase image, one can observe components

with different physical properties such as viscosity, adhesion, elasticity and others (Tamayo and Garcia 1997).

Another important feature concerning NPs that can be obtained with AFM measurements is the effectiveness of the encapsulation process. For example, NPs can be produced to obtain a core-shell structure with the goal of making precise drug and cosmetic delivery to the human body. The techniques used for verification of the encapsulation cannot provide accurate results; with AFM measurements, one can verify this package in two ways:

1. With the aid of AFM phase images, by observing the differences in the phases that compose the image due to the differences in physical properties of the materials comprising the core and the shell of the NP
2. Producing an indentation using the AFM tip as indenter, with a very controlled force, to determine the difference in Young's modulus between particles with and without core, using the AFM force curves

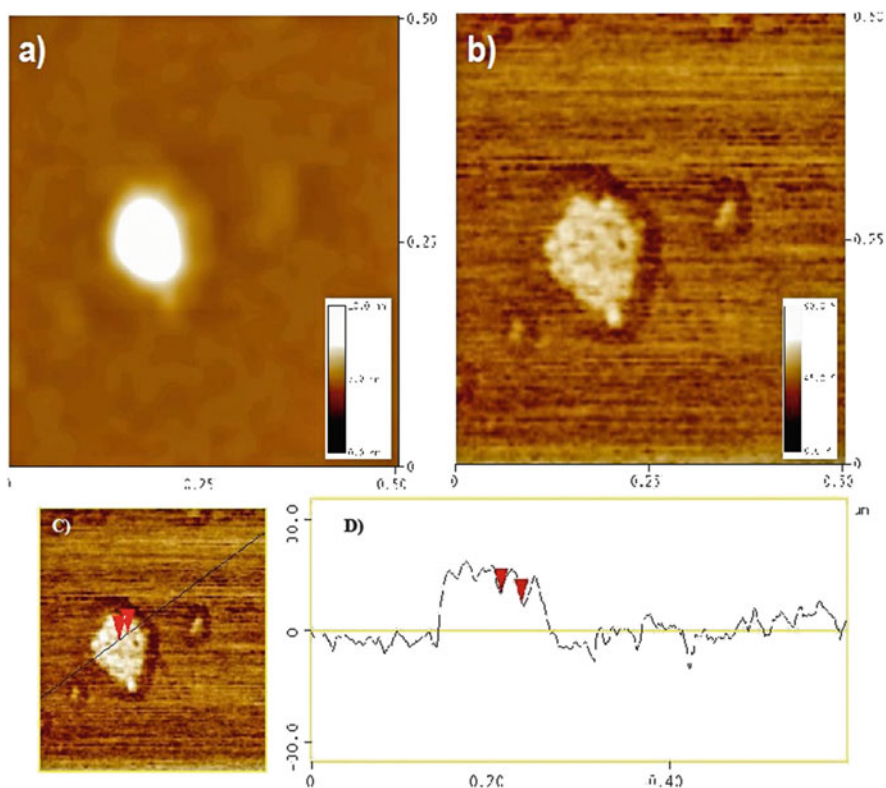


**Fig. 8.3** Nanoparticle agglomeration study: AFM topography image (a) and corresponding phase image (b) of carbon nanoparticles. The image reveals a cluster of nanoparticle with diameters of approximately 15 nm (d) (red arrows). (c) selection of carbon nanoparticles presented

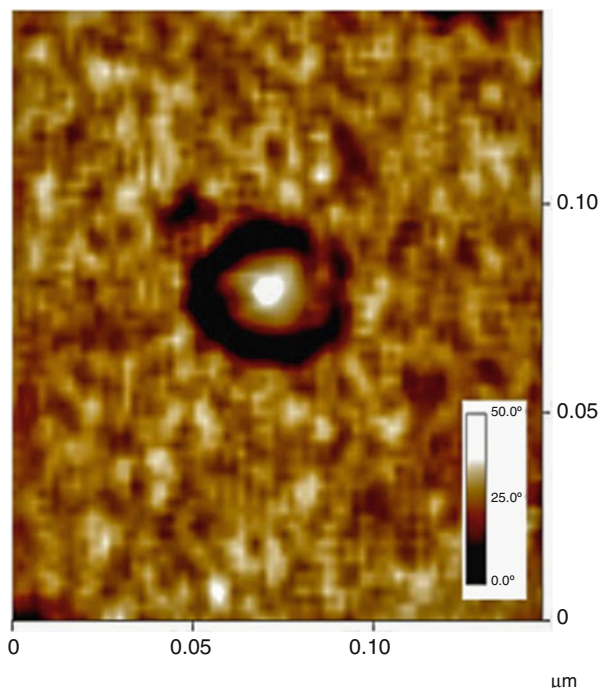
Magnetic or electric properties of NPs can also be evaluated by AFM [magnetic force microscope (MFM) and electrostatic force microscope (EFM)]. Using a probe coated with magnetic (conducting) material, one can image magnetic (electrostatic) domains of magnetic (charged) samples. This technique can provide the magnetic force gradient response of nanoparticles, simultaneously obtaining a topographic image, as well as a phase image, of these particles (Zhang et al. 2009). These images are performed in non-contact mode with the goal of sensing these long-range forces (Fig. 8.4).

The interaction of NPs and many compounds can also be evaluated using AFM force measurements. Using force versus displacement AFM curves, it is possible to measure quantitatively the interaction force between the functionalized AFM tip and the sample surface (Ong and Sokolov 2007). In the case of NP force interactions, the AFM tip can be mounted with NPs or functionalized with other chemical groups that react with the sample, so the force curve is acquired from this interaction. Ong and Sokolov (2007) used this kind of measurements to obtain the force between ceria nanoparticles and silica in aqueous media at different pH values.

### 8.3.7 Transmission Electron Microscopy

The first electron microscope was developed in 1929, based on the PhD thesis of Ernst Ruska, who studied magnetic lenses. In the microscope developed by Ernst

**Fig. 8.4** EFM image: electrostatic force microscopy (EFM) image of a metallic nanoparticle. Observe the difference in charges between the non-conductive shell and the metallic core





Ruska and Max Knoll, the sample surface was placed normal to the viewing direction and illuminated by an electron beam at a grazing incident angle. In 1938, scientists from the University of Toronto, Albert Prebus and James Hillier, developed the first practical transmission electron microscope. In order to get more information about TEM, the readers should consult *Transmission Electron Microscopy, Part 1: Basics* (Williams and Carter 2008), as well as *Fifty Years of Electron Diffraction* (Goodman 1981).

Electron microscopies (EM) utilize highly energetic beams of electrons that interact with the sample. The information obtained from this interaction is directly related to the chemical composition, morphology, topography and crystallographic structure.

The EM is suitable for characterization of both organic and inorganic materials. However, as EM employs a high-energy electron beam, a prolonged exposure may damage or destroy the materials. The incident electron beam causes secondary electrons to be emitted from the surface of the sample. Such secondary electrons can be monitored to produce a topological image.

TEM is a unique technique, which can be used to focus on a single NP in a sample, to indirectly identify its chemical and electronic structure. Furthermore, TEM provides atomic resolution lattice images at a spatial resolution of 1 nm.

Briefly, TEM operates with an electron beam passing through the sample, where only certain parts of it are transmitted, making an amplitude contrast image. The image passes through a magnifying lens and is then projected onto a charge-coupled device (CCD) or a phosphor screen, which allows for a quantitative data processing.

A simplified TEM setup is made with an electron gun which is a pin-shaped cathode that is commonly made from lanthanum hexaboride ( $\text{LaB}_6$ ), a long vacuum column, condenser objective and projective lenses, CCD surface or phosphor screen.

The electron beam from the heated cathode is accelerated by a high voltage and travels down a long column. Condenser lenses focus the beam into a small, coherent cylinder, while the condenser aperture removes electrons scattered at large angles. Thus, the beam strikes the specimen on the grid (sample holder), and the majority is transmitted, focused by the objective lens. Then it passes through the intermediate and projector lenses. The enlarged resulting beam strikes a CCD or phosphor screen, forming the image.

TEM has been extensively used by Sadykov et al. (2015) to characterize nickel alloy nanoparticles used to replace traditional Ni catalysts in the production of syngas from natural gas and biogas. The application of Ni alloy NPs can mitigate problems related with Ni catalyst deactivation by coke deposition during production of syngas. Further, a high syngas yield, similar to the best values reported by the literature at short contact times, was obtained.

Tang et al. (2015) used TEM to study  $\text{TiO}_2@\text{C}$ , used in a 3D electrode (LSC- $\text{TiO}_2@\text{C}$ ). TEM showed that  $\text{TiO}_2@\text{C}$  NPs have a core-shell structure. Moreover, selected area electron diffraction (SAED), a crystallographic experimental technique associated with TEM, revealed the highly crystalline nature of

TiO<sub>2</sub>NPs that, according to the authors, correlated with obtaining MFCs that produced energy more efficiently.

### 8.3.8 Scanning Electron Microscopy

SEM is one of the most commonly used techniques to characterize the morphologies of NPs used to produce biofuels and bioenergy. SEM can be used to obtain images of material with nanoscale resolution by scanning an electron probe beam across a surface and monitoring the secondary electrons emitted. Further, the SEM can provide a compositional analysis by studying X-rays produced by electron-specimen interaction. Detailed maps of elemental analysis can thus be obtained.

Briefly, SEM images are obtained by an electron beam (EB), which is emitted from a heated filament made from tungsten or lanthanum hexaboride (LaB<sub>6</sub>). The filament is heated by applying a voltage. The emitted electrons are accelerated towards the sample by applying an electric potential. The EB is focused by a condenser lens, which projects the image of the source onto a condenser aperture. It is then focused by an objective lens and raster-scanned the sample by scanning coils. Thus, a magnetic field is generated which deflects the beam back and forth in a controlled pattern. Subsequently, when the primary electrons strike the sample, they give their energy to electrons of the sample, resulting in the emission of secondary electrons. These secondary electrons are collected by a detector, converted to a voltage and amplified to build the image.

SEM provides topographical and morphological analyses of the samples. As an example of this, Tang et al. (2015) used SEM to characterize TiO<sub>2</sub>NPs@C-coated loofah sponge used to produce a MFC bioanode. Singh and Verma (2015) also used SEM to carry out such analyses and, in addition, used SEM-EDX to identify the NiNP distribution at an MFC electrode by the Ni mapping of the samples.

Santos et al. (2016) developed an analytical method to determine the total reducing sugars in residual water samples from sugarcane processing for ethanol. The authors modified a glassy carbon electrode with graphene oxide (GO) decorated with copper nanoparticles (CuNPs). The CuNPs-GO were investigated by SEM-EDX, XPS and Raman spectroscopy. SEM was first used to identify the deposition of CuNPs-GO at the electrode; subsequently EDAX was applied to identify regions decorated with copper.

## 8.4 Concluding Remarks

In this chapter, we present a resume of some techniques that are used to characterize NPs and NMs used in biofuel and bioenergy production. In order to give the reader, who may be unfamiliar with the techniques available, an insight into each technique, we briefly described the general instrument setup, as well as the underlying

physics behind of those techniques. Additionally, we presented some examples of application of these techniques in the literature of biofuel and bioenergy production. This is intended to help the reader of this chapter in making choices as to the best combination of techniques to use.

In choosing the techniques to be used and to obtain specific requirements concerning sample preparation procedures and data handling and manipulation techniques, the reader must then verify the choices through consultation with those competent in the techniques.

## References

- Agiotis L, Theodorakos I, Samothrakitis S, Papazoglou S, Zergioti I, Raptis YS (2016) Magnetic manipulation of superparamagnetic nanoparticles in a microfluidic system for drug delivery applications. *J Magn Magn Mater* 401(March):956–964. doi:[10.1016/j.jmmm.2015.10.111](https://doi.org/10.1016/j.jmmm.2015.10.111)
- Arsiwala A, Desai P, Patravale V (2014) Recent advances in micro/nanoscale biomedical implants. *J Control Release* 189(September):25–45. doi:[10.1016/j.jconrel.2014.06.021](https://doi.org/10.1016/j.jconrel.2014.06.021)
- Baer DR, Gaspar DJ, Nachimuthu P, Techane SD, Castner DG (2010) Application of surface chemical analysis tools for characterization of nanoparticles. *Anal Bioanal Chem* 396(3): 983–1002. doi:[10.1007/s00216-009-3360-1](https://doi.org/10.1007/s00216-009-3360-1)
- Bagus PS, Ilton ES, Nelin CJ (2013) The interpretation of XPS spectra: insights into materials properties. *Surf Sci Rep* 68(2):273–304. doi:[10.1016/j.surfrep.2013.03.001](https://doi.org/10.1016/j.surfrep.2013.03.001)
- Bounab L, Iglesias O, Pazos M, Sanromán MÁ, González-Romero E (2016) Effective monitoring of the electro-fenton degradation of phenolic derivatives by differential pulse voltammetry on multi-walled-carbon nanotubes modified screen-printed carbon electrodes. *Appl Catal Environ* 180(January):544–550. doi:[10.1016/j.apcatb.2015.07.011](https://doi.org/10.1016/j.apcatb.2015.07.011)
- Choi C, Cui Y (2012) Recovery of silver from wastewater coupled with power generation using a microbial fuel cell. *Bioresour Technol* 107(March):522–525. doi:[10.1016/j.biortech.2011.12.058](https://doi.org/10.1016/j.biortech.2011.12.058)
- Choi B, Ahn J-H, Lee J, Yoon J, Lee J, Jeon M, Kim DM, Kim DH, Park I, Choi S-J (2015) A bottom-gate silicon nanowire field-effect transistor with functionalized palladium nanoparticles for hydrogen gas sensors. *Solid-State Electron* 114(December):76–79. doi:[10.1016/j.sse.2015.07.012](https://doi.org/10.1016/j.sse.2015.07.012)
- Covarrubias C, Mattmann M, Von Martens A, Caviedes P, Arriagada C, Valenzuela F, Rodríguez JP, Corral C (2015) Osseointegration properties of titanium dental implants modified with a nanostructured coating based on ordered porous silica and bioactive glass nanoparticles. *Appl Surf Sci*. doi:[10.1016/j.apsusc.2015.12.022](https://doi.org/10.1016/j.apsusc.2015.12.022)
- Ebenstein Y, Nahum E, Banin U (2002) Tapping mode atomic force microscopy for nanoparticle sizing: tip–sample interaction effects. *Nano Lett* 2(9):945–950. doi:[10.1021/nl025673p](https://doi.org/10.1021/nl025673p)
- Feng M, Qu R, Zhang X, Sun P, Sui Y, Wang L, Wang Z (2015) Degradation of flumequine in aqueous solution by persulfate activated with common methods and polyhydroquinone-coated magnetite/multi-walled carbon nanotubes catalysts. *Water Res* 85(November):1–10. doi:[10.1016/j.watres.2015.08.011](https://doi.org/10.1016/j.watres.2015.08.011)
- Fiel LA, Rebelo LM, Santiago T de M, Adorne MD, Guterres SS, de Sousa JS, Pohlmann AR (2011) Diverse deformation properties of polymeric nanocapsules and lipid-core nanocapsules. *Soft Matter* 7(16):7240–7247. doi:[10.1039/C1SM05508A](https://doi.org/10.1039/C1SM05508A)
- França R, Zhang X-F, Veres T, Yahia L'H, Sacher E (2013) Core-shell nanoparticles as prodrugs: possible cytotoxicological and biomedical impacts of batch-to-batch inconsistencies. *J Colloid Interface Sci* 389(1):292–297. doi:[10.1016/j.jcis.2012.08.065](https://doi.org/10.1016/j.jcis.2012.08.065)

- Gong F, Gong Y, Liu H, Zhang M, Zhang Y, Li F (2016) Porous In<sub>2</sub>O<sub>3</sub> nanocuboids modified with Pd nanoparticles for chemical sensors. *Sens Actuators B* 223(February):384–391. doi:[10.1016/j.snb.2015.09.053](https://doi.org/10.1016/j.snb.2015.09.053)
- Goodman P (1981) Fifty years of electron diffraction. Springer Netherlands
- Johnson BFG (2003) Nanoparticles in catalysis. *Topics Catal* 24(1–4):147–159. doi:[10.1023/B:TOCA.000003086.83434.b6](https://doi.org/10.1023/B:TOCA.000003086.83434.b6)
- Junno T, Deppert K, Montelius L, Samuelson L (1995) Controlled manipulation of nanoparticles with an atomic force microscope. *Appl Phys Lett* 66(26):3627. doi:[10.1063/1.113809](https://doi.org/10.1063/1.113809)
- Kalantar-zadeh K, Fry B (2008) Nanotechnology-enabled sensors. Springer US, Boston, MA
- Kim Y-K, Park SE, Lee H, Yun JY (2014) Enhancement of bioethanol production in syngas fermentation with *Clostridium ljungdahlii* using nanoparticles. *Bioresour Technol* 159(May):446–450. doi:[10.1016/j.biortech.2014.03.046](https://doi.org/10.1016/j.biortech.2014.03.046)
- Klapetek P, Valtr M, Nečas D, Salyk O, Dzik P (2011) Atomic force microscopy analysis of nanoparticles in non-ideal conditions. *Nanoscale Res Lett* 6(1):514. doi:[10.1186/1556-276X-6-514](https://doi.org/10.1186/1556-276X-6-514)
- Kuppusamy P, Yusoff MM, Ichwan SJA, Parine NR, Maniam GP, Govindan N (2015) *Commelina nudiflora* L. Edible weed as a novel source for gold nanoparticles synthesis and studies on different physical–chemical and biological properties. *J Indus Eng Chem* 27(July):59–67. doi:[10.1016/j.jiec.2014.11.045](https://doi.org/10.1016/j.jiec.2014.11.045)
- Kuthati Y, Kankala RK, Lee C-H (2015) Layered double hydroxide nanoparticles for biomedical applications: current status and recent prospects. *Appl Clay Sci* 112–113(August):100–116. doi:[10.1016/j.clay.2015.04.018](https://doi.org/10.1016/j.clay.2015.04.018)
- Liu Y, Harnisch F, Fricke K, Sietmann R, Schröder U (2008) Improvement of the anodic bioelectrocatalytic activity of mixed culture biofilms by a simple consecutive electrochemical selection procedure. *Biosens Bioelectron* 24(4):1012–1017. doi:[10.1016/j.bios.2008.08.001](https://doi.org/10.1016/j.bios.2008.08.001)
- Magonov SN, Elings V, Whangbo M-H (1997) Phase imaging and stiffness in tapping-mode atomic force microscopy. *Surf Sci* 375(2–3):L385–L391. doi:[10.1016/S0039-6028\(96\)01591-9](https://doi.org/10.1016/S0039-6028(96)01591-9)
- Mansoorian HJ, Mahvi AH, Jafari AJ, Amin MM, Rajabizadeh A, Khanjani N (2013) Bioelectricity generation using two chamber microbial fuel cell treating wastewater from food processing. *Enzyme Microb Technol* 52(6–7):352–357. doi:[10.1016/j.enzmictec.2013.03.004](https://doi.org/10.1016/j.enzmictec.2013.03.004)
- Masood F (2015) Polymeric nanoparticles for targeted drug delivery system for cancer therapy. *Mater Sci Eng C*, November. doi:[10.1016/j.msec.2015.11.067](https://doi.org/10.1016/j.msec.2015.11.067)
- Nayak D, Ashe S, Rauta PR, Kumari M, Nayak B (2016) Bark extract mediated green synthesis of silver nanoparticles: evaluation of antimicrobial activity and antiproliferative response against osteosarcoma. *Mater Sci Eng C Mater Biologic Application* 58(January):44–52. doi:[10.1016/j.msec.2015.08.022](https://doi.org/10.1016/j.msec.2015.08.022)
- Ong QK, Sokolov I (2007) Attachment of nanoparticles to the AFM tips for direct measurements of interaction between a single nanoparticle and surfaces. *J Colloid Interface Sci* 310(2):385–390. doi:[10.1016/j.jcis.2007.02.010](https://doi.org/10.1016/j.jcis.2007.02.010)
- Pines D, Bohm D (1952) A collective description of electron interactions: II. Collective vs individual particle aspects of the interactions. *Phys Rev* 85(2):338–353. doi:[10.1103/PhysRev.85.338](https://doi.org/10.1103/PhysRev.85.338)
- Piyakis KN, Yang D-Q, Sacher E (2003) The applicability of angle-resolved XPS to the characterization of clusters on surfaces. *Surf Sci* 536(1–3):139–144. doi:[10.1016/S0039-6028\(03\)00571-5](https://doi.org/10.1016/S0039-6028(03)00571-5)
- Ramesh S, Cohen Y, Aurbach D, Gedanken A (1998) Atomic force microscopy investigation of the surface topography and adhesion of nickel nanoparticles to submicrospherical silica. *Chem Phys Lett* 287(3–4):461–467. doi:[10.1016/S0009-2614\(97\)01446-2](https://doi.org/10.1016/S0009-2614(97)01446-2)
- Ravi S, Vadukumpully, S (2015) Sustainable carbon nanomaterials: recent advances and its applications in energy and environmental remediation. *J Environ Chem Eng*, December. doi:[10.1016/j.jece.2015.11.026](https://doi.org/10.1016/j.jece.2015.11.026)

- Rodrigues ADG, Galzerani JC (2012) Infrared, Raman and photoluminescence spectroscopies: potentialities and complementarities. *Revista Brasileira de Ensino de Física* 34:4309
- Sadykov V, Mezentseva N, Simonov M, Smal E, Arapova M, Pavlova S, Fedorova Y et al (2015) Structured nanocomposite catalysts of biofuels transformation into syngas and hydrogen: design and performance. *Int J Hydrogen Energy* 40(24):7511–7522. doi:[10.1016/j.ijhydene.2014.11.151](https://doi.org/10.1016/j.ijhydene.2014.11.151)
- Salata OV (2004) Applications of nanoparticles in biology and medicine. *J Nanobiotechnol* 2 (April):3. doi:[10.1186/1477-3155-2-3](https://doi.org/10.1186/1477-3155-2-3)
- Samiei M, Farjami A, Dizaj SM, Lotfipour F (2016) Nanoparticles for antimicrobial purposes in endodontics: a systematic review of in vitro studies. *Mater Sci Eng C Mater Biologic Application* 58(January):1269–1278. doi:[10.1016/j.msec.2015.08.070](https://doi.org/10.1016/j.msec.2015.08.070)
- Santos FCU, Paim LL, da Silva JL, Stradiotto NR (2016) Electrochemical determination of total reducing sugars from bioethanol production using glassy carbon electrode modified with graphene oxide containing copper nanoparticles. *Fuel* 163(January):112–121. doi:[10.1016/j.fuel.2015.09.046](https://doi.org/10.1016/j.fuel.2015.09.046)
- Saravanakumar K, MubarakAli D, Kathiresan K, Thajuddin N, Alharbi NS, Chen J (2016) Biogenic metallic nanoparticles as catalyst for bioelectricity production: a novel approach in microbial fuel cells. *Mater Sci Eng B* 203(January):27–34. doi:[10.1016/j.mseb.2015.10.006](https://doi.org/10.1016/j.mseb.2015.10.006)
- Segura R, Pizarro J, Díaz K, Placencio A, Godoy F, Pino E, Recio F (2015) Development of electrochemical sensors for the determination of selenium using gold nanoparticles modified electrodes. *Sens Actuators B* 220(December):263–269. doi:[10.1016/j.snb.2015.05.016](https://doi.org/10.1016/j.snb.2015.05.016)
- Silverstein RM, Webster FX, Kiemle DJ (2005) Spectrometric identification of organic compounds, 7th edn. Wiley, Hoboken, NJ
- Singh S, Verma N (2015) Fabrication of Ni nanoparticles-dispersed carbon micro-nanofibers as the electrodes of a microbial fuel cell for bio-energy production. *Int J Hydrogen Energy* 40(2): 1145–1153. doi:[10.1016/j.ijhydene.2014.11.073](https://doi.org/10.1016/j.ijhydene.2014.11.073)
- Tamayo J, Garcia R (1997) Effects of elastic and inelastic interactions on phase contrast images in tapping-mode scanning force microscopy. *Appl Phys Lett* 71(16):2394. doi:[10.1063/1.120039](https://doi.org/10.1063/1.120039)
- Tang J, Yuan Y, Liu T, Zhou S (2015) High-capacity carbon-coated titanium dioxide core-shell nanoparticles modified three dimensional anodes for improved energy output in microbial fuel cells. *J Power Sources* 274(January):170–176. doi:[10.1016/j.jpowsour.2014.10.035](https://doi.org/10.1016/j.jpowsour.2014.10.035)
- Tougaard S (2005) XPS for quantitative analysis of surface nano-structures. *Microsc Microanal* 11 (S02). doi:[10.1017/S1431927605500229](https://doi.org/10.1017/S1431927605500229)
- Vesenska J, Manne S, Giberson R, Marsh T, Henderson E (1993) Colloidal gold particles as an incompressible atomic force microscope imaging standard for assessing the compressibility of biomolecules. *Biophys J* 65(3):992–997, <http://www.ncbi.nlm.nih.gov/pmc/articles/PMC1225815/>
- Viguié J-R, Sukmanowski J, Nölting B, Royer F-X (2007) Study of agglomeration of alumina nanoparticles by atomic force microscopy (AFM) and photon correlation spectroscopy (PCS). *Colloids Surf A Physicochem Eng Asp* 302(1–3):269–275. doi:[10.1016/j.colsurfa.2007.02.038](https://doi.org/10.1016/j.colsurfa.2007.02.038)
- Webster MS, Cooper JS, Chow E, Hubble LJ, Sosa-Pintos A, Wieczorek L, Raguse B (2015) Detection of bacterial metabolites for the discrimination of bacteria utilizing gold nanoparticle chemiresistor sensors. *Sens Actuators B* 220(December):895–902. doi:[10.1016/j.snb.2015.06.024](https://doi.org/10.1016/j.snb.2015.06.024)
- Williams DB, Carter CB (2008) Transmission electron microscopy. Part 1: Basics, 2nd edn
- Willner I, Willner, B (2002) Functional nanoparticle architectures for sensoric, optoelectronic, and bioelectronic applications. *Pure Appl Chem* 74(9). doi:[10.1351/pac200274091773](https://doi.org/10.1351/pac200274091773)
- Xie X, Li F, Zhang H, Lu Y, Lian S, Lin H, Gao Y, Lee J (2015) EpCAM aptamer-functionalized mesoporous silica nanoparticles for efficient colon cancer cell-targeted drug delivery. *Eur J Pharm Sci*. doi:[10.1016/j.ejps.2015.12.014](https://doi.org/10.1016/j.ejps.2015.12.014)
- Zhang C, Zhang Y, Miao Z, Ma M, Xin D, Lin J, Han B, Takahashi S, Anzai J-i, Chen Q (2016) Dual-function amperometric sensors based on poly(diallyldimethylammonium chloride)-

functionalized reduced graphene oxide/manganese dioxide/gold nanoparticles nanocomposite.

*Sens Actuators B* 222(January):663–673. doi:[10.1016/j.snb.2015.08.114](https://doi.org/10.1016/j.snb.2015.08.114)

Zhang Yu, Yang M, Ozkan M, Ozkan CS (2009) Magnetic force microscopy of iron oxide nanoparticles and their cellular uptake. *Biotechnol Prog* 25(4):923–928. doi:[10.1002/btpr.215](https://doi.org/10.1002/btpr.215)

Zhou W, Lin L, Wang W, Zhang L, Wu Q, Li J, Guo L (2011) Hierarchical mesoporous hematite with ‘electron-transport channels’ and its improved performances in photocatalysis and lithium ion batteries. *J Phys Chem C* 115(14):7126–7133. doi:[10.1021/jp2011606](https://doi.org/10.1021/jp2011606)

**Part III**  
**Nano-characterization and Role**  
**of Catalysts**

# Chapter 9

## From Biomass to Fuels: Nano-catalytic Processes

Mohammad Barati

**Abstract** Fossil fuel consumption has generated many environmental problems such as air pollution as a result of environment carbon balance disarrangement through releasing petroleum carbon content. New energy resources can reduce consumption of petroleum and environment damages. Sun, wind, sea waves, and biomass are renewable energy resources that can produce power. Biomass can also supply chemical energy because of its carbon-rich structure. The structure makes biomass an ideal alternative energy resource for petroleum. It can be converted to fuels, fuel additives, and chemicals. Conversion of biomass to gaseous and liquid fuels such as hydrogen, biodiesel, alcohols, ethers, and aromatics is an interesting field for research and larger scales of production. The processes often are performed in the presence of heterogeneous catalysts. Metals such as Ru, Ni, Pt, Pd, and Cu are used for catalyzing biomass to fuel (BTF) processes. It has been demonstrated that decreasing metal particle sizes to nano-scale can increase the processes productivity and selectivity. Very high production yields of biofuels up to 100% can be available in the presence of nano-catalysts.

In this chapter, BTF processes have been introduced, and performances for non-catalytic, catalytic, and nano-catalytic ones have been compared. Nano-catalytic preparation methods that were applied for BTF processes have been explained, and the use of nanotechnology for more productive and selective BTF processes has been concluded.

**Keywords** Biomass • Biofuel • Nano-catalyst • Chemical processes

### 9.1 Introduction

Biofuels as a type of renewable energy resources can be introduced to be interesting, especially in the case of their application for fuels as well as fuel additives. Direct burning was the first method for using biomass as fuel that has a history as old as fires (Faaij and Domac 2006). Methane production from animal and plant

---

M. Barati (✉)

Department of Applied Chemistry, Faculty of Chemistry, University of Kashan, Kashan, Iran  
e-mail: [barati.m@kashanu.ac.ir](mailto:barati.m@kashanu.ac.ir)



wastes via microbial processes was the way of biomass usage that passed a conversion step. Nowadays, reducing in petroleum resources, air pollution and global warming because of greenhouse gasses emission forces world society to find alternative energy resources. Biomass is a golden key for resolving the problem. Converting biomass to biofuels with chemical and biochemical treatments is a promising renewable and clean energy production method. Since energy content of biofuels is supplied from their carbon-rich organic structure and the structure has been made via a natural harmony of earth (atmosphere and ground) and sun, their combustion has net greenhouse gasses emission of zero. Therefore, using this type of fuel offers economic and environmental benefits (Huber and Iborra 2006; Kircher 2015; Withers et al. 2015).

Various non-catalytic and catalytic biomass conversion processes have been performed to produce fuels and chemicals. Catalytic processes have shown higher production yields and selectivities of fuels such as hydrogen, fatty acid methyl esters (FAME), and higher alcohols and ethers compared with non-catalytic processes. Reducing catalyst active metals particle sizes to nanoscale have promoted catalytic processes performances in fuel production (Amidon et al. 2008; Xie and Ma 2010; Liu et al. 2012).

The aim of the chapter is to discuss about reasons for preferring nanoscale materials to microscale ones as heterogeneous catalysts for biomass to fuel (BTF) conversion processes. It has been concluded that nanotechnology improves productivity and selectivity of BTF processes effectively so far as it seems necessary to perform them in the presence of nano-catalysts.

## 9.2 Processes for Biomass Conversion

Chemical and biochemical treatments have been carried out to obtain chemicals with high energy values. Transesterification can be the main method for biofuel production because of its wide researching area as well as potential applications for larger scales. The process converts triglycerides extracted from biomass to various value added chemicals such as some fatty acid esters that can be used as biodiesel. Figure 9.1 shows total reaction for transesterification of triglycerides in biofuels production (Boz et al. 2009; Patil et al. 2012).

Catalytic and non-catalytic transesterification processes have been evaluated. Biomass to fuels conversion via these processes is performed in at least three steps. Triglycerides extraction is the first one. Triglycerides are extracted from biomass via a physical process. In this step, oil and cellulose are separated, and oil is used as precursor of transesterification reaction. Vegetable oil is esterified to glycerol and fatty acid esters, subsequently. The last step contains various reactions for producing value added materials (Shuttleworth et al. 2014). Lignocellulosic biomass is another type of biomass with potential applications for biofuel production. It can be converted to solid, liquid, and gaseous fuels. Pyrolysis is defined as the conversion of biomass in the absence of water and oxygen to gaseous and liquid

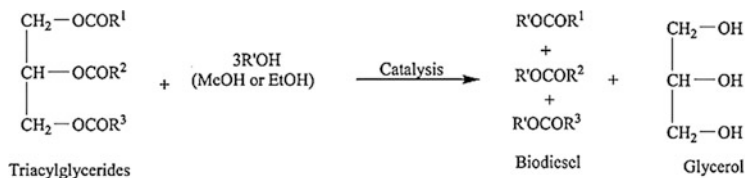


**Fig. 9.1** Biodiesel production via transesterification triglycerides (Boz et al. 2009; Patil et al. 2012)

products at higher temperatures. Biodiesel and hydrogen-rich syngas are value added products that are achieved from biomass pyrolysis. Hydrothermal treatments such as steam reforming as well as sub-, near-, and supercritical water gasification and liquefaction have been performed to convert biomass to chemicals, fuels, and fuel additives. The processes produce CO, CO<sub>2</sub>, CH<sub>4</sub>, and H<sub>2</sub> as gaseous products, bioethanol and biobutanol as liquid, and biochar as solid ones. All mentioned processes often are catalyzed using heterogeneous metal or metal oxide catalysts. However, both lignocelluloses and triglycerides have been used to produce biofuels via processes that are catalyzed with enzymes. Enzymes make the processes more selective and safer due to reacting in milder temperatures and pressures (Evans and Milne 1987; Rapagna 2000; Bridgwater et al. 2002; Tomishige et al. 2004).

### 9.2.1 Non-catalytic and Catalytic Processes

The biofuel production processes have been performed catalytically and non-catalytically. Non-catalytic transesterification has been performed widely in supercritical methanol for the conversion of triglycerides to fatty acid methyl esters (FAME) and glycerol (Sakdasri et al. 2015; Manuale et al. 2015). Three effective parameters in non-catalytic transesterification of *Jatropha curcas* oil have been investigated to find conditions for the best yield of products. Methanol to oil ratio has been changed with 20:1, 30:1, 50:1, and 60:1 moles, reaction temperature with 330, 360, 390, and 420 °C, and reaction time with 5, 10, 15, and 20 h. Reaction with 50:1 methanol to oil molar ratio, 330 °C, and 20 h reaction time has been simulated as the best one. The reaction yield has been compared with different catalysts. Table 9.1 shows reaction yields in the presence of different catalysts and with no catalyst. As shown in the table, catalytic reactions yields are higher than non-catalytic ones. Reaction in the presence of potassium hydroxide and sulfated tin oxide has shown maximum yields of 97.0 and 96.9, respectively (Kafuku et al. 2010).

Lignocellulosic biomasses conversion to fuels and chemicals also has been performed with and without catalysts. The aim in these processes is to produce higher alcohols and ethers as liquid and syngas and hydrogen-rich gas as gaseous products. The reaction condition for the conversion of sugarcane bagasse to

**Table 9.1** Catalytic and non-catalytic *Jatropha curcas* oil transesterification comparison (Kafuku et al. 2010)

Condition	Supercritical methanol method	Homogeneous catalyst		Heterogeneous catalyst	
		Potassium hydroxide	Sodium hydroxide	Montmorillonite KSF	Sulfated tin oxide
Methanol to oil molar ratio	50:1	8:1	8:1	15:1	15:1
Catalyst (wt%)	Not applicable	1	1	3	3
Temperature (°C)	330	50	50	180	180
Time (min)	20	60	60	120	120
Agitation rate (rpm)	Not applicable	400	400	360	360
Yield (%)	76.9	97.0	83.9	77.4	96.9

hydrogen-rich gas product has been optimized. Reaction time and feed content have been changed as two effective parameters in a supercritical water medium with 400 °C and 24 MPa. Both of the parameters have optimum amounts of 15 min and 0.05 g, respectively. Non-catalytic reaction has been compared with the reaction in the presence of Ru promoted catalyst. The catalyst with 5 wt% active metal can improve reaction performance to 15 mmol<sub>Hydrogen</sub> g<sup>-1</sup><sub>bagasse</sub> compared with non-catalytic ones with 7 mmol<sub>Hydrogen</sub> g<sup>-1</sup><sub>bagasse</sub> (Barati et al. 2014). Researches have demonstrated preference of catalytic processes for biofuel production with these two main plant biomasses. Researchers also have focused on catalyst particle size effect on reaction performance. The idea led researches to perform the processes in the presence of nano-catalysts.

## 9.3 Nano-catalytic Conversion of Biomass to Fuels

### 9.3.1 Nano-catalytic Processes

Reducing catalyst active metals particle size to nanoscales in BTF processes seems to be inevitable. According to recent researches, using nano-size active metals in catalyst formula (nano-catalysts) makes the BTF processes more productive and selective. In most cases, active metals have been loaded on nanoporous supports such as Y-Al<sub>2</sub>O<sub>3</sub>, CNT, and other metal oxides to achieve nanoscale sizes (Mehrani et al. 2014; Rashidi and Tavasoli 2015). To obtain glycerol and fatty acid esters from triglyceride, a developed mesoporous Mg-Fe bimetal oxides has been synthesized as supports for high performance transesterification catalysts of biodiesel production. The support has been impregnated with different amounts of KF in two water and methanol solvents, and catalysts prepared in methanol solvent have been found to be more effective for producing biodiesels. Also KF loading has shown an optimum point of 20 wt% in higher reaction times. Reaction in the presence of

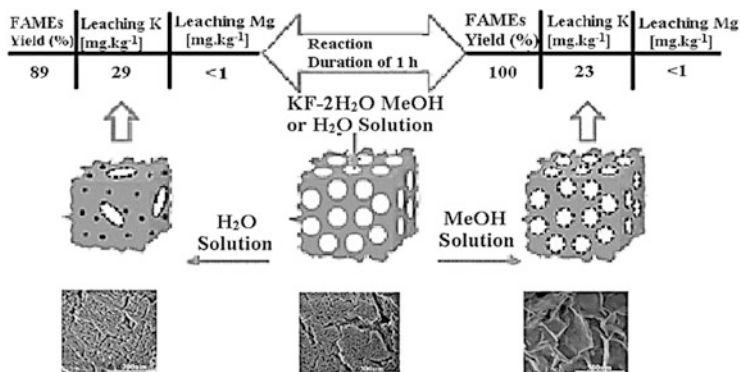


**Fig. 9.2** The schematic description for biodiesel production via transesterification in methanol and water media in the presence of K–F nano-catalysts (Tao et al. 2013)

20 wt% of KF with 60 min duration has had approximately 100 wt% yield. Figure 9.2 shows reported abstract of the process (Tao et al. 2013).

Nanocrystalline calcium oxide has been used as catalyst for transesterification of soybean oil and poultry fat for producing fatty acid methyl esters (FAME) as biodiesel. The soybean oil to methanol molar ratio has been changed, and reaction performance investigated in the presence of nanocrystalline CaO. Fatty acid conversion has increased with increase in methanol portion. The ratio has been changed from 1:3 to 1:30, and conversion increased from 75 to 99%. The research also has studied catalyst deactivation in different cycles of reaction. Results have shown a significant decreasing in reaction conversion after five cycles (Reddy et al. 2006).

Other nano-catalysts have been used for this reaction. Enzymes, especially lipase have been widely used as catalysts for this process. Enzymes make the processes more selective and safer due to milder temperatures and pressures of reaction (Xie and Ma 2010).

Produced glycerol has been converted to glyceric and lactic acids using gold and platinum nano-catalysts through an oxidation reaction. Nano-size CuO, Fe<sub>2</sub>O<sub>3</sub>, and Pd also have been used for converting glycerol to value added chemicals via hydrogenolysis and dehydration reactions. Produced FAME after a hydrogenation reaction has been converted to alkanes and ethers that are very suitable for transportation fuels. The famous catalyst for this reaction is palladium metallic. Nano-size Pd has shown better catalytic performance compared with micro-size ones (Huang et al. 2008; Liu et al. 2010; Maupin et al. 2010; Katryniok et al. 2011).

Nano-catalytic conversion of cellulosic biomasses to biofuels has been performed in the presence of different catalysts. Cellulose is a biopolymer with D-glucose monomers. Pyrolysis is a direct conversion of cellulose to liquid fuels that need high temperatures and pressures. The process proceeded in a non-oxidative atmosphere, and its products are a wide range of materials such as heavy alkanes and aromatics. Nano-size nickel and iron have been used as catalysts for pyrolysis of cellulosic biomass to biofuels (Ansari et al. 2014). Another method for direct

production of liquid fuels is liquefaction that proceeded in different media such as supercritical methanol, ethanol, and hexane. The processes have been catalyzed with copper and magnesium nano-catalysts. Metal particle sizes have been distributed in nano-range using nanoporous supports (Xu and Etcheverry 2008). In a promising research, conversion of model woody biomass to a wide range of alcohols and ethers that are desirable fuels and additives for transportation fuels has been performed. The process has been carried out in supercritical methanol solvent in the presence of Cu/Al<sub>2</sub>O<sub>3</sub>/MgO nano-catalyst. Reaction time effect also has been studied, and results have shown 96 % conversion of carbon source to liquid products in 8 h. Figure 9.3 shows a chromatogram of liquid products for this research. Actually, there are many attentions to higher alcohol synthesis from different sources, especially syngas, because they can be added to transportation fuels to increase the octane number and reduce air pollution. Finding these products from a renewable carbon source such as cellulosic biomasses that are major types of plant biomasses can be a very good idea for substitution of petroleum-based chemicals and fuels, especially that higher alcohol synthesis from syngas has no acceptable conversions (Akhtar and Amin 2011; Matson et al. 2011).

Potassium promoted copper nano-catalyst has been used in another research to convert sugarcane bagasse in subcritical water medium for higher alcohols and ethers production. Catalysts have been prepared with metal crystallite sizes between 9.1 and 17.6 nm on  $\gamma$ -Al<sub>2</sub>O<sub>3</sub>-MgO nanoporous support. Potassium has been added to catalyst formula, and its effect on higher alcohols and ethers production and selectivity has been evaluated. Figure 9.4 shows a chromatogram for liquid products of this process.

Catalyst characterization results have shown that potassium addition to copper-based catalyst can decrease average crystallite size of metals. So, better process selectivity for higher alcohols and ethers production has been related to decrease in

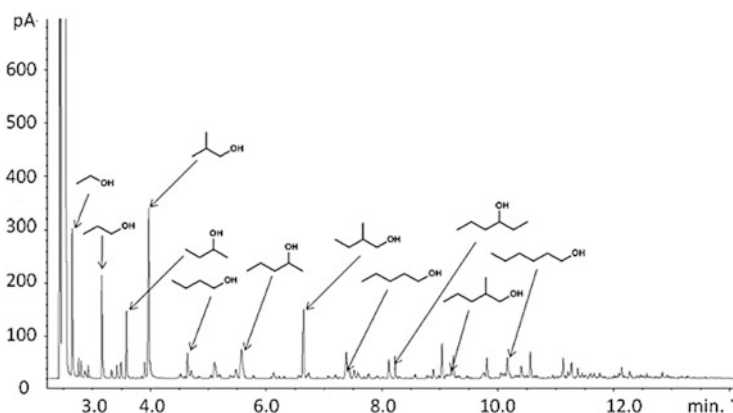


**Fig. 9.3** A chromatogram for liquid products of woody biomass conversion in supercritical methanol in the presence of Cu nano-catalyst (Akhtar and Amin 2011; Matson et al. 2011)

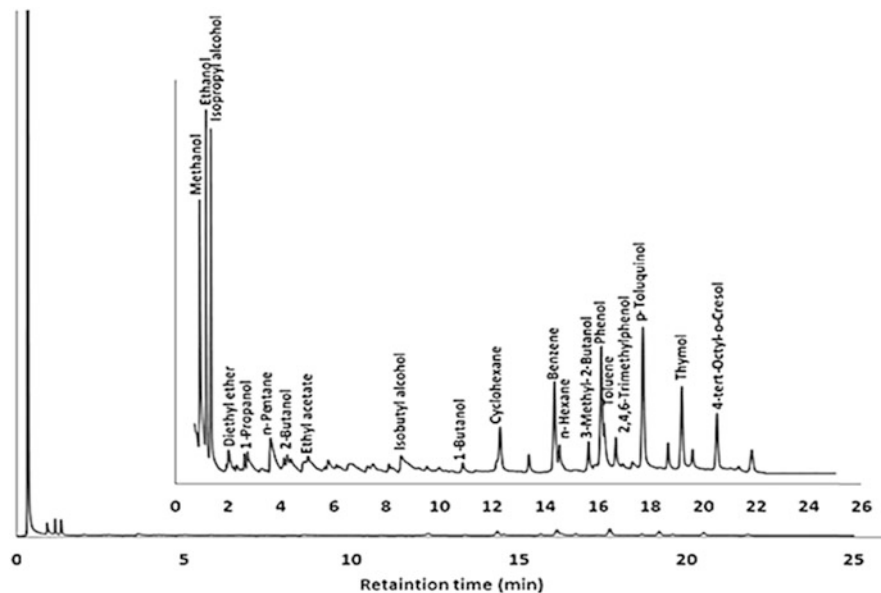


**Fig. 9.4** A chromatogram for liquid products of bagasse conversion in subcritical water in the presence of Cu nano-catalyst (Tavasoli et al. 2015)

active metals sizes to less than 10 nm. However, selectivity has decreased in very high amounts of promoter because of decrease in surface area of active metals.

Variety in liquid products (Fig. 9.4) can be related to biomass chemical structure. It contains lignin with aromatic-rich structure, cellulose, and hemicellulose that are biopolymers with oxygenated monomers. So, alcohols, ethers, hydrocarbons, and aromatics in liquid products are explainable (Tavasoli et al. 2015).

A mechanism has been suggested for cellulosic biomasses conversion to alcohols and ethers in the presence of Cu–K nano-catalyst. It passes a depolymerization step with cellulose hydrolysis to glucose monomers. Glucose losses a few oxygen in a dehydration reaction and produces another oxygenated species with higher tendency of adsorption on nano-size potassium surface (Fig. 9.5). Molecular adsorption of these oxygenates accelerates producing higher alcohols and ethers. Reducing potassium particle sizes to nanoscales increases surface area and helps the process to have a better performance and selectivity (Matson et al. 2011). Glucose also is converted to hydrocarbons via another reaction. In this reaction, glucose is reduced and losses its oxygen atoms via hydrogenation and produces aldehydes and hydrocarbons. According to suggested mechanism for this step, copper catalyzes the reaction (Fig. 9.6). Researchers have reported that increase in K percentage on Cu-based catalyst decelerates this reaction because of potassium unwillingness to adsorb hydrocarbons and saturated chains (Akhtar and Amin 2011).

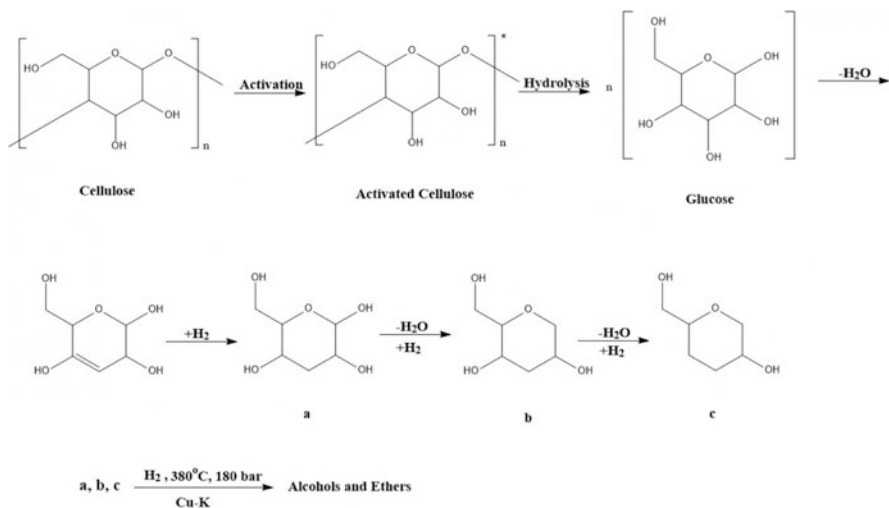


**Fig. 9.5** Suggested mechanism for cellulosic biomasses conversion to alcohols and ethers in subcritical water medium in the presence of Cu-K-based nano-catalysts (Matson et al. 2011)

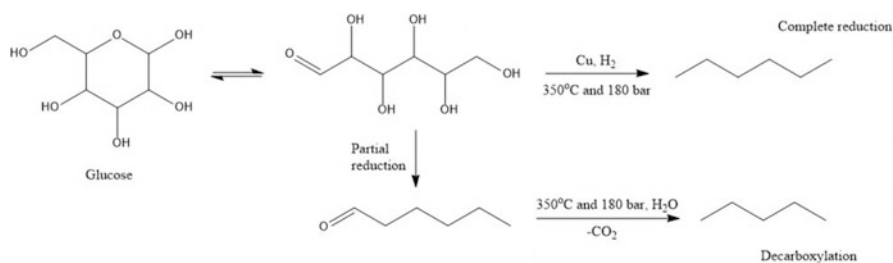


**Fig. 9.6** Suggested mechanism for cellulosic biomasses conversion to hydrocarbons in subcritical water medium in the presence of Cu-K-based nano-catalysts (Akhtar and Amin 2011)

During mentioned processes cellulose hydrolysis, glucose dehydration, and glucose reduction occur in one pot. However, the first step can be performed separately. Different methods such as basic, acidic, and enzyme hydrolysis have been used from cellulose depolymerization to glucose monomers. Nano-Fe<sub>3</sub>O<sub>4</sub> is a well-known nanostructure for enzyme immobilization. Cellulase on nano-Fe<sub>3</sub>O<sub>4</sub> showed to be an effective and selective catalyst for cellulose destruction to its monomers (Lupoi and Smith 2011).

Nano-catalytic production of hydrogen-rich gases from biomass is widely investigated. Hydrogen can be classified as transportation fuels because of its direct application as fuel cells feed. Hydrogen is produced from biomass via various thermal and hydrothermal processes. Pyrolysis, steam reforming, and sub- and supercritical water gasification are the most interesting and promising methods. The processes have been carried out in the presence of nano-size nickel-

et al. 2014), ruthenium- (Barati et al. 2014), platinum-, palladium- (Lee et al. 2015), and copper (Tavasoli et al. 2015)-based catalysts to achieve hydrogen-rich gas from biomass. The metals have been loaded on supports that are nanoporous materials. Cellulose as real and glucose as model biomasses have been gasified to CO, CO<sub>2</sub>, CH<sub>4</sub> and H<sub>2</sub>. The main reaction of hydrogen production in hydrothermal processes (steam reforming, sub and supercritical water gasification) is water–gas shift. In this reaction CO and H<sub>2</sub>O reacts to produce CO<sub>2</sub> and H<sub>2</sub>. It has been demonstrated that the reaction has tendency to accelerate in the presence of copper, nickel and ruthenium in such biomass gasification processes. Nano-catalytic supercritical water gasification of biomass has shown the best performance in hydrogen production compared with three other methods. The process can produce up to 60 mol<sub>gas</sub> g<sup>-1</sup><sub>biomass</sub> in the presence of nickel base nano-catalyst (Barati et al. 2014; Mehrani et al. 2014).

### 9.3.2 Nano-catalyst Preparation Methods for BTF Processes

Impregnation of nanoporous supports is a common method for preparation of BTF processes nano-catalysts. In this method, nanoporous supports are calcined to remove their water content and probable combustible impurities, and aqueous solution of active metals salts is prepared with considered amounts of water and metals. Two methods can be used for impregnation of supports. In dry impregnation method, aqueous solution is prepared with such concentration that its volume is equal with total pore volume of considered amount of support. Pretreated support is added to the solution to absorb it totally, dried in 100–120 °C, and calcined in 350–450 °C to form metal oxides and stabilize their nanoparticles in support pores. In wet impregnation method, aqueous solution is prepared with lower concentration (higher water content) than dry impregnation. Pretreated support is added to the solution slowly under stirring and mild heating until total vaporization of water. The wet solid is dried in 100–120 °C and calcined in 350–400 °C (Tavasoli et al. 2015).

Microemulsion is another method that commonly is used to prepare nano-catalysts for BTF processes. The method can be adjusted for increasing or decreasing particle sizes. In this method, the aqueous solutions of metals are prepared with target concentrations. Organic phase that is an immiscible solvent with water (generally n-hexane) and co-surfactant (generally n-butanol) are added to aqueous solution under stirring. Surfactant (generally Triton X-100) is added dropwise to the mixture to obtain a clear solution and make a microemulsion. The microemulsion contains micelles full of metal solution. Micelle size and subsequently metal particle size can be adjusted through protocol with changing in water to surfactant ratio. Decreasing this ratio can produce smaller particles as a result of producing smaller micelles. Also, metal particle size distribution in this method is in a narrower range compared with impregnation method because micelles are created in a narrow size range. Hydrazine is added in excess to improve nanoparticle formation in core of micelles by reducing metal oxides. Appropriate weight of



nanoporous support is added under stirring, and afterward tetrahydrofuran, (THF) as an emulsion destabilizing agent, is also added. The mixture is left to mature and settle slowly for hours and then decanted to achieve solid part. The solid is dried, calcined, and reduced before using as nano-catalyst in BTF processes (Barati et al. 2014).

### ***9.3.3 Nanotechnology Preference for BTF Processes***

BTF shows higher performances in activity and selectivity as two main parameters in the presence of nano-size heterogeneous catalysts compared with micro-size ones. Reducing particle sizes to nanoscales makes catalyst more effective in reactions because of higher available surface for reactants. Higher catalytic activity produces more products and higher catalyst selectivity accelerates specific product production versus others. In BTF process usually the base metal and its promoter are responsible for activity and selectivity, respectively. Catalysts show better activity and selectivity for fuel production when both of metals prepare in nano-scale. The difference is such higher enough to use nano-catalysts for BTF processes instead of micro-size ones. Nano-catalysts give higher and higher performances to the process even to 100% yields. So, using nano-size active metals for BTF catalyzing seems to be inevitable.

## **9.4 Conclusion**

Biomass conversion to liquid and gaseous fuels is a promising method to obtain stored energy amounts in chemical structure of biomass as clean and renewable energy resources. Triglycerides and lignocelluloses treatments have the main portion of biofuel production. Transesterification, pyrolysis, gasification, and liquefaction are processes for the conversion of biomass to fuels and value added chemicals. Fatty acid methyl esters (FAME), hydrogen gas, hydrocarbons, aromatics, and higher alcohols and ethers are main products of these processes that can be used as fuels and fuel additives. Heterogeneous catalysts show very good performances on BTF processes. Nickel, ruthenium, potassium fluoride, copper, potassium, and many other metals are used in these processes.

Studies demonstrated that reducing metal particle sizes to nanoscale has a specific positive effect on their activity and selectivity in BTF processes. The phenomenon is related to increasing catalyst surface area and active sites that are important parameters in proceeding a catalytic reaction. To prepare nano-catalysts, there are different methods that inserting active metals into nano-size pores of nanoporous supports is a common method.

## References

- Akhtar J, Amin N (2011) A review on process conditions for optimum bio-oil yield in hydrothermal liquefaction of biomass. *Renew Sustain Energy Rev* 15:1615–1624. doi:[10.1016/j.rser.2010.11.054](https://doi.org/10.1016/j.rser.2010.11.054)
- Amidon T, Wood C, Shupe A, Wang Y, Graves M, Liu S (2008) Biorefinery: conversion of woody biomass to chemicals, energy and materials. *J Biobased Mater Bioenergy* 2:100–120. doi:[10.1166/jbmb.2008.302](https://doi.org/10.1166/jbmb.2008.302)
- Barati M, Babatabar M, Tavasoli A, Dalai A, Das U (2014) Hydrogen production via supercritical water gasification of bagasse using unpromoted and zinc promoted Ru/Y-Al<sub>2</sub>O<sub>3</sub> nanocatalysts. *Fuel Process Technol* 123:140–148. doi:[10.1016/j.fuproc.2014.02.005](https://doi.org/10.1016/j.fuproc.2014.02.005)
- Boz N, Degirmenbasi N, Kalyon D (2009) Conversion of biomass to fuel: transesterification of vegetable oil to biodiesel using KF loaded nano-Y-Al<sub>2</sub>O<sub>3</sub> as catalyst. *Appl Catal Environ* 89:590–596. doi:[10.1016/j.apcatb.2009.01.026](https://doi.org/10.1016/j.apcatb.2009.01.026)
- Bridgwater A, Toft A, Brammer J (2002) A techno-economic comparison of power production by biomass fast pyrolysis with gasification and combustion. *Renew Sustain Energy Rev* 6:181–246. doi:[10.1016/s1364-0321\(01\)00010-7](https://doi.org/10.1016/s1364-0321(01)00010-7)
- Evans R, Milne T (1987) Molecular characterization of the pyrolysis of biomass. *Energy Fuel* 1:123–137. doi:[10.1021/ef00002a001](https://doi.org/10.1021/ef00002a001)
- Faaij A, Domac J (2006) Emerging international bio-energy markets and opportunities for socio-economic development. *Energy Sustain Dev* 10:7–19. doi:[10.1016/s0973-0826\(08\)60503-7](https://doi.org/10.1016/s0973-0826(08)60503-7)
- Hojjat Ansari M, Jafarian S, Tavasoli A, Karimi A, Rashidi M (2014) Hydrogen rich gas production via nano-catalytic pyrolysis of bagasse in a dual bed reactor. *J Nat Gas Sci Eng* 19:279–286. doi:[10.1016/j.jngse.2014.05.018](https://doi.org/10.1016/j.jngse.2014.05.018)
- Huang Z, Cui F, Kang H, Chen J, Zhang X, Xia C (2008) Highly dispersed silica-supported copper nanoparticles prepared by precipitation-gel method: a simple but efficient and stable catalyst for glycerol hydrogenolysis. *Chem Mater* 20:5090–5099. doi:[10.1021/cm8006233](https://doi.org/10.1021/cm8006233)
- Huber G, Iborra S, Corma A (2006) Synthesis of transportation fuels from biomass: chemistry, catalysts, and engineering. *Chem Rev* 106:4044–4098. doi:[10.1021/cr068360d](https://doi.org/10.1021/cr068360d)
- Kafuku G, Lee K, Mbarawa M (2010) The use of sulfated tin oxide as solid superacid catalyst for heterogeneous transesterification of *Jatropha curcas* oil. *Chem Papers*. doi:[10.2478/s11696-010-0063-1](https://doi.org/10.2478/s11696-010-0063-1)
- Katryniok B, Kimura H, Skrzynska E, Girardon J, Fongarland P, Capron M, Ducoulombier R, Mimura N, Paul S, Dumeignil F (2011) Selective catalytic oxidation of glycerol: perspectives for high value chemicals. *Green Chem* 13:1960. doi:[10.1039/c1gc15320j](https://doi.org/10.1039/c1gc15320j)
- Kircher M (2015) Sustainability of biofuels and renewable chemicals production from biomass. *Curr Opin Chem Biol* 29:26–31. doi:[10.1016/j.cbpa.2015.07.010](https://doi.org/10.1016/j.cbpa.2015.07.010)
- Lee I, Nowacka A, Yuan C, Park S, Yang J (2015) Hydrogen production by supercritical water gasification of valine over Ni/activated charcoal catalyst modified with Y, Pt, and Pd. *Int J Hydrogen Energy* 40:12078–12087. doi:[10.1016/j.ijhydene.2015.07.112](https://doi.org/10.1016/j.ijhydene.2015.07.112)
- Liu Y, Tuezsuez H, Jia C, Schwickardi M, Rinaldi R, Lu A, Schmidt W, Schueth F (2010) From glycerol to allyl alcohol: iron oxide catalyzed dehydration and consecutive hydrogen transfer. *ChemInform* 41. doi:[10.1002/chin.201025034](https://doi.org/10.1002/chin.201025034)
- Liu S, Lu H, Hu R, Shupe A, Lin L, Liang B (2012) A sustainable woody biomass biorefinery. *Biotechnol Adv* 30:785–810. doi:[10.1016/j.biotechadv.2012.01.013](https://doi.org/10.1016/j.biotechadv.2012.01.013)
- Lupoi J, Smith E (2011) Evaluation of nanoparticle-immobilized cellulase for improved ethanol yield in simultaneous saccharification and fermentation reactions. *Biotechnol Bioeng* 108:2835–2843. doi:[10.1002/bit.23246](https://doi.org/10.1002/bit.23246)
- Manuale D, Torres G, Vera C, Yori J (2015) Study of an energy-integrated biodiesel production process using supercritical methanol and a low-cost feedstock. *Fuel Process Technol* 140:252–261. doi:[10.1016/j.fuproc.2015.08.026](https://doi.org/10.1016/j.fuproc.2015.08.026)

- Matson T, Barta K, Iretskii A, Ford P (2011) One-pot catalytic conversion of cellulose and of woody biomass solids to liquid fuels. *J Am Chem Soc* 133:14090–14097. doi:[10.1021/ja205436c](https://doi.org/10.1021/ja205436c)
- Maupin C, Aradi B, Voth G (2010) The self-consistent charge density functional tight binding method applied to liquid water and the hydrated excess proton: benchmark simulations. *J Phys Chem B* 114:6922–6931. doi:[10.1021/jp1010555](https://doi.org/10.1021/jp1010555)
- Mehrani R, Barati M, Tavasoli A, Karimi A (2014) Hydrogen production via supercritical water gasification of bagasse using Ni-Cu/Y-Al<sub>2</sub>O<sub>3</sub> nano-catalysts. *Environ Technol* 36:1265–1272. doi:[10.1080/09593330.2014.984771](https://doi.org/10.1080/09593330.2014.984771)
- Patil P, Gude V, Mannarswamy A, Cooke P, Nirmalakhandan N, Lammers P, Deng S (2012) Comparison of direct transesterification of algal biomass under supercritical methanol and microwave irradiation conditions. *Fuel* 97:822–831. doi:[10.1016/j.fuel.2012.02.037](https://doi.org/10.1016/j.fuel.2012.02.037)
- Rapagna S (2000) Steam-gasification of biomass in a fluidised-bed of olivine particles. *Biomass Bioenergy* 19:187–197. doi:[10.1016/s0961-9534\(00\)00031-3](https://doi.org/10.1016/s0961-9534(00)00031-3)
- Rashidi M, Tavasoli A (2015) Hydrogen rich gas production via supercritical water gasification of sugarcane bagasse using unpromoted and copper promoted Ni/CNT nanocatalysts. *J Supercrit Fluids* 98:111–118. doi:[10.1016/j.supflu.2015.01.008](https://doi.org/10.1016/j.supflu.2015.01.008)
- Sakdasri W, Sawangkeaw R, Ngamprasertsith S (2015) Continuous production of biofuel from refined and used palm olein oil with supercritical methanol at a low molar ratio. *Energy Convers Manage* 103:934–942. doi:[10.1016/j.enconman.2015.07.027](https://doi.org/10.1016/j.enconman.2015.07.027)
- Shuttleworth P, De Bruyn M, Parker H, Hunt A, Budarin V, Matharu A, Clark J (2014) Applications of nanoparticles in biomass conversion to chemicals and fuels. *Green Chem* 16:573–584. doi:[10.1039/c3gc41555d](https://doi.org/10.1039/c3gc41555d)
- Tao G, Hua Z, Gao Z, Zhu Y, Zhu Y, Chen Y, Shu Z, Zhang L, Shi J (2013) KF-loaded mesoporous Mg-Fe Bi-metal oxides: high performance transesterification catalysts for biodiesel production. *ChemInform* 44. doi:[10.1002/chin.201346014](https://doi.org/10.1002/chin.201346014)
- Tavasoli A, Barati M, Karimi A (2015) Conversion of sugarcane bagasse to gaseous and liquid fuels in near-critical water media using K<sub>2</sub>O promoted Cu/Y-Al<sub>2</sub>O<sub>3</sub>-MgO nanocatalysts. *Biomass Bioenergy* 80:63–72. doi:[10.1016/j.biombioe.2015.04.031](https://doi.org/10.1016/j.biombioe.2015.04.031)
- Tomishige K, Asadullah M, Kunimori K (2004) Syngas production by biomass gasification using Rh/CeO<sub>2</sub>/SiO<sub>2</sub> catalysts and fluidized bed reactor. *Catal Today* 89:389–403. doi:[10.1016/j.cattod.2004.01.002](https://doi.org/10.1016/j.cattod.2004.01.002)
- Venkat Reddy C, Oshel R, Verkade J (2006) Room-temperature conversion of soybean oil and poultry fat to biodiesel catalyzed by nanocrystalline calcium oxides. *Energy Fuel* 20:1310–1314. doi:[10.1021/ef050435d](https://doi.org/10.1021/ef050435d)
- Withers M, Malina R, Barrett S (2015) Carbon, climate, and economic breakeven times for biofuel from woody biomass from managed forests. *Ecol Econ* 112:45–52. doi:[10.1016/j.ecolecon.2015.02.004](https://doi.org/10.1016/j.ecolecon.2015.02.004)
- Xie W, Ma N (2010) Enzymatic transesterification of soybean oil by using immobilized lipase on magnetic nano-particles. *Biomass Bioenergy* 34:890–896. doi:[10.1016/j.biombioe.2010.01.034](https://doi.org/10.1016/j.biombioe.2010.01.034)
- Xu C, Etcheverry T (2008) Hydro-liquefaction of woody biomass in sub- and super-critical ethanol with iron-based catalysts. *Fuel* 87:335–345. doi:[10.1016/j.fuel.2007.05.013](https://doi.org/10.1016/j.fuel.2007.05.013)

# Chapter 10

## Catalytic Conversion on Lignocellulose to Biodiesel Product

Samira Bagheri, Nurhidayatullaili Muhd Julkapli,  
and Rabi'atul Adawiyah Zolkepli

**Abstract** Biomass is considered to be an important renewable source for securing future energy supply, production of fine chemicals, and sustainable development. The brilliant advantage of employing reproducible sources to synthesize biofuels is the conversion of natural bioresources for independence and secure bioenergy supply. Although utilizing complex biomass feedstock is full of challenges, approaches based on the formation of simpler and more stable intermediate derivatives, denoted as platform molecules, appear to be an efficient biomass conversion to fuels and chemicals. As a means of upgrading biofuels, heterogeneous base catalysts can be employed to produce liquid hydrocarbon fuel using deoxygenation reactions. Therefore, this chapter presents a state-of-the-art overview of the most relevant catalytic strategies available today for this paradigmatic conversion. However, more research and development are necessary before confirming the heterogeneous catalyst alternatives become economically and technically viable.

**Keywords** Biomass • Biofuels • Refining process • Heterogeneous catalyst • Homogeneous catalysts

### 10.1 Introduction

The combination of economic and environmental factors, including soaring crude oil prices and climate change, has created a global interest in developing renewable energy sources that could replace fossil fuels (Arthur et al. 2006; Michael et al. 2007; Avinash 2007; Ayhan 2007; Peer et al. 2008). Besides, due to the rapid growth of energy consumption, fossil-based fuel is on the verge of extinction (Michael et al. 2007; Avinash 2007). Hence, it is needless to say that the world needs new energy resources to substitute the nonrenewable ones (Peer et al. 2008).

---

S. Bagheri • N.M. Julkapli (✉) • R.A. Zolkepli  
Nanotechnology & Catalysis Research Centre (NANOCAT), University of Malaya, IPS  
Building, 50603 Kuala Lumpur, Malaysia  
e-mail: [nurhidayatullaili@um.edu.my](mailto:nurhidayatullaili@um.edu.my)

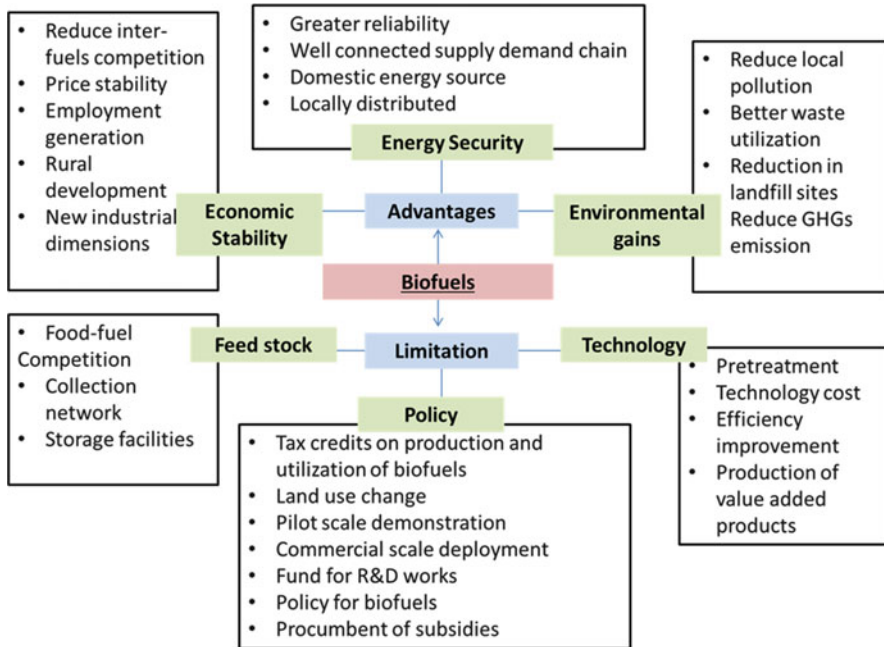


Fig. 10.1 Advantages and limitations of biofuels

Biofuels derived from renewable resources including lignocellulose biomass are considered the best potential alternative fuels for at least partially replacing fossil fuels in the future (Arthur et al. 2006; Avinash 2007). Some advantages and limitations of biofuels are shown in Fig. 10.1 (Ayhan 2007; Gregory 2007).

Biofuels are generally classified into two types: primary and secondary biofuels. The primary biofuels, including fuel wood, wood chips, and pellets (in raw form), are used mostly for heating, cooking, or electricity production (Gregory 2007; Edward 2008). The second type of biofuels, e.g., bioethanol and biodiesel, which can be used in the transportation sector as well as in many industrial processes, are synthesized through treatment of raw feedstocks such as biomass. The second type based on source material and technology used for their synthesis is further divided into three generations of biofuels (Table 10.1) (Seungdo and Bruce 2005; Jerry et al. 2009; Naika et al. 2010).

## 10.2 General Methods for the Production of Biofuels

Different methods used for the conversion of biomass into biofuels, i.e., chemical, physical, biological, or combination of procedures, are pivotal to their characteristics. The choice of which method to be used depends upon the quantity and type of

**Table 10.1** Classification of biofuels

	First generation	Second generation	Third generation	Fourth generation
Substrate	Sugar, starch, plant oil	– Lignocellulosic biomass – Waste plant/animal oil	Algae, microbes	High solar efficiency cultivations
Production method	– Biodiesel: transesterification of plant oils – Bioalcohols: fermentation of sugar or starch	Methanol, Fischer–Tropsch gasoline, mixed alcohol, diesel, dimethyl ether Green diesel: thermochemical conversion of, etc. Bio-methane: Anaerobic digestion of municipal, industrial or agricultural waste	H <sub>2</sub> from microbe Biodiesel and bioethanol from algae	Hydrolytic conversion/deoxygenating
Sources	Sugarcane, wheat, barley, potato, corn, sugar beet, vegetable oils (soybean, sunflower, coconut, rapeseed, etc.)	Firewood, wood chips, pellets, animal waste, forestry and crop residues, landfill gas, municipal wastes Non-edible energy crops	Microbes, algae	Vegetable oil

biomass feedstock, the preferred kind of fuels, economic conditions, environmental standards, and project factors (e.g., processing steps and time) (Seungdo and Bruce 2005; Ayhan 2008; Naika et al. 2010). In light of economic and environmental factors, it is imperative to select and develop a commercially viable process for converting a specific type of biomass into fuels.

### 10.2.1 Thermochemical Process

A number of thermochemical conversion equipment exist which could transform agricultural biomass into biofuels (Michele et al. 2005; Mark and Robert 2007; Andrew et al. 2008; Hanna and Raimo 2009; Damartzis and Zabaniotou 2011). Such thermochemical routes include gasification, liquefaction, and pyrolysis, which directly process whole lignocelluloses to upgradeable platforms, e.g., synthesis gas and bio-oil (Fig. 10.2). The specific features of thermochemical process, which ensure the maximum efficiency of the entire cycle of plant biomass conversion into heat and power, include cost-effectiveness and minimum technical complicity. The other advantages of fast thermochemical conversion process are the high performance rate, applied to various kinds of plant materials, the possibility to produce gas and liquid biofuels in one technological process, and the unique flexibility and

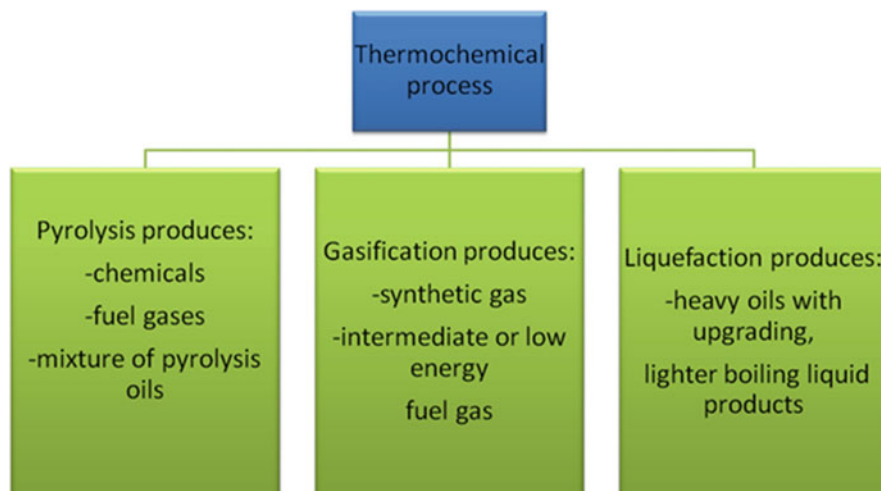


**Fig. 10.2** Thermochemical processes used in biomass management and conversion to biofuels

controllability (Michele et al. 2005; Thomas et al. 2009; Damartzis and Zabaniotou 2011). However, there exists a challenge for scientists to choose the best thermochemical route for such methods are still in their early stages of development (Manara and Zabaniotou 2012).

The difficulty of plant biomass and factors including moisture,  $O_2$ ,  $S_2$ ,  $N_2$ , and metal contents bring challenges to this process (Damartzis and Zabaniotou 2011). It is well believed that agricultural biomass could be a major and potentially substantial contributor to the existing energy demands, only if thermochemical conversion of different kinds of plant biomass could be achieved (Ajay et al. 2009; Rowbotham et al. 2012). Therefore, multi-products strategy could be regarded as a promising option for thermochemically based bio-refineries in order to reduce the risks of investment (Andrew et al. 2008). In fact, this would enhance the actual variety of products, provide better material and energy integration, and improve the effectiveness of the process (Thomas et al. 2009; Manara and Zabaniotou 2012). Such strategy has been previously proved highly profitable in conventional oil refineries (Hanna and Raimo 2009).

### 10.2.1.1 Pyrolysis Process

The thermochemical decomposition of an organic material at high temperatures in the absence of oxygen is called pyrolysis, which produces gas and liquid products and leaves behind a carbon-rich residue (Fig. 10.3). Many valuable reports have been published on various features of fast biomass pyrolysis, including quality and applications of bio-oil and bio-oil fractionation methods, as well as designs of fast pyrolysis systems and their process features (Edimar et al. 2006; Richard and Stefan

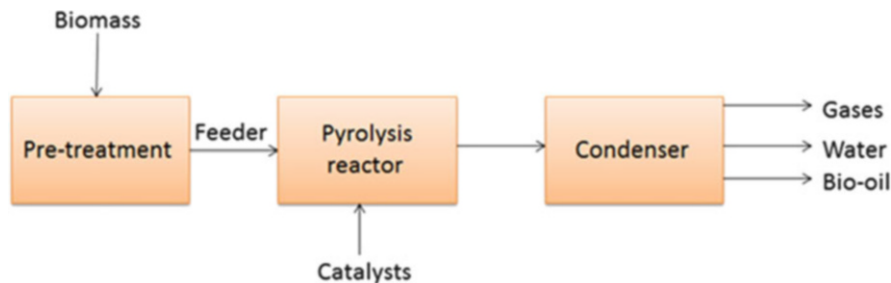


**Fig. 10.3** Pyrolysis process used for biomass conversion

2010; Mercadera et al. 2010). This liquid fuel, which was converted into industrial product feedstock by hydroprocessing, increased the pyrolysis oil intrinsic hydrogen, producing alcohols and polyols (Edimar et al. 2006; Zhenyi et al. 2011). The microalgae or seaweed represents a novel category of feedstock for pyrolysis, which, because of the nature of the environment of their growth coupled with their biochemistry, naturally has high metal content (Richard and Stefan 2010; Zhenyi et al. 2011).

### 10.2.1.2 Liquefaction Process

The use of this process resulted in a lower quantity of unsaturated products and less polymerization and absence of  $O_2$  from the final products. In general, the process is done in the self-designed reactor to study the special effects of the composition of molten salt, biomass materials, and process temperature on the liquefaction of biomass (Dong et al. 2010; Biller and Ross 2011; Peigao and Phillip 2011; Diego et al. 2013). The greatest yield reached to 35 % of bio-oil obtained when cellulose is liquefied in  $ZnCl_2$ , while the lowest 21 % of  $H_2O$  content in bio-oil obtained when it is liquefied in 66 %  $KCl-CuCl$ . Yield of bio-oil produced from cellulose was much greater than from rice straw liquefaction, while  $H_2O$  in bio-oil from cellulose was lower (Peigao and Phillip 2011). It indicated that biomass containing more cellulose was more proper for liquefaction process (Yu et al. 2011). Since liquefaction is greatly affected by temperature, the yield of bio-oil increased at first and then decreased when temperature increases. The best liquefaction temperatures of cellulose are recorded in a range of 450–530 °C (Javaid et al. 2010; Yu et al. 2011). Another study revealed the liquefaction of maize stalk in polyhydric alcohol under different reaction conditions and found that the liquefaction efficiency was high in mixed solvents of polyethylene glycol and glycerin (mass ratio 80:20) using  $H_2SO_4$  (mass fraction 3 %) as catalyst (Tylisha et al. 2010). The liquefied products contained oligomers of polyhydric alcohols,  $COOH$ , and their esters because of the oxidation and esterification of polyhydric alcohols and the decomposition of maize stalk (Rodrigo et al. 2011). Other liquefaction processes of maize salt are recorded in the production of heavy oil products composed of ketones, esters, and



small amount of alcohols and phenols, but furans were not detected (Huajun et al. 2011). The similar observation for the direct liquefaction of cyanobacteria in ethanol under supercritical conditions was that the optimum conditions were recorded at 270 °C, 40 min, and at the ratio of cyanobacteria to ethanol of 1:5 g mL<sup>-1</sup>. Under these conditions, the liquefaction conversion rate reached 83.13 % with the kinetic on activation energy of 50.793 kJ mol<sup>-1</sup>.

The produced cellulosic liquefaction fuel could not completely mix with diesel fuels; however, it could be mixed with fatty acid methyl ester and a diesel engine could be operated with the blend (Ting et al. 2007; Shuping et al. 2010; Umakanta et al. 2011).

### 10.2.1.3 Gasification Process

The thermochemical transformation of biomass at high temperature in the presence of restricted supply of oxygen is called gasification of biomass, which may be supplied as such or in the form of air or steam. In advance, concentrated solar reactor was enlisted in high-temperature biomass process (Lucasa et al. 2004; Krzysztof et al. 2007; Samuel et al. 2009). High-temperature biomass gasification compared to the traditional methods of synthesizing fuel represents many advantages and various types of end products (Fig. 10.4) (Samuel et al. 2009). An enhancement in the overall conversion, tar removing, and decreasing the product composition ratios occur at higher temperatures than 1000 °C (Lucasa et al. 2004).

Moreover, driving these processes using concentrated solar energy decreased consumption of energy and caused a portion of the product stream to heat up and part of the solar energy to be stored in the product stream as chemical energy (Krzysztof et al. 2007). Biomass is found to be the only significant factor with a 95 % confidence interval whose conversion reached 68 % with solar energy (Lucasa et al. 2004; Marbe et al. 2004; Samuel et al. 2009). Rather than that, the separation of H<sub>2</sub> from CO<sub>2</sub>, using high-pressure water, is explained for a biomass gasification process in supercritical H<sub>2</sub>O (Kurkela et al. 1993; Krzysztof 2008; Anna et al. 2010). Addition of excess H<sub>2</sub>O under high pressure to the product gas mixture based on the lowest solubility of H<sub>2</sub> than CO<sub>2</sub> in H<sub>2</sub>O results in H<sub>2</sub> with purity more than 90 % mol in gas phase (Anna et al. 2010). Utilized energy for the compression of H<sub>2</sub>O required to dissolve the CO<sub>2</sub> is negligible. H<sub>2</sub> dissolved in the H<sub>2</sub>O together with CO<sub>2</sub> is utilized for process heat (Kurkela et al. 1993; Karin and Simon 2010).

### 10.2.2 Hydrolysis Process

There are some reports on a highly yielding chemical method of hydrolyzing biomass to monosaccharide (Eiji and Shiro 2006; Robert et al. 2010; Sayantan et al. 2010). Aqueous phase processes for the conversion of carbohydrate-derived

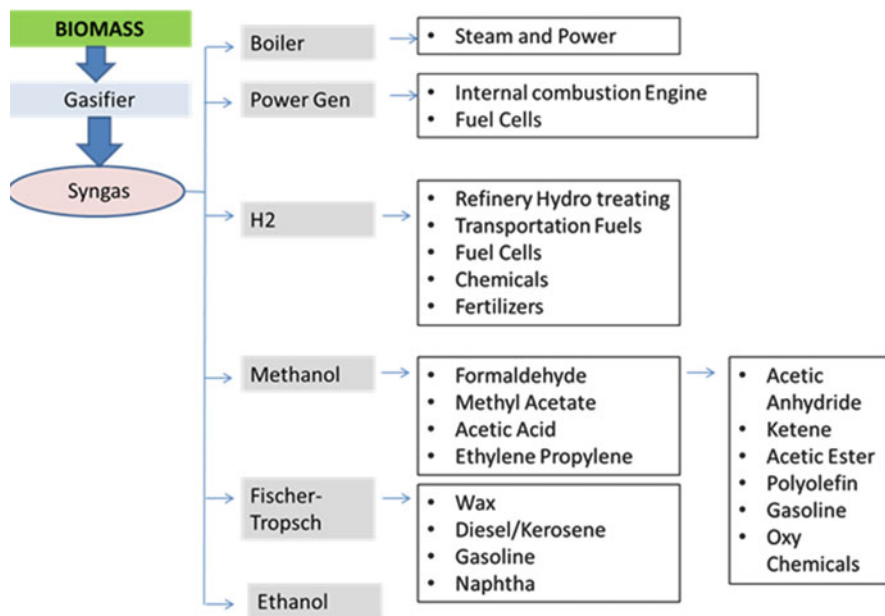


**Fig. 10.4** Biomass syngas productivity

compounds are potentially attractive in that they do not require concentration of the aqueous solution and generally yield a gas phase or hydrophobic product that separates spontaneously from water, which reduces the cost of separation steps in the catalytic processing strategies (Robert et al. 2010). Ninety percent cellulose conversion to glucose and 70–80 % sugar yield from untreated biomass will be achieved by gradually adding  $\text{H}_2\text{O}$  to a catalytic acid in chloride ionic solution. Another study revealed the hydrolysis of cellulose with concentrated phosphoric acid and 95 % ethanol and found that the overall glucose and xylose yields were 86 % and 82.6 % (Sayantan et al. 2010). Meanwhile, dilute acid hydrolysis mainly releases pentose from rice straw. In this case, the optimum yield of xylose produced is  $19.35 \text{ g L}^{-1}$  with only  $0.24 \text{ mol L}^{-1}$  of  $\text{H}_2\text{SO}_4$  for 30 min of reaction (Ching-Hung et al. 2010).

One of the main drawbacks of this process is that, as in the production of cellulosic ethanol, aqueous phase catalytic processing requires a pretreatment step to hydrolyze solid lignocellulose to soluble carbohydrates.

## 10.3 Heterogeneous Catalysis Technology

To date, metal particles including Pt, Ir, and Pd supported on metal oxide surfaces have been reportedly used in converting plant biomass into biofuel. Nano-catalysts, such as TiO<sub>2</sub>, ZnO, CaO, and MgO, have also shown potential applications. Also, bimetallic nanoparticles have shown major technological applications in heterogeneous catalysis (Kazuya et al. 2000; Hak-Joo et al. 2004; Bournaya et al. 2005). Although the use of bimetallic nanoparticles as catalysts for various chemical reactions is vividly studied, their application as catalysts for converting biomass to biofuel is largely unexplored (Gabriele et al. 2000; Kohsuke et al. 2004; Wenlei and Haitao 2006; Naomi et al. 2007). Instead, more attention has been paid to the homogeneous catalyst due to their higher activities compared to that of heterogeneous catalysts (Gabriele et al. 2000; Wenlei and Haitao 2006; Naomi et al. 2007). Thus, the challenge is to design an improved catalyst to overcome the disadvantages associated with heterogeneous catalysts (Bournaya et al. 2005).

### 10.3.1 Heterogeneous Catalytic Approach for the Production of Biofuels

Heterogeneous catalysts are environment friendly, reusable, and, unlike homogeneous catalysts, operated in continuous reactions (Andreozzi et al. 1996; Damsa et al. 2002; Wenlei and Xiaoming 2006; Young-Moo et al. 2008). There are some limitations on the application of heterogeneous catalysis including composition of alcohol and oil, concentration of catalyst, and extreme conditions of temperature and pressure. These series of limitations provide negative impact on the application of heterogeneous catalysis especially as metal oxide and supported metal oxide catalyst are concerned (Andreozzi et al. 1996; Young-Moo et al. 2008).

#### 10.3.1.1 Metal Oxide Heterogeneous Catalyst

The adsorption of reactant on the unsaturated metal oxide represented by O<sub>2</sub> atoms and the elimination of H<sub>2</sub> and O<sub>2</sub> during the chemical process are major factors that contribute on the catalytic activity and selectivity of metal oxide (Andreozzi et al. 1996; Young-Moo et al. 2008; Martino et al. 2008; Claire et al. 2008; Anton et al. 2008; Refaat 2011). With consideration on those factors, metal oxide families (e.g., alkali earth metal oxides and transition metal oxides) have found a promising catalytic application in oil transesterification process (Claire et al. 2008; Masoud et al. 2009). During the methanolysis process, sufficient adsorptive sites of ethanol are required to the breaking of O-H bonds into methoxide anions. The process continued with triglyceride reaction and resulted in the production of hydrogen cations and fatty acid methyl esters (Anton et al. 2008; Refaat 2011).

Due to its hollow and layered structure,  $\text{Co}_3\text{O}_4$  metal oxide catalyst has demonstrated promising catalytic and coupling properties with Mo(VI)/Mo(V) (Kirillov et al. 2011).

Meanwhile, the application of metal oxide catalyst such as  $\text{Co}_3\text{O}_4$ , KOH,  $\text{MoO}_3$ , NiO,  $\text{V}_2\text{O}_5$ , and ZnO in the cracking process of vegetable oil has been extensively studied. In this case, almost 87.6 % of products have been recorded (Claire et al. 2008). This encourages the application of  $\text{CeO}_2$ ,  $\text{TiO}_2$ ,  $\text{Al}_2\text{O}_3$ , and  $\text{ZrO}_2$  catalysts for the aldol condensation and the ketonization process of biomass (Refaat 2011). The catalytic efficiency in aldol condensation is strongly related to the bond of C-C in aldehyde groups for the production of diesel and jet fuel green hydrocarbon components (Sanjib and Anju 2005; Mathias et al. 2006; Helwania et al. 2009).

During the process, the C-C coupling would occur with the removal of  $\text{O}_2$ ,  $\text{CO}_2$ , and  $\text{H}_2\text{O}$  (Sanjib and Anju 2005).

Furthermore, transesterification of soybean oil and 99 % products is obtained using nanoparticle  $\text{MgO}_2$  under 523 °C and 24 MPa, respectively, for 10 min (Emin et al. 2009). It indicates when the pressures and temperatures are higher, the catalyst is more active. Meanwhile, in order to understand the function of  $\text{H}_2\text{O}$  and  $\text{CO}_2$  on catalytic performance in the air medium for different amount of times, some studies using the solid base activated CaO catalyst in the methanolysis of sunflower oil, which shows rapid hydration and carbonation of CaO in air ( $\text{H}_2\text{O}$  and  $\text{CO}_2$  has covered the poisoning active surface sites of CaO) (Shuli et al. 2008). As a result, in order to avoid reduction of CaO catalytic activity, the catalyst was thermally treated at 700 °C in order to chemically desorb  $\text{CO}_2$  before being used (Ayato et al. 2009). Ninety four percent of conversion at 60 °C was obtained with 13 alcohol to 1 oil molar ratio and 3 wt% catalyst content based on the weight of oil after 100 min reaction time. Not much work has been carried out using SrO catalyst (Xuejun et al. 2007; Miri et al. 2011). SrO is a highly soluble and active metal oxide (Xuejun et al. 2007). Using SrO as a solid base catalyst in soybean oil transesterification resulted in 90 % yields of methyl esters achieved after 30 min, although the specific surface area of the catalyst is as low as  $1.05 \text{ m}^2 \text{ g}^{-1}$  (Miri et al. 2011). The catalyst still can be reused and is stable even after ten reaction cycles.

Furthermore, support materials play an important role on the conversion and selectivity of biofuels with metal oxide catalyst (Kohsuke et al. 2004; Wenlei and Haitao 2006). For example,  $\text{V}_2\text{O}_5$  catalyst is used in the catalytic partial oxidation of hydrocarbon, and its activity and selectivity depend on the mode of dispersion, pretreatment conditions, and nature of the support (Tian et al. 2003; Xuejun et al. 2007; Shuli et al. 2008; Emin et al. 2009; Ayato et al. 2009; Betina et al. 2009; Miri et al. 2011). Pd-supported carbon resulted the greatest catalytic and selectivity properties for deoxygenation reactions of fatty acids and their esters (Siswati et al. 2008, 2009; Irina et al. 2010; Xuan et al. 2012). Almost 95 % of long-chain alkenes (compose of 87 % heptadecane and 9 % octadecane) have been successfully converted from viscous methyl ester during the hydrodeoxygenation process (Siswati et al. 2009). Therefore, most of Pd-supported carbon catalyst focused on catalytic deoxygenation of biofuel esters and stearic acid, forming n-heptadecane as the main product (Xuan et al. 2012). Meanwhile,  $\text{BaSO}_4$  is also

used as support on the Pd catalyst to deoxygenate sunflower oil using n-hexane as the solvent demonstrating high yield and selectivity (Santiago et al. 2012).

As a result of acidic characteristics, the attention was focused on ZrO<sub>2</sub>, TiO<sub>2</sub>, and ZnO among other transition metal oxides in the biofuel production process (Atsushi et al. 2008; Zhao et al. 2011; David et al. 2011). An investigation of the catalytic performance of ZnO and ZrO<sub>2</sub> as heterogeneous acid catalysts in palm kernel oil transesterification of the supercritical methanol showed 86.1 % yields for ZnO using methyl ester and 64.5 % for ZrO<sub>2</sub> after 60 min using 6:1 molar ratio of alcohol/oil and 3 wt% catalyst (Satoshi et al. 2006; Xiao-Rong et al. 2007; Sunitaa et al. 2008; Hui et al. 2010). Using sulfated ZrO<sub>2</sub>, the yields considerably increased to 90.3 %, which might be due to the high acidic strength of sulfate anions on the surface of ZrO<sub>2</sub> (Brito et al. 2007). A comparison of the catalytic activity in the triacetin methanolysis of the two super acid catalysts, ZrO<sub>2</sub>/SO<sub>4</sub><sup>2-</sup> and ZrO<sub>2</sub>/WO<sub>3</sub><sup>2-</sup>, has demonstrated the important role of specific surface area and active site concentration in the catalyst activity (Kourieh et al. 2009; Young-Moo et al. 2010a; Mongkolbovornkija et al. 2010). With similar process parameters of 60 °C and 8 h, ZrO<sub>2</sub>/SO<sub>4</sub><sup>2-</sup> compared to ZrO<sub>2</sub>/WO<sub>3</sub><sup>2-</sup> demonstrated more conversion of triacetins due to its greater active phase concentration and specific surface area. While the two solid strong acid catalysts, TiO<sub>2</sub>/SO<sub>4</sub><sup>2-</sup> and ZrO<sub>2</sub>/SO<sub>4</sub><sup>2-</sup>, have higher activity in the transesterification of cottonseed oil to methyl esters, higher methyl ester yields were obtained for sulfated TiO<sub>2</sub> due to its 99.5 m<sup>2</sup> g<sup>-1</sup> higher specific surface area compared to 91.5 m<sup>2</sup> g<sup>-1</sup> for sulfated ZrO<sub>2</sub>/SO<sub>4</sub><sup>2-</sup> (Young-Moo et al. 2010b). It was discovered that after the introduction of the sulfate anions, new Bronsted acid sites were formed on the catalyst surface. With only 2 wt% catalyst and 12:1 alcohol to oil molar ratio, after 8 h of reaction time, the methyl ester yields would be 90 % and 85 % produced by using the TiO<sub>2</sub>/SO<sub>4</sub><sup>2-</sup> and ZrO<sub>2</sub>/SO<sub>4</sub><sup>2-</sup>, respectively (Kourieh et al. 2009). Calcination at 800 °C with Bronsted acid site formation in 161 μmol g<sup>-1</sup> concentration presents the most active catalyst. Although the catalyst performs both transesterification and esterification, the reaction took a long time to complete. Calcination at 500 °C will offer the most active catalyst base of the studies evaluating the catalytic performance of ZrO<sub>2</sub>/WO<sub>3</sub><sup>2-</sup> associated with calcination temperature and effect of amount of WO<sub>3</sub> loading of the ZrO<sub>2</sub> for the esterification of palmitic acid with methanol that attributed to ZrO<sub>2</sub> tetragonal phase formation (Mongkolbovornkija et al. 2010). Beyond 500 °C the tetragonal phase switched to the monoclinic phase which caused the activity reduction from 98 % conversion of palmitic acid to 8 % for the catalyst calcined at 900 °C. The concentration of 1.04 mmol g<sup>-1</sup> at acid site is achievable with 5 wt% loading of WO<sub>3</sub> (Shuguang et al. 2009). Furthermore, excess coverage of WO<sub>3</sub> species on ZrO<sub>2</sub> decreased the acidity correlated activity. The soybean oil conversion over ZrO<sub>2</sub>/WO<sub>3</sub> establishes stability of catalyst activity up to 100 h of use. 94 % of oil changed with 40 alcohol and 1 oil molar ratio at 300 °C during 8 h of the reaction (Nikolaos et al. 2010).

Recently, Stefanidis et al. studied the catalytic performance of MCM41, silicalite, ZSM-5, and alumina for the pyrolysis of beech wood. The application of strongly acidic zeolite H-ZSM-5 resulted in the reduction of the total bio-oil by

decreasing the bio-oil organic phase and increasing its water content, accompanied by an increase of gases and formation of coke on the catalyst. The zeolite silicalite and Al-MCM-41 induced the same effect with those of H-ZSM-5 but to a less extent, except of the significantly higher production of coke that was deposited on Al-MCM-41. Regarding the composition of bio-oil, all the catalysts and mostly the strongly acidic H-ZSM-5 zeolite reduced the oxygen content of the organic fraction, mainly by decreasing the concentration of acids, ketones, and phenols.

### 10.3.1.2 Bimetallic Heterogeneous Catalysts

Au/Ag bimetallic catalyst is applied in the transesterification of sunflower oil to biofuels using methanol (Habriouxa et al. 2009; Banerjee et al. 2014). Synthesizing biofuels from sunflower oil is catalyzed heterogeneously, at 65 °C for 2.0 h, with 5:1 molar ratio of methanol to oil and 5 % catalyst concentration, with a 86.9 % biofuel yield obtained (Banerjee et al. 2014). This shows that Au/Ag core-shell nanoparticle is a promising catalyst in transesterificating sunflower oil to biofuel, which is reused over three cycles.

As part of concerted effort toward improving the isoparaffin content of biofuels via hydrodeoxygenation, synthesized bimetallic nickel including NiMo/SiO<sub>2</sub>, NiMo/c-Al<sub>2</sub>O<sub>3</sub>, and NiMo/SiO<sub>2</sub>-Al<sub>2</sub>O<sub>3</sub> has been promising. In another development, some researchers improved the bimetallic system by substituting it with fluoride ion in order to increase the acidity since the former could be of serious environmental concerns (Wijayapala et al. 2014). They reported that the isoparaffin content of the product was significantly greater by using NiMo/Al<sub>2</sub>O<sub>3</sub>/F compared to NiMo/Al<sub>2</sub>O<sub>3</sub> (Ayodele et al. 2014). This unique ability is due to their formation reaction, which does not permit significant changes in their molecular sizes due to the similar van der Waals radii of carbon and fluorine (Senol et al. 2006; David and Luděk 2010). Other factors include their high bond energy, low polarizability, and the presence of the perfluoro species that twists themselves so that the carbon chain is wrapped with the electronegative fluorine (Senol et al. 2006).

For deoxygenation of stearic acid, variety of catalysts was tested at 300 °C and 0.6 MPa of helium (Zhao et al. 2011). Catalyst screening was performed for Pd, Pt, Mo, Ni, Ru, Rh, Ir, and other metals, bimetallic Pd–Pt catalyst, as well as Raney nickel and oxides Ni–Mo/Al<sub>2</sub>O<sub>3</sub>. It was shown that Pt and Pd active metals on carbon as a support have the highest activity and selectivity to hydrocarbons (Table 10.2).

**Table 10.2** Conversion of stearic acid deoxygenation with different catalysts (Seungdo and Bruce 2005; Ayhan 2008; Naika et al. 2010; Zhao et al. 2011)

Catalyst	Conversion (%)	Selectivity (C17) (%)	Selectivity (C17) (%)
16 % Ni/Al <sub>2</sub> O <sub>3</sub>	17.8	46	<0.5
3 %, Ni–Mo/Al <sub>2</sub> O <sub>3</sub>	8.6	23	–
5 % Pd/Al <sub>2</sub> O <sub>3</sub>	23.7	42	–
5 % Pt/Al <sub>2</sub> O <sub>3</sub>	19.9	46	<0.5
2 % Ir/Al <sub>2</sub> O <sub>3</sub>	17.2	2	–
3 % Rh/SiO <sub>2</sub>	15.7	23	–
60 % Ni/SiO <sub>2</sub>	18.1	58	1

## 10.4 Heterogeneous Catalysis in Biomass: Selective Transformation of Biofuels

### 10.4.1 Bioethanol

Ethanol production commonly begins by releasing the fermentable sugars during the saccharification process from polysaccharides, known as substrate pretreatment. The following step is fermenting the released sugars and final separation of ethanol in distillation (Seungdo and Bruce 2004; Yusuf 2008; Alvira et al. 2010). During pretreatment step, polymer carbohydrate molecules, including cellulose, hemicellulose, and lignin, are separated and decomposed into their simple sugars by enzyme-catalyzed hydrolysis (Mustafa et al. 2008). Therefore, each of these polymers that contain great amounts of carbohydrates is a suitable source of raw materials for the biosynthesis of bioethanol from fermentable sugars using the optimized microbial fermentation procedure (Thangavelu et al. 2014; Hansdah and Murugan 2014).

Cellulase enzymes are applied in hydrolysis, while yeast or bacteria are used in fermentation (Gomez and Saadeddin 2014; Tan and Lee 2014). An increase of porosity, including accessible surface area, of waste materials, cellulose fiber crystallinity reduction, and removal of lignin and hemicellulose that facilitate the access of cellulase enzymes to cellulose are the factors that significantly improve the hydrolysis in pretreatment processes (Liu et al. 2014; Neto et al. 2014). Reducing the amount of produced inhibitor compounds by adding H<sub>2</sub>SO<sub>4</sub>/SO<sub>2</sub>/CO<sub>2</sub> in steam explosion significantly improves enzymatic hydrolysis process and results in complete removal of hemicellulose (Gomez and Saadeddin 2014). Lignin also can be degraded using polyphenol oxidases, laccases, H<sub>2</sub>O<sub>2</sub>-producing enzymes, and quinone-reducing enzymes (Liu et al. 2014; Möllers et al. 2014). The advantages of biological pretreatment include mild environmental conditions and lower energy requirement; nevertheless the hydrolysis rate is very low.

### 10.4.2 Biodiesel

An advanced method focused to exploit are pyrolysis and catalytic cracking (Andreozzi et al. 1996; Kazuya et al. 2000; Gabriele et al. 2000; Damsa et al. 2002; Hak-Joo et al. 2004; Kohsuke et al. 2004; Bournaya et al. 2005; Eiji and Shiro 2006; Wenlei and Haitao 2006; Wenlei and Xiaoming 2006; Naomi et al. 2007; Young-Moo et al. 2008; Robert et al. 2010; Sayantan et al. 2010; Ching-Hung et al. 2010). Through pyrolysis, vegetable oils are converted to biodiesel using high temperature or high temperature plus a catalyst. The selection is limited and a broad range of compounds is obtained commonly. Alkenes, aromatic compounds, esters, CO<sub>2</sub>, CO, water, and H<sub>2</sub> are the outcome of pyrolysis treatment based on the triglyceride source and the employed alkanes (Martino et al. 2008; Claire et al. 2008; Anton et al. 2008; Refaat 2011). Unfortunately, pyrolysis takes out O<sub>2</sub> from substrate molecules making the resulting fuel harmful to the environment compared to fossil fuels in terms of O<sub>2</sub> content. Furthermore, extra separation steps should carry out for solid residues and carbon created during pyrolysis (Mathias et al. 2006). Meanwhile, catalytic cracking used in an effort to control the types of products generated by triglyceride cracking, using a vast variety of catalysts and a gasoline-like fuel more likely formed than a diesel-like fuel (Sanjib and Anju 2005; Helwania et al. 2009). Among the four techniques, transesterification is the most promising solution (Emin et al. 2009). Biodiesel and glycerol are obtained by transesterification of oil with alcohol in the presence of a catalyst (Shuli et al. 2008). The reaction is normally a sequence of three consecutive reversible reactions. Through this three-step process, 1 mol of alkyl ester is released as the triglyceride molecule is broken down step-by-step first into diglyceride, then in monoglyceride, and, finally, in glycerin (Xuejun et al. 2007; Ayato et al. 2009; Miri et al. 2011).

Acid-catalyzed esterification followed by transesterification offers a better conversion for higher free fatty acids containing triglyceride stock, while stock with lower amount of free fatty acids, base-catalyzed in a relatively short time, is suitable (Satoshi et al. 2006; Xiao-Rong et al. 2007; Sunitaa et al. 2008; Hui et al. 2010). The stoichiometric reaction requires 1 mol of triglyceride and 3 mol of alcohol. Alkali-catalyzed transesterification method is generally preferred, which includes the use of a homogeneous catalyst including NaOH and KOH (Hak-Joo et al. 2004; Arzamendia et al. 2007). In order to get the highest yield from different types of oil, various kinds of catalysts and alcohols are used. For example, the optimum concentration for KOH catalyst to get an 83 % yield from crude *Karanja* oil (*Pongamia pinnata*) is 1 % KOH, while applying 0.5 % of NaOH provides almost 99 % yield from refined *Karanja* oil (Sharma and Singh 2008). The high performance of the alkaline catalysts is observed when high-quality vegetable oils were used. However, when the oils contain significant amounts of free fatty acids, they cannot be converted into biodiesel but instead to soaps (Hanny and Shizuko 2008). These soaps can prevent the separation of biodiesel from the glycerin fraction. These free fatty acids react with the alkaline catalyst to produce soaps that inhibit



the separation of ester, glycerin, and wash  $\text{H}_2\text{O}$ . Since base catalysts are less corrosive compared to acid compounds, the industry is interested in them (Meher et al. 2006; Alamu et al. 2008; Guo et al. 2014). Whereas acid-catalyzed transesterification is sensitive to  $\text{H}_2\text{O}$  concentration, the acid catalysts show low susceptibility to the presence of free fatty acids in the starting feedstock unlike base catalysts (Guo et al. 2014; Ezebor et al. 2014; Islam et al. 2014). The addition of the spectator polar compounds slows down the transesterification of small esters under acid-catalyzed conditions (Ezebor et al. 2014). High-efficiency conversion of vegetable oil is achievable when replacing alcohol to supercritical alcohol (and with no catalyst) (Islam et al. 2014). Higher temperature and pressure conditions would be required to overcome the absence of catalyst to achieve the nearly complete conversion. The palm oil and ground nut oil are converted to biodiesel without any catalyst at 200–400 °C and at 200 bar in the presence of supercritical methanol and ethanol (Teo et al. 2014).

However, the yield volume is low and the operating costs are high; the acid or base catalyst is involved in the transesterification. Moreover, the disadvantage of using a liquid catalyst is severe economic and ecological penalties (Di Serio et al. 2005). Continuous processes combine the esterification and transesterification steps, allowing higher productivity. However, most of these processes are still plagued by the disadvantages of using homogeneous catalysts although solid catalysts emerged in the last decade (Gemma et al. 2004; Edgar et al. 2005; Anton et al. 2006). The solid catalyst transesterification can withstand more extreme reaction conditions in comparison to homogeneously catalyzed process due to an immiscible liquid/liquid/solid three-phase system nature of the solid catalyzed mass transfer-limited process (Gemma et al. 2004).

### 10.4.3 Bioethers

Three groups of catalysts including base catalysts, acid catalysts, and enzymes have been studied in order to produce bioethers (Fabien et al. 2002). Utilizing enzymatic procedures to synthesize more pure bioethers by preventing soap formation has attracted much attention in recent years. However, enzymes used in a commercial production of biofuels are expensive (Thomas et al. 2008). The transesterification reaction without catalytic material is slow and normally high pressures and temperatures are required. Some studies demonstrate the water level-independent conversion of oil by transesterifying rapeseed oil in the absence of catalyst and in the supercritical methanol (Dilek et al. 2007). On the other hand, the production of methyl esters and esterification of free fatty acids in single stage could be enhanced using a certain amount of  $\text{H}_2\text{O}$ . Due to the absence of base or acid catalyst, the products can easily separate in supercritical temperature (250–400 °C) and pressure (35–60 MPa) (Gayubo et al. 2010). Numerous studies have carried out transesterification on vegetable oils using homogeneous acid and base catalysis. In the presence of high amount of free fatty acids and water, it was

suggested to use acid catalysts such as  $H_2SO_4$  and  $HCl$ , which handle esterification and transesterification of triglyceride simultaneously (João and Fausto 2006). Nonetheless, the process requires a high molar ratio of alcohol to oil and long reaction time. Since the environment is acidic, the instruments should be able to withstand corrosion (Thomas et al. 2008).  $NaOH$  and  $KOH$  are common homogeneous base catalysts, which are usually used in the industry. The transesterification can operate in modest conditions and shorter period of time. In addition, to prevent soap formation and increase the methyl ester yields, the oil with low amount of water and free fatty acids is preferred (Dilek et al. 2007).

Furthermore, the separation process of bioethers is further increased by the application of heterogeneous catalyst. Nevertheless, one of the main challenges is to decrease the rate of the reaction by limiting the diffusion rate using heterogeneous catalysts in three-phase alcohol and oil formation (João and Fausto 2006; Dilek et al. 2007). Interestingly, introducing a certain amount of cosolvent to stimulate miscibility of oil and methanol overcomes mass transfer challenge in heterogeneous catalysts and speeds up the reaction rate consequently. Usual cosolvents in vegetable oil transesterification by means of methanol and solid catalysts are THF, DMSO, n-hexane, and ethanol (Zhang 2003). Transesterifying rapeseed oil with methanol in the presence of  $CaO$  as a solid base catalyst in 170 min of reaction leads to 93 % yields of methyl ester (Emin et al. 2009). However, the reaction time could reduce to 120 min by adding a certain amount of THF into rapeseed oil/methanol mix without changing the yields (Shuli et al. 2008). In addition to applying cosolvent, using structure promoters or catalyst supports overcome mass transfer challenges associated with heterogeneous catalysts. Recently, researchers have developed a new bioether production process suitable for commercial continuous production, utilizing  $ZnO$  and  $Al_2O_3$  solid catalyst, no requirement for post-treatment catalyst removal, and with yields with a purity of approximately 98 %, not far from the theoretical value, achieved at high pressure and temperature (Wenlei and Xiaoming 2006).

## 10.5 Heterogeneous Catalysis in Biomass: Current Research and Prospective

Heterogeneous catalyst for biofuel production has offered the ability to process alternative and cheaper feedstock with simplified processes and cheaper manufacturing processes. In heterogeneous catalysis contrary to the homogenous system, adsorption of reactants and desorption of products have to take place on the surface of the solid catalyst for the reaction to take place at increased rate (Zhang 2003).

### 10.5.1 *Jatropha* Biofuels

In general, the conventional transesterification process with alkali catalyst cannot be employed in *Jatropha* oil. A solution to this problem is the use of heterogeneous alkali catalyst including CaO, microporous zeolite, and heteropoly acid (Alok et al. 2007; Amish et al. 2009; Houfang et al. 2009; Xin et al. 2011). It was found that CaO catalyst increases the mass transfer constraints of transesterification resulting four times increase in activation energy compared to homogenous alkali catalyzed system (Xin et al. 2011). It is also revealed that intense micro-convection induced by ultrasound enhances the mass transfer characteristics of the system with almost 20 % reduction in activation energy, as compared to mechanically agitated systems (Houfang et al. 2009). Catalyst concentration and alcohol to oil molar ratio of the transesterification yield are influenced by the formation of methoxy ions and their diffusion to the oil–alcohol interface, which in turn is determined by the volume fractions of the two phases in the reaction mixture (Foidla et al. 1996).

Microporous ZrO<sub>3</sub> catalysts including HY, H $\beta$ , HMOR, and HZSM-5It crack *Jatropha* oil readily. HZSM-5 reveals to be the most active catalyst in terms of conversion of *Jatropha* oil (65 %), yield of BLP (29 %), and selectivity toward green gasoline (50 %) compared to other microporous catalysts (Kazuhisa et al. 2010). However, modifying the catalytic system would improve the % yield and the selectivity toward green gasoline (Hui et al. 2006). The combined micro- and mesoporous materials in these composite catalysts with the core–shell arrangement inherit advantages of both micro- and mesoporous catalysts. In addition, restructuring mesoporous walls into ZrO<sub>3</sub> matrix has been applied such as in hydrocracking, cracking, and alkylation reactions (Kazuhisa et al. 2010).

The catalytic activity in the transesterification of *Jatropha* oil to fatty acid methyl ester was studied with sulfate zirconia as the heterogeneous catalyst. The study of the results of the calcination process indicates the quadratic effect of temperature and linear effects of duration on the obtained fatty acid methyl ester (Hui et al. 2006). Enlisting optimum calcination temperature at 490 °C and optimum calcination duration of 4 h, an optimal fatty acid methyl ester yield of 78.2 wt % is obtained (Ching-Hung et al. 2010).

## 10.6 Conclusion

The existing large amount of lignocellulosic biomass is a sustainable bioresource for producing biofuels and chemicals. Moreover, biofuels derived from renewable carbon sources could lead to diminished greenhouse gas emissions. They could be employed as drop-in replacements for petroleum fuels. In fact, the direct use of biomass feedstocks as biofuels is difficult owing to the complex structure, and therefore, they need to be converted using different non-catalyzed or catalyzed processes. As for the latter, homogeneous catalysts are generally used, but these

catalysts suffer from a number of drawbacks such as impossible separation of the catalyst from the reaction mixture and consequently impracticable catalyst recycling/reuse and the need for downstream separation/purification steps. An alternative is the application of heterogeneous catalysts, which eliminates the costs associated with separation and purification and, thus, could be used in commercial production systems.

**Acknowledgment** This work is financially supported by the University Malaya Research Grant (UMRG RP022-2012E) and Fundamental Research Grant Scheme (FRGS: FP049-2013B) by the University of Malaya and Ministry of High Education, Malaysia, respectively.

**Conflict of Interests** The authors declare that there is no conflict of interests regarding the publication of this paper.

## References

- Ajay K, David DJ, Milford AH (2009) Thermochemical biomass gasification: a review of the current status of the technology. *Energies* 2(3):556–581. doi:[10.3390/en20300556](https://doi.org/10.3390/en20300556)
- Alamu OJ, Akintola TA, Enweremadu CC, Adeleke AE (2008) Characterization of palm-kernel oil biodiesel produced through NaOH-catalysed transesterification process. *Scientific Res Essay* 3(7):308–311
- Alok KT, Akhilesh K, Hifjur R (2007) Biodiesel production from *Jatropha* oil (*Jatropha curcas*) with high free fatty acids: an optimized process. *Biomass Bioenergy* 31(8):569–575
- Alvira P, Tomás-Pejó E, Ballesteros M, Negro MJ (2010) Pretreatment technologies for an efficient bioethanol production process based on enzymatic hydrolysis: a review. *Bioresour Technol* 101(13):4851–4861
- Amish PV, Subrahmanyam N, Payal AP (2009) Production of biodiesel through transesterification of *Jatropha* oil using KNO<sub>3</sub>/Al<sub>2</sub>O<sub>3</sub> solid catalyst. *Fuel* 88(4):625–628
- Andreozzi R, Insolaa A, Capriob V, Marottab R, Tufano V (1996) The use of manganese dioxide as a heterogeneous catalyst for oxalic acid ozonation in aqueous solution. *Appl Catal Gen* 138(1):75–81
- Andrew AP, Frédéric V, Russell PL, Morgan F, Michael J Jr, Jefferson WT (2008) Thermochemical biofuel production in hydrothermal media: a review of sub- and supercritical water technologies. *Energy Environ Sci* 2008(1):32–65
- Anna S, Martin J, Krzysztof P (2010) Exergetic evaluation of 5 biowastes-to-biofuels routes via gasification. *Energy* 35(2):996–1007
- Anton AK, Alexandre CD, Gadi R (2006) Solid acid catalysts for biodiesel production towards sustainable energy. *Adv Synth Catal* 348(1):75–81
- Anton AK, Alexandre CD, Gadi R (2008) Biodiesel by catalytic reactive distillation powered by metal oxides. *Energy Fuels* 22(1):598–604
- Arthur JR, Charlotte KW, Brian HD, George B, John C, Charles AE, William JFJ, Jason PH, David JL, Charles LL, Jonathan RM, Richard M, Richard T, Timothy T (2006) The path forward for biofuels and biomaterials. *Science* 311(5760):484–489
- Arzamendia G, Campoa I, Arguiñarena E, Sánchezb M, Montesb M, Gandía LM (2007) Synthesis of biodiesel with heterogeneous NaOH/alumina catalysts: comparison with homogeneous NaOH. *Chem Eng J* 134(1):123–130
- Atsushi T, Caio T, Kazunari D. (2008) Glucose production from saccharides using layered transition metal oxide and exfoliated nano-sheets as a water-tolerant solid acid catalyst. *Chem Commun* (42):5363–5365

- Avinash KA (2007) Biofuels (alcohols and biodiesel) applications as fuels for internal combustion engines. *Prog Energy Combust Sci* 33(3):233–271
- Ayato K, Koh M, Katsuhisa H (2009) Acceleration of catalytic activity of calcium oxide for biodiesel production. *Bioresour Technol* 100(2):696–700
- Ayhan D (2007) Progress and recent trends in biofuels. *Prog Energy Combust Sci* 33(1):1–18
- Ayhan D (2008) Biofuels sources, biofuel policy, biofuel economy and global biofuel projections. *Energy Convers Manage* 49(8):2106–2116
- Ayodele OB, Abbas HF, Daud WMAW (2014) Catalytic upgrading of oleic acid into biofuel using Mo modified zeolite supported Ni oxalate catalyst functionalized with fluoride ion. *Energy Convers Manage* 88:1111–1119
- Banerjee M, Dey B, Talukdar J, Chandra KM (2014) Production of biodiesel from sunflower oil using highly catalytic bimetallic gold-silver core-shell nanoparticle. *Energy* 69:695–699
- Betina J, Steffen BK, Andreas JK-K, Rasmus F, Claus HC, Anders R (2009) Gas-phase oxidation of aqueous ethanol by nanoparticle vanadia/anatase catalysts. *Topics Catal* 52(3):253–257
- Billir P, Ross AB (2011) Potential yields and properties of oil from the hydrothermal liquefaction of microalgae with different biochemical content. *Bioresour Technol* 102(1):215–225
- Bournaya L, Casanavea D, Delfortb B, Hillionb G, Chodorge JA (2005) New heterogeneous process for biodiesel production: a way to improve the quality and the value of the crude glycerin produced by biodiesel plants. *Catal Today* 106(1):190–192
- Brito A, Borges ME, Otero N (2007) Zeolite Y as a heterogeneous catalyst in biodiesel fuel production from used vegetable oil. *Energy Fuels* 21(6):3280–3283
- Ching-Hung C, Wei-Heng C, Chieh-Ming JC, Shih-Ming L, Chien-Hsiun T (2010) Biodiesel production from supercritical carbon dioxide extracted *Jatropha* oil using subcritical hydrolysis and supercritical methylation. *J Supercrit Fluids* 52(2):228–234
- Claire SM, Adam PH, Adam FL, Karen W (2008) Evaluation of the activity and stability of alkali-doped metal oxide catalysts for application to an intensified method of biodiesel production. *Chem Eng J* 135(1):63–70
- Damartzis T, Zabaniotou A (2011) Thermochemical conversion of biomass to second generation biofuels through integrated process design—a review. *Renew Sustain Energy Rev* 15(1):366–378
- Damsa M, Drijkoningena L, Pauwelsb B, Tendeloo GV, Vosa DED, Jacobs PA (2002) Pd-zeolites as heterogeneous catalysts in heck chemistry. *J Catal* 209(1):225–236
- David K, Luděk K (2010) Deoxygenation of vegetable oils over sulfided Ni, Mo and NiMo catalysts. *Appl Catal Gen* 372(2):199–208
- David C, Françoise D, Yosslen A, Philippe S (2011) Stability of intermediates in the glycerol hydrogenolysis on transition metal catalysts from first principles. *Phys Chem Chem Phys* 13:1448–1456
- Di Serio M, Tessera R, Dimiccolia M, Cammarotaa F, Nastasib M, Santacesariaa E (2005) Synthesis of biodiesel via homogeneous Lewis acid catalyst. *J Mol Catal A Chem* 239(1):111–115
- Diego LB, Wolter P, Frederik R, Wim B (2013) Hydro thermal liquefaction (HTL) of microalgae for biofuel production: state of the art review and future prospects. *Biomass Bioenergy* 53:113–127
- Dilek V, Timur D, Gulsen D (2007) Ethylene and diethyl-ether production by dehydration reaction of ethanol over different heteropoly acid catalysts. *Chem Eng Sci* 62(18):5349–5352
- Dong Z, Liang Z, Shicheng Z, Hongbo F, Jianmin C (2010) Hydrothermal liquefaction of macroalgae *Enteromorpha prolifera* to bio-oil. *Energy Fuels* 24(7):4054–4061
- Edgar L, Yijun L, Dora EL, Kaewta S, David AB, Goodwin JG Jr (2005) Synthesis of biodiesel via acid catalysis. *Indus Eng Chem Res* 44(14):5353–5363
- Edimar D, Rafael LQ, Paulo AZS, Alexandre GSP (2006) Heats of combustion of biofuels obtained by pyrolysis and by transesterification and of biofuel/diesel blends. *Thermochim Acta* 450(1):87–90
- Edward MR (2008) Genomics of cellulosic biofuels. *Nature* 454:841–845

- Eiji M, Shiro S (2006) Kinetics of hydrolysis and methyl esterification for biodiesel production in two-step supercritical methanol process. *Fuel* 85(17):2479–2483
- Emin SU, Mert T, Erol S (2009) Transesterification of *Nannochloropsis oculata* microalga's lipid to biodiesel on Al<sub>2</sub>O<sub>3</sub> supported CaO and MgO catalysts. *Bioresour Technol* 100 (11):2828–2831
- Ezebor F, Khairuddean M, Abdullah AZ, Boey PL (2014) Esterification of oily-FFA and transesterification of high FFA waste oils using novel palm trunk and bagasse-derived catalysts. *Energy Convers Manage* 88:1143–1150
- Fabien A, Claude D, Daniel D (2002) Bio-ethanol catalytic steam reforming over supported metal catalysts. *Catal Commun* 3(6):263–267
- Foidla N, Foidla G, Sancheza M, Mittelbach M, Hackel S (1996) *Jatropha curcas* L. as a source for the production of biofuel in Nicaragua. *Bioresour Technol* 58(1):77–82
- Gabriele C, Siglinda P, Teresa T, Maria GV (2000) Catalytic wet oxidation with H<sub>2</sub>O<sub>2</sub> of carboxylic acids on homogeneous and heterogeneous Fenton-type catalysts. *Catal Today* 55 (1):61–69
- Gayubo AG, Valle B, Aguayo AT, Olazar M, Bilbao J (2010) Pyrolytic lignin removal for the valorization of biomass pyrolysis crude bio-oil by catalytic transformation. *J Chem Technol Biotechnol* 85(1):132–144
- Gemma V, Mercedes M, José A (2004) Integrated biodiesel production: a comparison of different homogeneous catalysts systems. *Bioresour Technol* 92(3):297–305
- Gomez EM, Saadeddin A (2014) The cellulolytic system of *thermobifidafusca*. *Crit Rev Microbiol* 40(3):236–247
- Gregory S (2007) Challenges in engineering microbes for biofuels production. *Science* 315 (5813):801–804
- Guo X, Chen L, Zhu Y, Zhang A, Wei D, Tang M (2014) A density functional theory study on lewis acid-catalyzed transesterification of  $\beta$ -oxodithioesters. *Int J Quantum Chem* 114 (13):862–868
- Habriouxa A, Servata K, Tingryb S, Kokoha KB (2009) Enhancement of the performances of a single concentric glucose/O<sub>2</sub> biofuel cell by combination of bilirubin oxidase/Nafion cathode and Au–Pt anode. *Electrochem Commun* 11(1):111–113
- Hak-Joo K, Bo-Seung K, Min-Ju K, Young MP, Deog-Keun K, Jin-Suk L, Kwan-Young L (2004) Transesterification of vegetable oil to biodiesel using heterogeneous base catalyst. *Catal Today* 93:1315–1320
- Hanna L, Raimo A (2009) Production of vegetable oil-based biofuels—thermochemical behavior of fatty acid sodium salts during pyrolysis. *J Anal Appl Pyrolysis* 86(2):274–280
- Hanny JB, Shizuko H (2008) Biodiesel production from crude *Jatropha curcas* L. seed oil with a high content of free fatty acids. *Bioresour Technol* 99(6):1716–1721
- Hansdah D, Murugan S (2014) Bioethanol fumigation in a di diesel engine. *Fuels* 130:324–333
- Helwania Z, Othman MR, Aziz N, Fernandob WJN, Kim J (2009) Technologies for production of biodiesel focusing on green catalytic techniques: a review. *Fuel Process Technol* 90 (12):1502–1514
- Houfang L, Yingying L, Hui Z, Ying Y, Mingyan C, Bin L (2009) Production of biodiesel from *Jatropha curcas* L. oil. *Comp Chem Eng* 33(5):1091–1096
- Huajun H, Xingzhong Y, Guangming Z, Jingyu W, Hui L, Chunfei Z, Xiaokai P, Qiao Y, Liang C (2011) Thermochemical liquefaction characteristics of microalgae in sub- and supercritical ethanol. *Fuel Process Technol* 92(1):147–153
- Hui Z, Houfang L, Bin L (2006) Solubility of multicomponent systems in the biodiesel production by transesterification of *Jatropha curcas* L. oil with methanol. *J Chem Eng Data* 51 (3):1130–1135
- Hui S, Yuqi D, Jinzhao D, Qijun Z, Zhiyong W, Hui L, Xiaoming Z (2010) Transesterification of sunflower oil to biodiesel on ZrO<sub>2</sub> supported La<sub>2</sub>O<sub>3</sub> catalyst. *Bioresour Technol* 101 (3):953–958

- Irina S, Olga S, Päivi M-A, Dmitry YM (2010) Decarboxylation of fatty acids over Pd supported on mesoporous carbon. *Catal Today* 150(1):28–31
- Islam A, Taufiq-Yap YH, Chan E-S, Moniruzzaman M, Islam S, Nabi Md N (2014) Advances in solid-catalytic and non-catalytic technologies for biodiesel production. *Energy Conver Manage* 88:1200–1218
- Javaid A, Soo KK, Nor Aishah SA (2010) Liquefaction of empty palm fruit bunch (EPFB) in alkaline hot compressed water. *Renew Energy* 35(6):1220–1227
- Jerry MM, John MR, David WK, Angelo CG, Timothy WC, Sergey P, Benjamin SF, Xiaodong W, Andrei PS, Adam SC (2009) Indirect emissions from biofuels: how important? *Science* 326 (5958):1397–1399
- João M, Fausto F (2006) Renewability and life-cycle energy efficiency of bioethanol and bio-ethyl tertiary butyl ether (bioETBE): assessing the implications of allocation. *Energy* 31 (15):3362–3380
- Karin P, Simon H (2010) CO<sub>2</sub> emission balances for different black liquor gasification biorefinery concepts for production of electricity or second-generation liquid biofuels. *Energy* 35 (2):1101–1106
- Kazuhiisa M, Yanyong L, Megumu I, Isao T (2010) Production of synthetic diesel by hydro treatment of *Jatropha* oils using Pt–Re/H-ZSM-5 Catalyst. *Energy Fuels* 24(4):2404–2409
- Kazuya Y, Kohsuke M, Tomoo M, Kohki E, Kiyotomi K (2000) Creation of a monomeric Ru species on the surface of hydroxyapatite as an efficient heterogeneous catalyst for aerobic alcohol oxidation. *J Am Chem Soc* 122:7144–7145
- Kirilov VA, Kuzin NA, Amosov YI, Kireenkov VV, Sobyenin VA (2011) Catalysts for the conversion of hydrocarbon and synthetic fuels for onboard syngas generators. *Catal Indus* 3 (2):176–182
- Kohsuke M, Takayoshi H, Tomoo M, Kohki E, Kiyotomi K (2004) Hydroxyapatite-supported palladium nanoclusters: a highly active heterogeneous catalyst for selective oxidation of alcohols by use of molecular oxygen. *J Am Chem Soc* 126(34):10657–10666
- Kourieh R, Bennici S, Auroux A (2009) Study of acidic commercial WO<sub>x</sub>/ZrO<sub>2</sub> catalysts by adsorption microcalorimetry and thermal analysis techniques. *J Thermal Anal Calorim* 90 (3):849–853
- Krzysztof JP (2008) Thermodynamic efficiency of biomass gasification and biofuels conversion. *Biofuels Bioprod Bioref* 2(3):239–253
- Krzysztof JP, Mark JP, Anke P (2007) Exergetic evaluation of biomass gasification. *Energy* 32 (4):568–574
- Kurkela E, Ståhlberg P, Laatikainen J, Simell P (1993) Development of simplified IGCC-processes for biofuels: supporting gasification research at VTT. *Bioresour Technol* 6(1):37–47
- Liu Y-H, Wu ZY, Yang J, Yuan YJ, Zhang WX (2014) Step enzymatic hydrolysis of sodium hydroxide-pretreated Chinese liquor distillers' grains for ethanol production. *Preparative Biochem Biotechnol* 44(5):464–479
- Lucasa C, Szweczyka D, Blasiaka W, Mochidab S (2004) High-temperature air and steam gasification of densified biofuels. *Biomass Bioenergy* 27(6):563–575
- Manara P, Zabaniotou A (2012) Towards sewage sludge based biofuels via thermochemical conversion – a review. *Renew Sustain Energy Rev* 16(5):2566–2582
- Marbe A, Harvey S, Bernatsson T (2004) Biofuel gasification combined heat and power—new implementation opportunities resulting from combined supply of process steam and district heating. *Energy* 29(8):1117–1137
- Mark MW, Robert CB (2007) Comparative economics of biorefineries based on the biochemical and thermochemical platforms. *Biofuels Bioprod Bioref* 1(1):49–56
- Martino DS, Riccardo T, Lu P, Elio S (2008) Heterogeneous catalysts for biodiesel production. *Energy Fuel* 22(1):207–217
- Masoud Z, Wan AWD, Mohamed KA (2009) Activity of solid catalysts for biodiesel production: a review. *Fuel Process Technol* 90(6):770–777

- Mathias S, Iva K, Päivi M-A, Kari E, Dmitry YM (2006) Heterogeneous catalytic deoxygenation of stearic acid for production of biodiesel. *Indus Eng Chem Res* 45(16):5708–5715
- Meher LC, Sagar DV, Naik SN (2006) Technical aspects of biodiesel production by transesterification—a review. *Renew Sustain Energy Rev* 10(3):248–268
- Mercaderia F d M, Groeneveld MJ, Kerstena SRA, Wayb NWJ, Schaverienb CJ, Hogendoorna JA (2010) Production of advanced biofuels: co-processing of upgraded pyrolysis oil in standard refinery units. *Appl Catal B Environ* 96(1):57–66
- Michael EH, Shi-You D, David KJ, William SA, Mark RN, John WB, Thomas DF (2007) Biomass recalcitrance: engineering plants and enzymes for biofuels production. *Science* 315 (5813):804–807
- Michele A, Angela D, Maria C, Teresa C, Carlo F (2005) Production of biodiesel from macroalgae by supercritical CO<sub>2</sub> extraction and thermochemical liquefaction. *Environ Chem Lett* 3 (3):136–139
- Miri K, Riam A-M, Aharon G (2011) Optimization of bio-diesel production from soybean and wastes of cooked oil: combining dielectric microwave irradiation and a SrO catalyst. *Bioresour Technol* 102(2):1073–1078
- Möllers KB, Cannella D, Jørgensen H, Frigaard NU (2014) Cyanobacterial biomass as carbohydrate and nutrient feedstock for bioethanol production by yeast fermentation. *Biotechnol Biofuels* 7(1), 64
- Mongkolbovornkija P, Champredab V, Sutthisripokc W, Laosiripojana N (2010) Esterification of industrial-grade palm fatty acid distillate over modified ZrO<sub>2</sub> (with WO<sub>3</sub>-, SO<sub>4</sub>-and TiO<sub>2</sub>-): effects of co-solvent adding and water removal. *Fuel Process Technol* 91(11):1510–1516
- Mustafa B, Havva B, Cahide Ö (2008) Progress in bioethanol processing. *Prog Energy Combust Sci* 34(5):551–555
- Naika SN, Vaibhav VG, Prasant KR, Ajay KD (2010) Production of first and second generation biofuels: a comprehensive review. *Renew Sustain Energy Rev* 14(2):578–597
- Naomi SK, Hiroki H, Homare K, Takuji T, Takuya F, Toshikuni Y (2007) Biodiesel production using anionic ion-exchange resin as heterogeneous catalyst. *Bioresour Technol* 98(2):416–421
- Neto AGB, Pestana-Calsa MC, de Morais MA Jr, Calsa T Jr (2014) Proteome responses to nitrate in bioethanol production contaminant *Dekkera bruxellensis*. *J Proteomics* 104:104–111
- Nikolaos S, Wu Z, Antonis CP, Alejandro JG, Eleni FI, Christopher JK, Israel EW, Michael SW (2010) Relating n-pentane isomerization activity to the tungsten surface density of WO<sub>x</sub>/ZrO<sub>2</sub>. *J Am Chem Soc* 132(38):13462–13471
- Peer MS, Skye RTH, Evan S, Ute CM, Jan HM, Clemens P, Olaf K, Ben H (2008) Second generation biofuels: high-efficiency microalgae for biodiesel production. *BioEnergy Res* 1 (1):20–43
- Peigao D, Phillip ES (2011) Hydrothermal liquefaction of a microalga with heterogeneous catalysts. *Indus Eng Chem Res* 50(1):52–61
- Refaat AA (2011) Biodiesel production using solid metal oxide catalysts. *Int J Environ Sci Technol* 8(1):203–221
- Richard F, Stefan C (2010) Catalytic pyrolysis of biomass for biofuels production. *Fuel Process Technol* 91(1):25–32
- Robert BL, Tanawan P, Phillip ES (2010) Biodiesel production from wet algal biomass through in situ lipid hydrolysis and supercritical transesterification. *Energy Fuels* 24(9):5235–5243
- Rodrigo B, Luis S, Rodrigo L-P, Jalel L (2011) Polyols obtained from solvolysis liquefaction of biodiesel production solid residues. *Chem Eng J* 175:169–175
- Rowbotham JS, Dyer PW, Greenwell HC, Theodorou MK (2012) Thermochemical processing of macroalgae: a late bloomer in the development of third-generation biofuels? *Biofuels* 3 (4):441–461. doi:10.4155/bfs.12.29
- Samuel S, Frédéric V, Christian L, Anca GH, Martin B (2009) Catalytic gasification of algae in supercritical water for biofuel production and carbon capture. *Energy Environ Sci* 2:535–541
- Sanjib KK, Anju C (2005) Preparation of biodiesel from crude oil of *Pongamiapinnata*. *Bioresour Technol* 96(13):1425–1429



- Santiago D, Jimmy F, M. Pilar Ruiz M, Jeffrey HH, Daniel ER (2012) Amphiphilic nanohybrid catalysts for reactions at the water/oil interface in subsurface reservoirs. *Energy Fuels* 26 (4):2231–2241
- Satoshi F, Hiromi M, Kazushi A (2006) Biodiesel fuel production with solid amorphous-zirconia catalysis in fixed bed reactor. *Biomass Bioenergy* 30(10):870–873
- Sayantan B, Daniel WA, Jacob WP (2010) Enzyme-catalyzed hydrolysis of cellulose in ionic liquids: a green approach toward the production of biofuels. *J Phys Chem B* 114 (24):8221–8227
- Senol OI, Viljava T-R, Krause AOI (2006) Hydrodeoxygenation of aliphatic esters on sulphidedNiMo/g-Al<sub>2</sub>O<sub>3</sub> and CoMo/g-Al<sub>2</sub>O<sub>3</sub> catalyst: the effect of water. *Catal Today* 106:186–189
- Seungdo K, Bruce ED (2004) Global potential bioethanol production from wasted crops and crop residues. *Biomass Bioenergy* 26(4):361–375
- Seungdo K, Bruce ED (2005) Life cycle assessment of various cropping systems utilized for producing biofuels: bioethanol and biodiesel. *Biomass Bioenergy* 29(6):426–439
- Sharma YC, Singh B (2008) Development of biodiesel from Karanja, a tree found in rural India. *J Fuel* 87(8):1740–1742
- Shuguang Z, Jinxia Z, Zhang CZ (2009) Isomerization and arylation of oleic acid on anion modified zirconia catalysts. *Catal Lett* 127(1):33–38
- Shuli Y, Houfang L, Bin L (2008) Supported CaO catalysts used in the transesterification of rapeseed oil for the purpose of biodiesel production. *Energy Fuels* 22(1):646–651
- Shuping Z, Yulong W, Mingde Y, Chun L, Junmao T (2010) Bio-oil production from sub- and supercritical water liquefaction of microalgae *Dunaliellatertiolecta* and related properties. *Energy Environ Sci* 3:1073–1078
- Siswati L, Irina S, Anton T, Päivi M-A, Kari E, Dmitry YM (2008) Synthesis of biodiesel via deoxygenation of stearic acid over supported Pd/C catalyst. *Catal Lett* 122(3):247–251
- Siswati L, Päivi M-A, Heidi B, Olga S, Rainer S, Jorge B, Max Lu GQ, Jukka M, Irina S, Dmitry YM (2009) Catalytic deoxygenation of stearic acid in a continuous reactor over a mesoporous carbon-supported Pd catalyst. *Energy Fuels* 23(8):3842–3845
- Sunitaa G, Biju MD, Ajayan V, Dhanashri PS, Balasubramanian VV, Halligudib SB (2008) Synthesis of biodiesel over zirconia-supported isopoly and heteropoly tungstate catalysts. *Catal Commun* 9(5):696–702
- Tan IS, Lee KT (2014) Enzymatic hydrolysis and fermentation of seaweed solid wastes for bioethanol production: an optimization study. *Energy* 78:53–62
- Teo SH, Taufiq-Yap YH, Ng FL (2014) Alumina supported/unsupported mixed oxides of Ca and Mg as heterogeneous catalysts for transesterification of *Nannochloropsis* sp. microalga's oil. *Energy Convers Manage* 88:1193–1199
- Thangavelu SK, Ahmed AS, Ani FN (2014) Bioethanol production from sago pith waste using microwave hydrothermal hydrolysis accelerated by carbon dioxide. *Appl Energy* 128:277–283
- Thomas S, Alexander Z, Alain C, Nikolaus M, Matthias B (2008) Bio-inspired copper catalysts for the formation of diaryl ethers. *Tetrahedron Lett* 49(11):1851–1855
- Thomas DF, Andy A, Abhijit D, Steven P (2009) An economic and environmental comparison of a biochemical and a thermochemical lignocellulosic ethanol conversion processes. *Cellulose* 16 (4):547–565
- Tian L, Ye D, Liang H (2003) Catalytic performance of a novel ceramic-supported vanadium oxide catalyst for NO reduction with NH<sub>3</sub>. *Catal Today* 78(1):159–170
- Ting Z, Yujie Z, Dehua L, Leo P (2007) Qualitative analysis of products formed during the acid catalyzed liquefaction of bagasse in ethylene glycol. *Bioresour Technol* 98(7):1454–1459
- Tylisha MB, Peigao D, Phillip ES (2010) Hydrothermal liquefaction and gasification of *nannochloropsis* sp. *Energy Fuels* 24(6):3639–3646
- Umakanta J, Das KC, Kastner JR (2011) Effect of operating conditions of thermochemical liquefaction on biocrude production from *Spirulina platensis*. *Bioresour Technol* 102 (10):6221–6229

- Wenlei X, Haitao L (2006) Alumina-supported potassium iodide as a heterogeneous catalyst for biodiesel production from soybean oil. *J Mol Catal A Chem* 255(1):1–9
- Wenlei X, Xiaoming H (2006) Synthesis of biodiesel from soybean oil using heterogeneous KF/ZnO catalyst. *Catal Lett* 107(1):53–59
- Wijayapala R, Yu F, Pittman CU Jr, Mlsna TE (2014) K-promoted Mo/Co- and Mo/Ni-catalyzed Fischer-Tropsch synthesis of aromatic hydrocarbons with and without a Cu water gas shift catalyst. *Appl Catal Gen* 480:93–99
- Xiao-Rong C, Yi-Hsu J, Chung-Yuan M (2007) Direct synthesis of mesoporous sulfated silica-zirconia catalysts with high catalytic activity for biodiesel via esterification. *J Phys Chem C* 111(50):18731–18737
- Xin D, Zhen F, Yun-hu L, Chang-Liu Y (2011) Production of biodiesel from *Jatropha* oil catalyzed by nanosized solid basic catalyst. *Energy* 36(2):777–784
- Xuan X, Yi L, Yutong G, Pengfei Z, Haoran L, Yong W (2012) Synthesis of palladium nanoparticles supported on mesoporous N-doped carbon and their catalytic ability for biofuel upgrade. *J Am Chem Soc* 134(41):16987–16990
- Xuejun L, Huayang H, Yujun W, Shenlin Z (2007) Transesterification of soybean oil to biodiesel using SrO as a solid base catalyst. *Catal Commun* 8(7):1107–1111
- Young-Moo P, Dae-Won L, Deog-Keun K, Jin-Suck L, Kwan-Young L (2008) The heterogeneous catalyst system for the continuous conversion of free fatty acids in used vegetable oils for the production of biodiesel. *Catal Today* 131(1):238–243
- Young-Moo P, JoonYeob L, Sang-Ho C, In SP, Seung-Yeon L, Deog-Keun K, Jin-Suk L, Kwan-Young L (2010a) Esterification of used vegetable oils using the heterogeneous WO<sub>3</sub>/ZrO<sub>2</sub> catalyst for production of biodiesel. *Bioresour Technol* 101(1):S59–S61
- Young-Moo P, Sang-Ho C, Hee JE, Jin-Suk L, Kwan-Young L (2010b) Tungsten oxide zirconia as solid superacid catalyst for esterification of waste acid oil (dark oil). *Bioresour Technol* 101(17):6589–6593
- Yu G, Zhang Y, Schideman L, Funk TL, Wang Z (2011) Hydrothermal liquefaction of low lipid content microalgae into bio-crude oil. *Am Soc Agric Biol Eng* 54(1):239–246
- Yusuf C (2008) Biodiesel from microalgae beats bioethanol. *Trend Biotechnol* 26(3):126–131
- Zhang SP (2003) Study of hydrodeoxygenation of bio-oil from the fast pyrolysis of biomass. *Energy Sources* 25(1):57–65
- Zhao HY, Li D, Buia P, Oyama ST (2011) Hydrodeoxygenation of guaiacol as model compound for pyrolysis oil on transition metal phosphide hydroprocessing catalysts. *Appl Catal Gen* 39(1):305–310
- Zhenyi D, Yecong L, Xiaoquan W, Yiqin W, Qin C, Chenguang W, Xiangyang L, Yuhuan L, Paul C, Roger R (2011) Microwave-assisted pyrolysis of microalgae for biofuel production. *Bioresour Technol* 102(7):4890–4896

# Chapter 11

## Heterogeneous Catalysts for Advanced Biofuel Production

Vorranutch Itthibenchapong, Atthapon Srifa,  
and Kajornsak Faungnawakij

**Abstract** The triglyceride-based feedstocks and biomass derivatives have been considered promising resources for production of advanced biofuels, namely, green diesel and biojet fuels. Among the series of deoxygenation reactions, hydrodeoxygenation is a majority in the green diesel production when utilizing the group of metal sulfides catalysts, namely, MoS<sub>2</sub> with various doping elements. Moreover, decarbonylation is predominant over sulfur-free catalysts including noble metals, e.g., Pd and Pt, and non-precious transition metal, e.g., Ni. The decarboxylation is an interesting pathway due to unconsumed H<sub>2</sub> reaction mechanism. As for biojet fuels, the composite of metal/metal sulfides with strong solid acids are promising approaches to catalyze hydroisomerization and cracking reactions of the straight-chain alkanes into the branch ones with proper carbon atoms. Alternatively, the alumina- and zeolite-supported metal catalysts have been extensively developed for the conversion of biomass derivatives into biojet fuels, fuel additives, and biochemical platforms. The research, development, and engineering of novel heterogeneous catalysts could be a key factor for commercialization and strong establishment of the biorefinery and biofuel industries.

**Keywords** Advanced biofuels • Bio-hydrogenated diesel • Biojet • Deoxygenation • Heterogeneous catalyst

### 11.1 Introduction

Biofuels are derived from biomass and its derivatives and used as fossil fuel substitutes. It is anticipated that biofuels produce less greenhouse gas emissions than fossil fuels, hence slowing down the global warming effect. This is due to the fact that biomass is a source of organic carbon in a carbon cycle that can be renewed faster. The heterogeneous catalysis is expected to be a key technology for effective

---

V. Itthibenchapong • A. Srifa • K. Faungnawakij (✉)  
National Nanotechnology Center (NANOTEC), National Science and Technology  
Development Agency (NSTDA), Khlong Luang, Pathumthani 12120, Thailand  
e-mail: [kajornsak@nanotec.or.th](mailto:kajornsak@nanotec.or.th)

and eco-friendly biorefinery. Not only biofuels and biochemicals but also various forms of solid materials can be produced from renewable resources. In the short-to-medium term solution, biofuels will largely contribute to the world energy supply. Lignocellulose materials, carbohydrates, and animal fats/vegetable oils are major groups of bio-based sources for biofuel and biochemical production (Bezergianni et al. 2011). The first generation biofuels have been widely used in various countries, while they are typically produced directly from food crops, including sugar and triglycerides via conventional technologies. The technology for production of bioethanol, biodiesel, and biogas has been well established. Currently, the biofuels are used in combustion engines by blending with fossil fuels to some extent, and the largest sector for liquid biofuel usage is in a transportation sector. Biodiesel is fatty acid methyl ester (FAMES), while bioethanol is alcohol. Therefore, the use of these biofuels still has some limitations due to their fuel properties.

More advanced and efficient conversion technologies thus are of importance to produce biofuels with improved fuel properties. In addition, the use of non-food feedstocks, namely, cellulosic biomass, is one of sustainable solution to serve the world energy consumption. In this context, advanced biofuels would refer to the next generation biofuels that provide better properties beyond the first generation biofuels. They would be produced from renewable and abundant feedstocks, such as fats, oils, or cellulosic materials. In particular, synthetic diesel, or called green diesel, and biojet fuels synthesized from catalytic hydro-processing will be focused. The heterogeneous catalysts are known to be key factors for the efficient conversion of the feedstocks to designed products. The novel nanostructured catalysts along with various state-of-the-art catalysts have been extensively used in the advanced biofuels production.

The simple chemical structure of glycerides makes it promising as biofuel feedstocks (Kubička and Kaluža 2010; Kumar et al. 2014). In particular, most vegetable oils contain long-chain fatty acids (C12–C20) which are suitable for green diesel and biodiesel. It is known that the direct combustion of triglycerides results in engine problems. Upgrading of triglycerides is therefore indispensable. One possibility is the reactions of triglycerides and alcohol into fatty acid methyl esters or biodiesel. In addition, the hydrotreating process can refine triglycerides into hydrocarbon-like biofuel (Peng 2012). It can be said that triglycerides would still play an important role as the most abundant biofuel feedstock in the present decades. Triglycerides, including waste cooking oil and animal fat, have been largely and continuously produced around the world when food-feed-waste management through a governmental policy is crucial (Peng 2012). On the other hand, the utilization of cellulosic material as an advanced biofuel has to be further developed to reduce the cost. A variety of product value-chains from biomass, such as biochemicals, bioplastics, advanced biofuels, and additives, etc., would make it cost-effective and economically feasible. This green carbon cycle would be realized by the integrated biorefinery concept.

The aim of this chapter is to present the recent developments of catalysts in the production of renewable advanced biofuels, especially green diesel and biojet fuels from vegetable oil, animal fat, and biomass derivatives. The focus is on the

heterogeneous catalysis concept of the related liquid-phase reactions, namely, hydrodeoxygenation, decarbonylation, decarboxylation, hydroisomerization, and cracking. The related gas-phase reactions are also discussed. In addition, the catalytic process and reaction behaviors are analyzed in detail to achieve the optimization operation of the process.

## 11.2 Nanocatalysts for Green Diesel Production

Biodiesel is alternative biofuel typically produced from triglyceride feedstock via transesterification reaction. Transesterification is generally defined as a chemical reaction between an ester bond and short-chain alcohol with or without a catalyst to generate esters and glycerol. A sequence of three reversible reactions starts from esterifying triglyceride to diglyceride and monoglyceride, respectively. Typically, 1 mol of triglyceride requires 3 mol of alcohol to generate 3 mol of their corresponding alkyl ester and 1 mol of glycerol. An excess of alcohol is generally applied to the reaction systems to increase the product yield. The use of biodiesel as a blend fuel with fossil diesel is recognized as one of the practical renewable energy policies, especially in the ASEAN countries. However, low thermal and oxidation stability of biodiesel due to the presence of the double bonds in the molecular structure showed major disadvantages in practical utilization (Liu et al. 2011; Wang et al. 2012).

Due to the disadvantages of biodiesel, green diesel, also known as green hydrocarbon and bio-hydrogenated diesel (BHD), which has similar molecular structure as petroleum diesel and provides better diesel properties, has attracted much attention for last decades. The deoxygenation process involves three main reaction pathways including decarbonylation, decarboxylation, and hydrodeoxygenation (Kubička and Kaluža 2010; Faungnawakij and Suriye 2013). As demonstrated in Fig. 11.1, firstly free fatty acids would be generated from hydrogenation of unsaturated triglyceride and hydrogenolysis of the resultant

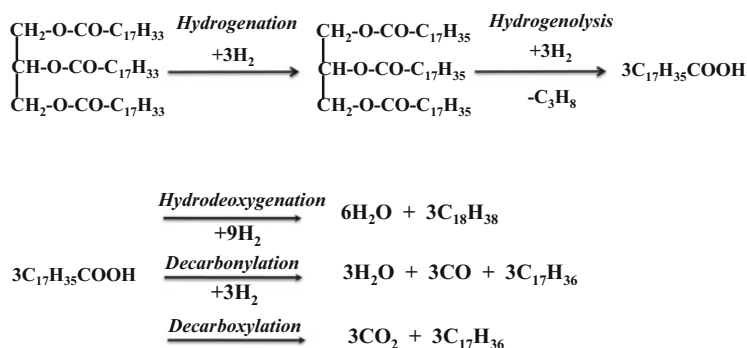


Fig. 11.1 Major reaction pathways of triglyceride deoxygenation

**Table 11.1** Overall deoxygenation reactions of fatty acid to green diesel, other related reactions, and thermodynamic data (Donnis et al. 2009; Kim et al. 2013; Satyarthi et al. 2013; Zhao et al. 2013)

Liquid phase	Reactions	$\Delta G_{533}$ (kJ/mol)	$\Delta H_{533}$ (kJ/mol)
Hydrodeoxygenation	$R-COOH + 3H_2 \rightarrow R-CH_3 + 2H_2O$	-88.0	-112.6
Decarbonylation	$R-COOH + H_2 \rightarrow R-H + CO + H_2O$	-59.5	49.7
Decarboxylation	$R-COOH \rightarrow R-H + CO_2$	-78.6	10.1
Gas phase	Reactions	$\Delta G_{533}$ (kJ/mol)	$\Delta H_{533}$ (kJ/mol)
Methanation	$CO + 3H_2 \rightarrow CH_4 + H_2O$	-88.4	-215.3
Methanation	$CO_2 + 4H_2 \rightarrow CH_4 + 2H_2O$	-69.2	-175.7
Water gas shift	$CO + H_2O \rightarrow CO_2 + H_2$	-19.1	-39.6

saturated triglyceride. Subsequently, hydrodeoxygenation, an exothermic reaction, eliminates oxygen from free fatty acids and yields *n*-alkane and water without a loss of carbon atom from their structures. On the other hand, endothermic reactions of decarbonylation and decarboxylation, respectively, produce CO/H<sub>2</sub>O and CO<sub>2</sub> during the deoxygenation process. As a result, one carbon atom is removed from the reactants (Snåre et al. 2006; Gong et al. 2012a). Other related gaseous reactions are methanation, cracking, hydrogenation, and water gas shift reactions. Typically, the decarbonylation, decarboxylation, and hydrodeoxygenation reactions can be proceed via free fatty acid intermediates (Table 11.1). The overall deoxygenation reaction of fatty acid to green diesel and thermodynamic data are summarized in Table 11.1. The hydrodeoxygenation combined with isomerization is the effective way to produce hydrocarbons with fuel property as good as found in conventional diesel, while the merit of transesterification is its mild reaction condition and easy operation (Priece et al. 2011).

The hydrodeoxygenation process optimization and catalysts have been intensively studied for upgrading of oil-based feedstocks, including vegetable oil, fats, and fatty acids. A sizable number of catalyst types have been employed in deoxygenation reactions. The conventional metal sulfide catalysts, namely, NiMo, CoMo, and NiW catalyst have been considered the state-of-the-art catalysts for deoxygenation. Alumina is known to a good catalyst support due to its excellent mechanical strength. Nonetheless, the strong interactions between Al<sub>2</sub>O<sub>3</sub> and metal or metal oxides gave some drawbacks on preventing complete sulfidation, resulting in low catalyst performance.

A study on the hydrotreating of sunflower oil over sulfide NiMo/Al<sub>2</sub>O<sub>3</sub> showed that the complete conversion with 70% product yield of alkanes (*n*-C<sub>15</sub> to *n*-C<sub>18</sub>) was achieved at 350 °C (Huber et al. 2007). The hydrotreating of triglycerides into alkanes proceeds via three major steps, namely, (1) hydrogenation of unsaturated triglycerides, (2) hydrogenolysis of saturated triglycerides to fatty acids and propane, and (3) deoxygenation of resultant fatty acids to alkanes. In the last step, the oxygen is removed in forms of CO and H<sub>2</sub>O for decarbonylation, CO<sub>2</sub> for decarboxylation, and H<sub>2</sub>O for hydrodeoxygenation.

In order to distinguish the role of each components in the sulfided NiMo, the deoxygenation of rapeseed oil over single- and bi-component was investigated in a fixed-bed reactor (Kubička and Kaluža 2010). The ability of the sulfided NiMo catalyst is superior to the sulfided Ni or Mo catalyst. NiS<sub>x</sub> catalysts were active in decarboxylation, while MoS<sub>x</sub> ones exclusively catalyzed hydrodeoxygenation pathway (Kubička and Kaluža 2010; Kubička and Tukač 2013). Likewise, in order to the understand the role of supports, Kubička et al. (2014) studied the interaction between the supports and NiMoS<sub>x</sub> in the deoxygenation of rapeseed oil. It turned out that TiO<sub>2</sub>-supported NiMo showed improved selectivity toward hydrodeoxygenation, while SiO<sub>2</sub>-supported one showed smaller extent of hydrogenation reactions and a higher selectivity to decarboxylation pathway.

Srifa et al. (2014) investigated the palm oil deoxygenation in a trickle-bed reactor with the aim at optimizing the operation conditions including temperature, H<sub>2</sub> pressure, LHSV, and H<sub>2</sub>/oil ratio. It turned out that the temperature played a crucial role on reaction pathways (decarbonylation, decarboxylation, hydrodeoxygenation, cracking, and isomerization reactions) over NiMoS<sub>2</sub>/γ-Al<sub>2</sub>O<sub>3</sub>, meanwhile the increase in the H<sub>2</sub> pressure promoted the hydrodeoxygenation. The recommended reaction conditions for high product yield (>95 %) were as follows: temperature, 300 °C; pressure, 3.0–5.0 MPa; LHSV, 1–2 h<sup>-1</sup>; and H<sub>2</sub>/oil ratio, 750–1000 N(cm<sup>3</sup>/cm<sup>3</sup>).

As mentioned above, the transition metal sulfide catalysts provided the high catalytic activity through the hydrodeoxygenation reaction. However, the metal sulfide can be deactivated during the triglyceride conversion. The sulfur leaching not only leads to catalyst degradation but also sulfur contamination in the product (Peng et al. 2012a, b, 2013; Liu et al. 2014). To avoid the catalyst degradation, sulfiding agents, e.g., CS<sub>2</sub> and DMDS, should be added into the oil feed (Ochoa-Hernández et al. 2013; Chen et al. 2014). Furthermore, water generated from the reactions brought about the sulfur leaching and shorten the catalysts' lifetime (Zhao et al. 2013). As reported in the literatures (Zhao et al. 2013), the rapeseed oil conversion during the hydrotreating process over a sulfided NiMo/Al<sub>2</sub>O<sub>3</sub> declined as a function of time when without a source of H<sub>2</sub>S co-feed. In contrast, the catalyst performances were significantly improved when dimethyl disulfide was co-fed along with rapeseed oil. It was suggested that the admixing of sulfiding agents suppressed the deactivation of catalyst. The examples of feedstocks and experimental conditions using metal sulfide catalysts reported in literatures are summarized in Table 11.2.

Recently, the sulfur-free metal catalysts such as Ni (Veriansyah et al. 2012; Zuo et al. 2012; Ochoa-Hernández et al. 2013; Santillan-Jimenez et al. 2013a; Kumar et al. 2014), Co (Ochoa-Hernández et al. 2013; Liu et al. 2014), Pd (Simakova et al. 2009; Mäki-Arvela et al. 2011; Duan et al. 2012), Pt (Chen et al. 2013), and Ru (Chen et al. 2011, 2012) have been proposed as green diesel production catalysts. Over these metallic catalysts, the major gaseous reactions were methanation and water gas shift reactions. It is worth noting that these reactions are not dominant over sulfide catalysts. The metal catalysts have become potential deoxygenation catalysts (Do et al. 2009; Murata et al. 2010) because of (1) good reactivity at

**Table 11.2** Deoxygenation of triglycerides over metal sulfide catalysts

Feedstock	Catalyst	Reactor type	Condition	Main product	Performance	Refs
Sunflower oil	1. CoMo/Al <sub>2</sub> O <sub>3</sub>	Fixed bed	$T = 360\text{--}380\text{ }^{\circ}\text{C}$ $P = 6\text{--}8\text{ MPa}$ $\text{LHSV} = 1.0\text{--}1.2\text{ h}^{-1}$ $\text{H}_2/\text{oil ratio} = 450\text{ Nm}^3/\text{m}^3$	n-paraffins and iso-paraffins C <sub>11</sub> –C <sub>19</sub>	1. Conversion: 94–99.8 % Yield: 63.1–71.5 % 2. Conversion: 81.8–97.4 % Yield: 42–52.9 % 3. Conversion: 86.7–95.6 % Yield: 9.4–49.3 %	Hancsók et al. (2012)
	2. NiMo/Al <sub>2</sub> O <sub>3</sub>					
	3. NiW/Al <sub>2</sub> O <sub>3</sub>					
Sunflower oil	NiMo/Al <sub>2</sub> O <sub>3</sub> –F	Fixed bed	$T = 350\text{--}370\text{ }^{\circ}\text{C}$ $P = 2\text{--}4\text{ MPa}$ $\text{LHSV} = 1.0\text{ h}^{-1}$ $\text{H}_2/\text{oil ratio} = 500\text{ Nm}^3/\text{m}^3$	n-paraffins C <sub>15</sub> –C <sub>18</sub>	Yield: 73.2–75.6 %	Kovács et al. (2011)
Sunflower oil	CoMo/Al <sub>2</sub> O <sub>3</sub>	Fixed bed	$T = 380\text{ }^{\circ}\text{C}$ $P = 4\text{--}6\text{ MPa}$ $\text{LHSV} = 1.0\text{ h}^{-1}$ $\text{H}_2/\text{oil ratio} = 500\text{--}600\text{ Nm}^3/\text{m}^3$	n-paraffins C <sub>15</sub> –C <sub>18</sub>	Yield: 73.7–73.9 %	Krář et al. (2010)
Palm oil	NiMo/Al <sub>2</sub> O <sub>3</sub>	Fixed bed	$T = 300\text{ }^{\circ}\text{C}$ $P = 5\text{ MPa}$ $\text{LHSV} = 1.0\text{ h}^{-1}$ $\text{H}_2/\text{oil ratio} = 1000\text{ Nm}^3/\text{m}^3$	n-paraffins C <sub>15</sub> –C <sub>18</sub>	Conversion 100 % Yield: 89.8 %	Sriifa et al. (2014)
Palm oil	NiMo/Al <sub>2</sub> O <sub>3</sub>	Fixed bed (Pilot plant)	$T = 350\text{ }^{\circ}\text{C}$ $P = 4\text{--}9\text{ MPa}$ $\text{LHSV} = 2\text{ h}^{-1}$	n-paraffins C <sub>15</sub> –C <sub>18</sub>	Molar yield: 100 %	Guzman et al. (2010)



Jatropha oil	NiMo/Al <sub>2</sub> O <sub>3</sub> - SiO <sub>2</sub>	Fixed bed	<p><math>T = 350\text{ }^{\circ}\text{C}</math>  <math>P = 3\text{ MPa}</math>  <math>\text{LHSV} = 2\text{ h}^{-1}</math>  <math>\text{H}_2/\text{oil ratio} = 600\text{ mL/mL}</math></p>	n-paraffins C <sub>15</sub> -C <sub>18</sub>	Yield: 82.4–88.2 %	Gong et al. (2012b)
Waste cooking oil	NiMo/Al <sub>2</sub> O <sub>3</sub>	Fixed bed	<p><math>T = 350\text{--}390\text{ }^{\circ}\text{C}</math>  <math>P = 1.37\text{ MPa}</math>  <math>\text{LHSV} = 0.5\text{--}2.5\text{ h}^{-1}</math>  <math>\text{H}_2/\text{oil ratio} = 1068\text{ m}^3/\text{m}^3</math></p>	n-paraffins C <sub>15</sub> -C <sub>18</sub>	Yield: 73–82 %	Bezegeanni and Kalogianni (2009)

relatively low temperature, (2) low H<sub>2</sub> consumption, (3) high energy efficiency, (4) no sulfur leaching, and (5) flexibility of catalyst design and synthesis.

The catalytic deoxygenation of fatty acids typically palmitic acid (Simakova et al. 2009; Peng et al. 2013), stearic acid (Lestari et al. 2009; Immer et al. 2010; Santillan-Jimenez et al. 2013a, b; Kumar et al. 2014), and oleic acid (Immer et al. 2010) has been extensively studied in the literatures. Hydrogenolysis of triglycerides produces free fatty acids which are the major intermediate components in the deoxygenation of triglycerides (Kim et al. 2013, 2014). Pd/C and Pt/C catalysts exhibited overwhelming activity among various types of metal catalysts, including Ru, Mo, Rh, Ir, and Os (Snåre et al. 2006). The decarboxylation and decarbonylation pathways were dominant over Pd/C and Pt/C catalysts, respectively. Besides, complex reaction networks of hydrogenation, dehydrogenation, cyclization, ketonization, dimerization, and cracking simultaneously underwent during the deoxygenation. Duan et al. (2012) investigated the sunflower oil hydrodeoxygenation over Pd/Al-SBA-15 and Pd/HZSM-5 with various Al/Si ratios in the temperature range of 250–300 °C. The Pd/Al-SBA-15(Si/Al = 300) showed the best activity, while the increment of the reaction temperature was in favor of C-C bond breaking. In comparison between Ni/C and Pd/C (Santillan-Jimenez et al. 2013b), Ni/C favors the adsorption and the cracking reactions due to the greater acidity.

Meanwhile, the high price of noble metal also limits its potential use in an industrial application. The use of non-precious metal catalyst for the deoxygenation reactions was more attractive than the use of noble metal ones. The Ni-based catalyst is one of the most promising non-precious metal catalysts, which exhibits the high catalytic deoxygenation activity in catalyzing the fatty acids and vegetable oil. Peng et al. (2012a) explored the catalytic deoxygenation of stearic acid over Ni supported on ZrO<sub>2</sub>, TiO<sub>2</sub>, CeO<sub>2</sub>, TiO<sub>2</sub>, and Al<sub>2</sub>O<sub>3</sub> at 260 °C under 4.0 MPa H<sub>2</sub> in the batch reactor. The results showed that pure ZrO<sub>2</sub> resulted in 13 % conversion of the stearic acid with 3.2 % *n*-heptadecane selectivity. The 10 % Ni/ZrO<sub>2</sub> was superior to the other catalysts and provided the 100 % conversion and 96 % selectivity to *n*-heptadecane. The 10 % Ni/TiO<sub>2</sub> and 10 % Ni/CeO<sub>2</sub> exhibited slightly lower selectivities to *n*-heptadecane. Besides, the Ni/Al<sub>2</sub>O<sub>3</sub> and Ni/SiO<sub>2</sub> gave the lowest activity of 45–63 % conversion with 80–90 % *n*-heptadecane selectivity. A non-pyrophoric RANEY-type Ni catalyst was proposed for the deoxygenation in a flow-through reactor at 340 °C and 2.1 MPa of H<sub>2</sub> (Onyestyák et al. 2012). High conversion was achieved over RANEY-type Ni catalyst through the decarbonylation and decarboxylation reactions. It also provided the higher activity in methanation and C–C bond scission, as compared with Ni/Al<sub>2</sub>O<sub>3</sub>.

The mechanism of the deoxygenation reactions was mostly exposed based on a model compound study. The hydrodeoxygenation of stearic acid to hydrocarbons was studied in a batch-type reactor using *n*-dodecane as solvent over Ni catalysts supported on different supports, including SiO<sub>2</sub>,  $\gamma$ -Al<sub>2</sub>O<sub>3</sub>, and HZSM-5 (Kumar et al. 2014). The *n*-pentadecane, *n*-hexadecane, *n*-heptadecane, *n*-octadecane, and 1-octadecanol were detected during the tests. A reaction mechanism of hydrodeoxygenation of stearic acid was described based on product distribution.

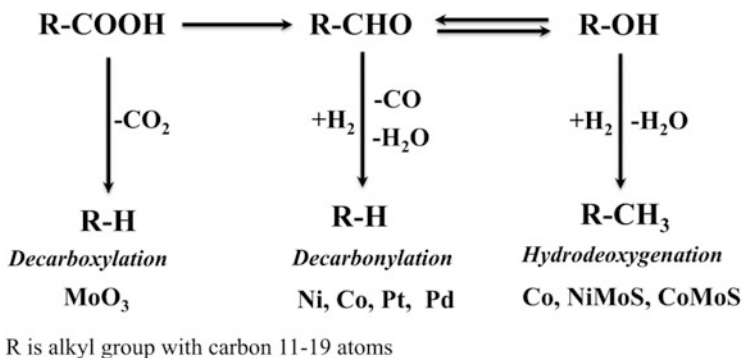


**Fig. 11.2** Deoxygenation of free fatty acids over different types of heterogeneous catalysts

Hydrogenolysis of stearic acid first proceeds to form octadecanal and water. Subsequently, octadecanal was hydrogenated to octadecanol. It should be noted that octadecanal was not observed during oleic acid deoxygenation, suggesting the good reaction rate of decarbonylation of octadecanal to heptadecane. The reaction mechanisms for the oleic acid deoxygenation was similar to those found in the case of stearic acid (Srifai et al. 2015a).

Figure 11.2 demonstrates the preferable reaction pathways over different types of catalysts. The free fatty acids would be similarly produced from hydrogenation/hydrogenolysis of triglycerides. After that, the produced fatty acids were converted to fatty acid aldehyde and/or alcohol. The hydrocarbon products were finally obtained from those intermediates. The decarbonylation is generally dominant on metallic sites of Ni and Pd. It is interesting that the Co species could effectively catalyzed both hydrodeoxygenation and decarbonylation pathways. In contrast, a major pathway is on hydrodeoxygenation when metal sulfide catalysts ( $\text{MoS}_2$ ,  $\text{NiMoS}_2$ , and  $\text{CoMoS}_2$ ) are used. Interestingly, decarboxylation, which needs no hydrogen gas reactant, can proceed over  $\text{MoO}_3$  catalyst, although its performance still needs significant improvement. The stability of the metal and metal oxide catalyst is considered a key factor for successful development and practical use. On the contrary, the green diesel can be produced by animal fat though the hydrodeoxygenation. Kaewmeesri et al. (2015) reported the effect of water and fatty acid on the deoxygenation of chicken fats on a supported nickel catalyst in a continuous flow process. Decarbonylation and/or decarboxylation were found to be the major reaction in producing green diesel. Meanwhile, methane, a major gas product, was formed via methanation and the propane cracking. The free fatty acid and water content showed a positive effect to yield the green diesel. Especially, the water expedited triglyceride conversion to fatty acids, mainly palmitic acid and stearic acid. Consequently, raw waste chicken fat is a potential feedstock for green diesel. Table 11.3 summarizes the feedstock, reaction parameters, and major products in the hydrodeoxygenation of triglycerides, fatty acids, and animal fat using metal catalysts.

**Table 11.3** Deoxygenation of triglycerides, fatty acids, and waste chicken fat over metal catalysts

Feedstock	Catalyst	Reactor type	Condition	Main product	Performance	Refs
Stearic acid	Pd, Pt, Ru, Mo, Ni, Rh, Ir, and Os supported on carbon, Al <sub>2</sub> O <sub>3</sub> , and SiO <sub>2</sub>	Batch	T = 300 °C P = 0.6 MPa	n-paraffins C <sub>17</sub>	Conversion: 4.6–100 % C <sub>17</sub> selectivity: 1–95 %	Snare et al. (2006)
Tall oil fatty acid	1 wt% Pd/C	Semi-batch	T = 300–325 °C P = 1.7 MPa	n-paraffins C <sub>17</sub>	Conversion: 32 % (1 % H <sub>2</sub> /Ar) 59 % (100 % H <sub>2</sub> ) Yield: 72 % (1 % H <sub>2</sub> /Ar) 91 % (100 % H <sub>2</sub> )	Mäki-Arvela et al. (2011)
Palm oil	Pd/C	Batch	T = 400 °C P = 4 MPa Reaction time = 2 h	n-paraffins C <sub>15</sub> –C <sub>18</sub>	Yield: 51–70 wt. %	Kiatkitipong et al. (2013)
Soybean oil	Ni/SiO <sub>2</sub> –Al <sub>2</sub> O <sub>3</sub>	Batch	T = 400 °C P = 9.2 Mpa	n-paraffins C <sub>17</sub> –C <sub>18</sub>	Diesel yield: 90 %	Kim et al. (2013)
Palm oil	Pd, Pt, Ni, and Co supported on Al <sub>2</sub> O <sub>3</sub>	Fixed bed	T = 300 °C P = 5 MPa LHSV = 1.0 h <sup>-1</sup> H <sub>2</sub> /oil ratio = 1000 Nm <sup>3</sup> /m <sup>3</sup>	n-paraffins C <sub>15</sub> –C <sub>18</sub>	Conversion: 100 % Yield: 70–90 %	Srifa et al. (2015b)
Palm oil	Ni/SAPO-11	Fixed bed	T = 200 °C P = 4 MPa LHSV = 2 h <sup>-1</sup>	n-paraffins and <i>iso</i> -paraffins	Yield: 80 %	Liu et al. (2013a, b)

Waste chicken fat	Ni/Al <sub>2</sub> O <sub>3</sub>	Fixed bed	H <sub>2</sub> /oil ratio = 1000 Nm <sup>3</sup> /m <sup>3</sup>	n-paraffins C <sub>15</sub> -C <sub>18</sub>	Conversion: 100 % Yield: 75 %	Kaewmeesri et al. (2015)
			T = 350 °C			
			P = 5 MPa			
			LHSV = 5 h <sup>-1</sup>			
			H <sub>2</sub> /oil ratio = 1000 Nm <sup>3</sup> /m <sub>3</sub>			

### 11.3 Nanocatalysts for Biojet Fuel Production

The petroleum jet fuel for transportation (e.g., Jet A, Jet A-1) and military aircrafts (e.g., JP-8, JP-4) typically comprise paraffins (kerosenes) as the main component with some of aromatics and naphtha. According to the Agency for Toxic Substances and Disease Registry (ATSDR), US, in 2015, the JP-4 (Jet A-1) fuel is provided by 60–80 % of straight-chain (*n*-alkanes) and branched chain (*i*-alkanes) hydrocarbon with carbon number in a range of C<sub>7</sub>–C<sub>15</sub> (C<sub>10</sub>–C<sub>12</sub> as a majority); the short-medium chains of hydrocarbon compared with those in diesel fuel.

The presence of branched alkanes and aromatics improves heating value, energy density, and cold flow properties, e.g., pour point and cloud point (Lown et al. 2014; Choi et al. 2015), enabling the application in a very low temperature condition which is crucial for the military and commercial aircrafts. Hydro-processing of triglyceride-based feedstocks have been approved for blending and have a defined ASTM specification. The natural fat and oil obtained from animal and plant contained an even number of carbon mostly in C<sub>12</sub>, C<sub>14</sub>, C<sub>16</sub>, and C<sub>18</sub> fatty acids; C<sub>16</sub> and C<sub>18</sub> fatty acids are much more abundant than those of C<sub>12</sub> and C<sub>14</sub> in both animal and plant triglycerides. For biojet fuel production, the C<sub>12:0</sub> fatty acid (lauric acid) found in coconut oil, laurel oil, babassu oil, and palm kernel oil (not to be confused with palm oil) is a favorable feedstock with minimum and simplified hydro-conversion steps. Nonetheless, the feedstocks containing long-chain fatty acids like C<sub>16</sub> and C<sub>18</sub> obtained from soybean oil, jatropha oil, palm oil, sunflower oil, rapeseed oil, cow fat, and chicken fat are also applicable with cracking to smaller units. Aside from fat and oil of animal and plant, biodiesel (FAMES), microalgae oil, and bio-oil produced by pyrolysis of biomass could be considered as alternative feedstocks for upgrading their fuel quality.

Depending on the characteristic of the triglyceride feedstocks, the hydro-process remains the major reactions including deoxygenation and hydrogenation to remove oxygenated compounds and obtain *n*-alkanes. Hydroisomerization becomes important to produce a certain amount of branched alkane mixture to reach low cloud point according to the ASTM standard. Hydrocracking is necessary to reduce the alkane chain if the fat and oil contain long-chain triglycerides, e.g., C<sub>16</sub> and C<sub>18</sub>. Degree of isomerization and cracking has to be controlled through catalysts and operating conditions. The hydro-process catalysts for jet fuel-ranged hydrocarbon production are similar to those in green diesel; however, the acidic property in catalysts is required to promote hydroisomerization and hydrocracking. The single-step production of *n*- and *i*-alkanes has been reported by using acidic solid supports especially ZSM-5 and SAPO-11 combined with metal and metal sulfide as the active phases for deoxygenation. The Ni, Pd, and Pt are common metallic catalysts, whereas MoS<sub>2</sub> and WS<sub>2</sub> with Ni and Co promoters, similar to HDS catalysts, are conventionally and widely used for deoxygenation catalysts. Since the molybdenum (Mo) and tungsten (W) are prepared in metal oxide form, i.e., MoO<sub>3</sub> and WO<sub>3</sub>, before sulfurization, NiMoS<sub>2</sub> or CoMoS<sub>2</sub> are similar to sulfided NiMo or CoMo in literatures. Interestingly, the NiO-MoO<sub>3</sub> oxide catalyst was observed as an acidic

property and then after reduction at 450 °C, the high surface density of Mo<sup>4+</sup> and Mo<sup>5+</sup> species can promote deoxygenation activity and selectivity toward isomerization, respectively. The synergetic effect of the nickel metal and Mo<sup>4+</sup> species at the catalyst surface by reduction at 450–500 °C is responsible for the high selectivity of hydrodeoxygenation (Chen et al. 2015a, b). For the acidic supporting material, the H-ZSM-5 (aluminosilicate zeolite, pore diameter of 0.53–0.56 nm) is well known for its high acidity among the microporous supporting materials and generally used in catalytic cracking and isomerization. The moderate acidity SAPO-11, aluminosilico-phosphate zeolite with 2D pore diameter of 0.39 nm × 0.63 nm, has been proposed as a good isomerization (Mériaudeau et al. 1999) over cracking. Zeolitic materials are good catalyst supports in many industrial catalytic processes due to their well-defined porous structure, high thermal stability, and strong acidity. The small pore size of zeolites however limits the access to bulky molecules such as fat and oil; therefore, the larger pore diameter, e.g., modified-mesoporous materials and hybrid micro-meso porous zeolites (Verma et al. 2011), is beneficial while remaining of acidity and crystalline pore structure for hydro-processing of triglyceride-based feedstock.

The catalytic condition for deoxygenation in the presence of high H<sub>2</sub> pressure of 2–8 MPa can be ranged from 270 to 400 °C, in typically 300–350 °C. The hydroisomerization is generally good activity with acid solid catalysts around 300–370 °C. The too high reaction temperature such as 400 °C or higher can lead to thermal cracking as a side reaction as well as the increasing of hydrocracking activity resulting in light hydrocarbon (C1–C4) as by-products and decreasing in the yield of jet fuel range alkanes. The examples of feedstocks and catalytic condition recently reported in literatures are represented in Table 11.4.

The hydroisomerization and cracking are generally proposed as the later steps of producing branched chain hydrocarbons from the straight-chain hydrocarbons obtained from deoxygenation of fat and oil feedstocks. The reaction pathways occurring in hydrocarbons cracking over strong acid zeolites such as H-ZSM-5 involve with a series of reaction steps where light olefins are generated mainly from β-scissions (through Brønsted acid sites) and also by a protolysis mechanism (forming carbenium species) on acid sites of zeolites (Maia et al. 2010). The Lewis acid sites, generated by metal or metal oxide loading on the catalyst support, promotes dehydrogenation reaction leading to isomerization, cyclization, and aromatization (Botas et al. 2012; Kim et al. 2014; Sattler et al. 2014; Musselwhite et al. 2015) as shown in Fig. 11.3; Mo-oxide catalysts are known for dehydrogenation of alkanes to produce alkenes. To maximize *i/n*-alkane ratio, mild acidity of the catalyst supporting material is preferable, e.g., SAPO-11, Al-SBA-15, and zeolite beta (Kordulis et al. 2016).

The commercial scale processes of green diesel and green aviation fuel have been successfully developed by a Finnish company, Neste Oil as NEXBTL (Jakkula et al. 2004) and UOP as Ecofining<sup>TM</sup> process (Kalnes et al. 2009). Both processes consist of (1) hydrodeoxygenation and (2) hydroisomerization/selective cracking. Nevertheless, to attain desirable hydrocarbons, a great amount of hydrogen is required, i.e., 300–500 m<sup>3</sup> of H<sub>2</sub>/m<sup>3</sup> of vegetable oil. The sufficient hydrogen

**Table 11.4** Hydrotreating of triglyceride-based feedstock into jet fuel-range hydrocarbons

Feedstock	Catalyst	Reactor type	Condition	Performance	Refs.
Waste soybean oil (majority = C <sub>16</sub> and C <sub>18</sub> )	Pd/zeolite beta	Batch reactor	300 °C, 6 h, N <sub>2</sub> = 1.5 MPa	C <sub>12</sub> -C <sub>18</sub> yield ≈ 31 %, C <sub>12</sub> -C <sub>18</sub> hydrocarbons selectivity = 60.77 %, 23.48 % of <i>n</i> -hydrocarbons and 16.15 % of <i>i</i> -hydrocarbons	Choi et al. (2015)
Palm fatty acid distillate (PFAD) (majority = C <sub>18</sub> )	Pd/zeolite beta	Batch reactor	300 °C, 6 h, N <sub>2</sub> = 1.5 MPa	C <sub>12</sub> -C <sub>18</sub> yield ≈ 31 %, C <sub>12</sub> -C <sub>18</sub> hydrocarbons selectivity = 67.07 %, 15.75 % of <i>n</i> -hydrocarbons and 16.78 % of <i>i</i> -hydrocarbons	Choi et al. (2015)
Waste cooking oil (majority = C <sub>18</sub> )	Ni/mesoporous zeolite Y	Batch reactor	400 °C, 8 h, H <sub>2</sub> = 3 MPa	Jet-ranged alkanes yield = 40.5 %, aromatics yield = 11.3 %, aliphatic selectivity = 53 %, aromatic selectivity = 13.4 %	Li et al. (2015a)
Bio-oil from pyrolysis of Douglas-fir sawdust (C <sub>8</sub> -C <sub>15</sub> = 60 %)	Rayney-Ni/ZSM-5	Batch reactor	300 °C, 12 h, H <sub>2</sub> = 3.4 MP	Jet-ranged alkanes selectivity = 12.63 %, aromatics selectivity = 19.48 %	Zhang et al. (2015)
Methyl laurate (lauric acid methyl ester)	Reduced NiMoO <sub>3-x</sub> /SAPO-11	Fixed bed reactor	300 °C, H <sub>2</sub> = 3 MPa, WHSV = 5 h <sup>-1</sup> , H <sub>2</sub> /feed = 800 (v/v)	Conversion = 75.72 %, C <sub>11</sub> selectivity = 6.4 %, C <sub>12</sub> selectivity = 65.1 %	Chen et al. (2015a, b)
Jatropha oil (majority = C <sub>18</sub> )	Sulfided Ni <sub>2</sub> W/SiO <sub>2</sub> -Al <sub>2</sub> O <sub>3</sub>	Continuous flow reactor	420 °C, H <sub>2</sub> = 8 MPa, LSHV = 1 h <sup>-1</sup> , H <sub>2</sub> :feed ratio = 1500 (v/v)	Conversion = 99 %, C <sub>9</sub> -C <sub>15</sub> yield = 33.2 %, <i>i</i> -alkanes/ <i>n</i> -alkanes ratio (C <sub>9</sub> -C <sub>15</sub> ) = 1.1	Verma et al. (2011)
Jatropha oil (majority = C <sub>18</sub> )	Sulfided Ni <sub>2</sub> W/HZSM-5	Continuous flow reactor	400 °C, H <sub>2</sub> = 6 MPa, LSHV = 1 h <sup>-1</sup> , H <sub>2</sub> :feed ratio = 1500 (v/v)	Conversion = 99 %, C <sub>9</sub> -C <sub>15</sub> yield = 39.6 %, <i>i</i> -alkanes/ <i>n</i> -alkanes ratio (C <sub>9</sub> -C <sub>15</sub> ) = 5.2	Verma et al. (2011)



Jatropha oil (majority = C <sub>18</sub> )	Sulfided NiMo/ HZSM-5	Continuous- flow reactor	400 °C, H <sub>2</sub> = 8 MPa, LHSV = 1 h <sup>-1</sup> , H <sub>2</sub> :feed ratio = 1500 (v/v)	Conversion = 99%, C <sub>9</sub> -C <sub>15</sub> yield = 38.3%, <i>i</i> -alkanes/ <i>n</i> -alkanes ratio (C <sub>9</sub> - C <sub>15</sub> ) = 13.5	Verma et al. (2011)
Algal oil (majority = C <sub>16</sub> and C <sub>18</sub> )	Sulfided NiMo/ HZSM-5	Continuous flow reactor	410 °C, H <sub>2</sub> = 5 MPa, LHSV = 1 h <sup>-1</sup> , H <sub>2</sub> :feed ratio = 1500 (v/v)	Conversion = 98%, C <sub>9</sub> -C <sub>15</sub> yield = 78.5%, <i>i</i> -alkanes/ <i>n</i> -alkanes ratio (C <sub>9</sub> - C <sub>15</sub> ) = 2.5	Verma et al. (2011)
Coconut oil (majority = C <sub>12</sub> and C <sub>14</sub> )	Bimetallic Mo-Ni/ $\gamma$ -Al <sub>2</sub> O <sub>3</sub>	Continuous -flow reactor	350 °C, H <sub>2</sub> = 0.8 MPa, LHSV = 1 h <sup>-1</sup> , molar ratio of H <sub>2</sub> :oil = 15	Conversion = 96.9%, C <sub>7</sub> -C <sub>16</sub> yield ≈ 70%, C <sub>11</sub> yield = 25.8%, C <sub>12</sub> yield = 13.5%	Kimura et al. (2013)
Soybean oil, sunflower oil, camelina oil, palm oil, tallow oil, castor oil (majority = C <sub>16</sub> and C <sub>18</sub> )	Pt/Al <sub>2</sub> O <sub>3</sub> /SAPO- 11	Trickle-bed reactor	370 °C, H <sub>2</sub> = 3.0 MPa, LHSV = 1 h <sup>-1</sup> , H <sub>2</sub> flow rate of 200 NmL/min	Liquid product yield = 78-85 wt%, aromatic content = 0.2-2.8 wt%	Rabaev et al. (2015)
Jatropha oil (majority = C <sub>16</sub> and C <sub>18</sub> )	NiMoS <sub>2</sub> / mesoporous SAPO-11	Trickle-bed reactor	450 °C, H <sub>2</sub> = 6.0 MPa, LHSV = 1 h <sup>-1</sup>	Conversion = 99+%, C <sub>9</sub> -C <sub>15</sub> yield = 37.5% yield, <i>i</i> -alkanes/ <i>n</i> -alkanes = 4.8, aromatics = 8%	Verma et al. (2015)
Castor oil (majority = C <sub>18</sub> )	25% Ni/USY-APTES- MCM-41 (APTES: 7.5%)	Continuous flow fixed- bed reactor	300 °C, H <sub>2</sub> = 3 MPa, WHSV = 2 h <sup>-1</sup> , H <sub>2</sub> flow rate = 160 mL/min	Conversion = 99%, C <sub>8</sub> -C <sub>15</sub> yield = 80.3%, <i>i</i> -alkanes/ <i>n</i> -alkanes (C <sub>8</sub> -C <sub>15</sub> ) = 4.4	Liu et al. (2015)

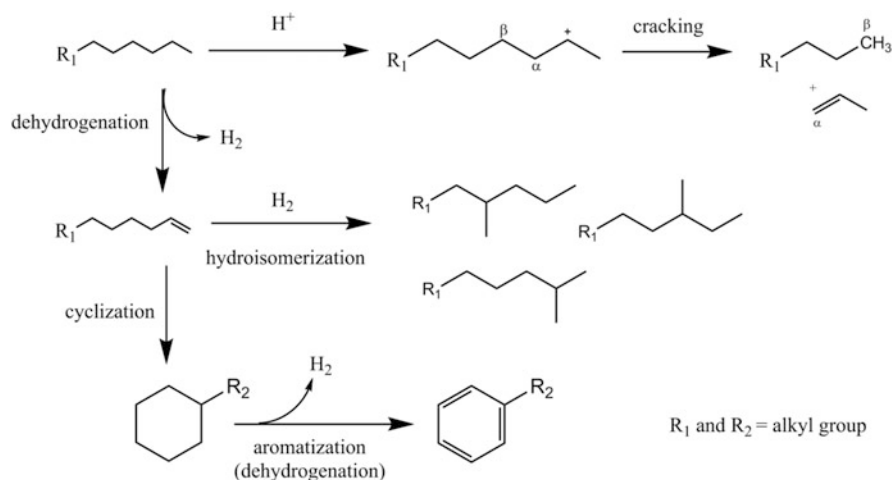


**Fig. 11.3** Cracking, isomerization, and cyclization pathways of *n*-alkanes to *i*-alkanes and cyclic products

source and production rate provided for large-scale production has become a great challenge for low cost and widespread utilization of this technology to produce renewable diesel and biojet fuel.

Hence, the approach of lower amount of H<sub>2</sub> consumption in hydro-processing has been attempted to overcome that issue. Unconventional deoxygenation conditions under low H<sub>2</sub> pressure or absence of H<sub>2</sub> at reaction temperature of 300–400 °C have been reported by using Pd (Kubičková et al. 2005; Snåre et al. 2006; Choi et al. 2015), Mo (Prasomsri et al. 2014), and Ni-Mo (Kimura et al. 2013) catalysts and fatty acid model compound (e.g., palmitic acid, stearic acid, and oleic acid) as reactants. The operating condition under the inert gas, e.g., N<sub>2</sub>, He, and Ar, leads to decarboxylation pathway (Snåre et al. 2006; Choi et al. 2015; Hermida et al. 2015) instead of hydrodeoxygenation which is dominant in an H<sub>2</sub>-rich atmosphere. However, the low or zero H<sub>2</sub> usage in deoxygenation process seems to face some problems related to catalyst stability and low alkane yield in comparison to those in conventional deoxygenation process. Reported in a work of Kubičková et al. (2005), the Pd/activated carbon catalyzed decarboxylation of stearic acid resulted in only conversion of 40% and C<sub>17</sub> selectivity of 70% under 1.7 MPa mixture of H<sub>2</sub>-Ar at 300 °C; while the reaction achieved the 100% conversion with C<sub>17</sub> selectivity of 45% at 360 °C and pressure of 4.0 MPa. Recently, the improvement of the decarboxylation product yield has been reported by using Pt over acidic supporting (Yang et al. 2015).

The hydrodeoxygenation process has been applied to the conversion of lignocellulosic and hemicellulosic biomass into jet fuel-ranged alkanes as the final step to remove oxygenated component in the product yielded by the prior pretreatment process including dehydration and aldol condensation. For example, demonstrated in Table 11.5, the xylose sugar from hemicellulosic biomass is converted to furfural through dehydration, then the aldol condensation of furfural (C<sub>5</sub>) with a ketone

**Table 11.5** Examples of catalytic conversion of biomass-based feedstock into jet fuel-ranged hydrocarbon

Feedstock	Catalyst	Reactor type	Condition	Performance	Refs
Furfural + 2-pentanone	1. CaO (aldol condensation) 2. Pd/HZSM-5 (HDO)	1. Batch reactor 2. Continuous flow reactor	1. 403 K, 6 h 2. 533 K, H <sub>2</sub> = 6 MPa, H <sub>2</sub> flow rate = 120 mL/min, feed flow rate = 0.04 mL/min	1. Conversion = 98.3 %, yield = 86.7 % 2. Conversion = 100 %, C <sub>9</sub> -C <sub>10</sub> yield ≈ 90 %	Yang et al. (2014)
Furfural + 3-pentanone	1. CaO (aldol condensation) 2. Co/SiO <sub>2</sub> , Ni/SiO <sub>2</sub> , Cu/SiO <sub>2</sub> (HDO)	1. Batch reactor 2. Continuous flow reactor	1. 443 K, 8 h 2. 623 K, H <sub>2</sub> = 6 MPa, H <sub>2</sub> flow rate = 120 mL/min, feed flow rate = 0.04 mL/min	1. Conversion = 80 %+, yield ≈ 60 % 2. Conversion = 100 %, C <sub>8</sub> -C <sub>10</sub> yield = 60–75 %	Chen et al. (2015a, b)
Furfural + acetone	1. THF + NaOH (aldol condensation) 2. Ru/Al <sub>2</sub> O <sub>3</sub> (Diels-Alder addition) 3. Pt/SiO <sub>2</sub> -Al <sub>2</sub> O <sub>3</sub> (HDO)	1. Batch 2. Batch 3. Continuous flow reactor	1. Room temperature, 1 h 2. 80–140 °C, 7 h, H <sub>2</sub> = 5.52–8.27 MPa 3. 300 °C, H <sub>2</sub> = 8.27 MPa, H <sub>2</sub> flow rate = 155 mL/min, feed flow rate = 0.02 mL/min	1. Yield = 16 % 2. Light products selectivity ≈ 5–20 % and heavy products selectivity ≈ 70–80 % 3. C <sub>13</sub> selectivity = 36.2 %	Olcay et al. (2013)

(continued)

Table 11.5 (continued)

Feedstock	Catalyst	Reactor type	Condition	Performance	Refs
Xylose + methyl isobutyl ketone (MIBK)	<ol style="list-style-type: none"> <li>1. HZSM-5, H-MOR, ZrP (dehydration)</li> <li>2. CaO, Ca(OH)<sub>2</sub> (aldol condensation)</li> <li>3. Ru/HZSM-5 (HDO)</li> </ol>	<ol style="list-style-type: none"> <li>1. Batch</li> <li>2. Batch</li> <li>3. Continuous flow reactor</li> </ol>	<ol style="list-style-type: none"> <li>1. 180 °C</li> <li>2. 180 °C, 5 h</li> <li>3. 300 °C, H<sub>2</sub> = 6 MPa, H<sub>2</sub> flow rate = 120 mL/min</li> </ol> <ol style="list-style-type: none"> <li>1. feed flow rate = 0.04 mL/min</li> </ol>	<ol style="list-style-type: none"> <li>1. Conversion = 60–90 %, furfural yield = 40–60 %, furfural selectivity = 60–70 %</li> <li>2. Conversion = 50–87 %, yield = 40–80 %, selectivity of FMI(BK (furan-2-yl)-5-methylhex-1-en-3-one = 83–92 %</li> <li>3. C<sub>8</sub>–C<sub>11</sub> yield = 68,4 %</li> </ol>	Pholjaroen et al. (2014)
2-methyl furan + n-butanol	<ol style="list-style-type: none"> <li>1. Protonated titanate nanotube (PTNT) (hydroxyalkylation/alkylation)</li> <li>2. Ni/HZSM-5 (HDO)</li> </ol>	<ol style="list-style-type: none"> <li>1. Batch</li> <li>2. Fixed bed reactor</li> </ol>	<ol style="list-style-type: none"> <li>1. 323 K, 4 h</li> <li>2. 533 K, H<sub>2</sub> = 6 MPa, WHSV = 1.3 h<sup>-1</sup>, H<sub>2</sub> flow rate = 120 mL/min</li> </ol>	<ol style="list-style-type: none"> <li>1. Conversion ≈ 70 %, yield = 67.6 %</li> <li>2. C<sub>9</sub>–C<sub>14</sub> yield ≈ 90 %, C<sub>14</sub> selectivity ≈ 80 % (isomerized C<sub>14</sub> = 20 %)</li> </ol>	Li et al. (2015b)

compound yields branched oxygenated hydrocarbons of  $C_8$ – $C_{13}$  before deoxygenation to obtain jet fuel-ranged branched alkanes; hydroisomerization and hydrocracking are not required for this approach. However, the selectivity of the products in each step of pretreatment varies significantly with operating conditions. Moreover, the organic acid by-products and acidic residuals prior to hydrodeoxygenation notably affect the performance of metal-based deoxy-catalysts. Other possible routes for production of biojet fuel have been reported as the oligomerization of lactone, e.g.,  $\gamma$ -valerolactone and alkene products from biomass pretreatment (Wright et al. 2008; Bond et al. 2010; Harvey and Meylemans 2013).

Alternatively, Fischer–Tropsch (F–T) process is often regarded as the key technology for converting synthesis gas (or “syngas”) which is a mixture of  $H_2$  and CO to transportation fuels and other liquid products (Liu et al. 2013a, b). The F–T synthesis could generate very long straight-chain hydrocarbon ( $>C_{20}$ ) with a variety of compositions depending on ratio of  $H_2$  and CO, catalyst, and operating conditions. The further cracking and isomerization of the F–T product is necessary to acquire proper carbon length and structure for desired liquid fuels. Starting materials for F–T process typically utilize coal, natural gas, steam reforming product, and woody biomass to produce  $C_9$ – $C_{15}$  paraffins (both *n*- and *i*-) and cyclic paraffins using Fe-based and Co-based catalysts (Zhang et al. 2006; Liu et al. 2013a, b; Yan et al. 2013; Hanaoka et al. 2015) under temperature of 250–350 °C. Nonetheless, with the current stage of technology, F–T synthesis can be economically feasible at very large-scale plant.

## 11.4 Conclusions

This chapter presents the green biorefinery concept of heterogeneous process for advanced biofuels production. The two categories of promising feedstocks are focused—(1) triglycerides or fatty acids in vegetable oils/animal fats and (2) biomass derivatives. The triglycerides are considered suitable sources for advanced biofuels, while the biomass derivatives can be suitable for jet fuels and fuel additives. The catalysts for production of green diesel and biojet fuels are presented and discussed in details. The series of hydrotreating reactions play a crucial role in the production process. Hydrodeoxygenation is a major contributor in the green diesel production when the catalysts used are metal sulfides, namely,  $MoS_2$  with various doping elements. In addition, the metal catalysts are proposed for the hydrotreating process since they are easy to prepare and sulfur-free. Basically, decarbonylation is a major reaction pathway when a precious metal (Pt, Pd) and non-precious metal (Ni) are employed in the process. The Co catalyst surprisingly is active for both hydrodeoxygenation and decarbonylation. Decarboxylation is an interesting pathway since  $H_2$  is not consumed in the reaction. As for biojet fuels, the composite of metal/metal sulfides with strong solid acids are promising approaches to drive hydroisomerization and cracking reactions over the straight-chain alkanes produced from the deoxygenation. The SAPO, zeolites, and  $ZrO_2$  exhibit excellent

performance to convert the straight-chain alkanes to branch ones with proper carbon atoms as jet fuels. Furthermore, supported metal catalysts have been extensively developed in the biomass derivatives conversion into various valued chemical platforms including biojet fuel and fuel additives. Alumina and zeolite are widely employed as oxide supports and simultaneously acid sites for the complex reaction network. The improvement of the catalysts in terms of activity, stability, selectivity, and cost effectiveness is still required for advanced biofuels production. The novel heterogeneous catalysts would be a key component to bring the biorefinery and biofuel industry to a reality in the near future.

**Acknowledgment** The authors acknowledge the financial support from the National Nanotechnology Center, NSTDA, Thailand, the Thailand Research Fund (TRF) to V.I. (TRG5880192) and K.F. (RSA5580055), and the National Research Council of Thailand (NRCT) to K.F. This work was also supported by the Collaboration Hubs for International Program (CHIRP) of Strategic International Collaborative Research Program (SICORP), Japan Science and Technology Agency (JST).

## References

- Agency for Toxic Substances and Disease Registry (ATSDR), U.S. <http://www.atsdr.cdc.gov/toxprofiles/tp76-c3.pdf>. Accessed 19 Nov 2015
- Bezergianni S, Kalogianni A (2009) Hydrocracking of used cooking oil for biofuels production. *Bioresour Technol* 100:3927–3932
- Bezergianni S, Dimitriadis A, Kalogianni A, Knudsen KG (2011) Toward hydrotreating of waste cooking oil for biodiesel production effect of pressure, H<sub>2</sub>/oil ratio, and liquid hourly space velocity. *Indus Eng Chem Res* 50:3874–3879
- Bond JQ, Alonso DM, Wang D, West RM, Dumesic JA (2010) Integrated catalytic conversion of  $\gamma$ -valerolactone to liquid alkenes for transportation fuels. *Science* 327:1110–1114
- Botas JA, Serrano DP, García A, de Vicente J, Ramos R (2012) Catalytic conversion of rapeseed oil into raw chemicals and fuels over Ni- and Mo-modified nanocrystalline ZSM-5 zeolite. *Catal Today* 195:59–70
- Chen L, Zhu Y, Zheng H, Zhang C, Zhang B, Li Y (2011) Aqueous-phase hydrodeoxygenation of carboxylic acids to alcohols or alkanes over supported Ru catalysts. *J Mol Catal A Chem* 351:217–227
- Chen L, Zhu Y, Zheng H, Zhang C, Li Y (2012) Aqueous-phase hydrodeoxygenation of propanoic acid over the Ru/ZrO<sub>2</sub> and Ru–Mo/ZrO<sub>2</sub> catalysts. *Appl Catal A* 411–412:95–104
- Chen N, Gong S, Shirai H, Watanabe T, Qian EW (2013) Effects of Si/Al ratio and Pt loading on Pt/SAPO-11 catalysts in hydroconversion of *Jatropha* oil. *Appl Catal A* 466:105–115
- Chen J, Shi H, Li L, Li K (2014) Deoxygenation of methyl laurate as a model compound to hydrocarbons on transition metal phosphide catalysts. *Appl Catal B* 144:870–884
- Chen F, Li N, Li S, Yang J, Liu F, Wang W, Wang A, Cong Y, Wang X, Zhang T (2015a) Solvent-free synthesis of C9 and C10 branched alkanes with furfural and 3-pentanone from lignocellulose. *Catal Commun* 59:229–232
- Chen N, Gong S, Qian EW (2015b) Effect of reduction temperature of NiMoO<sub>3-x</sub>/SAPO-11 on its catalytic activity in hydrodeoxygenation of methyl laurate. *Appl Catal B* 174–175:253–263
- Choi I-H, Hwang K-R, Han J-S, Lee K-H, Yun JS, Lee J-S (2015) The direct production of jet-fuel from non-edible oil in a single-step process. *Fuel* 158:98–104

- Do P, Chiappero M, Lobban L, Resasco D (2009) Catalytic deoxygenation of methyl-octanoate and methyl-stearate on Pt/Al<sub>2</sub>O<sub>3</sub>. *Catal Lett* 130:9–18
- Donnis B, Egeberg RG, Blom P, Knudsen KG (2009) Hydroprocessing of bio-oils and oxygenates to hydrocarbons understanding the reaction routes. *Top Catal* 52:229–240
- Duan J, Han J, Sun H, Chen P, Lou H, Zheng X (2012) Diesel-like hydrocarbons obtained by direct hydrodeoxygenation of sunflower oil over Pd/Al-SBA-15 catalysts. *Catal Commun* 17:76–80
- Faungnawakij K, Suriye K (2013) Chapter 4 – Current catalytic processes with hybrid materials and composites for heterogeneous catalysis. In: Suib SL (ed) *New and future developments in catalysis*. Elsevier, Amsterdam, pp 79–104
- Gong S, Shinozaki A, Qian EW (2012a) Role of support in hydrotreatment of jatropha oil over sulfided NiMo catalysts. *Indus Eng Chem Res* 51:13953–13960
- Gong S, Shinozaki A, Shi M, Qian EW (2012b) Hydrotreating of jatropha oil over alumina based catalysts. *Energy Fuels* 26:2394–2399
- Guzman A, Torres JE, Prada LP, Nuñez ML (2010) Hydroprocessing of crude palm oil at pilot plant scale. *Catal Today* 156:38–43
- Hanaoka T, Miyazawa T, Shimura K, Hirata S (2015) Jet fuel synthesis from Fischer–Tropsch product under mild hydrocracking conditions using Pt-loaded catalysts. *Chem Eng J* 263:178–185
- Hancsók J, Kasza T, Kovács S, Solymosi P, Holló A (2012) Production of bioparaffins by the catalytic hydrogenation of natural triglycerides. *J Clean Prod* 34:76–81
- Harvey BG, Meylemans HA (2013) 1-Hexene: a renewable C6 platform for full-performance jet and diesel fuels. *Green Chem* 16:770–776
- Hermida L, Abdullah AZ, Mohamed AR (2015) Deoxygenation of fatty acid to produce diesel-like hydrocarbons: a review of process conditions, reaction kinetics and mechanism. *Renew Sust Energy Rev* 42:1223–1233
- Huber GW, O'Connor P, Corma A (2007) Processing biomass in conventional oil refineries: production of high quality diesel by hydrotreating vegetable oils in heavy vacuum oil mixtures. *Appl Catal A* 329:120–129
- Immer JG, Kelly MJ, Lamb HH (2010) Catalytic reaction pathways in liquid-phase deoxygenation of C18 free fatty acids. *Appl Catal A* 375:134–139
- Jakkula J, Niemi V, Puroala VM (2004) Process for producing a hydrocarbon component of biological origin. US Patent 0230085
- Kaewmeesri R, Srifa A, Ithibenchapong V, Faungnawakij K (2015) Deoxygenation of waste chicken fats to green diesel over Ni/Al<sub>2</sub>O<sub>3</sub>: effect of water and free fatty acid content. *Energy Fuel* 29:833–840
- Kalnes TN, Koers KP, Marker T, Shonnard DR (2009) A technoeconomic and environmental life cycle comparison of green diesel to biodiesel and syndiesel. *Environ Prog Sustain Energy* 28:111–120
- Kiatkittipong W, Phimsen S, Kiatkittipong K, Wongsakulphasatch S, Laosiripojana N, Assabumrungrat S (2013) Diesel-like hydrocarbon production from hydroprocessing of relevant refining palm oil. *Fuel Process Technol* 116:16–26
- Kim SK, Brand S, Lee H, Kim Y, Kim J (2013) Production of renewable diesel by hydrotreatment of soybean oil: effect of reaction parameters. *Chem Eng J* 228:114–123
- Kim SK, Han JY, Lee HS, Yum T, Kim Y, Kim J (2014) Production of renewable diesel via catalytic deoxygenation of natural triglycerides: comprehensive understanding of reaction intermediates and hydrocarbons. *Appl Energy* 116:199–205
- Kimura T, Imai H, Li X, Sakashita K, Asaoka S, Al-Khattaf SS (2013) Hydroconversion of triglycerides to hydrocarbons over Mo–Ni/γ-Al<sub>2</sub>O<sub>3</sub> catalyst under low hydrogen pressure. *Catal Lett* 143:1175–1181
- Kordulis C, Bourikas K, Gousi M, Kordouli E, Lycourghiotis A (2016) Development of nickel based catalysts for the transformation of natural triglycerides and related compounds into green diesel: a critical review. *Appl Catal B* 181:156–196

- Kovács S, Kasza T, Thernesz A, Horváth IW, Hancsók J (2011) Fuel production by hydrotreating of triglycerides on NiMo/Al<sub>2</sub>O<sub>3</sub>/F catalyst. *Chem Eng J* 176–177:237–243
- Krás M, Kovács S, Kalló D, Hancsók J (2010) Fuel purpose hydrotreating of sunflower oil on CoMo/Al<sub>2</sub>O<sub>3</sub> catalyst. *Bioresour Technol* 101:9287–9293
- Kubička D, Kaluža L (2010) Deoxygenation of vegetable oils over sulfided Ni, Mo and NiMo catalysts. *Appl Catal* 372:199–208
- Kubička D, Tukač V (2013) Chapter Three – Hydrotreating of triglyceride-based feedstocks in refineries. In: Dmitry Yu M (ed) *Advances in chemical engineering*. Academic Press, Burlington, pp 141–194
- Kubička D, Horáček J, Setnička M, Bulánek R, Zukal A, Kubičková I (2014) Effect of support-active phase interactions on the catalyst activity and selectivity in deoxygenation of triglycerides. *Appl Catal B* 145:101–107
- Kubičková I, Snáre M, Eränen K, Mäki-Arvela P, Murzin DY (2005) Hydrocarbons for diesel fuel via decarboxylation of vegetable oils. *Catal Today* 106:197–200
- Kumar P, Yenumala SR, Maity SK, Shee D (2014) Kinetics of hydrodeoxygenation of stearic acid using supported nickel catalysts: effects of supports. *Appl Catal A* 471:28–38
- Lestari S, Mäki-Arvela P, Eränen K, Beltramini J, Max Lu GQ, Murzin DY (2009) Diesel-like hydrocarbons from catalytic deoxygenation of stearic acid over supported Pd nanoparticles on SBA-15 catalysts. *Catal Lett* 134:250–257
- Li S, Li N, Li G, Li L, Wang A, Cong Y, Wang X, Xu G, Zhang T (2015a) Protonated titanate nanotubes as a highly active catalyst for the synthesis of renewable diesel and jet fuel range alkanes. *Appl Catal B* 170–171:124–134
- Li T, Cheng J, Huang R, Zhou J, Cen K (2015b) Conversion of waste cooking oil to jet biofuel with nickel-based mesoporous zeolite Y catalyst. *Bioresour Technol* 197:289–294
- Liu Y, Sotelo-Boyas R, Murata K, Minowa T, Sakanishi K (2011) Hydrotreatment of vegetable oils to produce bio-hydrogenated diesel and liquefied petroleum gas fuel over catalysts containing sulfided Ni–Mo and solid acids. *Energy Fuels* 25:4675–4685
- Liu G, Yan B, Chen G (2013a) Technical review on jet fuel production. *Renew Sust Energy Rev* 25:59–70
- Liu Q, Zuo H, Wang T, Ma L, Zhang Q (2013b) One-step hydrodeoxygenation of palm oil to isomerized hydrocarbon fuels over Ni supported on nano-sized SAPO-11 catalysts. *Appl Catal A* 468:68–74
- Liu Q, Bie Y, Qiu S, Zhang Q, Sainio J, Wang T, Ma L, Lehtonen J (2014) Hydrogenolysis of methyl heptanoate over Co based catalysts: mediation of support property on activity and product distribution. *Appl Catal B* 147:236–245
- Liu S, Zhu Q, Guan Q, He L, Li W (2015) Bio-aviation fuel production from hydroprocessing castor oil promoted by the nickel-based bifunctional catalysts. *Bioresour Technol* 183:93–100
- Lown AL, Peereboom L, Mueller SA, Anderson JE, Miller DJ, Lira CT (2014) Cold flow properties for blends of biofuels with diesel and jet fuels. *Fuel* 117:544–551
- Maia AJ, Louis B, Lam YL, Pereira MM (2010) Ni-ZSM-5 catalysts: detailed characterization of metal sites for proper catalyst design. *J Catal* 269:103–109
- Mäki-Arvela P, Rozmysłowicz B, Lestari S, Simakova O, Eränen K, Salmi T, Murzin DY (2011) Catalytic deoxygenation of tall oil fatty acid over palladium supported on mesoporous carbon. *Energy Fuels* 25:2815–2825
- Mériaudeau P, Tuan VA, Sapaly G, Nghiem VT, Naccache C (1999) Pore size and crystal size effects on the selective hydroisomerisation of C8 paraffins over Pt–Pd/SAPO-11, Pt–Pd/SAPO-41 bifunctional catalysts. *Catal Today* 49:285–292
- Murata K, Liu Y, Inaba M, Takahara I (2010) Production of synthetic diesel by hydrotreatment of jatropa oils using Pt–Re/H-ZSM-5 catalyst. *Energy Fuels* 24:2404–2409
- Musselwhite N, Na K, Sabyrov K, Alayoglu S, Somorjai GA (2015) Mesoporous aluminosilicate catalysts for the selective isomerization of *n*-Hexane: the roles of surface acidity and platinum metal. *J Am Chem Soc* 137:10231–10237



- Ochoa-Hernández C, Yang Y, Pizarro P, O'Shea VA, Coronado JM, Serrano DP (2013) Hydrocarbons production through hydrotreating of methyl esters over Ni and Co supported on SBA-15 and Al-SBA-15. *Catal Today* 210:81–88
- Olcay H, Subrahmanyam AV, Xing R, Lajoie J, Dumesic JA, Huber JW (2013) Production of renewable petroleum refinery diesel and jet fuel feedstocks from hemicellulose sugar streams. *Energy Environ Sci* 6:205–216
- Onyestyák G, Harnos S, Szegedi Á, Kalló D (2012) Sunflower oil to green diesel over Raney-type Ni-catalyst. *Fuel* 102:282–288
- Peng B (2012) Transformation of triglycerides and fatty acids into biofuels with sulfur-free catalysts. Technische Universität München
- Peng B, Yao Y, Zhao C, Lercher JA (2012a) Towards quantitative conversion of microalgae oil to diesel-range alkanes with bifunctional catalysts. *Angew Chem Int Ed* 51:2072–2075
- Peng B, Yuan X, Zhao C, Lercher JA (2012b) Stabilizing catalytic pathways via redundancy: selective reduction of microalgae oil to alkanes. *J Am Chem Soc* 134:9400–9405
- Peng B, Zhao C, Kasakov S, Foraita S, Lercher JA (2013) Manipulating catalytic pathways: deoxygenation of palmitic acid on multifunctional catalysts. *Chemistry* 19:4732–4741
- Pholjaroen B, Li N, Yang J, Li G, Wang W, Wang A, Cong Y, Wang X, Zhang T (2014) Production of renewable jet fuel range branched alkanes with xylose and methyl isobutyl ketone. *Ind Eng Chem Res* 53:13618–13625
- Prasomsri T, Shetty M, Murugappan K, Roman-Leshkov Y (2014) Insights into the catalytic activity and surface modification of MoO<sub>3</sub> during the hydrodeoxygenation of lignin-derived model compounds into aromatic hydrocarbons under low hydrogen pressures. *Energy Environ Sci* 7:2660–2669
- Prielcel P, Kubička D, Čapek L, Bastl Z, Ryšánek P (2011) The role of Ni species in the deoxygenation of rapeseed oil over NiMo-alumina catalysts. *Appl Catal A* 397:127–137
- Rabaev M, Landau MV, Vidruk-Nehemya R, Koukouliev V, Zarchin R, Herskowitz M (2015) Conversion of vegetable oils on Pt/Al<sub>2</sub>O<sub>3</sub>/SAPO-11 to diesel and jet fuels containing aromatics. *Fuel* 161:287–294
- Santillan-Jimenez E, Morgan T, Lacny J, Mohapatra S, Crocker M (2013a) Catalytic deoxygenation of triglycerides and fatty acids to hydrocarbons over carbon-supported nickel. *Fuel* 103:1010–1017
- Santillan-Jimenez E, Morgan T, Shoup J, Harman-Ware AE, Crocker M (2013b) Catalytic deoxygenation of triglycerides and fatty acids to hydrocarbons over Ni–Al layered double hydroxide. *Catal Today* 237:136–144
- Sattler JJHB, Ruiz-Martinez J, Santillan-Jimenez E, Weckhuysen BM (2014) Catalytic dehydrogenation of light alkanes on metals and metal oxides. *Chem Rev* 114:10613–10653
- Satyarthi JK, Chiranjeevi T, Gokak DT, Viswanathan PS (2013) An overview of catalytic conversion of vegetable oils/fats into middle distillates. *Catal Sci Technol* 3:70–80
- Simakova I, Simakova O, Mäki-Arvela P, Simakov A, Estrada M, Murzin DY (2009) Deoxygenation of palmitic and stearic acid over supported Pd catalysts: effect of metal dispersion. *Appl Catal A* 355:100–108
- Snåre M, Kubičková I, Mäki-Arvela P, Eränen K, Murzin DY (2006) Heterogeneous catalytic deoxygenation of stearic acid for production of biodiesel. *Ind Eng Chem Res* 45:6875
- Srifa A, Faungnawakij K, Itthibenchapong V, Viriya-empikul N, Charinpanitkul T, Assabumrungrat S (2014) Production of bio-hydrogenated diesel by catalytic hydrotreating of palm oil over NiMoS<sub>2</sub>/γ-Al<sub>2</sub>O<sub>3</sub> catalyst. *Bioresour Technol* 158:81–90
- Srifa A, Faungnawakij K, Itthibenchapong V, Assabumrungrat S (2015a) Roles of monometallic catalysts in hydrodeoxygenation of palm oil to green diesel. *Chem Eng J* 278:249–258
- Srifa A, Viriya-empikul N, Assabumrungrat S, Faungnawakij K (2015b) Catalytic behaviors of Ni/γ-Al<sub>2</sub>O<sub>3</sub> and Co/γ-Al<sub>2</sub>O<sub>3</sub> during the hydrodeoxygenation of palm oil. *Catal Sci Technol* 5:3693–3705

- Veriansyah B, Han JY, Kim SK, Hong SA, Kim YJ, Lim JS, Shu YW, Oh SG, Kim J (2012) Production of renewable diesel by hydroprocessing of soybean oil: effect of catalysts. *Fuel* 94:578–585
- Verma D, Kumar R, Rana BS, Sinha AK (2011) Aviation fuel production from lipids by a single-step route using hierarchical mesoporous zeolites. *Energy Environ Sci* 4:1667–1671
- Verma D, Rana BS, Kumar R, Sibi MG, Sinha AK (2015) Diesel and aviation kerosene with desired aromatics from hydroprocessing of jatropha oil over hydrogenation catalysts supported on hierarchical mesoporous SAPO-11. *Appl Catal A* 490:108–116
- Wang C, Tian Z, Wang L, Xu R, Liu Q, Qu W, Ma H, Wang B (2012) One-step hydrotreatment of vegetable oil to produce high quality diesel-range alkanes. *ChemSusChem* 5:1974–1983
- Wright ME, Harvey BG, Quintana RL (2008) Highly efficient zirconium-catalyzed batch conversion of 1-butene: a new route to jet fuels. *Energy Fuels* 22:3299–3302
- Yan Q, Yu F, Liu J, Street J, Gao J, Cai Z, Zhang J (2013) Catalytic conversion wood syngas to synthetic aviation turbine fuels over a multifunctional catalyst. *Bioresour Technol* 127:281–290
- Yang J, Li N, Li S, Wang W, Li L, Wang A, Wang X, Cong Y, Zhang T (2014) Synthesis of diesel and jet fuel range alkanes with furfural and ketones from lignocellulose under solvent free conditions. *Green Chem* 16:4879–4884
- Yang L, Tate KL, Jasinski JB, Carreon MA (2015) Decarboxylation of oleic acid to heptadecane over Pt supported on zeolite 5A beads. *ACS Catal* 5:6497–6502
- Zhang C-H, Yang Y, Teng B-T, Li T-Z, Zheng H-Y, Xiang H-W, Li Y-W (2006) Study of an iron-manganese Fischer–Tropsch synthesis catalyst promoted with copper. *J Catal* 237:405–415
- Zhang X, Lei H, Zhu L, Wei Y, Liu Y, Yadavalli G, Yan D, Wu J, Chen S (2015) Production of renewable jet fuel range alkanes and aromatics via integrated catalytic processes of intact biomass. *Fuel* 160:375–385
- Zhao C, Brück T, Lercher JA (2013) Catalytic deoxygenation of microalgae oil to green hydrocarbons. *Green Chem* 15:1720–1739
- Zuo H, Liu Q, Wang T, Ma L, Zhang Q, Zhang Q (2012) Hydrodeoxygenation of methyl palmitate over supported ni catalysts for diesel-like fuel production. *Energy Fuels* 26:3747–3755

# Chapter 12

## An Overview of the Recent Advances in the Application of Metal Oxide Nanocatalysts for Biofuel Production

Mandana Akia, Esmail Khalife, and Meisam Tabatabaei

**Abstract** Fossil fuels are still primary resources of energy supply; however, they are undoubtedly responsible for most of the environmental pollutions. Over the last decades, renewable sources as clean alternative energies have received an increasing deal of attention due to the limitation of fossil fuel resources for reliable fulfillment of future energy demands and to address the environmental crises. Renewable energies predominately include solar, wind, biomass, hydrogen, and geothermal sources. Among these, biofuels derived from biomass are considered as the most promising candidate owing to a number of reasons such as direct conversion of biomass to liquid biofuels. Gases and liquid biofuels can be produced from biomass feedstock by three main approaches: thermochemical, biochemical, and microbiological technologies. Gasification, pyrolysis, liquefaction, hydrolysis, transesterification, and anaerobic digestion are main routes for biomass to biofuel conversion. In all biofuel production processes, developing the highest quality products with an optimized process (in terms of cost, energy consumption, etc.) is desirable which necessitates the exploitation of modern sciences such as nanotechnology. Among various aspects of nanotechnology, over the last several years,

---

M. Akia (✉)

Department of Mechanical Engineering, University of Texas Rio Grande Valley, Edinburg, TX, USA

Biofuel Research Team (BRTeam), Karaj, Iran

e-mail: [akia.mandana@gmail.com](mailto:akia.mandana@gmail.com); [mandana.akia@utrgv.edu](mailto:mandana.akia@utrgv.edu)

E. Khalife

Biofuel Research Team (BRTeam), Karaj, Iran

Department of Biosystems Engineering, Faculty of Agricultural Technology and Natural Resources, University of Mohaghegh Ardabili, 56199-11367 Ardabil, Iran

M. Tabatabaei (✉)

Biofuel Research Team (BRTeam), Karaj, Iran

Microbial Biotechnology Department, Agricultural Biotechnology Research Institute of Iran (ABRII), Agricultural Research, Education, and Extension Organization (AREEO), P.O. Box: 31535-1897, Karaj, Iran

e-mail: [meisam\\_tab@yahoo.com](mailto:meisam_tab@yahoo.com); [meisam\\_tabatabaei@abrii.ac.ir](mailto:meisam_tabatabaei@abrii.ac.ir)

utilization of highly active nanocatalysts for biofuel production has been growing quickly. Recent research studies have mainly focused on developing efficient nanocatalysts for improving conversion, accessing milder operating conditions, and lowering the process cost of biofuel production to collectively try to industrialize these green fuels. This chapter summarizes an overview of various biofuel production processes and, moreover, strives to comprehensively discuss metal oxide nanocatalysts used for biofuel production.

**Keywords** Biofuel production • Gasification • Pyrolysis • Liquefaction • Hydrolysis • Transesterification • Metal oxide nanocatalysts

## 12.1 Introduction

The present global energy demands are still mainly met by fossil fuels, i.e., petroleum, natural gas, and coal (Fig. 12.1). There are two major concerns associated with the wide use of fossil fuels, including rapid depletion of these nonrenewable resources and, more importantly, the environmental damages caused by their combustion [i.e., emissions of various greenhouse gases (GHGs)]. In order to address these challenges, the application of renewable energy carriers such as biofuels has been largely considered in many parts of the world.

Biofuels are generated from various renewable feedstocks such as agricultural crops, woody and herbaceous biomass, and waste materials. It is worth mentioning that although the combustion of biofuels also results in the release of CO<sub>2</sub>, the generated gases are utilized in the production cycle of the renewable feedstocks used for biofuel production. Hence, the biofuel production cycle is to some extent carbon neutral.

Production of biofuels from edible feedstocks (first-generation biofuels) has been condemned by many including the United Nations (Sachs 2007; Elbehri

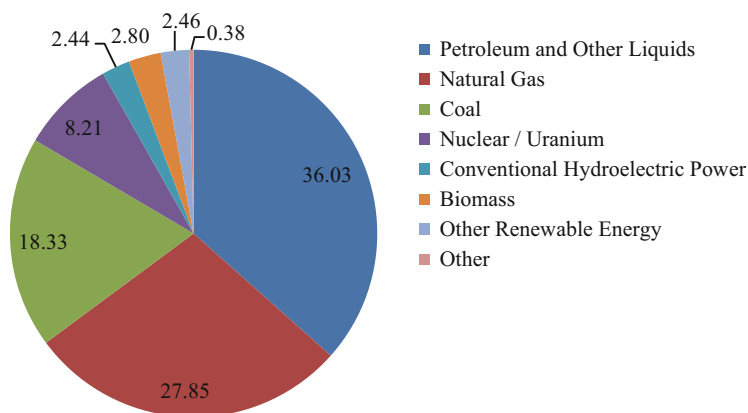


**Fig. 12.1** The consumption share of various energy carriers in the world in the year 2014 (EIA 2015)

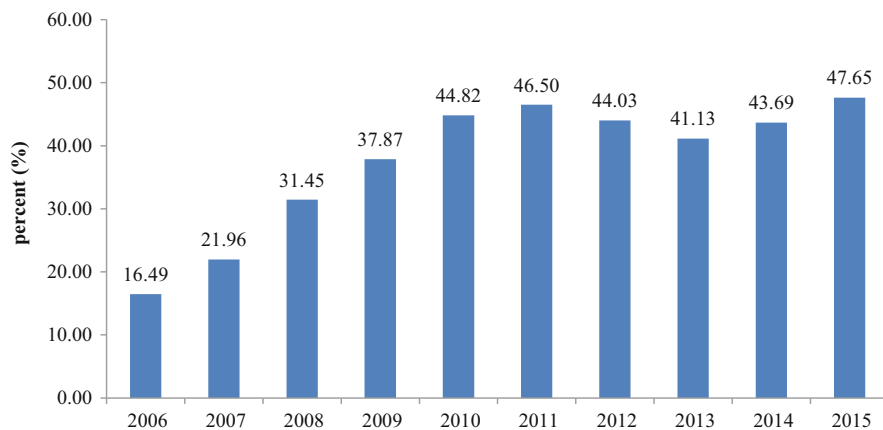


**Fig. 12.2** The trend showing the growing proportion of biomass (%) converted into biofuel (EIA 2015)

et al. 2013). As a result, there has been a growing interest in the conversion of biomass (wastes) into biofuels, i.e., second-generation biofuels (Fig. 12.2) (EIA 2015). The conversion methods used are divided into biochemical methods, such as hydrolysis and transesterification; thermochemical methods, such as direct combustion, pyrolysis, gasification, and liquefaction; as well as microbiological methods, such as anaerobic digestion (Hahn-Hägerdal et al. 2006). Figure 12.3 represents the various biofuel production methods.

Thermochemical conversions are the processes that can disintegrate the chemical bonds in biomass to disentangle the stored energy. Among these conversion methods, combustion is the most direct and technically easiest process, which converts organic matter to heat,  $\text{CO}_2$ , and  $\text{H}_2\text{O}$  using an oxidant and can directly release the energy by breaking primary bonds of biomass, while gasification and pyrolysis transfer the energy into secondary products (gas and liquid, respectively), which are likely to be ideal for fueling furnaces and engines (Asadullah 2014). Gasification has many advantages over combustion, including possibility of using low-value feedstock and converting them into electricity and also vehicle fuels (Alonso et al. 2010). Pyrolytic oil, also known as “tar or bio-oil” which has a high viscosity value, has high level of corrosiveness, is relatively unstable, and is chemically very complex, cannot be used as transportation fuel directly due to its high oxygen (40–50 wt%), high water (15–30 wt%) contents, and also low H/C ratios. Another method for producing biofuel is the transesterification method in which biodiesel is produced from vegetable oils and animal fats (Tabatabaei et al. 2011, 2015; Hasheminejad et al. 2011; Jingura and Kamusoko 2015).

In all the above mentioned methods, catalytic materials play an indisputable role in enhancing the speed of conversion. For instance, in the gasification, catalysts not only reduce the tar content but also improve the quality of gaseous products and the conversion efficiency (Akia et al. 2014; Goswami et al. 2015). In the liquefaction

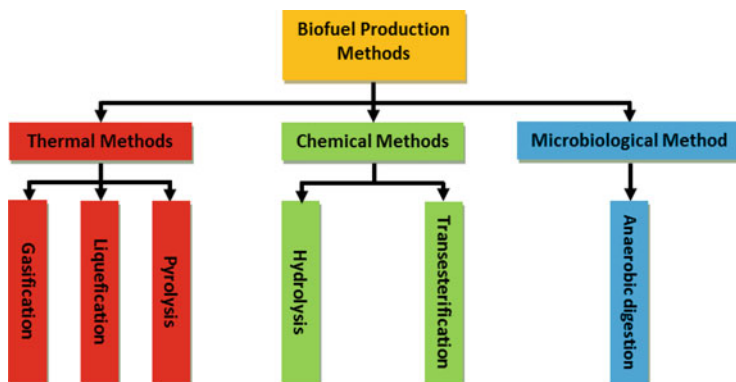


Fig. 12.3 Various biofuel production methods

process, alkaline salts,  $\text{Na}_2\text{CO}_3$ ,  $\text{KOH}$ , etc. are commonly used as homogenous catalysts (Duan and Savage 2010). Moreover, in the transesterification, the conversion of oil is catalyzed in presence of acidic, alkaline, or enzymatic catalysts.

During the last decades, the introduction of various nanomaterials has revolutionized the science of catalyst fabrication and application. The unique features of these materials have resulted in the production of more active, efficient, reusable, stable, and pollutant-free catalysts (Zhang et al. 2010). Recent catalyst developments based on nanomaterials have resulted in the improvement of biomass conversion processes. For instance, increased syngas production and reduced tar formation in the gasification processes were achieved by the application of nano- $\text{Fe}_3\text{O}_4$  (Yu et al. 2006). In nano-based catalytic biomass liquefaction, increased liquid yield and quality of products, i.e., heavy oil, were accomplished by the application of a nanocatalyst of  $\text{NaHCO}_3$  (Sun et al. 2010). Furthermore, high catalytic activity and high specific surface area of nano- $\text{KF}/\text{CaO}$  were also highlighted as instrumental in overcoming the known limitations on conventional alkalic heterogeneous catalysts for biodiesel production (Wen et al. 2010).

The present chapter aims to review a number of main biofuel production methods. Moreover, different nanocatalysts used in biofuel production such as alkali earth metal oxide nanocatalysts, transition metal oxide nanocatalysts, mixed metal oxide nanocatalysts, and supported nano-metal oxides are also elaborated.

## 12.2 Biofuel Production Methods

### 12.2.1 Gasification

Gasification is considered economical at any capacities beyond 5 kW (Kirubakaran et al. 2009). Therefore, there is a continued interest in the production of energy from

biomass through gasification. Gasification is in fact partial thermal oxidation, which leads to a high proportion of gaseous products (i.e., CO<sub>2</sub>, water, CO, H<sub>2</sub>, and gaseous hydrocarbons), slight amounts of char (solid product), ash, and condensable compounds (tars and oils). Steam, air, or oxygen is supplied to the reaction as oxidizing agent. The gas produced can be standardized in its quality and is easier and more versatile to use than the primary biomass. In better words, the generated gas can be consumed to power gas engines and gas turbines (Puig-Arnavat et al. 2010). Moreover, since the gas is rich in H<sub>2</sub> and CO, they can be separated to be utilized for a fuel cell as well (Park et al. 2011; Pakpour et al. 2014; Hosseini et al. 2015; Zahed et al. 2015) or to be converted into liquid fuels or chemicals by the Fischer–Tropsch synthesis method (Kim et al. 2013). Gasification adds value to low- or negative-value resources by transmuting them into valuable fuels and products. Overall, gasification is considered as one of the most efficient ways of converting the energy contained in biomass, and it is becoming one of the most suitable alternatives for the reuse of waste materials.

Despite the various benefits of biomass gasification, the technology is still in the developing step due to some problems. The presence of some impurities such as tars, particulate matters, NH<sub>3</sub>, H<sub>2</sub>S, HCl, and SO<sub>2</sub>, which are inescapably formed during the gasification process and generally sustained in the produced gas, leads to serious problems in downstream applications (Chiang et al. 2013). Among the impurities, tar is the infamous one. It is a sticky material representing several organic compounds, particularly aromatic compounds heavier than benzene (Asadullah 2014). These contaminants must be eliminated by other methods such as physical filtration, wet scrubbing, or catalytic hot gas cleaning (Asadullah 2014). The physical filtration is the simplest method but suffers from some disadvantages such as blocking the pores of filter and incapability to separate gaseous impurities (Asadullah 2014). It is worth mentioning that both the physical filtration and wet scrubbing methods do not efficiently remove tar (Asadullah 2014). These shortcomings cumulatively mark catalytic hot-gas cleaning as the most desirable option for eliminating pollutants from the gasification gas. In addition to that, this method is also beneficial in terms of energy efficiency as it removes the gas cooling step involved in physical filtration and the rewarming step of gas for downstream application (Asadullah 2014).

The gasification process consists of the following stages (Fig. 12.4) (Puig-Arnavat et al. 2010):

- *Drying stage*, where the moisture content of the biomass is reduced by heating at 100–200 °C. Through this stage, the moisture content of biomass typically ranging between 5 and 35 % is decreased down to <5 %.
- *Devolatilization (pyrolysis)*, representing the thermal decomposition of the biomass in the absence of oxygen or air which results in the release of hydrocarbon gases from the biomass. These gases can then be condensed at a sufficiently low temperature to generate liquid tars. In overall, the mechanism of devolatilization is still not fully understood. In better words, it is a complicated process including complex chemical pathways, multiphase reactions, and heat

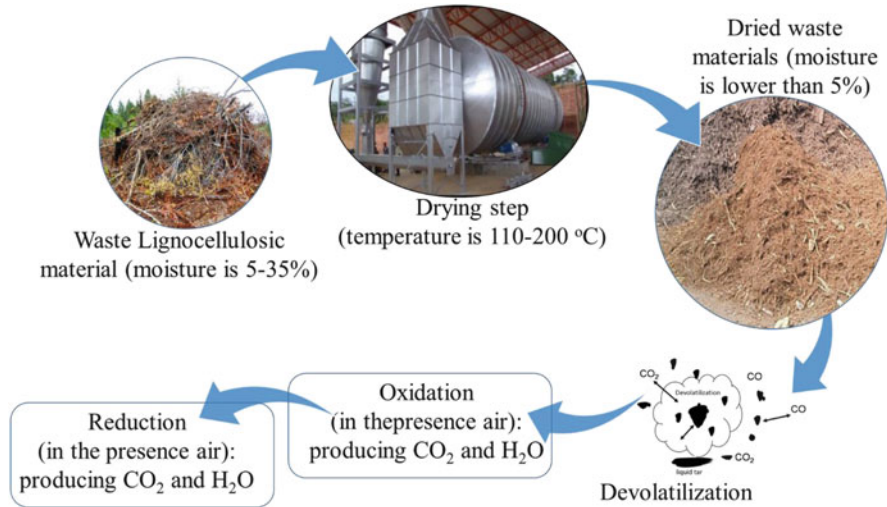
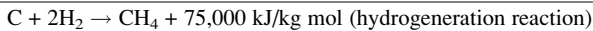
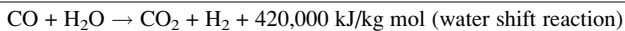
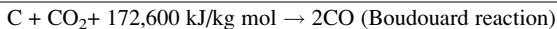
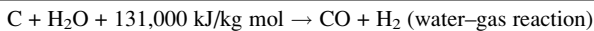


Fig. 12.4 Schematic flowchart of gasification process

and mass transfer effects (Moon et al. 2013). The product gases and tar obtained through this stage show a range of characteristics depending on the structure and composition of the biomass and the reaction conditions (Lin et al. 2009).

- *Oxidation* is a reaction between the solid carbonized biomass and oxygen in the air, through which  $\text{CO}_2$  is generated and the hydrogen contained in biomass is oxidized to produce water. During the course of the oxidation of carbon and hydrogen, a great deal of heat is also released. It is important to note that if oxygen is present in substoichiometric quantities,  $\text{CO}$  is generated as a result of partial oxidation of carbon (Puig-Arnavat et al. 2010).
- *Reduction* takes place in the absence of oxygen or in substoichiometric quantities of oxygen and in the temperature range of 800–1000 °C. These reactions which are mostly endothermic are as follows:



Hence, the final gas produced in the gasifier is composed of mainly  $\text{CO}$  and  $\text{H}_2$ .

In gasification technologies, gasifiers are classified according to different criteria, e.g., the direction of air/gas movement, types of bed, and types of fuel used (Brown et al. 2010). Among various factors involved, the bed type is probably the most important basis used for the classification of gasifiers. Accordingly, three main gasifiers are known, i.e., fixed bed, fluidized bed, and entrained flow.

**Fixed-Bed Gasifier** There are three principal designs of fixed-bed gasifiers, namely, (1) updraft, (2) downdraft, and (3) cross-draft as shown in Fig. 12.5 (Tiwari



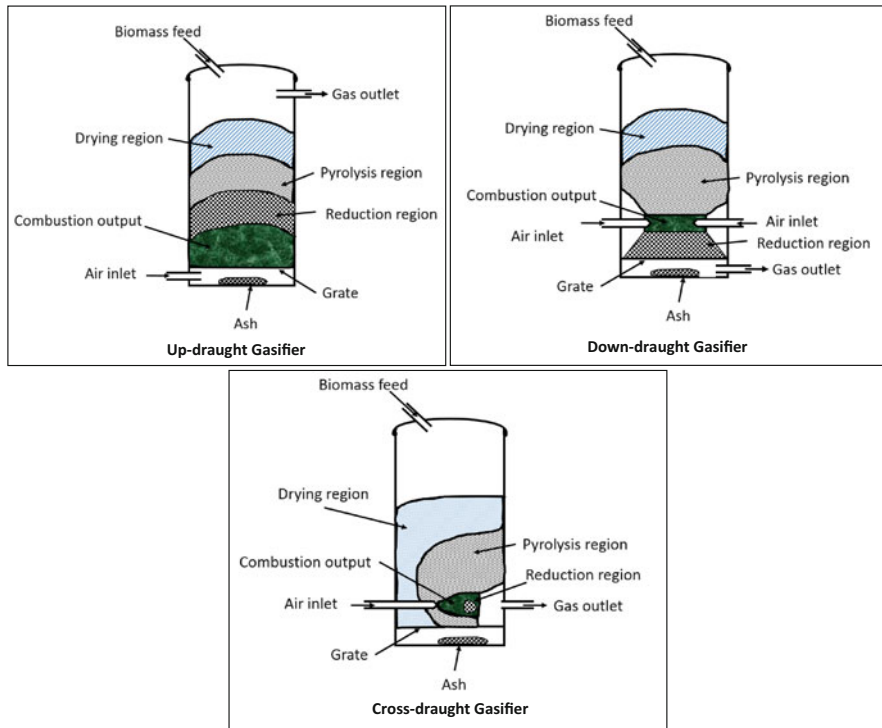
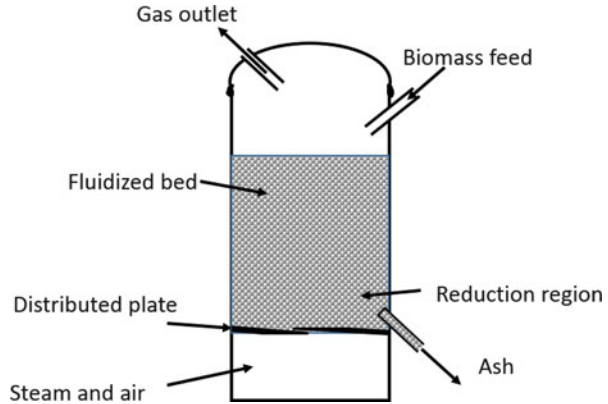


**Fig. 12.5** Different technologies of fixed-bed gasifiers (Tiwari and Mishra 2011). With permission from Elsevier, Copyright 2016

and Mishra 2011). In fact, the fixed-bed gasifier has a bed consisting of solid fuel particles through which the gasifying media and gas either move up (updraft), move down (downdraft), or are introduced from one side of the gasifier and are released from the opposite side on the same horizontal level (cross-draft) (Puig-Arnavat et al. 2010). This type of gasifier is the simplest, basically involving a cylindrical room for fuel and gasifying media, a fuel-feeding unit, an ash-removal unit, and a gas exit (Puig-Arnavat et al. 2010). These gasifiers are generally characterized by easy construction and operation with high carbon conversion, long solid residence time, low gas velocity, and low ash carryover (Carlos 2005). It is worth mentioning that as the gasification proceeds in fixed-bed gasifiers, the fuel bed moves slowly down the reactor (Puig-Arnavat et al. 2010).

**Fluidized Bed** In these reactors, the gasifying agent is blown through a bed consisting of solid materials at a velocity sufficient to maintain the particles in suspension (Fig. 12.6). The fuel particles introduced at the bottom of the reactor very quickly mix with the bed material and almost instantly reach the bed temperature. Consequently, fuel particles are pyrolyzed very fast, resulting in a relatively large amount of gaseous materials (Puig-Arnavat et al. 2010). Further gasification and tar conversion reactions happen in the gas phase (Knoef 2005).

**Fig. 12.6** Fluidized-bed gasifier (Tiwari and Mishra 2011). With permission from Elsevier, Copyright 2016



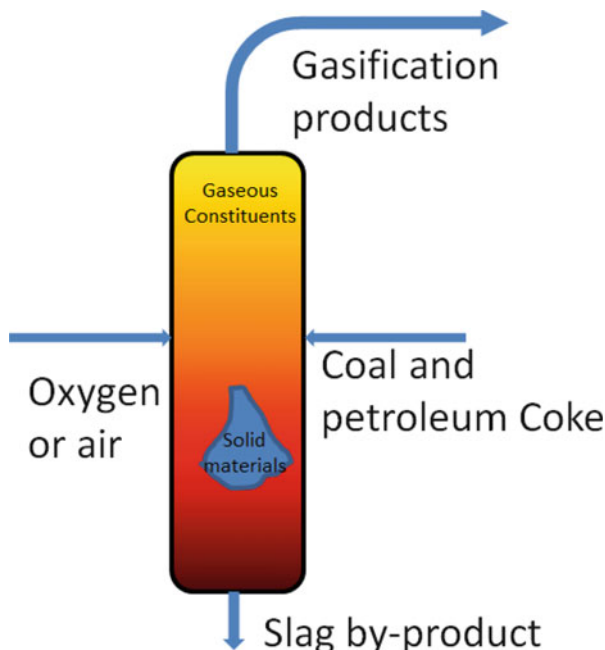
**Entrained-Flow** gasifier is commonly used for coal because these reactors can be slurry-fed in direct gasification mode, which makes solid fuel feeding at high pressures inexpensive (Mukherjee et al. 2014). This gasifier has also been used for biomass gasification (Qin et al. 2012). This gasifier is characterized by short residence time, high temperatures, high pressures, smaller particles, and large capacities, and regularly achieves a high carbon conversion, and produces syngas with high quality and minor methane and tar content (Fig. 12.7) (Qin et al. 2012).

Regardless of the type of the gasifier, their performance is also interfered by two more important parameters as well: produced-gas composition, which could directly influence the heating value of the gas, and gasification efficiency (Puig-Arnavat et al. 2010).

Catalysts play an important role in the gasification process. Catalysts could have different results depending on the stage of gasification process. For instance, Aradi et al. (2013) reported that char yield reduced during the final step of the gasification by using catalyst, while opposite results were obtained during the volatilization step. The role of catalysts is highlighted for the reduction of tar in the gasification as reported by Li et al. (2008a) who used metal-based catalysts of Ni and Al. Moreover, it seems that using catalytic cracking could be helpful for increasing yield of produced gas at lower-temperature condition (Han and Kim 2008). Similar studies were reported for using tri-metallic catalyst for high production of gas and also reducing a very impressive amount of tar (at 800 °C) (Li et al. 2009).

As mentioned before, hydrogen is one of the promising products of gasification, which could be recovered from the effluent gases by several means such as pressure-swing absorption by removing carbon dioxide (Onwudili 2014) and membrane separation processes (such as polymer electrolyte membrane) by removing methane and other gases (Ibeh et al. 2007). In a study, Fiori et al. (2012) demonstrated that hydrothermal gasification of biomass for hydrogen production could be energetically self-sustaining when biomass concentrations of between 15 and 25 wt% were used. The authors also showed that the energy balance of a conceptual reactor design could

**Fig. 12.7** Typical entrained-flow gasifier. With permission from Elsevier, Copyright 2016



provide 150 kW net energy per 1000 g feed. Hydrogen production via hydrothermal gasification has also been shown to occur much readily under supercritical water conditions (374 °C and 22 MPa) (Kruse 2009). In addition, Khan et al. (2014) argued that by using Ni catalyst, H<sub>2</sub> production was improved under supercritical water conditions.

### 12.2.2 Pyrolysis

Various types of biomass such as agro-wastes, animal manure, municipal solid wastes, and even the by-products/wastes of biofuel industries (e.g., biodiesel glycerin) can be converted into solid, liquid, and gaseous products through various thermochemical processes including pyrolysis (Boateng et al. 2015; Kojima et al. 2015). Through pyrolysis, biomass is heated and decomposed in the absence of oxygen for biofuel production (bio-oils and syngas), charcoal, and other chemicals (Boateng et al. 2015). It is worth quoting that syngas could contain high-value chemicals, such as carbon monoxide, methane, and short-chain hydrocarbons. Each biomass feedstock has an optimum fast pyrolysis temperature, and the resultant bio-oils from each biomass have distinct physical and chemical properties (Bok et al. 2013).

For instance, Xiu et al. in the year of 2010 studied the effect of components on the bio-oil yield and claimed that free fatty acid (FFA) content of biomass could

play a crucial role in the bio-oil yield. They experimented mixtures of swine manure and biodiesel crude glycerol at various ratios in a high-pressure batch reactor to produce bio-oil and revealed that the FFA present in the glycerol (at swine manure/crude glycerol weight ratio of 1:3) increased bio-oil yield intensely from 23.9% to 70.92%. Their findings confirmed that cohydrothermal pyrolysis of manure with biodiesel crude glycerol or FFA could lead to a relatively high yield of bio-oils at a moderately high temperature. Apart from the presence of a specific component in biomass such as FFA and its impact of bio-oil yield, the kinematic analysis of the components contained in a certain biomass would also be of significant importance. In fact, kinetics analysis is essential to comprehend the mechanism of decomposition and chemical reactions of biomass pyrolysis (Ren et al. 2012). Reaction kinetics of biomass pyrolysis is difficult to interpret due to the fact that three different main components are contained in biomass, i.e., hemicelluloses, cellulose, and lignin. Decomposition of these three components happens at different temperatures and rates. More specifically, hemicelluloses and cellulose are decomposed relatively fast at low temperatures of 200–350 °C, while lignin is decomposed slowly in a large range of temperatures from 280 to 500 °C (Mohan et al. 2006).

Conventional biomass pyrolysis is a thermal and chemical process conducted at 400–600 °C, also called low-temperature pyrolysis. More specifically, conventional pyrolysis is defined as the pyrolysis, which occurs under a slow heating rate. In these processes achieved in fixed and fluidized bed reactors, heating provided by heated surfaces, sands, and hot gas is used (Mohan et al. 2006; Ren et al. 2012). Conventional slow pyrolysis has been applied for many centuries and has been mainly used for the production of charcoal. However, the conventional pyrolysis is more difficult to reach the target temperature and to control the reaction. Therefore, over the last decade, the preferred technology has been fast pyrolysis at high temperatures with very short residence times (Demirbas 2007). A fast pyrolysis process includes drying the feed to a water content of typically <10% (although up to 15% can be acceptable), to reduce the water content in the product oil (Bridgwater 2006).

At the higher temperatures used in fast pyrolysis, the major products are gases, which can be continuously removed as they are formed. In fact, slow pyrolysis of biomass is associated with high charcoal content, while the fast pyrolysis is associated with tar at low temperatures and/or gas at high temperatures. Fast pyrolysis technique involves pyrolyzing the feedstock at modest temperatures in the range of 350–600 °C, at fast heating rates of ca. 1000 °C s<sup>-1</sup>. The liquid product can be upgraded to refinery-ready blend stocks or drop-in fuels. It should be noted that the presence of dissimilar phases such as solid, liquid aerosol, condensed melt, vapor, gas, and aromatic char makes fast pyrolysis a complex process.

Recently, many investigators have looked into alternative heating methods to be used during fast pyrolysis process such as microwave heating. Microwave pyrolysis is one of the novel thermochemical technologies in which biomass is heated by microwave irradiations. In fact, microwave-assisted pyrolysis (MAP) process has been successfully applied for processing wood (Miura et al. 2004), corn stover

(Yu et al. 2007), rice straw (Huang et al. 2010), coffee hulls (Dominguez et al. 2007), microalgae (Du et al. 2011), pine sawdust (Wang et al. 2009a), and wheat straw (Budarin et al. 2009). The major advantage of the microwave heating over conventional heating methods is the fast and uniform heating achieved by microwave irradiations (Ren et al. 2012). As a result, MAP offers several advantages over traditional pyrolysis processes, including uniform internal heating of large biomass particles, ease of control, and no requirement for agitation or fluidization, and hence minor ash particles in the bio-oil (Du et al. 2011). However, in a study, Ren et al. (2012) compared fluidized bed and microwave pyrolysis and claimed that the latter produced much lower liquid yield. They also reported that the highest bio-oil of 57.8 wt% based on dry biomass was obtained under the optimized conditions (i.e., reaction temperature of 471 °C and reaction time of 15 min). Moreover, compared with the conventional fast pyrolysis, microwave pyrolysis of biomass produced bio-oils with low yields (Bu et al. 2013).

Overall, the bio-oil yield reported by the MAP of biomass has been lower than 30 wt% (Huang et al. 2008; Lei et al. 2009; Salema and Ani 2011). For instance, Huang et al. (2008) studied biomass microwave pyrolysis of rice straw at the temperature of 407 °C with power input of 300 W and reported low yield bio-oil (22.6 wt%). This indicates that the high bio-oil yield efficiency is a big obstacle in microwave pyrolysis. Moreover, these findings also showed that about half of rice straw sample was transformed into H<sub>2</sub>-rich fuel gas, whose H<sub>2</sub>, CO<sub>2</sub>, CO, and CH<sub>4</sub> percentages were 55 vol%, 17 vol%, 13 vol%, and 10 vol%, respectively (Huang et al. 2008). Their results showed that the condensable part of the product was highly alkaline and oxygenated and the dangerous PAH content was quite less. In another study, microwave pyrolysis of distillers dried grain with soluble (DDGS) was investigated for the first time in the world by Lei et al. (2011) to conclude the impacts of pyrolytic conditions on the yield efficiency of bio-oil, syngas, and biochar. They ran the experiments under different conditions of reaction temperature, time, and power input. Based on their findings, the bio-oil yield was in the range of 26.5–50.3 wt% of the biomass. The energy content of the DDGS bio-oils obtained at 650 °C within 8 min was reportedly 28 MJ/kg (66.7 % of the heating value of gasoline).

Contrary to the abovementioned reports, biomass fast pyrolysis using conventional heating reactors, e.g., fluidized bed, has reportedly led to bio-oil yield of up to 60–70 wt% (Mohan et al. 2006). It is worth quoting that in some literatures the microwave absorption materials or catalysts were added to enhance the heating rate and bio-oil yield during the MAP (Chen et al. 2008; Moen et al. 2009). For instance, Ren et al. (2012) managed to enhance bio-oil yield by 33.8–57.8 wt% based on dry biomass basis. The highest bio-oil yield of 57.8 % was obtained under the optimization conditions (reaction temperature of 471 °C at 15 min) (Ren et al. 2012). However, their yield was still lower than that from fluidized bed pyrolysis. Overall, studies suggest that MAP is a highly scalable technology suitable for distributed conversion of bulky biomass (Du et al. 2011).

The particle size of biomass feedstock, as an essential factor in determining the efficacy of pyrolysis, could significantly affect pyrolysis oil and charcoal yields

(Şensöz et al. 2000). In a conventional pyrolysis system like fluidized bed, very fine feed material is used to achieve high heating rates and liquid production because large-sized particles are difficult to agitate and process (Weiming et al. 2008). In better words, in the fluidized bed pyrolysis system, big size particles incline to settle to the bottom of the gasifier bed and consequently heat transfer and speed of thermal processing are reduced. This has a negative impact on the efficiency of production of bio-oils, which is increased when the material size is reduced. But in microwave pyrolysis method, published results indicate that thermochemical conversion reactions can occur quickly in relatively large-sized biomass materials (Lei et al. 2009). Moreover in a study, Ren et al. (2012) using a central composite design (CCD) and response surface analysis investigated the microwave pyrolysis of Douglas fir sawdust pellet to produce bio-oil, syngas, and charcoal. Their results revealed that thermochemical conversion reactions could happen quickly in large-sized biomass pellet by using microwave pyrolysis.

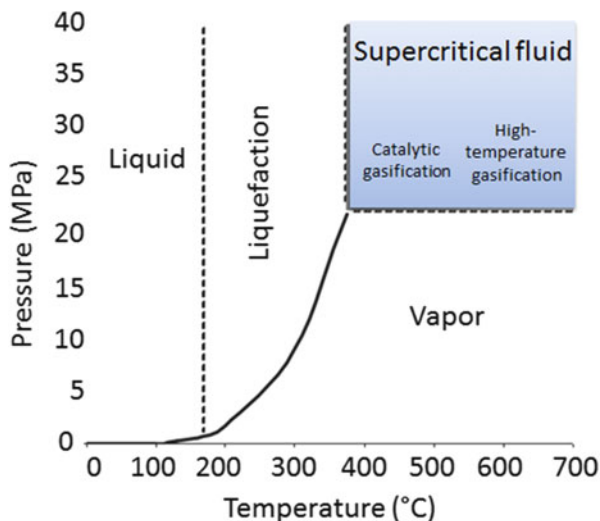
One of the other methods of application pyrolysis in biomass is smokeless biomass pyrolysis. Lee et al. (2010) studied the capacity of smokeless biomass pyrolysis for energy production, global carbon capture, and sequestration. They claimed that smokeless biomass pyrolysis for biochar and biofuel production is one of the most possible arsenals for global carbon capture at huge scales. Currently, the annual global biomass harvesting is more than 6.5 GtC/year and this huge amount of biomass could be converted to biochar (3.25 GtC/year) and biofuels by the smokeless biomass pyrolysis. On the other hand, the heating value equivalent of such a scenario equals at least 6500 million barrels of crude oil and could help achieve energy independence from fossil fuels (Lee et al. 2010).

### 12.2.3 Liquefaction

The pyrolysis and direct liquefaction with water processes are sometimes confused with each other, and hence a simplified comparison of the two has been presented herein. Both of these processes are thermochemical processes in which organic compounds contained in a specific feedstock are converted into liquid products. However, in hydrothermal liquefaction (HTL), water simultaneously acts as reactant and catalyst, and this makes the process meaningfully different from pyrolysis and thus the biomass can be directly converted without consuming energy for the drying step, as is the case of pyrolysis (Toor et al. 2011). It should be noted that HTL cannot compete with pyrolysis in terms of yields, but it has other basic privileges like a relatively stable oil product and an aqueous reaction environment, which does not require energy-consuming drying of the biomass.

HTL is generally conducted at 280–370 °C and between 10 and 25 MPa. Under these conditions water is still in a liquid state and has a range of exotic properties. At these temperatures, macromolecules in the biomass break down into smaller molecules that may afterward repolymerize into a viscous “bio-crude” oil product similar to crude petroleum (Peterson et al. 2008). Figure 12.8 shows the different

**Fig. 12.8** Different temperature and pressure ranges within which water is used for different hydrothermal processes (Adopted from Toor et al. 2011)



temperature and pressure ranges within which water is used for different hydrothermal processes.

Bio-oil (also known as bio-crude) as well as next to gaseous, aqueous, and solid by-products is generated during the HTL process. In general the energy content in bio-oils is in the range of 30–37 MJ/kg, i.e., considerably higher than the biomass (Toor et al. 2011). The oil still contains 10–20% of oxygen making it more polar than crude oil, and this causes a number of drawbacks, such as relatively high water content, corrosive characteristic, thermal instability, etc. (Hamaguchi et al. 2012). HTL offers several advantages compared with other hydrothermal approaches. For instance, HTL is a liquid-phase process that reduces consumed energy for vaporization of the process slurry. Moreover, HTL can process low-lipid algae, converting some carbohydrate and protein to bio-oils (Brown et al. 2010; Biller and Ross 2011).

It is worth quoting that the energy recovery from biomass to fuel (liquefaction) is often as high as 80%, which is very high in comparison with other biomass conversion processes. For instance, a process that currently receives much attention is bioethanol production from starch or lignocelluloses (Toor et al. 2011; Karimi et al. 2015). The most theoretical yield efficiency of starch is approximately 0.50 g/g, and taking the heating values of starch and bioethanol into account, this corresponds to an energy recovery of 88%. However, for lignocelluloses such as wood, yields on biomass are much lower than this, at approximately 30% corresponding to energy recoveries of approximately 50% (Toor et al. 2011; Mood et al. 2013a).

Although water acts as a catalyst in HTL processes (Toor et al. 2011), however to increase yield and reduce reaction time of the process, catalysts are important and are used for improving gasification efficiency, suppressing tar and char production, etc. Homogeneous catalysts like alkali salts have been often used, whereas heterogeneous catalysts such as Ni-containing catalysts have been less utilized in HTL

(de Sousa et al. 2012). It is well known that the addition of alkali salts has a positive influence on HTL processes by improving gasification, accelerating the water–gas shift (WGS), and increasing liquid yields (Xu et al. 2013). In a study, Song et al. in the year 2004 investigated the effect of addition of 1.0 wt% of  $\text{Na}_2\text{CO}_3$  catalyst on the liquefaction of corn stalk and concluded that the use of the catalyst increased the yield of bio-crude (from 33.4 to 47.2 %). Also, Karagöz et al. (2006) reported that HTL treatment of wood biomass at 280 °C for 15 min by using alkali catalyst (0.235–0.94 M  $\text{K}_2\text{CO}_3$ ) suppressed char formation and improved liquid yields' efficiency from 17.8 % to 33.7 %, respectively. With regard to homogeneous catalysts, alkalis appear to be a better option than organic acids as they lead to higher heating values and higher bio-crude oil yields (Barreiro et al. 2013).

In the previous decades, several pilot- and demo-scale projects started for HTL of terrestrial biomass, but none of them succeeded (Barreiro et al. 2013). In fact, developing of HTL technology started during the 1970s mostly through short-term projects for terrestrial biomass but failed to result in a demonstration scale, due to a combination of technological and economic problems. More specifically, the Pittsburgh Energy Research Center (in the year of 1973), the Shell (in the 1980s), and Dutch company Biofuel (1997) were the companies whose efforts to establish large-scale reactors for the commercialization of HTL biomass were not successful (Barreiro et al. 2013).

#### 12.2.4 Hydrolysis

Hydrolysis is one of the main and generally initial reactions taking place in the conversion of biomass. In this process, under hydrothermal conditions, cellulose and water react, and as a result the glycosidic bonds between sugar units are cleaved to form simpler sugars like glucose and partially hydrolyzed oligomers. The hydrolysis of cellulose is widely investigated due to the fact that a major fraction of plant biomass is made of cellulose and the resulting product, i.e., glucose, is a very important intermediate (Huang and Fu 2013).

Hydrolysis processes typically require a pretreatment step to expedite the breakdown of the polymers to a variety of sugars suitable for fermentation (Fig. 12.9). In fact, pretreatment is done to primarily remove lignin or hemicellulose, decrease the cellulose crystallinity, and subsequently to increase the surface area (Meena et al. 2015). The pretreatment step is currently performed using different physico-chemical methods such as dilute acids, alkali, microwave, steam explosion, ammonia fiber expansion (AFEX), etc. The second step is the hydrolysis step, which is currently accomplished by either acid or enzymatic digestion. This process could lead to the formation of different sugars like hexoses (glucose, galactose, etc.) and pentoses (xylose, arabinose, etc.).

Enzymatic hydrolysis is very effective on the yield, but at the same time, it has some drawbacks, for instance, it is expensive and its reusability is not practically feasible. The most known enzymes which play important roles in enzymatic



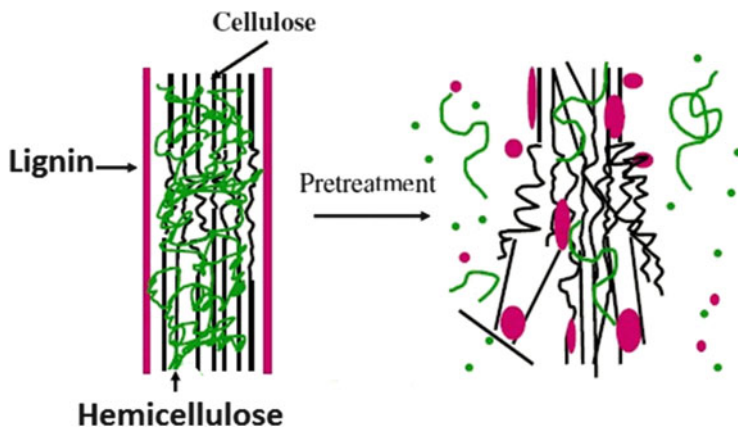


**Fig. 12.9** The effect of pretreatment on the biomass materials

hydrolysis are cellulase, xylanase,  $\beta$ -glucosidase, etc. (Khoshnevisan et al. 2011; Mood et al. 2013b). These enzymes act on the pretreated biomass at moderate conditions and resulted in releasing noticeably large amounts of sugars (Meena et al. 2015).

Acid-based hydrolysis can be used under both high temperature and pressure conditions when dilute acids are used at lower temperatures and atmospheric pressure when hydrolysis process is performed using concentrated acids (Meena et al. 2015). It is worth quoting that although acids are powerful agents for cellulose hydrolysis, due to the disadvantages of concentrated acids (i.e., toxicity, corrosiveness, hazardousness, etc.), the hydrolysis process, and the need to supply acid-proof reactors, the process becomes very costly. Also, the concentrated acid must be recovered after hydrolysis to make the process economically viable (Kumar et al. 2009). On the other hand, dilute acids can easily hydrolyze hemicellulose under moderate conditions, but hydrolyzing cellulose biomass requires very excessive conditions (Iranmahboob et al. 2002).

One of the important challenges faced in using acids in the hydrolysis step is recovering acids. Reusability is a major advantage of solid acid catalysts since they reduce pollution and can lower operation costs (Guo et al. 2012). Goswami et al. (2015) studied the hydrolysis of biomass using solid carbon acid catalyst. The milled biomass was pretreated using dilute alkali (4% w/w NaOH) at a temperature of 120 °C for 60 min. After biomass pretreatment by NaOH, hydrolysis process was carried out using the solid acid catalyst. The catalyst could liberate 262 mg/g (31% efficiency) of total reducing sugars (TRS) from the alkali-pretreated rice straw. Catalyst reusability was also checked by measuring the sugar release for the second cycle, and it was reported that water-washed and the methanol-washed catalysts retained 68% and 67% of their original activity after the first cycle (Goswami et al. 2015). Similar to these findings, Meena

et al. (2015) also reported that the solid acid catalyst used retained 57 % of its catalytic efficiency after the second round of hydrolysis.

The efficiency of enzymatic hydrolysis strongly depends on the quality of the pretreatment step conducted. In line with that, Eliana et al. (2014) studied the effects of the pretreatment method on enzymatic hydrolysis and ethanol fermentability of the cellulosic fraction from elephant grass. They stated that the best enzymatic hydrolysis results were with the alkaline pretreatments. Similar results were also reported previously by Mirahmadi et al. (2010) and Santos et al. (2012). In fact, the alkaline pretreatment removes lignin efficiently providing suitable conditions for enzymes to act (Chen et al. 2009; Khoshnevisan et al. 2011; Heredia-Olea et al. 2015). In another study, Rabelo et al. (2014) investigated on the alkaline hydrogen peroxide pretreatment and enzymatic hydrolysis of sugarcane bagasse to obtain ethanol. They reported that the alkali pretreatment eliminated the requirement for prior size reduction and removed lignin efficiently.

### 12.3 Transesterification

Plant oils usually contain FFAs, phospholipids, sterols, water, odorants, and other impurities, and consequently, the oil cannot be used as fuel directly (Murugesan et al. 2009). To overcome these problems, the oil requires slight chemical modification which could be mainly achieved through processes such as transesterification, pyrolysis, and emulsification (Murugesan et al. 2009). Among these, the transesterification is the key and foremost important step to produce biodiesel (monoalkyl esters of long-chain fatty acids) from animal fats or vegetable oil.

In other words, transesterification or alcoholysis is the replacement of alcohol from an ester by another in a process similar to hydrolysis, except than alcohol is used instead of water (Meher et al. 2006). Biodiesel could be a good possible substitute for conventional diesel fuel since it is nontoxic, is biodegradable, and results in very appreciable reduction of GHGs when used in the transportation sector (Tabatabaei et al. 2011; Talebi et al. 2013; Hamze et al. 2015).

Transesterification is catalyzed by acidic or alkaline catalysts or by lipase enzymes (Kirrolia et al. 2013). Nevertheless, biodiesel has been mainly produced through alkaline-catalyzed transesterification of vegetable oils and animal fats using homogeneous basic catalysts (Fig. 12.10).

In order to achieve an efficient transesterification reaction, the catalyst selection is of great importance. The traditional liquid acid and alkali catalysts, called homogeneous catalysts, act in the same liquid phase as the reaction mixture. Due to their simple usage and requirement of less time for lipid conversion, the homogeneous catalysts are widely used in the biodiesel industry. However, the transesterification catalyzed by homogeneous catalysts needs highly pure feedstock and complicated downstream processing. Consequently, catalysts such as solid

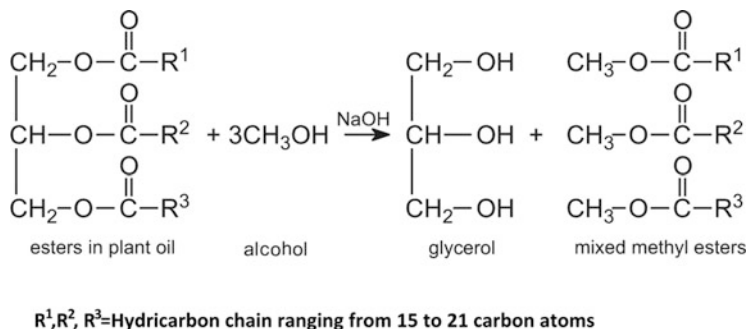


**Fig. 12.10** Transesterification of vegetable oil

acidic and alkaline catalysts, enzymes, supercritical catalyst systems, and ionic liquid catalysts have received a great deal of attention (Borges and Díaz 2012).

Enzymes such as lipase are biodegradable and nontoxic, while their application is accompanied with easy recovery of product and glycerol (Zheng et al. 2012). Moreover, enzyme-catalyzed transesterification requires moderate alcohol/oil molar ratio and mild reaction conditions (Zheng et al. 2012). Enzymes can also catalyze both esterification and transesterification and are thus suitable for feedstocks containing high FFA contents (Yan et al. 2012). Despite the advantages of enzyme-based transesterification, this process is still impractical because of the relatively high cost of the enzyme catalysts (Kirrolia et al. 2013).

Alkaline-catalyzed transesterification is about 4000 times faster than the acid-catalyzed reaction (Kirrolia et al. 2013). Sodium and potassium hydroxide are commonly used commercial basic catalysts at a concentration of about 1% by weight of oil. Alkaline-catalyzed transesterification is carried out at temperatures below the boiling point of methanol, i.e., 65 °C under atmospheric pressure, and takes about 60–90 min to complete (Khan et al. 2014). There is a trade-off between reaction time and temperature (Basha et al. 2009), i.e., a higher temperature along with higher pressure can be used to achieve a faster reaction, but this is expensive. Although alkaline-catalyzed transesterification leads to high conversion rates of triglycerides to their corresponding methyl esters in short reaction times, the reaction has several shortcomings, i.e., being energy intensive, difficulty of glycerol recovery, difficulty of removal of acidic or alkaline catalyst from the product, and formation of soap alkaline waste water which requires treatment (Meher et al. 2006).

Moreover, alkaline catalysts can be problematic when FFA content in the oil is above 3% which would result in increased soap formation (Vyas et al. 2010). Besides FFA, moisture content is also key challenge faced by alkaline-catalyzed transesterification.

Acid catalysts such as  $\text{H}_2\text{SO}_4$  catalyze reactions of fatty acid esterification and oil transesterification, thus allowing the use of feedstocks containing higher FFA content (Vyas et al. 2010). There are, however, several shortcomings associated with the application of acid-catalyzed biodiesel production compared to alkaline-catalyzed transesterification: (1) high molar ratios of alcohol to oil requirements

(approximately 5-fold to 50-fold), (2) longer reaction time, and (3) higher temperature requirements (60–90 °C) (Kirrolia et al. 2013). Reaction temperatures higher than the boiling point of the alcohol used in the reaction requires pressurized vessels to keep the alcohol, e.g., methanol in solution.

Among the most important variables affecting the production efficiency of biodiesel is the alcohol to triglyceride molar ratio. Stoichiometrically, for a successful transesterification, 3 mol of alcohol and 1 mol of triglyceride are required to yield 3 mol of fatty acid alkyl esters and 1 mol of glycerol. Nevertheless, since transesterification is an equilibrium reaction, a large excess of alcohol is required to drive the reaction toward the end products, i.e., glycerol and biodiesel. Therefore, molar ratios >6:1 are recommended to maximize the conversion of oil to esters (Meher et al. 2006).

## 12.4 Anaerobic Digestion

Anaerobic digestion (AD) is a versatile dual-purpose technology for treating various industries and domestic organic wastes and the production of biogas as an energy carrier (Madsen et al. 2011). The AD represents a system consisting of an active microbial community capable of effectively processing organic wastes under specific conditions (Lyberatos and Skiadas 1999). These microbes are very sensitive to the processing condition, and, thus, maximum biogas production by AD process will be only obtained under a proper management (Lin et al. 2014).

### 12.4.1 Influential Parameters on AD Process

#### 12.4.1.1 Temperature

The AD process at high temperature values (thermophilic AD) (55–70 °C) lead to higher yield of gas due to faster reaction rates compared with moderate temperature (mesophilic AD). However, high temperatures could also lead to acidic conditions and consequent diminished gas production (Mao et al. 2015). Thermophilic AD is also associated with some other drawbacks like higher instability, lower effluent quality, higher toxicity, higher susceptibility to environmental conditions, and more investment requirements (Mao et al. 2015). On the other hand, mesophilic systems have shown high process stability and higher microbial populations. However, these systems result in less methane production caused by their less biodegradability potentials and poor nutrient imbalance (Bowen et al. 2014). Therefore, the best conditions for an AD process would be thermophilic hydrolysis and mesophilic methanogenesis (Mao et al. 2015).

Overall, it should be noted that the microorganisms involved in the AD process are strongly sensitive to temperature changes, and this issue has direct impact on biogas production and the decomposition of organic substances. In fact, variations

in temperature could result in diminished substrate utilization and volatile fatty acid production rates and consequently increased “start-up” times. These consequently lead to decreased biogas yields (Bowen et al. 2014).

#### **12.4.1.2 pH**

The pH parameter has a direct impact on the AD process by affecting the growth rate of microorganisms, and an ideal pH ranges between 6.8 and 7.4. For instance, increasing pH from 4 to 7 increases the relative abundance of microbial species from 6 to 14 (Fang and Liu 2002). Controlling pH could be one potential technique to decrease ammonia toxicity and to obtain ideal microbial growth (Mao et al. 2015).

#### **12.4.1.3 C/N Ratio**

The C/N ratio shows the nutrient balance in a substrate, and therefore, it plays an important role in AD yield. Increasing C/N ratio decreases the amount of protein solubilization. Therefore, adjusting the C/N ratio is helpful for ammonia inhibition. However, if C/N ratio exceeds normal values, it could lead to the deficiency of the nitrogen required to maintain cell biomass resulting in decreased AD production yield. The optimum C/N ratio for the AD process has been reported at around 25 (Yen and Brune 2007; Zhang et al. 2013a).

#### **12.4.1.4 Organic Loading Rate**

Another key parameter which could influence the AD performance is organic loading rate which is the volatile solids fed per day under continuous feeding into digester. Increasing organic loading rate could disturb the equilibrium of the process and also temporarily restrains bacterial activity during primary phases of fermentation process. In fact, exerting a very high organic loading rate could result in a higher acidogenesis activity than methanogenesis activity and consequently increased volatile fatty acid production (Mao et al. 2015). Under the mesophilic conditions and based on the reports available, the maximum endurable organic loading rate is between 9.2 and 10.5 (Nagao et al. 2012; Gou et al. 2014).

#### **12.4.1.5 Retention Time**

The total time required to achieve a complete process of organic material digestion is called retention time. It is related to the microbial growth rate and organic loading rate. Retention time is mostly defined by two factors: the average spent time of solids in a digester which is called solids retention time (SRT) and the ratio of the

reactor volume/the influent flow rate (HRT) (Ekama and Wentzel 2008). It has been reported that 15–30 days is the average retention time for decomposition of waste under mesophilic conditions (Mao et al. 2015). Reducing the HRT generally increases volatile fatty acid, while increasing the HRT leads to inefficient utilization of the digester (Kwietniewska and Tys 2014).

## 12.5 Nanocatalysts in Biofuel Production

Investigation on different aspects of nanocatalysts for various applications has received more attention in recent years. Nanocatalysts due to their outstanding ability to provide high surface area perform a leading role in new fields of research. Metal oxide nanocatalysts have been applied extensively in many fields including chemistry and materials. They have special chemical and physical characteristics due to the size and high density of active catalytic sites (Gökdağ et al. 2010; Liu et al. 2012; Glaser 2012; Budarin et al. 2013). Metal oxide nanostructure catalysts could be appropriately classified as follows:

Alkali earth metal oxides (e.g., MgO, CaO)

Transition metal oxides (e.g., ZnO, NiO)

Mixed metal oxides (e.g., TiO<sub>2</sub>–ZnO)

Supported metal oxides (e.g., KF/Al<sub>2</sub>O<sub>3</sub>, KF/CaO, CaO/Fe<sub>3</sub>O<sub>4</sub>, Cs–Ca/SiO<sub>2</sub>–TiO<sub>2</sub>, KF/CaO–MgO, Li/CaO)

Indeed, these nanomaterials have been widely utilized in biodiesel and gasification/pyrolysis processes. Catalyst classifications and the number of published studies related to nanocatalytic conversion of biomass to biofuel (biodiesel and gasification process) from 2006 to 2015 have been presented in Fig. 12.11. In fact, this figure confirms that supported catalysts are the most used group of applied nanocatalysts. In Fig. 12.12, the catalysts with the number of recyclability along with their corresponding biodiesel yield have been shown.

### 12.5.1 Application of Nanocatalysts in Biodiesel Production

For biodiesel production, heterogeneous catalysts in comparison to homogenous catalysts provide more efficient separation steps for products and catalysts, eliminate quenching process, and offer conditions for continuous production process (Semwal et al. 2011; Banerjee et al. 2014). Based on a study on comparison of homogenous and heterogeneous catalysts in large-scale production process, it was revealed that for production of 8000 tons of biodiesel in the case of using NaOH as homogenous catalyst, the required amount of catalyst is nearly 88 tons of NaOH pellets, while by using supported MgO as heterogeneous catalyst, only 5.6 tons of this catalyst is required (Ullah et al. 2016). These results along with the other advantages of applying

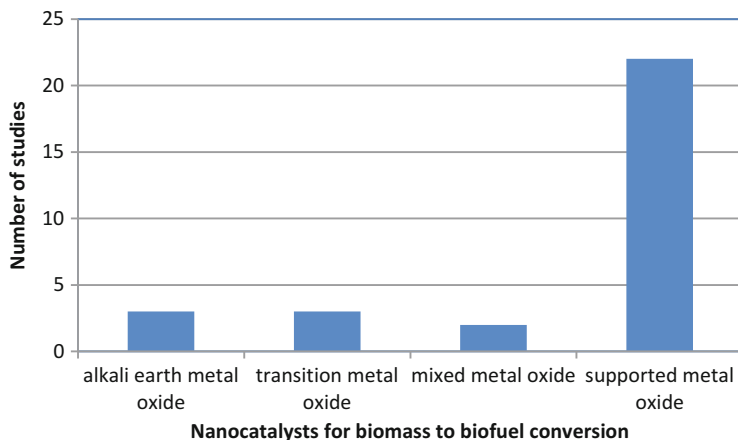


**Fig. 12.11** Metal oxide nanocatalysts applied in biodiesel production and gasification/pyrolysis processes

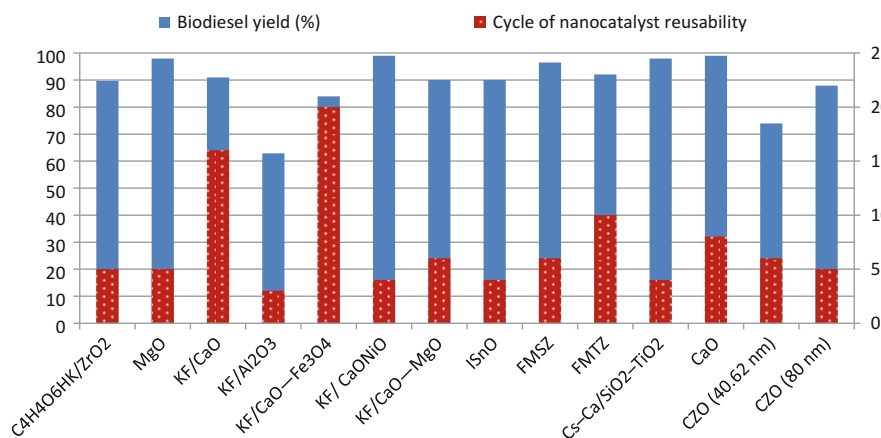


**Fig. 12.12** Cycles of metal oxide nanocatalysts reusability along with their corresponding biodiesel yield

heterogeneous catalysts emphasize the importance, priority, and superiority of heterogeneous catalysts for industrialization process. In heterogeneous catalytic reactions, two parameters solubility and diffusion play a fundamental role in the reaction besides the other operating parameters (Wang and Yang 2007). From a commercialization point of view, although heterogeneous catalysts offer some merits, still there are some limitations such as high reaction temperature, low stability of catalysts, and longer reaction time (Madhuvilakku and Piraman 2013).

Introduction and application of heterogeneous nanocatalysts have received great attention recently, which is mainly associated with providing higher surface area and increase in active sites besides reusability of the catalysts in more reaction

cycles (Glaser 2012; Madhuvilakku and Piraman 2013). In general, the main goal in designing and applying nanocatalysts is accessing green technologies with milder operating process besides providing higher catalytic activity.

Based on the investigations on the applications of nanocatalysts in biodiesel production, it was concluded that in the case of using nanocatalysts, the amount of required catalysts decreased to 30 % of the common catalysts. Additionally, the impacts of moisture and amount of FFA of the feedstock on the reaction were less in comparison to the common catalytic reactions (Zhang et al. 2013b).

In the following section, a survey of various nanocatalysts utilized in biodiesel production from both edible and nonedible feedstocks has been reviewed. In Table 12.1, all the related studies on nanocatalysts, which were employed in biodiesel production, have been summarized.

### 12.5.2 Alkali Earth Metal Oxides

Nanocrystalline calcium oxide was applied in transesterification reaction of soybean oil and poultry fat by Reddy et al. (2006). Four different types of CaO nanocatalysts with various surface areas (between 20–90 m<sup>2</sup> g<sup>-1</sup>) and different crystalline sizes (between 20 and 40 nm) were prepared, and their catalytic behavior was compared to the other nanocatalysts (MgO, TiO<sub>2</sub>, ZnO, CeO<sub>2</sub>). The transesterification reaction was completed with the conversion of 100 % after 12 h in the conditions of 1:27 oil to methanol molar ratio, 0.025 g of catalyst, and a temperature between 23 and 25 °C, while there is no reaction observed for the other nano-metal oxides at the same conditions. In the case of soybean as feedstock, maximum reusability of eight cycles with more than 99 % conversion was obtained using a catalyst with surface area and crystalline size of 90 m<sup>2</sup> g<sup>-1</sup> and 20 nm, respectively. The catalyst partly deactivated after eight cycles of reaction which was mainly attributed to polycrystallites and edge disappearances of the crystals. The results revealed that recyclability of catalyst in case of poultry fat as feedstock was almost less than half compared with soybean transesterification which associated with higher impurities in poultry fat. In mentioned research, the effect of surface area also was aimed to be investigated, and it was found that smaller crystalline size and defects (higher surface areas) led to higher catalytic performances. They scaled up the process to 1240 ml for sunflower, canola oils, and peanut as feedstock for biodiesel production. The operating conditions to reach more than 99 % of conversion were reported the same as the laboratory conditions in 24 h of reaction time at room temperature. It was also disclosed that by applying severe conditions of high temperature (between 240 and 280 °C) and high pressures (about 9 MPa), the feedstock with high FFA can be used without further treatment (neutralization). The obtained conversion was >99 % for three cycles of reactions.

Wang and Yang (2007) studied nano-MgO catalysts in subcritical and supercritical temperatures. They aimed to examine different parameters such as alcohol/oil molar ratio, amount of catalyst, and the temperature of reaction which resulted in different



Table 12.1 The diversity of metal oxide nanocatalysts applied in biodiesel production

Nanocatalyst	Feedstock	Preparation method	Catalyst specifications	Parameters	Recyclability	Result	Reference
CaO	Soybean oil (SBO) Poultry fat		BET = $90 \text{ m}^2 \text{ g}^{-1}$ (CS: 20 nm)	O/A: 1/27 C: 0.25 g Poultry fat O: 3.0 g A: 10 ml C: 1 mmol T: Room temperature t: 12 h		>99 % Conversion, scaled up to 1240 ml of oil feedstock	Reddy et al. (2006)
	Feedstock with high FFA			T: 240–280 °C P: 9 MPa	Three cycles for high FFA feedstock	High T and P conditions: conversion >99 %	
MgO	Soybean oil		PS: 60 nm	P: 30.0 MPa C: 3 wt% O/A: 1:36 S: 1000 rpm T: 260 °C		Biodiesel yield of 100 % in 10 min	Wang and Yang (2007)
MgO	Sunflower and rape-seed oils		MgO(I): $198 \text{ m}^2 \text{ g}^{-1}$ CS: 50–200 nm MgO(II): $80 \text{ m}^2 \text{ g}^{-1}$ CS: 8.8 nm MgO(III): $435 \text{ m}^2 \text{ g}^{-1}$ CS: 1–4.5 nm	Autoclave conditions O/A: 1/4 C: 300 mg S: 1200 rpm T: 69 °C t: 2 h		Biodiesel yield of approximately 86 %, 80 %, and 77 % for MgO(I), MgO(II), and MgO(III)	Verziu et al. (2008)
				Microwave conditions O/A: 1/4 C: 300 mg S: 1200 rpm T: 69 °C t: 40 min	Five cycles, conversion >99 %, with a biodiesel yield >98 %	>99 % biodiesel yield	

(continued)

Table 12.1 (continued)

Nanocatalyst	Feedstock	Preparation method	Catalyst specifications	Parameters	Recyclability	Result	Reference
KF/ $\gamma$ -Al <sub>2</sub> O <sub>3</sub>	Canola oil	Incipient wetness impregnation		KF (15 %) C: 3 wt% O/A: 1/15 T: 65 °C t: 8 h	Three cycles, 61.84 % biodiesel yield	99.84 % biodiesel yield	Boz et al. (2009)
KF/CaO-MgO	Rapeseed oil	Coprecipitation	PS: 35 nm 8:2 CaO to MgO mass ratio, 0.25:1 mass ratio of KF to CaO-MgO, and calcination temperature and time of 600 °C and 3 h	O/A: 1/12 C: 3 % T: 70 °C t: 3 h	Six cycles 90 % biodiesel yield (less than 5 % decrease)	95 % biodiesel yield	Wang et al. (2009a)
K <sub>2</sub> O/ $\gamma$ -Al <sub>2</sub> O <sub>3</sub>	Rapeseed oil			O/A: 1/12 C: 3 wt% T: 70 °C t: 3 h		94 % biodiesel yield	Han and Guan (2009)
CsNanoMgO	Tributyrin	Impregnation	PS: 25 nm	C: 50 mg T: 60 °C		40 % conversion after 24 h	Montero et al. (2010)
CsNanoMgO	Tributyrin	Coprecipitation	PS: 70 nm			100 % conversion within 3 h	Montero et al. (2010)
KF/CaO	Chinese tallow seed oil		PS: 30–100 nm Pore size: 97 nm BET: 109 m <sup>2</sup> g <sup>-1</sup>	O/A: 1/12 C: 4 % T: 65 °C t: 2.5 h	Sixteen cycles to achieve biodiesel yield 97–91 %	Up to 96 % biodiesel yield, good potential for industrialization	Wen et al. (2010)

CaO nanoparticles/ NaX zeolite		Impregnation	PS: 59.42 nm	O/A: 1/6 C: 16 wt% (CaO) P: atmospheric T: 60 °C t: 6 h	(93–95 %) biodiesel yield	Luz Martínez et al. (2010)
Potassium bitartrate on zirconia support (C <sub>4</sub> H <sub>4</sub> O <sub>6</sub> HK/ ZrO <sub>2</sub> )	Soybean oil	Incipient wetness impregnation	PS: 10–40 nm	O/A: 1/16 C: 6.0 % T: 60 °C t: 2 h	98.3 % biodiesel yield	Qiu et al. (2011)
Nanocrystalline lithium-impregnated calcium oxide	Karanja (3.4 wt% FFAs) and <i>Jatropha</i> oils (8.3 wt % FFAs)	Wet impregnation		O/A: 1/12 C: 1.75 wt% T: 65 °C	>99 % biodiesel yield	Kaur and Ali (2011)
KF/CaO— Fe <sub>3</sub> O <sub>4</sub>	Stillingia oil	Impregnation	PS: 50 nm BET = 20.8 m <sup>2</sup> g <sup>-1</sup> Pore diameter = 42 nm	O/A: 1/12 C: 4 wt% T: 65 °C t: 3 h	95 % biodiesel yield, 84 % in the twentieth cycle	Hu et al. (2011)
Nano-sulfated-TiO <sub>2</sub> (TiO <sub>2</sub> /SO <sub>4</sub> <sup>-2</sup> )	Different fatty acids	Sol-gel hydrothermal		T: 80 °C Molar ratio of acid/alcohol: 1/2 C: 0.2 wt%	98 % biodiesel yield for transesterification reaction	Hosseini-Sarvari and Sodagar (2013)

(continued)

Table 12.1 (continued)

Nanocatalyst	Feedstock	Preparation method	Catalyst specifications	Parameters	Recyclability	Result	Reference
$\text{TiO}_2\text{-ZnO}$	Palm oil			O/A: 1/6 C: 200 mg T: 60 °C t: 5 h		98 % conversion and 92 % biodiesel yield A good candidate for the large-scale biodiesel production from palm oil at the reduced temperature and time	Madhuvilakku and Piraman (2013)
$\text{Cs/Al/Fe}_3\text{O}_4$	Soybean oil	Precipitation	PS: 30–35 nm BET: 85.2 m <sup>2</sup> g <sup>-1</sup>	O/A: 1/14 S: 300 rpm T: 58 °C t: 2 h	Reused in different cycles with no significant changes	94.8 % biodiesel yield	Feyzi et al. (2013)
$\text{KF/CaONiO}$	WCO (5.8 wt% FFA)	Impregnation		O/A: 1/15 C: 5 wt% catalyst T: 65 °C t: 4 h	Fourth run of reaction Fifth catalytic run: 50 % conversion	>99 % biodiesel yield	Kaur and Ali (2014)
Cs-promoted MgO nanocatalysts	Olive oil	Supercritical sol-gel coprecipitation		O/A: 1/30 C: 2.8 wt% Butanol: 25 wt % T: 90 °C t: 24 h		93 % conversion	Woodford et al. (2014)
Iron/cadmium (ICdO)	Soybean		BET = 130.2 m <sup>2</sup> g <sup>-1</sup> Pore volume = 0.206 cm <sup>3</sup> g <sup>-1</sup> Pore size = 3.169 nm	Soybean oil: 20 g Methanol: 6 g C: 1 g P: 18.6 bar T: 200 °C t: 1 h		84 % biodiesel yield	Alves et al. (2014)

Iron/tin (ISnO) oxides	Macauba oil		BET = 49.9 m <sup>2</sup> g <sup>-1</sup> Pore volume = 0.0968 cm <sup>3</sup> g <sup>-1</sup> Pore size = 3.883 nm	Oil: 20 g Methanol: 6 g C: 1 g P: 18.6 bar T: 200 °C t: 3 h	Four cycles (no change)	90 % biodiesel yield	Alves et al. (2014)
Ferric manganese-doped sulfated zirconia (FMSZ) nanoparticle	Waste cooking oil	Impregnation		O/A: 1/20 C: 3 wt% S: 600 rpm T: 180 °C	Six times without loss in its activity	96.5 % biodiesel yield	Alhassan et al. (2015a)
Ferric manganese-doped tungstated zirconia (FMTZ) nanoparticles	Waste cooking oil containing 17.5 wt% FFAs	Impregnation calcined at 600 °C for 3 h	BET: 44 m <sup>2</sup> g <sup>-1</sup> Pore size: 79.0 nm Pore volume: 0.0897 cm <sup>3</sup> g <sup>-1</sup>	O/A: 1:25 C: 4 wt% S: 600 rpm T: 200 °C t: 4 h	Ten runs 92.1 % in the eleventh run	96.0 % biodiesel yield	Alhassan et al. (2015b)
Cs-Ca/SiO <sub>2</sub> -TiO <sub>2</sub>	Blend refined vegetable oil	Impregnation optimum calcination time is 6 h at 650 °C with heating rate of 5 °C min <sup>-1</sup>	PS: 45-50 nm BET = 169.6 m <sup>2</sup> g <sup>-1</sup> Pore volume = 0.595 cm <sup>3</sup> g <sup>-1</sup> Pore diameter = 5 nm	O/A: 1/12 S: 500 rpm T: 60 °C t: 2 h	Four cycles with small changes	98 % biodiesel yield	Feyzi and Shahbazi (2015)
CZO (copper-doped ZnO)	Waste cooking oil	Coprecipitation	PS: 80 nm	O/A: 1/10 (v) C: 10 wt% T: 55 °C t: 50 min	Five cycles, biodiesel yield of 87.94 %	97.71 % biodiesel yield	Gurunathan and Ravi (2015a)

(continued)

Table 12.1 (continued)

Nanocatalyst	Feedstock	Preparation method	Catalyst specifications	Parameters	Recyclability	Result	Reference
CZO	Neem oil		PS: 40.62 nm	O/A: 1/10 (v:v) C: 10 wt% T: 55 °C t: 1 h	Six cycles, biodiesel yield of 73.95 %	97.18 % biodiesel yield	Gurunathan and Ravi (2015b)

C catalyst concentration, O oil, A alcohol, O/A molar ratio of oil to alcohol, T temperature, P pressure, t time, S stirring speed, CS crystal size, PS particle size

conversions of soybean transesterification. In addition, stirring rate was found as an effective parameter on the diffusion and solubility. The best conditions to obtain 100 % of conversion were reaction temperature of 260 °C, pressure of 30 MPa, methanol to oil molar ratio of 36, catalyst loading of 3 wt%, and reaction time of 10 min.

Verziu et al. (2008) studied the effects of nanocrystalline samples of MgO in biodiesel production from sunflower or rapeseed oil. They prepared different nanocatalysts of MgO(I), MgO(II), and MgO(III) with (111), (110), and (100) lattice planes, respectively. They examined the catalysts under autoclave, ultrasound, and microwave conditions. Under the autoclave conditions (molar ratio of 1:4 for sunflower oil/methanol, temperature of 70 °C, and 2-h reaction time) for nanocatalysts of MgO(I), Mg(II), and MgO (III), biodiesel yield of approximately 86 %, 80 %, and 77 % was obtained, respectively. It was disclosed that activation temperature for providing the highest catalytic activity was dependent on the exposed facet of nanocatalysts, which was defined as temperature of 500 °C for MgO(I) and 310 °C for both Mg(II) and MgO(III). Under microwave condition the high conversion of 99 % and the biodiesel yield of 98 % (at 40 min of reaction time) were attained for the fifth run of recycling nanocatalysts. The result of applying ultrasound was different from microwave condition mainly associated with particle disruption which led to solving the nanoparticles in biodiesel and also glycerol to precede magnesium saponification reaction. They found that applying the microwave condition led to achieving higher biodiesel yield compared to autoclave and ultrasound conditions.

### 12.5.3 Transition Metal Oxides

Hosseini-Sarvari and Sodagar (2013) utilized nano-sulfated TiO<sub>2</sub> catalyst for esterification reaction of FFAs. Initial materials of Ti(OC<sub>4</sub>H<sub>9</sub>)<sub>4</sub>, HNO<sub>3</sub>, and H<sub>2</sub>SO<sub>4</sub> were implemented for catalyst preparation via sol-gel method. The prepared catalysts were applied in esterification reaction of different fatty acids with various alcohols. The results clearly indicated that esterification reaction occurred for all the fatty acids which resulted in fatty acid (methyl or ethyl) esters with the yield of 98 %.

### 12.5.4 Mixed Metal Oxides

Mixed oxide nanocatalysts displayed special characteristics that resulted in achieving efficient performances in transesterification reaction (Teo et al. 2014). Madhuvilakku and Piraman (2013) prepared nano-mixed oxide TiO<sub>2</sub>-ZnO by urea-glycerol combustion method. They examined the catalysts in transesterification of palm oil to synthesize biodiesel. The maximum conversion of 98 % and biodiesel yield of 92 % were achieved in the conditions of 200 mg nanocatalyst content (TiO<sub>2</sub>-ZnO), alcohol to oil molar ratio of 6:1, 5-h reaction time, and reaction temperature of 60 °C. It was explored that this method with

possessing great catalytic performances could provide an easy and cheap route with a promising potential to be implemented as an industrial method for biodiesel production.

Alves et al. (2014) utilized nano-mixed metal oxides of iron–cadmium (ICdO) and iron–tin (ISnO) in hydrolysis, transesterification, and esterification reactions. Soybean oil and macauba oil were used as feedstock for biodiesel production. Both ISnO and ICdO showed magnetic behavior as they were ferromagnetic and superparamagnetic, respectively. It was explained that nanomagnetic supports also took part in the reactions (such as oxidation reaction and alkylation). Moreover, nanomagnetic materials possessed high surface area and facilitated the separation of nanoparticles after reaction. The highest conversion of ISnO and ICdO catalysts was fulfilled at the conditions of 20/6 mass ratio of oil/methanol, 1 g catalyst loading, temperature of 200 °C, and pressure of 18.6 bar. The FAME conversions were reported as 90 % (macauba oil as feedstock, 3-h reaction time) and 84 % (soybean as feedstock, 1-h reaction time) for ISnO and ICdO catalysts, respectively. The reusability of ISnO and ICdO were examined and excellent results with almost no changes in catalytic performances were obtained for ISnO nanocatalyst. Meanwhile, the activity of ICdO catalyst slightly decreased after four cycles of reaction. It was revealed that the ratio of  $\text{Fe}^{3+}/\text{Sn}^{2+}$  remained almost constant, while the Cd content decreased after each cycle. Despite higher surface area of ICdO rather than ISnO (130.2 vs. 49.9  $\text{m}^2 \text{g}^{-1}$ ), both catalysts showed nearly the same catalytic activity.

### 12.5.5 Supported Metal Oxides

Supported metal oxide catalysts as the most used materials demonstrated adequate catalytic performances in biodiesel production. Boz et al. (2009) investigated biodiesel production from canola oil using KF supported on nano- $\gamma\text{-Al}_2\text{O}_3$ . The effect of operating parameters such as methanol to oil molar ratio, reaction temperature, catalyst loading, and reaction time was reviewed on the transesterification reaction. The catalyst preparation procedure was wet impregnation method, calcination temperature of 500 °C, and KF loading of 15 wt%. The optimum conditions to acquire the highest biodiesel yield of 99.84 were 3 wt% catalyst loading, reaction temperature of 65 °C, 8-h reaction time, and a molar ratio of 15:1 for methanol to oil. This comparative high conversion was attributed to high basicity of the surface and also high ratio of surface to volume for nanosized gamma alumina. The catalysts were analyzed for reusability, and it was found that the catalysts were stable for three cycles of reaction (38 % decrease in biodiesel yield for the third run). The main reason of 30–40 % reduction in catalytic performance after the first cycle was connected to partially decrease in KF content in catalyst composition after leaching.

Wang et al. (2009b) prepared mesoporous nanoparticles of KF/CaO–MgO (average size of 35 nm) by coprecipitation procedure and implemented for biodiesel



production process. The optimum catalyst preparation conditions were described as 8:2 for CaO/MgO mass ratio, 0.25:1 mass ratio of KF/(CaO–MgO), and calcination temperature and time of 500 °C and 3 h, respectively. The maximum biodiesel yield of 95 % was accomplished at 12:1 molar ratio of methanol to oil, catalyst dosage of 3 wt%, reaction temperature of 70 °C, and reaction time of 3 h. The recyclability of the prepared catalysts was tested for the sixth run of reaction (90 % biodiesel yield at the sixth cycle) which revealed less than 5 % decrease in biodiesel yield. Han and Guan (2009) prepared nano-heterogeneous base catalyst of  $K_2O/\gamma-Al_2O_3$  and utilized it in transesterification reaction of rapeseed oil for biodiesel synthesis. They investigated the impact of effective variables on the biodiesel production process. The optimum conditions were catalyst loading of 3 wt%, alcohol to oil molar ratio of 12:1, and reaction time and temperature of 3 h and 70 °C, respectively. The maximum biodiesel yield of 94 % was fulfilled at the optimum conditions. The optimum conditions for catalyst preparation were specified as calcination temperature of 600 °C for 3 h.

Montero et al. (2010) prepared CsNanoMgO through two methods of classical impregnation (I) and a novel coprecipitation (C) method and implemented it in transesterification reaction of tributyrin ( $(RCH_2)_2CHR$ ,  $R = CH_3CH_2CH_2COO$ ). CsNanoMgO-C demonstrated greater catalytic activity compared to the undoped and impregnated catalyst. Despite high catalytic performances of CsNanoMgO-C sample, it displayed poor reusability which mainly was associated with self-poisoning and instability of chemical structure and also coke buildup on the catalyst surface. Eventually, they found the exceptional ability of cesium as a dopant for MgO catalysts in tributyrin transesterification reaction. Wen et al. (2010) reported the preparation and application of KF/CaO as heterogeneous base nanocatalysts for transesterification reaction of Chinese tallow seed oil to biodiesel production. The catalysts were prepared using impregnation method with average pore size of 97 nm, specific surface area of  $109 \text{ m}^2 \text{ g}^{-1}$ , and particle size ranging between 30 and 100 nm. Maximum biodiesel yield of 96 % was achieved at the optimum conditions of 12:1 methanol/oil molar ratio, catalyst dosage of 4 wt%, temperature of 65 °C, and reaction time of 2.5 h. The recyclability of the prepared catalysts was examined for 16 cycles of reaction and the gained biodiesel yield was more than 91 %. From an industrial point of view, the presented results revealed the promising potential of the prepared catalyst for utilization in biodiesel production.

The catalytic performance of CaO on  $Fe_3O_4$  (as a nanosized magnetic support) was investigated by Liu et al. (2010). The highest activity was obtained at the conditions of 7:1  $Ca^{2+}$  to  $Fe_3O_4$ , 15:1 alcohol/oil molar ratio, catalyst loading of 2 wt%, and a temperature of 70 °C. The attained yield was 95 % after 80 min of reaction. One of the main reasons for applying magnetic supports was facilitating the separation steps of nanosized catalysts. Qiu et al. (2011) developed potassium bitartrate ( $C_4H_4O_6HK$ ) supported on zirconia as a new heterogeneous base nano-structured catalyst for biodiesel production from soybean oil. The effects of different operating parameters, molar ratio of methanol to oil, catalyst loadings, reaction temperature, and time were investigated. The best conditions to acquire 98.03 % yield of biodiesel were methanol to oil molar ratio of 6, catalyst loading of 6 %, and reaction time of 3 h.

temperature of 60 °C, and reaction time of 2 h. The prepared catalysts were tested in five cycles, and the results revealed a long lifetime for these catalysts with biodiesel yield of 89.65 % (8.5 % decrease in catalytic activity after five cycles). The prepared biodiesel displayed close properties with commercial diesel fuel which hinted its ability as a promising alternative for diesel.

Kaur and Ali (2011) prepared a nanocatalyst by using nanocrystalline Li impregnated on CaO support. The catalysts were applied for biodiesel production from *Jatropha* and Karanja oils (*Pongamia pinnata*) with 8.3 wt% and 3.4 wt% of FFA content, respectively. The optimum conditions which led to more than 99 % conversion were defined as molar ratio of 12:1, 65 °C, and 1.75 wt%, respectively, for methanol to oil, reaction temperature, and Li loading. These researchers stated that further investigation is required to improve the reusability of these catalysts. Hu et al. (2011) prepared nanocatalysts of KF supported on mixed oxides (CaO–Fe<sub>3</sub>O<sub>4</sub>) by using impregnation method and utilized in stillingia oil transesterification to produce biodiesel. The effects of calcination temperature and catalyst loading were examined on the biodiesel yield. The optimum reaction conditions to achieve 95 % of biodiesel yield were reported as a temperature of 65 °C, methanol/oil of 12:1, 4 wt% catalyst loading (25 wt% KF–5 wt% Fe<sub>3</sub>O<sub>4</sub> calcined at a temperature of 600 °C for 3 h) and 3-h reaction time. The prepared catalysts were tested for recyclability and the observed results were indicated 5 % reduction in biodiesel yield after 14 cycles of reaction (biodiesel yield of 90 % for the 14th run). Although for the 16th cycle the biodiesel yield reached to 84.4 % (6.5 % reduction compared to the 14th cycle), the catalysts almost demonstrated stable performances till the 20th cycle (84 % biodiesel yield).

Luz Martínez et al. (2010) reviewed the effects of nanoparticle concentration of CaO (weight percentages between 5 and 25 %) which was supported on NaX zeolite and employed in transesterification of sunflower oil to obtain biodiesel. It was confirmed that basicity of the catalysts strongly affected the methyl ester yield of the reaction. A temperature of 60 °C, catalyst loading of 16 wt%, molar ratio of 6:1 for methanol to oil, and reaction time of 6 h at the atmospheric pressure were specified as the best operating conditions to attain 93.5 % of biodiesel yield. Feysi et al. (2013) prepared nanocatalysts of Cs/Al/Fe<sub>2</sub>O<sub>3</sub> and utilized them in transesterification of soybean oil. They investigated the effects of different parameters in catalyst preparation (such as various loadings of Cs, Fe, and alumina and also different calcination procedures) and various operating conditions for transesterification reaction (such as methanol to oil molar ratio, reaction temperature, and reaction time). The maximum surface area of 85.2 m<sup>2</sup> g<sup>-1</sup> was obtained for the catalyst prepared at the conditions of molar ratio of 2.5:1 and 4:1 for Cs/Al and Cs/Fe, respectively, at the calcination temperature of 550 °C for 7 h with heating rate of 4 °C min<sup>-1</sup>. The optimum operating conditions to achieve 94.8 % of biodiesel yield were 1:14, 58 °C, and 120 min for methanol/oil molar ratio, temperature, and reaction time, respectively. The catalysts were employed in different cycles of reaction to examine the recyclability of catalysts. The results indicated no significant reduction in biodiesel yield at different cycles.

Woodford et al. (2014) utilized a supercritical sol-gel route to achieve nanoparticles of Cs–MgO catalyst. The surface area and range of crystalline diameter were reported as  $70 \text{ m}^2 \text{ g}^{-1}$  and between 12.2 nm and 22.8 nm, respectively. Pure triacylglycerides ( $\text{C}_3\text{H}_5(\text{OOR})_3$ , R:  $\text{C}_8$  and  $\text{C}_{12}$ ) and also olive oil were applied as feedstock for biodiesel production. The operating conditions to attain maximum conversion and selectivity of 93 and 78.4 % were methanol to oil molar ratio of 30:1, temperature of  $90^\circ\text{C}$ , reaction time of 24 h, catalyst dosage of 2.8 wt %, and 25 wt% of butanol for TAG solubilizing. High catalytic performance of Cs–MgO in low temperatures was associated with the high electron deficiency of Cs atoms in  $\text{CsMg}(\text{CO}_3)_2(\text{H}_2\text{O})_4$  nanospecies. Kaur and Ali (2014) prepared nanocatalysts of KF impregnated on CaO/NiO and applied for waste cooking oil (WCO) transesterification reaction. The best catalytic performances with complete transesterification reaction (>99 % biodiesel yield) were observed at the conditions of 1:15,  $65^\circ\text{C}$ , 5 wt%, and 4 h, respectively, for WCO/methanol molar ratio, temperature, catalyst loadings, and reaction time. The catalysts were recycled and employed in the fourth run with no significant loss in biodiesel yield.

Gurunathan and Ravi (2015a) evaluated biodiesel synthesis by using copper-doped ZnO (CZO) nanocatalyst. They prepared nanocatalysts of CZO with average particle size of 80 nm by coprecipitation method. The effects of oil to alcohol ratio, reaction time, and reaction temperature were studied on the biodiesel yield using WCO as feedstock. The optimum conditions were reported as 12 wt% of nanocatalyst content, volume percentage of 1:8 for oil to methanol, temperature of  $55^\circ\text{C}$ , and reaction time of 50 min which resulted in 97.71 % of biodiesel yield. The reusability of catalysts was defined, and it was found that after five cycles of reaction, the yield reduction rate was almost 10 %. Alhassan et al. (2015a) prepared  $\text{Fe}_2\text{O}_3$ – $\text{MnO}$ – $\text{SO}_4^{2-}$  supported on zirconia nanoparticle (FMSZ) via impregnation method and applied in biodiesel production from waste cooking oil. The prepared catalysts were categorized as heterogeneous solid acid catalysts which converted triglycerides into biodiesel. The most highlighted advantage of utilizing acidic catalysts was mentioned as their ability for converting low-price acidic feedstock to high-quality biodiesel. The catalysts performances were remarkable compared to biodiesel production using zirconia or sulfated zirconia catalysts. The optimum conditions were specified as oil to methanol molar ratio of 1:20, catalyst content of 3 wt%, temperature of  $180^\circ\text{C}$ , and 600 rpm stirring speed to obtain 96.5 % of biodiesel yield. In addition, the recyclability of FMSZ tested for six cycles of reaction and high catalytic stability without any losses in activity was revealed.

Alhassan et al. (2015b) investigated the preparation of nanoparticles of ferric manganese-doped tungstated zirconia (FMWZ) as a superacid catalyst and employed in biodiesel production. The feedstock was a kind of waste cooking oil with 17.5 wt% FFA value, and simultaneously reactions of esterification and transesterification were carried out using this acidic catalyst. Hydrate  $\text{ZrOCl}_2$ ,  $\text{Fe}(\text{NO}_3)_3 \cdot 9\text{H}_2\text{O}$ ,  $\text{Mn}(\text{NO}_3)_2 \cdot 4\text{H}_2\text{O}$ , and ammonium metatungstate hexahydrate as the starting materials were used for catalyst preparation via impregnation method at calcination temperature of  $600^\circ\text{C}$  for 3 h. The BET surface area, pore diameter, and pore volume of the catalyst were reported as  $44 \text{ m}^2 \text{ g}^{-1}$ , 79 nm, and  $0.0897 \text{ cm}^3 \text{ g}^{-1}$ , respectively. The best operating

conditions to achieve biodiesel yield of 96 % were defined as 1:25 molar ratio, 4 wt%, 4 h, 200 °C, and 600 rpm, respectively, for waste oil/alcohol, catalyst content, reaction time, temperature, and stirring speed. The XRF results were presented for fresh catalyst and used catalysts (after fifth and tenth cycle of reaction) and confirmed almost no significant changes in the contents of Fe, Mn, and W in the catalyst composition. The catalytic results indicated stable catalyst performances for almost ten runs. The biodiesel yield was 92.1 % at the 11th run, and this yield reduction mainly associated with the mass loss during the recovery of the catalyst. The authors claimed that FMWZ catalyst could be used for industrialization of biodiesel production from high-FFA value waste cooking oil feedstock.

Feyzi and Shahbazi (2015) synthesized nanocatalysts of Cs–Ca supported on mixed oxide of SiO<sub>2</sub>–TiO<sub>2</sub> and applied in transesterification reaction of a mix of refined plant oils. The impacts of calcination temperature and time were investigated, and the best calcination condition was specified as calcination temperature of 650 °C, time of 6 h, and heating rate of 5 °C min<sup>-1</sup>. The operating conditions to achieve 98 % of biodiesel yield were defined as methanol to oil molar ratio of 12:1, reaction temperature of 60 °C, stirring speed of 500 rpm, and reaction time of 2 h. The used catalysts were analyzed in four reaction cycles and displayed small losses in biodiesel yield. Gurunathan and Ravi (2015b) applied copper-doped ZnO (CZO) nanocatalysts in biodiesel production from neem oil as a low-cost feedstock. The optimization of process conditions were explained as oil/alcohol of 1:10 (v:v), temperature of 55 °C, nanocatalyst loading of 10 wt%, and reaction time of 60 min to achieve 97.18 % of biodiesel yield. The prepared catalysts were examined in six cycles of reaction and reduction in biodiesel yield determined as 24 % (73.95 % biodiesel yield for the sixth run of reaction).

## 12.6 Applications of Nanocatalysts in Gasification/Pyrolysis Reactions from Biomass Feedstock

Gasification process is one of the most important methods for converting biomass into gaseous products such as hydrogen, methane, and carbon monoxide. However, other undesired products such as tar and char are produced at high temperature and limited supply of oxygen (Chan and Tanksale 2014). Syngas can be converted to various sources of energies, renewable fuels, and chemicals via technological process such as Fischer–Tropsch (FT), methanol to olefins (MTO), and dimethyl ether (DME) (Heidenreich and Foscolo 2015).

There is an increasing interest of using biomass gasification process for energy production as it is an economical process even at lower production capacity (Kirubakaran et al. 2009). All kinds of biomass feedstocks can be used in gasification process. Carbon in biomass feedstock proceeds gasification process through partial oxidation reactions at relatively high temperature in the presence of an oxidant (e.g., air, steam, or pure oxygen) (Heidenreich and Foscolo 2015). The major gasification

reactions are including pyrolysis, oxidation, partial oxidation, steam reforming, reduction, and water–gas shift reactions (Chan and Tanksale 2014). Tar formation is a major hinder in commercialization of biomass gasification (Chan and Tanksale 2014). In fact, when the temperature decreases to below tar dew point temperature, tar compounds make blocking and fouling in different equipment such as filters and turbines. In general, utilizing thermal cracking and catalytic cracking can be applied for tar reduction. Although catalytic cracking is a useful method for modification of product gases at low temperature, still it has some defections such as catalyst deactivation by carbon and  $\text{H}_2\text{S}$  deposition (Han and Kim 2008).

In the following section, the metal oxide nanocatalysts employed in biomass gasification and pyrolysis reactions have been reviewed. The reported studies were specifically dedicated to the effective transition metal oxides and supported metal oxide nanocatalysts.

Yu et al. (2006) prepared char-supported nano- $\text{Fe}_3\text{O}_4$  and utilized it in hydrogen production from biomass. Char was obtained by using gasification reaction of brown coal in a fluidized-bed or fixed-bed reactor at a temperature of 800 °C. The prepared catalysts with less than 50 nm particle sizes demonstrated high activity in WGS reaction at relatively low temperature of 300 °C. It was indicated that applying nanomagnetic particles due to owning high surface area led to higher catalytic performance in WGS reaction.

Li et al. (2008a) prepared nano-NiO (12 wt% Ni) supported on  $\text{Al}_2\text{O}_3$  catalyst using deposition precipitation method and employed in tar reduction of pyrolysis or gasification reactions. The BET surface area, pore volume, and total pore diameter of the catalysts calcined at 400 °C were reported as  $124.6 \text{ m}^2 \text{ g}^{-1}$ ,  $0.37 \text{ cm}^3 \text{ g}^{-1}$ , and 12.3 nm, respectively. Sawdust particles were utilized as feedstock and a bench-scale fixed-bed reactor used for catalytic reactions. The catalysts were examined at temperatures of 600 °C, 700 °C, and 800 °C in pyrolysis reaction and maximum conversion of 99 % obtained for tar removal. Moreover, a significant increase in the produced-gas yield ( $\text{H}_2$  and CO contents) was revealed in the case of using NiO/ $\text{Al}_2\text{O}_3$  nanocatalyst in comparison with the condition without using catalyst. Li et al. (2008b) prepared nano-NiO as a catalyst for biomass pyrolysis reaction. The prepared nanocatalysts with specific surface area of  $179.2 \text{ m}^2 \text{ g}^{-1}$  were highlighted due to better catalytic performance in pyrolysis reaction of cellulose in comparison with micro-NiO ( $24.5 \text{ m}^2 \text{ g}^{-1}$ ) catalyst. The lower temperature and higher surface area of nanostructure NiO catalyst were specified as the advantages of this catalyst which led to better catalytic performances in pyrolysis and gasification reactions.

Li et al. (2009) studied the effect of tri-metallic catalyst that consisted of Ni–La–Fe supported on gamma alumina for tar reduction in the steam gasification of sawdust. The catalysts (8.6 % of NiO, 7.4 % of  $\text{Fe}_2\text{O}_3$ , and 5.9 % of  $\text{La}_2\text{O}_3$ ) were prepared using deposition precipitation method and examined in a fixed-bed reactor. The high surface area of  $214.7 \text{ m}^2 \text{ g}^{-1}$  for tri-metallic catalyst was indicated as a reason for its efficient catalytic performance. The results of experiments demonstrated longer lifetime in the case of using this catalyst rather than nanocatalyst of NiO/ $\gamma\text{-Al}_2\text{O}_3$ . Sintering effect and coke buildup were prevented in tri-metallic catalyst which was associated with the effects of doped La and Fe in this catalyst.

Based on the findings of this study, utilization of this catalyst led to a great increase in gasification yield (decrease in  $\text{CO}_2$  and  $\text{CH}_4$  content and a remarkable increase in the valuable hydrogen product); meanwhile, a high efficiency of 99 % for tar removal was attained at a temperature of 800 °C.

Gökdağ et al. (2010) compared the catalytic behavior of nano- $\text{SiO}_2$  with other catalysts such as red mud, HZSM-5,  $\text{K}_2\text{CO}_3$ , and bulk  $\text{SnO}_2$ . The highest gas yield was acquired using nano- $\text{SiO}_2$  at a temperature of 700 °C in hazelnut shell pyrolysis reaction. Applying higher temperature was reported as a method for reduction of char formation and increase in the gaseous yield. Higher surface area of  $\text{SnO}_2$  nanocatalyst was specified as a reason for improvement in the catalytic performance of biomass gasification and pyrolysis reactions. Jiang et al. (2012) developed a novel needle from nanocrystalline catalyst of  $\text{Ni}_5\text{TiO}_7/\text{TiO}_2/\text{Ti}$  (named nanoarchitected catalyst) and implemented in biomass gasification successfully. They utilized plasma oxidation reaction of  $\text{NiO}$  and  $\text{TiO}_2$  for needle-structured formation of nanocrystalline  $\text{Ni}_5\text{TiO}_7$ . Their findings indicated a significant increase in gas yields ( $\text{CH}_4$ ,  $\text{H}_2$ , and  $\text{CO}$ ) in the naphthalene reforming reaction at a temperature between 700 and 900 °C, and the obtained yield was almost two times more than gas yield of commercial catalyst. This catalyst demonstrated superior catalytic activity and higher stability (longer lifetime) even after 100 cycles of catalyst recyclability. It was outlined that this catalyst could improve the development of green technologies for biomass energy generation.

Wang et al. (2013) prepared bimetallic  $\text{Ni-Co}/\text{Al}_2\text{O}_3$  catalyst and studied their performances for steam reforming reaction of tar originated from the biomass (cedar wood) pyrolysis. The interaction between Ni and Co and confirmation of alloy formation were investigated and catalytic activities compared with single metallic Ni and Co catalysts. Higher catalytic activity and less coke formation (as the main reason of catalyst deactivation) were achieved in case of using  $\text{Co}/\text{Al}_2\text{O}_3$  catalyst. However, the performance of  $\text{Ni-Co}/\text{Al}_2\text{O}_3$  was better than  $\text{Ni}/\text{Al}_2\text{O}_3$  and lower than  $\text{Co}/\text{Al}_2\text{O}_3$ . It was revealed that addition of Co improved the catalytic performance of  $\text{Ni}/\text{Al}_2\text{O}_3$ . The catalytic activity of  $\text{Ni-Co}/\text{Al}_2\text{O}_3$  in the steam reforming reaction of tar content indicated almost no changes during 15 min of reaction at 550 °C. The best catalyst composition of  $\text{Ni-Co}/\text{Al}_2\text{O}_3$  was specified as 12 wt% of Ni and molar ratio of Co to Ni equal to 0.25:1. The stability of catalysts  $\text{Ni}$  (12 wt%)/ $\text{Al}_2\text{O}_3$ ,  $\text{Co}$  (12 wt%)/ $\text{Al}_2\text{O}_3$ , and  $\text{Ni-Co}$  ( $\text{Co}/\text{Ni} = 0.25$ )/ $\text{Al}_2\text{O}_3$  was examined at the same conditions and the results of 20 min, 40 min, and 60 min obtained, respectively.

## 12.7 Conclusion

Nanocatalysts provide a green and environmentally friendly process in biofuel production, which conducts the higher catalytic conversion and higher selectivity, economical process, milder operating conditions, and long-lasting catalysts. These investigations can be scrutinized from four different perspectives: feedstock,

operating conditions, durability, and potential of commercialization. As a matter of fact, the major cost of biodiesel production related to the feedstock, and therefore for biodiesel commercialization it is very important to find economical feedstock along with efficient technologies. In recent years converting WCO into biodiesel using heterogeneous nanocatalysts received considerable attentions. The nanocatalysts which were examined with waste oil as feedstock were KF/CaONiO, CZO, and acidic catalysts of FMSZ and FMTZ. Among these catalysts FMSZ and FMTZ were employed for high-FFA value feedstock (17.5 wt% FFAs) and demonstrated higher catalytic performances and higher recyclability compared to the other catalysts. In recent years, superacid nanocatalysts (e.g., sulfated zirconia) as a subgroup of heterogeneous catalysts for biodiesel production have received growing attention because they not only overcome many defects of homogenous acidic catalysts but also catalyze many reactions such as esterification, alkylation, cracking, and isomerization (Alhassan et al. 2015b).

Based on the reported studies on nanocatalysts for biodiesel production, the most effective parameters for nanocatalyst preparation were reported as catalyst composition, preparation method (such as impregnation and precipitation as the most used routes), and calcination procedure. The most important operating parameters which showed an influence on biodiesel yield were oil to alcohol molar ratio, temperature, stirring speed, catalyst loading, and reaction time. The range of applied operating parameters for oil/alcohol molar ratio, temperature, pressure, catalyst loading, and reaction time were 1:4–1:36, 23–280 °C, 1–90 bar, 0.2–16 wt%, and 10 min–24 h, respectively. Although applying severe operating conditions led to higher catalytic performances and further nanocatalyst reusability, it is not a recommended method in large-scale production process.

Durability of catalysts is one of the most important factors for developing heterogeneous catalysts in order to be applied industrially. In some research studies, the reusability of nanocatalysts was fully analyzed, and the number of runs for using the catalyst was presented, while in some studies the good recyclability of catalysts was mentioned generally without indicating specific information. Among the research studies, the more reusability of nanocatalysts for biodiesel production with best catalytic performances was reported for CaO, MgO, KF/CaO–MgO, KF/CaO, Cs/Al/Fe<sub>3</sub>O<sub>4</sub>, C<sub>4</sub>H<sub>4</sub>O<sub>6</sub>HK/ZrO<sub>2</sub>, KF/CaO–Fe<sub>3</sub>O<sub>4</sub>, ISnO, FMSZ, FMTZ, and Cs–Ca/SiO<sub>2</sub>–TiO<sub>2</sub> nanocatalysts. The most stable catalysts that attained the maximum life cycle were KF/CaO and KF/CaO–Fe<sub>3</sub>O<sub>4</sub> nanocatalysts with the biodiesel yield of 91 % at the 16th run and 84 % at 20th run, respectively. Based on the different studies on nanocrystalline CaO, it was revealed that presence of nanosized CaO as a highly active basic catalyst was highly effective in transesterification reaction due to its high surface area related to small crystalline particles and defects.

In brief, for the catalysts that showed poor reusability, the hypothesis is low stability of catalyst components during reaction and leaching of catalyst species into reaction mixture with the same mechanism as homogenous catalysts (Ullah et al. 2016). Applying higher calcination temperatures for catalyst preparations may be employed as a method for leaching reduction of components which is also a

trade-off between accessing higher surface area catalysts and more stable catalysts. Another hypothesis attributed the deactivation of catalysts to the existence of organic impurities or moisture and enolate formation which was caused by carboxyl group deprotonation (Reddy et al. 2006).

From a commercialization point of view, among the nanocatalysts applied for biodiesel production, CaO, KF/CaO, and TiO<sub>2</sub>-ZnO nanocatalysts were claimed to have a promising potential to be implemented for scale-up process of biodiesel production. It must be noted that for determining efficient technology for commercialization of nanocatalysts, not only criteria of higher catalytic performances and higher stability should be considered, but also other issues such as the ease of operating conditions, possibility for utilizing low-cost feedstocks, and low-energy consumption process should be regarded.

In biomass gasification and pyrolysis process, nanosized catalysts lead to higher performances compared to micro-scale catalysts due to possessing higher active site density per gram (Chan and Tanksale 2014). The main aim of most of the research studies has been focused on reduction of tar content in biomass pyrolysis and gasification (Li et al. 2009). Nickel was among the most applied transition metals in gasification and pyrolysis reactions which was also economically attractive. Applying this catalyst in pyrolysis/gasification process not only improved the gaseous products' quality but also reduced the tar formation. Based on the reported research studies, supported form of the catalyst and addition of some components such as Fe<sub>3</sub>O<sub>4</sub> and Co in the catalyst composition resulted in improvement in nanocatalytic performances of this catalyst.

Among the nanocatalysts employed for biomass gasification and pyrolysis, the best performance with the highest recyclability was revealed for Ni<sub>5</sub>TiO<sub>7</sub>/TiO<sub>2</sub>/Ti catalyst. Hence, this catalyst was proposed as an applied catalyst for green technology development in energy generation from biomass feedstock.

Despite the fact that metal oxides in nanocrystalline forms lead to increase in performances rather than common commercial catalysts, there are still difficulties such as catalyst reusability which necessitates more investigations in near future.

## References

- Akia M, Yazdani F, Motaee E, Han D, Arandiyani H (2014) A review on conversion of biomass to biofuel by nanocatalysts. *Biofuel Res J* 1(1):16–25
- Alhassan FH, Rashid U, Taufiq-Yap YH (2015a) Synthesis of waste cooking oil-based biodiesel via effectual recyclable bi-functional Fe<sub>2</sub>O<sub>3</sub>-MnO-SO<sub>4</sub><sup>2-</sup>/ZrO<sub>2</sub> nanoparticle solid catalyst. *Fuel* 142:38–45
- Alhassan FH, Rashid U, Taufiq-Yap YH (2015b) Synthesis of waste cooking oil based biodiesel via ferric-manganese promoted molybdenum oxide/zirconia nanoparticle solid acid catalyst: influence of ferric and manganese dopants. *J Oleo Sci* 64(5):505–514
- Alonso DM, Bond JQ, Dumesic JA (2010) Catalytic conversion of biomass to biofuels. *Green Chem* 12(9):1493–1513
- Alves MB, Medeiros F, Sousa MH, Rubim JC, Suarez PA (2014) Cadmium and tin magnetic nanocatalysts useful for biodiesel production. *J Brazil Chem Soc* 25(12):2304–2313



- Aradi A, Roos J, Jao TC (2013) U.S. Patent No. 8,404,155. U.S. Patent and Trademark Office, Washington, DC
- Asadullah M (2014) Biomass gasification gas cleaning for downstream applications: a comparative critical review. *Renew Sustain Energy Rev* 40:118–132
- Banerjee M, Dey B, Talukdar J, Kalita MC (2014) Production of biodiesel from sunflower oil using highly catalytic bimetallic gold–silver core–shell nanoparticle. *Energy* 69:695–699
- Barreiro DL, Prins W, Ronsse F, Brilman W (2013) Hydrothermal liquefaction (HTL) of microalgae for biofuel production: state of the art review and future prospects. *Biomass Bioenergy* 53:113–127
- Basha SA, Gopal KR, Jebaraj S (2009) A review on biodiesel production, combustion, emissions and performance. *Renew Sustain Energy Rev* 13(6):1628–1634
- Billar P, Ross AB (2011) Potential yields and properties of oil from the hydrothermal liquefaction of microalgae with different biochemical content. *Bioresour Technol* 102(1):215–225
- Boateng AA, Garcia-Perez M, Mašek O, Brown R, del Campo B (2015) Biochar production technology. In: *Biochar for environmental management: science, technology and implementation*. Routledge Taylor & Francis Group, New York, p 63
- Bok JP, Choi HS, Choi JW, Choi YS (2013) Fast pyrolysis of *Miscanthus sinensis* in fluidized bed reactors: characteristics of product yields and biocrude oil quality. *Energy* 60:44–52
- Borges ME, Diaz L (2012) Recent developments on heterogeneous catalysts for biodiesel production by oil esterification and transesterification reactions: a review. *Renew Sustain Energy Rev* 16(5):2839–2849
- Bowen EJ, Dolfing J, Davenport RJ, Read FL, Curtis TP (2014) Low-temperature limitation of bioreactor sludge in anaerobic treatment of domestic wastewater. *Water Sci Technol* 69(5):1004–1013
- Boz N, Degirmenbasi N, Kalyon DM (2009) Conversion of biomass to fuel: transesterification of vegetable oil to biodiesel using KF loaded nano- $\gamma$ - $\text{Al}_2\text{O}_3$  as catalyst. *Appl Catal Environ* 89(3):590–596
- Bridgwater T (2006) Biomass for energy. *J Sci Food Agric* 86(12):1755–1768
- Brown TM, Duan P, Savage PE (2010) Hydrothermal liquefaction and gasification of *Nannochloropsis* sp. *Energy Fuels* 24(6):3639–3646
- Bu Q, Lei H, Wang L, Wei Y, Zhu L, Liu Y, Liang J, Tang J (2013) Renewable phenols production by catalytic microwave pyrolysis of Douglas fir sawdust pellets with activated carbon catalysts. *Bioresour Technol* 142:546–552
- Budarin VL, Clark JH, Lanigan BA, Shuttleworth P, Breeden SW, Wilson AJ, Macquarrie DJ, Milkowski K, Jones J, Bridgeman T, Ross A (2009) The preparation of high-grade bio-oils through the controlled, low temperature microwave activation of wheat straw. *Bioresour Technol* 100(23):6064–6068
- Budarin V, Shuttleworth PS, Lanigan B, Clark JH (2013) Nanocatalysts for biofuels. In: *Nanocatalysis synthesis and applications*. Wiley, Hoboken, pp 595–614
- Carlos L (2005) High temperature air/steam gasification of biomass in an updraft fixed bed type gasifier (Thesis). Royal Institute of Technology, Energy Furnace and Technology. Stockholm, Sweden
- Chan FL, Tanksale A (2014) Review of recent developments in Ni-based catalysts for biomass gasification. *Renew Sustain Energy Rev* 38:428–438
- Chen MQ, Wang J, Zhang MX, Chen MG, Zhu XF, Min FF, Tan ZC (2008) Catalytic effects of eight inorganic additives on pyrolysis of pine wood sawdust by microwave heating. *J Anal Appl Pyrolysis* 82(1):145–150
- Chen M, Zhao J, Xia L (2009) Comparison of four different chemical pretreatments of corn stover for enhancing enzymatic digestibility. *Biomass Bioenergy* 33(10):1381–1385
- Chiang KY, Lu CH, Lin MH, Chien KL (2013) Reducing tar yield in gasification of paper-reject sludge by using a hot-gas cleaning system. *Energy* 50:47–53

- De Sousa HSA, Da Silva AN, Castro AJ, Campos A, Josue Filho M, Oliveira AC (2012) Mesoporous catalysts for dry reforming of methane: correlation between structure and deactivation behavior of Ni-containing catalysts. *Int J Hydrogen Energy* 37(17):12281–12291
- Demirbas A (2007) Producing bio-oil from olive cake by fast pyrolysis. *Energy Sour A Recov Util Environ Effects* 30(1):38–44
- Dominguez A, Menéndez JA, Fernandez Y, Pis JJ, Nabais JV, Carrott PJM, Carrott MR (2007) Conventional and microwave induced pyrolysis of coffee hulls for the production of a hydrogen rich fuel gas. *J Anal Appl Pyrolysis* 79(1):128–135
- Du Z, Li Y, Wang X, Wan Y, Chen Q, Wang C, Lin X, Liu Y, Chen P, Ruan R (2011) Microwave-assisted pyrolysis of microalgae for biofuel production. *Bioresour Technol* 102(7):4890–4896
- Duan P, Savage PE (2010) Hydrothermal liquefaction of a microalga with heterogeneous catalysts. *Indus Eng Chem Res* 50(1):52–61
- EIA U (2015) International energy outlook. US Energy Information Administration, Washington, DC
- Ekama G, Wentzel M (2008) Biological wastewater treatment: principles, modelling and design. IWA Publishing, London, pp 53–86
- Elbehri A, Segerstedt A, Liu P (2013) Biofuel and the sustainability challenge. Food and Agriculture Organization of the United Nations, Trade and Markets Division. Food and Agriculture Organization of the United Nations, Rome
- Eliana C, Jorge R, Juan P, Luis R (2014) Effects of the pretreatment method on enzymatic hydrolysis and ethanol fermentability of the cellulosic fraction from elephant grass. *Fuel* 118:41–47
- Fang HH, Liu H (2002) Effect of pH on hydrogen production from glucose by a mixed culture. *Bioresour Technol* 82(1):87–93
- Feyzi M, Shahbazi E (2015) Catalytic performance and characterization of Cs–Ca/SiO<sub>2</sub>–TiO<sub>2</sub> nanocatalysts for biodiesel production. *J Mol Catal A Chem* 404:131–138
- Feyzi M, Hassankhani A, Rafiee HR (2013) Preparation and characterization of Cs/Al/Fe<sub>3</sub>O<sub>4</sub> nanocatalysts for biodiesel production. *Energy Conv Manage* 71:62–68
- Fiori L, Valbusa M, Castello D (2012) Supercritical water gasification of biomass for H<sub>2</sub> production: process design. *Bioresour Technol* 121:139–147
- Glaser JA (2012) Green chemistry with nanocatalysts. *Clean Technol Environ Policy* 14(4):513–520
- Gökdağ Z, Sınag A, Yumak T (2010) Comparison of the catalytic efficiency of synthesized nano tin oxide particles and various catalysts for the pyrolysis of hazelnut shell. *Biomass Bioenergy* 34(3):402–410
- Goswami M, Meena S, Navatha S, Rani KP, Pandey A, Sukumaran RK, Prasad RB, Devi BP (2015) Hydrolysis of biomass using a reusable solid carbon acid catalyst and fermentation of the catalytic hydrolysate to ethanol. *Bioresour Technol* 188:99–102
- Gou C, Yang Z, Huang J, Wang H, Xu H, Wang L (2014) Effects of temperature and organic loading rate on the performance and microbial community of anaerobic co-digestion of waste activated sludge and food waste. *Chemosphere* 105:146–151
- Guo F, Fang Z, Xu CC, Smith RL (2012) Solid acid mediated hydrolysis of biomass for producing biofuels. *Prog Energy Combust Sci* 38(5):672–690
- Gurunathan B, Ravi A (2015a) Biodiesel production from waste cooking oil using copper doped zinc oxide nanocomposite as heterogeneous catalyst. *Bioresour Technol* 188:124–127
- Gurunathan B, Ravi A (2015b) Process optimization and kinetics of biodiesel production from neem oil using copper doped zinc oxide heterogeneous nanocatalyst. *Bioresour Technol* 190:424–428
- Hahn-Hägerdal B, Galbe M, Gorwa-Grauslund MF, Lidén G, Zacchi G (2006) Bio-ethanol the fuel of tomorrow from the residues of today. *Trends Biotechnol* 24(12):549–556
- Hamaguchi M, Cardoso M, Vakkilainen E (2012) Alternative technologies for biofuels production in kraft pulp mills—potential and prospects. *Energies* 5(7):2288–2309

- Hamze H, Akia M, Yazdani F (2015) Optimization of biodiesel production process from the waste cooking oil using response surface methodology. *Process Saf Environ Protect* 94:1–10
- Han H, Guan Y (2009) Synthesis of biodiesel from rapeseed oil using  $K_2O/\gamma-Al_2O_3$  as nano-solid-base catalyst. *Wuhan Univ J Nat Sci* 14(1):75–79
- Han J, Kim H (2008) The reduction and control technology of tar during biomass gasification/pyrolysis: an overview. *Renew Sustain Energy Rev* 12(2):397–416
- Hasheminejad M, Tabatabaei M, Mansourpanah Y, Javani A (2011) Upstream and downstream strategies to economize biodiesel production. *Bioresour Technol* 102(2):461–468
- Heidenreich S, Foscolo PU (2015) New concepts in biomass gasification. *Progress Energy Combust Sci* 46:72–95
- Heredia-Olea E, Pérez-Carrillo E, Serna-Saldívar SO (2015) Effect of extrusion conditions and hydrolysis with fiber-degrading enzymes on the production of C5 and C6 sugars from brewers' spent grain for bioethanol production. *Biofuel Res J* 2(1):203–208
- Hosseini SS, Aghbashlo M, Tabatabaei M, Najafpour G, Younesi H (2015) Thermodynamic evaluation of a photobioreactor for hydrogen production from syngas via a locally isolated *Rhodospseudomonas palustris* PT. *Int J Hydrogen Energy* 40(41):14246–14256
- Hosseini-Sarvari M, Sodagar E (2013) Esterification of free fatty acids (Biodiesel) using nano sulfated-titania as catalyst in solvent-free conditions. *Comptes Rendus Chimie* 16(3):229–238
- Hu S, Guan Y, Wang Y, Han H (2011) Nano-magnetic catalyst  $KF/CaO-Fe_3O_4$  for biodiesel production. *Appl Energy* 88(8):2685–2690
- Huang YB, Fu Y (2013) Hydrolysis of cellulose to glucose by solid acid catalysts. *Green Chem* 15(5):1095–1111
- Huang YF, Kuan WH, Lo SL, Lin CF (2008) Total recovery of resources and energy from rice straw using microwave-induced pyrolysis. *Bioresour Technol* 99(17):8252–8258
- Huang YF, Kuan WH, Lo SL, Lin CF (2010) Hydrogen-rich fuel gas from rice straw via microwave-induced pyrolysis. *Bioresour Technol* 101(6):1968–1973
- Ibeh B, Gardner C, Terman M (2007) Separation of hydrogen from a hydrogen/methane mixture using a PEM fuel cell. *Int J Hydrogen Energy* 32(7):908–914
- Iranmahboob J, Nadim F, Monemi S (2002) Optimizing acid-hydrolysis: a critical step for production of ethanol from mixed wood chips. *Biomass Bioenergy* 22(5):401–404
- Jiang X, Zhang L, Wybornov S, Staedler T, Hein D, Wiedenmann F, Krumm W, Rudnev V, Lukiyanchuk I (2012) Highly efficient nanoarchitected  $Ni_5TiO_7$  catalyst for biomass gasification. *ACS Appl Mater Interf* 4(8):4062–4066
- Jingura RM, Kamusoko R (2015) A multi-factor evaluation of *Jatropha* as a feedstock for biofuels: the case of sub-Saharan Africa. *Biofuel Res J* 2(3):254–257
- Karagöz S, Bhaskar T, Muto A, Sakata Y (2006) Hydrothermal upgrading of biomass: effect of  $K_2CO_3$  concentration and biomass/water ratio on products distribution. *Bioresour Technol* 97(1):90–98
- Karimi K, Tabatabaei M, Sárvári Horváth I, Kumar R (2015) Recent trends in acetone, butanol, and ethanol (ABE) production. *Biofuel Res J* 2(4):301–308
- Kaur M, Ali A (2011) Lithium ion impregnated calcium oxide as nano catalyst for the biodiesel production from karanja and jatropha oils. *Renew Energy* 36(11):2866–2871
- Kaur M, Ali A (2014) Potassium fluoride impregnated  $CaO/NiO$ : an efficient heterogeneous catalyst for transesterification of waste cottonseed oil. *Eur J Lipid Sci Technol* 116(1):80–88
- Khan Z, Yusup SS, Ahmad MM, Fui L, Chin B (2014) Performance study of Ni catalyst with quicklime (CaO) as  $CO_2$  adsorbent in palm kernel shell steam gasification for hydrogen production. *Adv Mater Res* 917:292–300
- Khoshnevisan K, Bordbar AK, Zare D, Davoodi D, Noruzi M, Barkhi M, Tabatabaei M (2011) Immobilization of cellulase enzyme on superparamagnetic nanoparticles and determination of its activity and stability. *Chem Eng J* 171(2):669–673
- Kim K, Kim Y, Yang C, Moon J, Kim B, Lee J, Lee U, Lee S, Kim J, Eom W, Lee Y (2013) Long-term operation of biomass-to-liquid systems coupled to gasification and Fischer–Tropsch processes for biofuel production. *Bioresour Technol* 127:391–399

- Kirrolia A, Bishnoi NR, Singh R (2013) Microalgae as a boon for sustainable energy production and its future research and development aspects. *Renew Sustain Energy Rev* 20:642–656
- Kirubakaran V, Sivaramakrishnan V, Nalini R, Sekar T, Premalatha M, Subramanian P (2009) A review on gasification of biomass. *Renew Sustain Energy Rev* 13(1):179–186
- Knoef H (2005) Practical aspects of biomass gasification. In: *Handbook of biomass gasification*. BTG Biomass Technology Group BV, Enschede, pp 13–37
- Kojima Y, Kato Y, Akazawa M, Yoon SL, Lee MK (2015) Pyrolysis characteristic of kenaf studied with separated tissues, alkali pulp, and alkali lignin. *Biofuel Res J* 2(4):317–323
- Kruse A (2009) Hydrothermal biomass liquefaction. *J Supercrit Fluids* 47:391–399
- Kumar P, Barrett DM, Delwiche MJ, Stroeve P (2009) Methods for pretreatment of lignocellulosic biomass for efficient hydrolysis and biofuel production. *Indus Eng Chem Res* 48(8):3713–3729
- Kwietniewska E, Tys J (2014) Process characteristics, inhibition factors and methane yields of anaerobic digestion process, with particular focus on microalgal biomass fermentation. *Renew Sustain Energy Rev* 34:491–500
- Lee JW, Hawkins B, Day DM, Reicosky DC (2010) Sustainability: the capacity of smokeless biomass pyrolysis for energy production, global carbon capture and sequestration. *Energy Environ Sci* 3(11):1695–1705
- Lei H, Ren S, Julson J (2009) The effects of reaction temperature and time and particle size of corn stover on microwave pyrolysis. *Energy Fuels* 23(6):3254–3261
- Lei H, Ren S, Wang L, Bu Q, Julson J, Holladay J, Ruan R (2011) Microwave pyrolysis of distillers dried grain with solubles (DDGS) for biofuel production. *Bioresour Technol* 102(10):6208–6213
- Li J, Yan R, Xiao B, Liang DT, Du L (2008a) Development of nano-NiO/Al<sub>2</sub>O<sub>3</sub> catalyst to be used for tar removal in biomass gasification. *Environ Sci Tech* 42(16):6224–6229
- Li JF, Bo XIAO, Du LJ, Rong YAN, Liang TD (2008b) Preparation of nano-NiO particles and evaluation of their catalytic activity in pyrolyzing cellulose. *J Fuel Chem Technol* 36(1):42–47
- Li J, Xiao B, Yan R, Xu X (2009) Development of a supported tri-metallic catalyst and evaluation of the catalytic activity in biomass steam gasification. *Bioresour Technol* 100(21):5295–5300
- Lin YC, Cho J, Tompsett GA, Westmoreland PR, Hube GW (2009) Kinetics and mechanism of cellulose pyrolysis. *J Phys Chem C* 113(46):20097–20107
- Lin Y, Ge X, Li Y (2014) Solid-state anaerobic co-digestion of spent mushroom substrate with yard trimmings and wheat straw for biogas production. *Bioresour Technol* 169:468–474
- Liu C, Lv P, Yuan Z, Yan F, Luo W (2010) The nanometer magnetic solid base catalyst for production of biodiesel. *Renew Energy* 37(7):1531–1536
- Liu S, Bai SQ, Zheng Y, Shah KW, Han MY (2012) Composite metal–oxide nanocatalysts. *ChemCatChem* 4(10):1462–1484
- Luz Martínez S, Romero R, López JC, Romero A, Sánchez Mendieta V, Natividad R (2010) Preparation and characterization of CaO nanoparticles/NaX zeolite catalysts for the transesterification of sunflower oil. *Indus Eng Chem Res* 50(5):2665–2670
- Lyberatos G, Skiadas I (1999) Modelling of anaerobic digestion—a review. *Glob Nest Int J* 1(2):63–76
- Madhuvilakku R, Piraman S (2013) Biodiesel synthesis by TiO<sub>2</sub>–ZnO mixed oxide nanocatalyst catalyzed palm oil transesterification process. *Bioresour Technol* 150:55–59
- Madsen M, Holm-Nielsen JB, Esbensen KH (2011) Monitoring of anaerobic digestion processes: a review perspective. *Renew Sustain Energy Rev* 15(6):3141–3155
- Mao C, Feng Y, Wang X, Ren G (2015) Review on research achievements of biogas from anaerobic digestion. *Renew Sustain Energy Rev* 45:540–555
- Meena S, Navatha S, Devi BP, Prasad RBN, Pandey A, Sukumaran RK (2015) Evaluation of Amberlyst15 for hydrolysis of alkali pretreated rice straw and fermentation to ethanol. *Biochem Eng J* 102:49–53
- Meher LC, Sagar DV, Naik SN (2006) Technical aspects of biodiesel production by transesterification—a review. *Renew Sustain Energy Rev* 10(3):248–268

- Mirahmadi K, Kabir MM, Jeahanipour A, Karimi K, Taherzadeh M (2010) Alkaline pretreatment of spruce and birch to improve bioethanol and biogas production. *BioResources* 5(2):928–938
- Miura M, Kaga H, Sakurai A, Kakuchi T, Takahashi K (2004) Rapid pyrolysis of wood block by microwave heating. *J Anal Appl Pyrolysis* 71(1):187–199
- Moen J, Yang C, Zhang B, Lei H, Hennessy K, Wan Y, Le Z, Liu Y, Chen P, Ruan R (2009) Catalytic microwave assisted pyrolysis of aspen. *Int J Agric Biol Eng* 2(4):70–75
- Mohan D, Pittman CU, Steele PH (2006) Pyrolysis of wood/biomass for bio-oil: a critical review. *Energy Fuels* 20(3):848–889
- Montero JM, Wilson K, Lee AF (2010) Cs promoted triglyceride transesterification over MgO nanocatalysts. *Topics Catal* 53(11–12):737–745
- Mood SH, Golfeshan AH, Tabatabaei M, Abbasalizadeh S, Ardjmand M (2013a) Comparison of different ionic liquids pretreatment for barley straw enzymatic saccharification. *Biotech* 3(5):399–406
- Mood SH, Golfeshan AH, Tabatabaei M, Jouzani GS, Najafi GH, Gholami M, Ardjmand M (2013b) Lignocellulosic biomass to bioethanol, a comprehensive review with a focus on pretreatment. *Renew Sustain Energy Rev* 27:77–93
- Moon J, Lee J, Lee U, Hwang J (2013) Transient behavior of devolatilization and char reaction during steam gasification of biomass. *Bioresour Technol* 133:429–436
- Mukherjee S, Kumar P, Hosseini A, Yang A, Fennell P (2014) Comparative assessment of gasification based coal power plants with various CO<sub>2</sub> capture technologies producing electricity and hydrogen. *Energy Fuels* 28(2):1028–1040
- Murugesan A, Umarani C, Chinnusamy TR, Krishnan M, Subramanian R, Neduzchezain N (2009) Production and analysis of bio-diesel from non-edible oils—a review. *Renew Sustain Energy Rev* 13(4):825–834
- Nagao N, Tajima N, Kawai M, Niwa C, Kurosawa N, Matsuyama T, Yusoff EM, Toda T (2012) Maximum organic loading rate for the single-stage wet anaerobic digestion of food waste. *Bioresour Technol* 118:210–218
- Onwudili JA (2014) Hydrothermal gasification of biomass for hydrogen production. In: Jin F (ed) *Application of hydrothermal reactions to biomass conversion*. Springer, Berlin, pp 219–246
- Pakpour F, Najafpour G, Tabatabaei M, Tohidfar M, Younesi H (2014) Biohydrogen production from CO-rich syngas via a locally isolated *Rhodopseudomonas palustris* PT. *Bioprocess Biosyst Eng* 37(5):923–930
- Park SK, Ahn JH, Kim TS (2011) Performance evaluation of integrated gasification solid oxide fuel cell/gas turbine systems including carbon dioxide capture. *Appl Energy* 88(9):2976–2987
- Peterson AA, Vogel F, Lachance RP, Fröling M, Antal MJ Jr, Tester JW (2008) Thermochemical biofuel production in hydrothermal media: a review of sub- and supercritical water technologies. *Energy Environ Sci* 1(1):32–65
- Puig-Arnavat M, Bruno JC, Coronas A (2010) Review and analysis of biomass gasification models. *Renew Sustain Energy Rev* 14(9):2841–2851
- Qin K, Lin W, Jensen PA, Jensen AD (2012) High-temperature entrained flow gasification of biomass. *Fuel* 93:589–600
- Qiu F, Li Y, Yang D, Li X, Sun P (2011) Heterogeneous solid base nanocatalyst: preparation, characterization and application in biodiesel production. *Bioresour Technol* 102(5):4150–4156
- Rabelo SC, Andrade RR, Maciel Filho R, Costa AC (2014) Alkaline hydrogen peroxide pretreatment, enzymatic hydrolysis and fermentation of sugarcane bagasse to ethanol. *Fuel* 136:349–357
- Reddy C, Reddy V, Oshel R, Verkade JG (2006) Room-temperature conversion of soybean oil and poultry fat to biodiesel catalyzed by nanocrystalline calcium oxides. *Energy Fuels* 20(3):1310–1314
- Ren S, Lei H, Wang L, Bu Q, Chen S, Wu J, Julson J, Ruan R (2012) Biofuel production and kinetics analysis for microwave pyrolysis of Douglas fir sawdust pellet. *J Anal Appl Pyrolysis* 94:163–169

- Sachs I (2007) The biofuels controversy. UNCTAD, New York, NY
- Salema AA, Ani FN (2011) Microwave induced pyrolysis of oil palm biomass. *Bioresour Technol* 102(3):3388–3395
- Santos RB, Lee JM, Jameel H, Chang HM, Lucia LA (2012) Effects of hardwood structural and chemical characteristics on enzymatic hydrolysis for biofuel production. *Bioresour Technol* 110:232–238
- Semwal S, Arora AK, Badoni RP, Tuli DK (2011) Biodiesel production using heterogeneous catalysts. *Bioresour Technol* 102(3):2151–2161
- Şensöz S, Angin D, Yorgun S (2000) Influence of particle size on the pyrolysis of rapeseed (*Brassica napus* L.): fuel properties of bio-oil. *Biomass Bioenergy* 19(4):271–279
- Song C, Hu H, Zhu S, Wang G, Chen G (2004) Nonisothermal catalytic liquefaction of corn stalk in subcritical and supercritical water. *Energy Fuels* 18(1):90–96
- Sun P, Heng M, Sun S, Chen J (2010) Direct liquefaction of paulownia in hot compressed water: influence of catalysts. *Energy* 35(12):5421–5429
- Tabatabaei M, Tohidfar M, Jouzani GS, Safarnejad M, Pazouki M (2011) Biodiesel production from genetically engineered microalgae: future of bioenergy in Iran. *Renew Sustain Energy Rev* 15(4):1918–1927
- Tabatabaei M, Karimi K, Sárvári Horváth I, Kumar R (2015) Recent trends in biodiesel production. *Biofuel Res J* 2(3):258–267
- Talebi AF, Mohtashami SK, Tabatabaei M, Tohidfar M, Bagheri A, Zeinalabedini M, Mirzaei HH, Mirzajanzadeh M, Shafaroudi SM, Bakhtiari S (2013) Fatty acids profiling: a selective criterion for screening microalgae strains for biodiesel production. *Algal Res* 2(3):258–267
- Teo SH, Rashid U, Taufiq-Yap YH (2014) Biodiesel production from crude *Jatropha Curcas* oil using calcium based mixed oxide catalysts. *Fuel* 136:244–252
- Tiwari GN, Mishra RK (2011) Advanced renewable energy sources. Royal Society of Chemistry, London
- Toor SS, Rosendahl L, Rudolf A (2011) Hydrothermal liquefaction of biomass: a review of subcritical water technologies. *Energy* 36(5):2328–2342
- Ullah F, Dong L, Bano A, Peng Q, Huang J (2016) Current advances in catalysis toward sustainable biodiesel production. *J Energy Inst* 89(2):282–292
- Verziu M, Cojocar B, Hu J, Richards R, Ciuculescu C, Filip P, Parvulescu VI (2008) Sunflower and rapeseed oil transesterification to biodiesel over different nanocrystalline MgO catalysts. *Green Chem* 10(4):373–381
- Vyas AP, Verma JL, Subrahmanyam N (2010) A review on FAME production processes. *Fuel* 89(1):1–9
- Wang L, Yang J (2007) Transesterification of soybean oil with nano-MgO or not in supercritical and subcritical methanol. *Fuel* 86(3):328–333
- Wang XH, Chen HP, Ding XJ, Yang HP, Zhang SH, Shen YQ (2009a) Properties of gas and char from microwave pyrolysis of pine sawdust. *BioResources* 4(3):946–959
- Wang Y, Hu SY, Guan YP, Wen LB, Han HY (2009b) Preparation of mesoporous nanosized KF/CaO–MgO catalyst and its application for biodiesel production by transesterification. *Catal Lett* 131(3–4):574–578
- Wang L, Li D, Koike M, Watanabe H, Xu Y, Nakagawa Y, Tomishige K (2013) Catalytic performance and characterization of Ni–Co catalysts for the steam reforming of biomass tar to synthesis gas. *Fuel* 112:654–661
- Weiming Y, Xueyuan B, Zhihe L, Lihong W, Nana W, Yanqiang Y (2008) Laboratory and pilot scale studies on fast pyrolysis of corn stover. *Int J Agric Biol Eng* 1(1):57–63
- Wen L, Wang Y, Lu D, Hu S, Han H (2010) Preparation of KF/CaO nanocatalyst and its application in biodiesel production from Chinese tallow seed oil. *Fuel* 89(9):2267–2271
- Woodford JJ, Parlett C, Dacquin JP, Cibin G, Dent A, Montero J, Wilson K, Lee AF (2014) Identifying the active phase in Cs-promoted MgO nanocatalysts for triglyceride transesterification. *J Chem Technol Biotechnol* 89(1):73–80

- Xiu S, Shahbazi A, Shirley V, Mims MR, Wallace CW (2010) Effectiveness and mechanisms of crude glycerol on the biofuel production from swine manure through hydrothermal pyrolysis. *J Anal Appl Pyrolysis* 87(2):194–198
- Xu ZR, Zhu W, Gong M, Zhang HW (2013) Direct gasification of dewatered sewage sludge in supercritical water. Part 1: Effects of alkali salts. *Int J Hydrogen Energy* 38(10):3963–3972
- Yan J, Li A, Xu Y, Ngo TPN, Phua S, Li Z (2012) Efficient production of biodiesel from waste grease: one-pot esterification and transesterification with tandem lipases. *Bioresour Technol* 123:332–337
- Yen HW, Brune DE (2007) Anaerobic co-digestion of algal sludge and waste paper to produce methane. *Bioresour Technol* 98(1):130–134
- Yu J, Tian FJ, McKenzie LJ, Li CZ (2006) Char-supported nano iron catalyst for water-gas-shift reaction: hydrogen production from coal/biomass gasification. *Process Saf Environ Protect* 84(2):125–130
- Yu F, Deng S, Chen P, Liu Y, Wan Y, Olson A, Kittelson D, Ruan R (2007) Physical and chemical properties of bio-oils from microwave pyrolysis of corn stover. *Appl Biochem Biotechnol* 137(1–12):957–970
- Zahed O, Jouzani GS, Abbasalizadeh S, Khodaiyan F, Tabatabaei M (2015) Continuous co-production of ethanol and xylitol from rice straw hydrolysate in a membrane bioreactor. *Folia Microbiol* 61:179–189
- Zhang L, Xu CC, Champagne P (2010) Overview of recent advances in thermo-chemical conversion of biomass. *Energy Conv Manage* 51(5):969–982
- Zhang T, Liu L, Song Z, Ren G, Feng Y, Han X, Yang G (2013a) Biogas production by co-digestion of goat manure with three crop residues. *PLoS One* 8(6), e66845
- Zhang XL, Yan S, Tyagi RD, Surampalli RY (2013b) Biodiesel production from heterotrophic microalgae through transesterification and nanotechnology application in the production. *Renew Sustain Energy Rev* 26:216–223
- Zheng J, Xu L, Liu Y, Zhang X, Yan Y (2012) Lipase-coated  $K_2SO_4$  micro-crystals: preparation, characterization, and application in biodiesel production using various oil feedstocks. *Bioresour Technol* 110:224–231

# Chapter 13

## Nanocatalysis for the Conversion of Nonedible Biomass to Biogasoline via Deoxygenation Reaction

Hwei Voon Lee and Joon Ching Juan

**Abstract** Deoxygenation of nonedible biomass is one of the main challenges for the development of technologies to produce biofuels, which possess high thermal and chemical stability to be used in combustion engines. Generally, deoxygenation reaction is facilitated by a suitable catalyst based on the surface area, particle size, porosity, and acidity–basicity. Lately, catalysis in nanodimension (nanocatalyst) has received a great attention as deoxygenation catalyst. Due to high surface area to volume ratios of nanocatalyst, it is able to tune the physicochemical properties toward higher catalytic activity. This is because nanocatalyst can overcome several limitations in a heterogeneous system, such as mass transfer, long reaction time, catalyst deactivation, and poisoning. Thus, many attempts have been made to develop new forms of nanocatalysts for deoxygenation. The catalytic conversion system of biomass to biogasoline has been reported using different edible and nonedible feedstock. Recent studies have focused on the synthesis and manipulation of nanocatalysts to improve the product yield and selectivity under mild operating conditions. In this chapter, the establishment of nanocatalysts for converting nonedible oil to bio-olefin (biogasoline) via deoxygenation process (e.g., hydrodeoxygenation, hydrocracking, and decarboxylation) has been highlighted.

**Keywords** Nanodimension • Nanostructure • Nanocatalyst • Deoxygenation • Biogasoline

---

H.V. Lee  
Nanotechnology & Catalysis Research Centre (NANOCAT), Institute of Postgraduate Studies,  
University of Malaya, 50603 Kuala Lumpur, Malaysia

J.C. Juan (✉)  
Nanotechnology & Catalysis Research Centre (NANOCAT), Institute of Postgraduate Studies,  
University of Malaya, 50603 Kuala Lumpur, Malaysia

School of Science, Monash University, Sunway Campus, Jalan Lagoon Selatan, 47500 Bandar  
Sunway, Malaysia  
e-mail: [jcjuan@um.edu.my](mailto:jcjuan@um.edu.my)



## 13.1 Introduction

Gasoline, also known as petrol, is a petroleum-derived liquid that is used globally as fuel in internal combustion engines in the transportation sector and the petrochemical-based industry (Galadima and Muraza 2015). This liquid hydrocarbon comprises mainly of light to medium ( $C_5$ – $C_{12}$ ) aliphatic chains and isomers, where propane, butane, pentane, heptane, and nonane are the most common alkane components. Besides that, aromatics, cycloalkane, and others are also found in the liquid hydrocarbon (Table 13.1) (Sanders and Maynard 1968; Johansen et al. 1983; Sheppard et al. 2016).

With the expansion of automobile sector, the global demand and consumption of gasoline grow progressively every year. Both gasoline (42 %) and diesel (22 %) production carry around 2/3 of each barrel of petroleum in the refinery process in the United States, which indicates the high demand for fuel in the automotive sector. The remainder yields are jet fuels (9 %), liquefied petroleum gasses (5 %), heavy fuel oils (4 %), distillates (2 %), and other by-products (16 %) (Wallington et al. 2006).

The reduction of oil reserves, fluctuation of oil prices, deterioration of health due to high sulfur content, and declination of the environment caused by greenhouse gas (GHG) have led to world demand for the exploitation of renewable carbon sources for bio-based gasoline (Deneyer et al. 2015). The alternatives for petroleum-based gasoline include bioalcohol and bio-based hydrocarbon-range gasoline.

Generally, conventional alcohol (methanol, ethanol, propanol, and butanol) consists of similar fuel characteristics as gasoline, which allows it to be used in internal combustion engines. As shown in Table 13.2, alcohol-based fuels have a similar energy density (~33 MJ/L) and high octane number values as gasoline. The

**Table 13.1** Chemical composition of gasoline fuel (Sanders and Maynard 1968; Johansen et al. 1983; Sheppard et al. 2016)

Chemical composition	Percentage (wt%)
(1) Alkane	49.5
Propane	0.1
n-Butane	3.7
Isopentane	9.3
n-Pentane	7.8
2-Methylpentane	4.2
3-Methylpentane	2.7
n-Hexane	4
2-Methylhexane	1.4
3-Methylhexane	1.5
n-Heptane	2
n-Octane	1.2
n-Nonane	0.7
(2) Aromatics	33.2
(3) Cycloalkane	6.9
(4) Other	10.4

**Table 13.2** Comparison of fuel properties for gasoline and alcohol-based fuel

Fuel	Energy density (MJ/L)	Average octane (AKI rating/RON) <sup>a</sup>
Gasoline	~33	85–96/90–105
Methanol	~16	98.65/108.7
Ethanol	~20	99.5/108.6
Propanol	~24	108/118
Butanol	~30	97/103

<sup>a</sup>AKI—Anti-Knock Index: This octane rating is used in countries like Canada and the United States; RON—Research Octane Number: This octane rating is used in Australia and most of Europe

presence of higher octane values than that of gasoline indicate that alcohol fuels burn slower, which reveals a more energy efficient fuel in terms of distance per volume metrics. Within the C<sub>1</sub>–C<sub>4</sub> alcohol range, butanol owns the highest fuel efficiency rating for engine usage. However, unfavorable hygroscopicity and corrosivity of alcohol pose difficulties to storage systems, and the low chemical stability of alcohol influences its fuel performance. Thus, alcohol was not used directly, but it served as a gasoline additive to increase octane rating and improve vehicle emissions (Owen and Coley 1996; Shah and Sen 2011).

In order to reduce the dependence on fossil fuel for alcohol production, bio-based alcohol (e.g., bioethanol) can be derived from renewable cellulosic biomass, such as trees and grass. Chemically, there is no characteristic difference between biologically produced (from biomass) and chemically produced from petroleum alcohols. For example, bioethanol is a bio-based alcohol made by fermenting the sugar components of plant materials and is mostly made from sugar and starch crops (Gray et al. 2006). Similar to petroleum-based butanol, biobutanol also has the advantage in combustion engines. The energy density of biobutanol is very close to gasoline (while still retaining over 25 % higher octane rating), but it is difficult to produce as compared to bioethanol (Kumar and Gayen 2011).

With the limitations of bioalcohol as a gasoline alternative, biomass-based gasoline (biogasoline) tends to be developed as a substitute for gasoline in existing internal combustion engines. Like petroleum-based gasoline, biogasoline composed of hydrocarbon components in alkane range of C<sub>6</sub> (hexane) to C<sub>12</sub> (dodecane) carbon atoms, while the molecular structures are chemically different from biobutanol and bioethanol (Hassan et al. 2015).

Conventionally, the main source of carbon-type components in gasoline is extracted via petroleum refinery process. In order to sustain the transition to renewable carbon sources, biorefinery systems with the use of biomass feedstock such as carbohydrate-based feedstocks (hemicellulose and cellulose), lignin, and plant-based triglycerides have been initiated. This will help to reduce humanity's dependence on fossil fuels as energy sources in daily and industrial activities. Recently, the focus on the usage of nonfood-based biomass resources has received worldwide attention as debates surround the food versus fuel competition. There are

two types of potential biogasoline feedstock: (1) lignocellulosic biomass composed of mainly sugar-based materials (cellulose and hemicellulose) and lignin and (2) nonedible plant oil (triglyceride) from lipid biomass (Regalbuto 2009).

The transition to petroleum-based gasoline into nonfood-biomass-based gasoline provides several advantages: (1) full compatibility of biogasoline to conventional gasoline makes it applicable to all types of transport vehicles that run on existing gasoline engines, (2) provides a replacement that will force the reduction on petroleum dependence and subsequent reduction in environmental impacts, and (3) no competition with the food purposes. Hence, biogasoline is a promising biofuel that ensures full energy security and maintains safer environment without sacrificing engine operating performance at a relatively cheaper price with the usage of low-cost biofuel feedstock (Hassan et al. 2015).

However, for successful execution of biogasoline into a commercial investment, technological issues such as catalyst and reactor design should be addressed. Catalytic deoxygenation is a prominent technology for the conversion of liquid biomass into alkane-range biogasoline. The process involves removing oxygen from the oxygenated feedstock into a mixture of hydrocarbons and aromatic compounds via cracking, decarboxylation, decarbonylation, and hydrodeoxygenation pathways (Harlin et al. 2012; Brandvold and McCall 2013). Although, these processes have shown promising findings in the laboratory, there are technical barriers that need to be tackled in order to scale up to a manufacturing plant. This includes the need for extremely high temperatures for deoxygenation process in the presence of a liquid acid catalyst. These issues may not disqualify this method for future manufacturing scale, and hence, further improvement needs to be assessed in light of better benign catalytic pathways available.

In the twenty-first century, nanocatalysts have attracted many researchers to develop a feasible and renewable energy production scheme. Nanocatalysts have been proposed as effective tools for cracking large refractories of biomass-based organic molecules into desirable products. Typically, nanocatalysts possess large surface area to the volume ratio as compared to bulk materials, and this makes them the key to increase the reactivity of biomass conversion. Furthermore, the tunable acid–base properties, type of active metal nanoparticles, and porosity of nanosized catalysts are additional features affecting the efficiency in biomass conversion.

The present chapter is an overview of the various nanocatalysts used to produce biogasoline via deoxygenation reaction from renewable biomass. It has been observed that the type of nanocatalyst and the nature of the biomass feedstock (lignocellulosic biomass and lipid biomass) influence the extent of deoxygenation and the selectivity of the gasoline range. Nonedible biogasoline production and the future outlook of nanocatalyst application in biorefinery scheme have also been discussed.

## 13.2 Nanocatalysts

Catalysis plays a crucial role in controlling deoxygenation reaction mechanisms and reaction kinetics by which oxygenated biomass transformations take place, thus enabling the viable creation of desired biogasoline-range alkane products. Deoxygenation catalysts are categorized into homogeneous [inorganic acids (HCl, H<sub>2</sub>SO<sub>4</sub>), alkali (NaOH, KOH), and transition metal salts (FeCl<sub>3</sub>, FeSO<sub>4</sub>)] (Fischmeister et al. 2012; Deuss et al. 2014), and heterogeneous [(noble metals—Ni, Co, Mo, and Fe) supported on porous-structured catalysts] (Lin and Huber 2009; Rinaldi and Schüth 2009). Both of the homogeneous and heterogeneous catalysts have their own superior properties and weaknesses. Nanocatalysts have combined positive characteristics of both the homogeneous and heterogeneous catalytic systems (Fig. 13.1). Nanocatalytic systems allowed a rapid, selective, highly active reaction coupled with the ease of catalyst separation and recovery. Catalyst reusability is one of the important criteria of biomass conversion before being acceptable for commercial scale biofuel/chemical manufacturing processes. Furthermore, the nanoparticle size of the catalysts leads to a high surface area to volume ratio, which increases the contact between the bulky biomass reactants and the catalysts during the reaction. Therefore, the catalytic activities and yield are comparable to the homogeneous catalytic system. In another word, nanocatalysts mimic the homogeneous catalytic system and can be easily recycled (Singh and Tandon 2014).

In principle, nanocatalysts are defined as catalytically active materials comprising either (1) particles smaller than 100 nm in at least one dimension or (2) porous compounds having pore diameters not bigger than 100 nm (Oliveira et al. 2014). Besides, nanocatalysts are also known as “semi-heterogeneous” or “soluble heterogeneous” catalysts, which consist of unique aspects of biorefinery process, such as

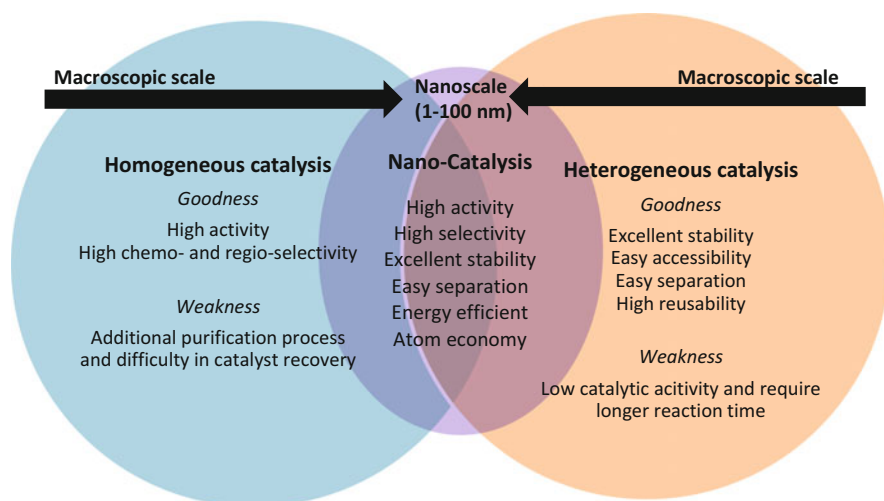


**Fig. 13.1** Characteristics of bulk (homogeneous and heterogeneous) catalysts and nanocatalysts

high reactivity and selectivity, homogeneous mimic-like structure, lower process energy consumption (high catalytic activity as compared to the same amount of bulk catalysts with lower reaction temperature), longer lifetime of the catalyst systems and enhanced possibilities to isolate and reuse the active nanomaterial (Widegren and Finke 2003; Astruc et al. 2005). Thus, nanocatalysts are prominent examples to illustrate the efforts toward “green chemistry” in sustainable biomass conversion, for which they fulfill the criteria that reduce the generation of hazardous substances during the manufacturing process.

### ***13.2.1 Characteristics of Nanocatalyst***

The properties of nanocatalysts are strongly influenced by three factors (1) size, (2) shape, and (3) surface composition by controlling these parameters that tailor the optimal characteristics for biomass conversion (Gellman and Shukla 2009; Somorjai et al. 2009).

**Particle size:** Reduction in particle size of catalysts to nanoscale leads to the increase of surface atom to bulk atom ratio. Thus, more catalytically active sites are accessible for substrate molecules, which can increase catalytic activities (turnover frequency, TOF). The nanoscale materials do not merely lead to an increase in S/V but evoke novel properties differing from their macroscopic counterparts (e.g., mechanical, electronic, and optical properties).

**Catalyst shape and structure:** The catalytic activity and selectivity of nanocatalysts are influenced by tuning the shape of particles (i.e., tetrahedral, cubic, and spherical). Even though a catalyst has the same size, tetrahedral particles featuring a larger number of edges and corners are considerably more active than spherical shape.

**Surface composition:** Higher selectivity can be achieved by adjusting the chemical composition of the catalysts’ surface. This can be done via the employment of bimetallic system, core–shell type, or the use of support. The co-adsorbing molecules (such as electron donors or acceptors) attached to the surface of the catalysts improve the activation energy of the reaction pathways and therefore, the respective selectivity can be influenced as the stability of the reaction intermediates are affected. In addition, surface composition is an important contributor to nanocatalyst durability and reusability. Since nanoparticle catalysts have a high tendency to agglomerate, it is important to stabilize the catalytic system. One possibility to reduce agglomeration tendency and stabilize the nanocatalysts is by functionalization of the surface with capping agents, such as polymers or surfactants.

**Surface area to volume ratio:** Smaller particles comprise of large surface areas with respect to their volume. Thus, this will contribute a positive effect on reaction rate and enhance the catalytic activity of nanocatalysts.

### 13.2.2 Performance of Nanocatalyst

The optimal dimensions to determine the performance of nanocatalyst catalyzed biomass conversion include (a) high activity, (b) high selectivity, and (c) high durability and reusability. All these advantages will enable the deoxygenation process become more efficient, consume less energy, and produce less waste, which helps to counter environmental and sustainable impact due to conventional fuel (Li and Somorjai 2010; Oliveira et al. 2014).

- (a) *Selectivity*: Highly selective catalysts are able to produce ideally 100 % of the desired product even the competing reaction pathways would lead to thermodynamically more stable molecules. Moreover, complicated separation steps can be eliminated, and the raw material is converted more efficiently to the product without generating unnecessary by-products that have to be disposed of. From an economic point of view, the process costs can potentially be reduced.
- (b) *Activity*: High activity ensures that the raw material is completely converted into the product by the catalyst per unit time. Theoretically, turnover frequency (TOF) is used to measure the catalytic activity of catalysts. For industrial applications, high catalytic activities lead to higher output per time, which indicates higher plant capacity utilization.
- (c) *The lifetime of a catalyst*: The durability and reusability of catalysts can be determined by the total number of catalytic cycles. The productivity of catalysts can be measured by turnover number (TON), which denotes the total amount of product (in moles) that can be formed by a given amount (in moles) of a catalyst. Therefore, a highly durable catalyst will enable more economic production in larger quantities of the desired compound by avoiding frequent interruption due to the replacement of catalyst.

### 13.2.3 Synthesis of Nanocatalysts

Nanocatalysts that are applied for biomass conversion can be categorized into: (a) nanoparticle catalysts and (b) porous nanocatalysts. Figure 13.2 illustrates the different active metal nanoparticles and nanoporous support materials that are potentially employed for deoxygenation reaction. The nanoparticle catalysts comprised of particle sized between 1 and 100 nm. Preparation of stabilized nanoparticles (e.g., Ni, Pd, and Pt) is the main challenge in nanochemistry. In general, nanoparticles can be prepared by two techniques, namely “top-down” and “bottom-up.” The top-down approach involves mechanical grinding, metal vapor, thermal breakdown, chemical breakdown, and spontaneous chemisorption. In contrast, bottom-up methods involve solgel, precipitation, chemical reduction of salts, solvothermal processing, electrochemistry, template directed, sonochemistry,

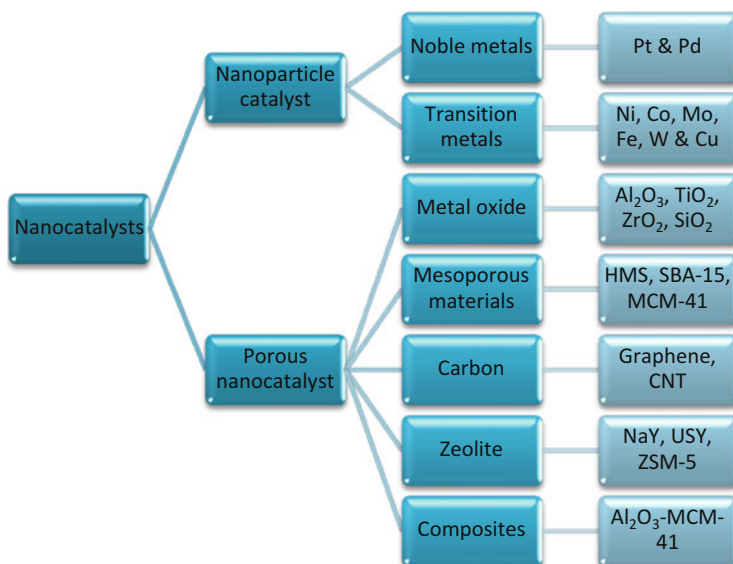


**Fig. 13.2** Different types of nanocatalysts for biomass conversion

microwave irradiation, and microemulsion (Zhou et al. 2005; Horikoshi and Serpone 2013).

The top-down approach is to break the bulk material down mechanically, thermally, or chemically into smaller particles. However, this method is being criticized because of its inability to yield particles with uniform characteristics. The bottom-up approach involves the formation of nanocatalysts by reaction or agglomeration of suitable starting molecules with or without structure-directing agents. This approach is more favorable than the former approach, as it allows the synthesis of well-defined and stabilized catalysts at the nanoscale, with regard to size, shape, and surface composition. This is due to the use of stabilizing agents such as ligands, surfactants, polymers, dendrimers, ions, or polyoxoanions used to control the size of the nanoparticles (Horikoshi and Serpone 2013).

There are two main challenges that need to be solved during the usage of nanoparticle catalysts in a liquid medium for biomass conversion: (1) the tendency to agglomerate associated with deterioration in their unique characteristics and (2) the difficulties encountered in the catalyst recovery from the viscous mixture after the reaction. To overcome the aggregation problem, active metal nanoparticle catalysts can be deposited on different kinds of catalyst supports. As the catalyst supports consist of defined and regularly structured pores and channels on the nanoscale, wherein the catalytic processes take place, they are named porous nanocatalysts. Furthermore, the unique pore structure of nanocatalysts act as “nanoreactors” to promote regio- and stereoselectivity of the reaction process (Oliveira et al. 2014; Singh and Tandon 2014). The most prominent representatives of this class are zeolite, mesoporous silica, mesoporous/macroporous resins,

mesoporous metal oxides, graphene, and interconnected carbon nanosheets (Sinağ 2012).

Supported active metal nanocatalysts are one of the most potential heterogeneous catalysts for biofuel and petrochemical industries such as hydrogenation, deoxygenation, methanation, reforming, and hydrocracking. Active metal nanoparticles (Ni, Cu, Pt, and Pd) play an important role in the reaction process, while the use of catalyst supports (e.g., mesoporous metal oxide, carbon, zeolite) helps to prevent agglomeration and improves the stability/durability of the active metal catalysts. Suitable metal nanoparticle dispersion on the catalyst supports is capable of increasing the accessible active center for reaction. Furthermore, large pore sizes of the catalyst support render greater diffusion of bulky biomass and products during the course of the reaction. Hence, high dispersion of small particles of active metal and high catalyst porosity are desirable at all time (Akia et al. 2014).

## 13.3 Deoxygenation of Nonedible Feedstock

### 13.3.1 *Potential of Nonedible-Based Biomass*

There is a high demand for a shift to alternative industrial feedstock and sustainable processes to synthesize green fuel from renewable biomass resources. Conversion of biomass into paraffin based (biofuel) has received great attention to overcome the scenario of high petroleum consumption, as well as the environmental interest of renewable energy, and reduction of gas emissions. Application of renewable bio-based feedstock as fuel resources has shown good returns pertaining to economic, social, and environmental aspects: (1) constant supply of feedstock, (2) decrease in carbon footprint from the biofuel usage, and (3) money-making agricultural industry (Huber et al. 2006). Currently, efforts have been made on searching high-performance, sustainable alternative second-generation feedstock (nonfood-based feedstock) that can substitute petrol fuel without greenhouse gas emissions or cause a food crop crisis. The foremost conflict to the usage of cultivated crops for the biofuel production is its effect on food supply. Thus, exploitation of nonfood-based biomass or farming of nonedible crops for fuel production becomes a future transition to renewable carbon resources for biofuel production (Naik et al. 2010).

Generally, the potential renewable biomass feedstock is carbohydrate-based materials (i.e., hemicellulose and cellulose), lignin, and glycerides (Fig. 13.3) (Ashraful et al. 2014; Arun et al. 2015). Lignocellulosic biomass, such as agricultural, industrial, and forest waste, is the cheapest and most abundant carbon source for biofuel production. However, the presence of high oxygen functionality (40–45 wt% of oxygen) in lignocellulosic biomass needs to be converted into transportation fuel mimicked structure, by the removal of oxygen in the form of



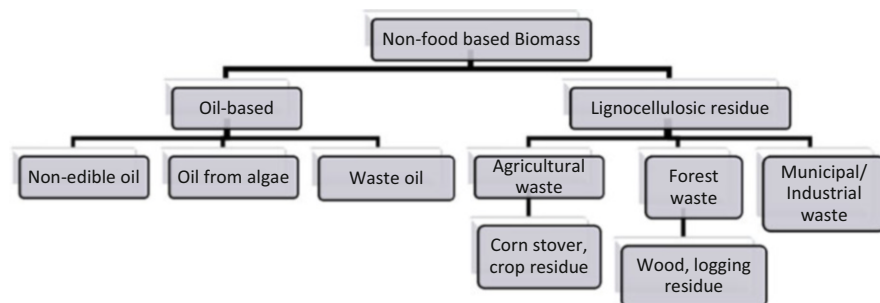


Fig. 13.3 Overview of nonfood-based biomass feedstock

CO<sub>2</sub> or H<sub>2</sub>O, and conversion into a higher-grade liquid fuel (Huber et al. 2006; Cherubini 2010).

The structured portion of lignocellulose biomass is composed of cellulose (35–50 wt%), hemicellulose (25–30 wt%), and lignin (15–30 wt%). Generally, cellulose and hemicellulose are composed of 60–90 wt% of native biomass (Huber et al. 2006). Cellulose is a homopolymer, which is composed of a linear polysaccharide with  $\alpha$ -1,4 linkages of D-glucopyranose monomers. The degree of polymerization of cellulose is about 10,000–15,000 glucopyranose monomer units in softwood. The mild acid hydrolysis will cause cellulose to depolymerize into cellobiose (glucose dimer), cellotriose (glucose trimer), cellotetraose (glucose tetramer), or glucose unit. Hemicellulose is composed of five-carbon sugars xylose and arabinose) and six-carbon sugars (galactose, glucose, and mannose), with the most abundant building block of hemicellulose, xylan (a xylose polymer linked at the 1 and 4 positions). Starting from cellulose and hemicellulose, a wide range of alkanes (C<sub>5</sub>–C<sub>31</sub>) with/without the presence of cyclic and/or branched structures can be synthesized in three stages: (1) decoupling of polysaccharides into sugars, followed by (2) dehydration and hydrogenation into hydrocarbons, and (3) further aldol condensation, radical reaction, oligomerization, or alkylation will yield longer chains of alkanes. Lignin is an irregular large polyaromatic compound that is formed from three phenolic building blocks (coniferyl, sinapyl, and coumaryl alcohols) that linked through ether and C–C interunit connections. The lignin-derived alkanes, such as mixture of phenolic monomers (C<sub>6</sub>–C<sub>11</sub>) and dimers (C<sub>12</sub>–C<sub>22</sub>) can be produced via (1) decoupling reaction and further (2) deoxygenation and hydrogenation into short (C<sub>6</sub>–C<sub>9</sub>) and mid-range (C<sub>12</sub>–C<sub>18</sub>) cyclic alkane products (Deneyer et al. 2015).

Another type of biomass (lipid biomass) used to produce biofuel utilizes energy crops that consist of high energy density and structural similarities to petroleum-based fuels are vegetable oils. Currently, the focus is concentrated on nonedible oils, which include *Jatropha*, algae oil, waste cooking oils, and fats. The use of nonedible oils compared to edible oils is significant in developing countries because of the great demand for edible vegetable oils as food; these edible vegetable oils are expensive for biofuel production. Generally, a huge amount of nonedible oil plants

is naturally available (Taufiqurrahmi and Bhatia 2011). Energy crops such as *Jatropha curcas*, *Maduca indica*, *Pongamia pinnata*, *Simmondsia chinensis*, *Linum usitatissimum*, *Nicotiana tabacum*, *Calophyllum inophyllum*, *Hevea brasiliensis*, *Croton megalocarpus*, *Carmellia*, *Simarouba glauca*, desert date, *Sapindus mukorossi*, algae, etc. represent second-generation biofuel feedstock. Furthermore, nonedible vegetable oil crops are grown in wastelands (unproductive lands, degraded forests, cultivators' fallow lands, irrigation canals, and boundaries of roads and fields), and their farming cost is lower than that of edible oil crops because intensive care is not required to sustain a reasonably high yield (Ashraful et al. 2014).

Triglycerides can be decomposed into one glycerol molecule and three fatty acid molecules. The carbon chain length and the number of unsaturated bonds in the fatty acids depend on the source of oil crops. The feedstock oils cannot apply directly as petrol fuels due to their high oxygen content (>50%), which leads to some technical limitations such as low heating value, immiscibility with petrol fuels, tendency to polymerize, thermal instability, and high viscosity. Thus, production of alkanes via deoxygenation process is able to enhance energy density of the product by reducing the oxygen content in triglyceride system. During the deoxygenation reaction, a fatty acid with unsaturated bond is saturated via hydrogenation, and oxygen is removed in the form of water and CO or CO<sub>2</sub> gas via decarboxylation or decarbonylation. The dominant alkane products in the range of C<sub>15</sub>–C<sub>18</sub> will be produced (Snåre et al. 2008). Figure 13.4 shows an overview of the chemo-catalytic process for the production of biogasoline-range alkanes based on carbohydrate-based materials, lignin, and triglyceride. There is a necessity to change and modify the chemical structure and the carbon skeleton of ligno-cellulosic and lipid biomass in order to produce biofuel (Deneyer et al. 2015).

### 13.3.2 Deoxygenation Reaction

In order to chemically mimic biomass-based gasoline as petroleum-based gasoline (biogasoline), deoxygenation approach is used to remove oxygen from a bio-based feedstock. As mentioned earlier, if large amounts of oxygenated compounds are present in the products, this would hinder the application as fuel due to the challenges both in storage and usage in internal combustion engines. Various combinational reaction pathways of the deoxygenation of biomass can take place, depending on the feedstock composition, catalyst choice, and reaction conditions. Decarboxylation, decarbonylation, and hydrodeoxygenation are the main reaction routes in deoxygenating biomass to biogasoline fuel (Gosselink et al. 2013).

*Deoxygenation* covers all reaction pathways involving the removal of oxygen from a molecule in the form of H<sub>2</sub>O, CO<sub>2</sub>, or CO.

*Decarbonylation/decarboxylation* covers the deoxygenation reactions where CO<sub>2</sub> (decarboxylation) or CO (decarbonylation) is removed from a molecule. For

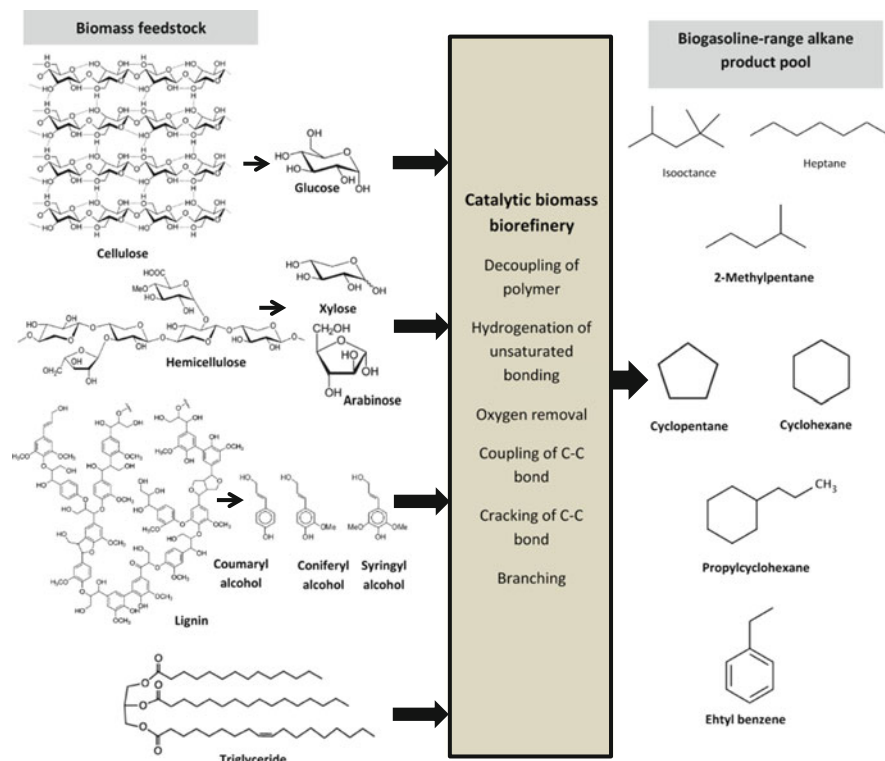
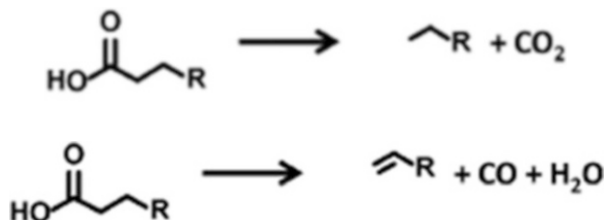
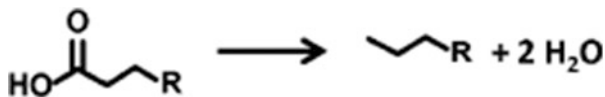


**Fig. 13.4** Overview of the biomass biorefinery for the production of biogasoline-range alkanes starting from sugar-based materials, lignin, and triglyceride-based oil

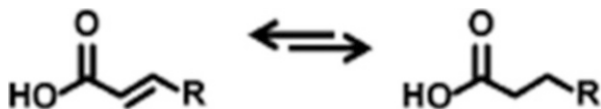
fatty acids, deoxygenation process yield paraffin and  $\text{CO}_2$ , while decarbonylation yield olefins,  $\text{CO}$ , and  $\text{H}_2\text{O}$ .



*Hydrodeoxygenation* is the reaction pathway where oxygen is removed from a feedstock in the presence of hydrogen gas. In the case of fatty acids, hydrodeoxygenation will lower the oxidation state of the carbon atom by using  $\text{H}_2$  to form hydrocarbons and  $\text{H}_2\text{O}$ .



*Hydrogenation* is the hydrogen addition reactions without the cleavage of bonds.



### 13.3.3 Reaction Mechanism of Deoxygenation Process

#### 13.3.3.1 Deoxygenation Mechanism of Triglyceride-Based Feedstock

In general, the main component of lipid biomass consists of triglycerides, which are divided into two parts, namely, glycerol and fatty acid backbone. The long chain of fatty acid backbone varies in chain length from 14 to 30 carbon atoms depending on the source of the biomass. To produce paraffin with the same length ( $C_n$ ) or one carbon atom shorter ( $C_{n-1}$ ), three proposed decomposition pathways (1)  $\beta$ -elimination, (2)  $\gamma$ -hydrogen transfer, and (3) direct deoxygenation were presented (Fig. 13.5). Among the reaction pathways,  $\beta$ -elimination is the preferred route for alkane production. Firstly, fatty acids from triglycerides will decouple from glycerol via hydrolysis,  $\beta$ -elimination, or hydrogenolysis pathways. The fatty acid was further converted in desired saturated chain via hydrogenation and formation of oxygen-free alkane after the oxygen-removal process. There are several pathways for oxygen removal of fatty acids including hydrodeoxygenation, decarbonylation, and decarboxylation. The hydrodeoxygenation is able to produce same carbon chain lengths of alkane's product, while decarbonylation and decarboxylation yield shorter carbon chain as the reaction involve consumption of hydrogen molecule. Typically, the lengths of fatty acid chains from vegetable oil vary between  $C_{12}$  and  $C_{22}$ , which the majority group is between  $C_{16}$  and  $C_{18}$  chains. This indicates that the yielded hydrocarbons are mostly attributed to the range of  $C_{15}$ – $C_{18}$ . Nevertheless, shorter and branched alkanes are also produced during deoxygenation reaction, where further cracking and isomerization of the formed  $C_{15}$ – $C_{18}$  alkanes are required. Kinetically, the formation of fatty acids from triglycerides is a relatively fast process; thus, the deoxygenation (hydrodeoxygenation, decarboxylation, or decarbonylation) of fatty acids to hydrocarbons is regarded as rate-determining step (Fig. 13.6) (Gosselink et al. 2013; Mohammad et al. 2013).

Formation of  $C_{n-2}$  hydrocarbons via  $\gamma$ -hydrogen migration during thermal decomposition at 450 °C was reported by Gosselink's research group. Generally, the deoxygenation process was performed at a reaction temperature of 250–380 °C; thus,  $\gamma$ -hydrogen transfer decomposition pathway is presumed to only occur at increased reaction temperatures during pyrolysis process (Gosselink et al. 2013).

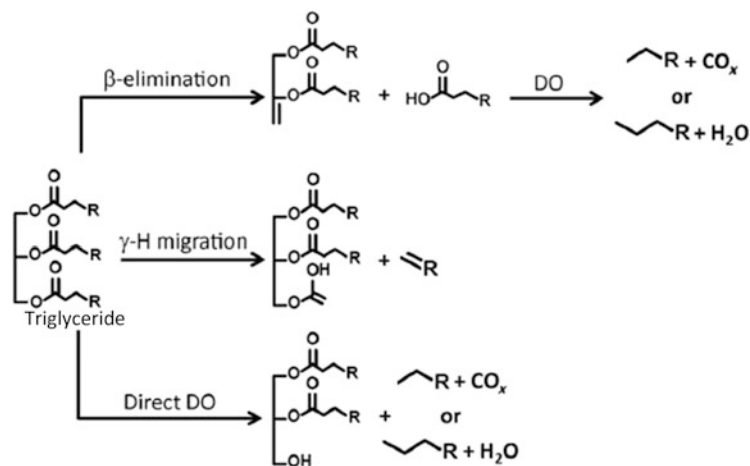


Fig. 13.5 Plausible deoxygenation pathways of triglycerides

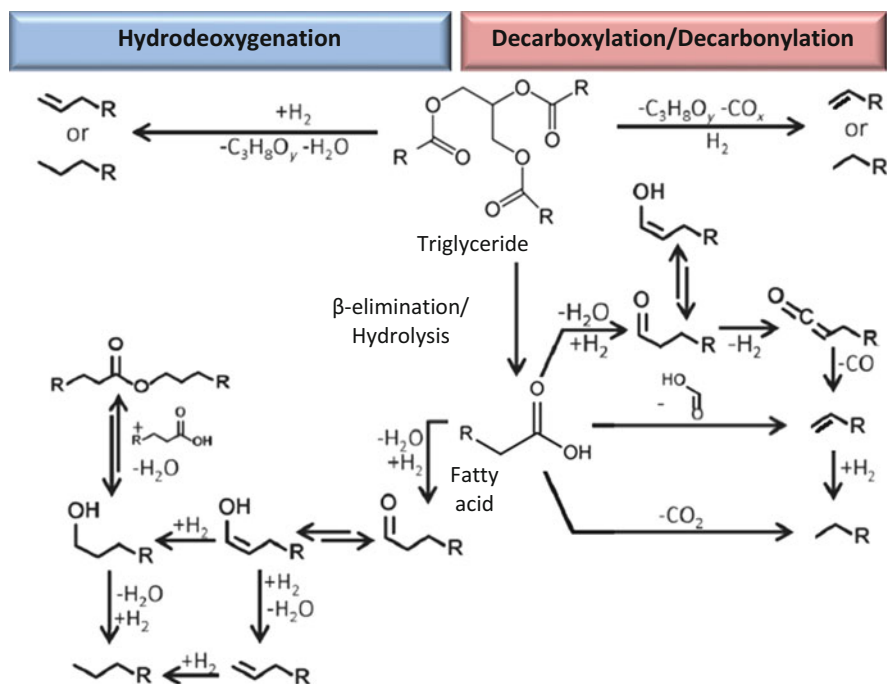


Fig. 13.6 Reaction mechanism for decarboxylation/decarbonylation and hydrodeoxygenation of triglyceride feedstock

### 13.3.3.2 Deoxygenation Mechanism of Lignocellulosic Biomass Feedstock

#### Sugar-Based Feedstock

Glucose is a potential feedstock derived from nonfood cellulosic biomass (sugar-based feedstock). It can be directly converted into the biomass platform chemical 5-hydroxymethylfurfural (HMF), which can then be converted into 5-hydroxymethyl tetrahydrofuran-2-carbaldehyde (HMTHFA), a promising biogasoline component with high energy density than ethanol fuel (Dunn et al. 2013). Deoxygenation of sugar monomers usually occurs via (Ho et al. 2012);

1. Dehydration of sugar monomers to 5-hydroxymethylfurfural (HMF).
2. Hydrogenation to 5-hydroxymethyl tetrahydrofuran-2-carbaldehyde (HMTHFA).
3. The two intermediates formed further undergo aldol condensation reactions to form large molecules with more carbons.
4. Multistep hydrogenation/dehydration processes to form C<sub>9</sub>–C<sub>15</sub> alkanes.

#### Lignin-Based Model Compounds

As lignin is a complex polyaromatic matrix made up of alkoxy substituted phenylpropyl units, a model component (guaiacol) is discussed herein to avoid complexity. Guaiacol (2-methoxyphenol) can be represented as a lignin model component, which is composed of simple monomeric structures and product distribution compared to real lignin (Asmadi et al. 2011; Nguyen et al. 2016). Generally, guaiacol conversion routes are mainly determined by methoxy group, phenolic group, and the benzene ring. The overview of plausible reaction pathways is discussed below (Ho et al. 2012):

##### *Methoxy group reaction routes*

1. Demethylation of guaiacol to produce catechol, which is subsequently deoxygenated to phenol
2. Demethoxylation of guaiacol to produce phenol directly

##### *Phenolic group reaction route*

3. Cleavage of C–O between hydroxyl group and the aromatic ring of guaiacol to produce methoxybenzene

##### *Benzene ring reaction route*

4. Hydrogenation of guaiacol's aromatic ring followed by the rupture of methyl group or hydroxyl group

*Phenol is one of the major intermediates formed from deoxygenation of guaiacol. It can be further upgraded via two parallel reaction routes as discussed below:*

5. Hydrogenolysis–hydrogenation: direct hydrogenolysis of C–O bonds, then followed by hydrogenation of benzene ring to cyclohexane
6. Hydrogenation–hydrogenolysis: hydrogenation of aromatic ring followed by dehydration forming C=C bonds and rehydrogenation of the double bonds to cyclohexane

## 13.4 Nanocatalysts for Deoxygenation Reaction

### 13.4.1 Precious and Non-precious Metal Catalyst

The efficiency of removing oxygen from biomass via HDO or DCO is highly dependent on the type of catalyst. In general, metal sulfide shows higher selectivity toward HDO products, while precious metals, which are group 10 metals (e.g., Pd, Pt, and Ni), take place via DCO route (Peng et al. 2012b; Gosselink et al. 2013; Ding et al. 2014). For example, Pt supported on activated carbon is highly active for deoxygenation of oleic acid to C<sub>17</sub> hydrocarbons (Na et al. 2012). In addition, results also revealed that activated carbon, which has a large surface area, achieved better metal dispersion than silica support at similar metal loading. These promising results are also supported by Yang et al. (2013) (Table 13.3, Entry 1) in which 5 wt % Pt supported on carbon nanotubes showed the high conversion of stearic acid and selectivity toward heptadecane. The conversion and selectivity were up to 52 % and 97 % toward heptadecane, respectively. Although Pd and Pt are proven to be active and selective toward deoxygenation process (Na et al. 2012; Yang et al. 2013), the high costs of these noble metals represent a major drawback from an economic standpoint, especially in large-scale production.

Therefore, non-precious metals have been actively studied for deoxygenation reaction. This is because non-precious metals are in abundance with cheaper price. Nevertheless, the fundamental understanding between non-precious and precious metals is still not well understood. It was reported that a series of metal comprised of Pd, Pt, Ru, Mo, Ni, Rh, Ir, and Os have been screened for deoxygenation of fatty acids (Snåre et al. 2006). The deoxygenation activity was found to be in the following order: Pd>Pt>Ni>Rh>Rh >Ir>Ru>Os. Among the non-precious metals, Ni is the most potential alternative to replace the use of noble metals. The catalytic activity of Ni-based catalysts can be improved when the supported Ni content is increased. It is worth to note that the cost of Ni is approximately 1000 and 2500 times cheaper than that of Pd and Pt, respectively (Santillan-Jimenez and Crocker 2012). Moreover, Ni-based catalysts are capable of producing green hydrocarbons with shorter chain lengths. This is an important characteristic for green gasoline and jet fuel production.

**Table 13.3** Catalytic conversion of nonedible oils

Entry	Catalyst	Reactor	T (°C)	P (bar)	t (h)	Conv (%)	Selectivity (%)			Ref
							HDO	DCO	Isomerization	
1	5 wt% Pt/MWCNT	Batch	330	N/A	0.5	52.4	N/A	97	N/A	Yang et al. (2013)
2	10 wt% Ni/ZrO <sub>2</sub>	Batch	260	6	8	N/A	N/A	26	N/A	Peng et al. (2012b)
3	10 wt% Ni/ZrO <sub>2</sub>	Batch	260	40	8	N/A	N/A	66	N/A	Peng et al. (2012b)
4	10 wt% Ni/ZrO <sub>2</sub>	Batch	260	70	8	N/A	N/A	59	N/A	Peng et al. (2012b)
5	10 wt% Ni/ZrO <sub>2</sub>	Batch	270	40	8	76	N/A	68	N/A	Peng et al. (2012b)
6	10 wt% Ni/ZrO <sub>2</sub>	Trickle bed	270	40	8	75	N/A	70	N/A	Peng et al. (2012b)
7	Ni-Al LDH	Continuous	260	40	1	65	N/A	Major	N/A	Santillan-Jimenez et al. (2015)
8	Ni-Al LDH	Continuous	260	40	4	55	N/A	Major	N/A	Santillan-Jimenez et al. (2015)
9	NiMoS/TiO <sub>2</sub>	Batch	300	35	4	100	56	5	N/A	Kubička et al. (2014)
10	10 wt% Ni/HBEA (Si/Al = 180)	Batch	260	40	8	75	54	8.9	6.3	Peng et al. (2012a)
11	Fe-MSN	Batch	290	30	6	67	C <sub>18</sub> :C <sub>17</sub> 6.4:1			Kandel et al. (2014)



Peng et al. (2012b) used 10 wt% Ni/ZrO<sub>2</sub> to convert microalgae oil to alkanes at 270 °C and 40 bar H<sub>2</sub> (Table 13.3, Entry 2–6). A total of 76 wt% yield and high selectivity toward C<sub>17</sub> hydrocarbon (66 %) were achieved after 4 h of reaction. The product in the liquid phase mainly comprised of C<sub>17</sub> *n*-heptadecane followed by minor amounts of C<sub>13</sub>–C<sub>21</sub>. Ni with the particle size of 11.6 nm was homogeneously dispersed on ZrO<sub>2</sub>. This Ni/ZrO<sub>2</sub> catalyst was highly stable, and its catalytic activity remained active even after 72 h. This result is in accordance with the literature where DCO is favored over group 10 metals (Pt, Pd, and Ni). Besides that, Ni–Al layered double hydroxide (Ni–Al LDH) was also used as a catalyst in the conversion of oil to fuel-like hydrocarbons (Table 13.3, Entry 7–8) (Santillan-Jimenez et al. 2015). The interlayer distance of the Ni–Al LDH of 7.1 nm allows the long-chain triglycerides to easily diffuse into the active site. However, this catalyst showed a poor stability as the reaction time increased from 1 h to 4 h, the conversion dropped 15 %. Kubička et al. (2014) found that NiMoS/TiO<sub>2</sub> (Table 13.3, Entry 9) deoxygenates rapeseed oil to *n*-octadecane (C<sub>18</sub>) as the main product, and the minor amount is *n*-heptadecane (C<sub>17</sub>). The ratio of C<sub>18</sub>/C<sub>17</sub> is 10, which would mean deoxygenation is selective toward HDO. It is believed that the adsorption of oxygenated compounds onto TiO<sub>2</sub> plays an important role in the transformation:  $\sigma$ -bonding adsorption through the oxygen atom would give C–O hydrogenolysis, while  $\pi$ -bonding of the double bond would allow hydrogenation.

As mentioned earlier, DCO route is normally catalyzed by group 10 metals. It was surprising to observe that Ni showed higher selectivity toward HDO when supported on zeolite. Zeolite is widely used in the cracking of petroleum products due to its outstanding properties such as high surface area, strong acid strength, and high density of acid sites. In this aspect, HDO has been conducted at 260 °C and 40 bar H<sub>2</sub> over 10 wt% Ni/HBEA zeolite (Si/Al ratio = 180) (Table 13.3, Entry 10). This catalyst works well because Ni efficiently catalyzes hydrogenolysis of fatty acid esters, which is the rate-determining step. Then this is followed by zeolite's Brønsted acid sites catalyzing dehydration of alcohol intermediates. Besides, Brønsted acid sites are also believed to catalyze hydroisomerization and hydrocracking of alkane products (Velichkina et al. 2008; Peng et al. 2012a). A 75 wt% yield of liquid alkanes was successfully achieved after 8 h. The channel system of zeolite beta has pore diameters of 5.6 × 5.6 Å and 7.7 × 6.6 Å (Bárcia et al. 2005); thus, triglycerides could not diffuse into the pores. This would also mean that the catalytic activity occurs on the surface. The acidity properties of zeolites can be tuned by selecting the most appropriate silica–alumina ratio (Si/Al ratio) (Macario et al. 2008). Zeolite with low Si/Al ratio exhibited higher acid strength and favored cracking reaction. Under similar reaction conditions, Ni/HBEA (Si/Al = 45) only achieved 26 % liquid yield (Song et al. 2013). The low catalytic activity and selectivity can be due to a weaker Brønsted acid strength (low Si/Al ratio) as a support. Cracking was more prominent (HDO/cracking ratio of 2.49 and 8.57) over HBEA with Si/Al ratio of 45 and 180, respectively, regardless of metal loading. These results demonstrate that acidity of the support plays a more prominent role as compared to Ni as an active metal. When Si/Al ratio of HZSM-5 was increased

from 45 to 200, selectivity toward cracking gradually decreased from 42.7 % to 7.2 % (Peng et al. 2012a). Meanwhile, selectivity toward HDO increased from 41 % to 80 %. The Ni loading increased with the selectivity of HDO from 82.8 % to 84.6 %. This is because the acid density of HBEA was reduced by 23 % with the increase of Ni from 5 to 10 wt% loading.

### ***13.4.2 Mesoporous Catalyst for Deoxygenation Reaction of Triglyceride to Biofuel***

Catalytic performance can be affected by diffusion limitations even in the case of small organic molecules. The dimension of triglyceride molecules is around 5 nm depending on the fatty acid chains, which is larger than the micropore size of zeolite (<2 nm) (Lukic et al. 2010). For example, only less than 10 % of zeolite active sites might actually be involved in a catalytic reaction due to the limited mass transport (Perez-Ramirez et al. 2008). Slow diffusion can cause polymerization of by-products within microporous channels. This will normally lead to coke formation which is associated with loss of catalytic activity (Na et al. 2013). Therefore, mesoporous materials between 2 and 50 nm are desirable in solving diffusional issues. The common mesoporous material is mesoporous molecular sieves (MCM-41) with varying Si/Al ratio (Kubička et al. 2010) and SBA-15 (Lee and Ramli 2013). As expected, the conversion of triglycerides and selectivity increased with the incorporation of Al into the framework of MCM-41. This is because acidity increases with Al and selectivity are also contributed by Co and Mo sulfides. The high surface area and large pore size enhance the catalytic activity of deoxygenation. The presence of mesopores can also catalyze isomerization of hydrocarbon and thus produce green jet fuel (C<sub>9</sub>–C<sub>15</sub> hydrocarbons with high *i/n* ratios). Fe nanoparticles supported on mesoporous silica (Fe–MSN) have been used to catalyze the HDO reaction of crude oil to green diesel (Kandel et al. 2014). The reaction was carried out at 290 °C, 30 bar H<sub>2</sub> for 6 h to give 67 % conversion (Table 13.3, Entry 11). The C<sub>18</sub>/C<sub>17</sub> ratio of 6.4 shows that the Fe–MSN favors HDO over DCO.

## **13.5 Conclusion**

Catalytic deoxygenation has become an alternative to remove oxygenated compounds from biomass feedstock especially nonedible oils. The removal of oxygen from biomass through deoxygenation, namely, HDO, DCO, cracking, and isomerization, for the production of paraffin is a very important process. This is because biomass serves a sustainable resource for hydrocarbons, which can be an alternative to petroleum-based derivatives. As global demand and consumption of gasoline and diesel progressively grow every year, sustainable resources are desirable. Presently,

catalytic deoxygenation of biomass is primarily based on supported metal catalysts. The metal site varies from sulfide metal comprised of Co and Mo suffered from catalytic deactivation. Noble metals such as Pt and Pd exhibit limitations because they are cost ineffective, while low-cost non-precious metals (Fe and Ni) have lower activity as compared to those of noble metals. The catalytic activity of deoxygenation for non-precious metals such as Ni can be further enhanced by supported on a suitable material. For example, the catalytic activity and selectivity of the Ni-based catalyst were enhanced significantly when supported on HZSM-5. In addition, mesoporous supports with bigger pore sizes could be used to overcome diffusion limitations of large molecules such as triglycerides. For the production of biogasoline, Ni/HBEA and Fe-MSN, which exhibit Brønsted acid sites, will be preferable because Brønsted acid sites can crack the products into shorter-chain hydrocarbons for green gasoline production. In the production of green diesel in the range of C<sub>10</sub>-C<sub>18</sub>, Ni/ZrO<sub>2</sub> and Ni-Al LDH are more suitable without any cracking reaction. Further research in developing the upstream and downstream technologies will speed up the commercial production of green biogasoline.

**Acknowledgment** The authors would like to thank Malaysia Ministry of Education (MOE) for sponsoring this work under FRGS Grant (Nos. FP056-2013B and FP054-2013B), University of Malaya (UMRG Grant No.RP 025A/025B/025C-14AET).

## References

- Akia M, Yazdani F, Motae E, Han D, Arandiyani H (2014) A review on conversion of biomass to biofuel by nanocatalysts. *Biofuel Res J* 1(1):16–25
- Arun N, Sharma RV, Dalai AK (2015) Green diesel synthesis by hydrodeoxygenation of bio-based feedstocks: strategies for catalyst design and development. *Renew Sustain Energy Rev* 48: 240–255
- Ashrafual A, Masjuki H, Kalam M, Fattah IR, Imtenan S, Shahir S, Mobarak H (2014) Production and comparison of fuel properties, engine performance, and emission characteristics of bio-diesel from various non-edible vegetable oils: a review. *Energy Conver Manage* 80:202–228
- Asmadi M, Kawamoto H, Saka S (2011) Thermal reactions of guaiacol and syringol as lignin model aromatic nuclei. *J Anal Appl Pyrolysis* 92(1):88–98
- Astruc D, Lu F, Aranzas JR (2005) Nanoparticles as recyclable catalysts: the frontier between homogeneous and heterogeneous catalysis. *Angew Chem Int Ed* 44(48):7852–7872
- Bárca PS, Silva JAC, Rodrigues AE (2005) Adsorption equilibrium and kinetics of branched hexane isomers in pellets of BETA zeolite. *Micropor Mesopor Mater* 79(1–3):145–163
- Brandvold TA, McCall MJ (2013) Hydrogenation and deoxygenation of glycerides and pyrolysis oil to form renewable diesel, biogasoline, or biojet fuel. Google Patents
- Cherubini F (2010) The biorefinery concept: using biomass instead of oil for producing energy and chemicals. *Energy Conver Manage* 51(7):1412–1421
- Deneuer A, Renders T, Van Aelst J, Van den Bosch S, Gabriëls D, Sels BF (2015) Alkane production from biomass: chemo-, bio- and integrated catalytic approaches. *Curr Opin Chem Biol* 29:40–48
- Deuss PJ, Barta K, de Vries JG (2014) Homogeneous catalysis for the conversion of biomass and biomass-derived platform chemicals. *Catal Sci Technol* 4(5):1174–1196
- Ding R, Wu Y, Chen Y, Liang J, Liu J, Yang M (2014) Effective hydrodeoxygenation of palmitic acid to diesel-like hydrocarbons over MoO<sub>2</sub>/CNTs catalyst. *Chem Eng Sci* 135:517–525

- Dunn EF, Liu DD, Chen EY-X (2013) Role of N-heterocyclic carbenes in glucose conversion into HMF by Cr catalysts in ionic liquids. *Appl Catal Gen* 460:1–7
- Fischmeister C, Bruneau C, De K, Vigier O, Jérôme F (2012) Catalytic conversion of biosourced raw materials: homogeneous catalysis. *Biorefin Biomass Chem Fuels* 232
- Galadima A, Muraza O (2015) From synthesis gas production to methanol synthesis and potential upgrade to gasoline range hydrocarbons: a review. *J Nat Gas Sci Eng* 25:303–316
- Gellman AJ, Shukla N (2009) Nanocatalysis: more than speed. *Nat Mater* 8(2):87–88
- Gosselink RW, Hollak SA, Chang SW, van Haveren J, de Jong KP, Bitter JH, van Es DS (2013) Reaction pathways for the deoxygenation of vegetable oils and related model compounds. *ChemSusChem* 6(9):1576–1594
- Gray KA, Zhao L, Emptage M (2006) Bioethanol. *Curr Opin Chem Biol* 10(2):141–146
- Harlin E, Turunen H, Selin J-F, Tiitta M, Lashdaf M (2012) Deoxygenation of materials of biological origin. Google Patents
- Hassan SN, Sani YM, Abdul Aziz AR, Sulaiman NMN, Daud WMAW (2015) Biogasoline: an out-of-the-box solution to the food-for-fuel and land-use competitions. *Energy Conver Manage* 89:349–367
- Ho S-H, Chen C-Y, Chang J-S (2012) Effect of light intensity and nitrogen starvation on CO<sub>2</sub> fixation and lipid/carbohydrate production of an indigenous microalga *Scenedesmus obliquus* CNW-N. *Bioresour Technol* 113:244–252
- Horikoshi S, Serpone N (2013) *Microwaves in nanoparticle synthesis: fundamentals and applications*. Wiley, Hoboken, NJ
- Huber GW, Iborra S, Corma A (2006) Synthesis of transportation fuels from biomass: chemistry, catalysts, and engineering. *Chem Rev* 106(9):4044–4098
- Johansen N, Ettore L, Miller R (1983) Quantitative analysis of hydrocarbons by structural group type in gasolines and distillates: I. Gas chromatography. *J Chromatogr A* 256:393–417
- Kandel K, Anderegg JW, Nelson NC, Chaudhary U, Slowing II (2014) Supported iron nanoparticles for the hydrodeoxygenation of microalgal oil to green diesel. *J Catal* 314:142–148
- Kubička D, Bejblova M, Vlk J (2010) Conversion of vegetable oils into hydrocarbons over CoMo/MCM-41 catalysts. *Topics Catal* 53(3–4):168–178
- Kubička D, Horáček J, Setnička M, Bulánek R, Zukal A, Kubičková I (2014) Effect of support-active phase interactions on the catalyst activity and selectivity in deoxygenation of triglycerides. *Appl Catal B Environ* 145:101–107
- Kumar M, Gayen K (2011) Developments in biobutanol production: new insights. *Appl Energy* 88(6):1999–2012
- Lee S-P, Ramli A (2013) Methyl oleate deoxygenation for production of diesel fuel aliphatic hydrocarbons over Pd/SBA-15 catalysts. *Chem Central J* 7(1):149
- Li Y, Somorjai GA (2010) Nanoscale advances in catalysis and energy applications. *Nano Lett* 10(7):2289–2295
- Lin Y-C, Huber GW (2009) The critical role of heterogeneous catalysis in lignocellulosic biomass conversion. *Energy Environ Sci* 2(1):68–80
- Lukic I, Krstic J, Glisic S, Jovanovic D, Skala D (2010) Biodiesel synthesis using K<sub>2</sub>CO<sub>3</sub>/Al-O-Si aerogel catalysts. *J Serb Chem Soc* 75(6):789–801
- Macario A, Moliner M, Diaz U, Jorda JL, Corma A, Giordano G (2008) Biodiesel production by immobilized lipase on zeolites and related materials. In: Antoine Gédéon PM, Florence B (eds) *Studies in surface science and catalysis*, vol 174B. Elsevier, Amsterdam, pp 1011–1016
- Mohammad M, Hari TK, Yaakob Z, Sharma YC, Sopian K (2013) Overview on the production of paraffin based-biofuels via catalytic hydrodeoxygenation. *Renew Sustain Energy Rev* 22:121–132

- Na J-G, Yi BE, Han JK, Oh Y-K, Park J-H, Jung TS, Han SS, Yoon HC, Kim J-N, Lee H, Ko CH (2012) Deoxygenation of microalgal oil into hydrocarbon with precious metal catalysts: optimization of reaction conditions and supports. *Energy* 47(1):25–30
- Na K, Choi M, Ryoo R (2013) Recent advances in the synthesis of hierarchically nanoporous zeolites. *Micropor Mesopor Mater* 166:3–19
- Naik S, Goud VV, Rout PK, Dalai AK (2010) Production of first and second generation biofuels: a comprehensive review. *Renew Sustain Energy Rev* 14(2):578–597
- Nguyen T, He S, Lefferts L, Brem G, Seshan K (2016) Study on the catalytic conversion of lignin-derived components in pyrolysis vapour using model component. *Catal Today* 259:381–387
- Olveira S, Forster SP, Seeger S (2014) Nanocatalysis: academic discipline and industrial realities. *J Nanotechnol*. Article ID 324089:19
- Owen K, Coley T (1996) Automotive fuels reference book. *Fuel Energy Abstr* 1(37):10
- Peng B, Yao Y, Zhao C, Lercher JA (2012a) Towards quantitative conversion of microalgae oil to diesel-range alkanes with bifunctional catalysts. *Angew Chem Int Ed* 51(9):2072–2075
- Peng B, Yuan X, Zhao C, Lercher JA (2012b) Stabilizing catalytic pathways via redundancy: selective reduction of microalgae oil to alkanes. *J Am Chem Soc* 134(22):9400–9405
- Perez-Ramirez J, Christensen CH, Egeblad K, Christensen CH, Groen JC (2008) Hierarchical zeolites: enhanced utilisation of microporous crystals in catalysis by advances in materials design. *Chem Soc Rev* 37(11):2530–2542
- Regalbuto JR (2009) Cellulosic biofuels—got gasoline. *Science* 325(5942):822–824
- Rinaldi R, Schüth F (2009) Design of solid catalysts for the conversion of biomass. *Energy Environ Sci* 2(6):610–626
- Sanders W, Maynard J (1968) Capillary gas chromatographic method for determining the C3-C12 hydrocarbons in full-range motor gasolines. *Anal Chem* 40(3):527–535
- Santillan-Jimenez E, Crocker M (2012) Catalytic deoxygenation of fatty acids and their derivatives to hydrocarbon fuels via decarboxylation/decarbonylation. *J Chem Technol Biotechnol* 87(8):1041–1050
- Santillan-Jimenez E, Morgan T, Loe R, Crocker M (2015) Continuous catalytic deoxygenation of model and algal lipids to fuel-like hydrocarbons over Ni–Al layered double hydroxide. *Catal Today* 258:284–294
- Shah YR, Sen DJ (2011) Bioalcohol as green energy—a review. *Int J Cur Sci Res* 1(2):57–62
- Sheppard MJ, Kunjapur AM, Prather KL (2016) Modular and selective biosynthesis of gasoline-range alkanes. *Metab Eng* 33:28–40
- Snaž A (2012) Catalysts in thermochemical biomass conversion. In: *Biomass conversion*. Springer, pp 187–197
- Singh SB, Tandon PK (2014) Catalysis: a brief review on nano-catalyst. *J Energy Chem Eng* 2(3):106–115
- Snáře M, Kubičková I, Mäki-Arvela P, Eränen K, Murzin DY (2006) Heterogeneous catalytic deoxygenation of stearic acid for production of biodiesel. *Indus Eng Chem Res* 45(16):5708–5715
- Snáře M, Kubičková I, Mäki-Arvela P, Chichova D, Eränen K, Murzin DY (2008) Catalytic deoxygenation of unsaturated renewable feedstocks for production of diesel fuel hydrocarbons. *Fuel* 87(6):933–945
- Somorjai GA, Frei H, Park JY (2009) Advancing the frontiers in nanocatalysis, biointerfaces, and renewable energy conversion by innovations of surface techniques. *J Am Chem Soc* 131(46):16589–16605
- Song W, Zhao C, Lercher JA (2013) Importance of size and distribution of ni nanoparticles for the hydrodeoxygenation of microalgae oil. *Chemistry* 19(30):9833–9842
- Taufiqurrahmi N, Bhatia S (2011) Catalytic cracking of edible and non-edible oils for the production of biofuels. *Energy Environ Sci* 4(4):1087–1112
- Velichkina LM, Pestryakov AN, Vosmerikov AV, Tuzovskaya IV, Bogdanchikova NE, Avalos M, Farias M, Tiznado H (2008) Catalytic activity in the hydrocarbon conversion of systems containing platinum, nickel, iron, and zinc nanoparticles (communication 2). *Petrol Chem* 48(5):355–359

- Wallington T, Kaiser E, Farrell J (2006) Automotive fuels and internal combustion engines: a chemical perspective. *Chem Soc Rev* 35(4):335–347
- Widegren JA, Finke RG (2003) A review of the problem of distinguishing true homogeneous catalysis from soluble or other metal-particle heterogeneous catalysis under reducing conditions. *J Mol Catal A Chem* 198(1):317–341
- Yang C, Nie R, Fu J, Hou Z, Lu X (2013) Production of aviation fuel via catalytic hydrothermal decarboxylation of fatty acids in microalgae oil. *Bioresour Technol* 146:569–573
- Zhou B, Balee R, Groenendaal R (2005) Nanoparticle and nanostructure catalysts: technologies and markets. *Nanotech L Bus* 2:222

# Chapter 14

## Impact of Nanoadditive Blended Biodiesel Fuels in Diesel Engines

J. Sadhik Basha

**Abstract** Innovative techniques are underway to utilize various additives with the diesel and biodiesel fuels to improve the working attributes of internal combustion engines. Many researchers have proposed various techniques on adopting different types of additives to enhance the working attributes of CI (compression ignition) or diesel engines. Recently, nanoparticles or nanoadditives are mixed with the various fuels and have become widespread among the technical community. With regard to some potential characteristics of nanoadditives, it plays a vital role in all the fields of modern technology. Recently, nanoadditives such as alumina, ceria, aluminum, carbon nanotubes (CNT), etc. are considered as potential additive with all the available fuels. Owing to some peculiar characteristics of nanoadditives (such as shortened ignition delay, enhanced burning rate, catalytic activity, reaction efficiency, and higher cetane number), research have been carried out and thereby lead to potential usage in improvisation of fuel properties. Research information also revealed that on incorporating the nanoparticles as additives with the biodiesel, the magnitude of hazardous gaseous pollutants (such as unburnt hydrocarbons (UBHC), carbon monoxide (CO), nitrogen oxides (NO<sub>x</sub>), smoke) was reduced without inducing any negative effect with regard to performance attribute of a diesel engine. This chapter emphasizes on various investigations carried out by several researchers on utilization of several types of nanoadditives with biodiesel fuels and their experimental outcomes in internal combustion engines.

**Keywords** Nanoadditive • Biodiesel • Emulsion fuel • Ignition delay • Diesel engine

### Nomenclature

BTE	Brake thermal efficiency
CNT	Carbon nanotubes

---

J. Sadhik Basha (✉)

Mechanical Engineering, International Maritime College Oman, Al Liwa, Sultanate of Oman  
e-mail: [mailsadhik@gmail.com](mailto:mailsadhik@gmail.com)

CO	Carbon monoxide
HC	Hydrocarbons
JBD	Biodiesel of <i>Jatropha</i>
JBD25A	Biodiesel of <i>Jatropha</i> mixed with alumina (25 ppm)
JBD50A	Biodiesel of <i>Jatropha</i> mixed with alumina (50 ppm)
JBD100A	Biodiesel of <i>Jatropha</i> mixed with alumina (100 ppm)
JBD2S15W	Biodiesel of <i>Jatropha</i> mixed with 15 % of water and 2 % of surfactants
JBD2S15W25A	Biodiesel of <i>Jatropha</i> mixed with 15 % of water 2 % of surfactants, and 25 ppm of alumina
JBD2S15W50A	Biodiesel of <i>Jatropha</i> mixed with 15 % of water 2 % of surfactants, and 50 ppm of alumina
JBD2S15W100A	Biodiesel of <i>Jatropha</i> mixed with 15 % of water 2 % of surfactants, and 100 ppm of alumina
NO <sub>x</sub>	Nitrogen oxides

## 14.1 Introduction

Compression ignition engines or diesel engines are utilized in various modern applications (such as in captive power plants, automobile, marine, etc.) owing to their robustness and fuel economy. On the other hand, they emit harmful gaseous emissions (unburnt hydrocarbons (UBHC), nitrogen oxides (NO<sub>x</sub>), particulate matter (PM), carbon monoxide (CO), smoke, etc.) and thereby caused perturbing concern for the technical community. These pollutants have depleted the ecological equilibrium, and therefore, this situation has triggered on the quest of new sources to commensurate the world oil demand and to reduce the harmful pollutants. In order to improve the working attributes of diesel engines, several approaches have been materialized. One of the recent approaches is the nanoscience technology.

Nanotechnology is one of the recent development in modern science which deals with the materials of one billionth of meter or smaller and involves in developing materials or devices within that size. The application of nanotechnology has led to synthesis of metallic or nonmetallic particles (in terms of nanosize dimensions) which has played in various engineering fields (Vicky et al. 2010; Sadhik Basha 2015b). The nanosize of particles often overcomes the several rheological problems like abrasion, settling, friction, and clogging compared to micro-sized particles during the static and dynamic conditions (Sadhik Basha and Anand 2010a, 2014). The technical community all over the world is actively questing hundreds of applications in nanotechnology like nano-materials, nano-electronics, bio-nanotechnology, nanostructured catalysts, etc. Nanoparticles have excellent physical, chemical, and thermal properties (Sadhik Basha and Anand 2010a, b, c; Sadhik Basha 2015b) compared to that of micro-sized particles. Henceforth, nanoparticles have been materialized to ameliorate the properties of fuels which are utilized in automobiles (Sadhik Basha and Anand 2014; Sadhik Basha 2015a, b). The effect of nanoparticle applications is quite remarkable in improving the



working attributes (such as brake thermal efficiency, reducing harmful emissions, and improved combustion) of internal combustion engines. The concept of blending additives (as a catalyst) to any fuel is to obtain better working characteristics of compression ignition engines (Sadhik Basha 2014). Recently, a number of researchers (Arianna et al. 2005; Scattergood 2006; Roos et al. 2008; Justin et al. 2009; Sajith et al. 2010) have dispersed nanoparticles in a base fuel to attain favorable thermal properties. The following sections describe the critical review conducted on the reported literature with regard to the potentiality, compatibility, and feasibility of nanoparticles with the various biodiesel fuels and their emulsions (fuel derived from mixing water, biodiesel, and surfactant) in compression ignition engines.

## 14.2 Characteristics of Nanoparticle Blended Fuels

The important aspect of this chapter is to focus on the utilization of potential nanoadditives with the various fuels in compression ignition engines. In this division, the following attributes are discussed:

1. Improvisation attributes of fuels on adding potential nanoadditives
2. Stability attributes of nanoadditive mixed biodiesel emulsions
3. Working attributes of diesel engine using nanoadditive mixed biodiesel fuels and emulsions
4. Hot-plate evaporation attributes of nanoadditive mixed biodiesel emulsions

### 14.2.1 *Improvisation Attributes of Fuels on Adding Potential Nanoadditives*

Numerous types of additives have been materialized for many years to enhance the fuel properties (Signer et al. 1996; Zanier 2001; Moy et al. 2002; Nubia et al. 2007; Imdadul et al. 2015; Tayfun et al. 2015) and tried out on mixing the diesel and biodiesel to assess the working attributes of internal combustion engine. The incorporation of additives for both the ordinary fuel and emulsion fuel is essential to prevent the engine starting problems in cold weather as well as to enhance the fuel quality. To overcome those problems, ignition improvers such as alkyl nitrates were incorporated, but they were found to be toxic and corrosive (Danilov 2001). To improve the combustion quality of the inferior and low cetane fuels (biodiesel emulsion fuels), many researchers have incorporated some ignition promoters or oxygenated additives (such as diglyme, diethyl ether) or catalytic additives to ameliorate the fuel properties. Mimani and Patil (2001) have revealed that the alumina nanoparticles possess enhanced surface area/volume ratio characteristics to act as a catalyst.

In this perspective, some researchers have reported on incorporating additives (derived from metals) with the water-based biodiesel emulsion fuels to ameliorate

the performance and lower the deleterious pollutants and explained the phenomenon in the following ways. Firstly, the metal presence in the emulsion fuel reacts with water to produce OH ions, to reduce soot accumulation, and, secondly, reacts with the carbon reducing excess oxidation (Miyamoto et al. 1987; Yang et al. 1998).

Guru Metin et al. (2002) synthesized organic-based metal compounds (such as Mn, Mg, Cu, and Ca) dissolved in ethanol (2 % by vol.), and subsequently, the solution was mixed with the neat diesel, to investigate the better working attributes of compression ignition engine. They observed that an optimum organic-based manganese drop of 54.2  $\mu\text{mol/l}$  greatly lowered the diesel fuel freezing point and thereby facilitated better combustion and reduced harmful pollutants. Fazliakmetov and Shpiro (1997) used iron, manganese, and cerium additives mixed with the neat diesel to determine the particulate matter (PM) in a compression ignition engine. They observed a reduced particulate emission for the metal mixed diesel fuels than those of neat diesel owing to significant catalytic combustion. Hinkova and Stanimirov (1997) reported that on adding a percentage of 0.2–0.5 % of manganese metallic additive with diesel, 22–25 % of smoke was reduced on comparison with neat diesel. Kao et al. (2008) revealed that mixing the metal oxide additives in the emulsion fuel will facilitate better working attributes in a diesel engine than that of using neat diesel.

Heejung et al. (2005) utilized a four-cylinder turbocharged diesel engine fueled with ceria nanoparticles mixed diesel. They found that there is a significant change in reduction in the light-off temperature and enhanced kinetic oxidation of the diesel fuel. Sajith et al. (2010) utilized a compression ignition engine for investigating the properties of cerium oxide nanoadditive with biodiesel fuel. They pointed out that ceria mixed *Jatropha* biodiesel fuel exhibited better brake thermal efficiency and lowered gaseous emissions than those of pure biodiesel.

Tyagi et al. (2008) devised an exhaustive work employing a hot-plate setup to investigate the ignition prospects of nanoadditives (aluminum and alumina) mixed diesel fuels. Aforementioned nanoadditives are mixed with diesel fuels for one hour utilizing an ultrasonicator. The prepared nanoadditive fuels were dropped at a certain height on the hot plate to investigate the ignition probability. The hot plate was heated by means of an electric heater attached to its base. They conducted the ignition probability test for both the aluminum and alumina nanoparticles of size 15 and 50 nm with a volume fraction of 0, 0.1, and 0.5 % mixed with the diesel fuel. At 0.1 and 0.5 % volume fractions of diesel-aluminum nanoparticle mixture, the magnitude of the ignition probability was 50, 80, and 100 % and 45, 90, and 100 %, whereas it was 10, 50, and 80 % for the neat diesel at 708, 728, and 748 °C. Likewise, they have also conducted the experiments by changing nanoparticle material and size. They investigated the ignition probability characteristics by mixing diesel and alumina nanoadditives (50 nm) for a particle volume fraction of 0.1 % and 0.5 %, respectively. At 0.1 and 0.5 % volume fractions of diesel-alumina nanoparticle mixture, the magnitude of the ignition probability was 62, 80, and 100 % and 60, 80, and 100 %, whereas it was 10, 50, and 80 % for the neat diesel at the same aforementioned temperatures. They have also investigated adding aluminum oxide nanoparticle size of 15 nm to the diesel fuel for the particle

volume fraction of 0.1 % and 0.5 %, respectively. They observed that ignition probability of the nanoadditive mixed diesel fuels was higher than those of diesel fuel, and they affirmed that such an effect will facilitate significant enrichment in the ignition temperature, improvement in the radiative and heat transfer properties, and lessening in the evaporation time and thereby may lead to shorter ignition delay in compression ignition engines.

Many researchers (Sadhik Basha 2011, 2014, 2015a, b) have shown their interest on utilizing alumina nanoparticles with diesel and biodiesel fuel as additives (since aluminum is one of the widely available metals on the earth crust and cost of production is lesser compared to that of other nanoparticles). Moreover, the alumina nanoparticles are stable at high oxidation temperatures to undergo catalytic reactions (Mul et al. 1995). Very recently, many investigators (Sadhik Basha 2011, 2014, 2015a, b; Sadhik Basha and Anand 2010a, b, c, 2011a, b, c, d, 2012, 2013, 2014) have carried out intense investigations on using carbon nanotubes (CNT) and alumina as potential additives with various fuels to ameliorate the fuel quality.

#### ***14.2.2 Stability Attributes of Nanoadditive Mixed Biodiesel Emulsions***

Nanoparticles in general tend to agglomerate when mixed with a fluid. There are many techniques to de-agglomerate and disperse nanoparticles in a base fluid to overcome the bonding forces after wetting the powder. Ultrasonic dispersion is widely adopted by several researchers (Putra et al. 2003; Sadhik Basha 2015a) to break up the agglomerate structures in aqueous and nonaqueous suspensions, leading to utilize the full potentiality of nanosize materials for various applications.

Recently, researchers (Sadhik Basha and Anand 2010a, 2011c, d, 2013, 2014; Sadhik Basha 2015a) prepared nanoparticle mixed biodiesel fuels systematically with the aid of an ultrasonicator. Further, the same research team also incorporated nanoparticles in water-biodiesel emulsion fuels (in presence of surfactants) with the help of ultrasonicator and mechanical homogenizer. They revealed that the prepared fuels were stable for more than five days as illustrated in Fig. 14.1. In addition, they also revealed that if the agitation speed of mechanical homogenizer is enhanced (during the mixing of nanoadditives), then the stability of prepared fuels may increase. Currently, several researchers have proposed their valiant techniques to enhance the stability of nanoadditive emulsion fuels so that the prepared fuels can be utilized for a longer time in internal combustion engines.

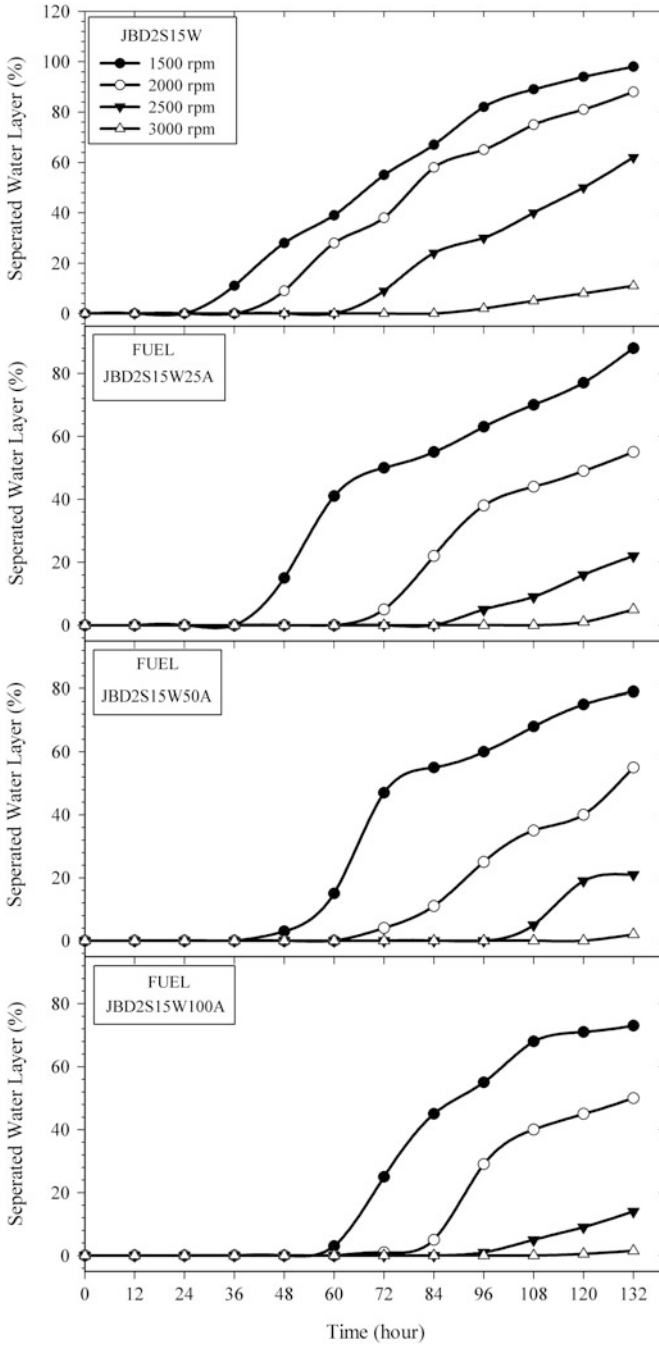
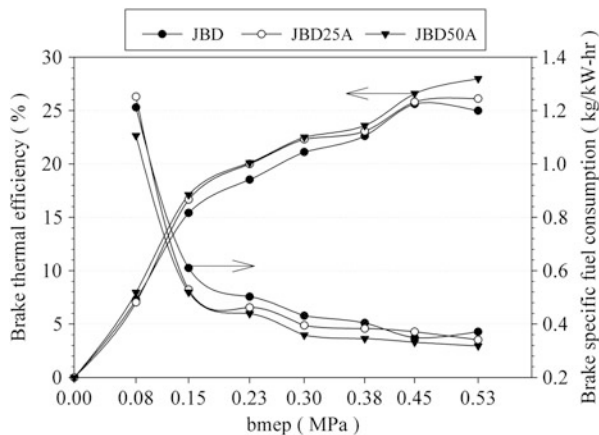
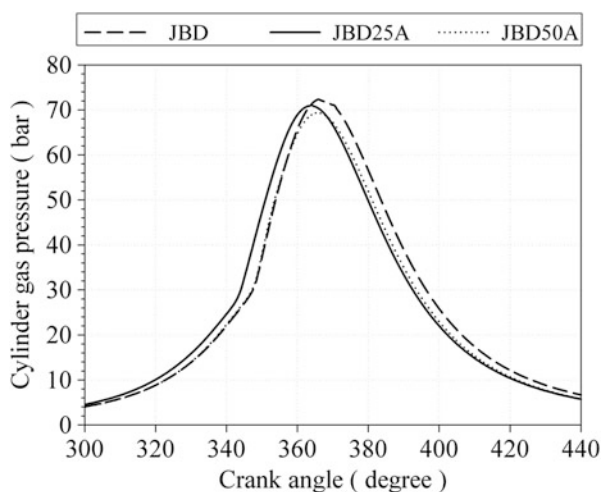


Fig. 14.1 Stability characteristics of alumina nanoadditive mixed water-biodiesel emulsions (Sadhik and Anand 2011c)

**Fig. 14.2** Performance attributes of BTE and BSFC of alumina nanoparticle mixed diesel fuels (Sadhik and Anand 2011d)



**Fig. 14.3** Combustion attributes of alumina nanoparticle mixed biodiesel fuels full (Sadhik and Anand 2011d)



### 14.2.3 Working Attributes of Diesel Engine Using Nanoadditive Mixed Biodiesel Fuels and Emulsions

The technical community has materialized many innovative techniques to eradicate the harmful gaseous emissions from compression ignition engine. One of the techniques is the incorporation of nanoadditives with the fuel to act as an ignition promoter or catalyst. Very recently, researchers (Sadhik Basha and Anand 2010a, 2011c, d, 2013, 2014; Sadhik Basha 2015a) reported enhanced brake thermal efficiency of nanoadditive mixed biodiesel fuels than those of neat fuels (Fig. 14.2). In addition, they also reported an appreciable reduction in the ignition delay in favor of nanoadditive mixed biodiesel fuels than those of neat diesel and biodiesel fuels. Owing to this result, they pointed out reduced cylinder pressure (Fig. 14.3) and gaseous emissions (Fig. 14.4) for the nanoadditive mixed biodiesel

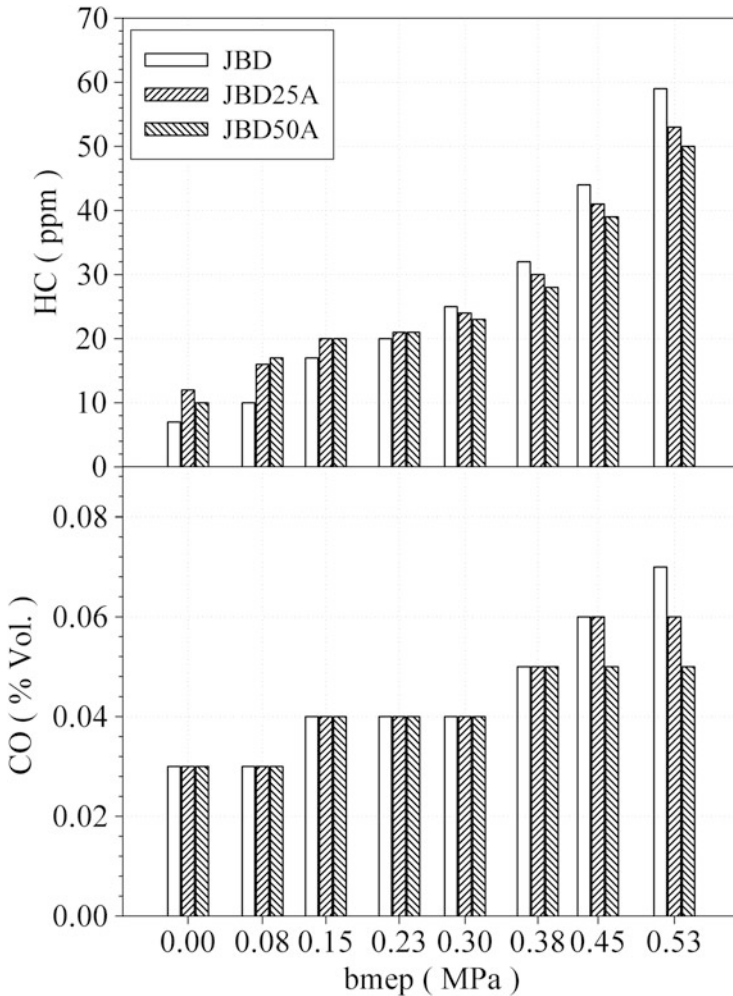


**Fig. 14.4** Variation of HC, CO of alumina nanoparticle mixed biodiesel fuels (Sadhik and Anand 2011d)

fuels than those of neat fuels. The same team (Sadhik Basha and Anand 2010a, 2011c, d, 2013, 2014; Sadhik Basha 2015a) incorporated nanoparticles with the biodiesel emulsion fuels. They observed enhanced brake thermal efficiency, reduced peak cylinder pressure, shortened ignition delay, reduced heat release rate, and minimum pressure rise rate for nanoadditive mixed biodiesel emulsions than those of neat fuels (Figs. 14.5 and 14.6). The researchers revealed that owing to the existence of nanoadditives in the emulsions, homogeneous mixing of air, fuel, and nanoadditives could take place in the engine cylinder during the combustion and thereby improve the catalytic combustion and reaction efficiency.

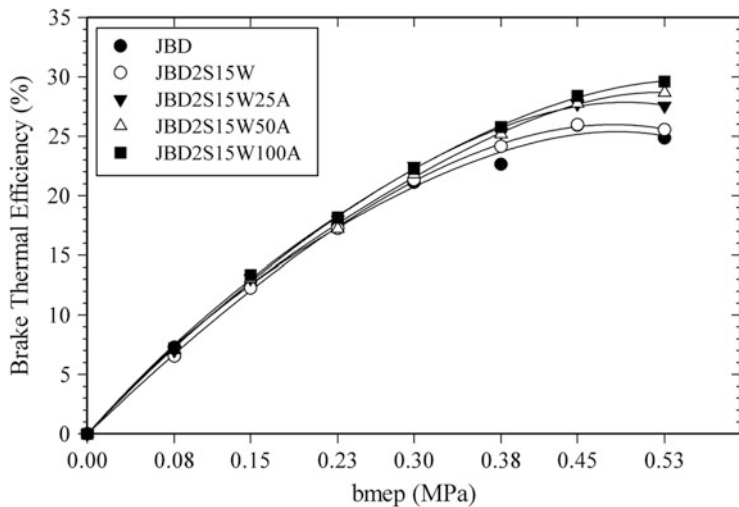


**Fig. 14.5** Performance attributes of alumina nanoadditive mixed water-biodiesel emulsions (Sadhik and Anand 2011c)

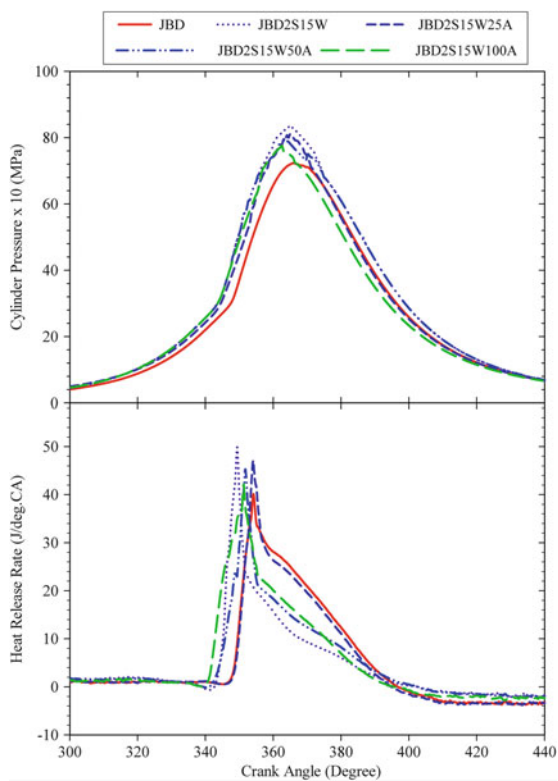


**Fig. 14.6** Combustion attributes of alumina nanoadditive mixed water-biodiesel emulsions (Sadhik and Anand 2011c)

With regard to emission attributes, the nanoadditive mixed emulsions exhibited a lesser emissions (nitrogen oxides and smoke in particular) than that of pure biodiesel (due to secondary atomization and micro-explosion) as illustrated in Fig. 14.7. Similar effect of reduced unburnt hydrocarbons and carbon monoxide emissions was observed for the nanoadditive mixed emulsions than those of neat biodiesel as depicted in Fig. 14.8. The reason behind the emission reduction on using the nanoadditive mixed biodiesel emulsion fuels is due to the improved degree of mixing of air-fuel in the presence of potential additives exhibiting better catalytic combustion. In addition, the researchers also revealed that the presence of nanoadditives in the inner cylinder service surfaces (which accumulated during the prior combustion cycle) will also impart in the improvement of performance, combustion, and emission attributes of CI engine. Currently, nanoscience researchers are also investigating the working attributes of the internal combustion engines on mixing the nanoadditives with the lubricant oil.

**Fig. 14.7** Emission attributes of  $\text{NO}_x$  and exhaust gas temperature of alumina nanoparticles mixed biodiesel emulsions (Sadhik and Anand 2011c)

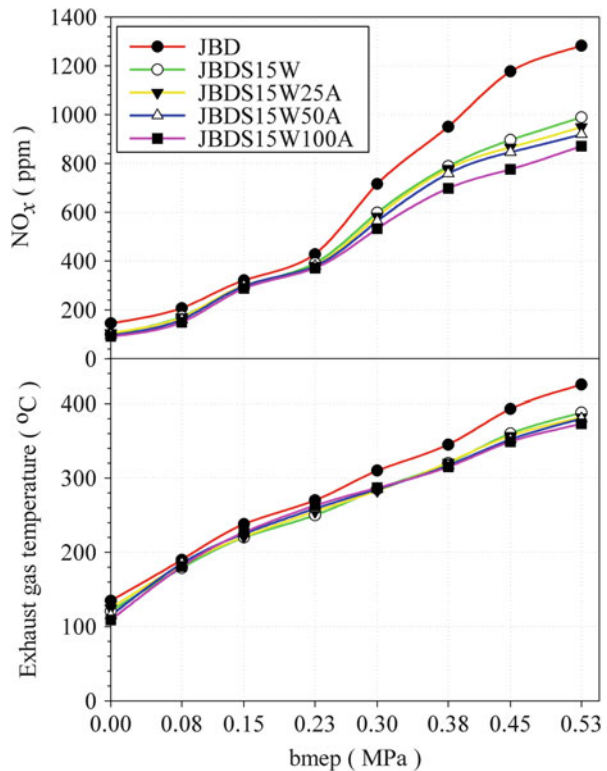
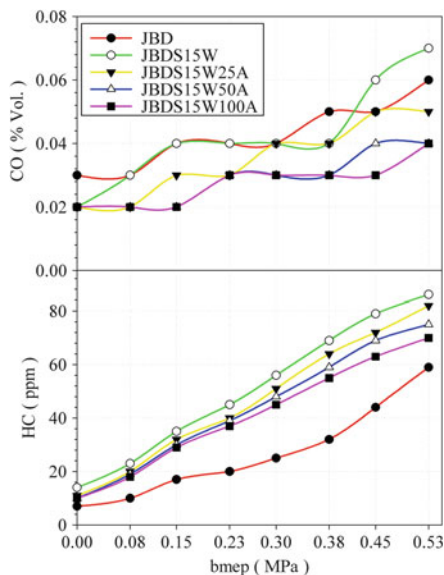




**Fig. 14.8** Emission attributes of CO and HC (Sadhik and Anand 2011c)



#### 14.2.4 Hot-Plate Evaporation Attributes of Nanoadditive Mixed Biodiesel Emulsions

Hot-plate evaporation test is one of the latest experimentation techniques to investigate the time period of ignition delay of various fuels in the field of combustion science (Lefebvre 1983; Cho et al. 1991; Xiong and Yuen 1991; Gogos et al. 2003; Abu-Zaid 2004; Toshikazu Kadota et al. 2007). Recently, researchers (Sadhik Basha and Anand 2011a, c, 2012, 2013) carried out hot-plate test and proved that nanoadditive mixed fuels exhibited minimum evaporation time than those of neat diesel and neat biodiesel fuels. The schematic of hot-plate experimental setup is shown in Fig. 14.9 and explained in detail by recent researchers (Sadhik Basha and Anand 2011a, c, 2012, 2013).

It is observed from Fig. 14.10 that the evaporation rate is maximum for the emulsions of biodiesel fuel and minimum for the nanoadditive mixed emulsions of biodiesel. The rate of evaporation was minimum for nanoadditive mixed biodiesel emulsion fuels (owing to catalytic attributes) of nanoadditives (Sadhik Basha and Anand 2010a, 2011c, d, 2013, 2014; Sadhik Basha 2015a). It was also observed from Fig. 14.10 that the nanoadditive mixed emulsion fuels attained the critical surface temperature in advance (reflecting minimum evaporation time and enhanced catalytic activity of potential nanoadditives).

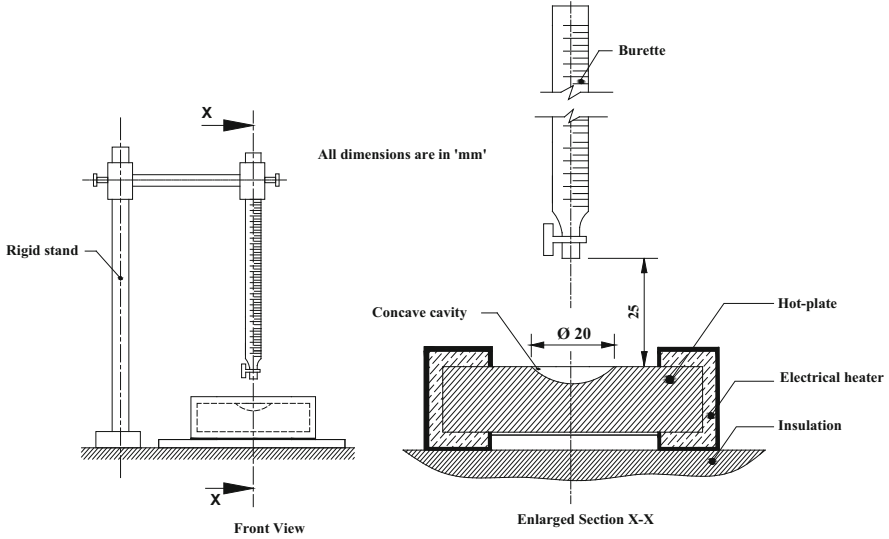


Fig. 14.9 Schematic layout of hot-plate experimental setup (Sadhik and Anand 2011c)

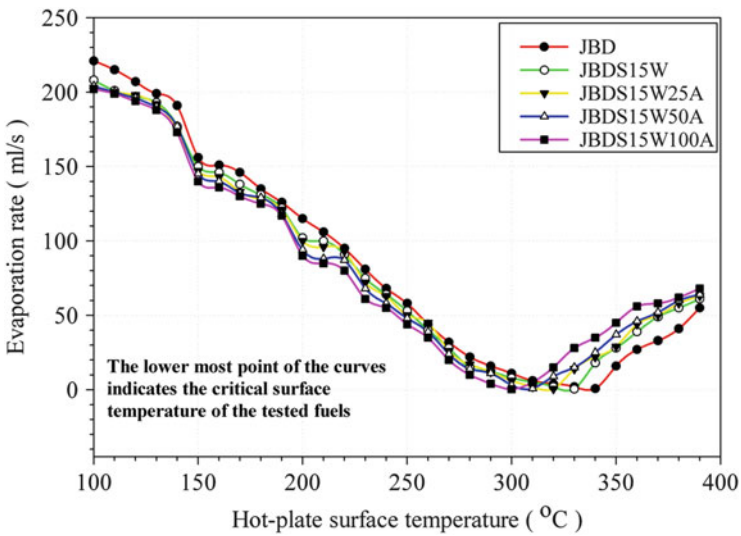


Fig. 14.10 Hot-plate evaporation characteristics of alumina nanoparticle mixed biodiesel emulsions (Sadhik and Anand 2011c)

### 14.3 Conclusion and Future Perspectives

It is evident from this chapter that the nanoparticles have found potential applications in fuel modifications. The physical and thermal properties of nanoparticles have attracted the researchers to utilize in various applications (such as in heat transfer, electronic systems, pipe coatings, fuel modification systems, etc.). With regard to unique properties of nanoadditives, they have resulted better performance, emission, and combustion attributes in diesel engines. The mixing of nanoadditives with biodiesel (fuel produced by transesterification) has ameliorated the better working characteristics of diesel engine in comparison with pure diesel and pure biodiesel.

Applications of nanoadditives in the future mostly rely in thermal and automotive sectors. The unique properties of nanoadditives have led to their usage in those sectors. The enhancement of thermal conductivity and improved rheological property associated with the nanoparticles has attracted the researchers to utilize in thermal applications. In case of automotive sector (particularly in the field of fuel engineering science), the addition of nanoadditives to the fuels has enhanced the ignition quality, enhanced performance characteristics and cetane number, reduced soot and smoke emissions, and reduced harmful pollutants. Owing to those improved properties of nanoadditives mixed with fuels, several researchers have contributed their valiant efforts to investigate its feasibility, compatibility, and potentiality in compression ignition engines. However, the addition of nanoadditives mixed with biodiesel has led to complications in trapping the unburnt nanoparticles in the exhaust. Henceforth, research is also in progress to filter the unburnt nanoadditives from the exhaust pipe of diesel engines.

### References

- Abu-Zaid M (2004) An experimental study of the evaporation characteristics of emulsified liquid droplets. *J Heat Mass Transfer* 40:737–741
- Arianna F, Covadonga A, Giorgio M, Urbano M, Anne M, Maria R, Giovanni D, Alois K, Larsen R (2005) Effect of water/fuel emulsions and a cerium-based combustion improver additive on HD and LD diesel exhaust emissions. *Environ Sci Technol* 39:6792–6799
- Cho P, Law C, Mizomoto M (1991) Effect of pressure on the micro-explosion of water/oil emulsion droplets over a hot plate. *Trans ASME* 113:272–273
- Daniilov A (2001) Fuel additives: evolution and use in 1996–2000. *Chem Technol Fuels Oils* 37:444–455
- Fazliakmetov R, Shpiro GS (1997) Selection and manufacture technology of antismoke additives for diesel fuel and boiler fuels oils. *Izdetal Stvo Neft I Gaz* 4:43–55
- Gogos G, Siang S, Daniel N (2003) Effects of gravity and ambient pressure on liquid fuel droplet evaporation. *J Heat Mass Transfer* 46:283–296
- Guru M, Karakaya U, Altiparmak D, Alicilar A (2002) Improvement of diesel fuel properties by using additives. *Energy Conver Manage* 43:1021–1025
- Heejung J, David B, Michael R (2005) The influence of a cerium additive on ultrafine diesel particle emissions and kinetics of oxidation. *Combust Flame* 142:276–288

- Hinkova M, Stanimirov L (1997) Synthesis and oxidation action of ecological additives for diesel fuel. *Res Inst Pet Hydrocarbon Gases* 39:21–32
- Imdadul H, Masjuki H, Kalam M, Zulkifli N, Rashed M, Rashedul H, Monirul I, Mosarofa M (2015) A comprehensive review on the assessment of fuel additive effects on combustion behavior in CI engine fuelled with diesel biodiesel blends. *J RSC Adv* 5:67541–67567
- Justin S, Daniel M, Yetter RA, Frederick L, Ilhan A (2009) Functionalized graphene sheet colloids for enhanced fuel/propellant combustion. *ACS Nano* 3:3945–3954
- Kao M, Chen C, Bai F, Tsing T (2008) Aqueous aluminium nanofluid combustion in diesel fuel. *J Test Eval*. 36 Paper ID JTE100579
- Lefebvre A (1983) Gas turbine combustion. Hemisphere Publishing Corporation, New York, NY
- Mimani T, Patil KC (2001) Solution combustion synthesis of nanoscale oxide and their composites. *Mater Phys Mech* 4:134–137
- Miyamoto N, Hou Z, Ogawa H, Murayama T (1987) Characteristics of diesel soot suppression with soluble fuel additives. SAE Technical Paper No 871612
- Moy D, Niu C, Tennent H, Hoch R (2002) Carbon nanotubes in fuels. United States Patent 6419717
- Mul G, Neeft JPA, Kapteijn F, Moulijn JA (1995) Soot oxidation catalyzed by a Cu/K/Mo/Cl catalyst: evaluation of the chemistry and performance of the catalyst. *J Appl Catal* 6:339
- Nubia M, Angelo C, Cristina M, Gisele O, Leonardo SG, Lilian L, Maria D, Marcia C, Michelle R, Rosenira S, Ana M, Ednildo A, Jailson B (2007) The role of additives for diesel and diesel blended (ethanol or biodiesel) fuels: a review. *Energy Fuel* 21:2433–2445
- Putra N, Wilfried R, Das S (2003) Natural convection of nano-fluids. *Heat Mass Transfer* 39:775–784
- Roos W, Duncan R, David J (2008) Diesel fuel additives containing cerium or manganese and detergents. US Patent No. US2008/0066375 A1
- Sadhik Basha J (2011) Impact of nano-additives on the performance, emission and combustion characteristics of direct injection compression ignition engine. PhD Dissertation, National Institute of Technology, Trichy, India
- Sadhik Basha J (2014) An experimental analysis of a diesel engine using alumina nanoparticles blended diesel fuel. SAE Technical Paper 2014-01-1391
- Sadhik Basha J (2015a) Preparation of water-biodiesel emulsion fuels with CNT & Alumina nano-additives and their impact on the diesel engine operation. SAE Technical Paper 2015-01-0904
- Sadhik Basha J (2015b) Chemical functionalization of carbon nanomaterials: chemistry and applications, Chap. 23. Taylor & Francis, Boca Raton, FL
- Sadhik Basha J, Anand RB (2010a) Effects of nanoparticle blended water-biodiesel emulsion fuel on working characteristics of a diesel engine. *J Glob Warm* 2:330–346
- Sadhik Basha J, Anand RB (2010b) Applications of nanoparticles/nanofluid in compression ignition engines – a case study. *J Appl Eng Res* 4:697–708
- Sadhik Basha J, Anand RB (2010c) Performance and emission characteristics of a DI compression ignition engine using carbon nanotubes blended diesel. *J Adv Thermal Sci Eng* 1:67–76
- Sadhik Basha J, Anand RB (2011a) An experimental study in a CI engine using nano-additive blended water-diesel emulsion fuel. *J Green Energy* 8:332–348
- Sadhik Basha J, Anand RB (2011b) An experimental investigation in a diesel engine using CNT blended water-diesel emulsion fuel. *J Power Energy* 225:279–288
- Sadhik Basha J, Anand RB (2011c) Role of nano-additive blended biodiesel emulsion fuel on the working characteristics of a diesel engine. *J Renew Sustain Energy* 3:1–17
- Sadhik Basha J, Anand RB (2011d) Effects of alumina nanoparticles blended jatropha biodiesel fuel on working characteristics of a diesel engine. *J Indus Eng Technol* 2:53–62
- Sadhik Basha J, Anand RB (2012) Effects of nanoparticle additive in the water-diesel emulsion fuel on the performance, emission and combustion characteristics of a diesel engine. *J Vehicle Des* 59:164–181
- Sadhik Basha J, Anand RB (2013) The influence of nano additive blended biodiesel fuels on the working characteristics of a diesel engine. *J Brazil Soc Mech Sci Eng* 35:257–264

- Sadhik Basha J, Anand RB (2014) Performance, emission and combustion characteristics of a diesel engine using carbon nanotubes blended jatropha methyl esters emulsions. *Alexandria Eng J* 53:259–273
- Sajith V, Sobhan CB, Peterson GP (2010) Experimental investigations on the effects of cerium oxide nanoparticle fuel additives on biodiesel. In: *Advances in Mechanical Engineering*. Article ID 581407, 6 pp
- Scattergood R (2006) Cerium oxide nanoparticles as fuel additives. US Patent No. US2006/0254130 A1
- Signer M, Heinze P, Mercogliano R, Stein J (1996) European (EPEEFE)-heavy duty diesel study. SAE Paper No. 961074
- Tayfun O, Mustafa O, Kadir A (2015) Investigation of nanoparticle additives to biodiesel for improvement of the performance and exhaust emissions in a compression ignition engine. *J Green Energy* 12:51–56
- Toshikazu K, Hajime T, Daisuke S, Shinji N, Hiroshi Y (2007) Microexplosion of an emulsion droplet during Leidenfrost burning. *Proc Combust Inst* 31:2125–2131
- Tyagi H, Patrick P, Ravi P, Robert P, Taewoo L, Jose R, Paul A (2008) Increased hot plate ignition probability for nanoparticle-laden diesel fuel. *Nano Lett* 8:1410–1416
- Vicky M, Rodney S, Ajay S, Hardik R (2010) Introduction to metallic nanoparticles. *J Pharm Bioallied Sci* 2:282–289
- Xiong T, Yuen M (1991) Evaporation of a liquid droplet on a hot plate. *J Heat Mass Transfer* 34:1881–1894
- Yang H, Lee W, Mi H, Wong CH, Chen CB (1998) PAH emissions influenced by Mn-based additive and turbocharging from a heavy-duty diesel engine. *Environ Int* 24:389–403
- Zanier A (2001) High-resolution TG for the characterization of diesel fuel additives. *J Thermal Anal Calorim* 64:377–384

**Part IV**  
**Risk Management**

# Chapter 15

## Nanotechnologies and the Risk Management of Biofuel Production

**Maria de Lourdes Oshiro, Edgar Oshiro, Tânia Elias Magno da Silva, William Waissmann, and Wilson Engelmann**

**Abstract** Nonrenewable energy derived from fossil fuels accounts for around 80 % of the primary energy usage in the world. The main problem is that petroleum reserves are limited and fossil fuels generate pollution. Therefore, it establishes essential need to acquire more sustainable energy alternatives. A well-known alternative is the development of biofuels produced from biomass, and the possible use of nanotechnology in the stages of production and process of biofuels may serve to improve and to overcome technical, economical, and environmental barriers. The present chapter discusses the problems generated by nanomaterials used for the production of biofuels. It has been observed that nanotechnology may have transversal action in the production of biofuels, including the improvement of raw material, and assist in processes and products developed in the sugarcane industry, extending its progress to automobile sector, transportation, and so on. We agree that

---

M. de Lourdes Oshiro

Dr. Jorge David Nasser Public Health School, Mato Grosso do Sul State Health Secretariat, University Católica Dom Bosco, Av. Senador Felinto Muller, 1480, Vila Ipiranga, CEP: 79074-460 Campo Grande, Mato Grosso do Sul, Brazil

E. Oshiro

Dr. Jorge David Nasser Public Health School, Mato Grosso do Sul State Health Secretariat, Av. Senador Felinto Muller, 1480, Vila Ipiranga, CEP: 79074-460 Campo Grande, Mato Grosso do Sul, Brazil

T.E.M. da Silva

Social Sciences Graduation and Research Group, Itinerary, Intellectuals, Image and Society, Sergipe Federal University, Cidade Universitária Prof. Aloyso de Campos, Jardim Rosa Elze, CEP: 49000-000 São Cristovão, Sergipe, Brazil

W. Waissmann

Research Group, Labour's Health and Human Ecology Studies Center, Sérgio Arouca National Public Health School, Oswaldo Cruz Foundation, Rua Leopoldo Bulhões 1480, CEP: 21041-210 Rio de Janeiro, Brazil

W. Engelmann (✉)

Vale do Rio Sinos University – UNISINOS, Avenida Unisinos, 950, CEP: 93022-000 São Leopoldo, RS, Brazil

e-mail: [wengelmann@unisinos.br](mailto:wengelmann@unisinos.br)

it is beneficial to increase the use of more effective catalysts in the production of biofuel. However, there should be concern of nanotoxicity research, regulation, governance, and social perspectives aiming the use of nanomaterials in order to develop sustainable future.

**Keywords** Nanotechnology • Risk Management • Biofuel • Regulation • Social perspectives

## 15.1 Introduction

Currently the energy consumption is pointed out as one of the largest generators of pollution worldwide, as its pollutants come in many forms such as carbon dioxide, methane, nitrogen oxide, and chlorinated fluorocarbon, all associated to the “greenhouse effects.” The production and consumption levels of nonrenewable energy are clearly unsustainable to the environment, economics, and society, which makes it a necessity to review the current policies in a way to include renewable energy alternatives (Rangel and Carvalho 2003).

Studies show that nearly 80 % of the energy usage in the world is nonrenewable energy derived from fossil fuels, mainly from oil, coal, and natural gas. As the oil continues to be the dominant form of fuel, its market advances in many fields, as it is essentially used in a large number of different final products.

The negative impacts of human behavior over the environment led many of the countries in earlier decades to majorly discuss environmental sustainability as a primary and fundamental issue. Several conferences were organized by the United Nations (UN), such as the Kyoto Protocol, held in 1997, which established reduction measures for the greenhouse gases and the need to replace fossil fuels with renewable energy sources, in order to preserve economic development without compromising the life of the current and future generations by protecting the structural integrity of the essential natural systems (Silva 2009).

Although it seems that a political cooperation exists, the legislative plan to assure the procedures of democracy needs to achieve scientific, economic, political, and legal subsystems that should be articulated in many ways. Under those circumstances, it must be understood that “the risk parameters can be set in very different ways, either one could be part of the risk as the decision maker or one could be affected by those decisions” (Luhmann 1992). The interpretation of environmental issues must be directly included in the development discussion. According to Jamieson (2010), “previous technological generations were developed to solve problems and decrease the labor in a world where the environmental costs were not meaningful.” This vision reveals to be incompatible with the present environmental logic, which comes from a redefinition of concept and limit of development in order to fight with the “dominant force of the unsustainable hegemonic thought” (Leff 2010). Along these thoughts, we can find the proposition of this chapter, which is intended to be addressed considering an approach under a perspective of



human and social sciences, focused at planning mechanisms and measures to override the unsustainability of the current model that “gain strength with the support and the reinforcement of the ecological critics” (Jamieson 2010).

Therefore, in the Brazilian scenario, the *Agenda 21*, as described by MMA, is “defined as a planning tool for the building of sustainable societies, within different geographical base, that reconcile environmental protection methods, social justice and economic efficiency” (MMA 2015a; MMA 2015b). The *Rio Statement* is also relevant in this matter (reaffirmed by the political commitment with the sustainable development signed in Rio+20: Conference which marked 20 years since the realization of the United Nation Conference about Environment and Development (Rio-92) and contributed to define the agenda of the sustainable development for the new decades, as well as to renew the political commitment with the sustainable development by way of the assessment of the progress and the gaps in the decisions implementation adopted by the main summits about the issue and the treatment given to new and emergent themes), which aims to establish a new global partnership in search of agreements and interests that benefits everyone (Nações Unidas sobre o Meio Ambiente 2016).

The effectiveness of these goals, expressed in the Brazilian Constitution of 1988 [Art. 3—The fundamental goals of the Federal Republic of Brazil are constituted by: (I) building a free, fair and supportive society; (II) guaranteeing the national development; (III) eradicating poverty and the marginalization and decreasing the social and regional inequalities; (IV) promoting the welfare for all, without origin, race, gender, color or age prejudice, or even any other ways of discrimination (Brasil 2016)], is characterized by the actions and the sustainable processes, focused on the human need dynamics, be them on the current or future time, harmonized with the socioeconomic and industrial development, in face of the conservation, protection, and improvement of the ecosystem in regeneration, reproduction, and coevolution (Boff 2012).

The researches of alternative energy sources involve solar, wind, and hydraulic energy from rivers and freshwater currents, tide and wave driving, and biomass (organic materials) among many others (Domingos et al. 2012). However, the current statistics estimates that the world energy offer for alternative sources will not be greater than 14% worldwide by 2030 (IEA 2013). According to data referring the year 2014, it is verified that, in Brazil, 39.4% of the energy used is derived from renewable sources, an important contribution of biomass usage (Brasil 2015).

The biofuels are obtained mainly from sugarcane, maize, soybean, sunflower seed, wood, cellulose, and other organic materials, generating products such as alcohol, ethanol, and biodiesel (Brasil 2007). Undeniably, the demand for biofuels is visibly increasing, and there are many companies and universities interested in investing on the development of such technologies. It's clear that with all ongoing improvements, the potential of biofuels as substitute of oil is promising (Teixeira et al. 2012).

## 15.2 From the Biofuels to the Nanotechnologies: Courses of the Nanotechnological Revolution

The world production of biofuels constantly increased specially throughout this last decade. In 2000, it was estimated that 16 billion liters were produced, and in 2011, more than 100 billion liters were achieved (IEA 2014). The biomass can be considered as an indirect way of conversion of solar energy. It is formed by the combination of carbon dioxide from the atmosphere and water by the plant photosynthesis process, which has carbon hydrates as a by-product. When the biomass burns, the release of carbon dioxide and water takes place, closing the cyclical process. Therefore, the biomass is said to be a renewable resource (Goldemberg 2009).

In Brazil, biofuels have a strategic role as an alternative energy source; the biomass produced from sugarcane, the same way as ethanol, presents as a renewable alternative in order to substitute the oil derivatives. For example, a report published at *Scientific American Brasil* is quoted, which highlights: “The next biofuel generation: companies tend to become commercially viable with alternatives from graminaceous plants, algae and the insuperable source: the genetically manipulated micro-organisms” (Wenner n. 32, no date indication in the original). Besides the advantage of possessing extended areas and climatic conditions for planting, ethanol from sugarcane has revealed itself to be the best option so far, because it consumes 1 energy unit of fossil energy for 8 units of renewable energy produced, while for the production of maize or wheat ethanol, this comparison is around 1.1 units for 1.5 (Leite and Leal 2007).

Brazilian spur for the intensification of ethanol production was initiated by the 1973 oil crisis, due to the decision of nations that participated from OPEC (Organization of the Petroleum Exporting Countries) of increasing the oil prices in international market, generating economic insecurity in countries that depended on oil supply, consequently impacting the Brazilian trade balance (Traumann 2007).

From this point on, in 1975, the Brazilian government created “Pró-Alcool” (Alcohol National Program, in Portuguese) which aimed to replace the petroleum for ethanol, using sugarcane as the main raw material for researches and production on large scale (Kohlhepp 2010). The sugar-alcohol sector chain stands out due to its relevance in the national scenario, which goes from the investments in production and processing until the consumption of raw material. According to Novacana (2015), Brazil has 408 sugar and ethanol stations, mainly concentrated in the southeast (55.6%), northeast (17.9%), and central-western region (17.1%). The extraction of ethanol from the sugarcane demands a sugar fermentation of micro-organisms, which is a necessary process to assure the release of alcohol and carbon gas that results in a fermented wine with 10% of alcohol. The next step is followed by a distillation process, where the hydrated alcohol is obtained. The liquid with 96% of alcohol is the final product sold in the gas stations (Novacana 2015).

The projection is that by 2035, the biofuels will practically be supplied to one third of the domestic demand of fuel for road transportation, which in 2013, was already around 19 % (IEA 2013). Brazil and the United States are the leaders in ethanol production. Brazilian production of ethanol in 2013 was equal to 23.2 billion liters (Unica 2014). But the progress of ethanol production in the earlier years was halted due to the lack of investments, which forced Brazilian companies to import sugarcane from the United States (Milanez et al. 2012).

Another good alternative for the use of biofuels in Brazil is the biodiesel, which can be used solely or be mixed with common diesel. In 2005, Brazil launched the National Program of Production and Use of Biodiesel, as an incentive in order to stimulate the biodiesel chain, aiming for social inclusion and regional development. The creation of this policy gave the researchers new possibilities in achieving different results. They were able to work with several biosources, such as castor oil, palm oil, babassu palm, canola oil, soybean, and others: “Scientists are transforming agriculture surplus, wood and graminaceous plants of fast growth in several biofuel types—even jet fuel. But, in order to popularize it, this new generation of biofuel will have to compete with oil costing US\$ 60 each barrel” (Huber and Dale 2009). Oleaginous plants have been sought in order to allow a greater yield in the production scale. In the vegetable diesel field, the soybean is the main input used in Brazil for biodiesel production (Mattei 2010).

An extensive research must be conducted in order to economically enable large-scale production of biodiesel. Undeniably, this race for better and cheaper results has launched a great number of patent requests. It is observed, in a report of the Brazilian National Institute of the Industrial Property (INPI—Instituto Nacional da Propriedade Industrial), that China and the United States represent more than 50 % of the patent requests (INPI 2011). The data shows the number of patent requests originated from China (76), the United States (46), Brazil (22), Japan (20), and South Korea (14).

The biodiesel production process is made through the reaction of transesterification of the vegetable oils with an alcohol (methanol or ethanol) in the presence of an acid or basic catalyst. From this reaction, an ester (biodiesel) and several by-products are generated (glycerin, lecithin, etc.). The choice of one or another route (methyl or ethyl) depends on various variables such as the price of products used on these routes, as well as the energy consumption in the reactive process (Mattei 2010).

Biotechnology has been playing a key role in new developments. For example, there is a continuous expansion of genetically modified seeds with greater resistance to dry periods and pest infestations, greater farm and oil production yield, and a smaller production cost. That is the great part of the research purposes, which leads to a greater yield within the refineries, allowing economic advantages (Malajovich 2012).

The Brazilian Agency of Industrial Development (ABDI—Agência Brasileira de Desenvolvimento Industrial) and the Center of Management and Strategic Studies (CGEE—Centro de Gestão e Estudos Estratégicos) performed a study about the

future of the biotechnology application in areas with promising development in the energy sector (Biotecnologia 2008).

With all the advancement made in biofuel technologies, it is inevitable to add nanotechnologies to the equation. Nanotechnologies may have transversal action in the biofuel production techniques, including the raw material improvement, sugarcane industry processes and products, as well as automobile, transportation industries, etc. According to a study performed by ABDI, “[. . .] the nanotechnology will have a great economic impact in the generation, distribution and energy storage sectors, with a decisive participation in several devices. Initially, its impact will only be noticed in a more rational use of the existing energy sources and in the evolution of the alternative sources use. In Brazil, the theme nano-energy is translated into many strategic opportunities, such as application in the oil refining, in the increase of the industrial processes efficiency and in the ethanol production and use. The processes of biodiesel generation may use heterogeneous nano particulate catalysts and or nano structured ones, in replacement of the homogeneous catalysts, currently employed. The last ones generate a great quantity of wastes, making it difficult to separate and to purify the products, which leads to an increase in the production costs. In the case of the ethanol production, the nano catalysts may compete or even substitute the enzymatic catalysts, which are the most promising ones for this process” (ABDI 2010). The researchers aim to introduce and use structures at nanoscale in order to try to improve the cost-benefit relation for the biofuel production (Brasil 2012).

Nanotechnologies refer to a group of technologies and sectors, which have conditions to develop processes and products with new characteristics, when compared with their similar products in a macroscale. In accordance with the concept adopted by ISO (International Organization for Standardization), through the Technical Committee 229 (ISO 2015): “*Standardization in the field of nanotechnologies that includes either or both of the following: (i) understanding and control of matter and processes at the nanoscale, typically, but not exclusively, below 100 nanometers in one or more dimensions where the onset of size-dependent phenomena usually enables novel applications; (ii) utilizing the properties of nanoscale materials that differ from the properties of individual atoms, molecules, and bulk matter, to create improved materials, devices, and systems that exploit these new properties.*”

In the farm, the nanometric scale effects over the farmers and the food may be greater than the ones of the Green Revolution, which had began in the decades of 1960 and 1970. The perspective is that the new technologies may reinvigorate the agri-chemistry and agri-biotechnological industries, unleashing a more intense debate, which is currently about nanotechnologically modified food (ETC 2004).

Generally, nanoparticles and nano-capsules may serve as tanks and vectors of pesticides, fertilizers, drugs, genes, etc. in order to facilitate the penetration and the control of the slow and constant release of active substances through the plant cuticles and tissues; nano-sensors may be used for monitoring the soil conditions, plant development and germination, rational water use, cattle treatment and feeding, etc. (Granziera et al. 2012; Isaaa 2015a).

Nanoparticles have been used for gene transfer into plants, aiming to induce greater pest infestation resistance and increase of the storage time and variety in the nutrient content. This can be performed through bombardment of silica nanoparticles—DNA conjugate, which penetrates into protoplasts and nucleus (Monica 2007). Such nanomaterials include carbon nanotubes (CNT), nano-porous silica, and gold nanoparticles (Galbraith 2007; Monica 2007).

Oak Ridge National Lab, from the United States of America Energy Department, developed a technique that uses millions of carbon nano-fibers in order to inoculate them into thousands of cells simultaneously. The nano-fibers grow and adhered to the silica part, which is full of synthetic DNA. Different from the other genetic engineering methods, Oak Ridge technicians argue that their technique does not pass the modified traces to the following generations. Theoretically, the DNA remains connected to the carbon nano-fibers, not being able to integrate itself completely to the plant genome. The implication is that this would enable “programming” the plants to reproduce themselves only once. According to Oak Ridge scientists, this would relieve the concerns about the gene flow associated to genetically modified plants, where the genes are transferred among non-related, removed organisms or ones which were rearranged among species (Biodiversidade en América Latina y el Caribe 2005).

Genetic manipulation may result in an increase in sugarcane sucrose level through its accumulation into the stem storage, offering the probability of transforming that in an alternative product for the biofuel production. Thus, the possibility of investigating new genes inserted into the plant is opened, turning it into the most effective raw material made of sucrose (Isaaa 2015b).

The increase in ethanol production, according to the industrial processing point of view, can be made basically in two distinct ways: by improvement of the technologies for ethanol production of the first generation, from the sugars, the same way as it is with sugarcane, or by the scientific and technological development of the lignocellulosic ethanol (denominated as second-generation ethanol), produced from a complex of mixing three types of natural polymers, constituted by cellulose, hemicellulose, and lignin (Embrapa 2011).

The lignocellulosic biomass can be converted through biochemical processes (such as fermentation) or thermochemical ones (such as pyrolysis, liquefaction, gasification, or combustion) originating from solid, liquid, or gaseous fuel (Araujo 2010). The current knowledge border for the production of second-generation ethanol corresponds to the difficulty of breaking the vegetable cell wall, constituted by cellulose polymer, therefore, the search for economically feasible ways of decomposing the cellulose and then extracting the sugar for fermentation and production of ethanol (Fapesp 2015).

The use of enzymes as catalyst in order to break the cellulose is an important issue concerning bioethanol production. However, the enzyme cost is high, which makes the process not feasible economically, once the enzymes suffer alterations in their structure and lose their catalytic activity with time (Palmer 2015). The production of enzymes is resorted by nanotechnological methods from plant wastes (Isaaa 2015a). This option becomes interesting once it's possible to produce ethanol

without compromising the quality of sucrose and enabling the recovery of cellulose (Isaaa 2015b).

Alves et al. (2012) demonstrated an alternative use of the sugarcane bagasse, besides its use for burning into boilers in order to generate electric energy and steam. Tomato seeds exposed to CNT by researches of Arkansas University, in the United States, germinated more quickly, and the seedlings were bigger and became more resistant than the seeds not exposed from the same lineage.

The analysis of seeds indicated that the CNT penetrated into the harder layer from the seeds, increasing the capacity of water absorption and the stimulus for the plant growth. The technique employed may increase the biomass production, be it of food or biofuel production (Khodakovskaya et al. 2009).

The role of nanotechnology for the biomass production in the sugarcane sector seems to enable the solution of some problems, which exist today in productive terms. Possibilities of the existence of fuel with greater economic and environmental advantages are pointed out. On the other hand, the surveillance about inadequate effects in agricultural environment showed as poor in national soil. The promised reduction of pesticide use with the introduction of the transgenic soybean was not confirmed, and the usage inspection has been insufficient. As the greatest world consumer, the risks are relevant for Brazil. The introduction of new technologies must be closely checked for assessments of potential environmental impacts whether in human or animal health (Martins 2007). This is also the scenario for the risk analysis, which shall flank the nanotechnology implementation, prominently in their biofuel usage.

### **15.3 Assessment and Management of the Risks Generated by the Usage of the Nanoscale materials in Biofuels**

Combustion vehicles are responsible for increasing air pollution to a great extent. One of the most adequate alternatives to decrease high concentration of pollutants is by the use of more effective catalysts. The advantage of using nano-catalysts is due to the great surface area and the increase of the contact area among the reagents and catalyst, consequently increasing the catalytic activity. The most used catalysts are made of noble metals, which are less reactive: platinum, silver, nickel, and gold (Ferreira and Rangel 2009). Platinum is extensively used in the gasoline engine catalysts, fuel cells, etc.; however, this is expensive and that's why the use of other nanoparticles may reduce the cost (Moreira 2013).

Nanotechnologies enable paths to improve the development and increase the engine capacity, which are also present in the energy search from the low economic cost of raw materials. Among the functionalities of nanotechnology, the catalyst efficiency is verified in the additive development for lubricants, production of fuel cells, and other devices, which involve the energy generator process (Herbst et al. 2004). In order to generate catalysis, a substance able to increase the velocity

of chemical reaction is necessary to decrease the energy of activation from the reaction. There are two types of catalysis: in one of them, the reagents, products, and catalysts are dispersed in a single phase, normally liquid, as well as in biodiesel production (vegetable oil, alcohol, and a catalyst) and, another, where the reagents, products, and catalysts are into different phases (reagents/products are liquid or gaseous and the catalyst is normally solid), such as in the catalytic converter used in the automobile exhausters that transforms toxic gases in a lesser quantity of pollutant (Dias et al. 2012).

The interest for searching less pollutant transports and new energy sources began to be researched from 1973, with fuel cells for motorized cars using hydrogen as fuel, that is, technology that transform oxygen and hydrogen in order to generate electric energy, thermal energy, and water. Hydrogen has great capacity to store energy, and for this reason, its usage as renewable energy source and also a thermal one has been widely researched (Silva et al. 2003). The increase in the nanotechnology presence also provokes the increase of the nanoparticle presence in the air and into the ecosystem as a whole. This generates nanotoxicological possibilities with effects still unknown (Joachim and Plévert 2009).

For more accurate risk assessment, be it in relation to human beings or the environment, nanotechnologies will demand the creation of additional human resources and the organization of laboratories equipped in order to study the nanoscale passing by regulatory and ethics issues. One of the conditions identified is related to global warming and its effects, which can lead to increased government and industrial interest, to replace supplies, technology generation, and distribution of energy with a socio-environmental effect not as negative (ABDI 2010). The figure 15.1 below presents the emerging issues, where the call is “nano-economy,” which is one of the eight new world economies, with promising effects:

It is observed that “nano-economy” is born in a period, which was initiated in 2010 and presents a fast growth, being inserted in the *Knowledge Era*. “Nano-economy” is closely related to the conditions pointed out by ABDI studies, demanding responsibility and environmental compromise. Since 2008, the “green economy” agenda intensification can be verified, and the idea related to the “green growth” concentrated itself about the articulation of these speeches within the economic institutions and international environments, involving the beginning of an institutional transformation in the sense of a world ecologically sustainable economy. The “green economy” may have the capacity of supporting within a transition of the current social and ecologically non-sustainable economic growth [...] through strong articulations of the green economy and alternative measures of progress of the gross domestic product are widely adopted. The concept of “rearticulating,” found within the poststructural discourse theory, proposes to guide this transition. This offers a structure to rebuild notions of prosperity, progress, and security, avoiding direct discursive conflict, which is disabling, with currently hegemonic pro-growth discourses (Ferguson 2015). Anyway, this kind of economy can progress alone, jointly with other “economies,” such as neuron, hydrogen, bio, knowledge, information, and industrial and source economies.

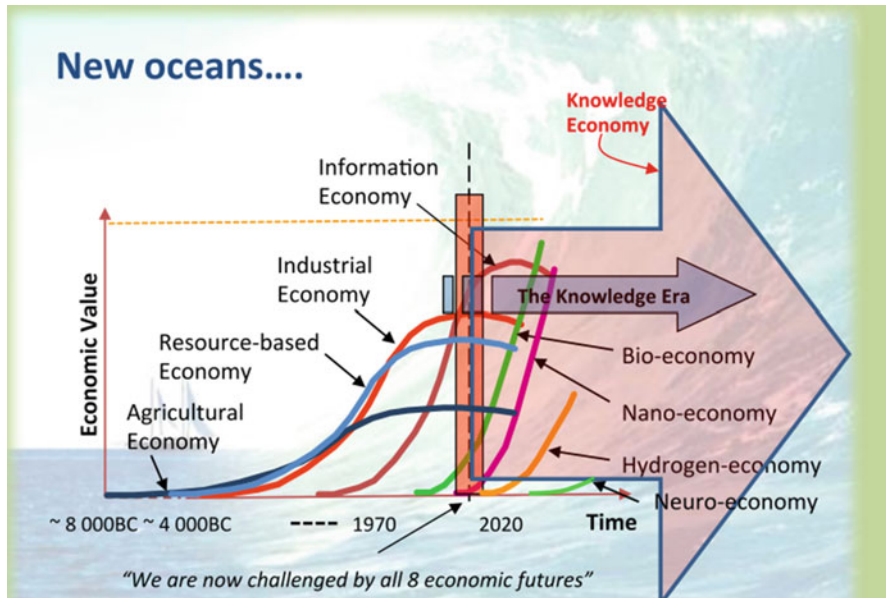


**Fig. 15.1** The new economies. *Source:* Botha (2015)

The chain of new economies and the challenges that they would bring are met within the growth, crisis, and certain stabilization of several sources overview, all related to the eight new economies referred that will be very important for the coming years. As some pessimistic projections (Casti 2012), there will be a collapse of everything around the year 2030 and subsequent years: with the great growth and the decline, the break, the sources, food, and industrial growth crisis at the same time in which the population growth and the pollution levels are verified. That is to say, this scenario will have a negative effect in the economic development projected above by the eight emergent economies. Nanotechnologies effectively will have a fundamental role in this catastrophic context rollback. Thus, the nanotechnologies applied to the biofuels will perform an important factor, which deserves attention.

Because of this, it is worth deepening the studies about the use of nanometric scale in biofuels. The production process needs a catalyst, generally platinum, in order to accelerate the oxidation reaction of hydrogen (Lorenzi 2009). Within a cell fuel system, the usage of pure hydrogen reveals advantages for not requiring reformers (equipment used to extract hydrogen from a source of this fuel, such as natural gas, methanol, ethanol, and others), decreasing the size and the cost of the system, without contaminating the membranes and electrodes that are sensitive to some composites (Moreira 2013).

Nowadays, nano-catalysts are being employed in this process, and a comparison of the efficiency between the conventional fuel cell and a cell using nanotechnology was performed. A higher efficiency percentage was verified; in other words, with 70 % less platinum applied in the shape of nanoparticles, there was an increase of



15% in efficiency (Moreira 2013). In Brazil, the theme nano-energy is translated into many strategic opportunities, such as application in the oil refining, in the increase of the industrial process efficiency, and in the ethanol production and use. The processes of biodiesel generation may use heterogeneous nanoparticulate catalysts and/or nanostructured ones, in replacement of the homogeneous catalysts, currently employed. The last ones generate a great quantity of wastes, making it difficult to separate and to purify the products, which leads to an increase in the production costs. “In the case of the ethanol production, the nano-catalysts may compete or even substitute the enzymatic catalysts, which are the most promising ones for this process” (ABDI 2010).

From this model, several researches concerning nanotechnology optimize catalysts. Catalysts based on nanospheres aroused, which react with vegetable oils, animal fat, and methanol in order to produce biodiesel. This process may turn the production cheaper, faster, and less toxic (Nanowerk News 2007a). A nanostructured catalyst with ruthenium nanoparticles fixed into the walls of the solid support pores has improved the catalytic performance (Nanowerk News 2007b). Graphene impregnated with nitrogen showed as an effective catalyst for fuel cells, demonstrating high efficiency at low cost in relation to hydrogen fuel cells with direct methanol/ethanol fuel. Graphene impregnated with nitrogen offers desirable electro-catalytic characteristics such as catalysts into alkaline solution and as catalysts that support for platinum and catalysts in acid solution of platinum-ruthenium (Nanowerk News 2013a). Nanoparticles of graphene with low-cost iodine and metal-free showed a better throughput than the high-cost platinum (Nanowerk News 2013a), that is to say, the fuel cell without platinum, based on magnesium and iron. This mixing, when heated under sulphur, at 800 °C, decomposes into shapes made of magnesium nitrate, nanoparticles of magnesium oxide, iron nitrate, and iron carbide (Nanowerk News 2013b).

Nanotechnologies provided throughout their history progresses and benefits in several areas, and due to their properties, considering this measure dimension, they enabled researches in several locations of the world innovating the creation of products and processes or even recreating some already existent, improving their performance, mainly considering the search for a new energy source and the sustainability in the technologies of energy generation with less emission of toxic gases.

Jovanovic (2006) developed several micro reactors for the production of oils. One of them, which produces biodiesel by combining alcohol and vegetable oil directly, is a device of the size of a bank card containing a series of parallel canals (nanoscalar), through which the vegetable oil and the alcohol are bombed simultaneously. Even though the quantity of biodiesel produced from a single microreactor is considerably low, the reactors may be connected and piled in benches in order to increase the production.

Basha and Anand (2011) used a mechanic agitator to create an emulsion of *Jatropha* biodiesel (*Jatropha curcas*), water, and a surfactant, with different proportions of nanoparticles of aluminum oxide. They accomplished a substantial

improvement in the performance and reduction pollutant emission when compared to the pure biodiesel.

Hydrogen is one of the best alternatives as a fuel in the future, but there are diverging about how to use it, as well as issues such as transport and gas storage, which limit its use dissemination. That is why the British company Cella Energy developed a method that captures hydrogen into plastic spheres in micro or nanoparticles, behaving as a liquid and facilitating the gas transportation and storage (Abegás 2015). Other authors developed new proposals on the use of nanotechnology in the energy production, such as the use of gold nanoparticles to the electro-catalytic reduction of oxygen, avoiding the corrosion applied to fuel cells (Wei and Liu 2013), platinum-cobalt nanoparticles into the optimization of the catalyst performance (Wang et al. 2012), mixed titanium oxide and zinc oxide nano-catalysts in the production of biodiesel from palm oil (Madhuvilakku and Piraman 2013), and a nano-catalyst containing copper, zinc, and aluminum oxides for the synthesis of an ecological fuel (Khoshbin and Haghighi 2013).

Kimura et al. (2012) presented an alternative in order to decrease the consumption of oil, from the biomass with the production of biofuels extracted from the microalgae oil, using hybrid catalysts with nano-pores constituted by aluminum oxide nanoparticles. Yang et al. (2013) introduced a diesel with an emulsion with nano-organic additives and showed a better performance (of 14.2%), comparing to the pure diesel, and the nitrogen oxide emission (NO<sub>x</sub>) was also reduced in 30.6%. The results indicated that the phenomenon of microexplosion of the water droplets in a nanometric size into the diesel with such emulsion may accelerate the fuel evaporation and the process of mixing with the air, reducing the combustion global duration (Yang et al. 2013).

After 15 years of study conducted in China, in 2004, an equipment with nanotechnology use was developed, which is patented in more than 20 countries and can be installed into cars. This would lead to a decrease of 50% up to 90% of the residual gas, savings of up to 20% or 30% and 10% up to 30% of increase of the power, besides engine noise reduction, combustion chamber cleaning, and increase of the engine life cycle, which may serve as a model to new advances in the area as they are mobile and installed in the own vehicle (Most 2004). During the last years, there was a decrease in the cost of glycerol in the world due to the biodiesel production, so that the environmental interest in new energy sources from this product is increased. Thus, researches are being performed in the electro-oxidation of glycerol using platinum nanoparticles directed, especially, to the possibility of using such alcohol into fuel cells (Fernández et al. 2013). Other researches with alcohols, such as methanol, ethanol, and ethylene glycol were important in the electro-catalysis process, particularly for fuel cells (Lima et al. 2013).

In the nanotechnology scenario, two difficulties are designed: the absence of a specific regulatory remark and the disagreement about the results obtained by exact science, particularly concerning nanotoxicology according to a study pointed out by Harald F. Krug, which aimed to review the literature of the last 15 years in order to establish if an assessment of the human toxicological criteria of engineering

nanomaterials (ENMs) is possible. The researchers pointed out the errors in the investigation methods and criteria of toxicological analysis used. From this analysis, an exponential increase in the number of publications in the last 15 years was observed, so that until 2000, there was a limited number of about 200 articles which were directly related to the theme of nanomaterials and the human and environmental health effect analysis. However, from 2001 onward, there are more than 10,000 registers, mostly disabled and contradictory, without a clear approach about the safety of nanomaterials and performed with inadequate methodology. It is affirmed that the most important literature results do not deal directly with a toxicological approach, but with mechanistic studies instead. Although the most relevant toxicological results are indirectly discussed, such results are confusing, and in some cases, frequently misleading, because as a matter of fact, the experiments were performed in higher concentrations or high dosage, providing only perceptions, which are not always useful for a toxicological risk assessment (Krug 2014).

In fact, there is a real problem for any regulation attempt and a bottleneck for the commercial advancement of nanotechnologies (about the nanotechnology regulation theme in Brazil, please review: Engelmann 2015). This shall not inhibit the investment progress of the researches, namely, *in vivo*, because most of the researches are *in vitro* yet. Moreover, there are other points that deserve attention as summarized by Kulinowski (2015): (a) the generalization process obtained in a result for all categories of nanotechnology ; (b) not taking the investigation results seriously, once there is a considerable number of publications pointing out the potential risks of some nanoparticles; and (c) taking greater scale materials in consideration in order to organize decisions about the risk management.

With all the new economies presented above, there is the need for a reconfiguration of complex arrangements of social and technological development. This reorganization will create new ways of risks, allowing its spread through systems that will be difficult, if not impossible, to predict or analyze using conventional risk assessment paradigm. For anticipating potential risks (here is situated the practical relevance of the precautionary principle), new approaches shall be necessary in order to model the dynamics among systems, using methods that integrate successfully and synthesize several knowledge ways about the countable and uncountable resources of multiple systems, as well as assure innovations in their initial stage, which are transparent enough to evaluate the wide systems reconfigurations associated to the new market development (Miller 2015). The author strengthens the argument of developing risk management in a wider perspective of governance to the generated challenges in the nanometric scale. It will not be possible to perform governance activities of the nanoscale from similar premises to the macroscale activities, because the physicochemical characteristics are different, consequently increasing the uncertainty scenario. Besides, one must pay attention to the following aspect: “The nanoparticles are used since the Bronze Age, but the quantity produced was always low. The great scale production of materials based on nanoparticles, without sanitary and toxicological control, as well

as their usage in the manufacture of consumption goods, might posit great risks for the population” (Joachim and Plévert 2009).

The sum of such factors will demand a decision making, implying a new risk involved, by the moment, the decision act about the way of approaching and crossing qualitative elements of the risk characterization posited by nanotechnologies. The future of the Earth life is at stake as a consequence of the decisions that will be made in the present. There rests a fundamental point: the caution with the so-called future generation, that is to say the current and future generations. The responsibility of current generations in relation to the future ones is opened. For this purpose, according to Hottois (2009): “We entered an era in which substituting a more or less stable and durable technical system for another through a revolution is not proceeding anymore. We are in a mobility era, of continuous changing and evolution; an era in which generated invention/discovery processes compete with each other and/or enter in conflict with the inertias caused by traditions and surpassed technologies.”

The speed in which technological novelties are presented and where the ones related with nanotechnologies are inserted is “almost frightening.” There is not enough time for a reflection about their necessity and adjustment to the human needs. In the decision of structuring models, ethical elements concerning current and future generations’ welfare and safety shall be included. Without such element, the decision may not be considered as correct, since it is not focused with future, which is always uncertain.

Therefore, the ethical issues connected with the judicial one may not be forgotten. In this sense, we propose the *nanotechnological risk governance* as a concrete contribution, which is mediated by ethical and judicial components, without which the technical, scientific, exact component should not have legitimacy structure and authorization to proceed. The governance includes studies about the risks, especially throughout the nanomaterial life cycle. However, “it requires the consideration of legal, institutional, social and economic contexts within which the risk is evaluated, as well as the involvement of the interested parties that represent them. Risk governance analyses the complex web of actors, rules, conventions, processes and mechanisms involved with the way that the relevant risk information are collected, analyzed communicated, and how the management decision are made. Engaging or combining relevant decisions about the risk and the government and private actors actions, the risk governance is particularly important, but not restricted to situations where there is no single authority to make a management decision of connection risk, but instead, where the risk nature requires collaboration and co-ordination among a range of different interested parties. Risk governance, nonetheless, does not include a multi-actor, multifaceted risk process, but also demands the consideration of context factors, such as institutional arrangements and political culture, including different risk perceptions. Thus, the framework includes several from these dimensions, abridging concerns assessment and an explicit discussion about the participation of interested parties” (Renn 2008).

A face of the *nanotechnological risk governance* will demand a compromise that goes beyond the States border limits: it is about the effective transnational

governance of biofuel sustainability and its interaction with the trade regime from the World Trade Organization (WTO). The Renewable Energy Directive (RED) stands out for modeling biofuel transnational governance, presenting deep and mutual dependency among public and private sectors. EU counts on a private system of enforcement and verification, but private certification systems depend on the incentives conceded by RED in order to expand themselves commercially. A way that presents positivity is the “transnational hybrid governance” (THG) of biofuels, anchored in the mutual formation of biofuel sustainability, discussing the institutional characteristics, process, webs, and socio-technical devices through which the markets are organized and the economic and political orders that are shaped (Ponte and Daugbjerg 2015).

With such elements, the conception of web in order to structure the *nanotechnological risk governance* is evinced. It is not an isolated initiative—be it public or private—but a combination of forces and visions, where the responsibility of current generations with the future ones can be aimed. Another example may be taken from Latin America and Caribbean region (ALC, in Portuguese), where a world production of biofuels is verified, responsible for 27 % of the offer and led by a proliferation of goals, which requires an increase of biofuel usage all over the world. The production of environmentally unsustainable biofuels may alter landscapes and point out socio-ecological systems. In order to mitigate such effects, different governance mechanisms were introduced, including national regulations, voluntary certification schemes, sustainability standards, meta-norms, and behavior codes. The voluntary certification stood out in the region, with more than 220 producers and processors into 12 countries of ALC recognized with the certification obtainment. Nevertheless, due to potential social and environmental effects in the region, the voluntary certification may not be enough and more binding sustainability mechanisms may be justified (Bailis et al. 2014). Therefore, it is necessary to pay attention to governance and risk management in an unknown effect scenario. The knowledge of positive aspects as well as of some risks is available, but the last ones are mostly unknown. Considering this perspective, Slater (2009) examined the governance issues from three “known unknowns,” which are the financial system, the biofuels, and the nanotechnology. The focus is aimed only for the last ones.

In the case of the biofuels, Slater (2009) raises a doubt about efficacy of green biofuels: “it is not certain if we are helping or damaging the environment through the promotion of their usage. This lack of knowledge did not stop the political decision makers of tagging current biofuels as green ones, besides of subsidizing their production strongly.”

The first level of ignorance strengthens the organization of the second level of known unknowns: “also we do not know if future comprehensive studies will tarnish the biofuels image and not even if current and future damage from biofuels industries will occur” (Slater 2009). Both levels presented are signaling the necessity of real investigation committed with the risk issue, all the more when particles in nanometric scale are added.

As verified in Krug (2014) study, research data about the effects of nanomaterials in human and environmental health are very scarce in this

moment—partly because there is not any regulatory demand in any jurisdiction obliging the producers to perform specific researches about the safety of nanomaterials (Slater 2009) and partly due to the disagreements and self-contradictions of the studies already published.

The “known unknown” aspect of the regulation of nanotechnology products may be structured as follows, according to Slater (2009): “We know that we are dealing with materials and substances that might be dangerous for human and environmental health. We don’t know if any of the products that are already available in the market is dangerous. We don’t know either for sure if the existent regulatory requirements (for instance, the clinical trials) are enough to cover the most important risks.”

The group of elements that are not known may receive one more ingredient, which is precisely what is the bearable limit that might be exerted over the nanotechnology regulation: meeting the balance point between an adequate regulation, aligned with ethical and judicial elements, particularly the human rights, and the production cost that the regulation might exert over the research continuity, development, industrialization, and commercialization of products based on nanotechnologies. Consequently, a preventive effective action (or even a precaution one) in the new technology regulation gets so difficult. Slater (2009) pointed out the reasons for such difficulty: (1) lack of knowledge about risks and benefits; (2) most part of the specialists is implied in innovation, and then, they could be into conflict of interests when manifesting about the regulation; (3) new technologies lead many times to the creation of several beginner small companies, which are vulnerable to administrative and regulatory charges; and (4) a political issue, in the sense that many politicians avoid to abridge the discussion of themes that may posit comprehensive difficulties to the population, which ends to be their electorate. These issues must be considered because they posit difficulties to an effective and democratic discussion process, as well as to the development of a normative nano-specified remark, reaching the usage of nanotechnologies in research and the development and production of biofuels as well.

An attempt to comprehend the risks and the uncertainty scenario is developing an assessment structure, analysis, and specification of several stages of the possibility of risk occurrence, searching for information, which are not enough yet. It will be necessary to organize and systematize the information about the risks that might be generated from the nanometric scale insertion into the biofuels. The risk governance shall initiate precisely from the already known risk recognition in relation to the nanoparticles to be handled. From this point on, obtaining conditions to evaluate the several levels of risks, initiating one’s management, and inserting the risk monitoring. In order to accomplish all of this, in each stage, the registers and the critical evaluation of the findings are fundamental in order to know some of the interaction periods of the nanoparticles, putting in their exposition in the lab with their reactions in the industrial environment and in the consumption environment.

As observed, *nanotechnological risk governance* will demand the knowledge of the risk outlines in each stage of their possible characterization, besides not being

possible to generalize any model, because the risk face designs are diverse in each nanoparticles. There lies a very interesting problem that was not adequately faced yet. Some stages for generating information can be summarized as follows: creating nanotechnology divisions, production of information on manufacturing the nano-scale, quantitative risk assessment, development of guidelines and regulations, and adjusting nanotechnology divisions for addressing risks (Reese 2013).

Therefore, the risk governance generated from the nanoscale is a group of actions and measures aiming the information generation and the detainment of specific actions for each type of nanomaterial or nanomaterial group, put together due to their common characteristics, which opens the possibility of knowing life cycle of nanomaterials and their toxicological characteristics. With all of this, it will be possible to make political decisions about the most adequate way of regulating nanotechnologies: the option by traditional regulation or the usage of other regulation, mixing the legislative regulation with a dialog among the sources of law, particularly through the precautions and principle of handling (Engelmann et al. 2014).

## 15.4 Conclusion

Nanotechnologies may bring several productive benefits including production of biofuels. Nevertheless, one has to compare the advantages with possible environmental and health risks posed by nanomaterials.

This observation is according to several international determinations, of which Brazil is one of the signatories. For instance, in the Rio-92 Conference statement, about environment and sustainable development, Principle No. 15 is specified as the precaution principle: “In order to protect the environment, preventive measures will be applied by the States, according to their capacity. Where there are real or permanent risk threats, the lack of total scientific certainty will not be applied as a postponement of efficient measures, in terms of cost in order to avoid the environmental degradation” (Brasil 2015). The principle is used in other contexts, aimed to life, and served as a moral paradigm to the productive logic.

The precaution principle will be the main theme that will interrelate with the several stages of nanotechnological risk governance, always aiming the systematization of information to be generated throughout several periods of the governance: creating nanotechnological divisions, production of information about the manufacture, quantitative risk evaluation, development of guidelines and regulation (signalizing the hybrid and flexible way of creating a nanospecific regulation), and always elaborating adjustments in the nanotechnologies, precisely aiming to comprehend new findings about the risks of different nanoparticles.

Checking the concepts, it is observed that prevention is a way to anticipate the processes and activities harmful to health, when is a probable risk and many times known.

The precautionary principle, on the other hand, impose actions even if there is no certainty about the risk, such as nanotechnologies. In fact, it is a concept of strong scientific and public health linkage. If there are indicatives of danger, one shall not let it happen as risks and damages to, only after their happening, try to repair them. Precaution respects life and the scientific uncertainty.

A great advance in the researches and the beginning of the existence of products from nanotechnological origin in the markets, even so late, alerted some regulation bodies and the executive body to understand the relevance of the regulatory aspects and the environmental and health risks related to the nanocomposites. And then, the National Sanitary Vigilance Agency (ANVISA), the Brazilian Industrial Development Agency (ABDI), the Brazilian Nanotechnology Initiative (IBN), and other academic and civil society bodies organized seminars and meetings as well as started to consider the regulatory process as a fundamental issue (Brasil 2012).

The final destination of wastes and products with nanomaterials in the environment leads to risks mainly provoked by inhalation and contact with the nanoparticles. The risks of diesel combustion particles to the cardiovascular and respiratory systems are known (Barath et al. 2010), but there is still need to understand about the effects of nanomaterials used in biodiesel production, such as catalysts and so on. One must take to debate if the doubts related to the potential risks are enough to suspend or relativize the nanotechnological production of biofuels to the society and its representatives. Up to the moment, there is no complete harmonization of methods to identify, quantify, and evaluate the potential damage caused by the nanomaterials to environment and to food and agriculture products (Bandyopadhyay et al. 2013).

The environmental exposure to nanomaterials shall be constant as its presence becomes more common and available for consumption. That's the main reason of its relevancy to society and why it must bring concerns and demand for nanotoxicity researches, regulations, governance, and social perspectives aimed to the use of those nanomaterials.

## References

- Abdi – agência brasileira de desenvolvimento industrial (2010) Estudo prospectivo nanotecnologia, vol XX. ABDI, Brasília
- Abegás (2015) Hidrogênio veio para desafiar os combustíveis fósseis. 2013. <http://www.abegas.org.br/site/?p=28068>. Accessed 20 July
- Alves JO, Zhuo C, Levendis YA, Tenório JAS (2012) Síntese de nanotubos de carbono a partir do bagaço da cana-de-açúcar. REM: R. Esc. Minas, Ouro Preto, 65(3):313–318, jul. set
- Araujo LR (2010) Pirólise: estudo do uso de catalisadores neste método e análise dos principais produtos obtidos na unidade piloto de pirólise rápida de ufu (ppr -10). Monografia da disciplina de projeto de graduação do curso de engenharia química. 2010. Universidade Federal de Uberlândia
- Bailis R, Solomon BD, Moser C, Hildebrandt T (2014) Biofuel sustainability in latin américa and the caribbean – a review of recent experiences and future prospects. Biofuels 5:469–485



- Bandyopadhyay S, Peralta-Videa JR, Gardea-Torresdey JL (2013) Advanced analytical techniques for the measurement of nanomaterials in food and agricultural samples: a review. *Environ Eng Sci* 30:118–125
- Barath S, Mills NL, Lundbäck M, Törnqvist H, Lucking AJ, Langrish JP, Söderberg S, Boman C, Westerholm R, Löndahl J, Donaldson K, Mudway IS, Sandström T, Newby DE, Blomberg A (2010) Impaired vascular function after exposure to diesel exhaust generated at urban transient running conditions. *Particle Fibre Toxicol Lond* 7:19–29
- Basha JS, Anand RB (2011) Role of nanoadditive blended biodiesel emulsion fuel on the working characteristics of a diesel engine. v. 3, n. 2. <http://scitation.aip.org/content/aip/journal/jrse/3/2/10.1063/1.3575169>. Accessed 20 July 2015
- Biotechnologia: iniciativa nacional de inovação (2008) – estudo prospectivo visão de futuro e agenda INI – biotecnologia 2008 – 2025
- Boff L (2012) Sustentabilidade: O que é: o que não é. Petrópolis, Jozes
- Botha A (2015) Future thinking and MOT. In: IAMOT. <http://www.iamot2015.com/documents/futurethinkingandmot-iamot2015.pdf>. Accessed 21 July
- Brasil (2007) Biocombustíveis: 50 perguntas e respostas sobre este novo mercado. Cartilha da Petrobras
- Brasil (2012) Anvisa. Nanotecnologia em debate na Anvisa. <http://portal.anvisa.gov.br/wps/content/anvisa+portal/anvisa/sala+de+imprensa/menu+-+noticias+anos/2012+noticias/nanotecnologia>. Accessed 25 July
- Brasil (2015) Empresa de pesquisa energética. Balanço energético nacional 2015. Ano base 2014: relatório síntese. EPE, Rio de Janeiro
- Brasil (2016) Brazilian Constitution of 1988. [http://www.planalto.gov.br/ccivil\\_03/constituicao/constituicaoconsolidado.htm](http://www.planalto.gov.br/ccivil_03/constituicao/constituicaoconsolidado.htm). Accessed 11 June 2016
- Casti JL (2012) O colapso de tudo: os eventos extremos que podem destruir a civilização a qualquer momento. Tradução de Ivo Korytowski e Bruno Alexandre. Intrínseca, Rio de Janeiro
- Dias FRF, Ferreira VF, Cunha AC (2012) Uma visão geral dos diferentes tipos de catálise em síntese orgânica. *Rev. Virtual Química* 4:840–871
- Domingos CA, Pereira DD, Cardoso LS, Teodoro RA, Castro VA (2012) Biodiesel – proposta de um combustível alternativo. *Revista brasileira de gestão e engenharia* 5:134–178. <http://www.periodicos.cesg.edu.br/index.php/gestaoeengenharia>. Accessed 25 July 2015
- Biodiversidade en América Latina y el Caribe (2005) Alerta sobre nova técnica de transgenia com nanofibras de carbono. <http://www.biodiversidadla.org/content/view/full/18206>. Accessed 20 July 2015
- Embrapa, Pacheco TF (2011) Produção de etanol: primeira geração ou segunda geração? <http://www.embrapa.br/imprensa/artigos/2011/producao-de-etanol-primeira-ou-segunda-geracao>. Accessed 20 July 2015
- Engelmann W (2015) Primeras tentativas de reglamentación de las nanotecnologías en Brasil. In: Foladori G, Hasmy A, Invernizzi N, Lau EZ (coords) *Nanotecnologías en América Latina: trabajo y regulación*, v. 1. Miguel Ángel Porrúa, Universidad Autónoma de Zacatecas; México, D.F., p 41–56
- Engelmann W, Aldrovandi A, Berger Filho AG (2014) Nanotecnologias aplicadas aos alimentos: construindo modelos jurídicos fundados no princípio da precaução. In: da Silva TEM, Waissmann W (Org) *Nanotecnologias: alimentação e biocombustíveis: um olhar transdisciplinar*. Criação, Aracaju, p 49–98
- ETC Group (2004) A invasão invisível do campo. O impacto das nanotecnologias na alimentação e na agricultura
- Fapesp (2015) <http://agencia.fapesp.br/13068>. Accessed 20 July
- Ferguson P (2015) The green economy agenda: business as usual or transformational discourse? *Environ Politics* 24:17–37
- Fernández PS, Martins CA, Martins ME, Camara GA (2013) Electro oxidation of glycerol on platinum nanoparticles: deciphering how the position of each carbon affects the oxidation pathways. *Electrochim Acta* 112:686–691

- Ferreira HS, Rangel MC (2009) Nanotecnologia: aspectos gerais e potencial de aplicação em catálise. *Química Nova* [online] 32:1860–1870
- Galbraith DW (2007) Nanobiotechnology: silica breaks through in plants. *Nat Nanotechnol* 2:272–273
- Goldemberg J (2009) Biomassa e Energia. *Rev. Química Nova* 32(3):582–587
- Granziera LS, de Assis OBG, Brumatti CR, de Jesus KRE (2012) Nanotecnologia na agricultura: prospecção dos indicadores de impactos ambientais e sociais. In: Congresso Interinstitucional de Iniciação Científica, 6, Jaguariúna. [Anais. . .] Jaguariúna: Embrapa Meio Ambiente. <http://www.alice.cnptia.embrapa.br/alice/bitstream/doc/951865/1/2012AA87.pdf>. Accessed 12 June 2016
- Herbst MH, Macedo MIF, Rocco AM (2004) Tecnologia dos nanotubos de carbono: tendências e perspectivas de uma área multidisciplinar. *Química Nova* 27:986–992
- Hottot G (2009) Qual é o quadro temporal para pensar nas gerações futuras? Uma abordagem filosófica. In: Schramm FR, Oliva A, Macial EMGS (Org) *Bioética: riscos e proteção*. 2. ed. UFRJ; FIOCRUZ, Rio de Janeiro, p 32–49
- Huber GW, Dale BE (2009) Gasolina de capim e outros vegetais. In: *Scientific American Brasil*, São Paulo, ano 8, 87:24–31
- INPI. Instituto Nacional da Propriedade Industrial (2011) Pedidos de patentes com tecnologias relativas ao biodiesel. [http://www.inpi.gov.br/menu-servicos/informacao/arquivos/biodiesel\\_pedidos\\_de\\_patentes.pdf](http://www.inpi.gov.br/menu-servicos/informacao/arquivos/biodiesel_pedidos_de_patentes.pdf). Accessed 25 Dec 2015
- IEA. International Energy Agency (2013) World energy outlook. [http://www.worldenergyoutlook.org/media/weowebiste/2013/weo2013\\_ch06\\_renewables.pdf](http://www.worldenergyoutlook.org/media/weowebiste/2013/weo2013_ch06_renewables.pdf). Accessed 15 July 2015
- IEA. International Energy Agency (2014) Biofuels. <http://www.iea.org/topics/biofuels/>. Accessed 15 July 2015
- Isaaa (2015a) International service for the acquisition of agri-biotech applications. <http://www.isaaa.org/resources/publications/pocketk/39/default.asp>. Accessed 20 July
- Isaaa (2015b) International service for the acquisition of agri-biotech applications. <http://www.isaaa.org/resources/publications/pocketk/45/default.asp>. Accessed 20 July
- ISO (International Organization for Standardization) (2015) Comitê técnico 229. [http://www.iso.org/iso/iso\\_technical\\_committee?commid=381983](http://www.iso.org/iso/iso_technical_committee?commid=381983). Accessed 20 July
- Jamieson D (2010) *Ética e Meio Ambiente: uma introdução*. SENAC, São Paulo
- Joachim C, Plévert L (2009) *Nanociências: a revolução do invisível*. Tradução de André Telles. Zahar, Rio de Janeiro
- Jovanovic G (2006) Tiny microreactor for biodiesel production could aid farmers, nation. <http://oregonstate.edu/ua/ncs/archives/2006/feb/tiny-microreactor-biodiesel-production-could-aid-farmers-nation>. Accessed 21 July 2015
- Khodakovskaya M, Dervishi E, Mahmood M, Xu Y, Li Z, Watanabe F, Biris AS (2009) Carbon nanotubes are able to penetrate plant seed and dramatically affect seed germination and plant growth. *ACS Nano* 3:3221–3227
- Khoshbin R, Haghghi M (2013) Preparation and catalytic performance of CuO-znO-AlO<sub>3</sub>/clinoptilolite nano catalyst for single-step synthesis of dimethyl ether from syngas as a green fuel. *J Nanosci Nanotechnol* 13(7):4996–5003
- Kimura T, Liu CX, Maekawa T, Asaoka S (2012) Conversion of isoprenoid oil by catalytic cracking and hydrocracking over nanoporous hybrid catalysts. *J Biomed Biotechnol* 2012:1–9
- Kohlhepp G (2010) Análise da situação da produção de etanol e biodiesel no Brasil. *Estud Av* [online] 24:223–253
- Krug HF (2014) Nanosafety research – are we on the right track? *Angew Chem Int Ed* 53:12304–12319. <http://onlinelibrary.wiley.com/doi/10.1002/anie.201403367/epdf>. Accessed 21 July 2015
- Kulinowski KM (2015) Tentación, tentación, tentación: ¿por qué es probable que respuestas simples sobre los riesgos de los nanomateriales sean erróneas? In: Foladori G, Hasmy A, Invernizzi N, Lau EZ (coord) *Nanotecnologías en América Latina: trabajo y regulación*, v. 1. Miguel Ángel Porrúa, Universidad Autónoma de Zacatecas, México, D.F., p 149–154

- Leff E (2010) *Discursos sustentáveis*. Cortez, São Paulo, 296p
- Leite RCC, Leal MRLV (2007) *O biocombustível no Brasil*. Cebrap 78, São Paulo
- Lima RB, Araujo HR, Camara GA (2013) Insights into the electro oxidation of glycolaldehyde on platinum. *Acidic Media J Electroanal Chem* 709:77–82
- Lorenzi CE (2009) *Impactos ambientais e energéticos provocados pela substituição de motores de combustão interna por células a combustível em veículos automotores*. São Caetano do Sul. Dissertação [Mestrado em Engenharia de Processos Químicos e Bioquímicos], Mauá
- Luhmann N (1992) *Sociología del Riesgo*. Universidade Iberoamericana, Guadalajara
- Madhuvilakku R, Piraman S (2013) ZnO mixed oxide nanocatalyst catalyzed palm oil transesterification process. *Bioresour Technol* 150:55–59
- Malajovich MA (2012) *Biotecnologia*. Rio de Janeiro, Edições da Biblioteca Max Feffer do Instituto de Tecnologia Ort
- Martins PR (2007) *Desenvolvimento recente da nanotecnologia no Brasil: reflexões sobre a política de riscos, impactos sociais, econômicos e ambientais em nanotecnologia*. In: Emerick MC, Montenegro KBM, Degraive W (org) *Novas tecnologias na genética humana: avanços e impactos para a saúde*. Gestec-Nit, Rio de Janeiro
- Mattei LF (2010) Programa nacional para produção e uso do biodiesel no Brasil (PNPB): trajetória, situação atual e desafios. *Revista Econômica do Nordeste*, Fortaleza 41:731–740
- MMA – Ministério do Meio Ambiente (2015a) Princípio da precaução. <http://www.mma.gov.br/biodiversidade/biosseguranca/organismos-geneticamente-modificados/item/7512>. Accessed 19 July
- MMA – Ministério do Meio Ambiente (2015b) Agenda 21. <http://www.mma.gov.br/responsabilidade-socioambiental/agenda-21>. Accessed 24 Jun
- Nações Unidas sobre o Meio Ambiente (2016) Sobre a Rio+20. [http://www.rio20.gov.br/sobre\\_a\\_rio\\_mais\\_20.html](http://www.rio20.gov.br/sobre_a_rio_mais_20.html). Accessed 24 July
- Milanez AY, Nyko D, Garcia JLF, Reis BLSFS (2012) O déficit de produção de etanol no Brasil entre 2012 e 2015: determinantes, consequências e sugestões de política BNDES setorial. *BNDES*, Rio de Janeiro 35:277–302
- Miller CA (2015) Modeling risk in complex bioeconomies. *J Responsible Innov* 2:124–127
- Monica JC Jr (2007) Nanoparticles successfully used in plant cell delivery study nanotechnology. Law Report. <http://www.nanolawreport.com/2007/05/articles/nanoparticles-successfully-used-in-plant-cell-delivery-study/#axzz2rafm5uk6>. Accessed 20 July 2015
- Moreira AJ (2013) *Obtenção de nanopartículas de platina para aplicação em células a combustível através do uso de plasma a baixa pressão*. Tese (doutorado), Escola Politécnica da Universidade de São Paulo
- Most Newsletter (2004) E3 fuel systems: a nano technology company. <http://www.alphapower.com/etech.htm>. Accessed 21 July 2015
- Nanowerk News (2007a) Nanosphere-based catalyst could revolutionize biodiesel production. <http://www.nanowerk.com/news/newsid=2161.php>. Accessed 20 July 2015
- Nanowerk News (2007b) Nanotechnology optimizes catalyst systems. <http://www.nanowerk.com/spotlight/spotid=2680.php>. Accessed 20 July 2015
- Nanowerk News (2013a) Graphene catalyst outperforms platinum in fuel cell. <http://www.nanowerk.com/news2/newsid=30786.php>. Accessed 21 July 2015
- Nanowerk News (2013b) Fuel cells from gelatin. <http://www.nanowerk.com/spotlight/spotid=32637.php>. Accessed 20 July 2015
- Novacana (2015) *As usinas de açúcar e etanol do Brasil*. <http://www.novacana.com/usinas-brasil>. Accessed 20 July
- Palmer J (2015) Cleaner cheaper fuels. *Nano the magazine for small science*. [http://www.nanomagazine.co.uk/index.php?option=com\\_content&view=article&id=385:cleaner-cheaper-fuels&catid=70&itemid=151](http://www.nanomagazine.co.uk/index.php?option=com_content&view=article&id=385:cleaner-cheaper-fuels&catid=70&itemid=151). Accessed 20 July
- Ponte S, Daugbjerg C (2015) Biofuel sustainability and the formation of transnational hybrid governance. *Environ Polit* 24:96–114

- Rangel MC, Carvalho MFA (2003) Impacto dos catalisadores automotivos no controle da qualidade do ar. *Química Nova* [online] 26:265–277
- Reese M (2013) Nanotechnology: using co-regulation to bring regulation of modern technologies into the 21st century. *Health Matrix* 23:537–572
- Renn O (2008) Risk governance. Coping with uncertainty in a complex world. Earthscan, London
- Silva DH (2009) Protocolos de Montreal e Kyoto: pontos em comum e diferenças fundamentais. *Rev Bras Polít Int* [online] 52:155–172
- Silva EP, Camargo JC, Sordi A, Santos AM (2003) Recursos energéticos, meio ambiente e desenvolvimento. *Multiciência*. <http://www.multiciencia.unicamp.br/art04.htm>. Accessed 21 July 2015
- Slater R (2009) The regulation of known unknowns: toward good regulatory governance principles. *Regulatory Governance Brief*, School of Public Policy and Administration, Carleton University. [www.regulatorygovernance.ca](http://www.regulatorygovernance.ca). Accessed 21 July 2015
- Teixeira LPB, Sales MN, Porto CM (2012) Necessidade de P&Dem biocombustíveis: o papel da Agência Nacional do Petróleo, Gás Natural e Biocombustíveis (ANP). *Diálogos ciência – Revista da Faculdade de Tecnologia e Ciências – Rede de Ensino FTC* 10
- Traumann AP (2007) Diplomacia dos petrodólares: relações do Brasil com o mundo árabe (1973–1985). Assis. Dissertação [Mestrado em História] – UNESP
- UNICA (2014) Relatório final da safra 2013/2014. Região Centro-Sul. [www.uni-cadata.com.br](http://www.uni-cadata.com.br). Accessed 28 August 2016
- Wang Y, Zhang X, Zhang H, Lu Y, Huang H, Dong X, Chen J, Dong J, Yang X, Hang H, Jiang T (2012) Coiled-coil networking shapes cell molecular machinery. *Mol Biol Cell* 23 (19):3911–3922
- Wei G-F, Liu Z-P (2013) Optimum nanoparticles for electrocatalytic oxygen reduction: the size, shape and new design. *Phys Chem Chem Phys* 15:18555–18561
- Wenner MA. próxima geração de biocombustíveis. In: *Scientific American Brasil*, São paulo, n. 32, [No date indication in the original], edição especial – todas as fontes de energia
- Yang WM, An H, Chou SK, Vedharaj S, Vallinayagam R, Balaji M (2013) Emulsion fuel with novel nano-organic additives for diesel engine application. *Fuel* 104:726–773

# Index

## A

Absorbance, 177  
Acidogenesis activity, 273  
Activity, 307  
Additives, 327, 328  
Adsorption, 43  
Advanced biofuel, 231–250  
AFEX. *See* Ammonia fiber/freeze explosion (AFEX)  
AFM. *See* Atomic force microscopy (AFM)  
Alcohol, 345–347, 351, 353, 354  
Alcoholysis, 270  
Alkali earth metal-oxides, 258  
Alkylation, 277, 291  
Al<sub>2</sub>O<sub>3</sub>, 234–238, 240, 241, 245, 247  
Alumina, 327, 328, 330–332, 337  
Ammonia fiber/freeze explosion (AFEX), 158  
Anaerobic digestion, 272–274  
Animal fats, 257, 270  
Applications, 91–111  
Atomic force microscopy (AFM), 22, 24, 26, 27, 182–185  
Atomization, 333  
Au nanoparticle, 48  
Aviation fuel. *See* Biojet fuel

## B

Beer-Lambert law, 177  
β-elimination, 313  
β-glucosidase, 166  
Bimetallic heterogeneous catalysts, 217, 218  
Bioalcohol, 302, 303  
Biochemical, 257  
Biodegradable, 270, 271

Biodiesel, 6, 8–11, 196, 198, 199, 207–223, 257, 258, 263, 264, 270–272, 274–282, 284, 325–337, 347  
Bioenergy, 174, 179, 187  
Bioethanol, 11–13, 154, 208, 218  
Bioethers, 220–221  
Biofuels, 3–15, 93, 94, 107, 109–111, 154, 174, 187, 196, 197, 199, 208–222, 255–293  
    production process, 255–293  
Biogas, 7–8, 272, 273  
Biogasoline, 301–320  
Biojet fuel, 232, 242–250  
Biological pretreatment methods, 157–158  
Biomass, 196, 204, 208–215, 218–222, 301–320, 345, 346, 349, 350, 354  
Biomass carbon, 40  
Biomass to fuel (BTF), 196, 198–204  
Biomaterials, 21, 22, 34  
Bio-oil, 257, 263, 265, 266  
Bio-organosolv, 158–159  
Biorefinery, 303–305  
BTF. *See* Biomass to fuel (BTF)

## C

Calcination temperature, 41  
Carbon-based nanomaterials, 39–56  
Carbon hollow fibers, 40  
Carbon nanotubes (CNTs), 45, 161, 329  
Catalyst deactivation, 283, 284  
Catalysts, 102, 107, 109, 110  
Catalytic, 327–329  
    activity, 258, 275, 276, 278, 279, 284  
    process, 233–238

C/Cu hybrids, 42  
 Cellobiose, 310  
 Cellotetraose, 310  
 Cellotriose, 310  
 Cellulose, 118–123, 130, 134, 135, 139, 155,  
 264, 268, 269, 283, 303, 309, 310  
 accessibility, 134, 136, 139, 144  
 nanocrystals, 43  
 susceptibility, 122–123  
 Ceria, 328  
 Cetane, 327  
 Chemical compositions of lignocellulose,  
 118–128  
 Chemical features of cellulose, 119–121  
 Chemical pretreatment methods, 136–139, 157  
 Cheong, H.K., 49  
 Chitosan–CNT–enzyme, 49  
*Chlorella vulgaris*, 102  
 C/N ratio, 273  
 CNTs. *See* Carbon nanotubes (CNTs)  
 Coating, 175, 180, 182  
 Co catalyst, 235, 242, 247, 249  
 Cohydrothermal, 264  
 Coke formation, 284  
 Combustion, 256, 257, 277, 327–329,  
 331–335  
 Commercialization, 268, 275, 282, 284  
 CoMoS<sub>2</sub>, 239, 242  
 CoMo sulfide. *See* CoMoS<sub>2</sub>  
 Concentration, 177  
 Conventional pyrolysis, 264, 266  
 Cracking, 262, 282, 291, 304, 313, 318, 319.  
*See also* Hydrocracking  
 Cross-draft, 260  
 Crystalline structures of cellulose, 121–122  
 Crystallinity, 175  
 Cu(OH)<sub>2</sub>/CuO, 41  
 Cyclic voltammetry curve, 40

## D

Decarbonylation, 233–235, 238, 239, 249,  
 304, 311–313  
 Decarboxylation, 233–235, 238, 239, 246,  
 249, 304, 311–313  
 Deoxygenation, 233–243, 246, 249, 301–320  
 Development, 344, 345, 347–350, 352, 355,  
 358, 359  
 Devolatilization, 259–260  
 Diesel, 325–337  
 Downdraft, 260  
 Drawbacks, 56  
 Dynamic light scattering (DLS), 175, 182

## E

EBFCs. *See* Enzymatic biofuel cells (EBFCs)  
 Efficiency, 326, 332  
 Electronic energy, 175  
 Electropun, 107, 109  
 Emissions, 326, 331, 333, 336  
 Emulsion, 327–330, 333–335  
 Energy, 344–348, 350, 351, 353, 354  
 Entrained-flow gasifier, 262–263  
 Environmentally-friendly methods, 56  
 Enzymatic biofuel cells (EBFCs), 45, 47,  
 53–56  
 Enzymatic hydrolysis, 21, 23, 24, 28, 29, 33,  
 123, 159  
 Enzyme immobilization, 159  
 Enzymes, 44  
 Esterification, 271, 277, 281, 291  
 Ethanol, 345–349, 352–354  
 Ethanol microfluidic, 56  
 Explosion, 333

## F

Fast pyrolysis, 263–265  
 Fatty acid methyl esters (FAME), 197,  
 199, 204  
 Fe<sub>3</sub>O<sub>4</sub>/C nanocomposites, 43  
 Fermentation, 268, 273  
 Ferromagnetism, 43  
 Fibers analysis, 23–26  
 First-generation biofuels, 154  
 Fluidized bed, 261–262  
 Fossil fuels, 5, 92, 93, 344  
 Fourier transform infrared spectroscopy  
 (FTIR), 174, 175  
 Fuels, 195–204, 302, 303, 307, 309, 311, 316,  
 318, 319  
 Fixed-bed gasifiers, 260–261

## G

Gaseous fuels, 94  
 Gaseous impurities, 259  
 Gasification, 94, 97–102, 106–110, 212,  
 257–263, 267, 274, 282–284  
 Gasifiers, 260–262, 266  
 D-Glucopyranose, 310  
 Glucose oxidase, 54  
 Glucose/oxygen biofuel cells, 55  
 Glycerol, 264, 271, 272, 277  
 Glycosidic bonds, 268  
 Graphene/enzyme, 55  
 Graphene oxide (GO), 47

Green diesel, 232–243, 249  
Greenhouse gas (GHG), 92  
Green technologies, 275, 284  
Guaiacol, 315, 316

## H

HC. *See* Hydrocarbons (HC)  
Hemicelluloses, 119, 123–125, 264, 303, 309, 310  
Heterogeneous catalysts, 214–222, 231–250, 258, 267, 274, 291, 305, 309  
Hierarchical, 50  
Hierarchy structure of cell wall, 129–133  
Higher alcohols and ethers, 196, 197, 200, 201, 204  
Highest surface area, 40, 49, 52, 56  
High stability, 47  
HMF. *See* 5-Hydroxymethylfurfural (HMF)  
HMTHFA. *See* 5-Hydroxymethyl tetrahydrofuran-2-carbaldehyde (HMTHFA)  
Homogeneous catalysts, 214, 219, 220, 222–223, 275  
Homopolymer, 310  
HTL. *See* Hydrothermal liquefaction (HTL)  
Hybrids, 41  
Hydrocarbons (HC), 326, 336  
Hydrocracking, 242, 243, 309, 318  
Hydrodeoxygenation, 233–235, 238, 239, 243, 246, 249, 304, 311, 313  
Hydrogen, 202  
Hydrogenation, 309–311, 313, 315, 316, 318  
Hydrogenolysis, 313, 316, 318  
Hydrogen transfer, 313  
Hydroisomerization, 233, 242, 243, 249  
Hydrolysis, 212–213, 257, 268–270, 272, 277  
Hydrothermal gasification, 262  
Hydrothermal liquefaction (HTL), 266  
5-Hydroxymethylfurfural (HMF), 315  
5-Hydroxymethyl tetrahydrofuran-2-carbaldehyde (HMTHFA), 315

## I

Ignition, 326–328, 336  
Immobilization of enzymes, 12, 164–167  
Impregnation, 278–281  
Infrared (IR) spectroscopy, 176–177  
Internal conversions, 175  
Intersystem crossings, 175  
Isomerization, 291. *See also* Hydroisomerization

## J

*Jatropha*, 222, 328

## K

Kinetic modeling, 106–108  
Krzysztof, S., 45  
Kyoto Protocol, 344

## L

Lignin, 20, 24, 27–29, 32, 119, 126–128, 137, 139, 264, 268, 270, 303, 309–311, 315–316  
Lignocellulose, 117–145, 207–223  
  biorefinery, 118, 119  
Lignocellulosic biomass, 19–34, 155  
Lignocellulosic materials, 8, 11  
Lipase, 270, 271  
Liquefaction, 211–212, 257, 258, 266–268  
Liquid fuels, 259  
Liquor, 33–34  
Long term stability, 56

## M

Magnetic nanocatalysts, 10  
Magnetic nanoparticles, 7, 13, 160–163  
Magnetophoretic separation, 62  
Mechanical pretreatment, 133–134  
Membrane/mediator-free enzymatic biofuel cells, 47  
Membrane separation processes, 262  
Mesophilic, 272–274  
Mesoporous, 308, 309, 319, 320  
  carbon nanoparticles, 52, 53  
  films, 52  
Metal-oxide nanocatalysts, 255–293  
Metal oxides, 107, 214–217  
Methanation, 234, 235, 238, 239, 309  
Methanogenesis activity, 273  
Methanol to oil molar ratio, 276, 278, 280, 282  
MFC. *See* Microbial fuel cell (MFC)  
Microalgae, 60, 265, 318  
  harvesting, 62  
Microalgal, 91–111  
Microalgal biorefinery, 60  
  conversion, 61  
  cultivation, 60  
  harvesting, 60  
  lipid extraction, 60  
Microbial fuel cell (MFC), 179, 187  
Microbiological, 257

- Microfibril, 24, 25, 28, 30–32  
 Microporous, 319  
 Microwave condition, 277  
 Microwave pyrolysis, 264  
 Mixed metal oxides, 258  
 Mode synthesizing atomic force microscopy (MSAFM), 24, 26  
 Molar absorptivity, 177  
 Molar extinction coefficient, 177  
 MoO<sub>3</sub>, 239, 242  
 MoS<sub>2</sub>, 239, 242, 249  
 Mo sulfide. *See* MoS<sub>2</sub>  
 MSAFM. *See* Mode synthesizing atomic force microscopy (MSAFM)  
 Multifunctional nanoparticles, 61  
 Multilayered architecture, 129–130  
 Multi-walled carbon nanotubes (MWCNTs), 48–51
- N**  
 NADH. *See* Nicotinamide adenine dinucleotide (NADH)  
 Nanoarchitected catalyst, 284  
 Nanocatalysts, 8–13, 305–309, 316–319  
   for biojet fuel production, 242–249  
   for green diesel production, 233–241  
 Nano-catalytic process, 195–204  
 Nanocellulose, 26, 30–33  
 Nanochemistry, 307  
 Nanocrystalline cellulose (NCC), 30, 33–34  
 Nanomagnetic materials, 277  
 Nanomaterials (NMs), 8, 39, 173, 355, 357–360  
 Nanoparticle-aided conversion of oil to biodiesel  
   acid nanocatalyst, 77–80  
   base nanocatalyst, 80–81  
   fatty acid methyl ester (FAME), 76  
   heterogeneous solid catalysts, 76  
   hierarchical nanocrystalline zeolite, 77  
   homogeneous catalysts, 76  
   sulfonated carbon-based catalyst, 77  
   upgrading to high-grade fuels, 77  
   ZrO<sub>2</sub>-promoted Ni catalysts, 81  
 Nanoparticle-aided lipid extraction, 73–76  
   aminoclay-based lipid extraction, 74, 75  
   enzyme pretreatment, 76  
   hydroxyl radicals, 74  
   potential engineered nanoparticles, 75–76  
   rigid cell wall, 73  
   surfactant-functionalized, 75  
 Nanoparticle-aided microalgae harvesting, 62–73  
 aminoclay-conjugated TiO<sub>2</sub> composites, 69, 74  
 aminoclay nanoparticles, 65, 68  
 APTES-functionalized BaFe<sub>12</sub>O<sub>19</sub> nanoparticles, 64, 70  
 attached-to, 63  
 cationic polyacrylamide (CPAM)-modified Fe<sub>3</sub>O<sub>4</sub> nanocomposites, 64  
 chitosan-functionalized Fe<sub>3</sub>O<sub>4</sub> nanoparticles, 65  
 detachment efficiency, 70  
 diethylaminoethyl (DEAE)-coated magnetic beads, 64  
 dually functionalized magnetic nanoparticles (dMNPs), 73  
 extended Derjaguin-Landau-Verwey-Overbeek (XDLVO) theory, 63, 64, 71  
 functionalized magnetic nanoparticles, 62–67  
 humic acid/Mg-aminoclay, 68  
 immobilized-on, 63  
 integrated use, 69–70  
 lipophilicity-controlled MNPs, 73  
 Mg-aminoclay-coated nZVI nanoparticles, 68  
 PDDA-coated magnetic nanoparticles, 63  
 PEI-coated magnetic beads, 63  
 PVP/Fe<sub>3</sub>O<sub>4</sub> composites, 65, 69  
 recyclable nanoparticles, 70–73  
 SA-coated Fe<sub>3</sub>O<sub>4</sub>-ZnO nanocomposites, 73  
 sonication-aided method, 72  
 surface wetting property, 73  
 TBD-Fe<sub>3</sub>O<sub>4</sub>@Silica NPs, 69, 81  
 tri-functionality, 69  
 water-nonpolar organic solvent (NOS) interface, 73  
 Nanoparticles, 173–188, 326–335, 359  
   immobilization, 29  
 Nanoporosity, 130–133  
 Nanoscale catalyzers/materials, 22  
 Nanoscale instrumentation, 21–26  
 Nano-shear hybrid alkaline (NSHA), 26–29  
 Nanotechnology, 3–15, 19–34, 39, 91–111, 154, 346–352, 354–356, 358, 359  
 Nanotoxicity, 160  
 NCC. *See* Nanocrystalline cellulose (NCC)  
 Ni catalyst, 235, 238, 240–242, 244, 245, 248  
 Nicotinamide adenine dinucleotide (NADH), 45  
 NiMoS<sub>2</sub>, 235, 242, 245  
 NiMo sulfide. *See* NiMoS<sub>2</sub>  
 Nitrogen oxides (NO<sub>x</sub>), 326  
 Non-renewable energy, 344



- NSHA. *See* Nano-shear hybrid alkaline (NSHA)
- Nuclear magnetic resonance (NMR), 175
- O**
- Operating conditions, 276, 278, 280–282, 284
- Optimum conditions, 278, 279, 281
- P**
- Partial thermal oxidation, 259
- Pd catalyst, 235, 238–240, 242, 244, 246, 247
- Performance, 328, 331, 333, 335, 336
- Phenylpropane units, 126
- Physical pretreatment methods, 156–157
- Physicochemical pretreatment, 134–136
- Physicochemical properties, 174
- Plasmon, 175, 177, 181
- Platinum nanoparticles, 48
- Pollutants, 326, 328, 336
- Pollution, 344, 350, 352
- Porosity of cell wall, 139–144
- Porous carbon, 52–53
- Porous carbon inks, 52
- Power output, 56
- Precipitation, 278, 279, 281, 283
- Pressure, 331, 332
- Pretreatment methods, 19–34, 133–139, 156–158
- Problems, 56
- Productivity, 196
- Pt catalyst, 235, 238, 240, 242, 245, 247, 249
- Pyrolysis, 210–211, 257, 259–260, 263–266, 270, 274, 282–284
- R**
- Ramie fibers, 40
- Rayleigh scattering, 181, 182
- Reaction time, 265, 267, 271, 272, 275–282
- Reactive oxygen species (ROS), 158
- Recalcitrance of cell wall, 130–133
- Renewable, 94, 110
- energy, 4, 20, 30, 256, 344, 346, 351
- sources, 345
- Reusability, 268, 269, 275, 276, 278–281
- ROS. *See* Reactive oxygen species (ROS)
- S**
- Saccharification, 29
- Saccharomyces cerevisiae*, 13
- Safety issues, 13–14
- SAPO-11, 240, 242–245
- Saturation magnetization, 43
- Scanning electron microscopy (SEM), 24, 174, 187
- Second-generation biofuels, 154
- Selectivity, 196, 200, 201, 204, 307
- Self-assembly, 48
- Silica, 51
- Single-walled carbon nanotubes (SWCNTs), 44–48
- Slow pyrolysis, 264
- Smoke, 328, 336
- Sonochemistry, 41, 43
- Specific capacitance, 40
- Stability, 327, 329–330
- Stearic acid deoxygenation, 217, 218
- Stirring speed, 281, 282
- Structure of hemicelluloses, 125
- Sugarcane, 345–350
- Superacid catalyst, 281
- Supercritical sol-gel route, 280
- Supported nano-metal oxides, 258
- Surface area, 258, 268, 274–277, 279–281, 283, 284
- Sustainability, 344, 345, 357
- Sustainable development, 359
- Sustainable energy, 110
- SWCNTs. *See* Single-walled carbon nanotubes (SWCNTs)
- T**
- Tar, 257–259, 261, 262, 264, 267, 282–284
- TEM. *See* Transmission electron microscopy (TEM)
- Theoretical and computer simulations, 56
- Thermochemical, 91–111, 209–212, 257, 263, 266
- Thermogravimetric, 98
- Thermophilic, 272
- 3D CNT/carbon microfiber-modified graphite electrode, 50
- Time of flight of secondary ion mass spectrometry (TOF-SIMS), 181
- Toxicity, 13, 14
- Transesterification, 257, 258, 270–272, 276–282
- Transition metal-oxides, 258
- Transmission electron microscopy (TEM), 24–26, 174, 185–187
- Triglyceride, 272, 304, 311, 313, 314, 319
- Tri-metallic catalyst, 262, 283

**U**

Ultraviolet-visible (UV-Vis) spectroscopy, 177–178  
Updraft, 260

**V**

Vegetable oils, 257, 270  
Vibrational and rotational relaxations, 175  
Volatilization step, 262

**W**

Waste cooking oil feedstock, 282  
Water–gas shift (WGS), 282, 283  
WO<sub>3</sub>, 242

**X**

X-ray diffraction (XRD), 175, 178–179  
X-ray photoelectron spectroscopy (XPS), 174, 175, 179–181  
Xylan, 310

**Y**

Y-shaped, 56

**Z**

Zeolite, 243, 249, 250, 308, 309, 318  
Zeta potential, 175  
ZnCl<sub>2</sub>, 40